Energy, Mines and Resources Canada | Énergie, Mines et Ressources Canada

CANMET

Canada Centre for Mineral and Energy Technology | Centre canadien de la technologie des minéraux et de l'énergie

STRENGTH DETERMINATION OF MONTAUBAN MINE ROCKS

B. Gorski, M. Little, M.C. Bétournay

Canadian Mine Technology Laboratory

January 1988

This document [illegible] report prepared [illegible] to [illegible] reporting purposes. It [illegible] represent a final expression [illegible] the opinion of the Centre [illegible] for Mineral and Energy T[illegible] (CANMET)

Ce document est un rapport [illegible] révisé et rédigé [illegible] fin de [illegible] documentation [illegible] nulle[illegible] définitive de [illegible] du Centre canadien de la technologie des minéraux et de l'énergie (CANMET)

353 pp

MICROMEDIA

MINING RESEARCH LABORATORIES
DIVISION REPORT MRL 87-169(TR)

STRENGTH DETERMINATION OF MONTAUBAN MINE ROCKS

by

B. Gorski*, M. Little**, M.C. Bétournay***

ABSTRACT

Laboratory tests were conducted on drill cores originating from previous diamond drilling activity at Montauban Mine, Quebec. The results of compressive strength and tests of ninety-two specimens are presented in this report.

Keywords : compression test, multiple failure state test, uniaxial strength, triaxial strength, m & s constants.

*Rock Mechanics & Development Technologist, Canadian Mine Technology Laboratory
Mining Research Laboratories, Energy, Mines and Resources Canada, Ottawa, Canada.

**Student, Civil Engineering, University of Waterloo

***Physical Scientist, Canadian Mine Technology Laboratory
Mining Research Laboratories, Energy, Mines and Resources Canada, Ottawa, Canada.

ÉVALUATION DE LA RÉSISTANCE DES ROCHES DE LA MINE MONTAUBAN

par

B. Gorski*, M. Little**, M.C. Bétournay***

RÉSUMÉ

Des essais en laboratoires out été faits sur des carottes de forage provennants de la mine Montauban, Québec. Les résultats de quatre - vingt douze essais en compression sont présentés dans ce rapport.

Mots clé : essais en compression, essais à résistances multiples résistance en compression uniaxiale, résistance en compression triaxiale, valeurs m & s.

*Technologue du développement et de la mécanique des roches Laboratoire de technologie, minière canadienne,Laboratoire de recherches minières, Énergie, Mines et Ressources Canada Ottawa, Canada.

** Étudiante, Génie Civil, Université de Waterloo

***Chercheur en science physiqe, Laboratoire de technologie minière canadienne, Laboratoire de recherches minières, Énergie, Mines et Ressources Canada Ottawa, Canada.

TABLE OF CONTENTS

		Page
	ABSTRACT	i
	RÉSUMÉ	ii
1.0	INTRODUCTION	1
2.0	TEST PROCEDURE	1
	SPECIMEN SELECTION	1
	SPECIMEN PREPARATION	1
	BASIC GEOLOGICAL DESCRIPTION	2
	UNIAXIAL POST-FAILURE TEST	2
	MULTI - STAGE TRIAXIAL TEST	2
	DATA ACQUISITION/REDUCTION	2
3.0	TEST RESULTS	3
	UNIAXIAL COMPRESSIVE STRENGTH	3
	ELASTIC CONSTANTS	3
	TRIAXIAL COMPRESSIVE STRENGTH	4
	FAILURE MODE	4
4.0	ANALYSIS OF TEST RESULTS	4
	STATISTICAL TREATMENT OF DATA	4
	STRENGTH ENVELOPES	4
	ROCK CLASSIFICATION	4
5.0	REFERENCES	6

TABLES

	Summary Table	5
1	Geological classification of drill cores	7
2	Specimen selection data	8, 9, 10, 11, 12
3	Uniaxial compressive test results	13, 14, 15
4	Multi - stage triaxial test results	16, 17, 18
5	Failure mode	19, 20, 21

APPENDICES

1 Stress-strain curves of uniaxial tests using axial LVDT #1 22
2 Stress-strain curves of uniaxial tests using axial strain gauges 23
3 Stress-strain curves of uniaxial tests using circumferential extensometer 24
4 Stress-strain curves of uniaxial tests using circumferential strain gauges . . . 25
5 Stress-strain curves of triaxial tests using axial LVDT #1 26
6 Stress-strain curves of triaxial tests using circumferential extensometer 27
7 Post-failure strength - confining pressure curves 28
8 Strength envelopes 29

1. INTRODUCTION

Drill core samples were received at MRL from Montauban Mine boreholes NQ1, 2, 3 and 4. The results of strength and deformation property tests performed on an MTS 815 test system are presented in this report. The program was completed in January 1988 and forms an integral part of the Montauban mine stability study. Results will be used in rock mass characterization, pillar strength determination, back analyses and numerical modelling.

2. TEST PROCEDURE

SPECIMEN SELECTION

Sample selection followed the need to obtain strength results for various geological units found around mine openings; footwalls, hanging walls and pillars.

Triaxial and uniaxial tests were conducted on rock specimens cut from each received core. The individual test specimens were coded as follows:

Example M36T

M - mine name

36 - specimen number

T - test type

The codes used for identification of test types are:

U - uniaxial test

T - triaxial test

The geological classification for the depth intervals of the drill cores are provided in Table 1. The specimen location, test type, dimensions and density, δ, of each tested specimen are listed in Table 2.

SPECIMEN PREPARATION

Rock core sample specimens selected for uniaxial and triaxial tests were prepared with length to diameter ratios of approximately 2:1. All specimens were lapped to within the specified tolerances, oven dried, weighed and dimensioned. Prior to testing planes of discontinuity, if any, or potential weaknesses were highlighted on the specimens with ink. The specimen preparation was performed according to the procedures used at MRL [1,2].

BASIC GEOLOGICAL DESCRIPTION

The rock types tested displayed varying degrees of gneissocity. This planar feature was oriented about 70° to core axes. Variations in quartz, mica and sulphide content are reflected in density values.

UNIAXIAL POST-FAILURE TEST

The specimen is uniaxially loaded, under load control mode, at the rate of 1kN/s. When the circumferential dilation of the specimen has reached 0.02 mm magnitude the axial load is reduced by 20%. The control mode is then switched over to circumferential displacement control. The test is continued, at a circumferential displacement rate of 0.0013 mm/s, through the peak strength until the residual strength is visually established, as indicated by a plateau in the graph recorded by the X Y recorder. The test is then terminated.

MULTI - STAGE TRIAXIAL TEST

The specimen is triaxially loaded, under load control mode, by the simultaneous application of axial load and confining pressure, at the rate of 1 kN/s. When the desired confining pressure of the first stage is reached, the axial loading is continued, at the rate of 1 kN/s while the confining pressure is kept constant. When circumferential dilation of the specimen has reached 0.02 mm magnitude the axial load is reduced by 20%. The control mode is then switched over to circumferential displacement control. The test is continued, at a circumferential displacement rate of 0.0013 mm/s, until an initial failure has occured as detected by an axial load drop.

The desired confining pressure of the second stage is applied, and so on, until the procedure is completed for each predetermined increment of confining pressure.

The confining pressure of the last stage is held through the peak strength until the residual strength is visually established, as indicated by a plateau in the graph recorded by the X Y recorder. The control is then switched over to axial displacement control mode. The specimen is further compressed axially for an additional displacement of 0.125 mm, at a rate of 0.002 mm/s, while the confining pressure is linearly reduced to zero within the time period of 60 seconds. This last phase of the test is required for residual strength data.

DATA ACQUISITION/REDUCTION

Data was scanned and stored by the computer every 3 seconds. Signals from the load cell, circumferential extensometer, axial LVDT#1, confinement pressure, and axial and circumferential strain gauges were scanned. Real time plotting of load versus axial displacement was obtained using a HP7046B X Y1 Y2 pen recorder wired to a MTS 448.85 controller.

The raw signals were reduced to engineering units and stored on hard disk for later recall. Measurements from axial LVDT#1 were corrected for end platen compression in the sensing gauge length. Reduced data was transferred to a VAX 750 computer for determination of specimen material constants. Mohr envelope plots were obtained using a laser printer. Hard copy plots of test results for report purposes were obtained using the DEC LVP16 pen plotter. The DEC LA50 printer was used to provide hard copies of reduced data for analyses.

3. TEST RESULTS

UNIAXIAL COMPRESSIVE STRENGTH

The peak strain values, ϵ_{peak}, listed in Table 3, were determined from the axial LVDT#1 readings. The uniaxial compressive strength results, Q_u, are also listed in Table 3.

Appendix 1 contains stress-strain curve plots utilizing signals from LVDT#1 for strain measurement. Appendix 2 provides stress-strain plots using signals from axial strain gauges mounted on the specimen surface. The gauges failed prior to test completion due to specimen fracture propagation. The plots in Appendix 3 are based on signals from the circumferential extensometer. The extensometer was located at mid-height of the specimen over mylar tape. The tape minimized rock spalling and reduced adverse extensometer signals. Appendix 4 contains curve plots derived from signals from strain gauges circumferentially mounted on the specimen surface. Specimen fracture propagation resulted in the gauges failing prior to test completion.

ELASTIC CONSTANTS

The modulus of elasticity, E, and the Poisson's ratio, ν, were established in each uniaxial compressive test case using load cell and strain gauge data. Modulus of elasticity values are based on axial strain gauge values. Poisson's ratio was calculated using axial and circumferential strain gauge readings. The obtained results are listed in Table 3.

Some values of Poisson's ratio appear erroneous; greater than 0.5, an impossibility, or very near to it indicating highly plastic behaviour. This is not very likely in this material as can be seen from the peak strains. Consequently, those values were rejected from statistical information. Relatively high values can be accounted for by gauge bonding either from material porosity or higher gneissocity that prevented good adhesive bonding.

TRIAXIAL COMPRESSIVE STRENGTH

The triaxial compressive strengths of the selected specimens were determined at successive confining stages of: 5 MPa, 10 MPa, 15 MPa and 20 MPa.

The stress-strain curve plots of the multi-stage triaxial tests are found in Appendix 5. Strain measurements were provided from LVDT #1 signals. Appendix 6 contains stress-strain curve plots using circumferential extensometer signals. The plots in Appendix 7 demonstrate the relationships between post-failure strength and confining pressure.

The results of the multi-stage tests are tabulated in Table 4.

FAILURE MODE

The information on test specimen failure modes are provided in Table 5.

4. ANALYSIS OF TEST RESULTS

STATISTICAL TREATMENT OF DATA

The test data, separated for each borehole and geologic type, were statistically reduced. The calculated mean and standard deviation values are shown in Tables 2, 3, 4, and 5.

The arithmetic mean values of the rock properties are listed in the Summary Table on page 5. It appears that there is no correlation between the rock name given by the mine and mechanical properties, ie. the strength and rock mass parameters are quite variable for each rock type. Strength and rock mass parameters are strata specific.

STRENGTH ENVELOPES

The peak strength envelopes of the boreholes are given in Appendix 8. These envelopes are based on the empirical failure criterion of rocks, established by Hoek and Brown [3].

The derived material constant values of m and s corresponding to the peak strength envelopes are given for each borehole in the relevant graph of Appendix 8. Residual m and s values were not considered valid due to the generally poor specimen response in the uniaxial residual stage and the calculation of higher residual values than intact.

ROCK CLASSIFICATION

The rocks may be classified on the basis of uniaxial compressive strength, as had been suggested by Coates and Parsons [5].

Accordingly, the rocks of borehole NQ1 are classified as weak to strong, NQ2 and 4 as strong, and NQ3 as strong to very strong. All rock types exhibited elastic behaviour, essentially for the entire range of loading, and brittle failure characteristics.

Summary Table

Borehole	Rock Type *	Rock Position +	δ (g/cm^3)	Q_u (MPa)	σ_t † (MPa)	E (GPa)	ν	ϕ ‡	m	s
NQ1	2	FW	2.74	118.89	—	47.32	0.29	46	7.83	1.00
NQ1	1	O,HW	2.85	87.03	—	38.82	0.24	30	14.16	1.00
NQ2	2	FW	2.74	84.68	—	44.19	0.24	48	8.75	1.00
NQ2	2	HW	2.72	44.68	-16.63	33.84	0.21	30	3.78	1.00
NQ3	1	FW	2.70	115.18	—	53.91	0.28	46	13.11	1.00
NQ3	2	O,HW	2.76	128.02	—	52.33	0.28	42	4.43	1.00
NQ4	2	O	2.77	59.76	—	27.46	0.22	20	1.23	1.00
NQ4	1	HW	2.69	78.44	-7.75	29.86	0.42	20	4.82	1.00

* [1] Q-B-M Gneiss, [2] Q-M-B Gneiss

+ FW - footwall, O - ore zone, HW - hanging wall

† obtained from hanging wall blocks and Brazilian tests [4]

‡ based on uniaxial failure plane angle

5. REFERENCES

1. Gorski, B. "Strength determinations of Prince Mine rocks"; Division Report RML/MRL 85-128(INT); CANMET, Energy, Mines and Resources Canada; 1985.

2. Gorski, B. "The design and operation of a stiff triaxial assembly for post-failure rock property testing"; Division Report MRP/MRL 82-81(TR); CANMET, Energy, Mines and Resources Canada; 1982.

3. Hoek, E. and Brown, E.T. "Underground excavations in rock"; Institution of Mining and Metallurgy, 527p; 1980.

4. Bétournay, M.C. , Lee, C. and Little, M. "Tensile strengths of Montauban Mine rocks"; Division Report MRL 87-169(TR); CANMET, Energy, Mines and Resources Canada; 1987.

5. Coates, D.F. and Parsons, R.C. "Experimental criteria for classification of rock substances"; Inst. of Rock Mechanics Sci. Vol. 3; Pergamon Press Ltd.; 1966.

Table 1 Geological classification of drill cores

Bore hole	Box number	Depth (m)	Geological Classification
NQ1	1,2	0-7.75	Quartz-Biotite-Muscovite Gneiss
	2	7.75-11.75	Quartz-Muscovite-Biotite Gneiss
	2,3	11.75-15.45	Quartz-Biotite-Muscovite Gneiss
	3,4	15.45-19.55	Amphibolite
NQ2	1,2	0-11.40	Quartz-Biotite-Muscovite Gneiss
	2,3,4	11.40-18.85	Quartz-Muscovite-Biotite Gneiss
	4	18.85-19.30	Tremolite Calc silicate
	4	19.30-21.96	Quartz-Muscovite-Biotite Gneiss
NQ3	1,2	0-6.40	Quartz-Biotite-Muscovite Gneiss
	2,3,4	6.40-16.75	Quartz-Muscovite-Biotite Gneiss
NQ4	1	0-2.65	Quartz-Muscovite-Biotite Gneiss
	1,2	2.65-5.34	Quartz-Biotite Gneiss
	2	5.34-7.75	Quartz-Muscovite-Biotite Gneiss
	2	7.75-8.30	Hornblende-Biotite Gneiss
	2,3	8.30-10.00	Quartz-Biotite Gneiss
	3	10.00-11.35	Amphibolite
	3	11.35-11.45	Quartz-Biotite Gneiss
	3	11.45-11.75	Garnet Amphibolite
	3	11.75-12.81	Quartz-Biotite Gneiss

Table 2 Specimen selection data

Sample Number	Depth (m)	Borehole & Box#	Test Type	Length (mm)	Diameter (mm)	δ (g/cm^3)
FW[2]						
M81U	9.17	NQ1-2	Uniaxial	95.04	47.48	2.75
M82U	9.65	NQ1-2	Uniaxial	95.92	47.50	2.78
M83U	10.65	NQ1-2	Uniaxial	93.68	47.48	2.64
M84U	11.28	NQ1-2	Uniaxial	97.52	47.48	2.67
M85U	11.45	NQ1-2	Uniaxial	95.44	47.50	2.66
mean						2.70
std.dev.						±0.06
FW[2]						
M44T	9.33	NQ1-2	Triaxial	96.74	47.46	2.75
M45T	9.43	NQ1-2	Triaxial	96.30	47.48	2.77
M46T	9.53	NQ1-2	Triaxial	96.40	47.50	2.79
M47T	8.56	NQ1-2	Triaxial	98.36	47.50	2.77
M48T	8.66	NQ1-2	Triaxial	96.24	47.50	2.75
mean						2.77
std.dev.						±0.02
O,HW[1]						
M3U	12.87	NQ1-3	Uniaxial	97.96	47.44	2.69
M4U	12.97	NQ1-3	Uniaxial	98.48	47.44	2.69
M5U	13.08	NQ1-3	Uniaxial	98.82	47.48	2.69
M6U	13.18	NQ1-3	Uniaxial	99.98	47.46	2.69
M7U	13.90	NQ1-3	Uniaxial	98.30	47.44	2.73
M8U	14.00	NQ1-3	Uniaxial	97.16	47.46	2.72
M9U	14.13	NQ1-3	Uniaxial	95.42	47.44	2.90
M10U	14.24	NQ1-3	Uniaxial	95.14	47.48	3.10
M11U	14.35	NQ1-3	Uniaxial	98.24	47.48	3.11
M12U	14.65	NQ1-3	Uniaxial	94.58	47.46	2.72
mean						2.80
std.dev.						±0.17
O,HW[1]						
M49T	14.93	NQ1-3	Triaxial	99.52	47.54	2.76
M50T	15.29	NQ1-3	Triaxial	99.18	47.50	2.90
M51T	15.39	NQ1-3	Triaxial	99.44	47.46	2.90
mean						2.85
std.dev.						±0.08

FW - footwall, O - ore zone, HW - hanging wall

[1] Q-B-M Gneiss [2] Q-M-B Gneiss [3] Amphibolite [4] Calc Silicate

Table 2 (continued)

Sample Number	Depth (m)	Borehole & Box#	Test Type	Length (mm)	Diameter (mm)	δ (g/cm^3)
HW[3]						
M52T	15.49	NQ1-3	Triaxial	99.80	47.46	2.85
M53T	15.60	NQ1-3	Triaxial	99.12	47.50	2.89
M54T	15.70	NQ1-3	Triaxial	99.50	47.48	2.9
M55T	15.91	NQ1-3	Triaxial	98.62	47.46	2.93
M56T	16.01	NQ1-3	Triaxial	100.10	47.46	2.90
mean						2.90
std.dev.						±0.03
FW[2]						
M13U	18.20	NQ2-4	Uniaxial	94.90	47.74	2.67
M14U	18.30	NQ2-4	Uniaxial	95.90	47.80	2.64
M15U	18.40	NQ2-4	Uniaxial	97.40	47.80	2.64
M16U	18.50	NQ2-4	Uniaxial	95.40	47.80	2.63
M17U	18.60	NQ2-4	Uniaxial	95.70	47.80	2.73
M18U	18.70	NQ2-4	Uniaxial	94.92	47.80	3.00
M19U	18.83	NQ2-4	Uniaxial	92.80	47.80	2.91
mean						2.75
std.dev.						±0.15
FW[2]						
M57T	12.21	NQ2-3	Triaxial	100.04	47.72	2.72
M58T	12.32	NQ2-3	Triaxial	99.90	47.72	2.74
M59T	12.42	NQ2-3	Triaxial	99.56	47.72	2.69
M60T	12.52	NQ2-3	Triaxial	99.80	47.70	* 2.27
M61T	12.63	NQ2-3	Triaxial	99.92	47.70	2.77
mean						2.73
std.dev.						±0.03
O[4]						
M20U	19.12	NQ2-4	Uniaxial	95.40	47.80	2.70
HW[2]						
M62T	20.13	NQ2-4	Triaxial	87.62	47.72	2.73
M63T	20.25	NQ2-4	Triaxial	82.20	47.74	2.72
M64T	20.34	NQ2-4	Triaxial	83.16	47.72	2.73
M65T	20.82	NQ2-4	Triaxial	91.46	47.74	2.70
mean						2.72
std.dev.						±0.01

* excluded from mean and standard deviation

Table 2 (continued)

Sample Number	Depth (m)	Borehole & Box#	Test Type	Length (mm)	Diameter (mm)	δ (g/cm^3)
HW[2]						
M21U	19.33	NQ2-4	Uniaxial	95.16	47.80	2.77
M22U	19.70	NQ2-4	Uniaxial	93.40	47.80	2.74
M23U	19.90	NQ2-4	Uniaxial	85.90	47.80	2.68
mean						2.73
std.dev.						±0.05
FW[1]						
M86U	0.31	NQ3-1	Uniaxial	95.82	47.44	2.75
M87U	1.16	NQ3-1	Uniaxial	90.64	47.52	2.79
M88U	1.79	NQ3-1	Uniaxial	98.04	47.44	2.68
M89U	3.13	NQ3-1	Uniaxial	96.64	47.52	2.69
M90U	4.42	NQ3-1	Uniaxial	94.89	47.44	2.69
mean						2.72
std.dev.						±0.05
FW[1]						
M66T	4.62	NQ3-2	Triaxial	100.70	47.52	2.67
M67T	4.72	NQ3-2	Triaxial	99.82	47.52	2.68
M68T	4.82	NQ3-2	Triaxial	99.38	47.50	2.67
M69T	5.03	NQ3-2	Triaxial	100.00	47.52	2.69
M70T	5.13	NQ3-2	Triaxial	100.04	47.54	2.68
mean						2.68
std.dev.						±0.00
O,HW[2]						
M24U	7.66	NQ3-2	Uniaxial	96.18	47.56	2.70
M25U	7.86	NQ3-2	Uniaxial	95.89	47.56	2.74
M26U	7.95	NQ3-2	Uniaxial	95.44	47.50	2.80
M27U	8.06	NQ3-2	Uniaxial	94.30	47.50	2.76
M28U	8.15	NQ3-2	Uniaxial	94.94	47.52	2.78
M29U	8.30	NQ3-2	Uniaxial	95.50	47.52	2.77
M30U	8.40	NQ3-2	Uniaxial	95.84	47.50	2.87
M31U	8.50	NQ3-2	Uniaxial	95.18	47.50	2.74
M32U	8.60	NQ3-2	Uniaxial	95.82	47.52	2.75
M33U	8.91	NQ3-2	Uniaxial	95.54	47.54	2.72
mean						2.76
std.dev.						±0.05

Table 2 (continued)

Sample Number	Depth (m)	Borehole & Box#	Test Type	Length (mm)	Diameter (mm)	δ (g/cm^3)
O,HW[2]						
M71T	11.26	NQ3-3	Triaxial	99.36	47.52	2.72
M72T	11.62	NQ3-3	Triaxial	99.52	47.56	2.74
M73T	11.94	NQ3-3	Triaxial	99.84	47.52	2.72
M74T	12.26	NQ3-3	Triaxial	99.90	47.50	2.78
M75T	12.46	NQ3-3	Triaxial	99.48	47.50	2.74
mean						2.74
std.dev.						±0.02
O[2]						
M34U	0.86	NQ4-1	Uniaxial	93.30	47.06	2.71
M35U	0.96	NQ4-1	Uniaxial	94.78	47.96	2.74
M36U	1.07	NQ4-1	Uniaxial	94.80	47.92	2.79
M37U	1.27	NQ4-1	Uniaxial	95.64	47.14	2.76
M38U	1.68	NQ4-1	Uniaxial	95.20	47.12	2.78
M39U	1.87	NQ4-1	Uniaxial	94.66	47.20	2.74
M40U	2.03	NQ4-1	Uniaxial	94.96	47.26	2.80
M41U	2.24	NQ4-1	Uniaxial	92.46	47.12	2.77
M42U	2.42	NQ4-1	Uniaxial	93.94	47.40	2.70
M43U	2.55	NQ4-1	Uniaxial	95.24	47.36	2.72
mean						2.75
std.dev.						±0.03
O[1]						
M93M	0.09	NQ4-1	Triaxial	97.24	47.40	2.77
M94M	0.39	NQ4-1	Triaxial	96.02	47.28	2.79
M95M	0.64	NQ4-1	Triaxial	89.76	47.46	2.75
mean						2.77
std.dev.						±0.02
HW[1]						
M91U	5.00	NQ4-2	Uniaxial	94.26	47.44	2.62
M92U	5.34	NQ4-2	Uniaxial	93.00	47.46	2.73
mean						2.68
std.dev.						±0.08

Table 2 (continued)

Sample Number	Depth (m)	Borehole & Box#	Test Type	Length (mm)	Diameter (mm)	δ (g/cm^3)
HW[1]						
M76T	2.73	NQ4-1	Triaxial	91.56	47.44	2.72
M77T	3.35	NQ4-1	Triaxial	95.78	47.32	2.73
M78T	3.56	NQ4-1	Triaxial	95.52	47.40	2.64
M79T	4.17	NQ4-1	Triaxial	95.60	47.44	2.67
M80T	4.60	NQ4-2	Triaxial	92.64	47.42	2.72
mean						2.70
std.dev.						$\pm$0.04

Table 3 Uniaxial compressive test results

Sample Number	Borehole & Box#	Depth (m)	Q_u (MPa)	ε_{peak} %	E (GPa)	ν
FW[2]						
M81U	NQ1-2	9.17	78.62	0.30	35.20	0.27
M82U	NQ1-2	9.65	55.14	0.35	28.81	* 0.96
M83U	NQ1-2	10.65	157.40	0.37	58.51	0.36
M84U	NQ1-2	11.28	172.68	0.28	64.68	0.25
M85U	NQ1-2	11.45	130.61	0.38	49.38	0.27
mean			118.89	0.34	47.32	0.29
std.dev.			±50.50	±0.04	±15.17	±0.05
O,HW[1]						
M3U	NQ1-3	12.87	122.68	0.27	46.68	0.26
M4U	NQ1-3	12.97	120.98	0.21	53.67	0.28
M5U	NQ1-3	13.08	94.91	0.31	38.81	0.31
M6U	NQ1-3	13.18	76.46	0.25	32.63	0.24
M7U	NQ1-3	13.90	83.36	0.27	46.10	0.25
M8U	NQ1-3	14.00	107.25	0.38	35.49	0.30
M9U	NQ1-3	14.13	29.61	0.13	25.61	0.21
M10U	NQ1-3	14.24	108.12	0.09	* 117.95	0.21
M11U	NQ1-3	14.35	70.01	0.16	* 113.21	0.13
M12U	NQ1-3	14.65	57.61	0.28	31.72	0.20
mean			87.12	0.24	38.84	0.24
std.dev.			±29.69	±0.03	±9.33	±0.05
FW[2]						
M13U	NQ2-4	18.20	110.36	0.45	35.98	0.15
M14U	NQ2-4	18.30	102.29	0.32	33.42	0.31
M15U	NQ2-4	18.40	70.03	0.23	40.34	0.25
M16U	NQ2-4	18.50	83.54	0.17	36.22	0.18
M17U	NQ2-4	18.60	87.08	0.16	48.59	0.35
M18U	NQ2-4	18.70	104.23	0.13	66.93	0.30
M19U	NQ2-4	18.83	30.69	0.16	47.84	0.12
mean			84.03	0.23	44.19	0.24
std.dev.			±27.34	±0.12	±11.63	±0.09
O[4]						
M20U	NQ2-4	19.12	67.21	0.25	31.26	0.43

* excluded from mean and standard deviation

Table 3 (continued)

Sample Number	Borehole & Box#	Depth (m)	Q_u (MPa)	ε_{peak} %	E (GPa)	ν
HW[2]						
M21U	NQ2-4	19.33	46.42	0.20	31.46	0.26
M22U	NQ2-4	19.70	57.34	0.36	35.23	0.16
M23U	NQ2-4	19.90	30.29	0.28	34.83	* 1.70
mean			44.68	0.28	33.84	0.21
std.dev.			±13.61	±0.08	±2.07	±0.07
FW[1]						
M86U	NQ3-1	0.31	106.73	0.35	43.72	0.29
M87U	NQ3-1	1.16	119.03	0.32	48.91	0.32
M88U	NQ3-1	1.79	177.22	0.35	67.26	0.24
M89U	NQ3-1	3.13	94.73	0.25	49.48	* 0.43
M90U	NQ3-1	4.42	78.20	0.28	60.20	* 0.44
mean			115.18	0.31	53.91	0.28
std.dev.			±37.82	±0.04	±9.57	±0.04
O,HW[2]						
M24U	NQ3-2	7.66	104.54	0.31	49.75	0.24
M25U	NQ3-2	7.86	128.38	0.27	50.56	0.26
M26U	NQ3-2	7.95	202.67	0.25	75.29	0.24
M27U	NQ3-2	8.06	129.85	0.30	47.13	0.38
M28U	NQ3-2	8.15	76.66	0.38	30.26	* 0.56
M29U	NQ3-2	8.30	114.25	0.25	43.28	0.37
M30U	NQ3-2	8.40	161.07	0.21	62.14	0.22
M31U	NQ3-2	8.50	137.78	0.27	45.27	* 0.46
M32U	NQ3-2	8.60	120.06	0.27	73.46	* 0.48
M33U	NQ3-2	8.91	104.89	0.31	46.14	0.22
mean			128.02	0.28	52.33	0.28
std.dev.			±34.55	±0.05	±14.00	±0.07

* excluded from mean and standard deviation

Table 3 (continued)

Sample Number	Borehole & Box#	Depth (m)	Q_u (MPa)	ε_{peak} %	E (GPa)	ν
O[2]						
M34U	NQ4-1	0.86	53.26	0.27	24.76	0.07
M35U	NQ4-1	0.96	65.23	0.25	39.36	0.19
M36U	NQ4-1	1.07	60.46	0.27	28.30	0.21
M37U	NQ4-1	1.27	72.60	0.29	32.85	0.26
M38U	NQ4-1	1.68	67.64	0.26	24.57	0.30
M39U	NQ4-1	1.87	81.53	0.35	31.04	0.19
M40U	NQ4-1	2.03	58.34	0.32	23.05	0.20
M41U	NQ4-1	2.24	38.31	0.37	13.28	0.25
M42U	NQ4-1	2.42	49.14	0.19	36.97	0.13
M43U	NQ4-1	2.55	51.10	0.19	20.43	0.05
mean			59.76	0.28	27.46	0.22
std.dev.			±12.58	±0.06	±7.89	±0.05
HW[1]						
M91U	NQ4-2	5.00	110.28	0.20	40.99	* 0.49
M92U	NQ4-2	5.34	46.60	0.33	18.74	0.42
mean			78.44	0.26	29.86	0.42
std.dev.			±45.03	±0.09	±15.73	±0.00

* excluded from mean and standard deviation

Table 4 Multi - stage triaxial test results

Sample indentification			σ_3=5.00 MPa		σ_3=10.00 MPa		σ_3=15.00 MPa		σ_3=20.00 MPa	
Sample Number	Borehole & Box#	Depth (m.)	σ_1 (MPa)	ε_{peak} (%)	σ_1 (MPa)	ε_{peak} (%)	σ_1 (MPa)	ε_{peak} (%)	σ_1 (MPa)	ε_{peak} (%)
FW[2]										
M44T	NQ1-2	9.33	169.83	0.48	200.63	0.58	225.83	0.65	248.10	0.74
M45T	NQ1-2	9.43	127.00	0.44	149.94	0.53	168.65	0.60	184.86	0.65
M46T	NQ1-2	9.53	161.53	0.40	188.23	0.50	208.91	0.57	224.93	0.61
M47T	NQ1-2	8.56	102.52	0.42	126.46	0.55	135.86	0.58	152.05	0.72
M48T	NQ1-2	8.66	109.49	0.61	124.40	0.70	137.49	0.79	148.95	0.87
mean			134.07	0.47	157.93	0.57	175.35	0.64	191.78	0.72
std.dev			±30.34	±0.08	±35.07	±0.08	±40.96	±0.09	±43.96	±0.10
O,HW[1]										
M49T	NQ1-3	14.93	118.26	0.38	131.42	0.47	143.29	0.55	154.56	0.69
M50T	NQ1-3	15.29	194.00	0.31	225.45	0.40	254.31	0.48	280.32	0.55
M51T	NQ1-3	15.39	225.23	0.38	254.91	0.43	278.64	0.47	295.90	0.51
mean			179.16	0.36	203.93	0.43	225.41	0.50	243.59	0.58
std.dev			±55.01	±0.04	±64.50	±0.04	±72.15	±0.04	±77.50	±0.09
HW[3]										
M52T	NQ1-3	15.49	226.87	0.40	270.36	0.50	309.71	0.61	340.95	0.68
M53T	NQ1-3	15.60	232.00	0.36	276.96	0.47	319.09	0.58	352.86	0.66
M54T	NQ1-3	15.70	216.77	0.32	261.30	0.41	308.85	0.55	348.46	0.67
M55T	NQ1-3	15.91	207.02	0.34	240.42	0.42	269.75	0.51	295.73	0.58
M56T	NQ1-3	16.01	226.26	0.31	279.94	0.43	310.49	0.49	355.62	0.72
mean			221.78	0.36	265.80	0.45	303.58	0.55	338.72	0.66
std.dev			±9.92	±0.03	±15.89	±0.04	±19.35	±0.05	±24.67	±0.05
FW[2]										
M57T	NQ2-3	12.21	120.87	0.35	143.23	0.42	163.97	0.50	181.38	0.57
M58T	NQ2-3	12.32	96.37	0.32	118.48	0.43	134.27	0.49	149.80	0.58
M59T	NQ2-3	12.42	192.57	0.44	230.98	0.55	253.51	0.60	279.04	0.69
M60T	NQ2-3	12.52	146.51	0.29	164.28	0.32	-	-	-	-
M61T	NQ2-3	12.63	190.86	0.27	215.61	0.30	217.49	0.34	240.80	0.38
mean			149.44	0.33	174.52	0.40	192.31	0.48	212.75	0.56
std.dev			±42.48	±0.07	±47.70	±0.10	±53.39	±0.11	±58.10	±0.13

Table 4 (continued)

Sample indentification			σ_3=5.00 MPa		σ_3=10.00 MPa		σ_3=15.00 MPa		σ_3=20.00 MPa	
Sample Number	Borehole & Box#	Depth (m.)	σ_1 (MPa)	ε_{peak} (%)	σ_1 (MPa)	ε_{peak} (%)	σ_1 (MPa)	ε_{peak} (%)	σ_1 (MPa)	ε_{peak} (%)
HW[2]										
M62T	NQ2-4	20.13	84.16	0.51	100.30	0.59	114.55	0.66	126.84	0.74
M63T	NQ2-4	20.25	103.20	0.74	—	—	—	—	—	—
M64T	NQ2-4	20.34	107.72	0.42	111.39	2.82	126.93	3.04	136.15	3.08
M65T	NQ2-4	20.82	103.28	0.27	120.51	0.31	135.95	0.35	149.42	0.41
mean			99.59	0.48	110.73	1.24	125.81	1.35	137.47	1.41
std.dev.			±10.50	±0.20	±10.12	±1.38	±10.74	±1.47	±11.35	±1.46
FW[1]										
M66T	NQ3-2	4.62	192.48	0.29	225.36	0.38	252.88	0.44	275.88	0.49
M67T	NQ3-2	4.72	226.73	0.41	270.38	0.50	303.09	0.57	338.72	0.71
M68T	NQ3-2	4.82	206.67	0.47	241.47	0.55	275.16	0.65	304.79	0.75
M69T	NQ3-2	5.03	214.94	0.38	246.96	0.45	269.43	0.50	285.53	0.54
M70T	NQ3-2	5.13	198.16	0.38	229.12	0.44	252.52	0.49	272.81	0.54
mean			207.80	0.39	242.66	0.46	270.60	0.53	295.55	0.61
std.dev.			±13.58	±0.07	±17.83	±0.06	±20.74	±0.08	±27.17	±0.12
HW[2]										
M71T	NQ3-3	11.26	113.11	0.33	131.53	0.38	145.90	0.44	156.32	0.48
M72T	NQ3-3	11.62	34.72	0.16	67.46	0.31	78.37	0.37	92.47	0.48
M73T	NQ3-3	11.94	82.29	0.19	94.17	0.23	104.50	0.27	111.13	0.27
M74T	NQ3-3	12.26	143.87	0.31	161.33	0.37	168.33	0.42	184.87	0.48
M75T	NQ3-3	12.46	149.38	0.42	169.62	0.49	186.60	0.54	201.93	0.59
mean			104.67	0.28	124.82	0.36	136.74	0.41	149.34	0.46
std.dev.			±47.44	±0.11	±43.63	±0.10	±44.76	±0.10	±46.83	±0.12
O[2]										
M93M	NQ4-1	0.09	57.35	0.24	65.39	0.26	72.57	0.29	80.18	0.34
M94M	NQ4-1	0.39	54.42	0.26	63.29	0.30	71.20	0.33	77.90	0.37
M95M	NQ4-1	0.64	68.95	0.29	82.67	0.34	96.40	0.40	113.48	0.52
mean			60.24	0.26	70.45	0.30	80.06	0.34	90.52	0.41
std.dev.			±7.68	±0.03	±10.63	±0.04	±14.17	±0.06	±19.92	±0.10

Table 4 (continued)

Sample indentification			σ_3=5.00 MPa		σ_3=10.00 MPa		σ_3=15.00 MPa		σ_3=20.00 MPa	
Sample Number	Borehole & Box#	Depth (m.)	σ_1 (MPa)	ε_{peak} (%)	σ_1 (MPa)	ε_{peak} (%)	σ_1 (MPa)	ε_{peak} (%)	σ_1 (MPa)	ε_{peak} (%)
HW[1]										
M76T	NQ4-1	2.73	86.97	0.22	98.03	0.27	105.02	0.31	133.87	1.07
M77T	NQ4-1	3.35	216.33	0.28	237.51	0.32	255.39	0.35	-	-
M78T	NQ4-1	3.56	105.28	0.18	123.54	0.22	143.44	0.44	163.94	0.40
M79T	NQ4-1	4.17	86.19	0.36	100.96	0.45	113.31	0.50	124.11	0.57
M80T	NQ4-2	4.60	80.65	0.41	-	-	-	-	-	-
mean			115.08	0.29	140.01	0.32	154.29	0.40	140.64	0.68
std.dev.			±57.35	±0.10	±65.99	±0.10	±69.39	±0.09	±20.76	±0.35

Table 5 Failure mode

Sample Number	Failure angle (Degrees)	Failure mode
FW[2]		
M81U	68	diagonal
M82U	* 40	discontinuity
M83U	-	single cone
M84U	-	axial split
M85U	-	single cone
mean	68	
std.dev.	±0	
FW[2]		
M44T	-	twin slabbing
M45T	48	shear failure
M46T	51	shear failure
M47T	43	shear failure
M48T	39	shear failure
O[1]		
M3U	64	diagonal
M4U	66	diagonal & discontinuity
M5U	51	diagonal
M6U	65	diagonal
M7U	48	diagonal
M8U	62	diagonal
M9U	56	diagonal & discontinuity
M10U	-	discontinuity & axial split
M11U	-	twin slabbing
M12U	69	diagonal
mean	60	
std.dev.	±8	
O[1]		
M49T	55	shear failure
M50T	61	shear failure
M51T	72	shear failure
HW[3]		
M52T	66	shear failure
M53T	66	shear failure
M54T	69	shear failure
M55T	75	shear failure
M56T	-	twin slabbing
FW[2]		
M13U	68	diagonal
M14U	58	diagonal
M15U	76	diagonal & discontinuity
M16U	-	twin slabbing
M17U	70	diagonal & discontinuity
M18U	71	diagonal & discontinuity
M19U	* 38	discontinuity
mean	69	
std.dev.	±7	

* excluded from mean and standard deviation

Table 5 (continued)

Sample Number	Failure angle (Degrees)	Failure mode
FW[2]		
M57T	63	shear failure
M58T	57	shear failure
M59T	66	shear failure
M60T	60	shear failure
M61T	70	shear failure
O[4]		
M20U	66	diagonal & discontinuity
HW[2]		
M62T	33	shear failure
M63T	53	shear failure
M64T	47	shear failure & discontinuity
M65T	57	shear failure & discontinuity
HW[2]		
M21U	55	diagonal
M22U	60	diagonal & discontinuity
M23U	66	diagonal
mean	60	
std.dev.	±6	
FW[1]		
M86U	70	diagonal
M87U	70	diagonal
M88U	–	axial split
M89U	–	single slab
M90U	55	discontinuity
mean	68	
std.dev.	±9	
FW[1]		
M66T	42	shear failure & discontinuity
M67T	–	twin slabbing
M68T	68	shear failure
M69T	57	shear failure & discontinuity
M70T	69	shear failure
O[2]		
M24U	60	diagonal
M25U	–	twin slabbing
M26U	–	twin slabbing
M27U	70	diagonal
M28U	66	diagonal
M29U	–	twin slabbing & discontinuity
M30U	–	twin slabbing & discontinuity
M31U	66	diagonal
M32U	–	discontinuity & axial split
M33U	–	discontinuity & axial split
mean	66	
std.dev.	±4	

Table 5 (continued)

Sample Number	Failure angle (Degrees)	Failure mode
HW[2]		
M71T	55	shear failure
M72T	48	discontinuity
M73T	49	discontinuity
M74T	55	shear failure
M75T	61	shear failure
O[2]		
M34U	* 48	diagonal & discontinuity
M35U	52	diagonal & discontinuity
M36U	53	diagonal
M37U		discontinuity & axial split
M38U	60	diagonal
M39U	* 77	diagonal & discontinuity
M40U	57	diagonal & discontinuity
M41U	54	diagonal
M42U	* 44	diagonal & discontinuity
M43U	* 37	diagonal & discontinuity
mean	55	
std.dev.	±3	
O[1]		
M93M	43	discontinuity
M94M	43	discontinuity
M95M	45	shear failure
HW[1]		
M91U	-	axial split
M92U	55	discontinuity
mean	55	
std.dev.	±0	
HW[1]		
M76T	36	shear failure & discontinuity
M77T	68	shear failure & discontinuity
M78T	45	shear failure & discontinuity
M79T	44	shear failure & discontinuity
M80T	33	shear failure & discontinuity

* excluded from mean and standard deviation

Appendix 1.

Stress-strain curves of uniaxial tests using axial LVDT #1

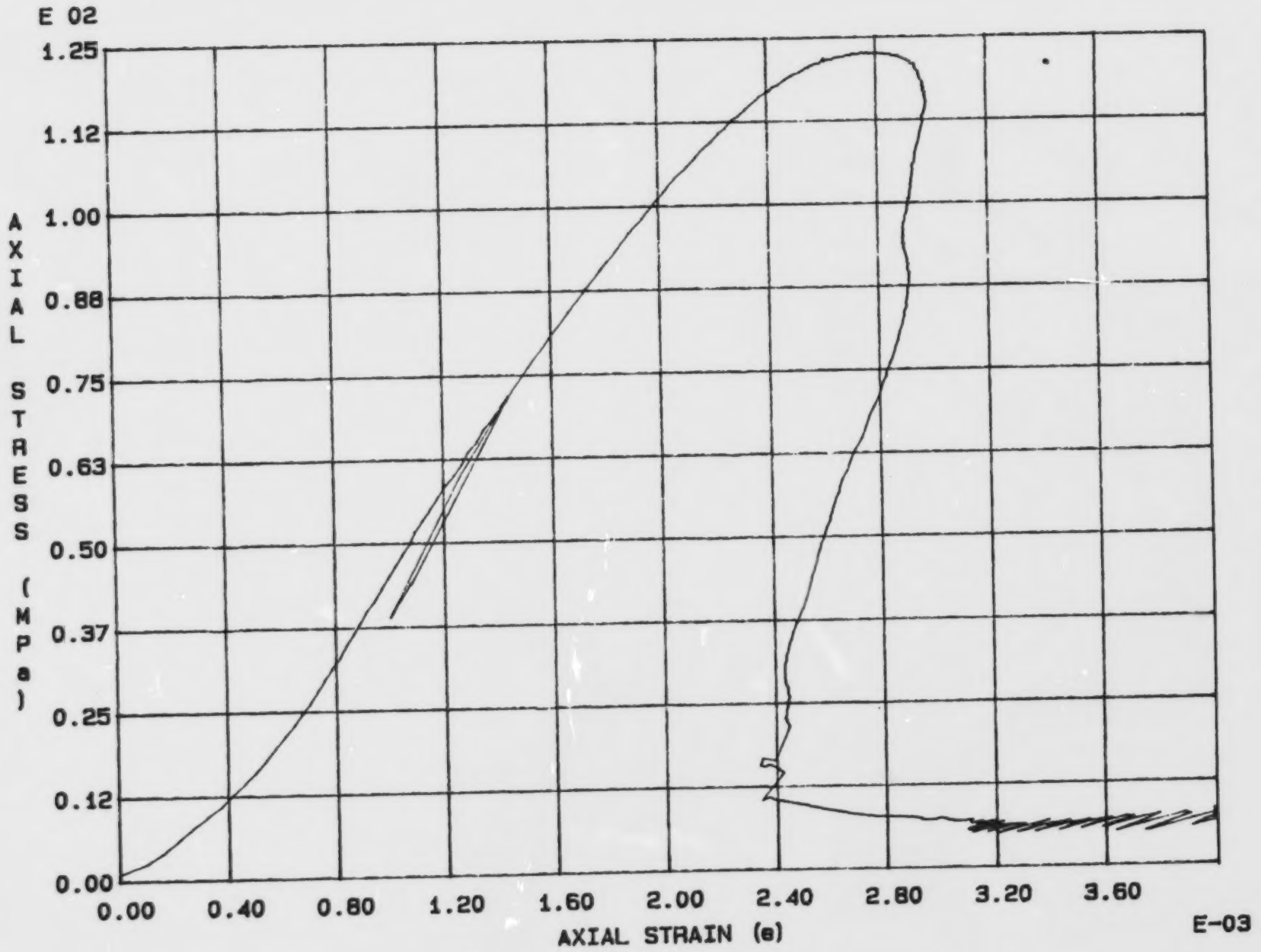

Fig. 1 - 1 Specimen M3U

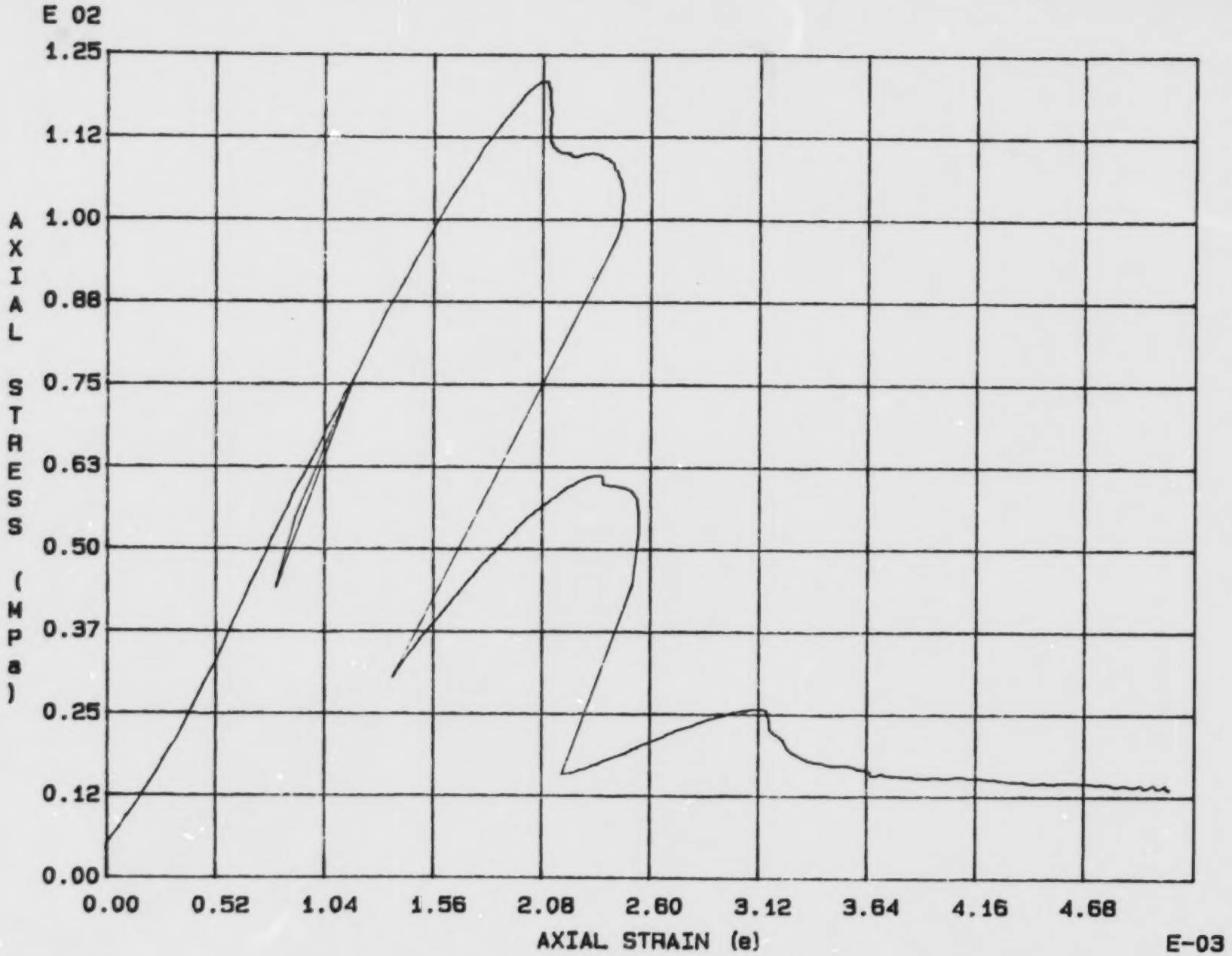

Fig. 1 - 2 Specimen M4U

Fig. 1 - 3 Specimen M5U

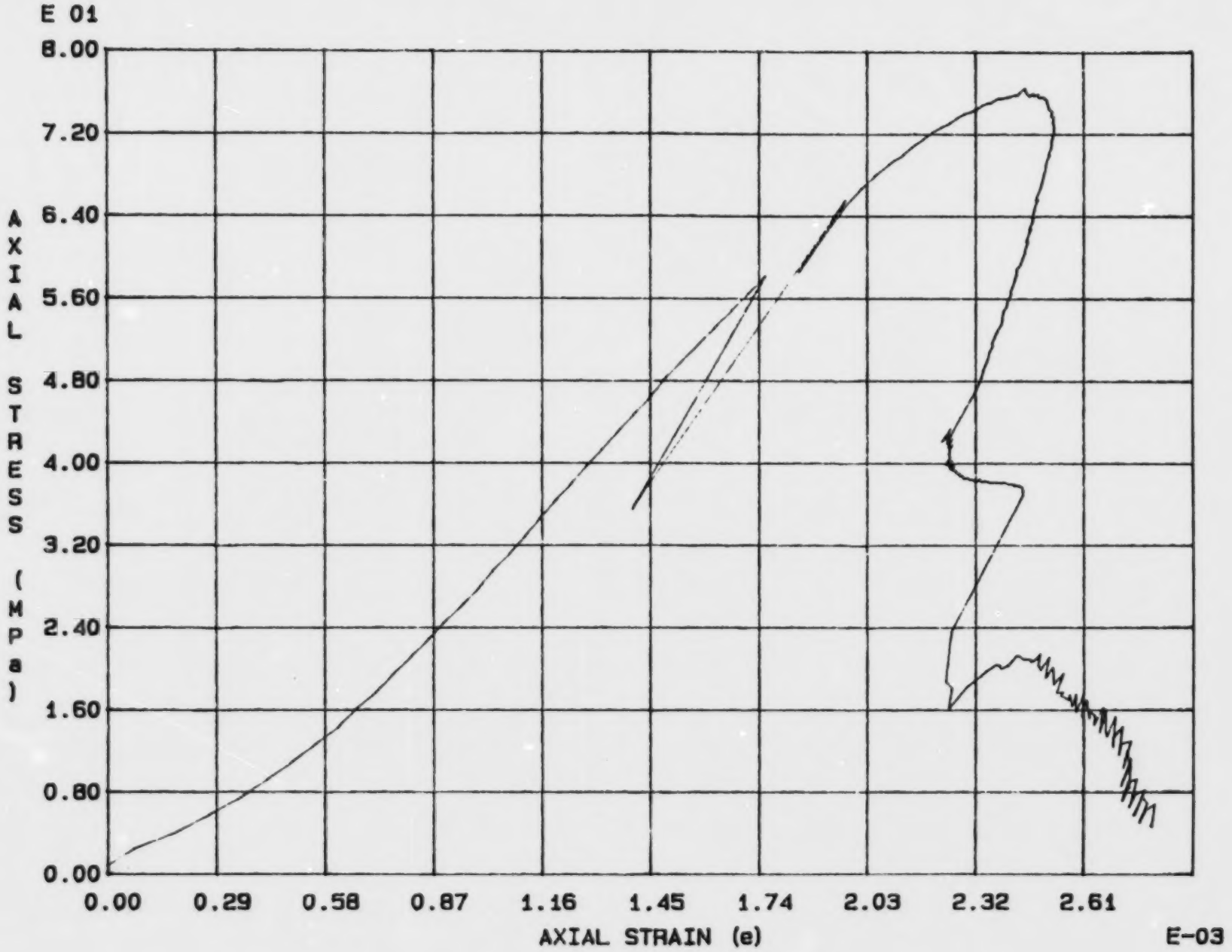

Fig. 1 - 4 Specimen M6U

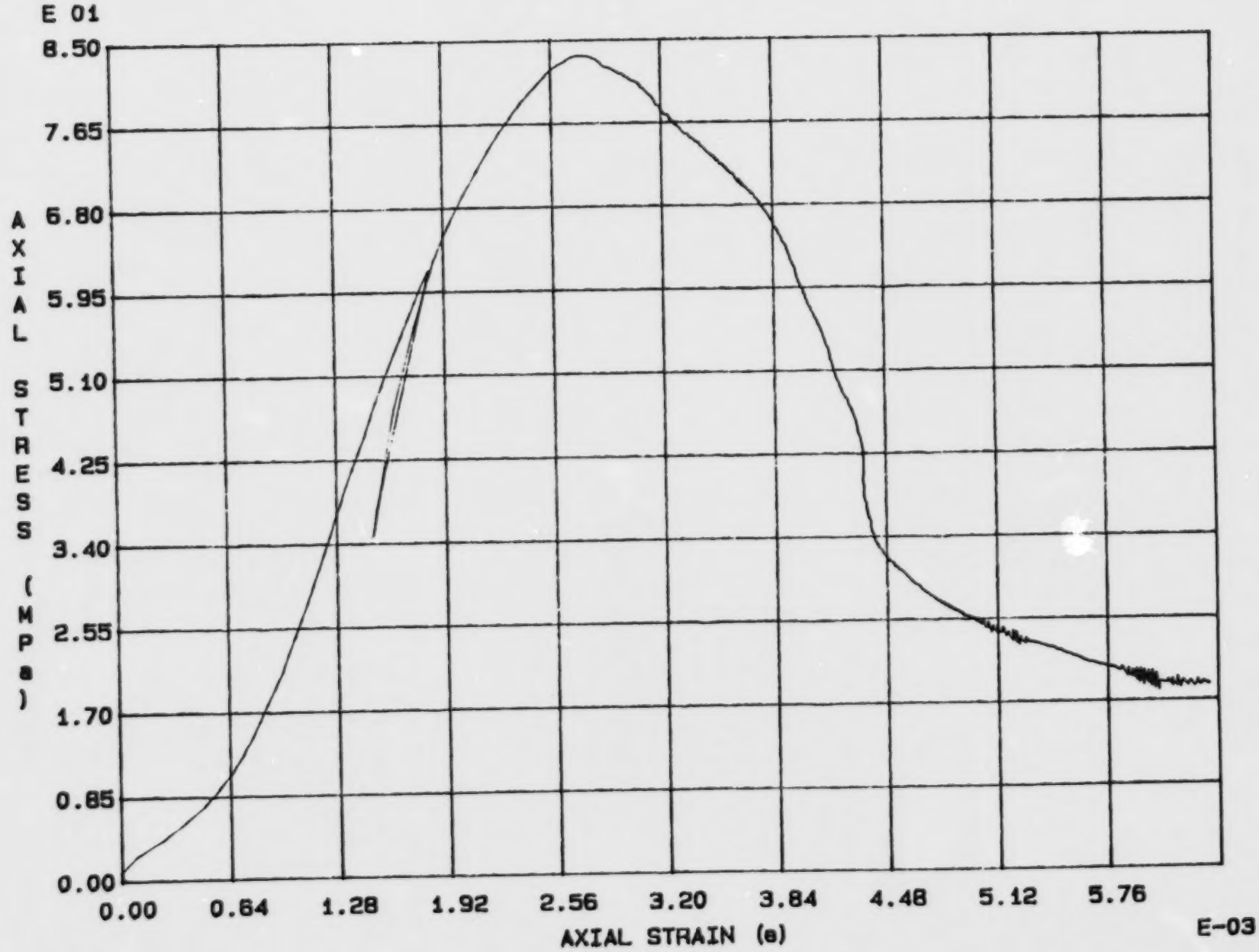

Fig. 1 - 5 Specimen M7U

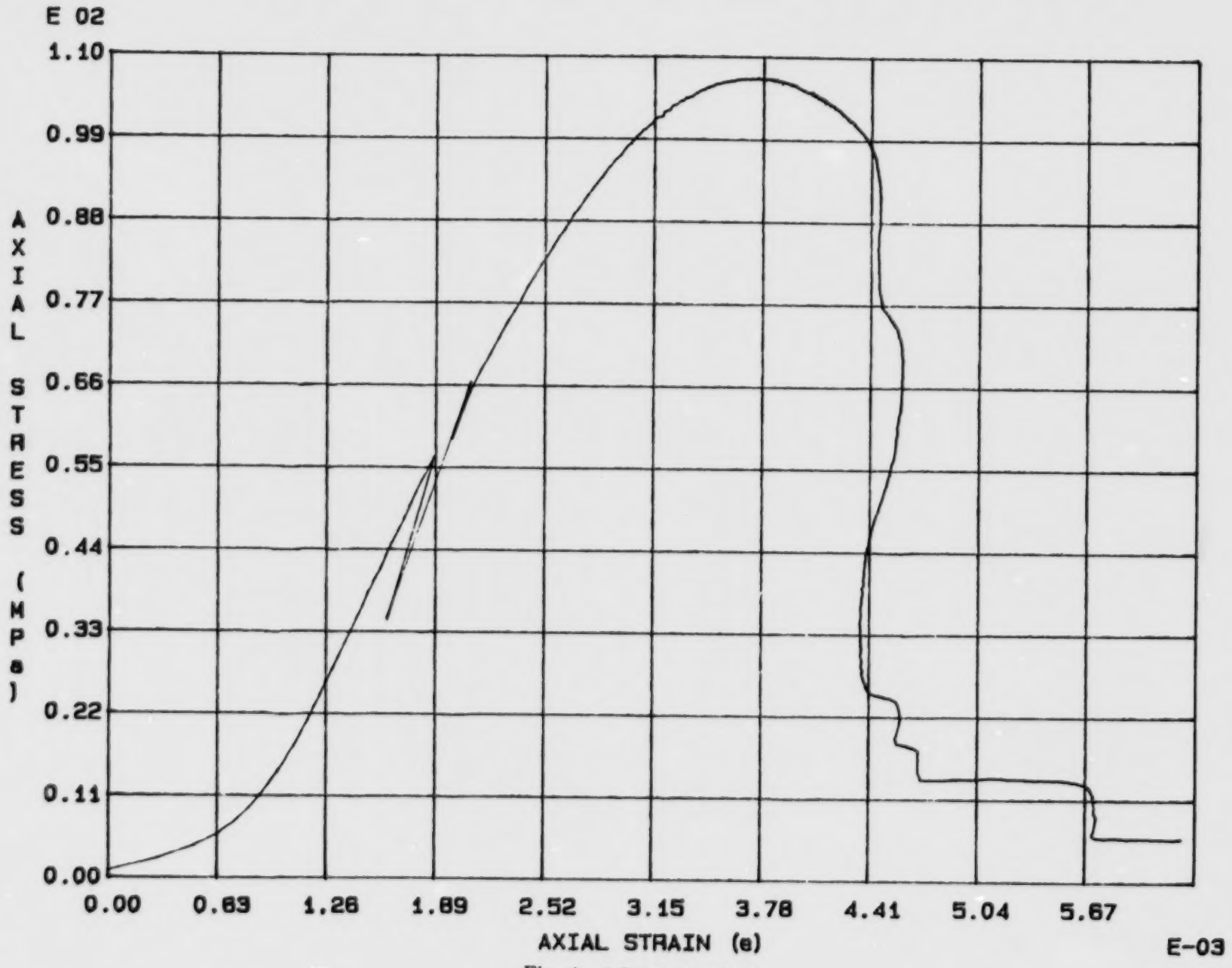

Fig. 1 - 6 Specimen M8U

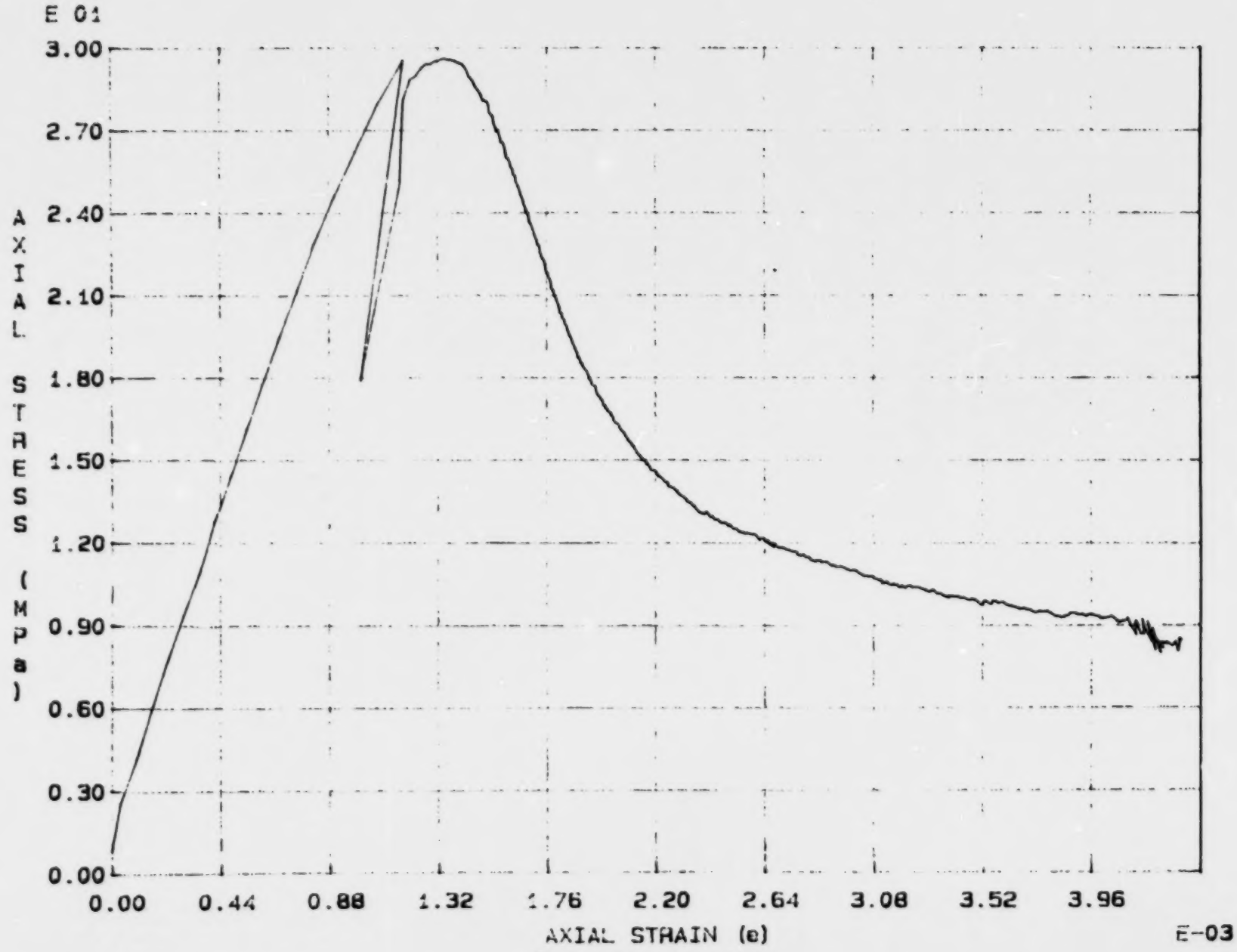

Fig. 1 - 7 Specimen M9U

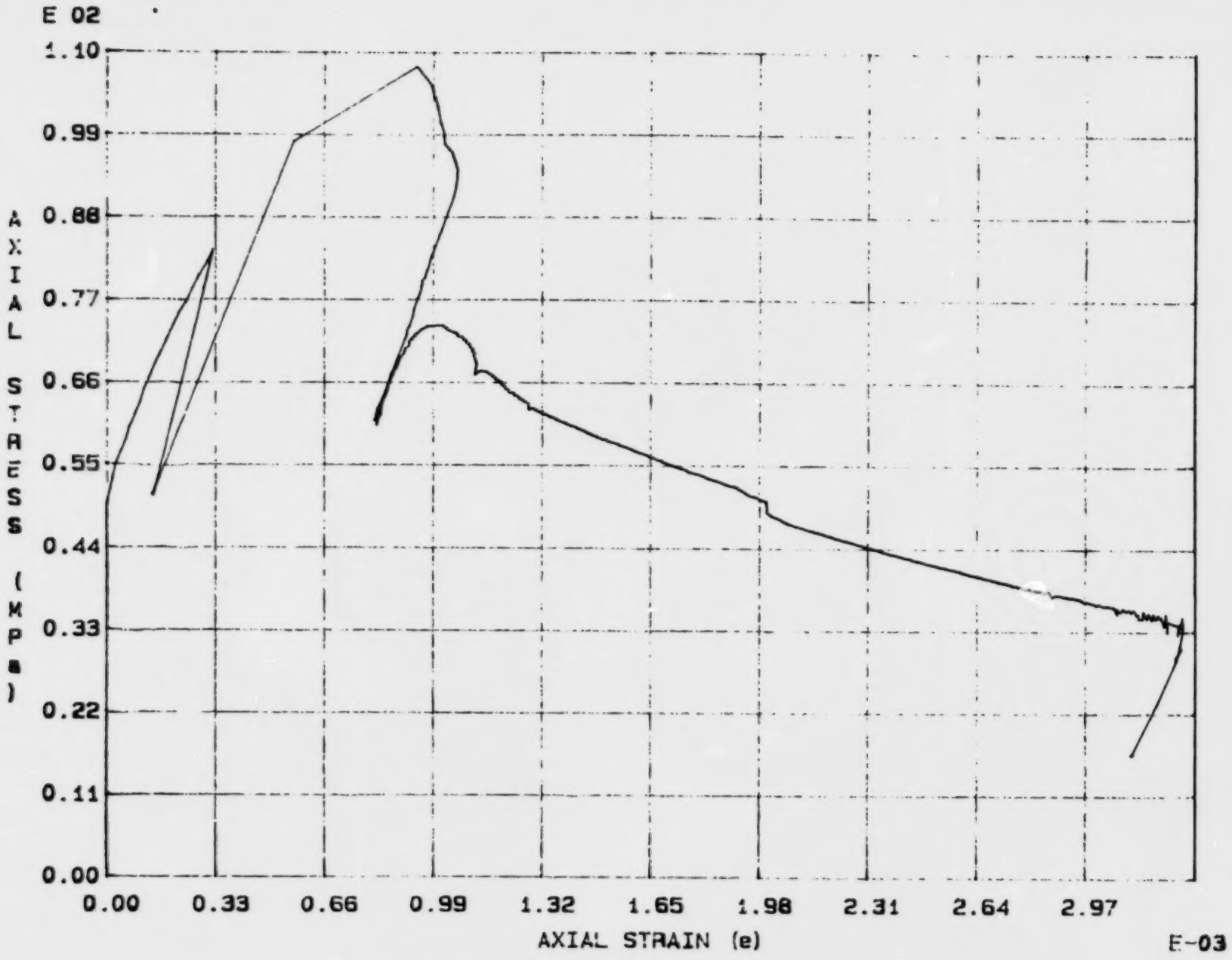

Fig. 1 - 8 Specimen M10U

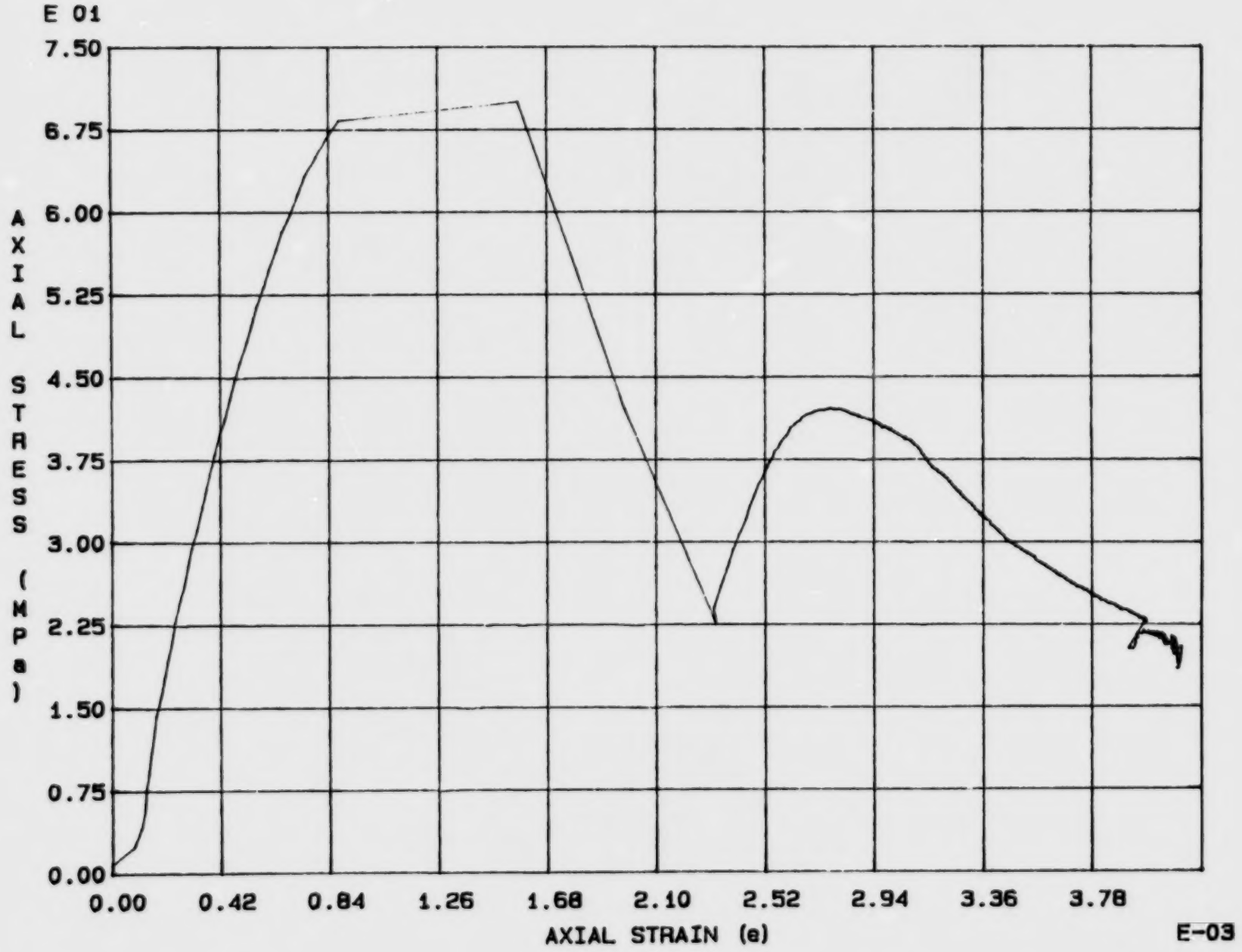

Fig. 1 - 9 Specimen M11U

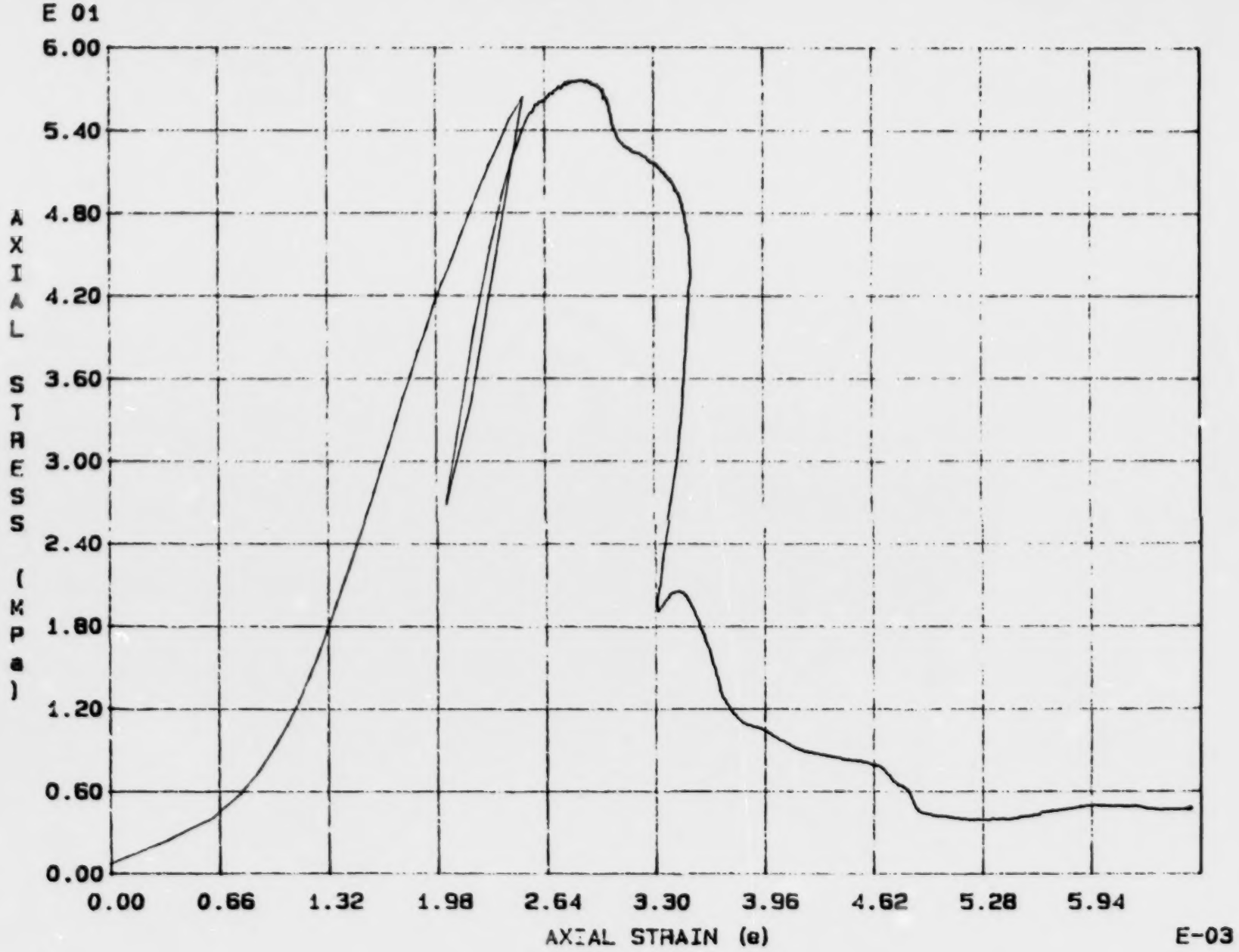

Fig. 1 - 10 Specimen M12U

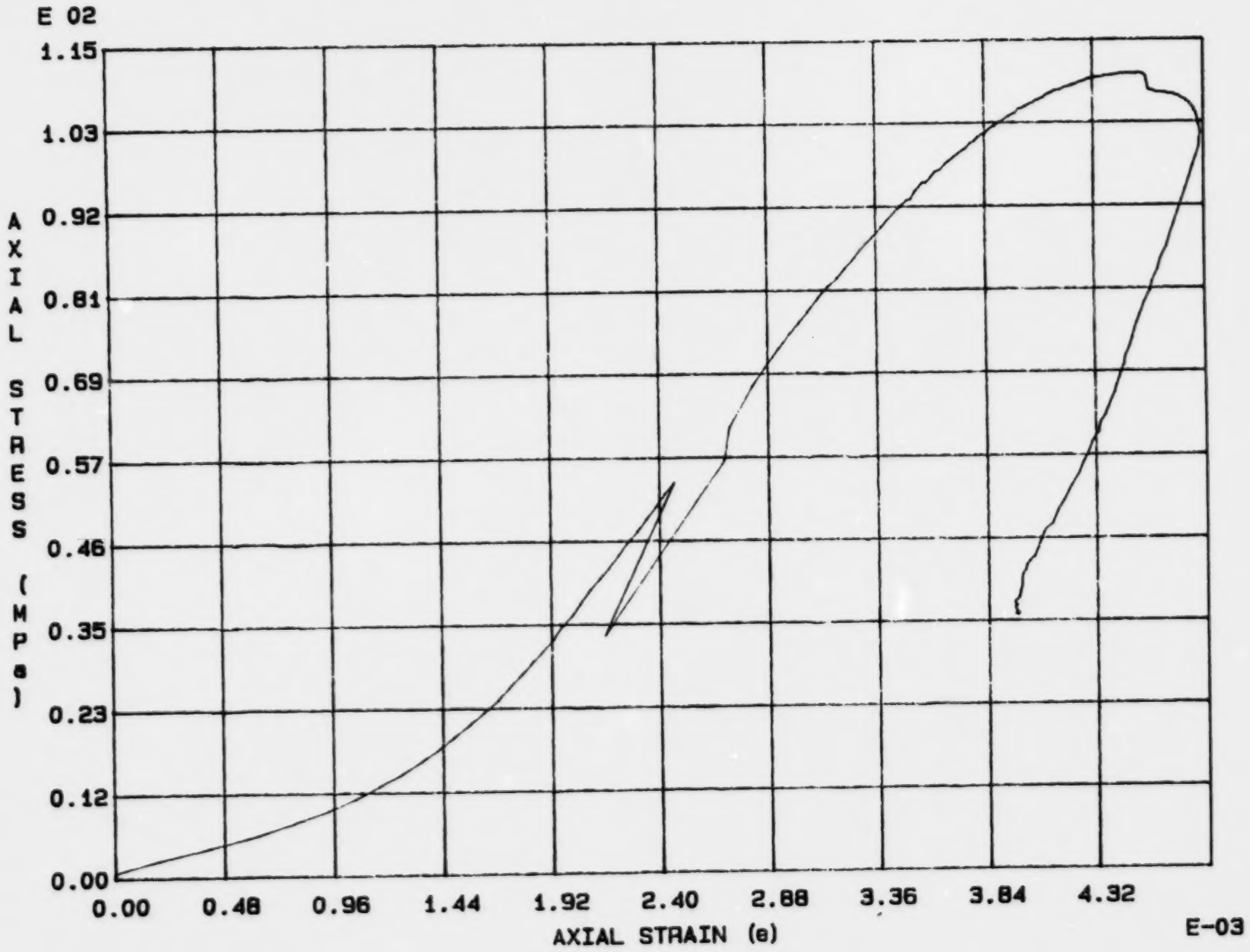

Fig. 1 - 11 Specimen M13U

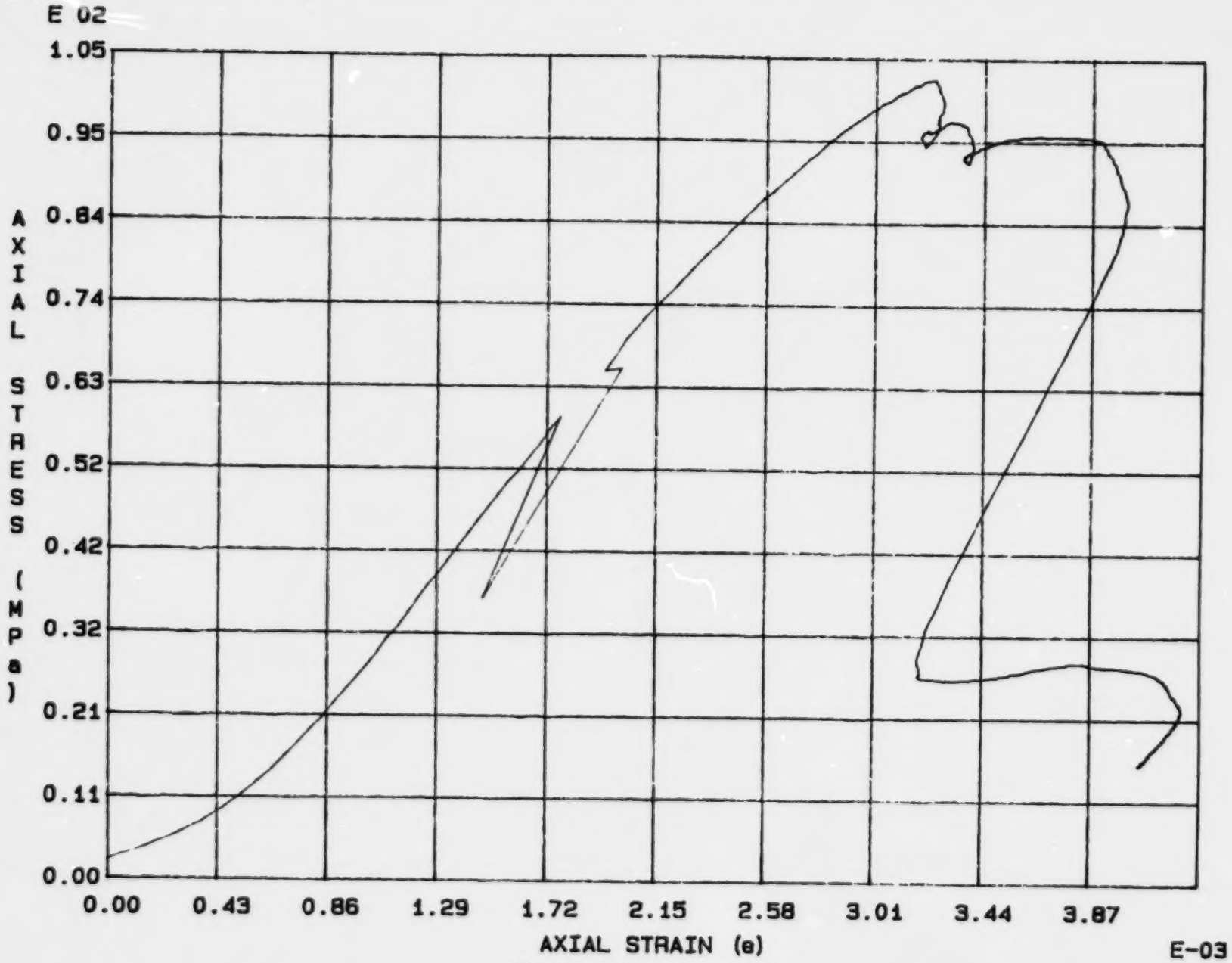

Fig. 1 - 12 Specimen M14U

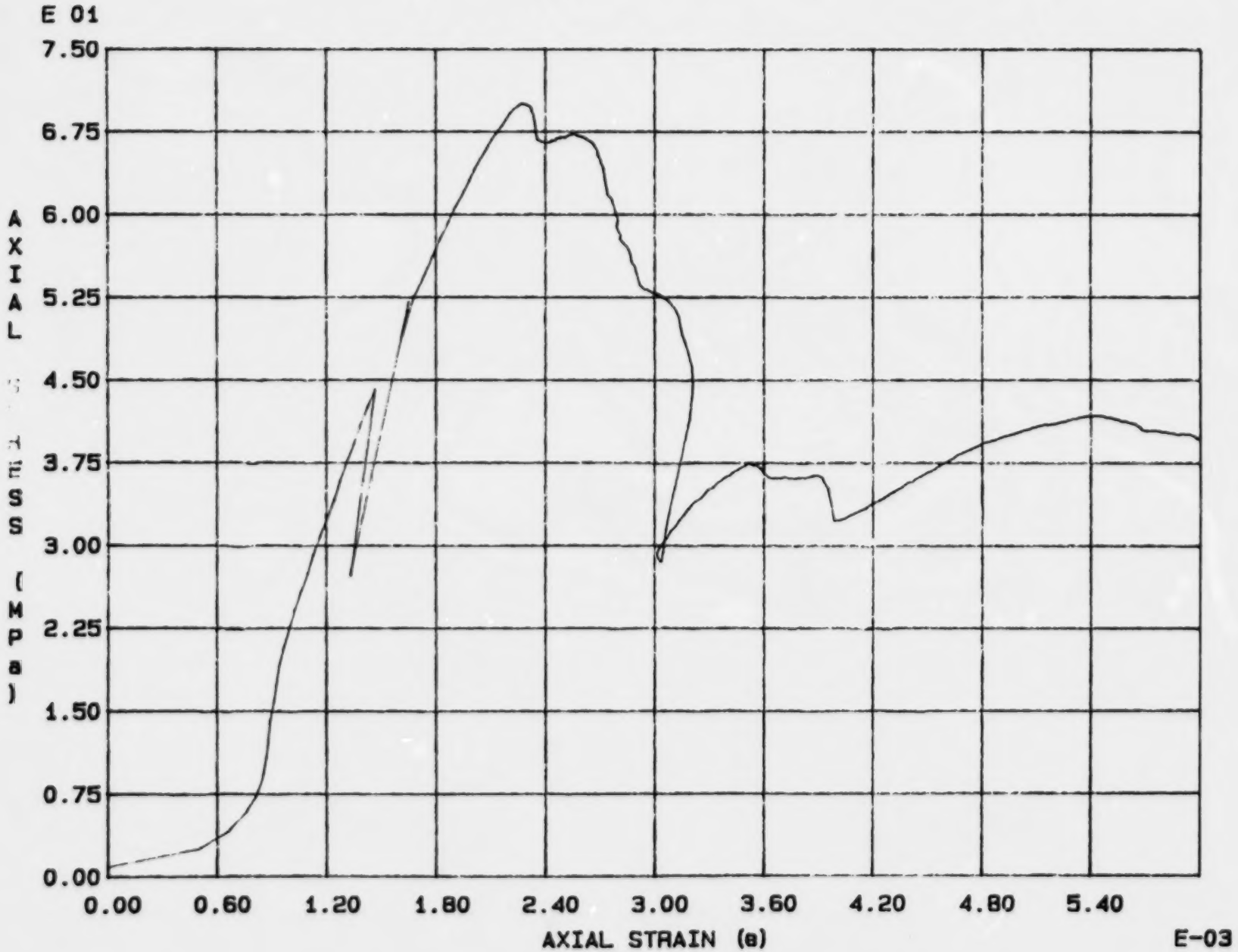

Fig. 1 - 13 Specimen M15U

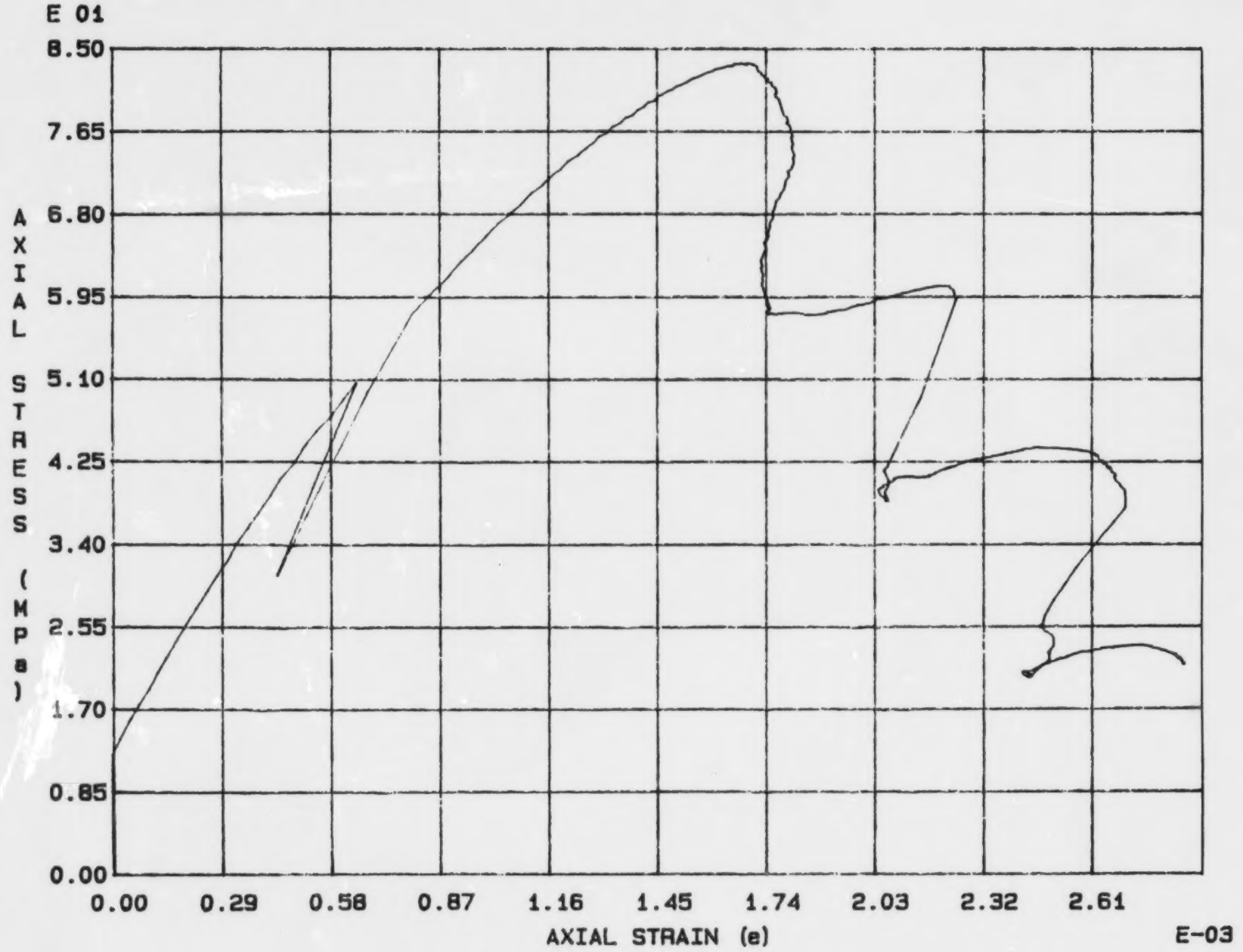

Fig. 1 - 14 Specimen M16U

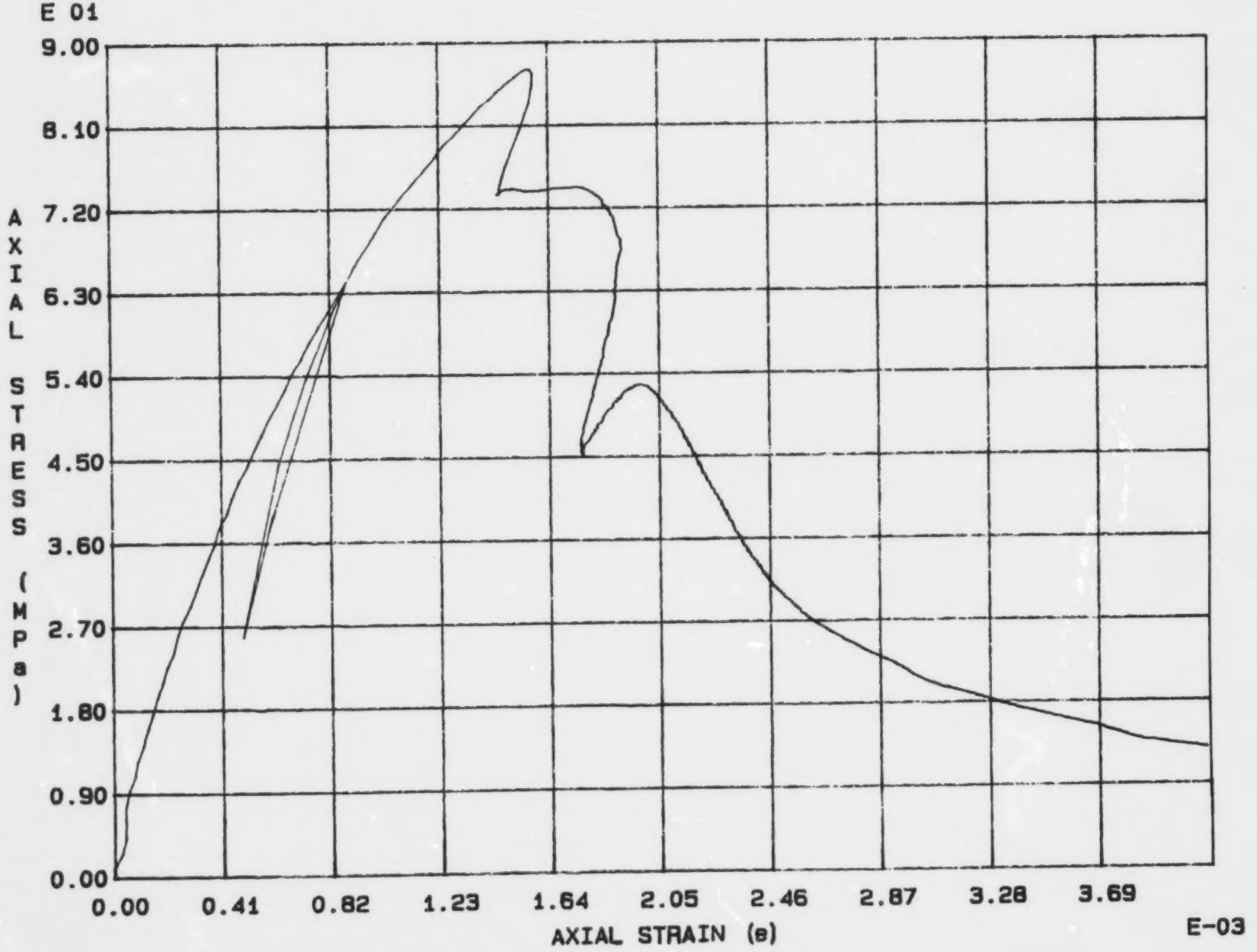

Fig. 1 - 15 Specimen M17U

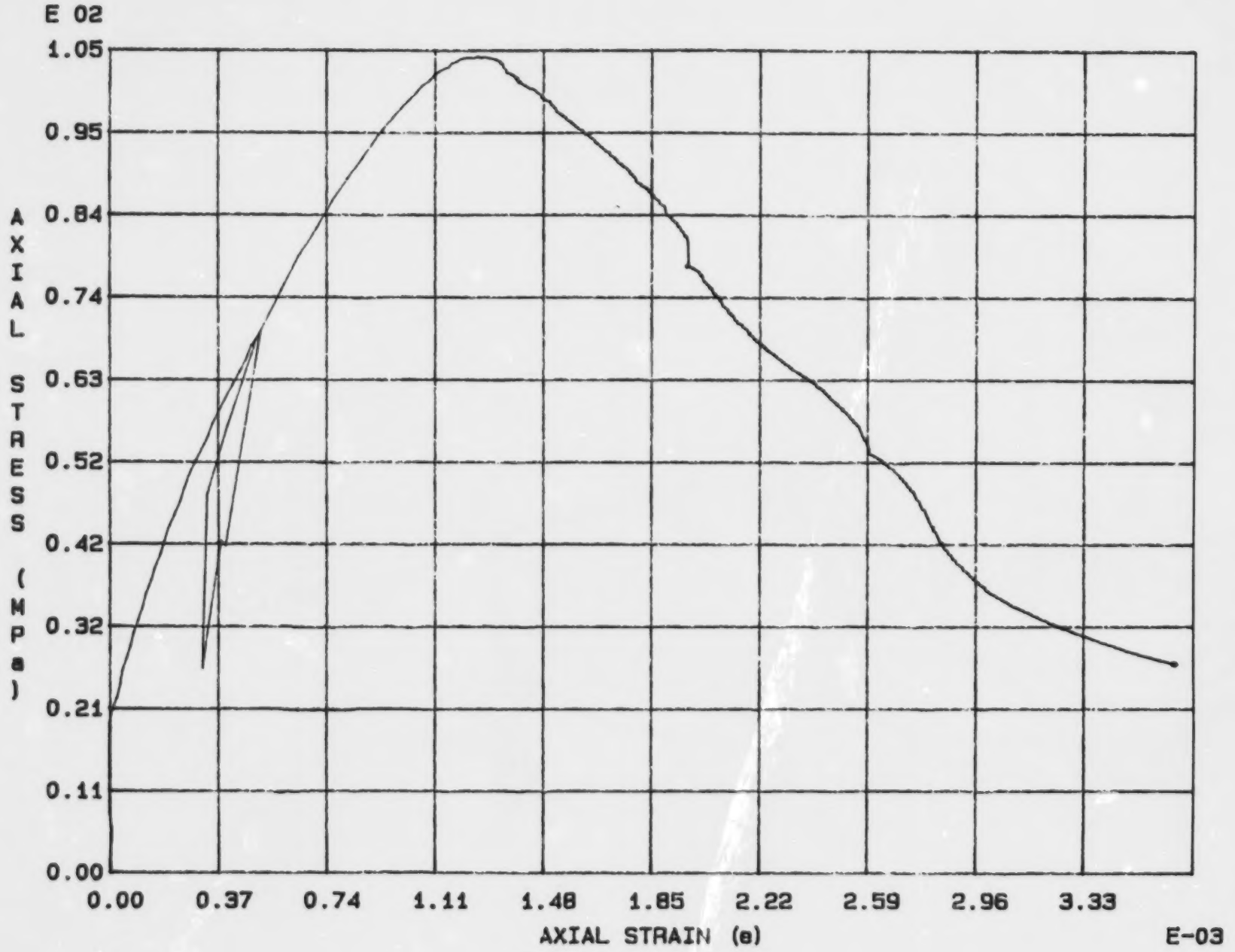

Fig. 1 - 16 Specimen M18U

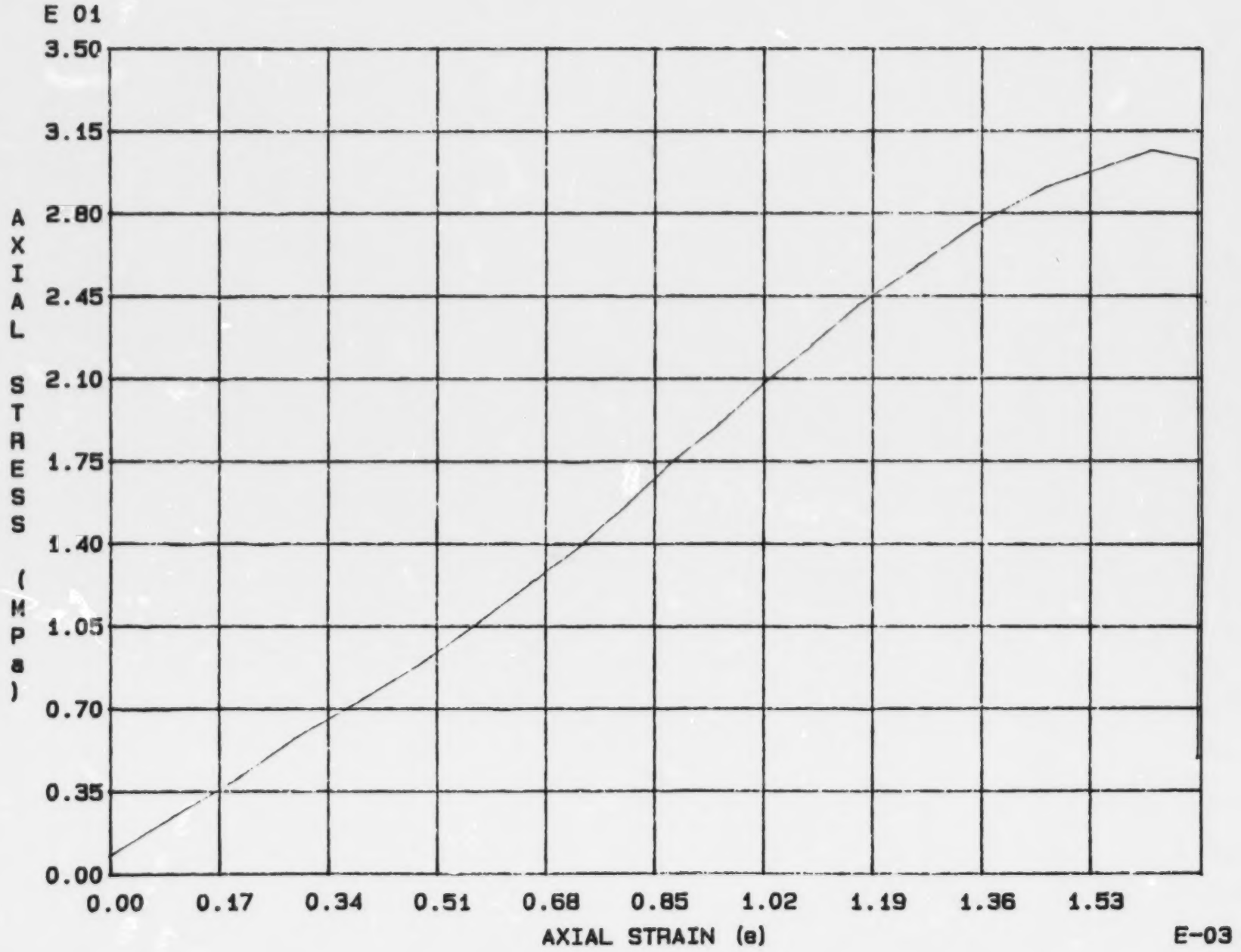

Fig. 1 - 17 Specimen M19U

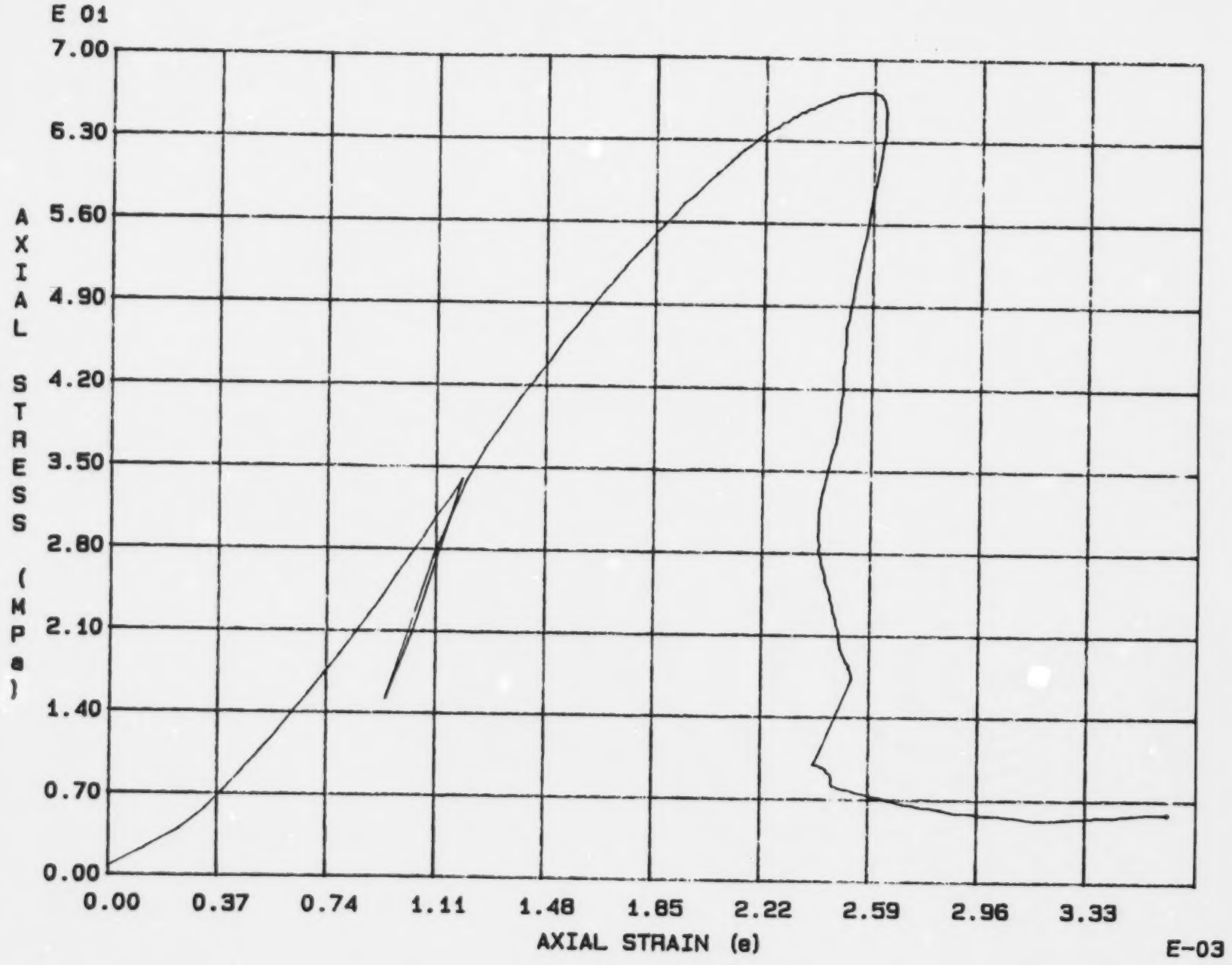

Fig. 1 - 18 Specimen M20U

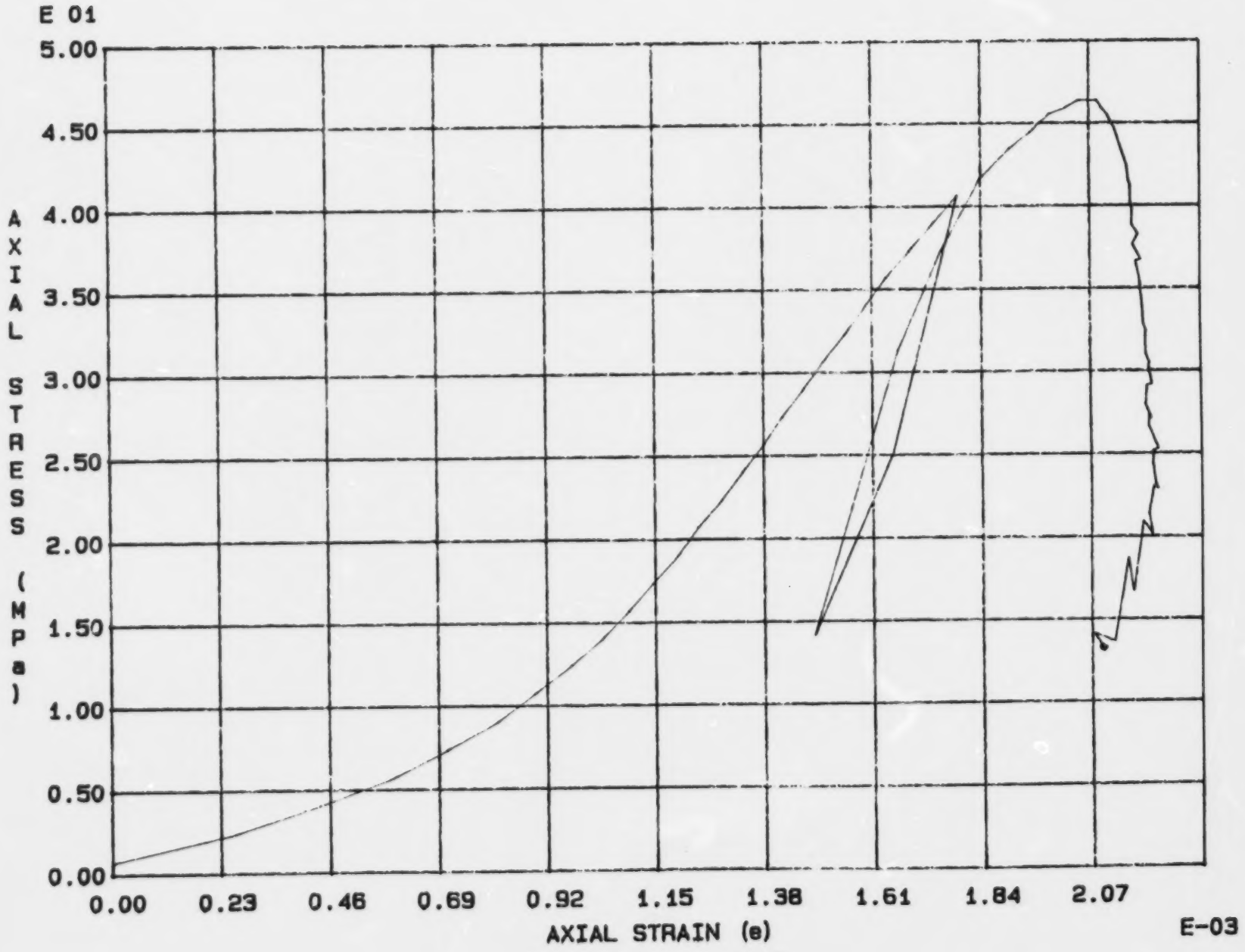

Fig. 1 - 19 Specimen M21U

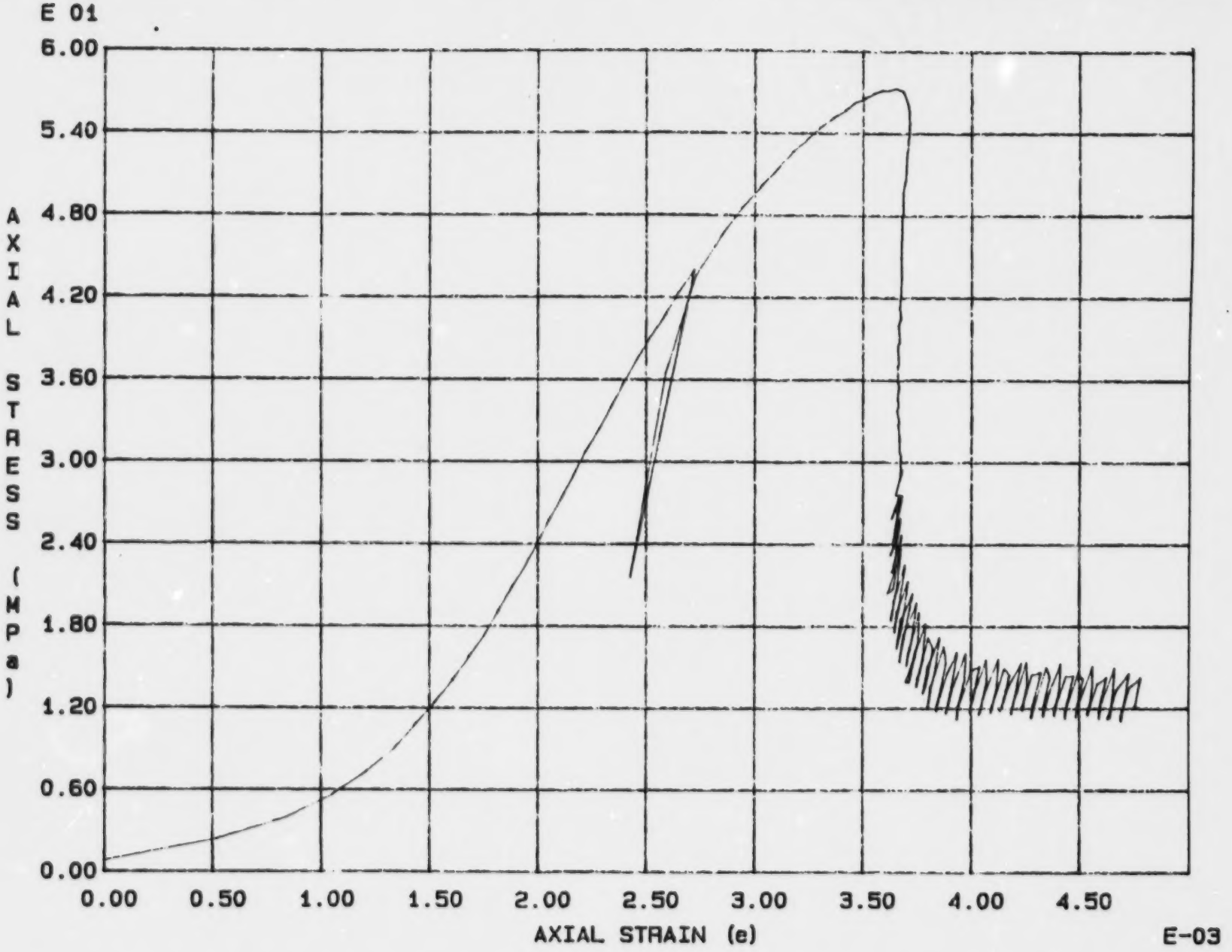

Fig. 1 - 20 Specimen M22U

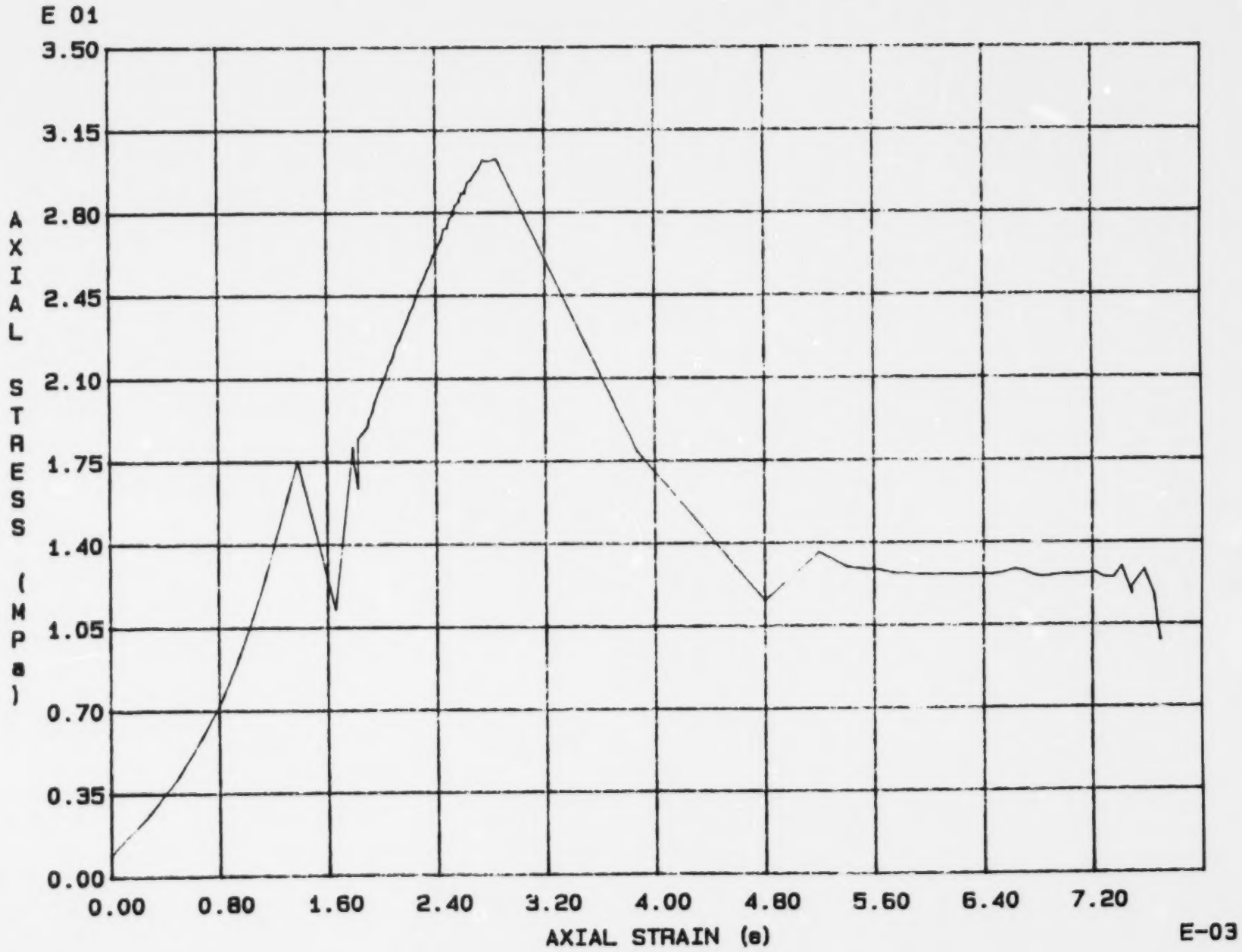

Fig. 1 - 21 Specimen M23U

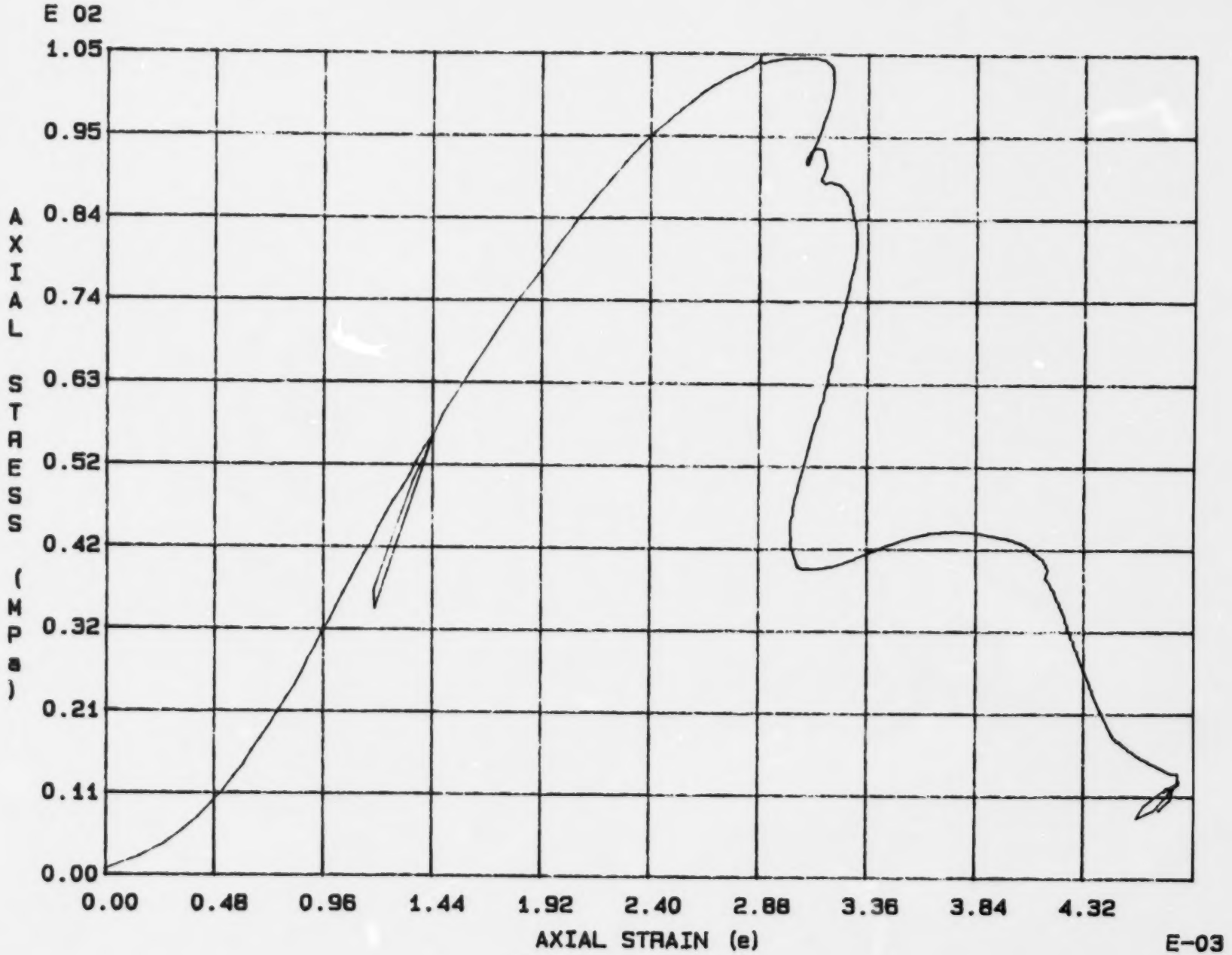

Fig. 1 - 22 Specimen M24U

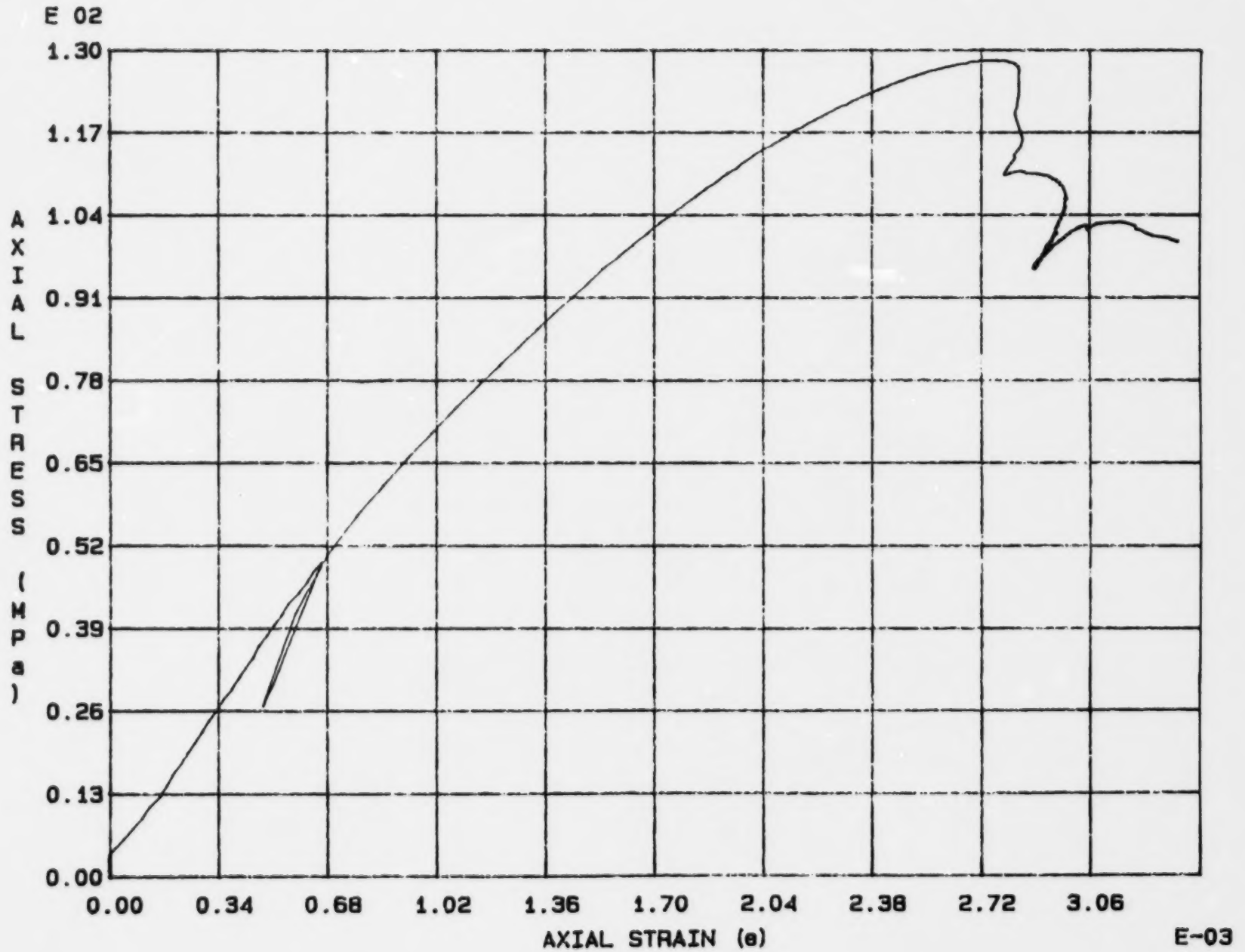

Fig. 1 - 23 Specimen M25U

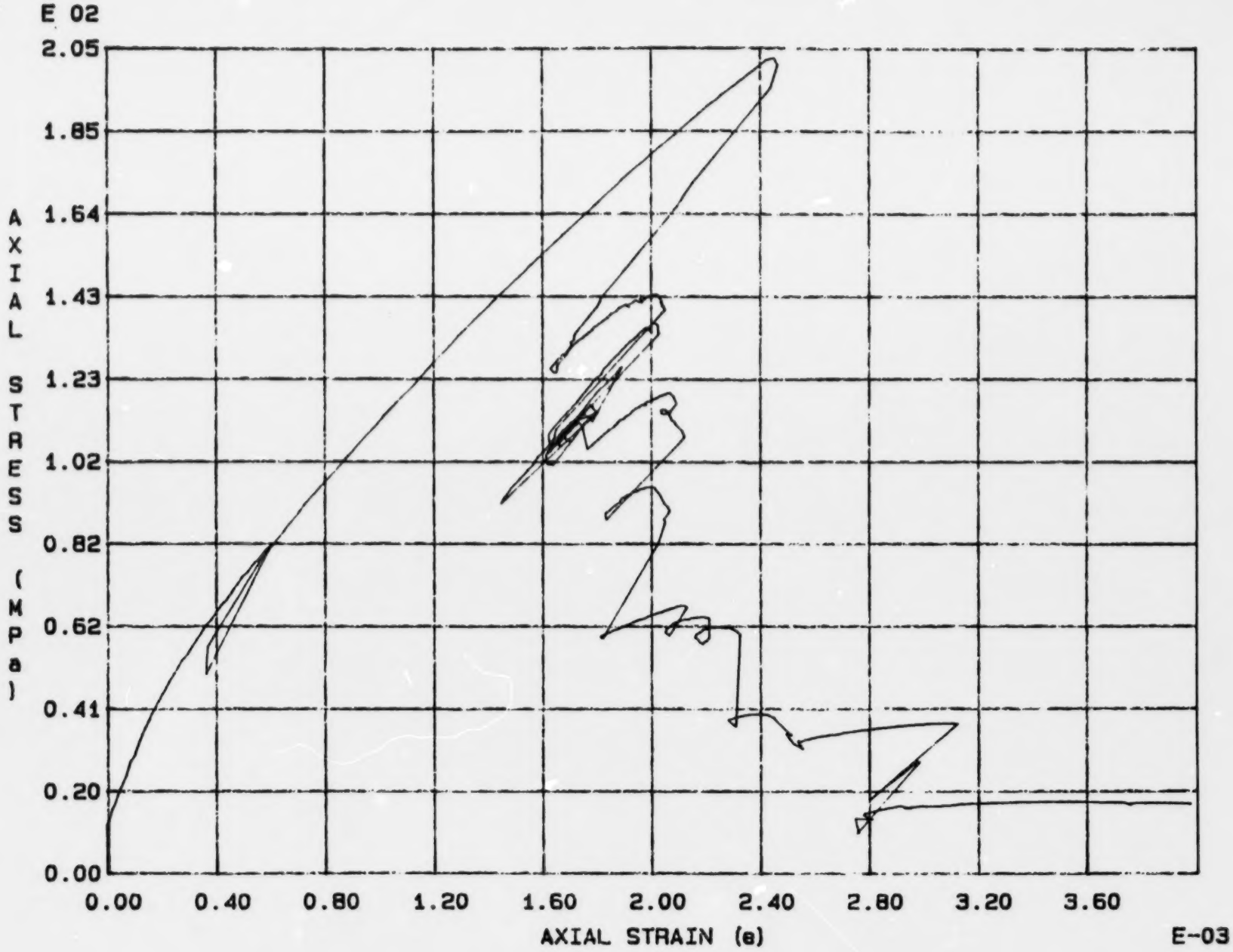
E 02
2.05
1.85
1.64
1.43
1.23
1.02
0.82
0.62
0.41
0.20
0.00
AXIAL STRESS (MPa)
0.00
0.40
0.80
1.20
1.60
2.00
2.40
2.80
3.20
3.60
AXIAL STRAIN (e)
E-03

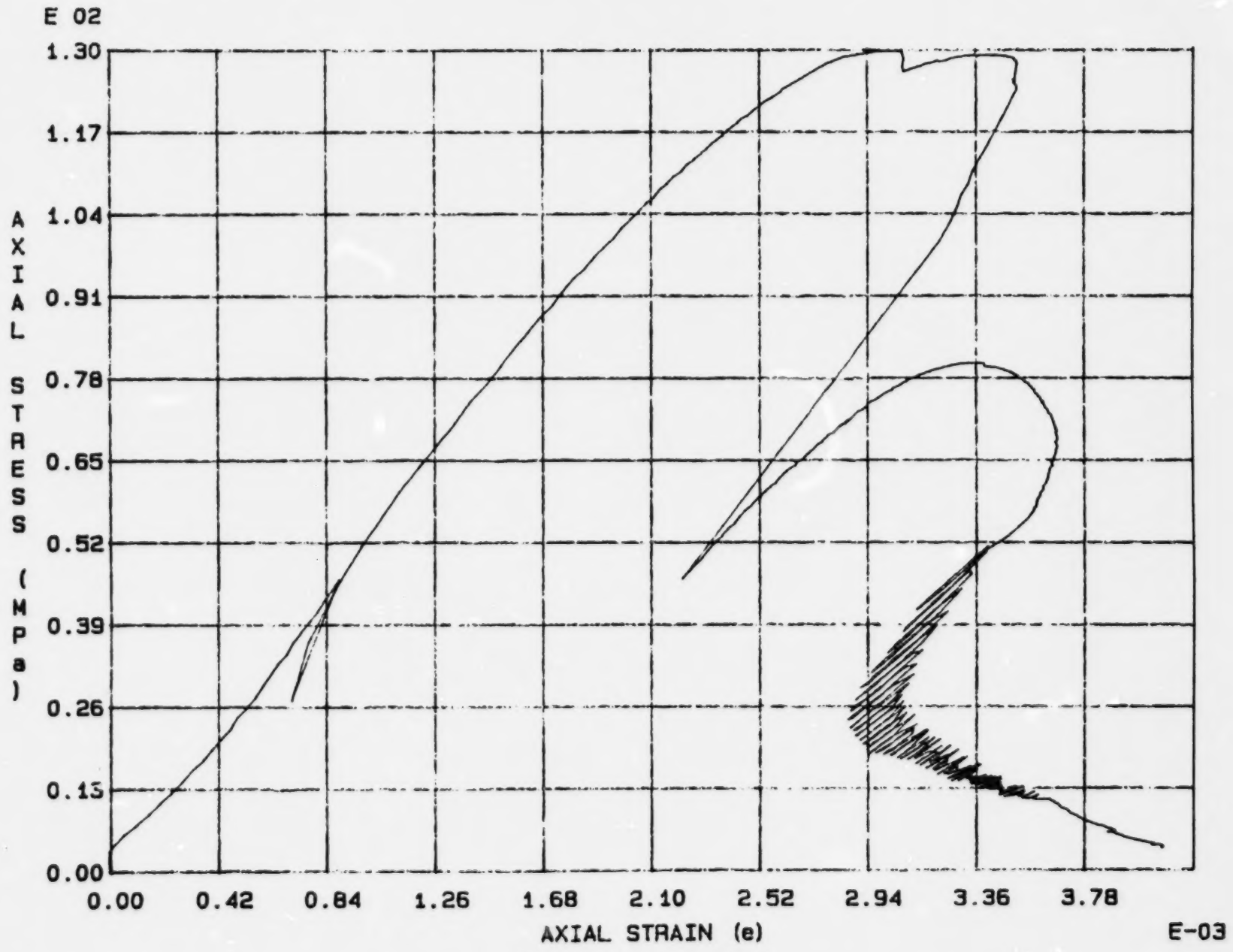

Fig. 1 - 25 Specimen M27U

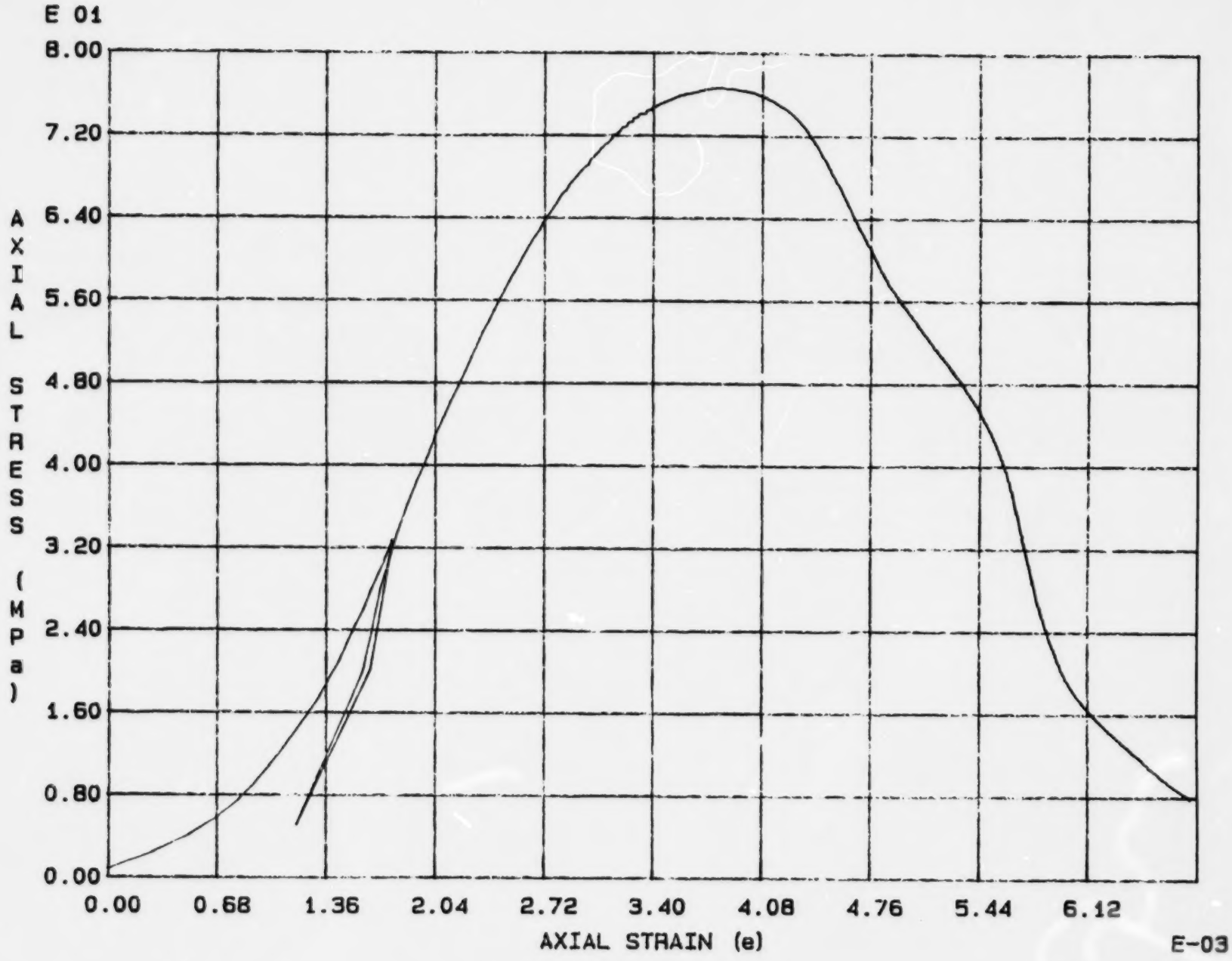

Fig. 1 - 26 Specimen M28U

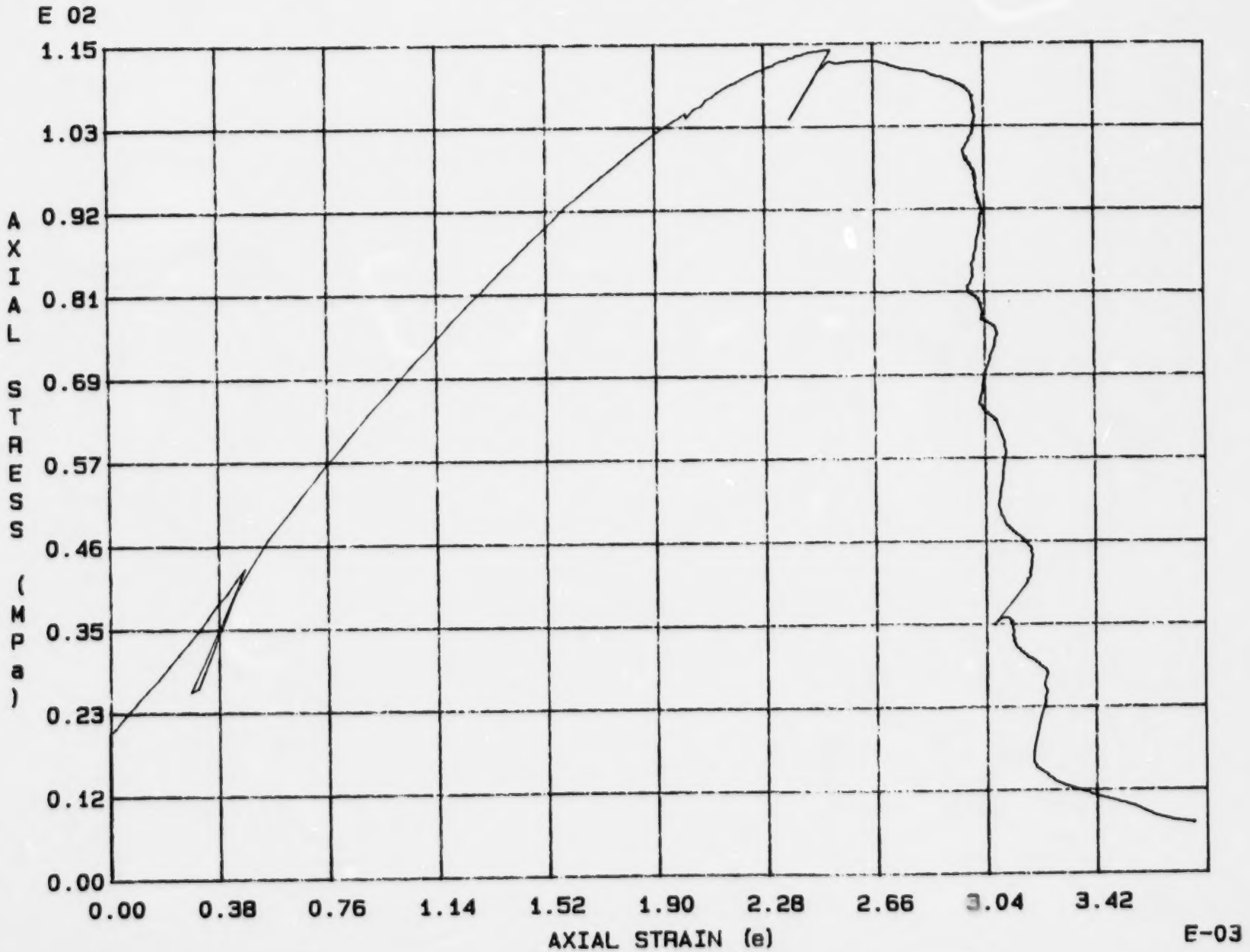

Fig. 1 - 27 Specimen M29U

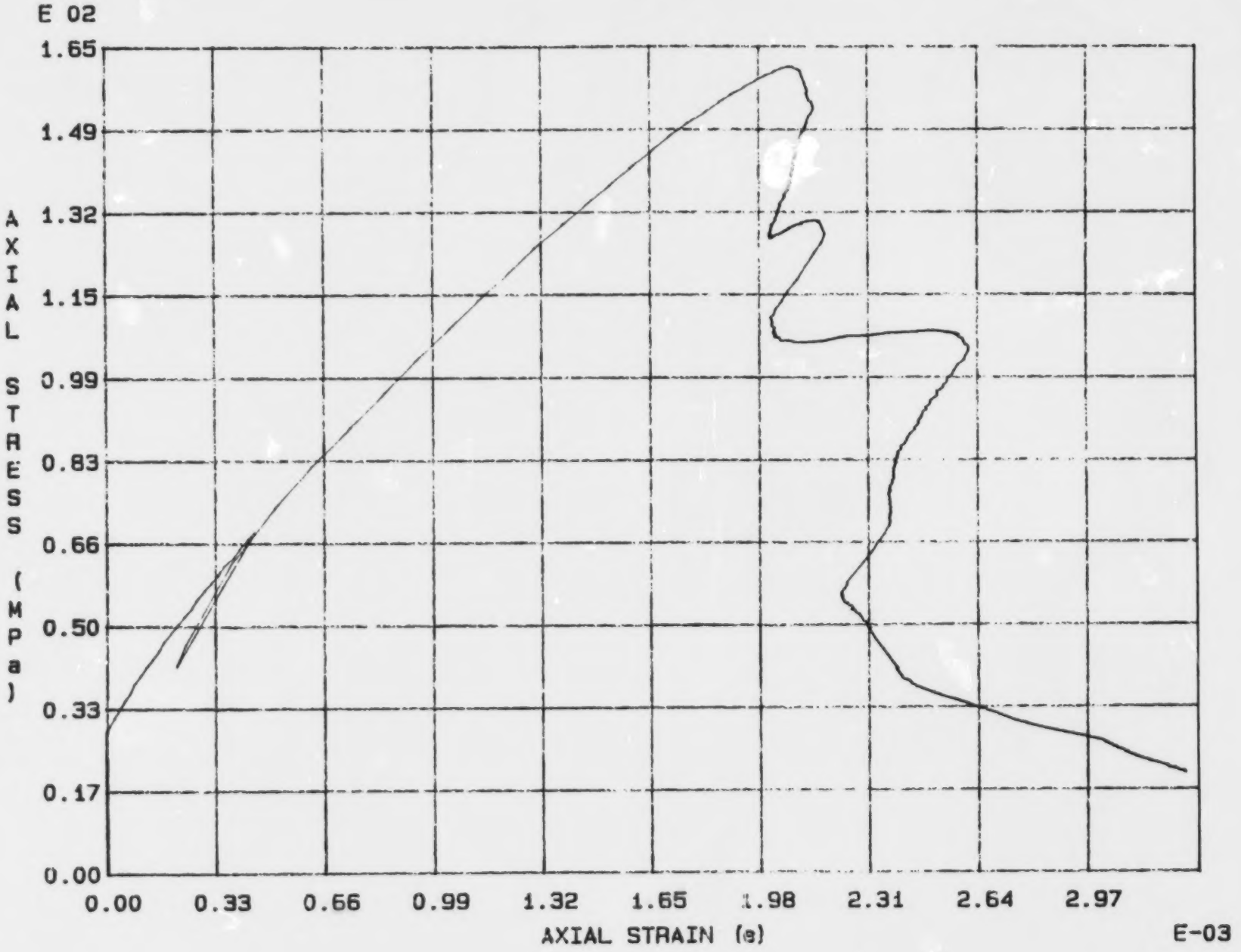

Fig. 1 - 28 Specimen M30U

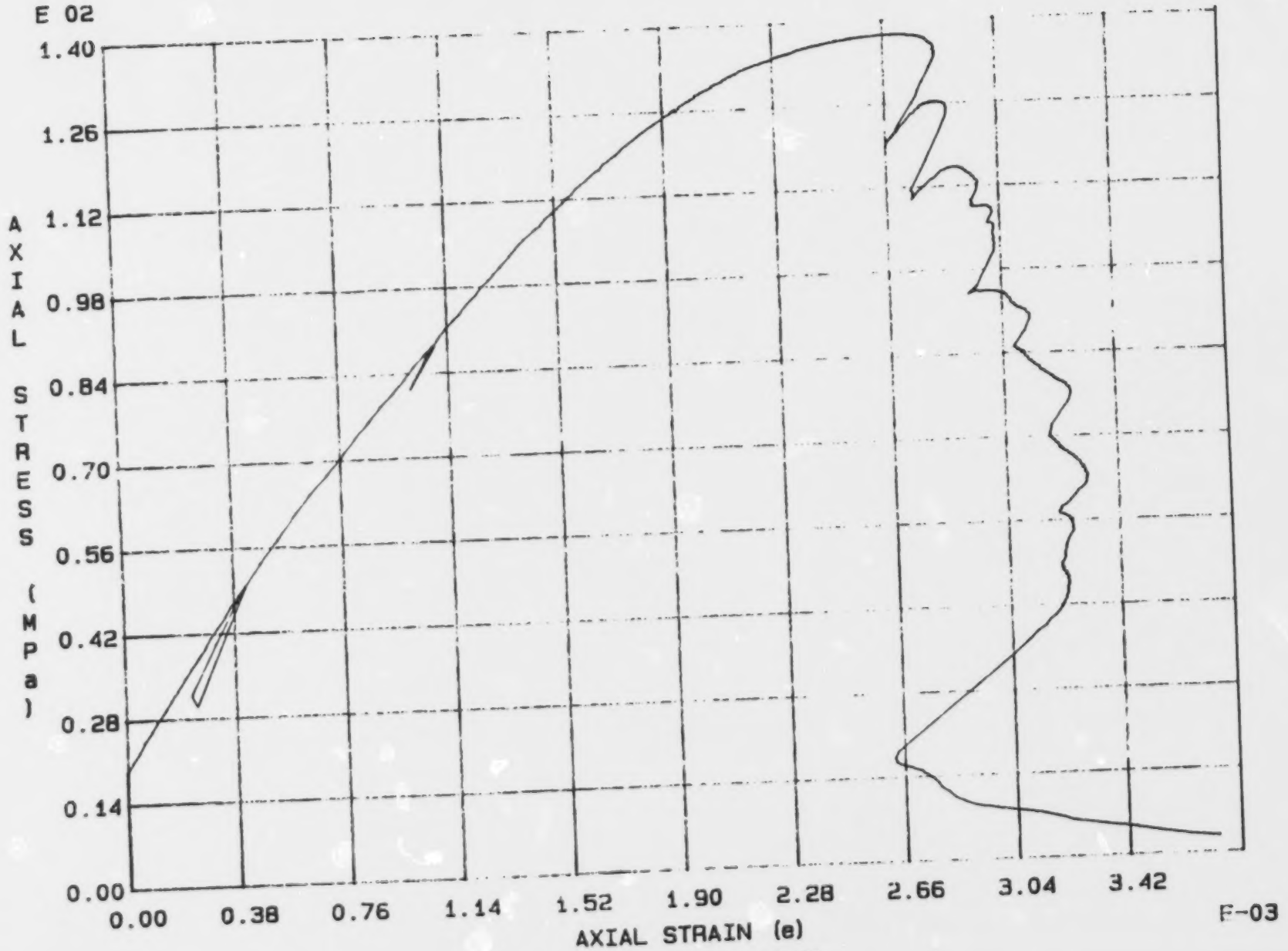

Fig. 1 - 29 Specimen M31U

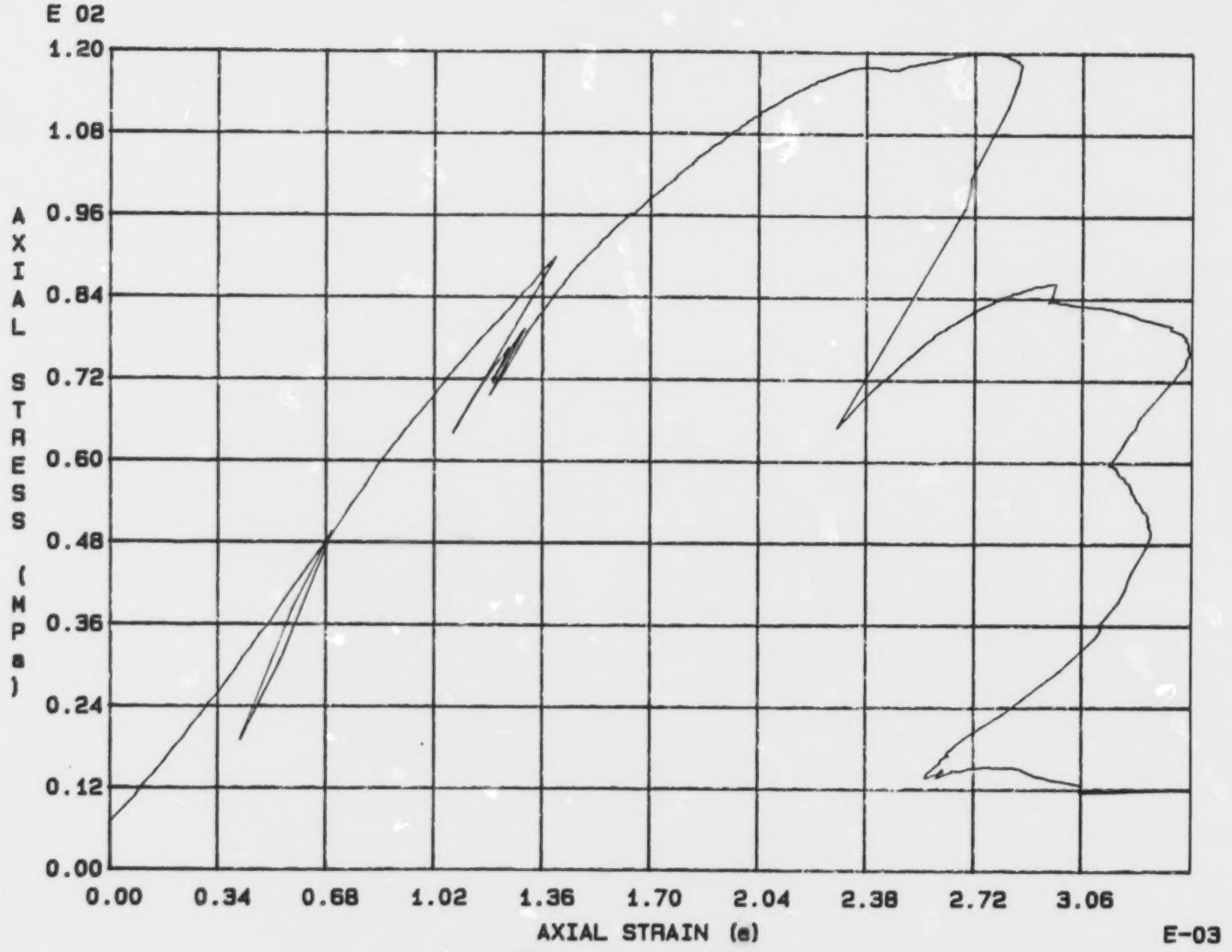

Fig. 1 - 30 Specimen M32U

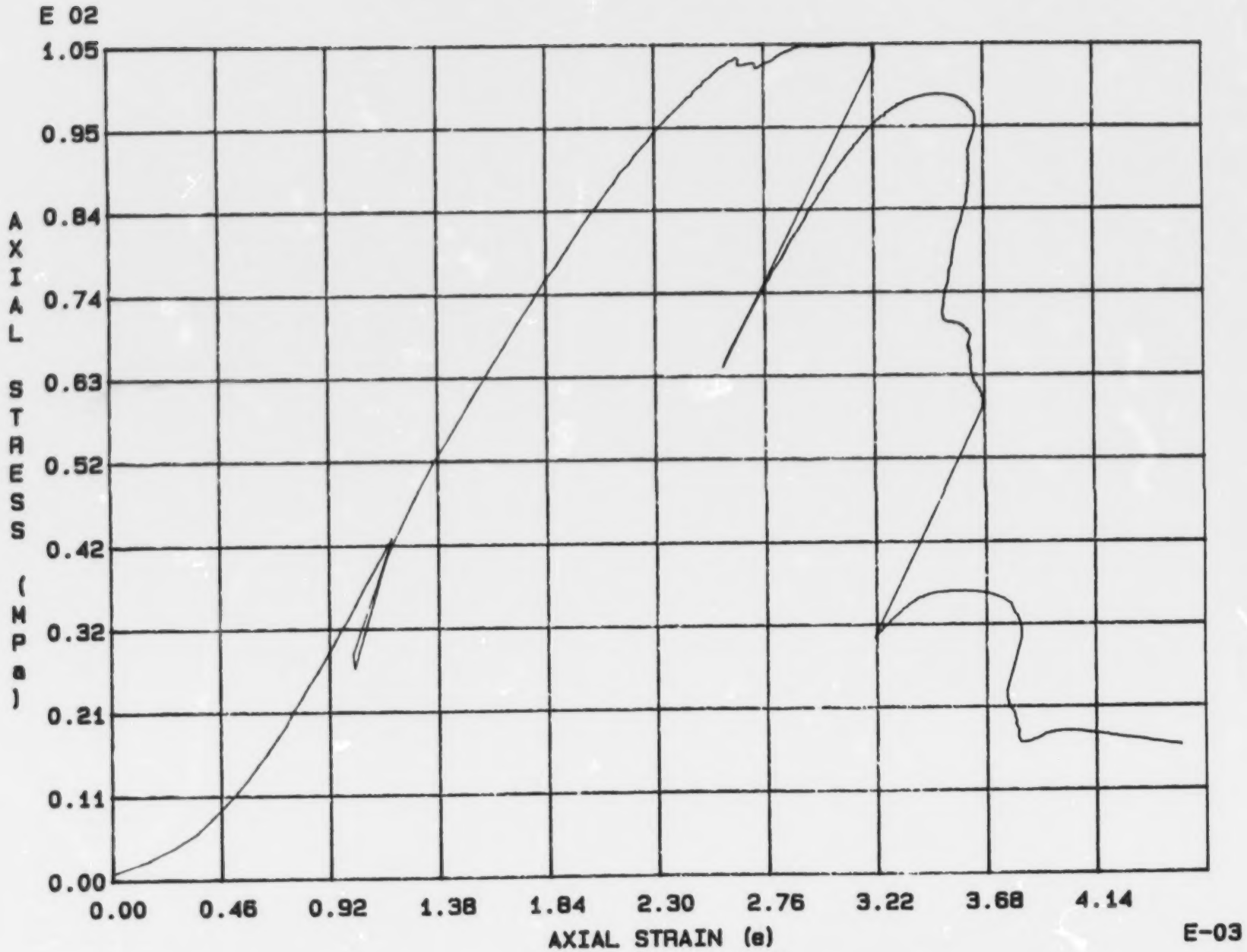

Fig. 1 - 31 Specimen M33U

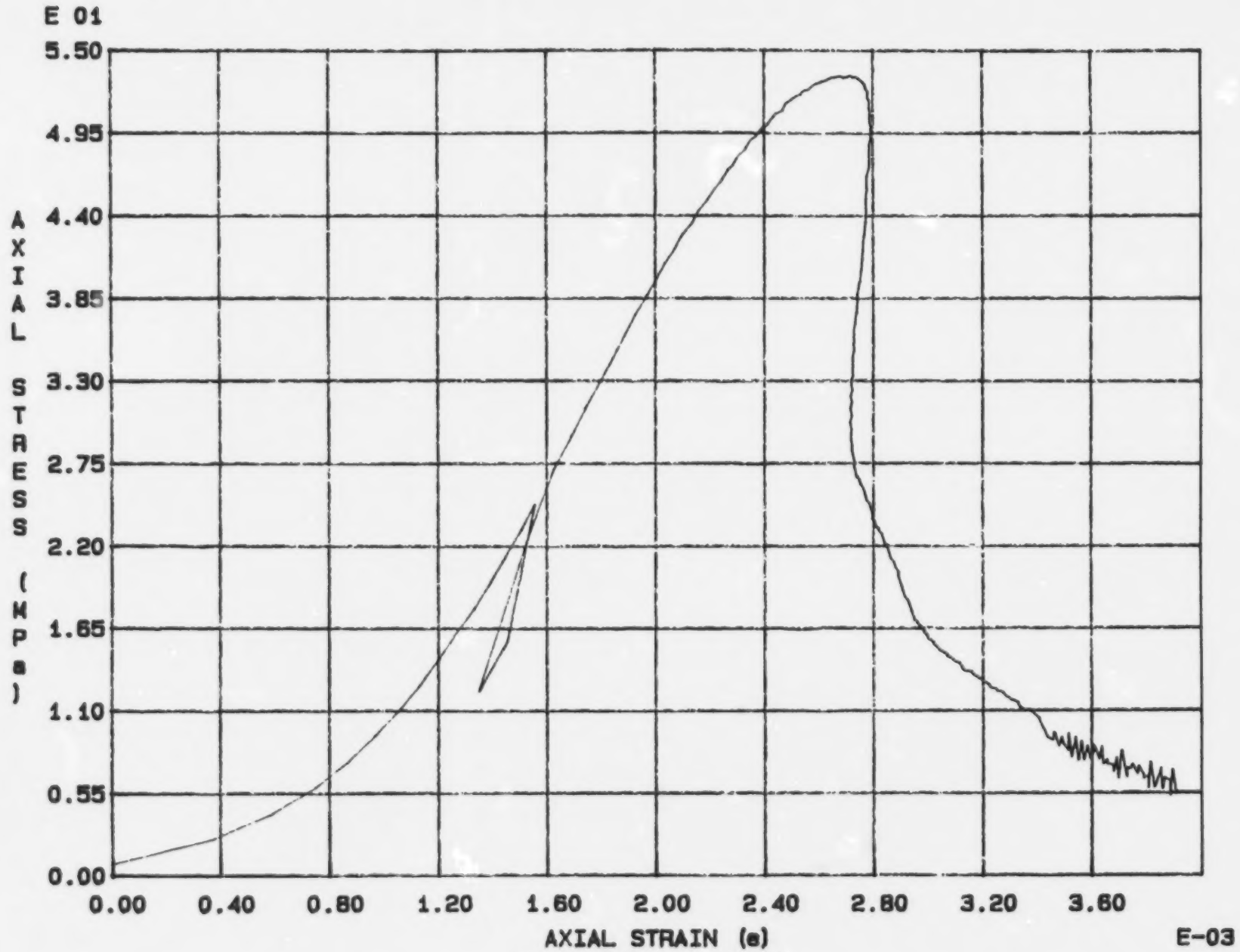

Fig. 1 - 32 Specimen M34U

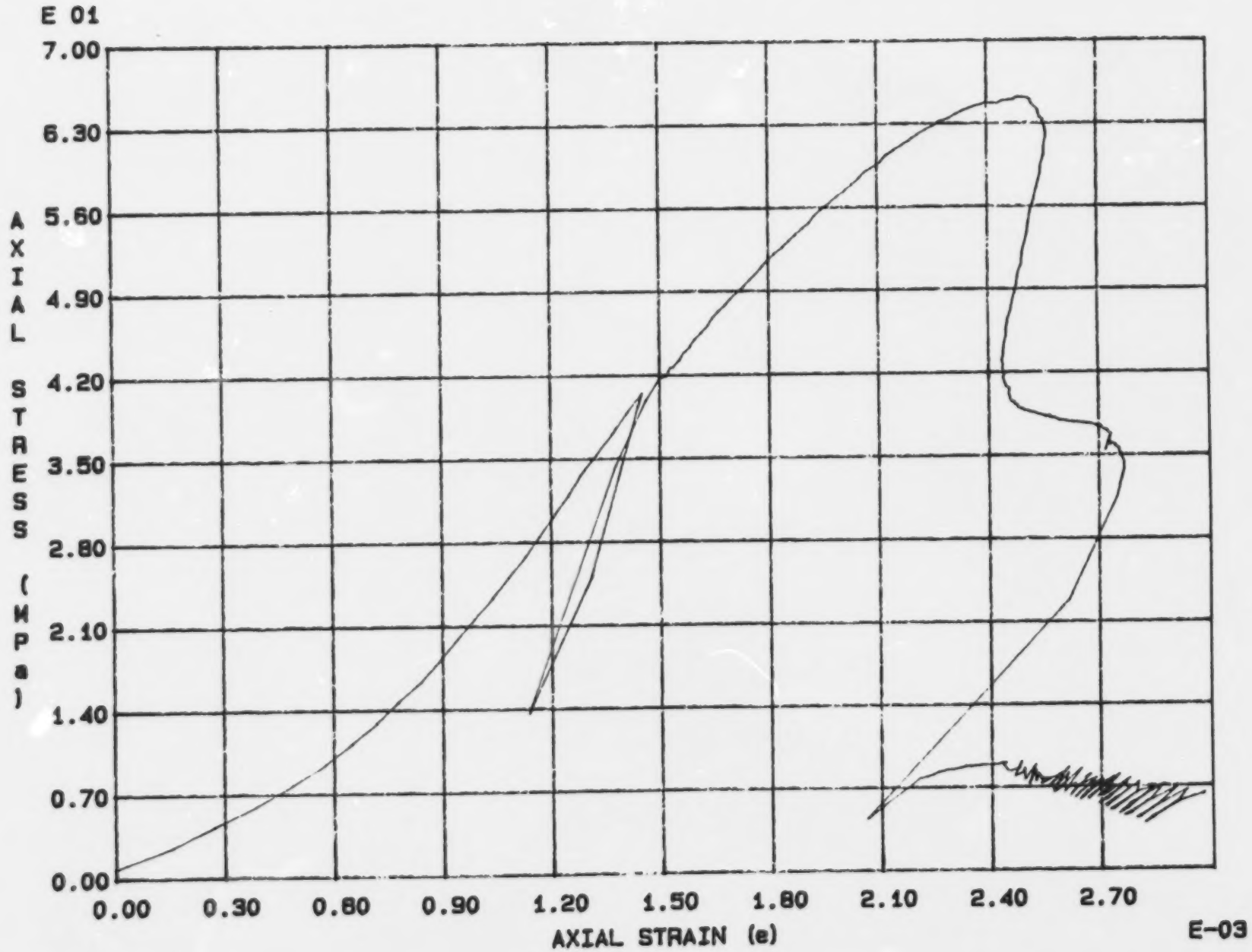

Fig. 1 - 33 Specimen M35U

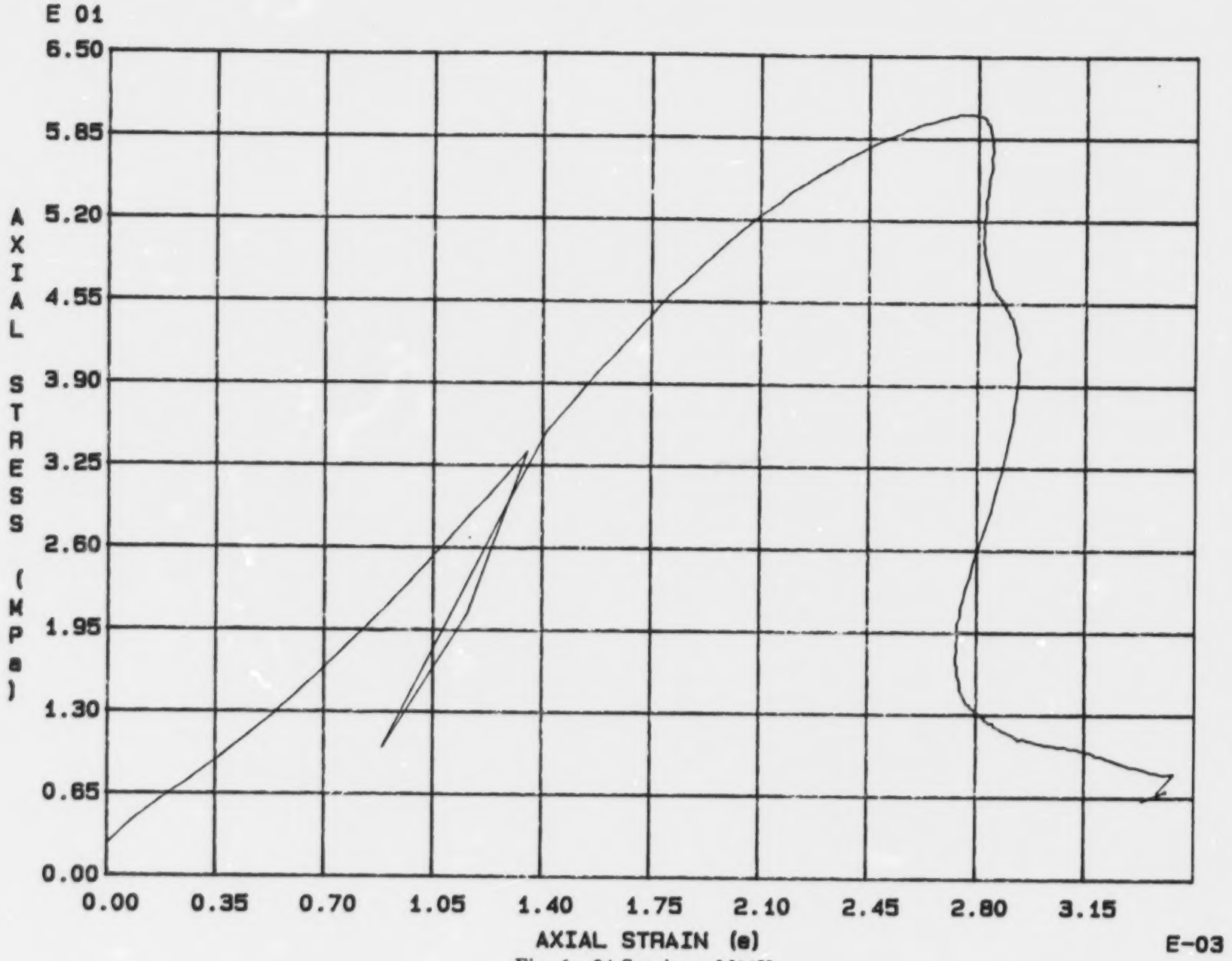

Fig. 1 - 34 Specimen M36U

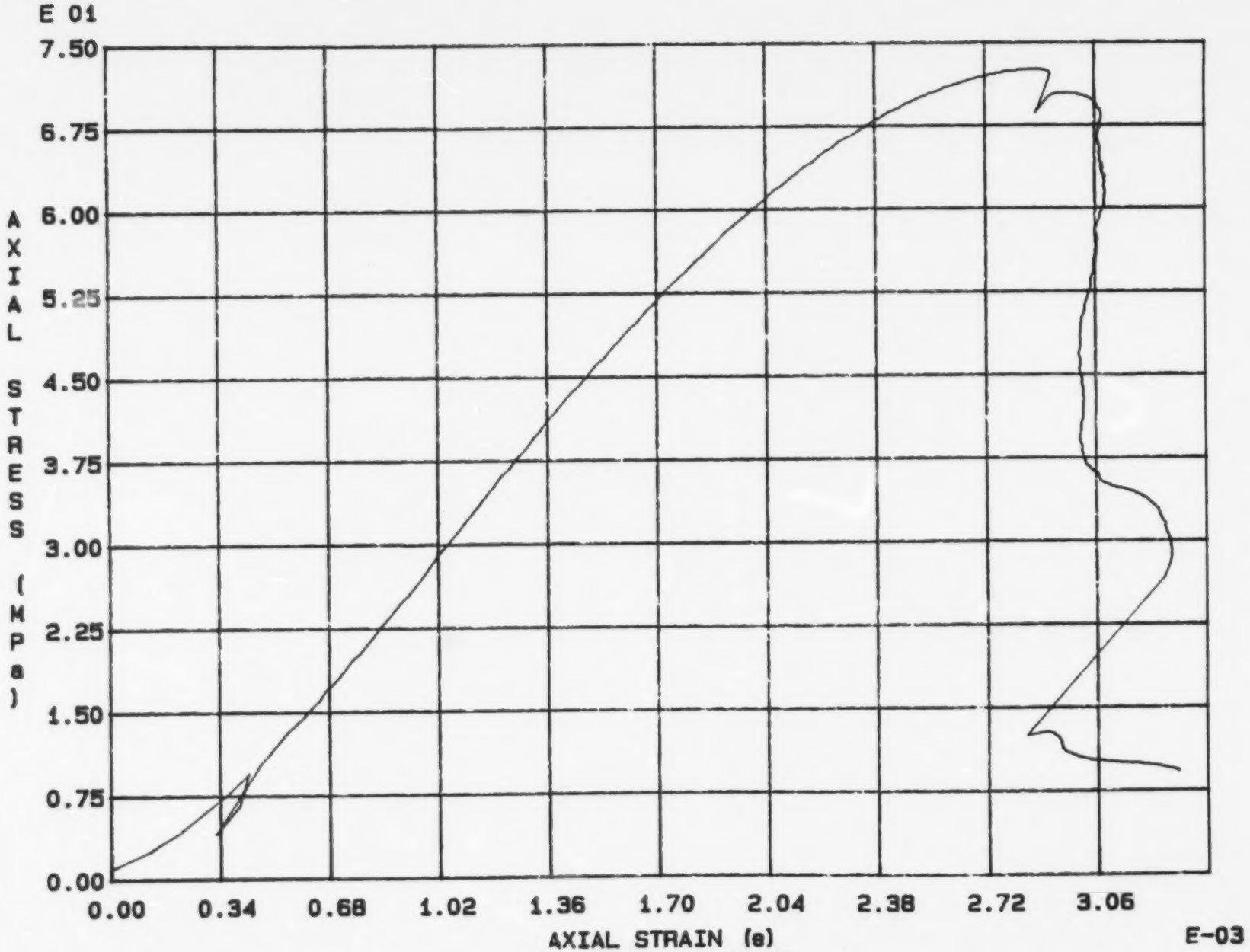

Fig. 1 - 35 Specimen M37U

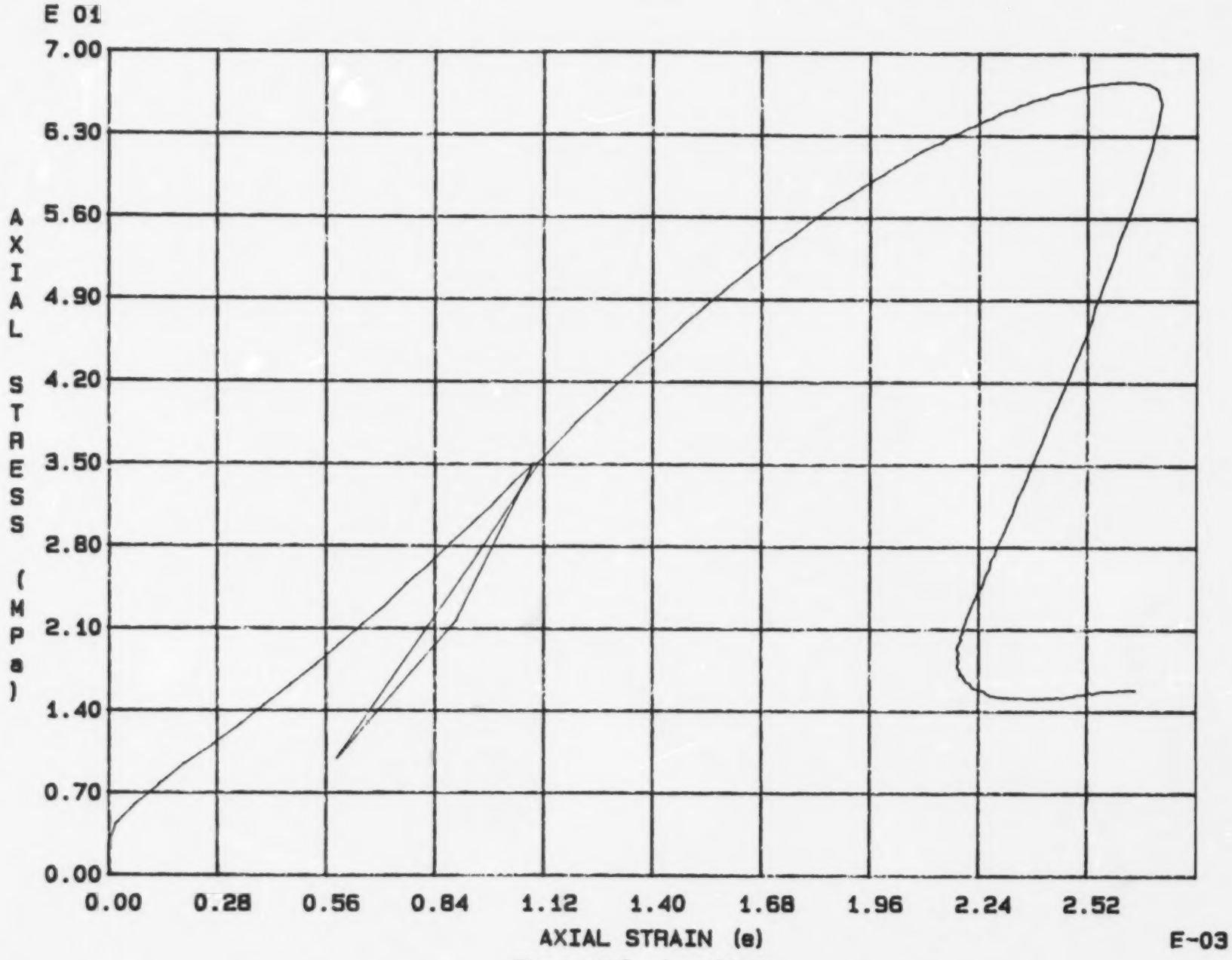

Fig. 1 - 36 Specimen M38U

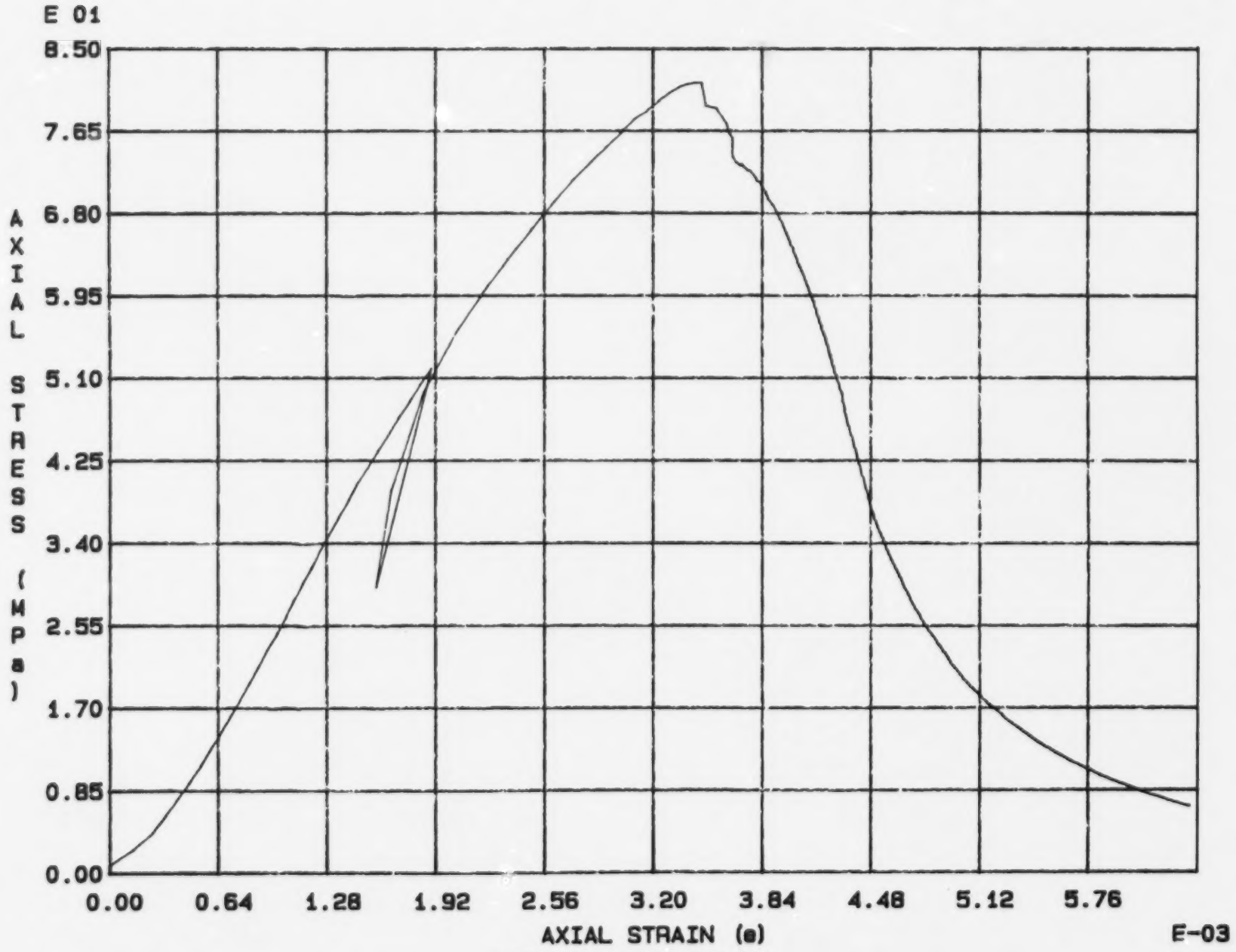

Fig. 1 - 37 Specimen M39U

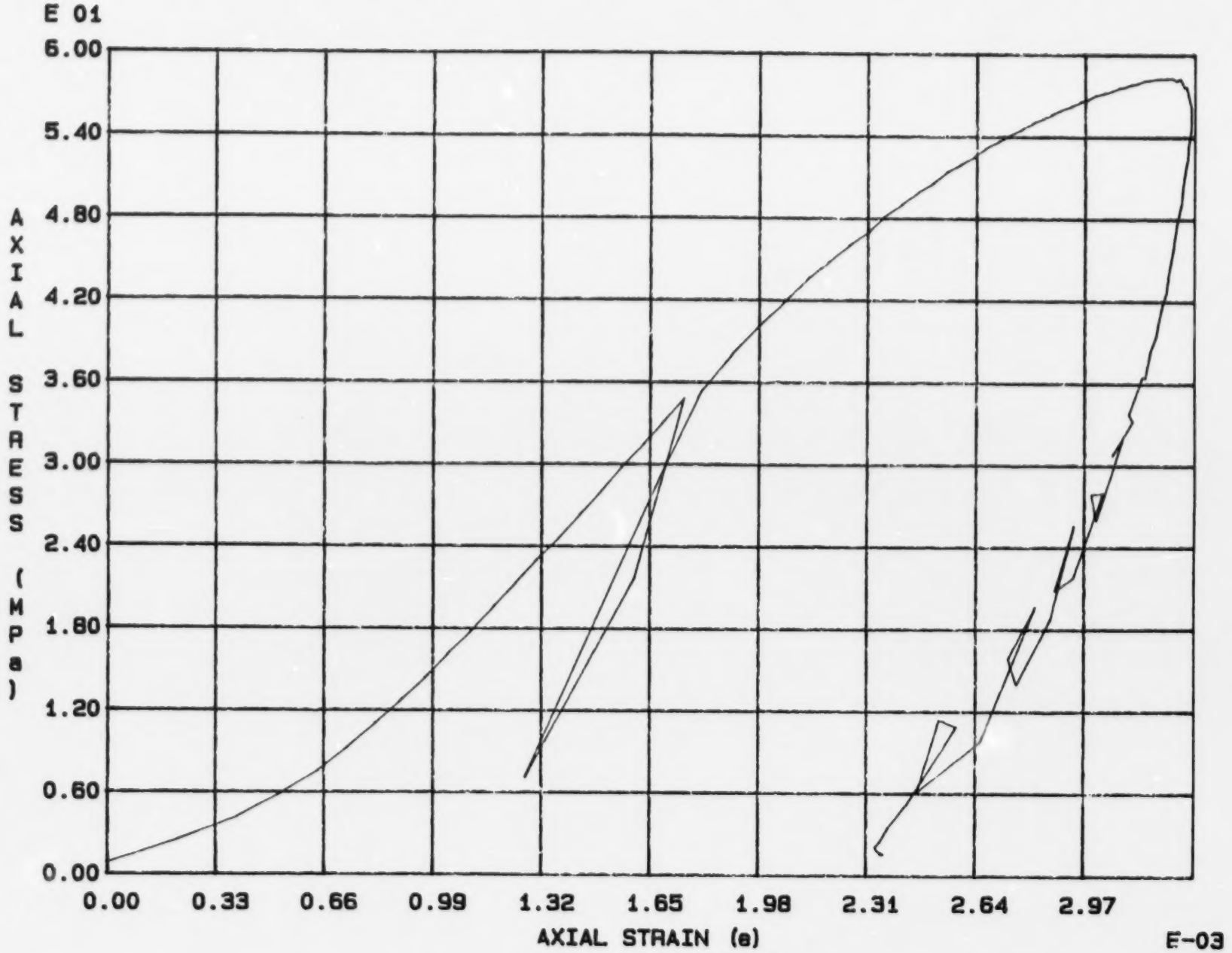

Fig. 1 - 38 Specimen M40U

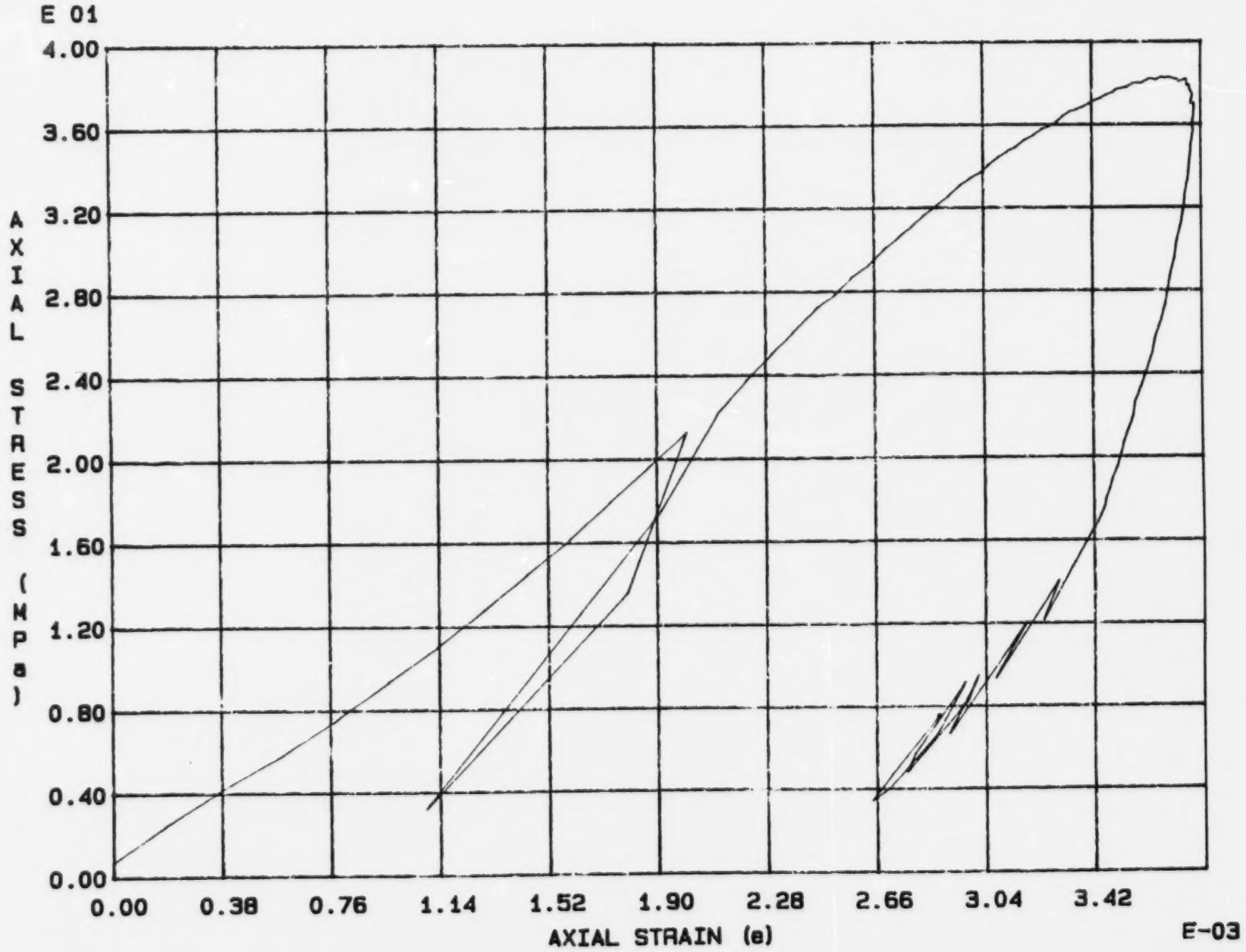

Fig. 1 - 39 Specimen M41U

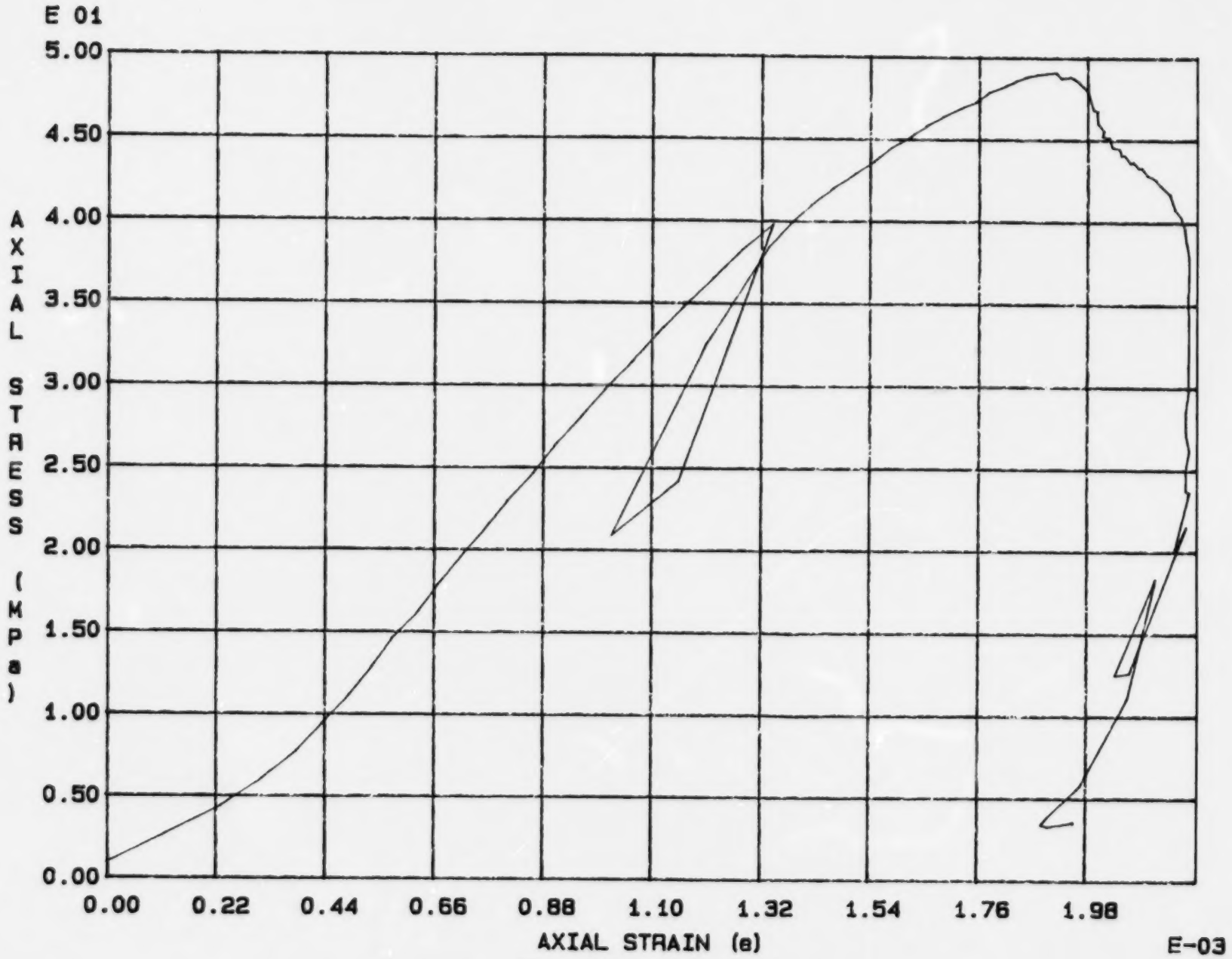

Fig. 1 - 40 Specimen M42U

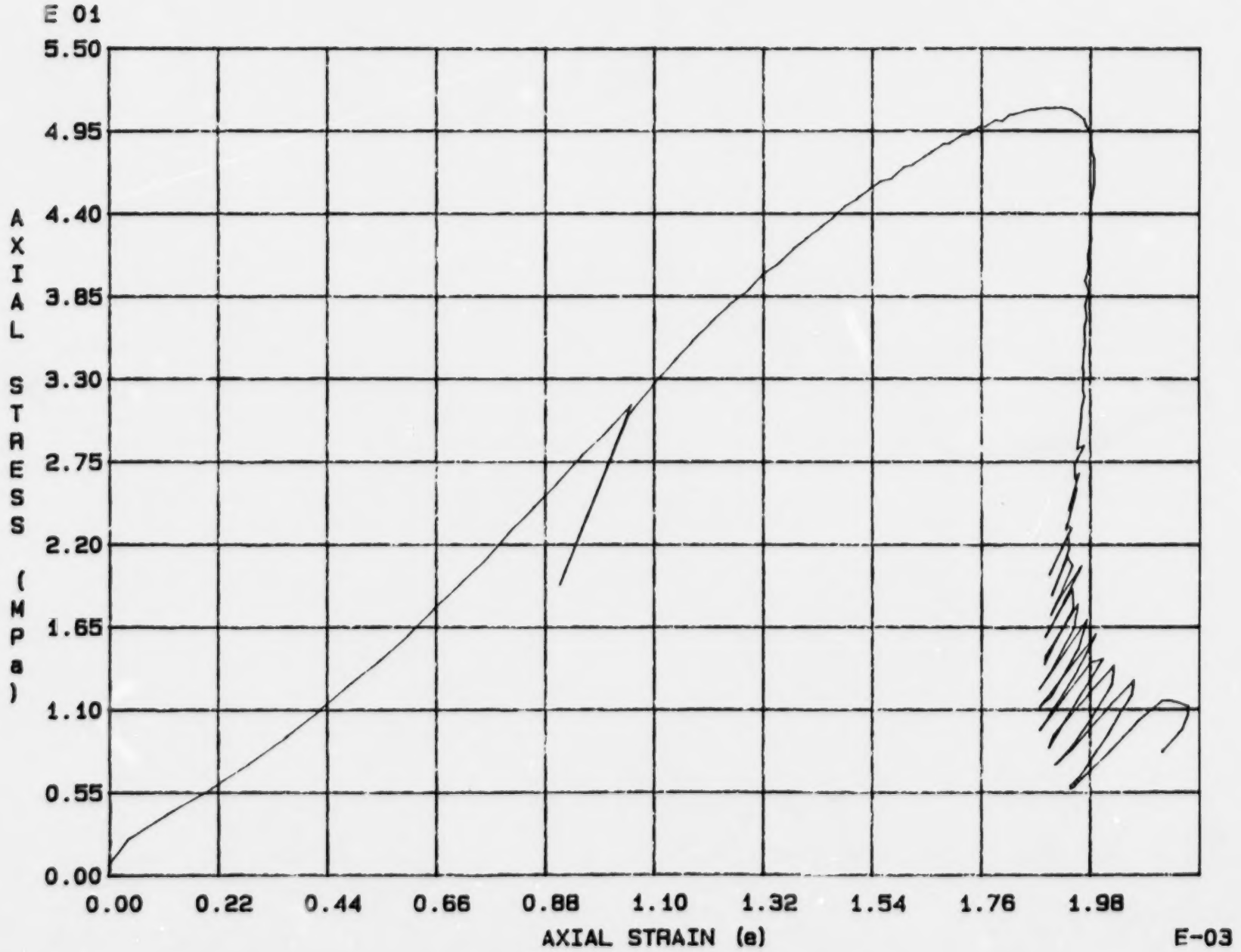

Fig. 1 - 41 Specimen M43U

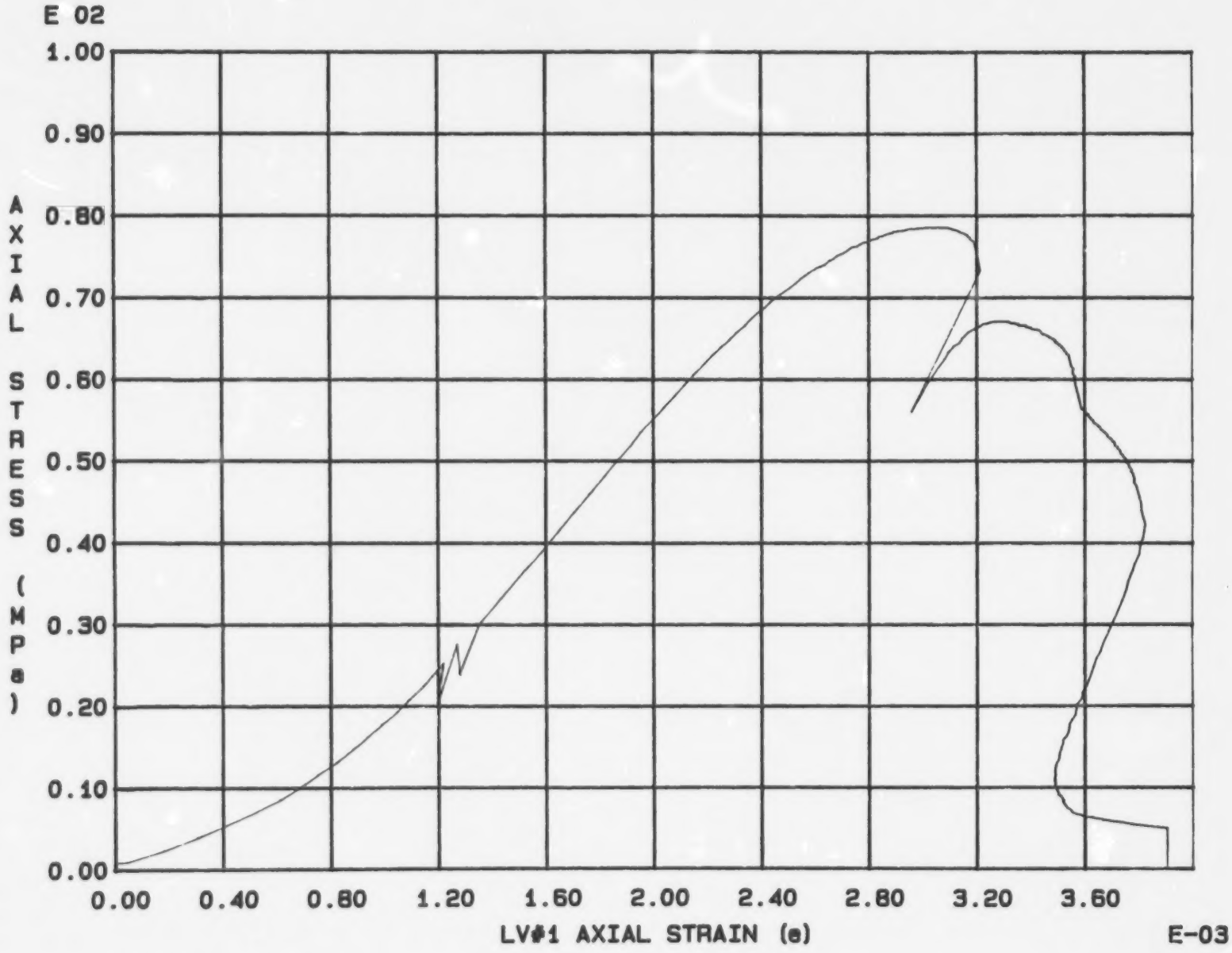

Fig. 1 - 42 Specimen M81U

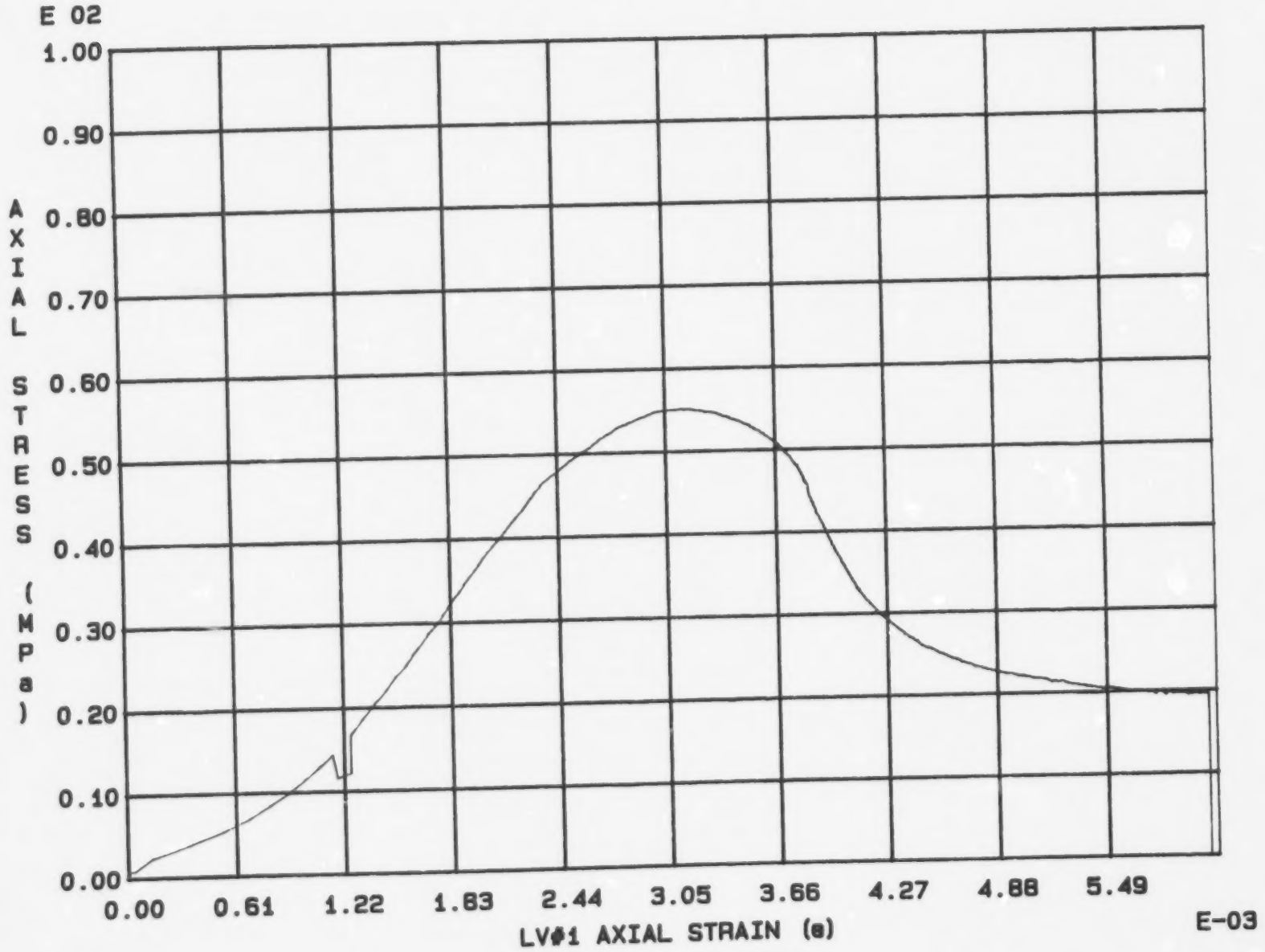

Fig. 1 - 43 Specimen M82U

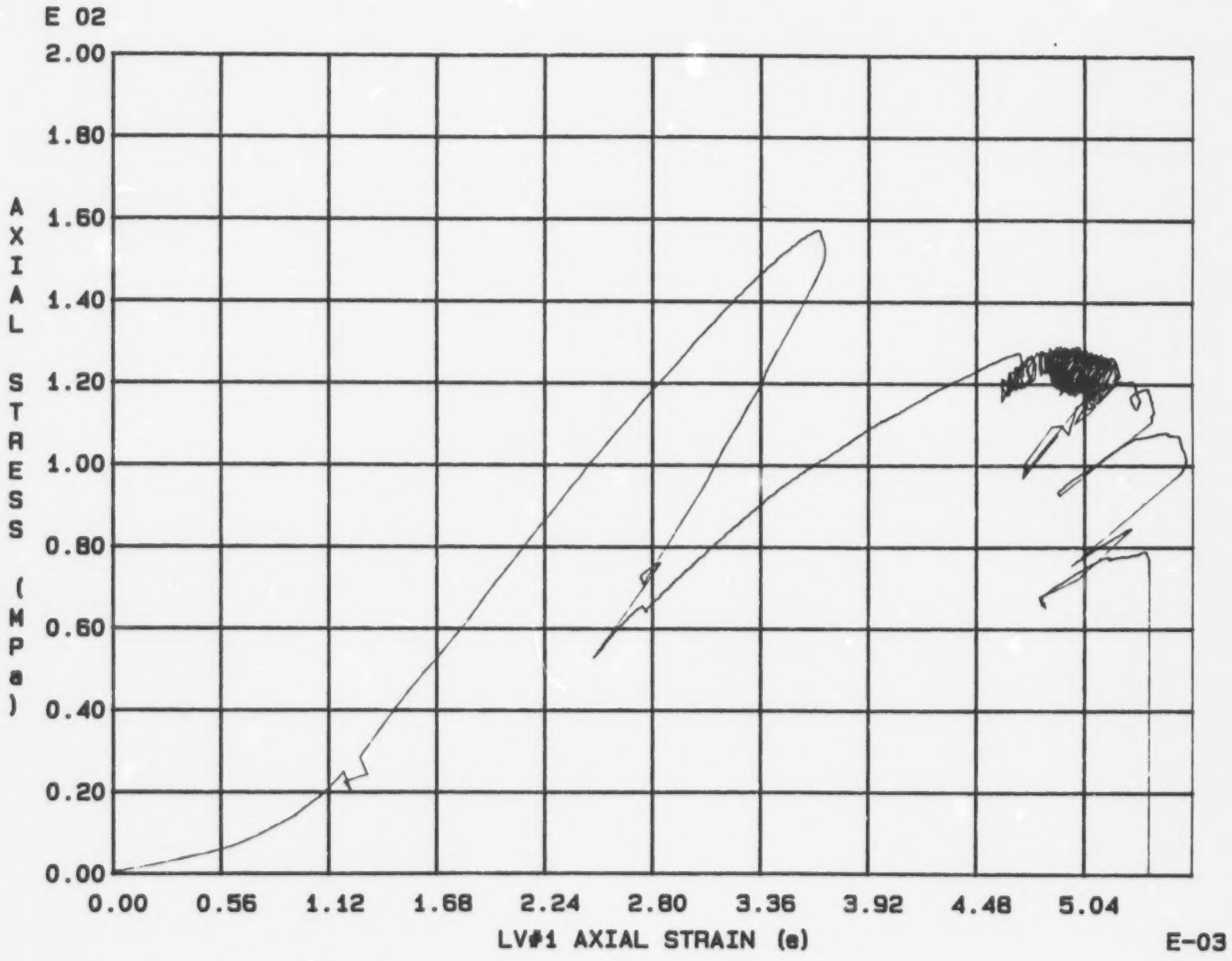

Fig. 1 - 44 Specimen M83U

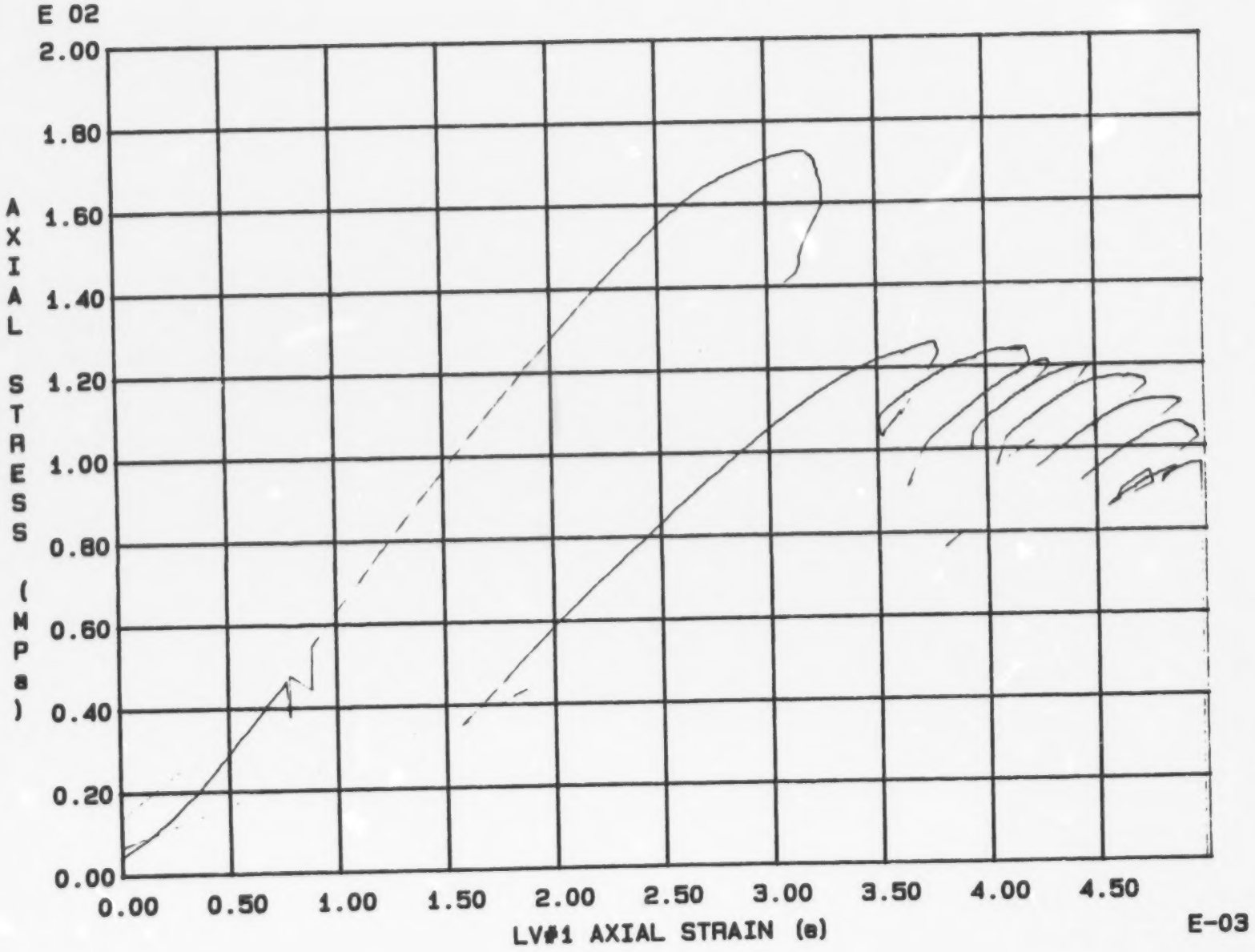

Fig. 1 - 45 Specimen M84U

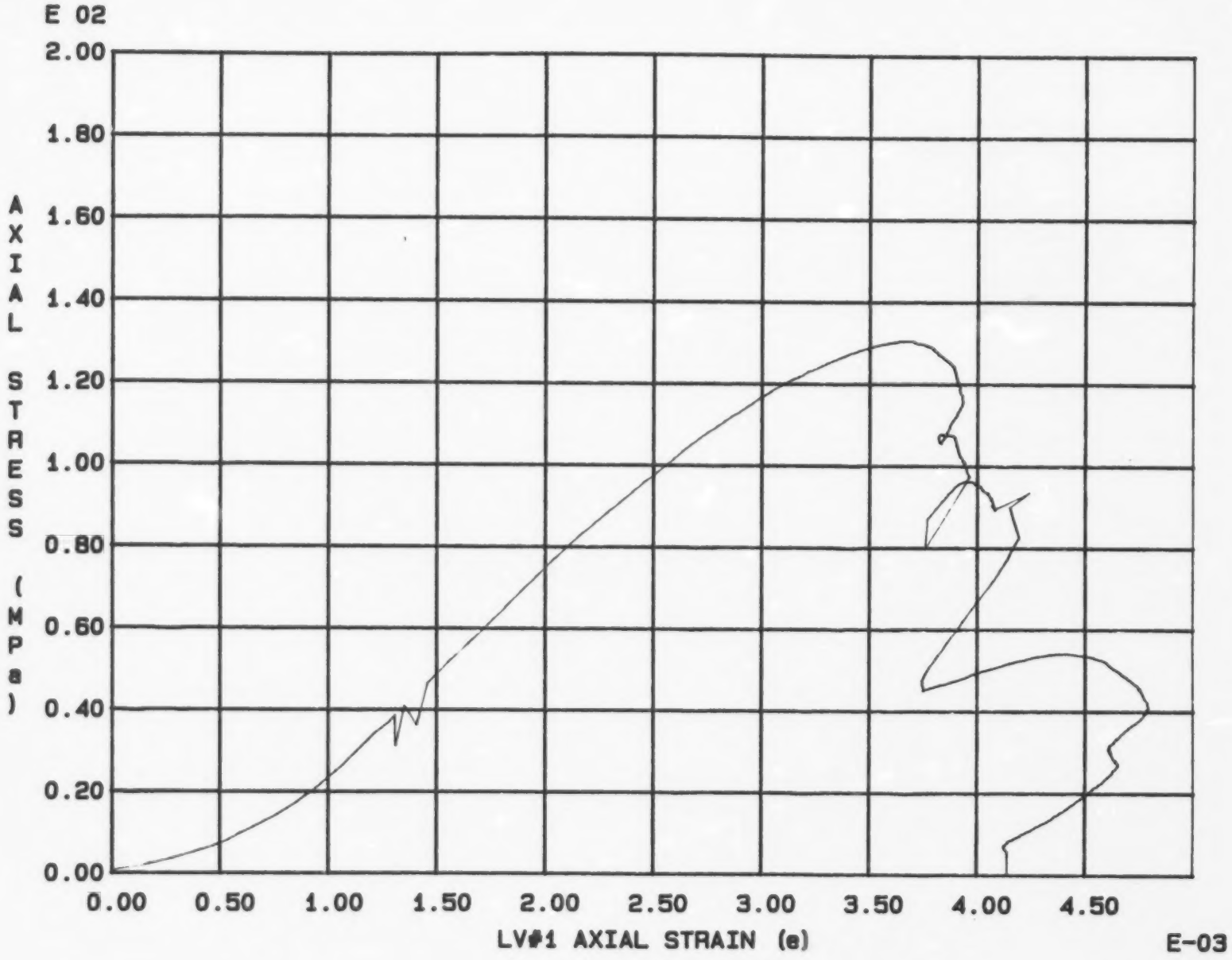

Fig. 1 - 46 Specimen M85U

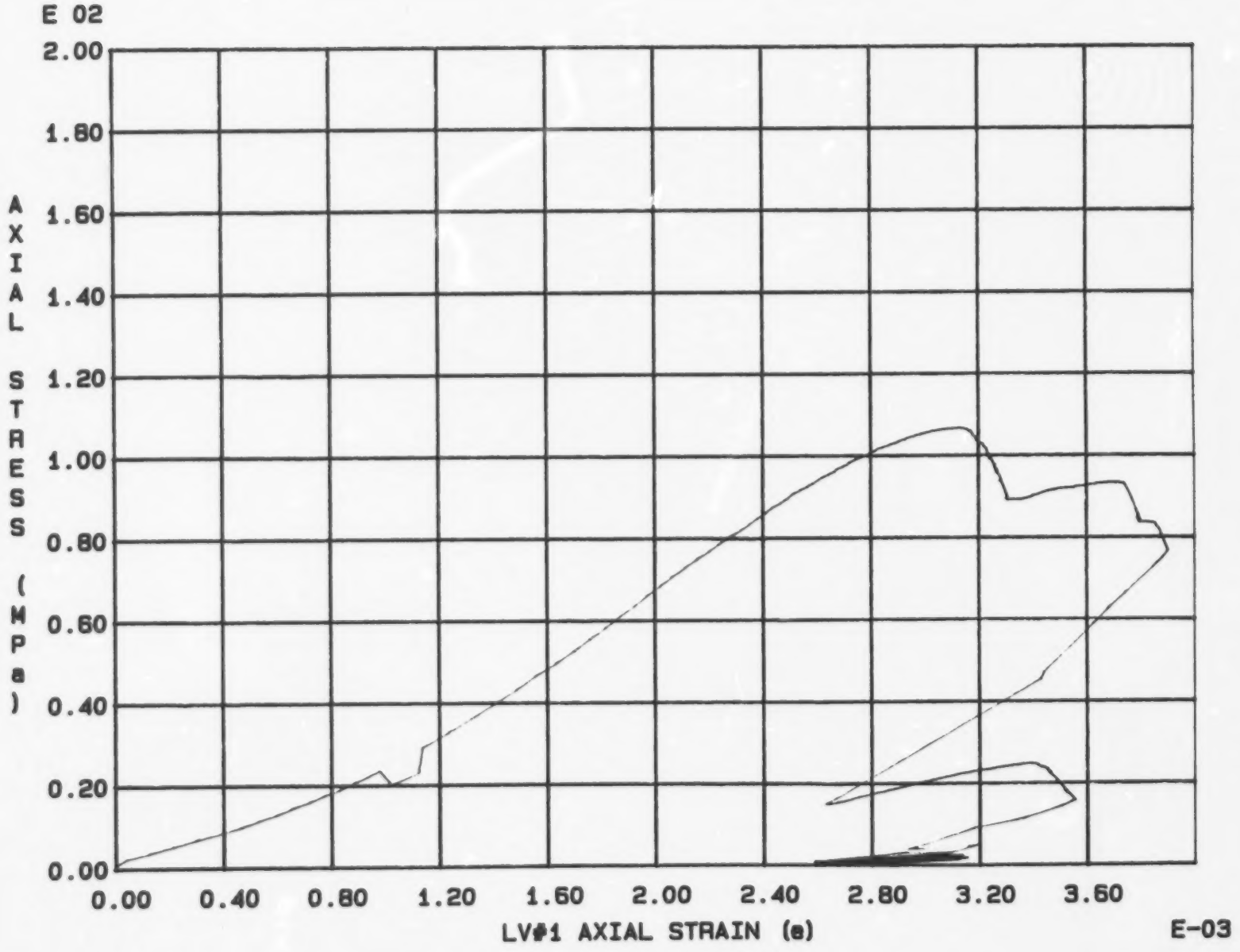

Fig. 1 - 47 Specimen M86U

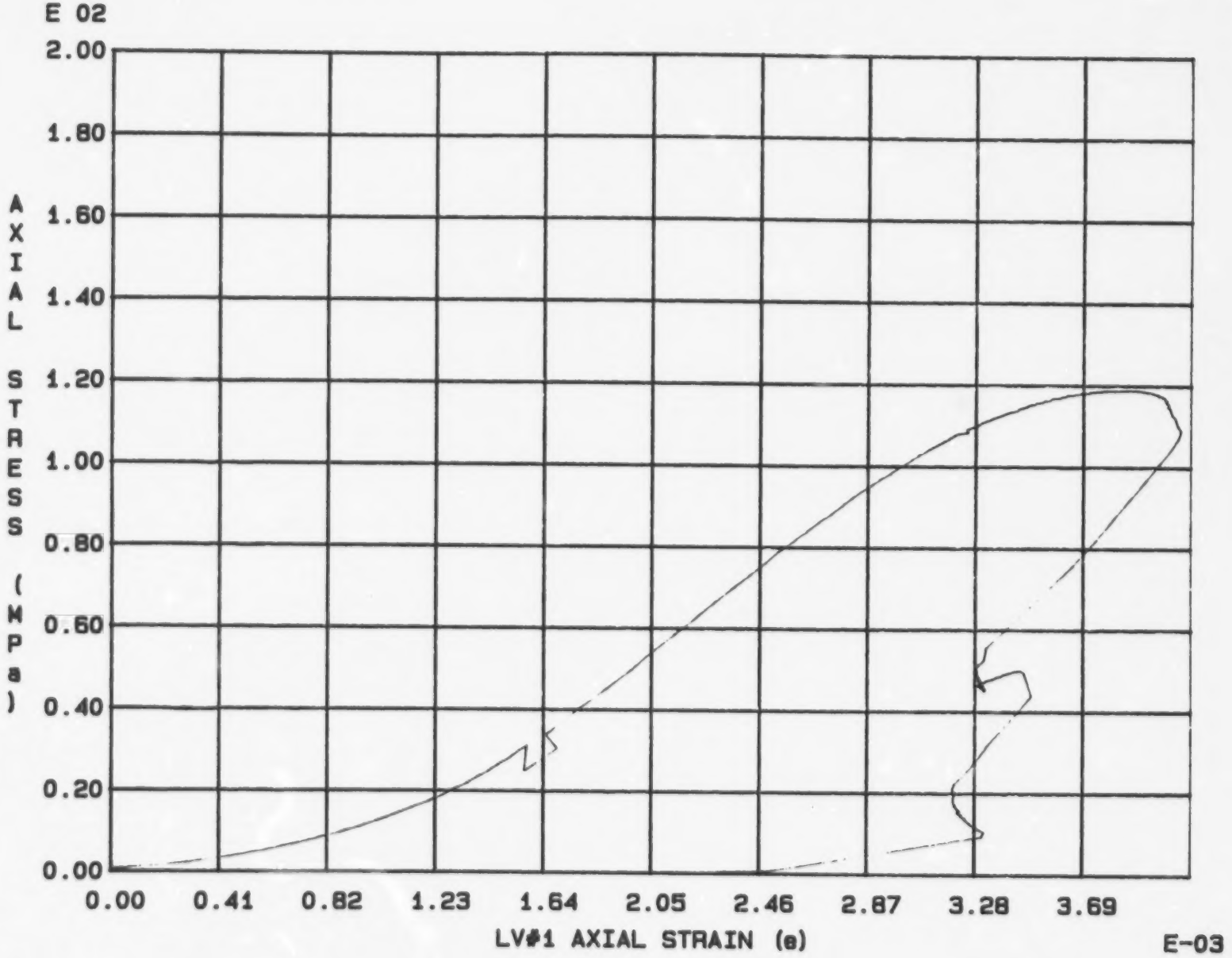

Fig. 1 - 48 Specimen M87U

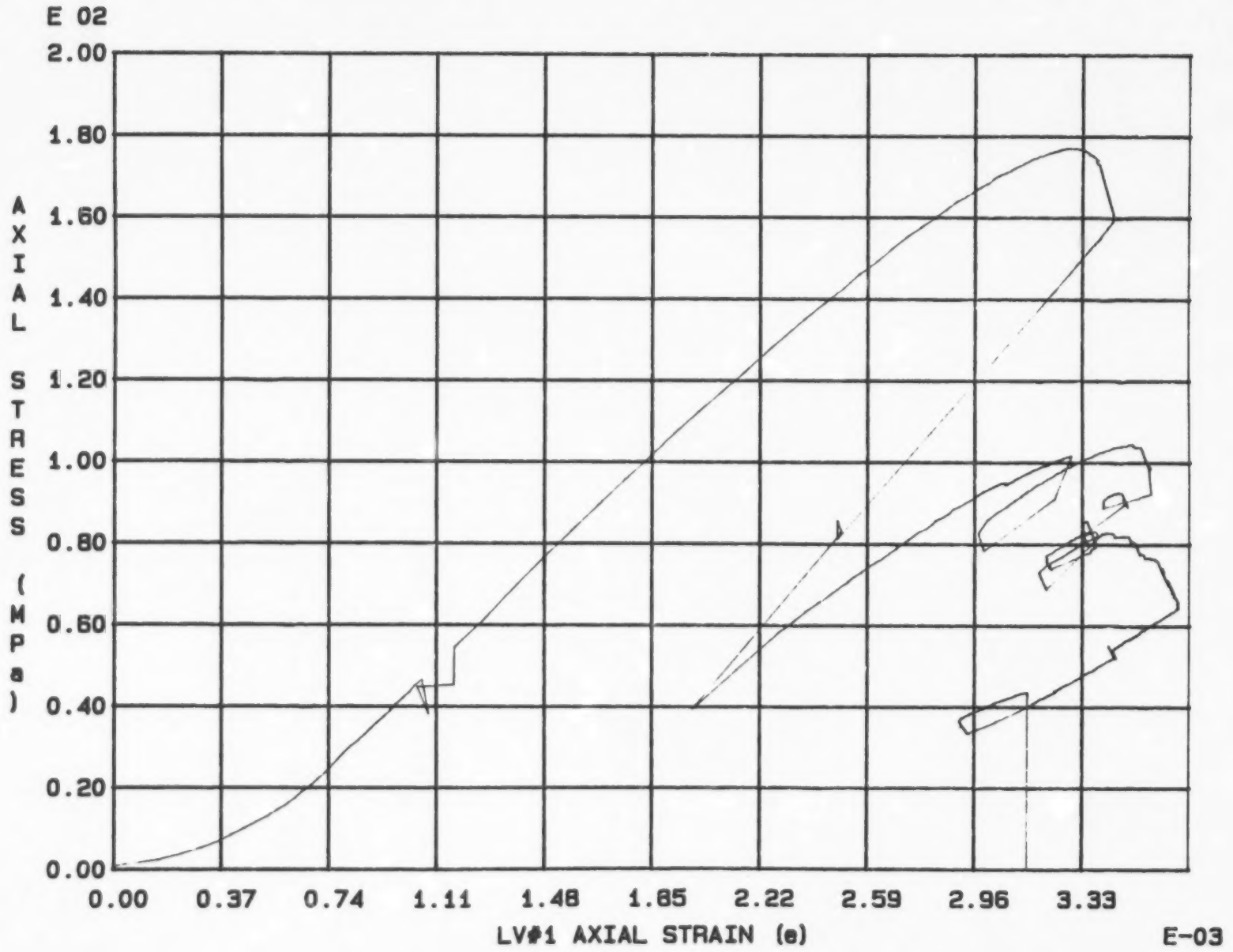

Fig. 1 - 49 Specimen M88U

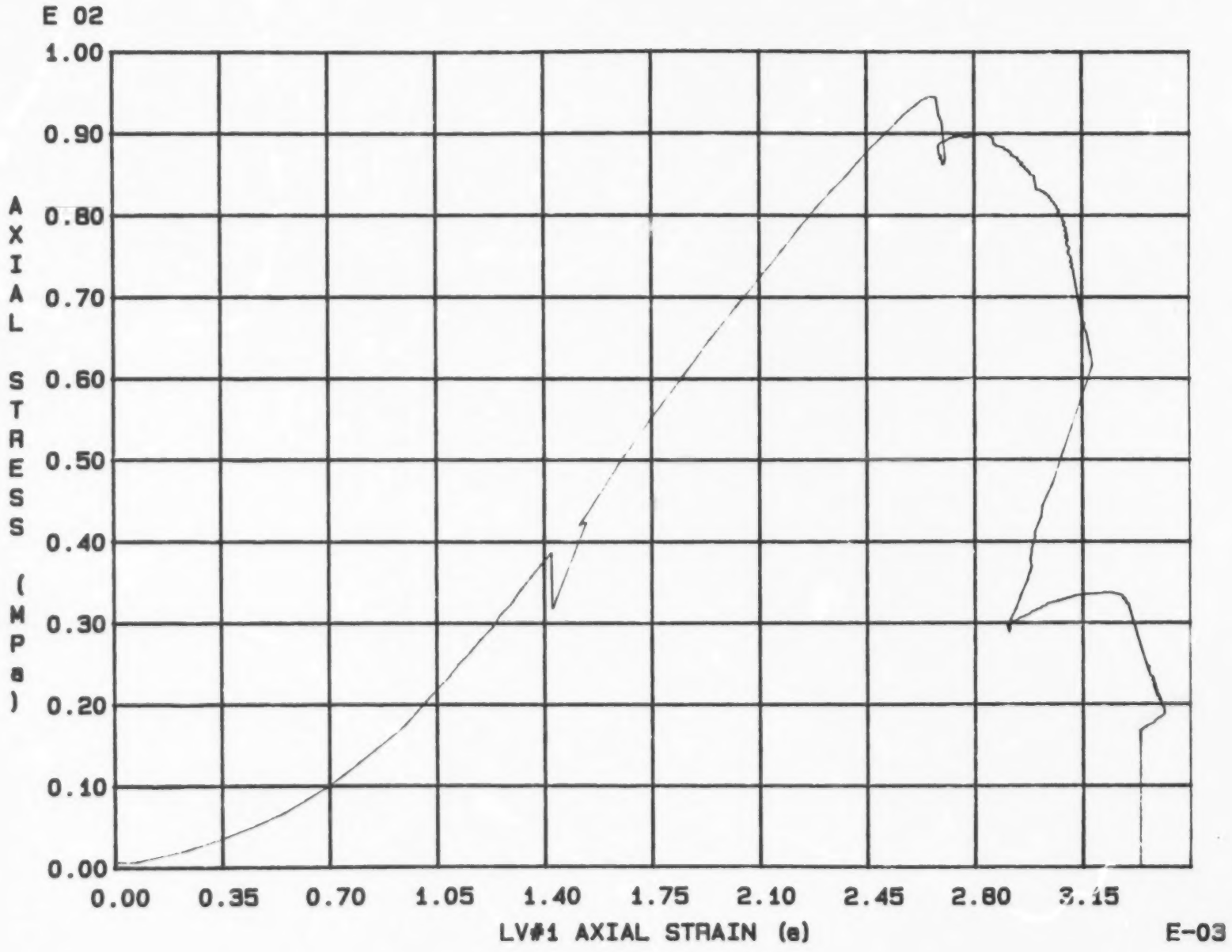

Fig. 1 - 50 Specimen M89U

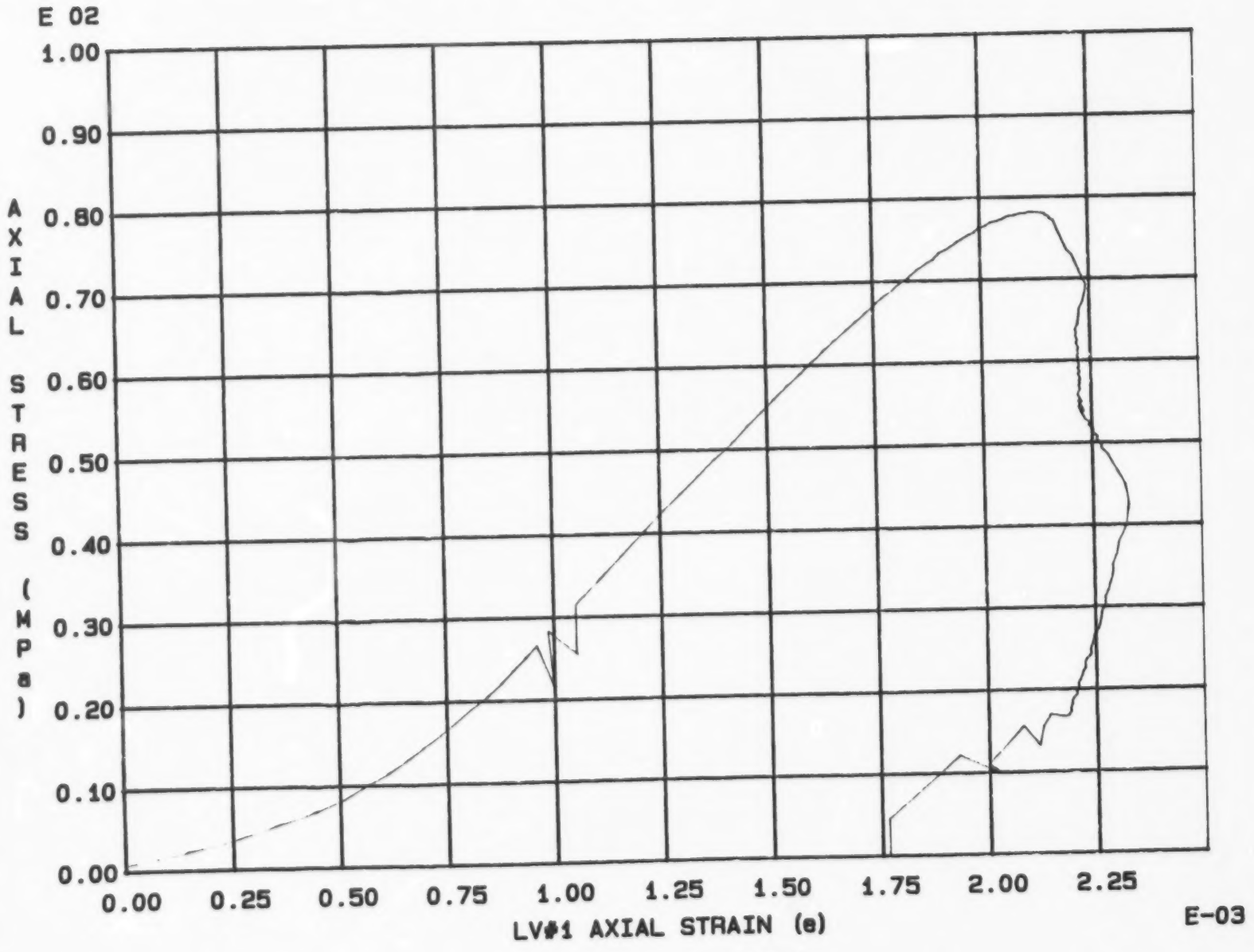

Fig. 1 - 51 Specimen M90U

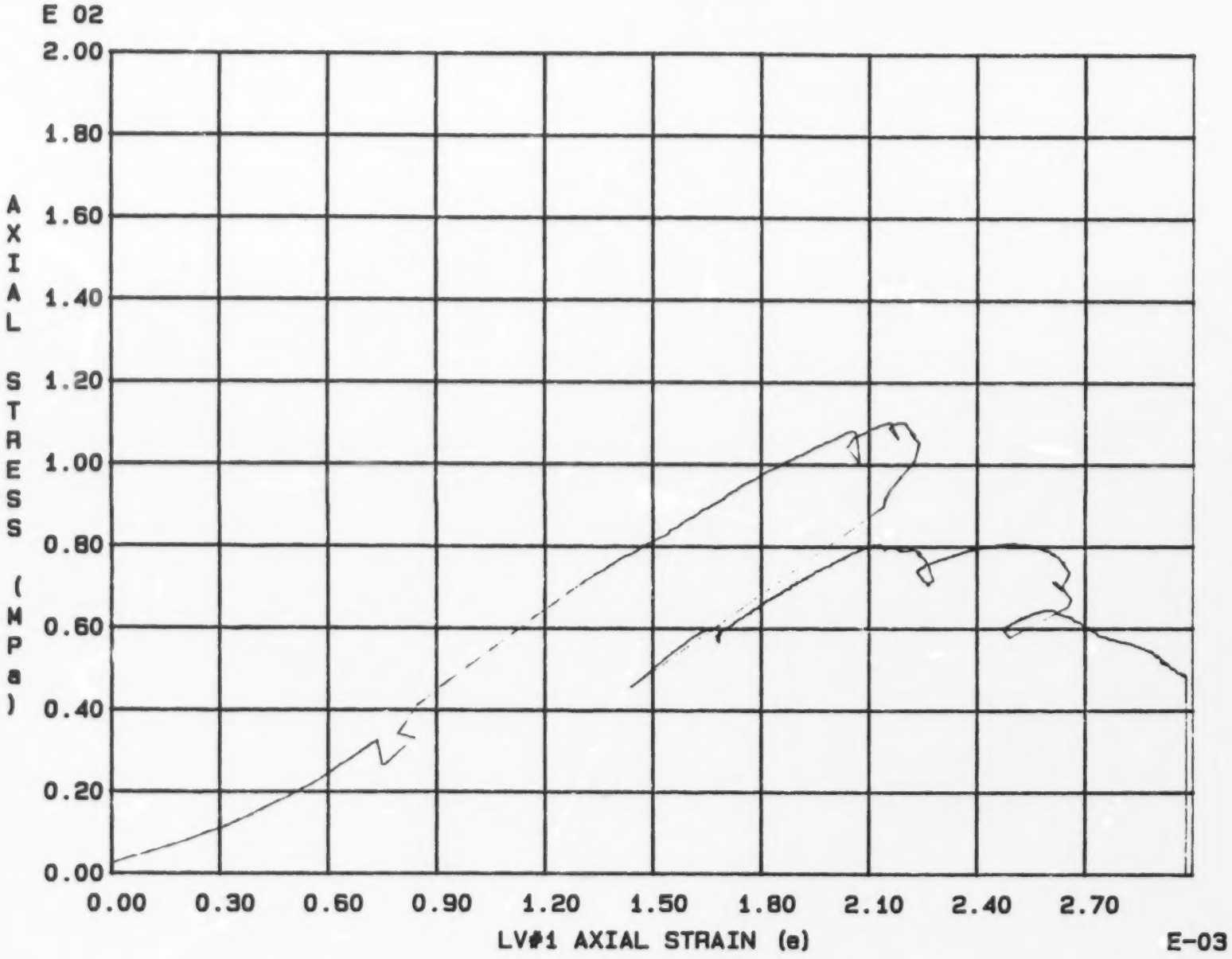

Fig. 1 - 52 Specimen M91U

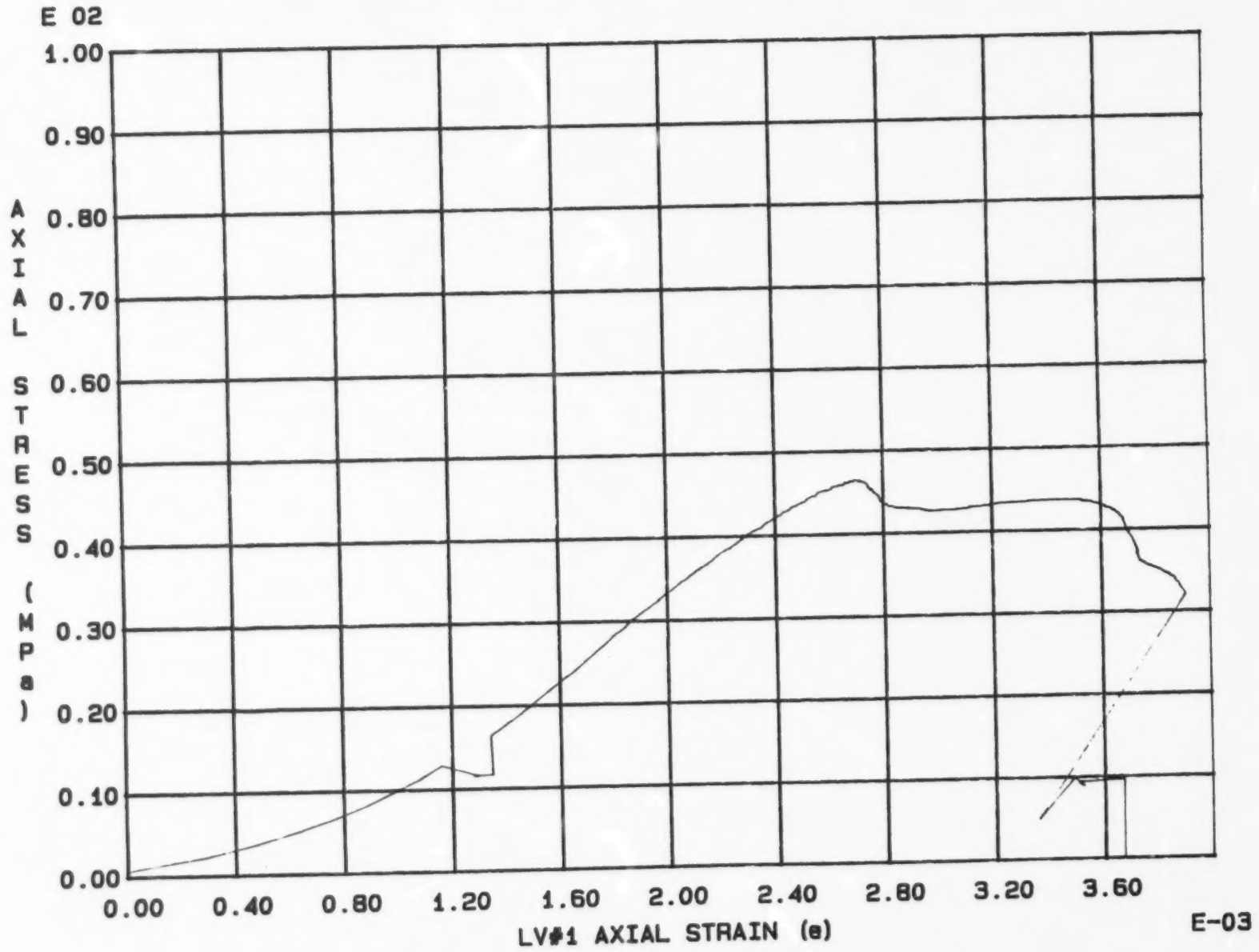

Fig. 1 - 53 Specimen M92U

Appendix 2.

Stress-strain curves of uniaxial tests using axial bonded strain gauges

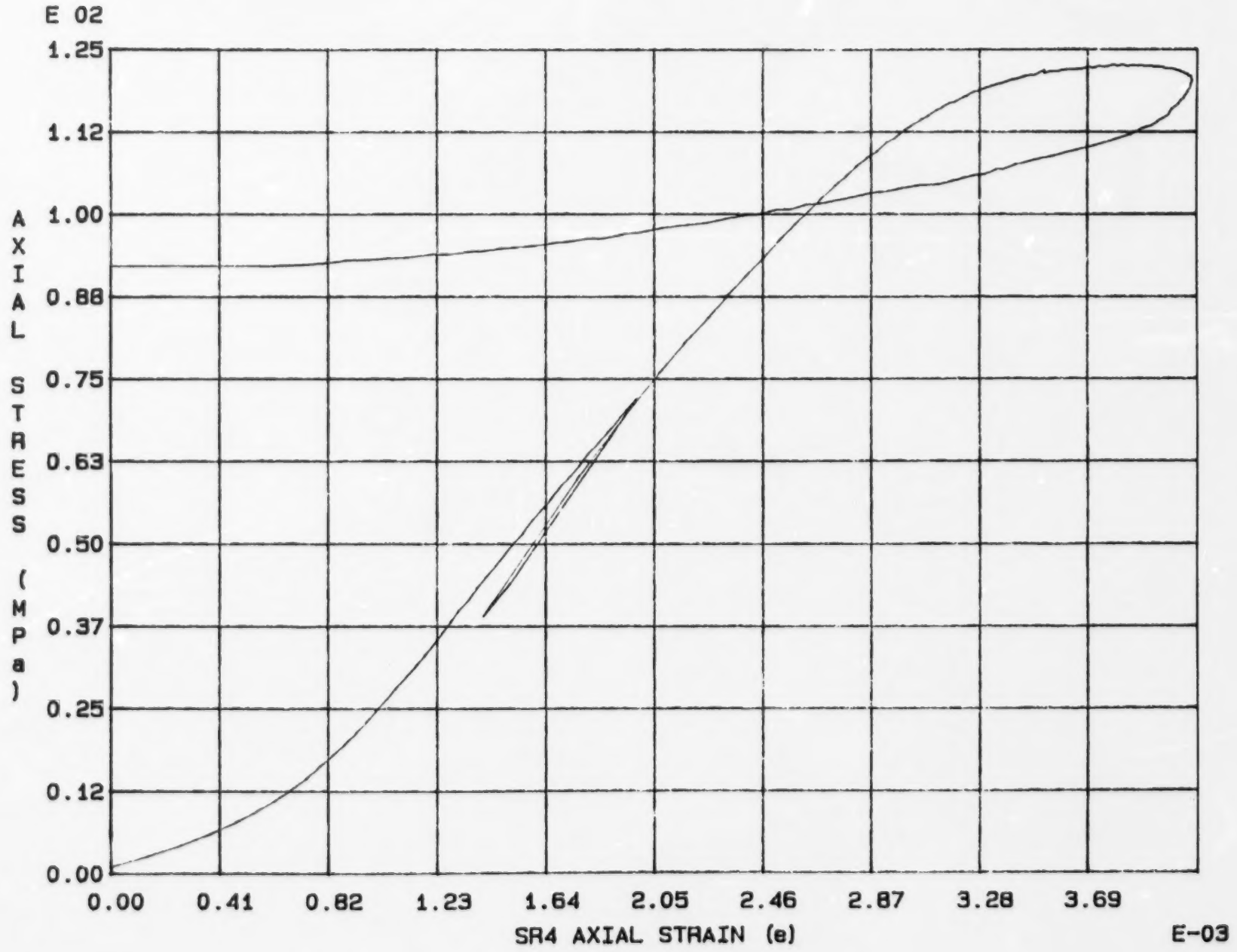

Fig. 2 - 1 Specimen M3U

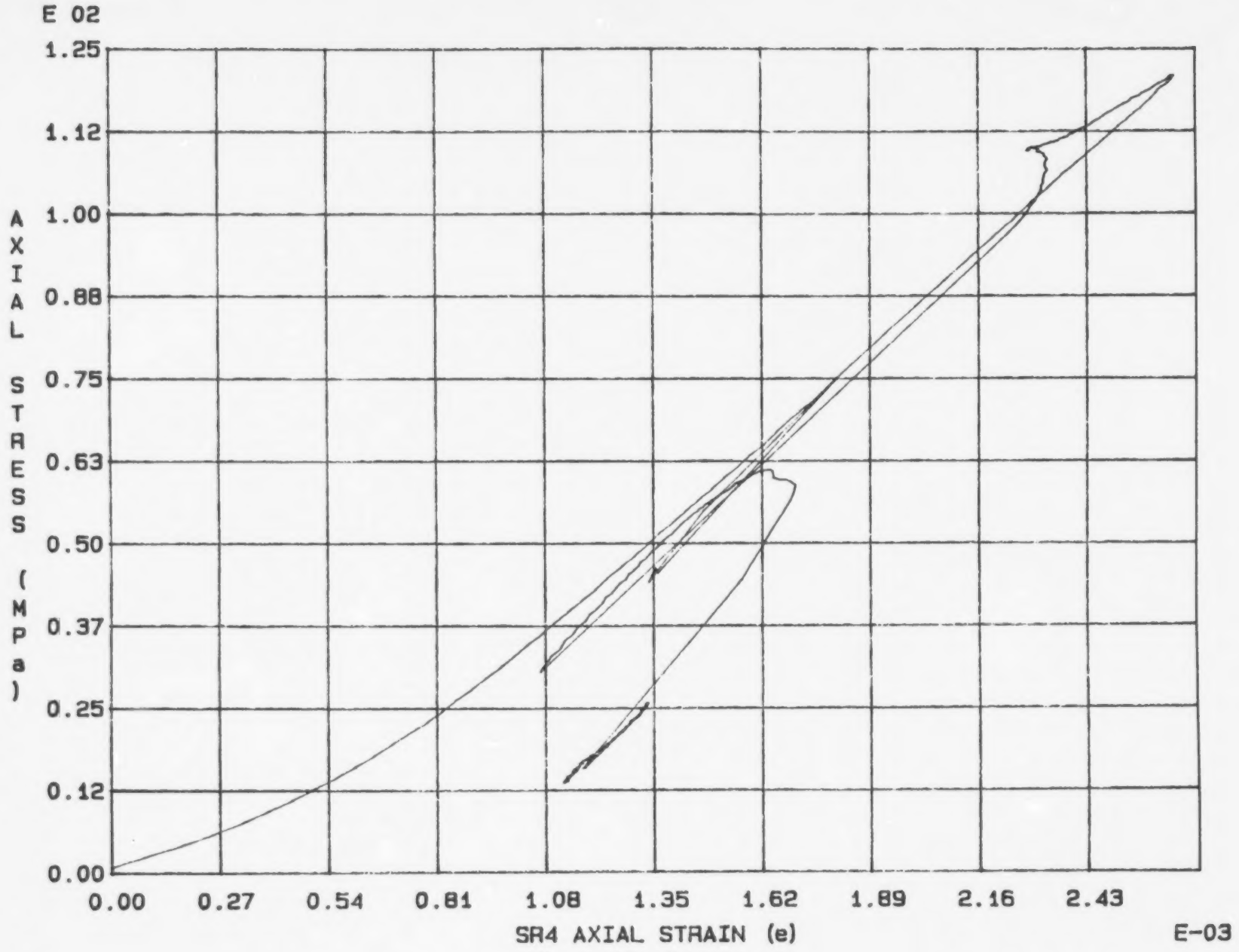

Fig. 2 - 2 Specimen M4U

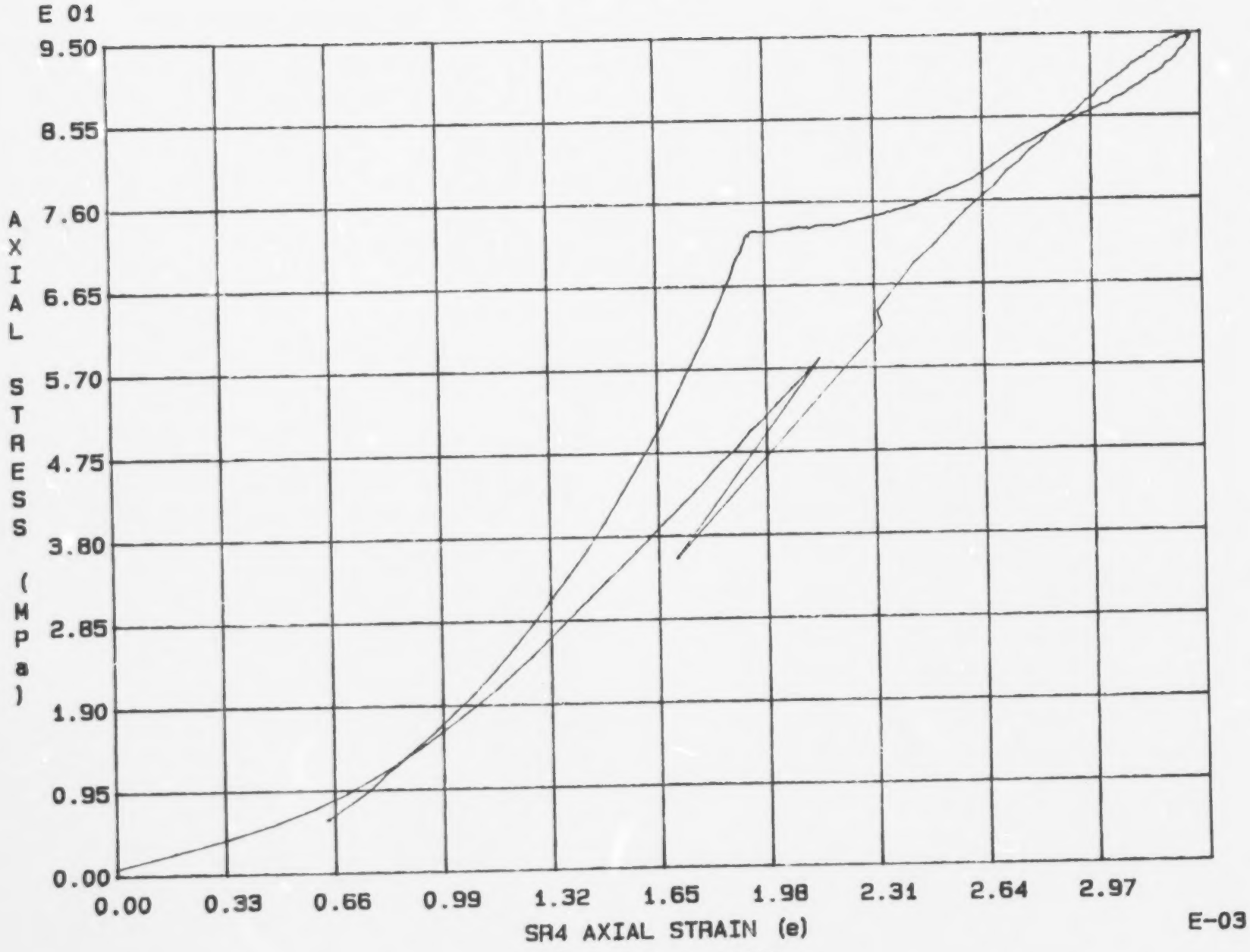

Fig. 2 - 3 Specimen M5U

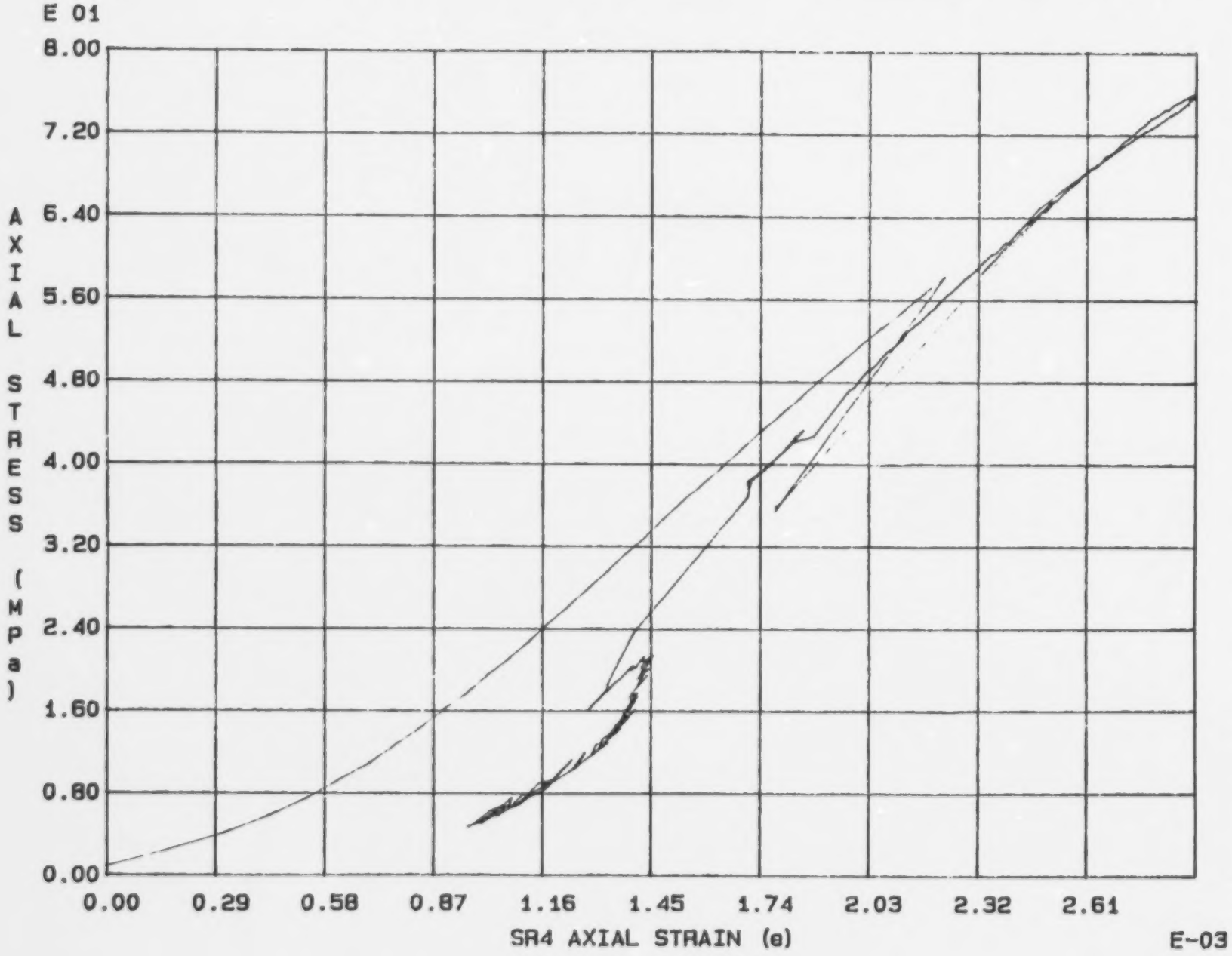

Fig. 2 - 4 Specimen M6U

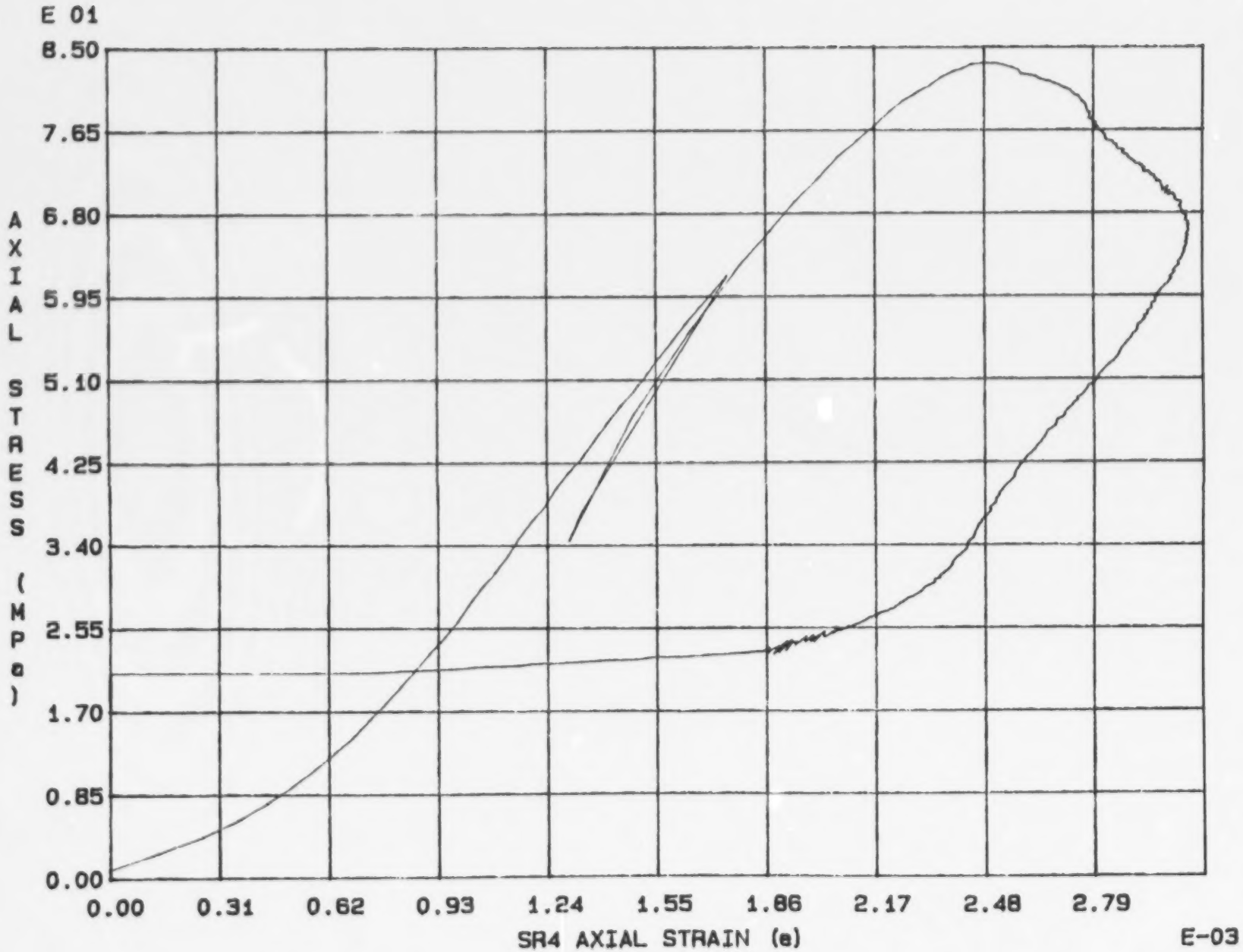

Fig. 2 - 5 Specimen M7U

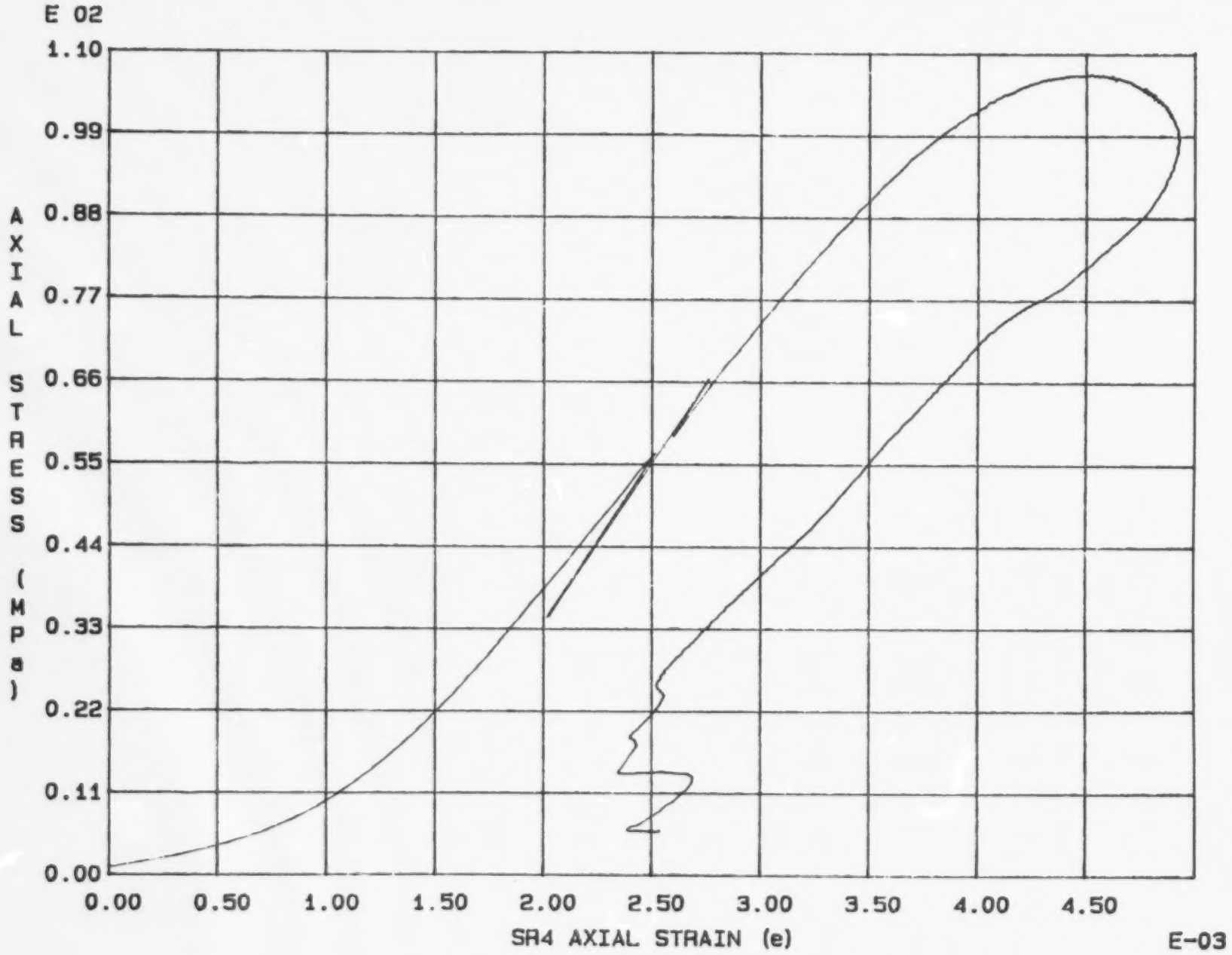

Fig 2 - 6 Specimen M8U

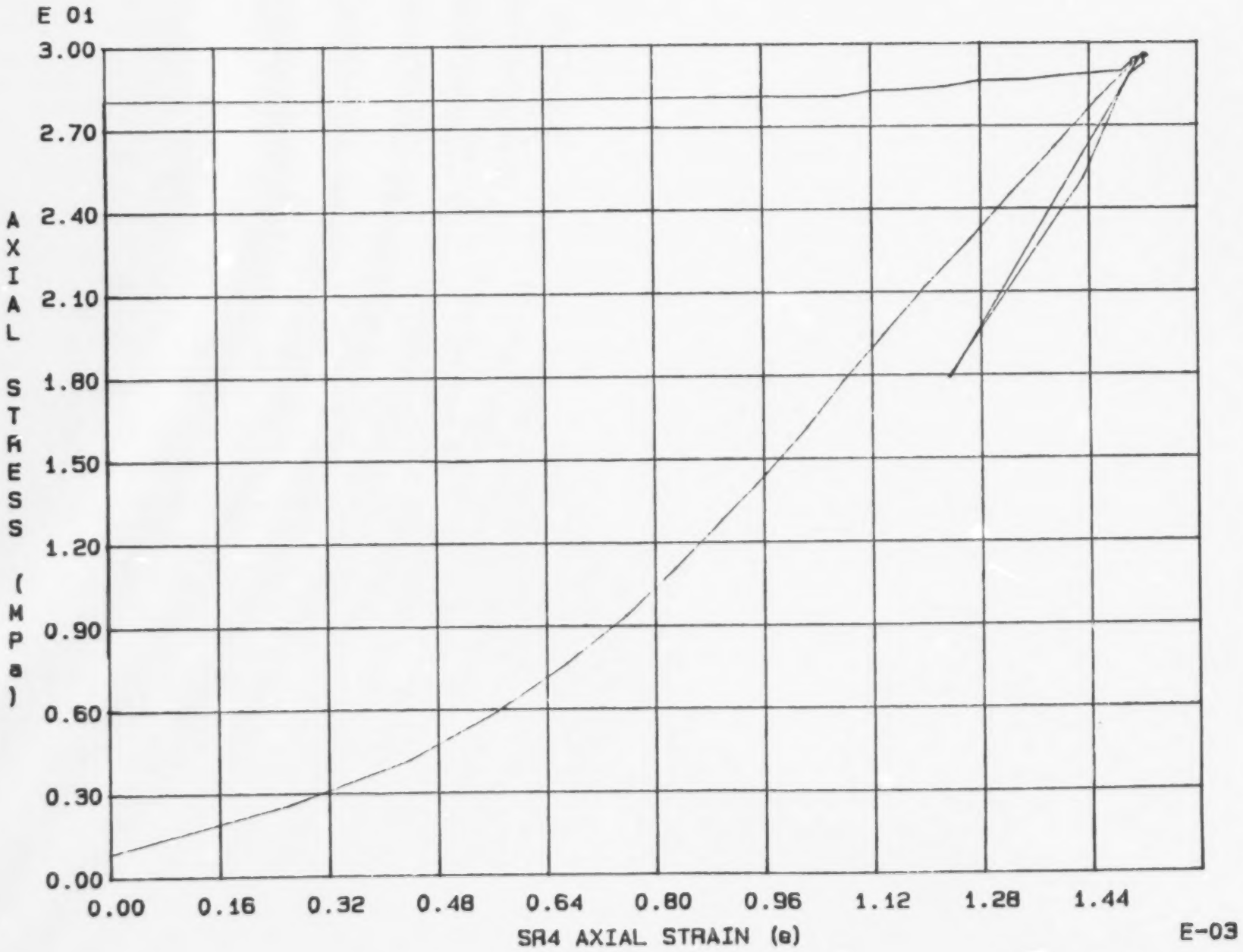

Fig. 2 - 7 Specimen M9U

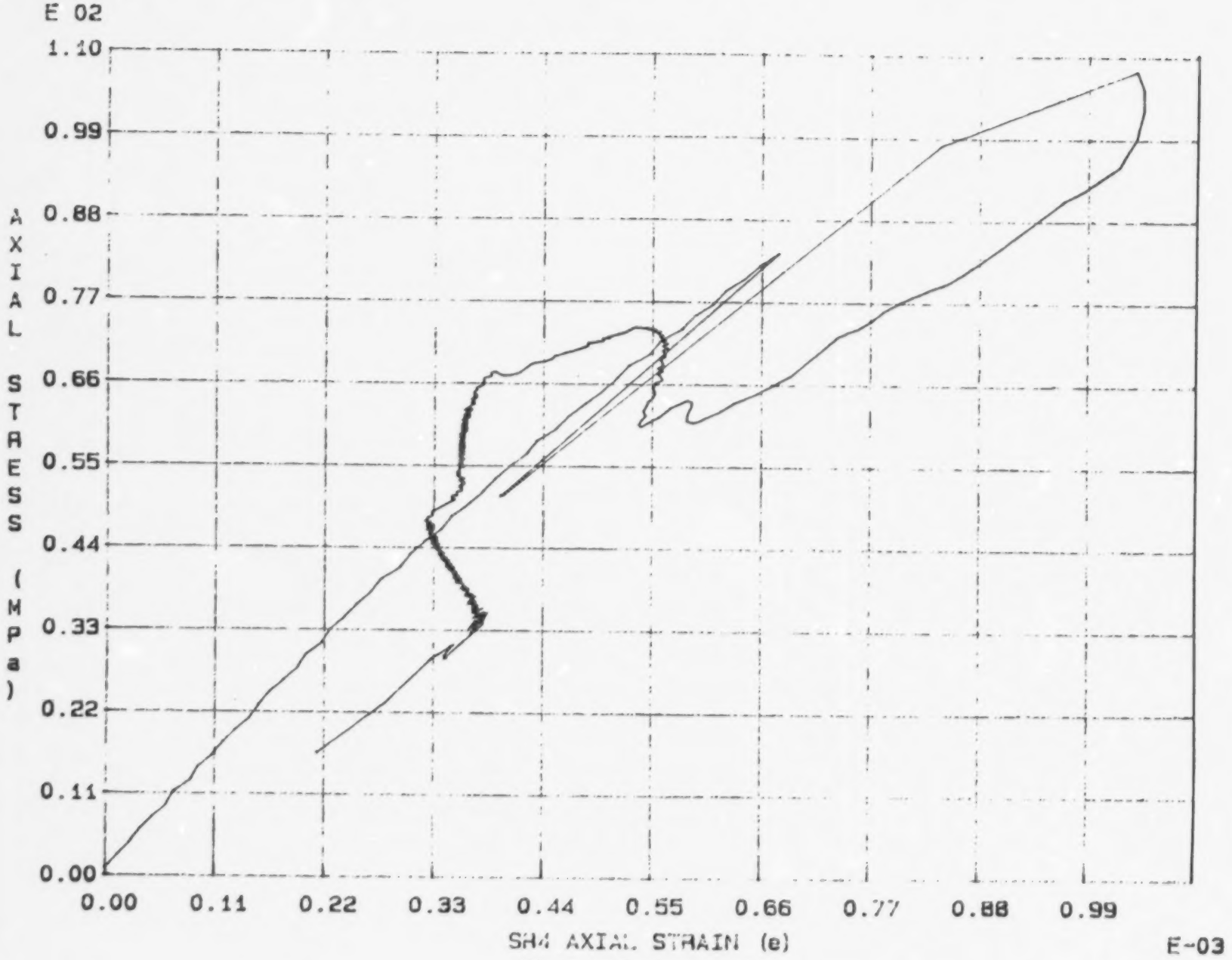

Fig. 2 - 8 Specimen M10U

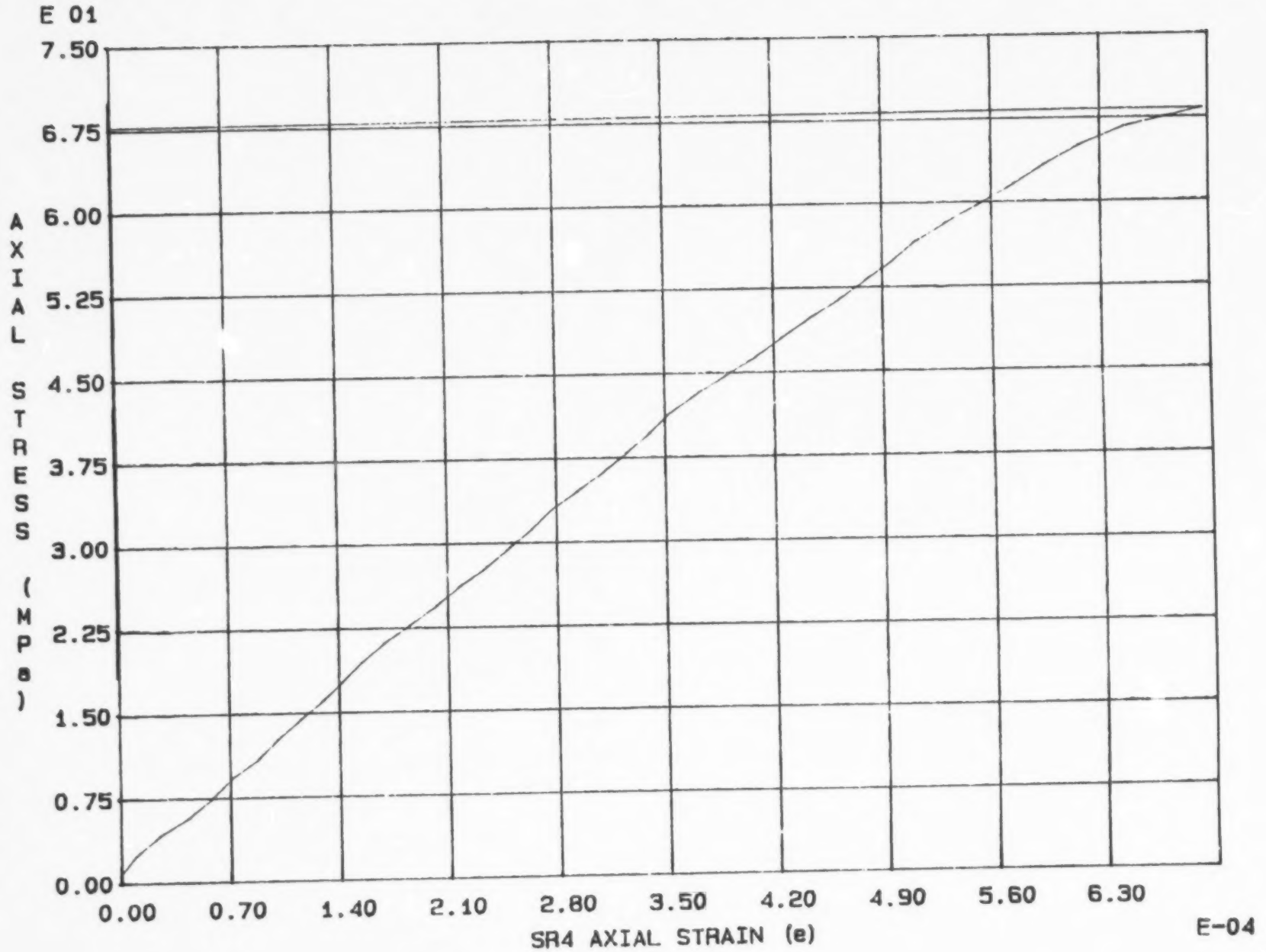

Fig. 2 - 9 Specimen M11U

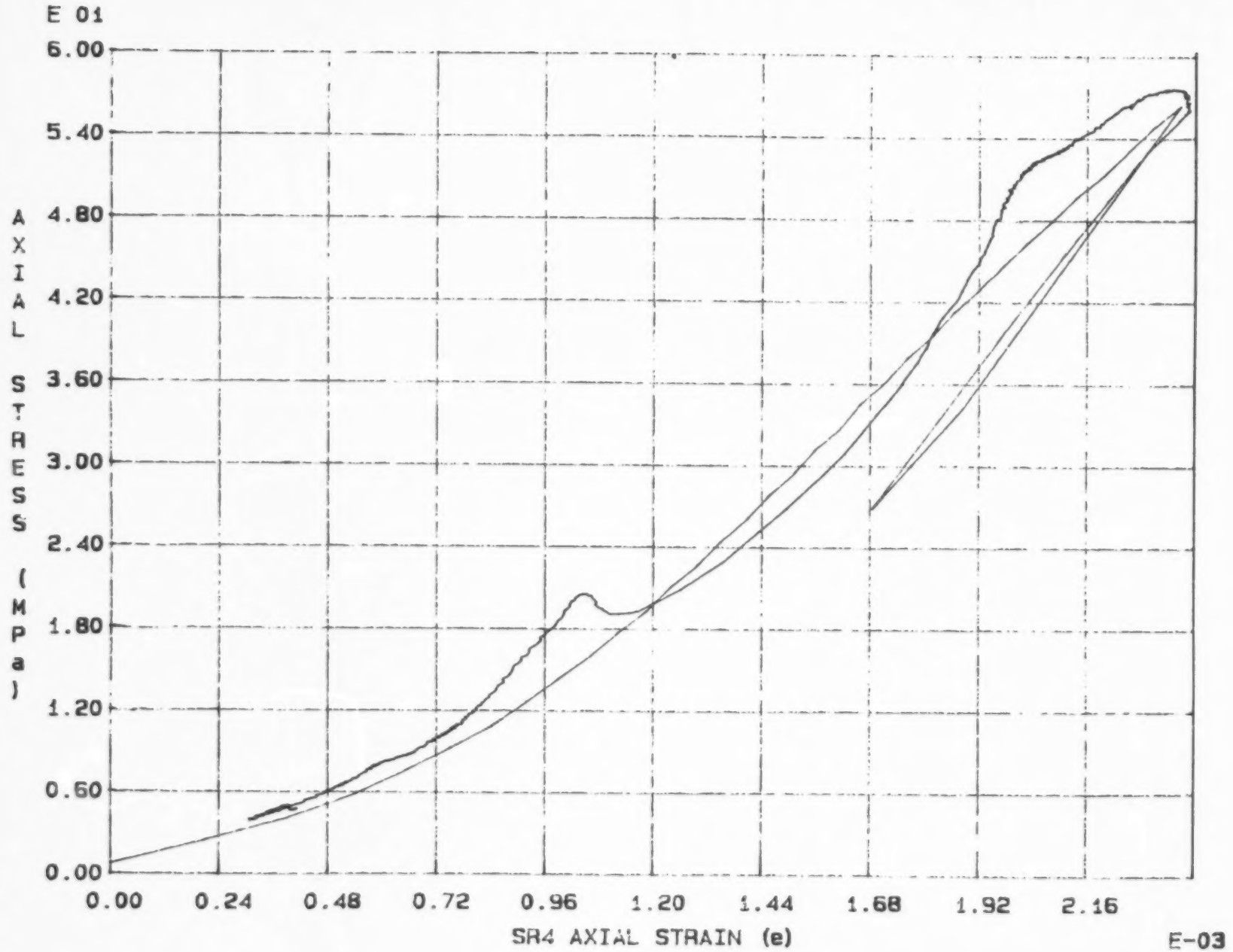

Fig. 2 - 10 Specimen M12U

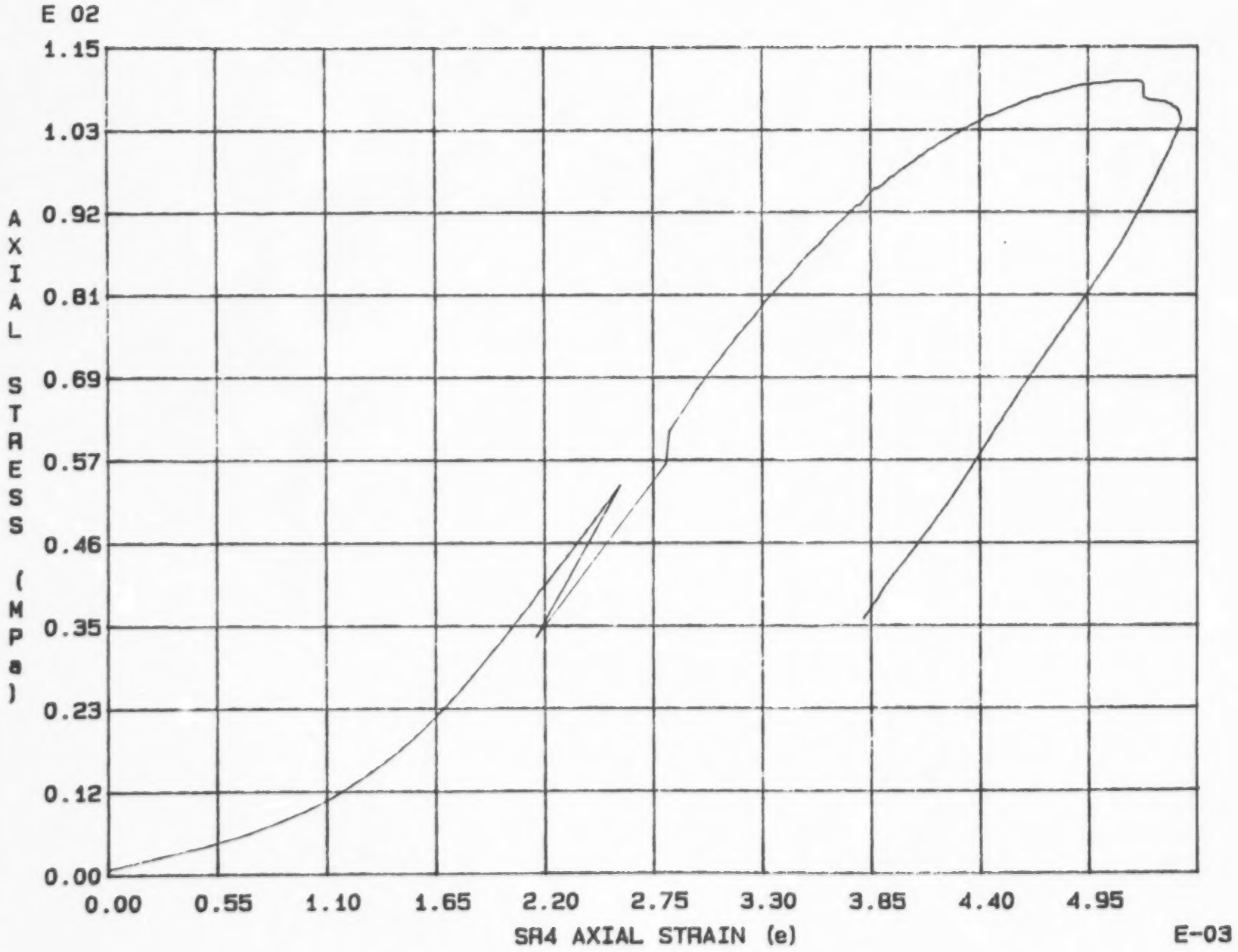

Fig. 2 - 11 Specimen M13U

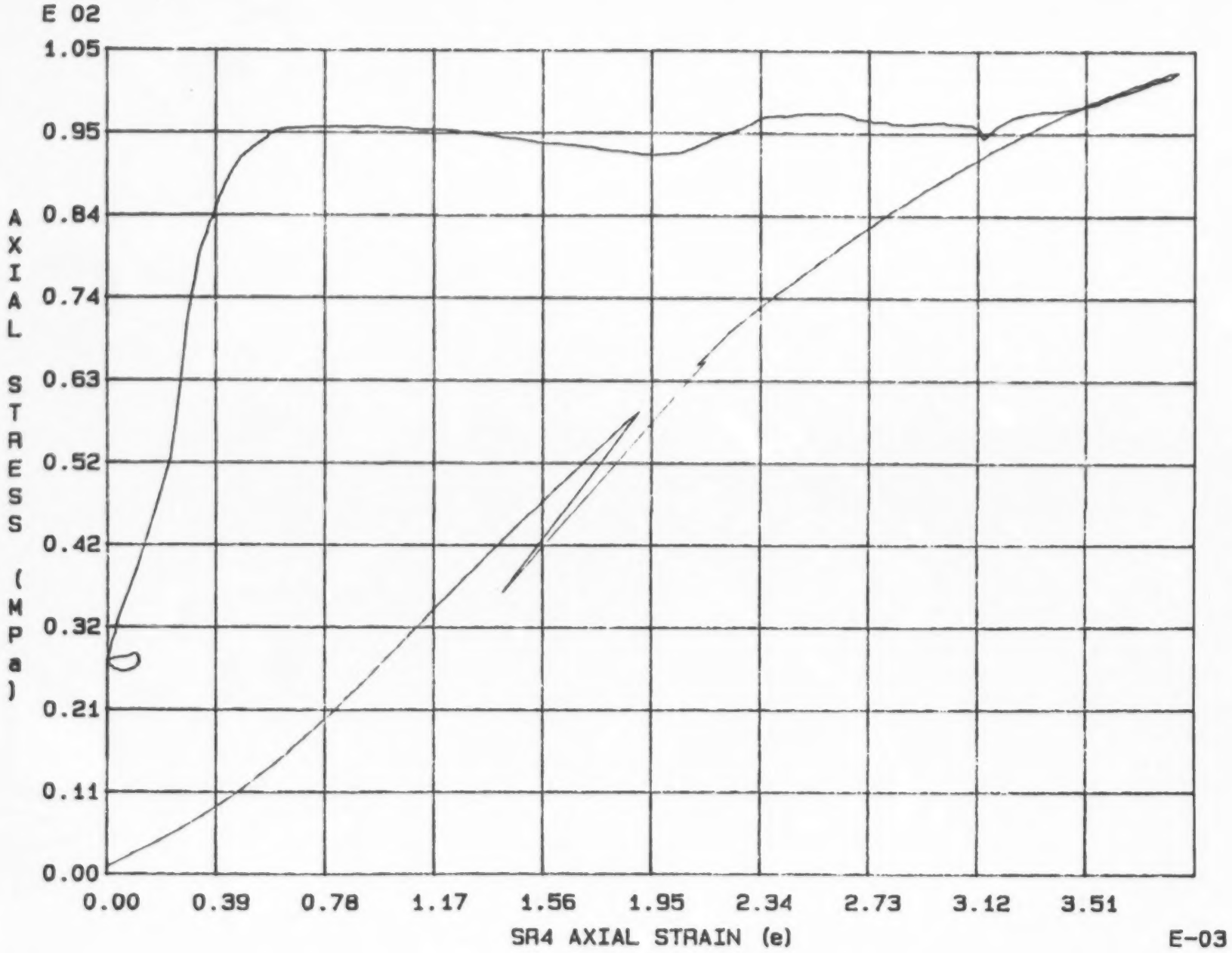

Fig. 2 - 12 Specimen M14U

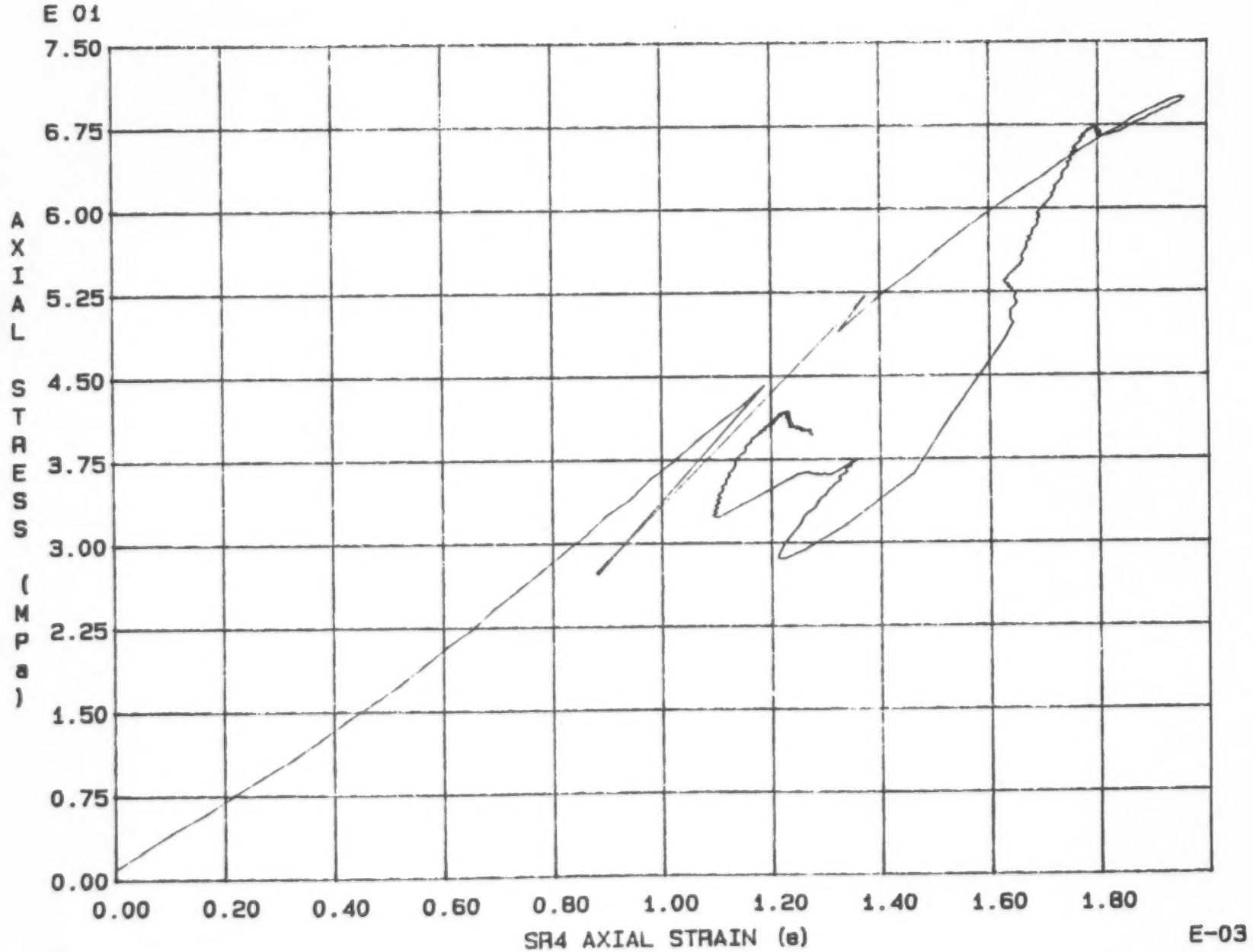

Fig. 2 - 13 Specimen M15U

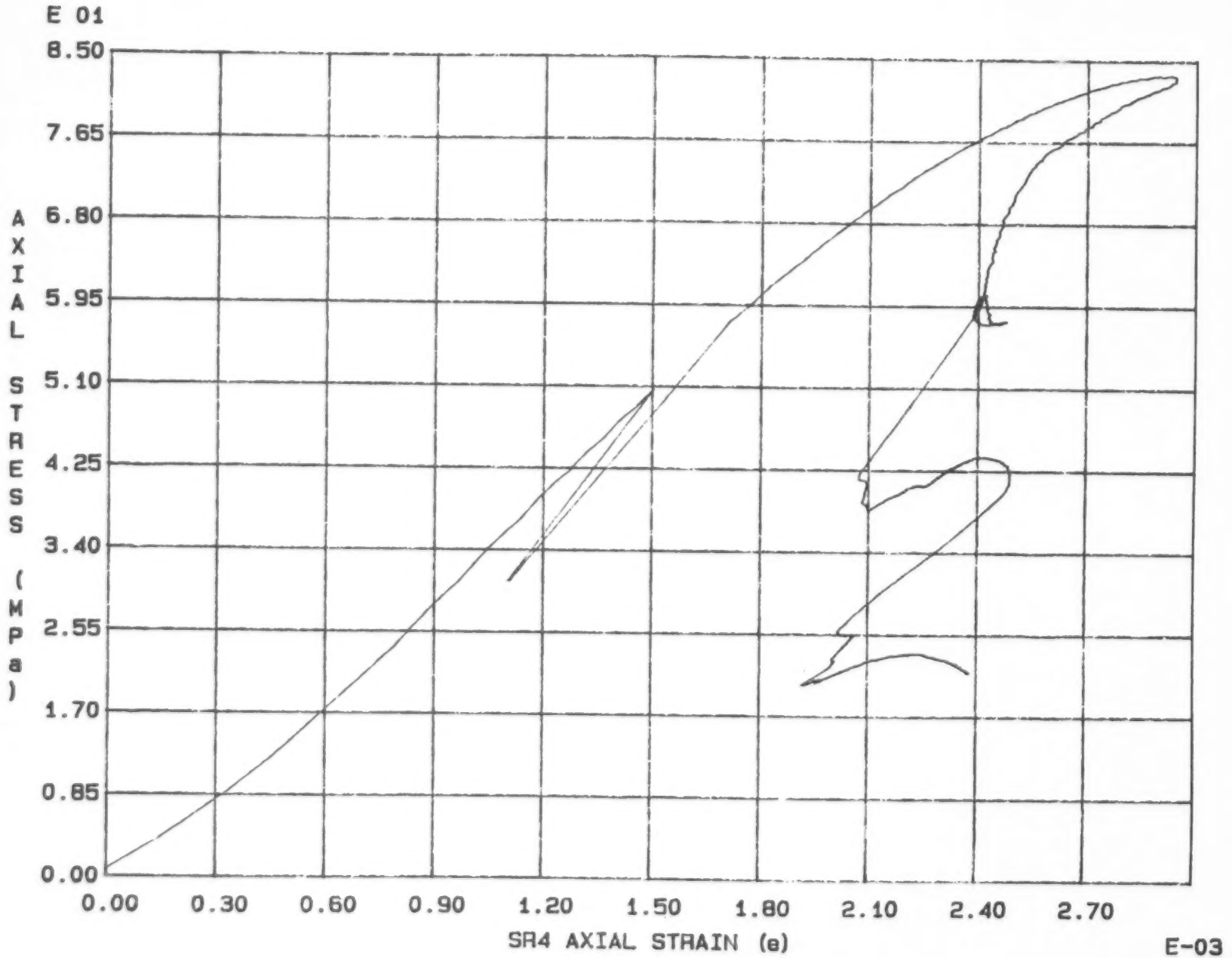

Fig. 2 - 14 Specimen M16U

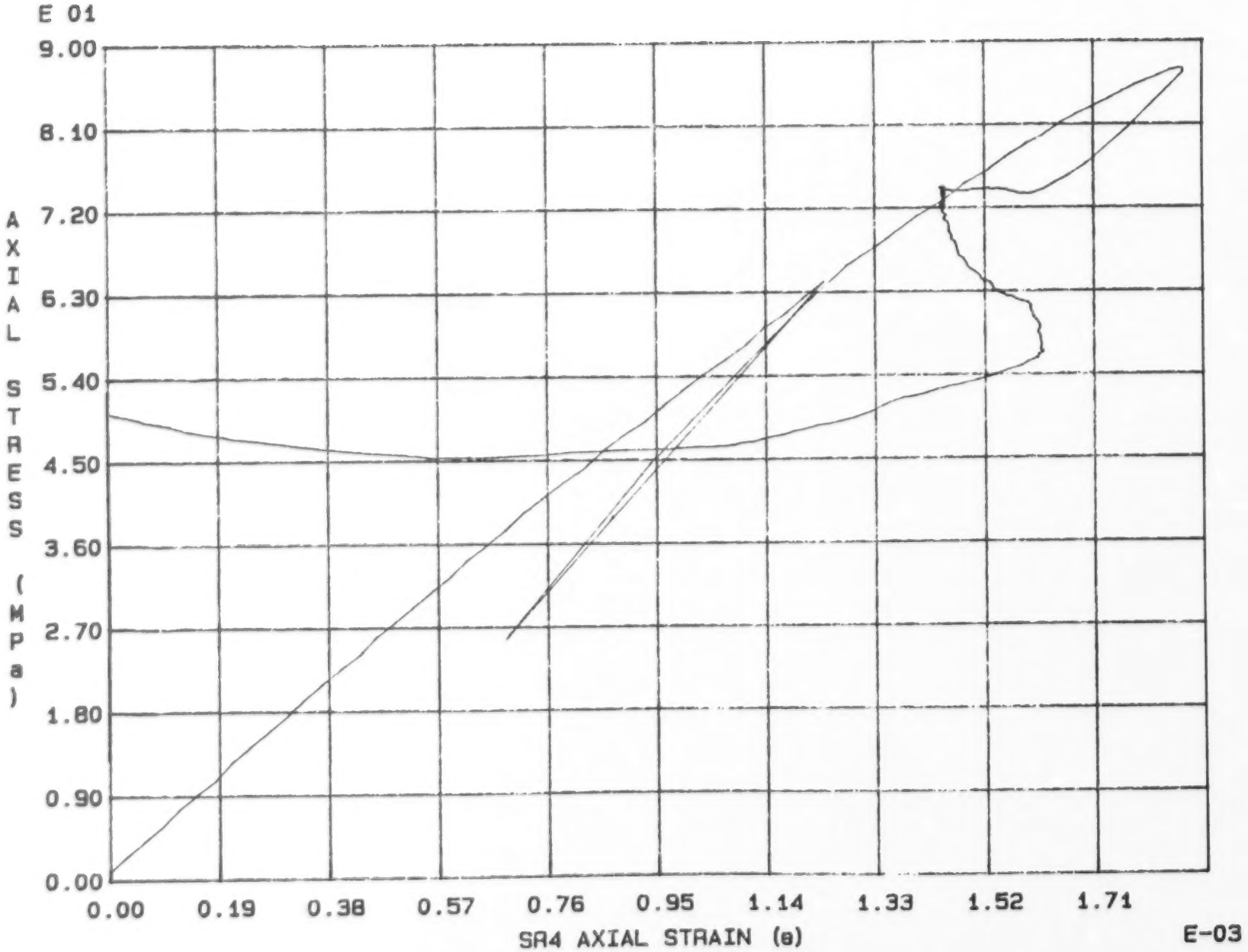

Fig. 2 - 15 Specimen M17U

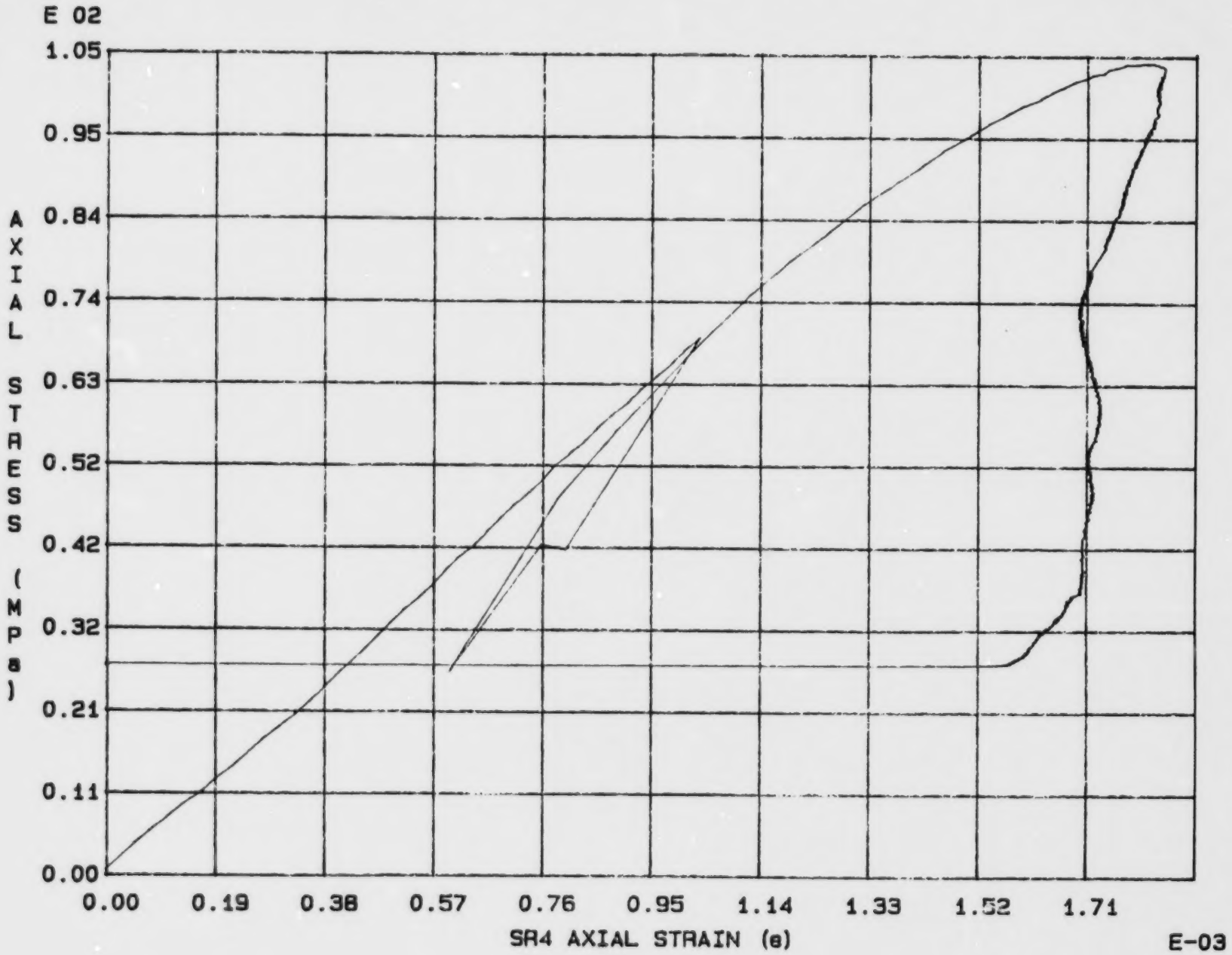

Fig. 2 - 16 Specimen M18U

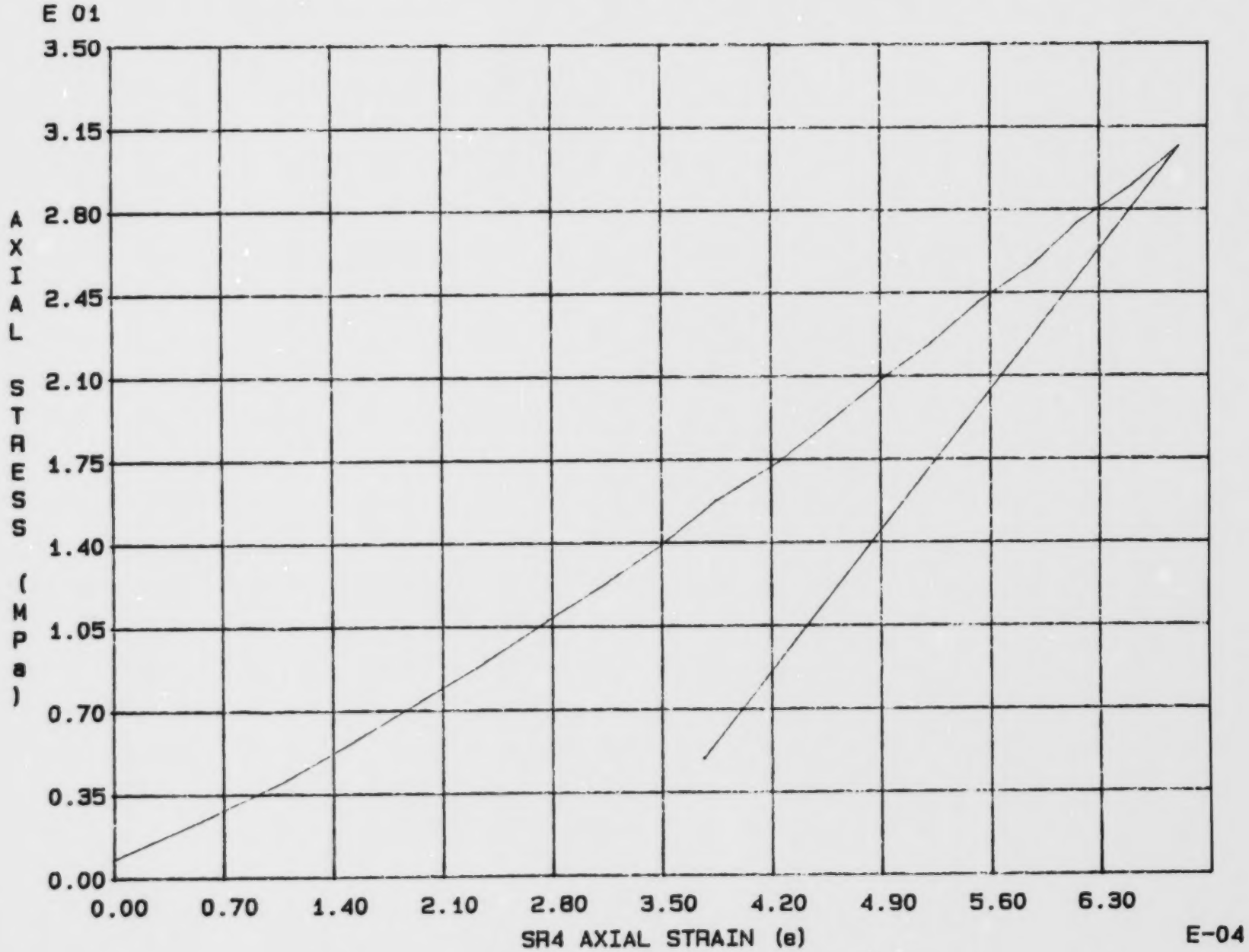

Fig. 2 - 17 Specimen M19U

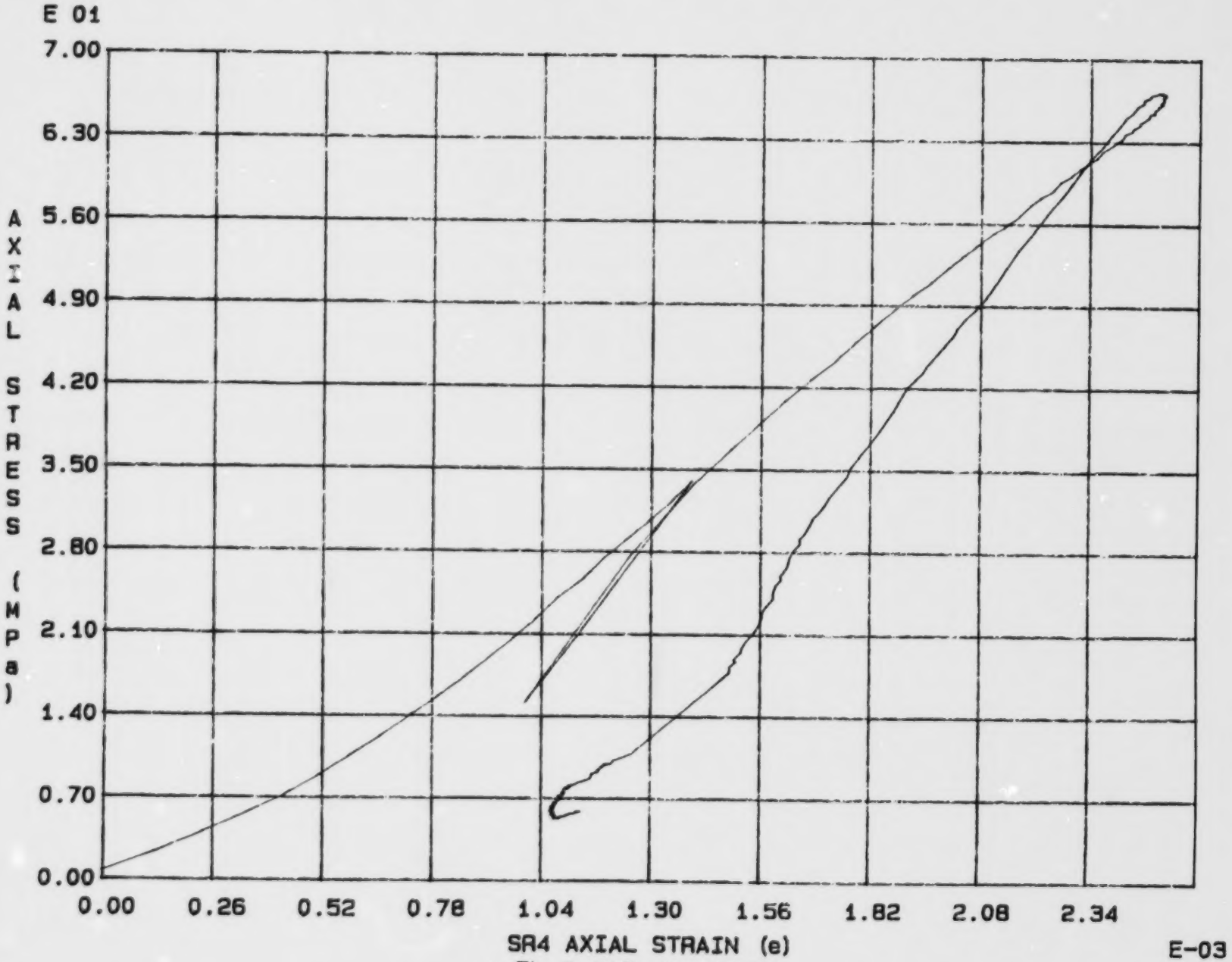

Fig. 2 - 18 Specimen M20U

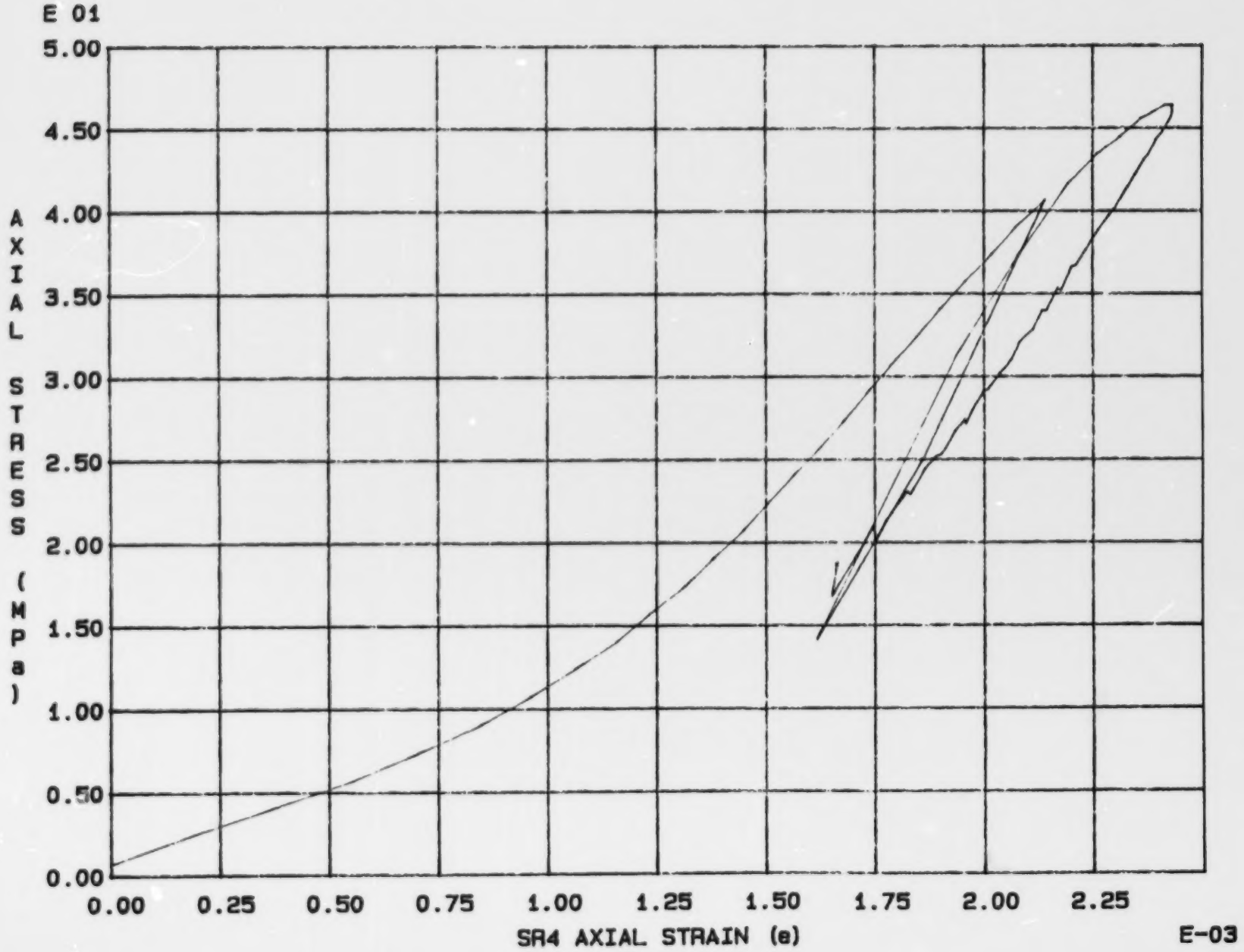

Fig. 2 - 19 Specimen M21U

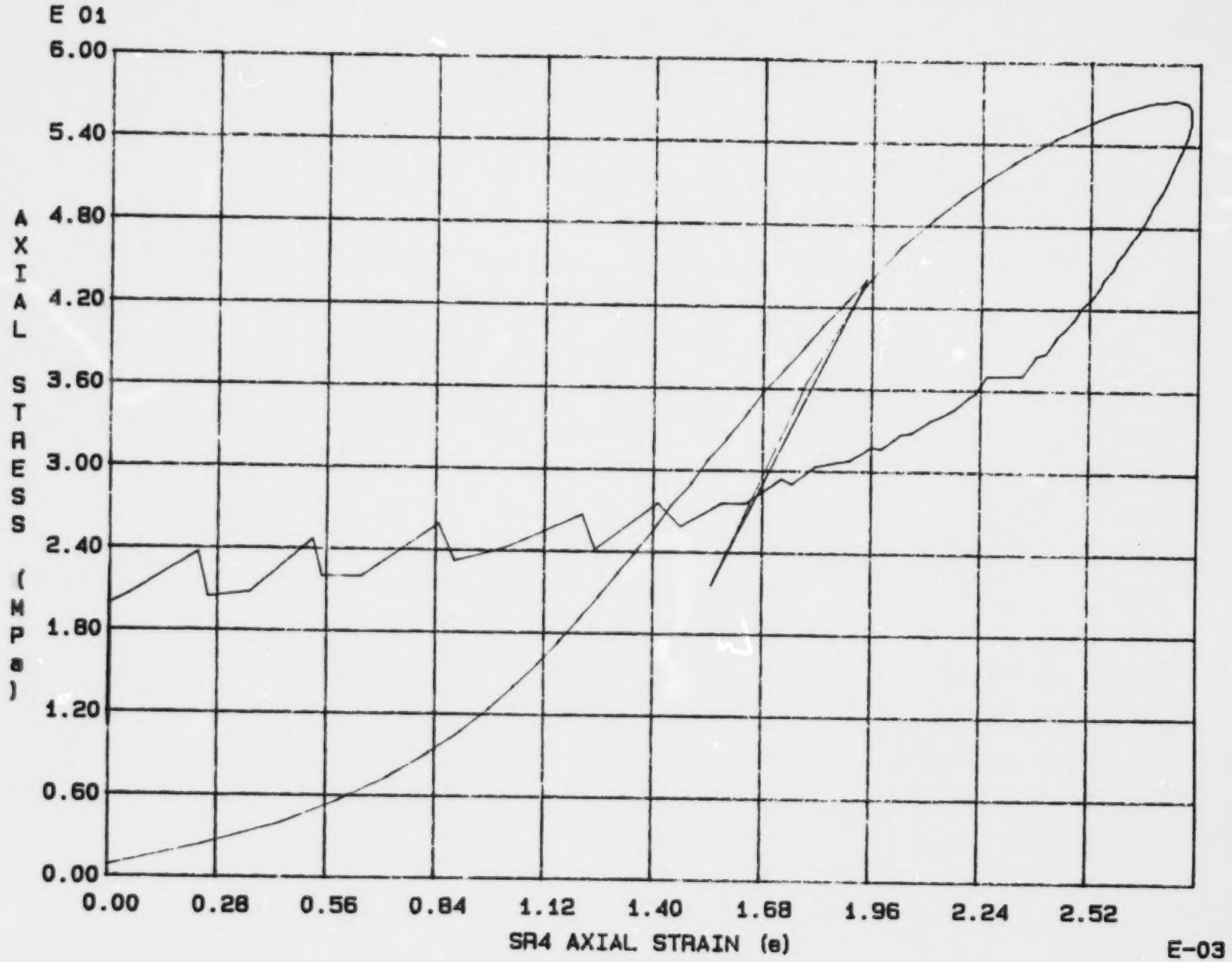

Fig. 2 - 20 Specimen M22U

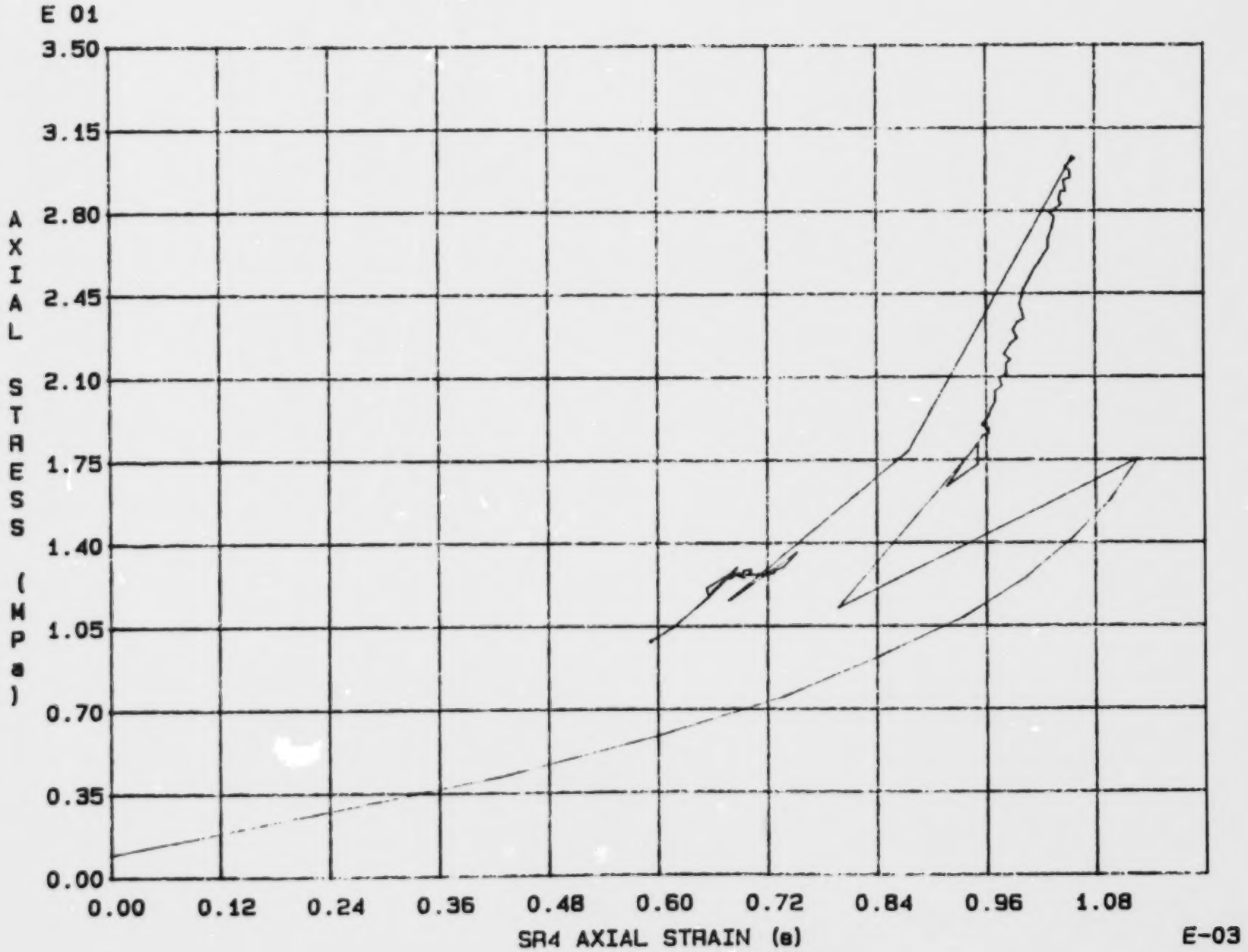

Fig. 2 - 21 Specimen M23U

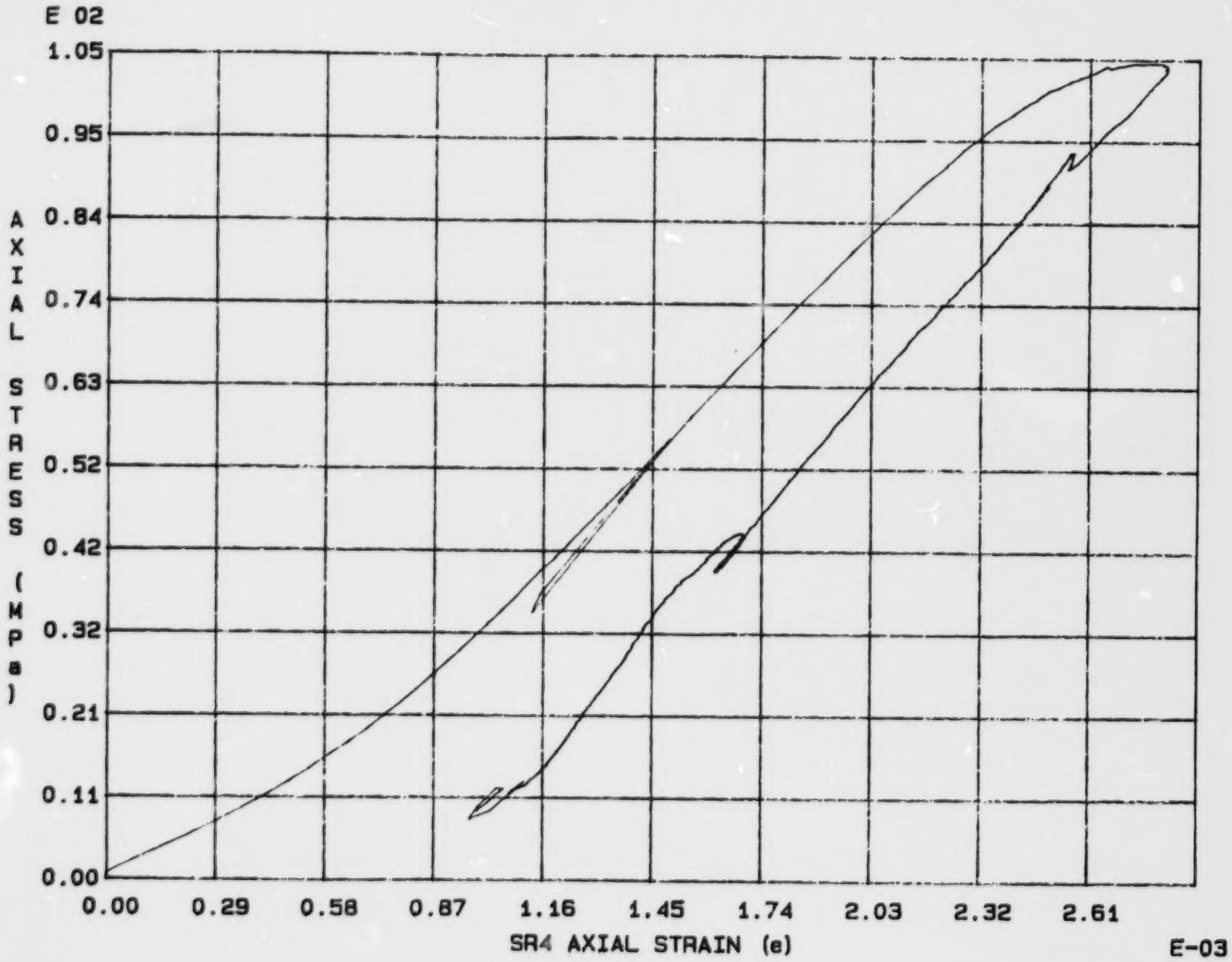

Fig. 2 - 22 Specimen M24U

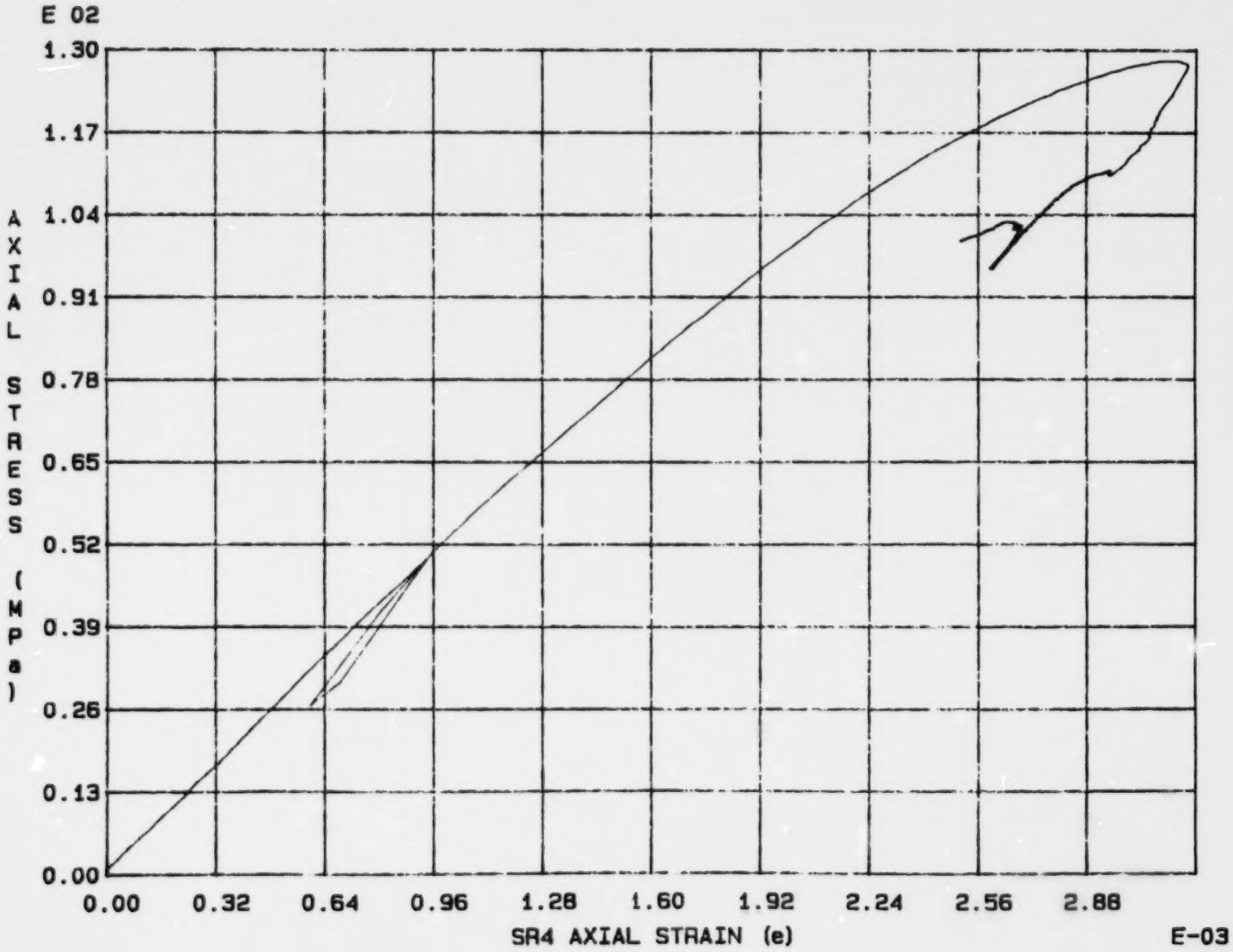

Fig. 2 - 23 Specimen M25U

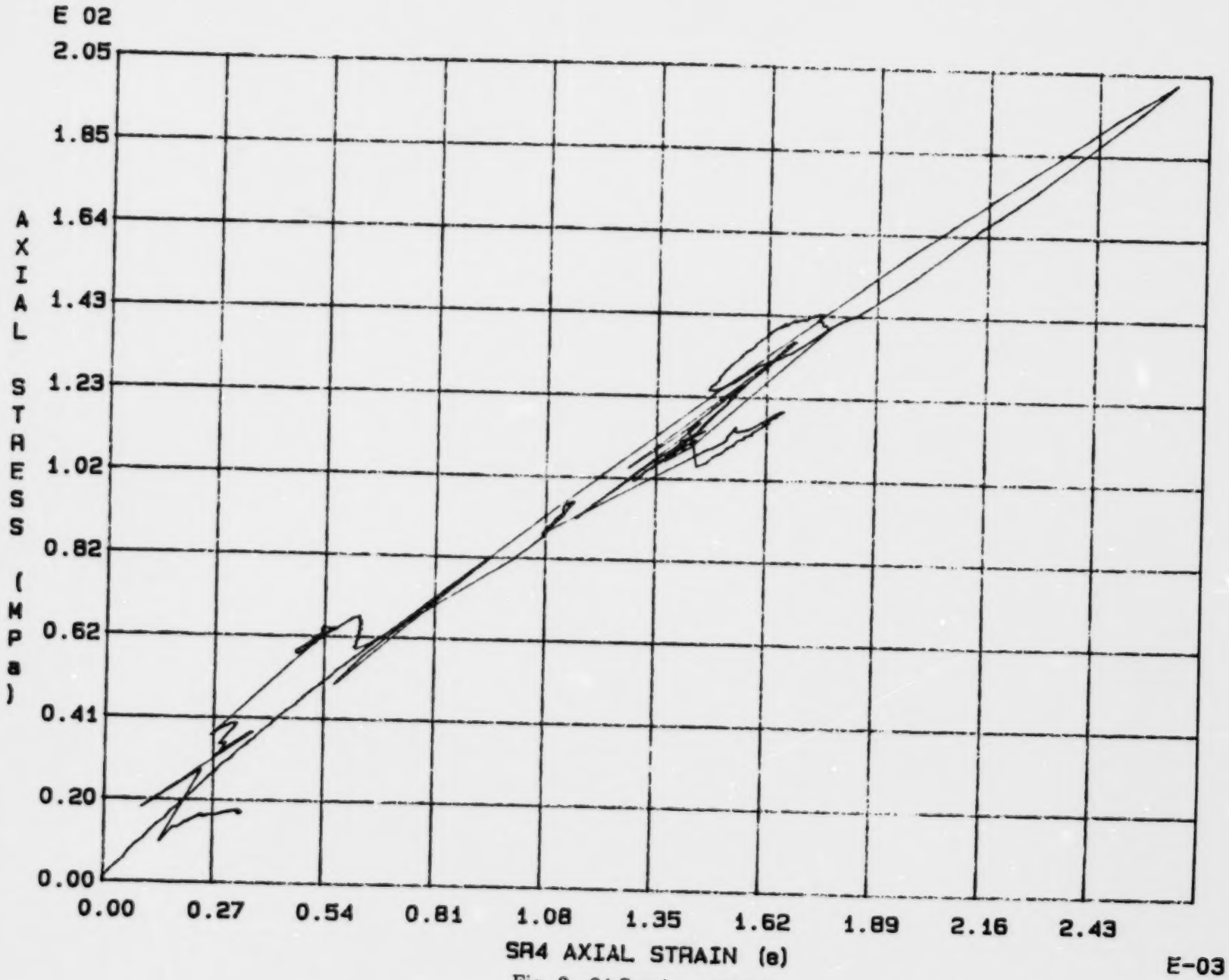

Fig. 2 - 24 Specimen M26U

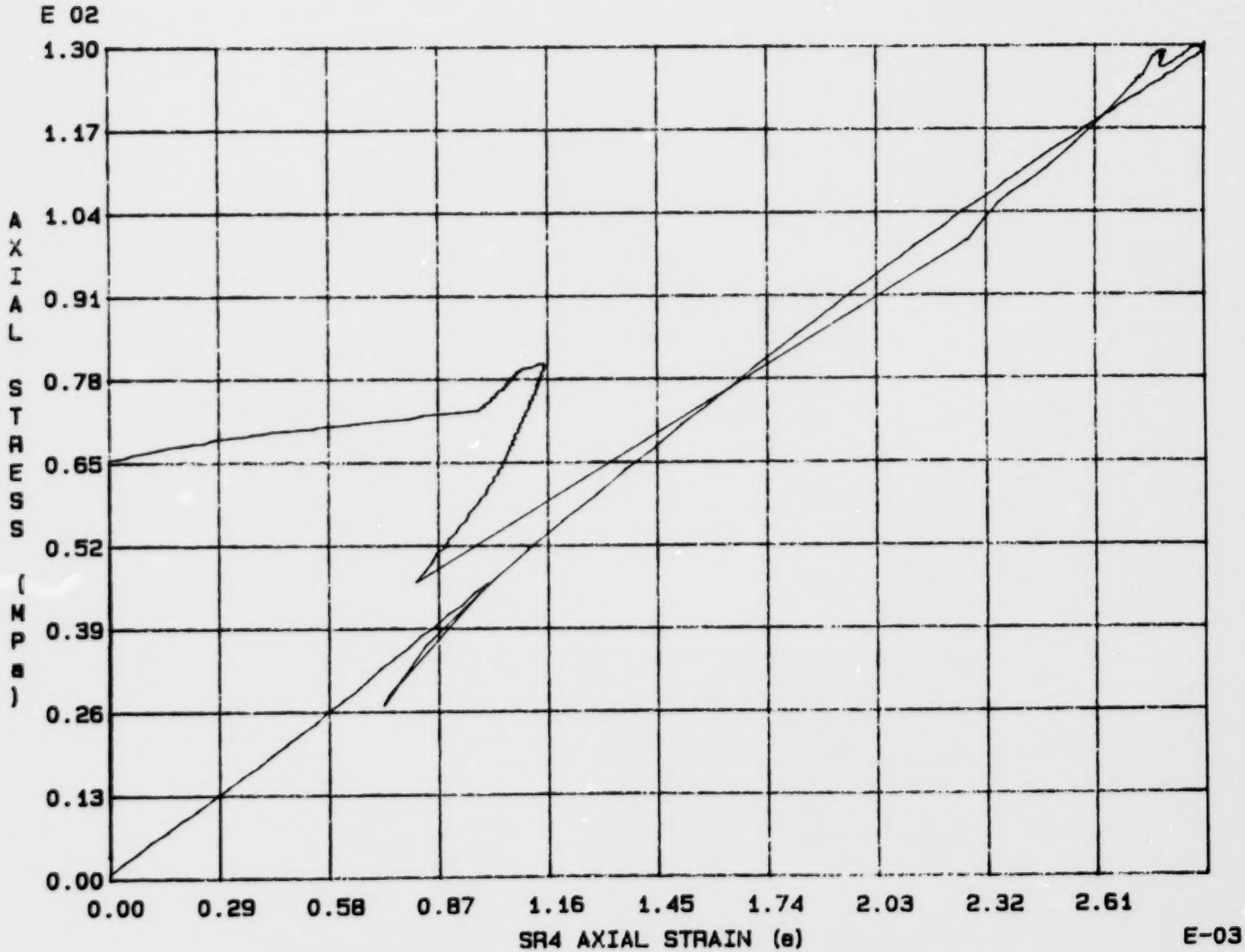

Fig. 2 - 25 Specimen M27U

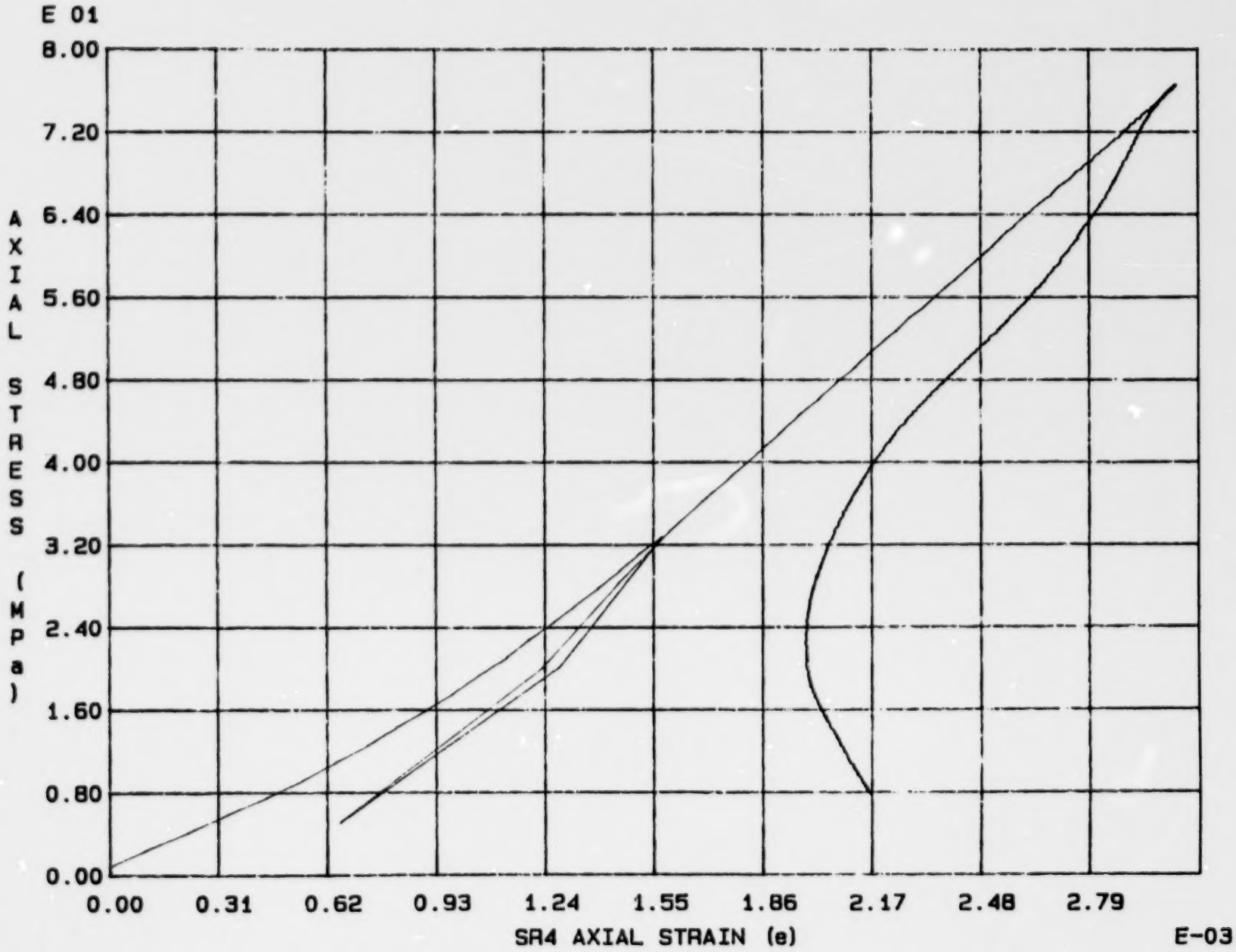

Fig. 2 - 26 Specimen M28U

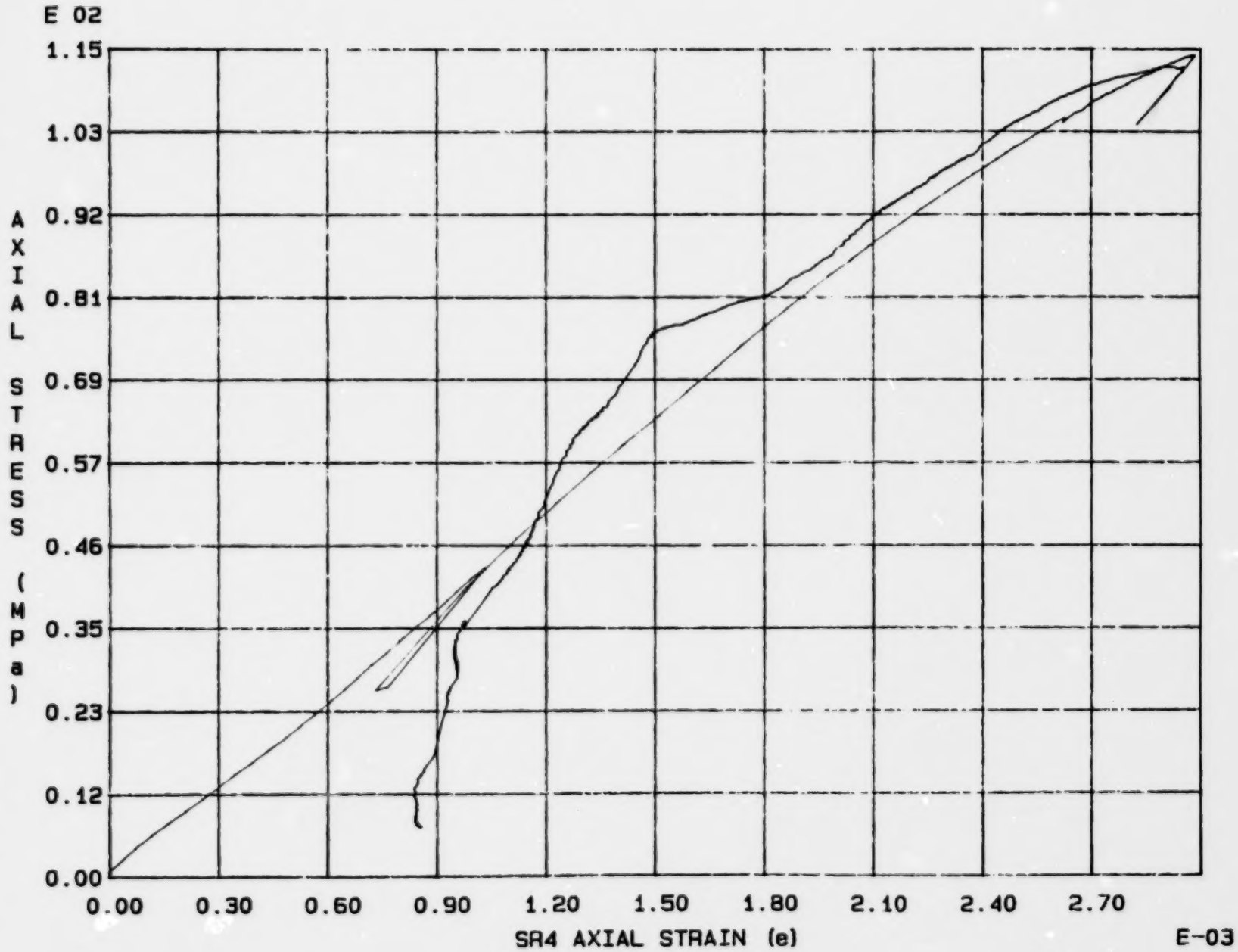

Fig. 2 - 27 Specimen M29U

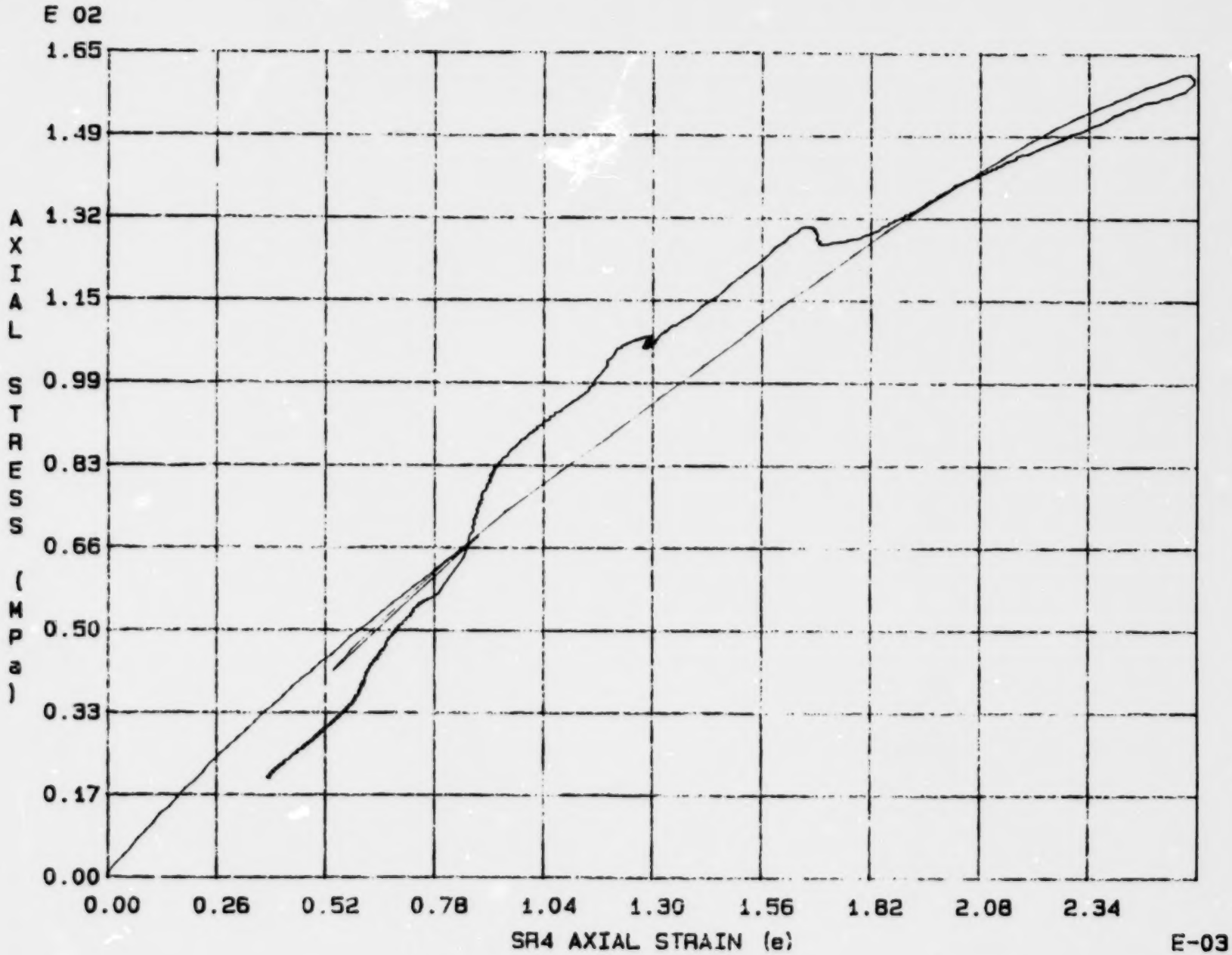

Fig. 2 - 28 Specimen M30U

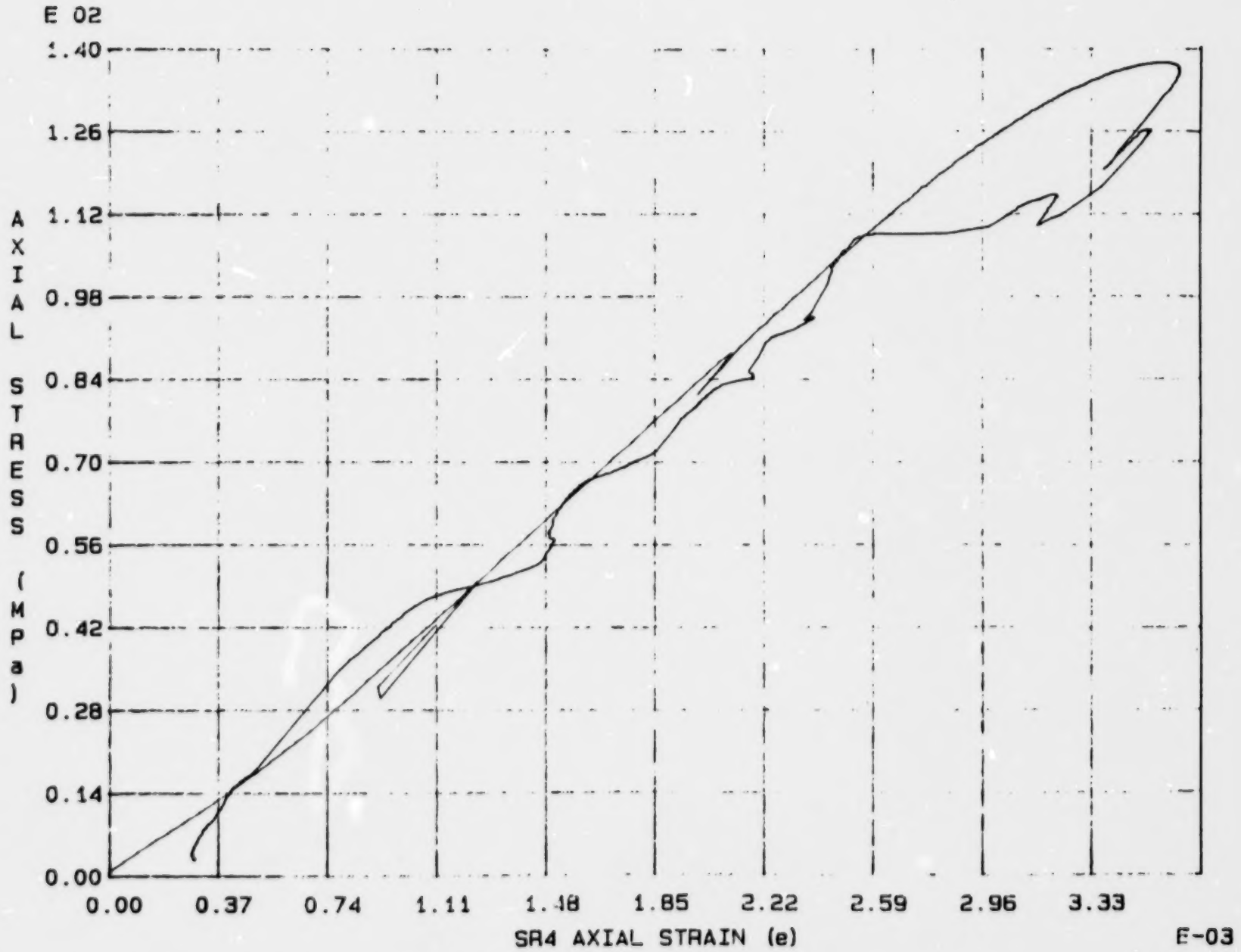

Fig. 2 - 29 Specimen M31U

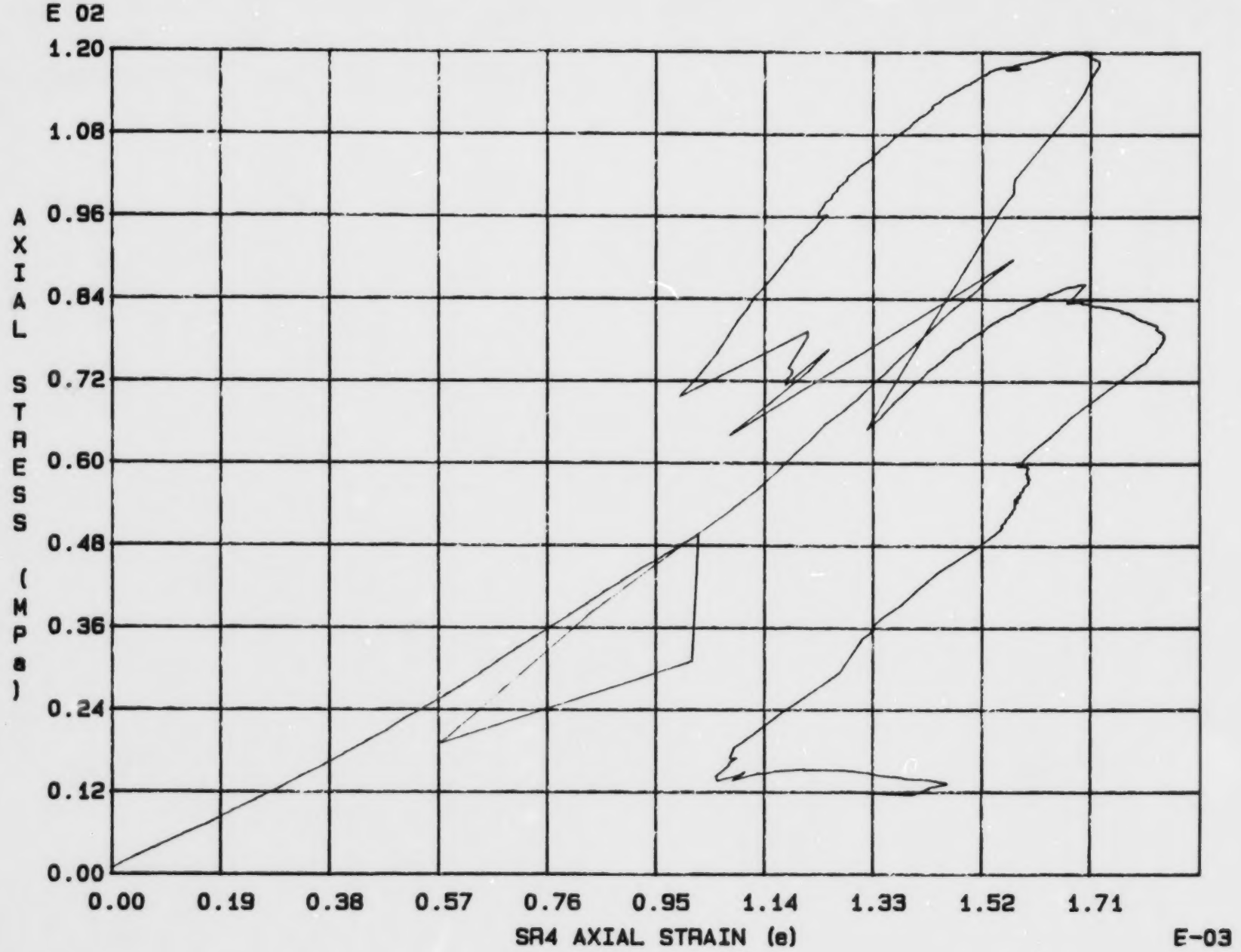

Fig. 2 - 30 Specimen M32U

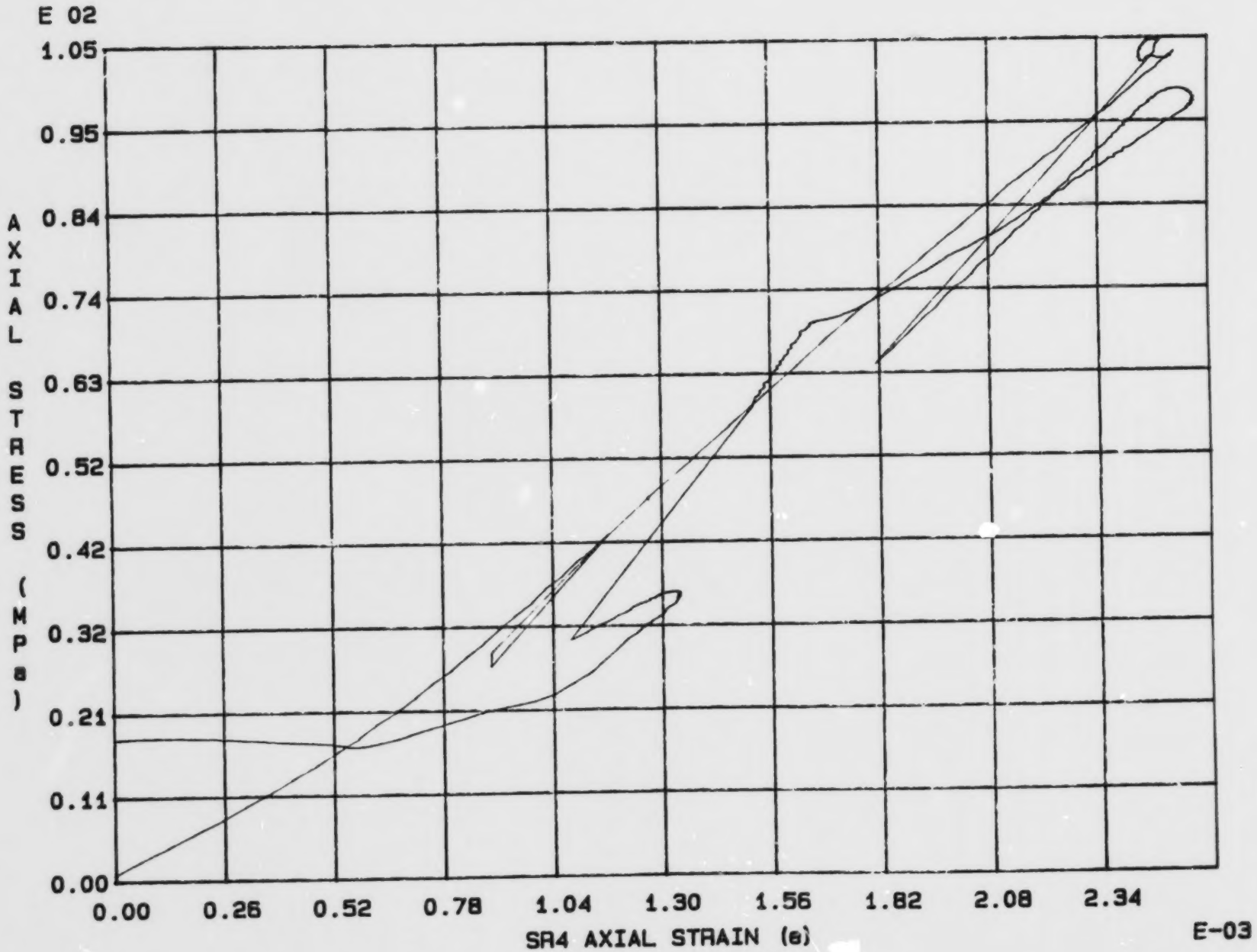

Fig. 2 - 31 Specimen M33U

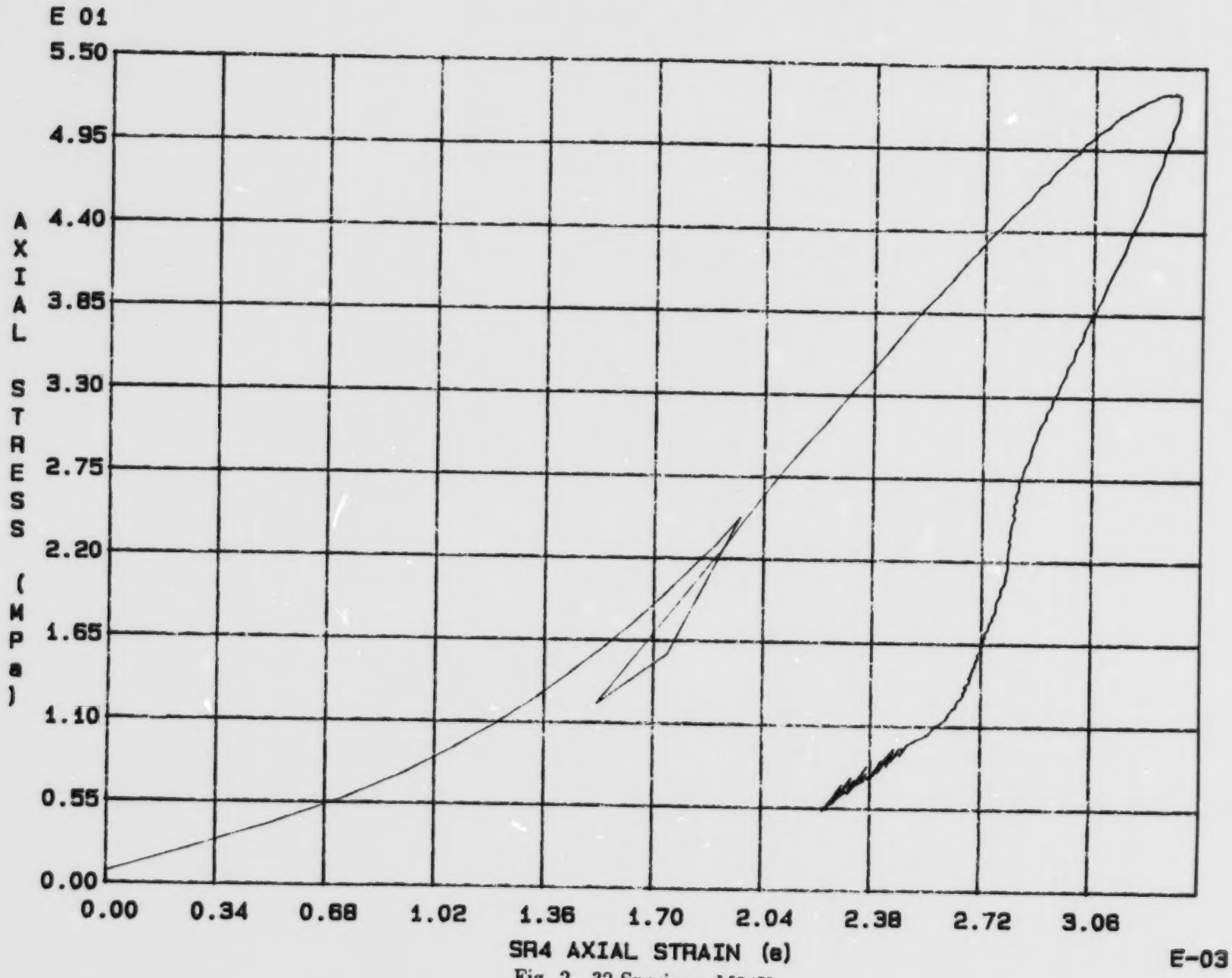

Fig. 2 - 32 Specimen M34U

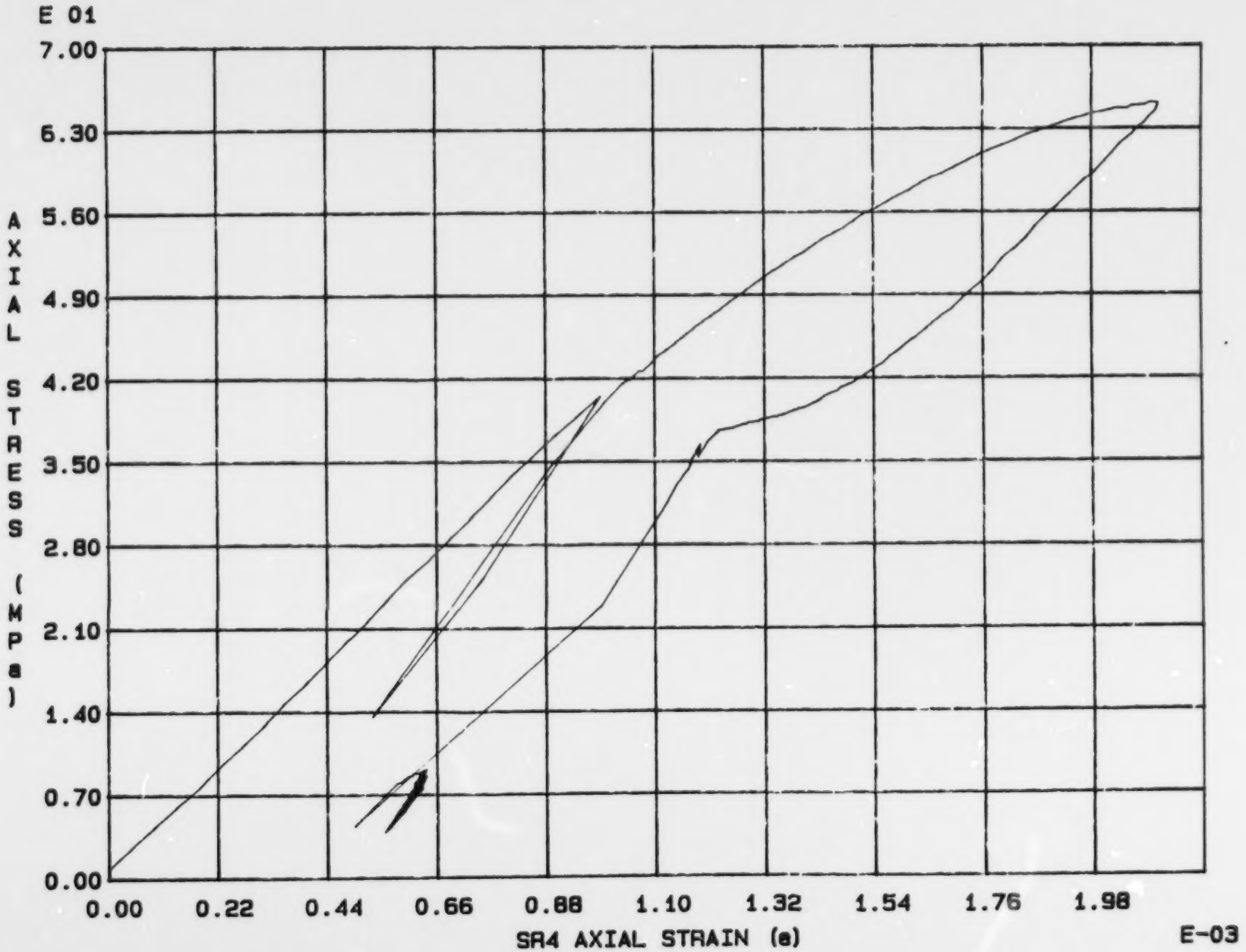

Fig. 2 - 33 Specimen M35U

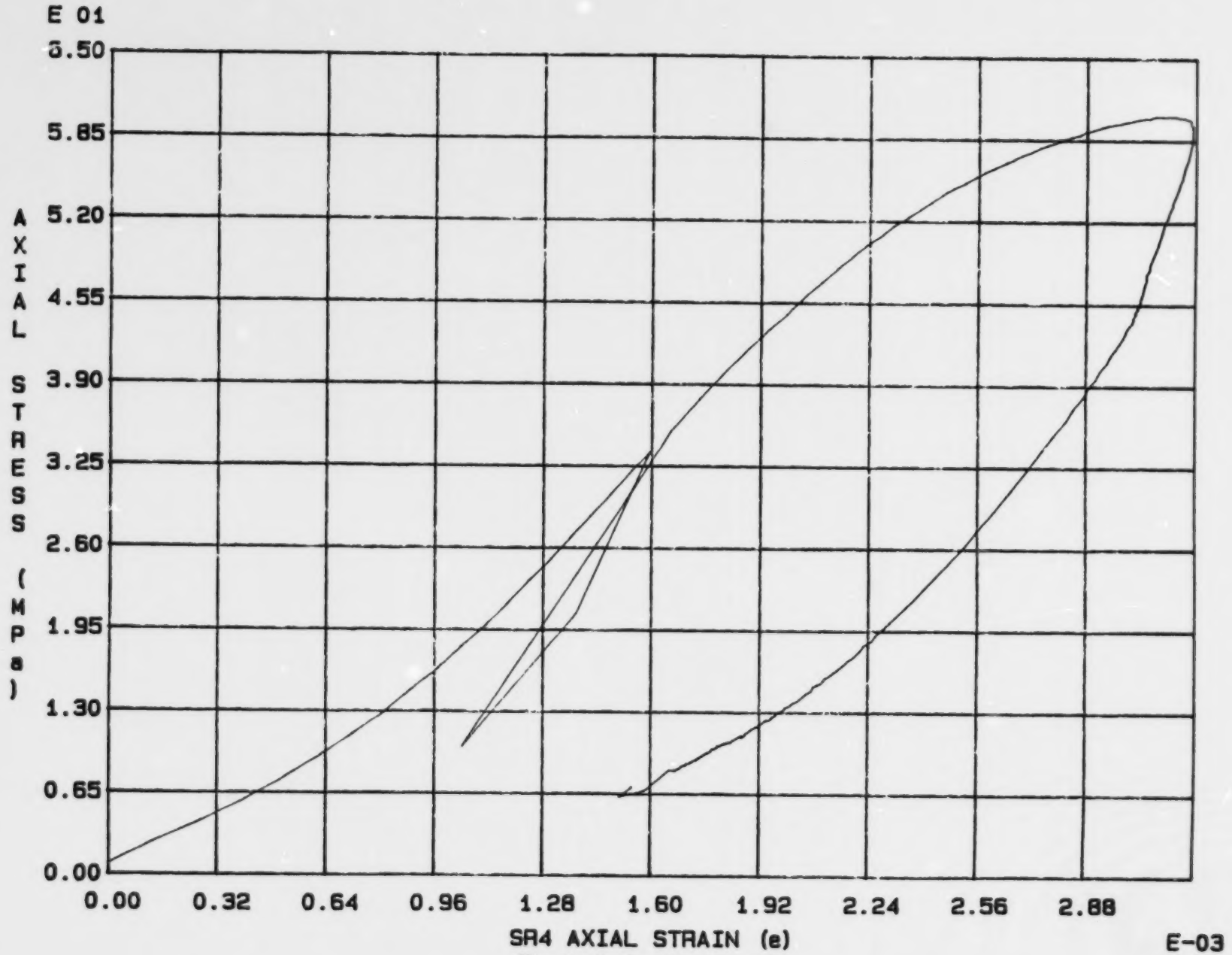

Fig. 2 - 34 Specimen M36U

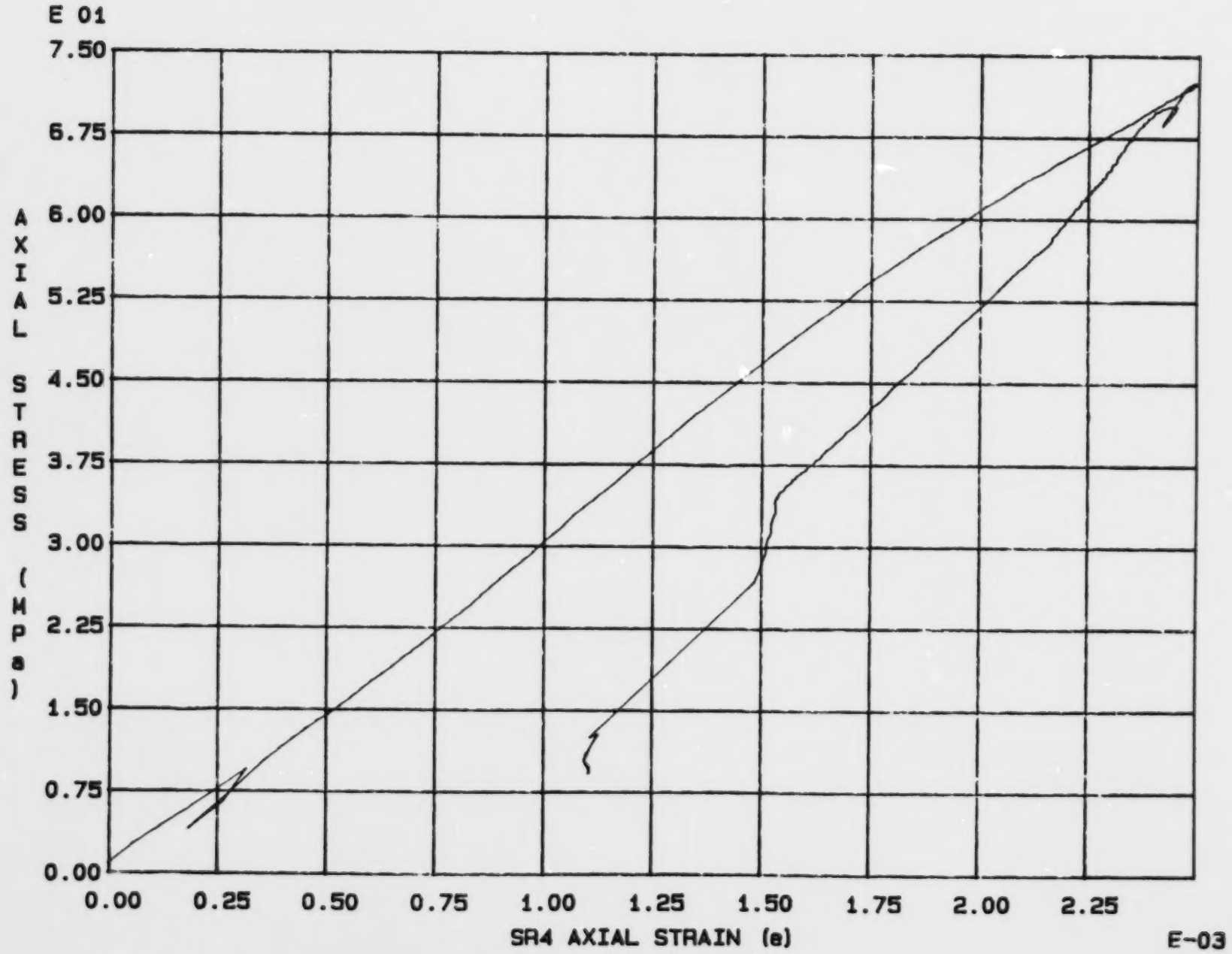

Fig. 2 - 35 Specimen M37U

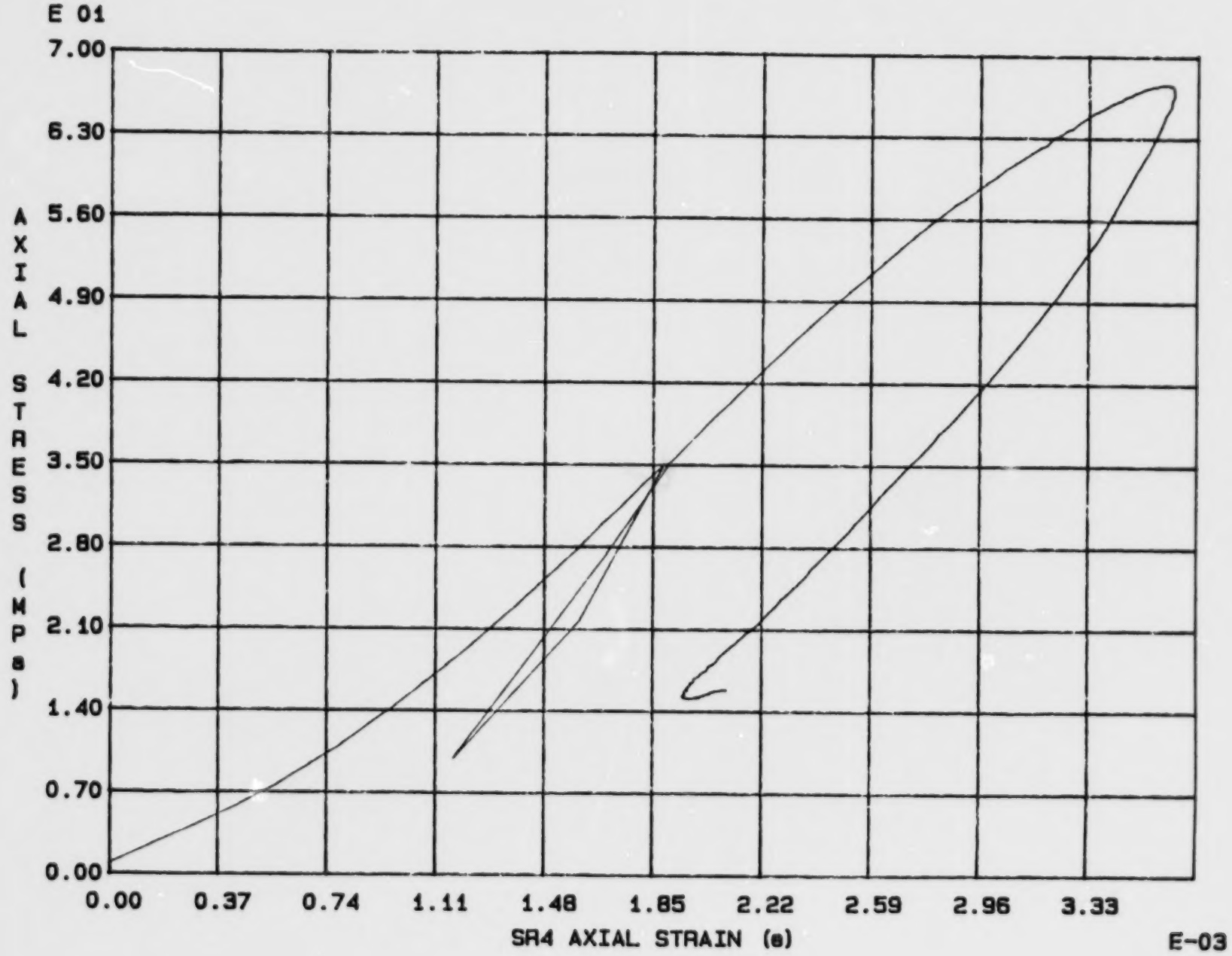

Fig. 2 - 36 Specimen M38U

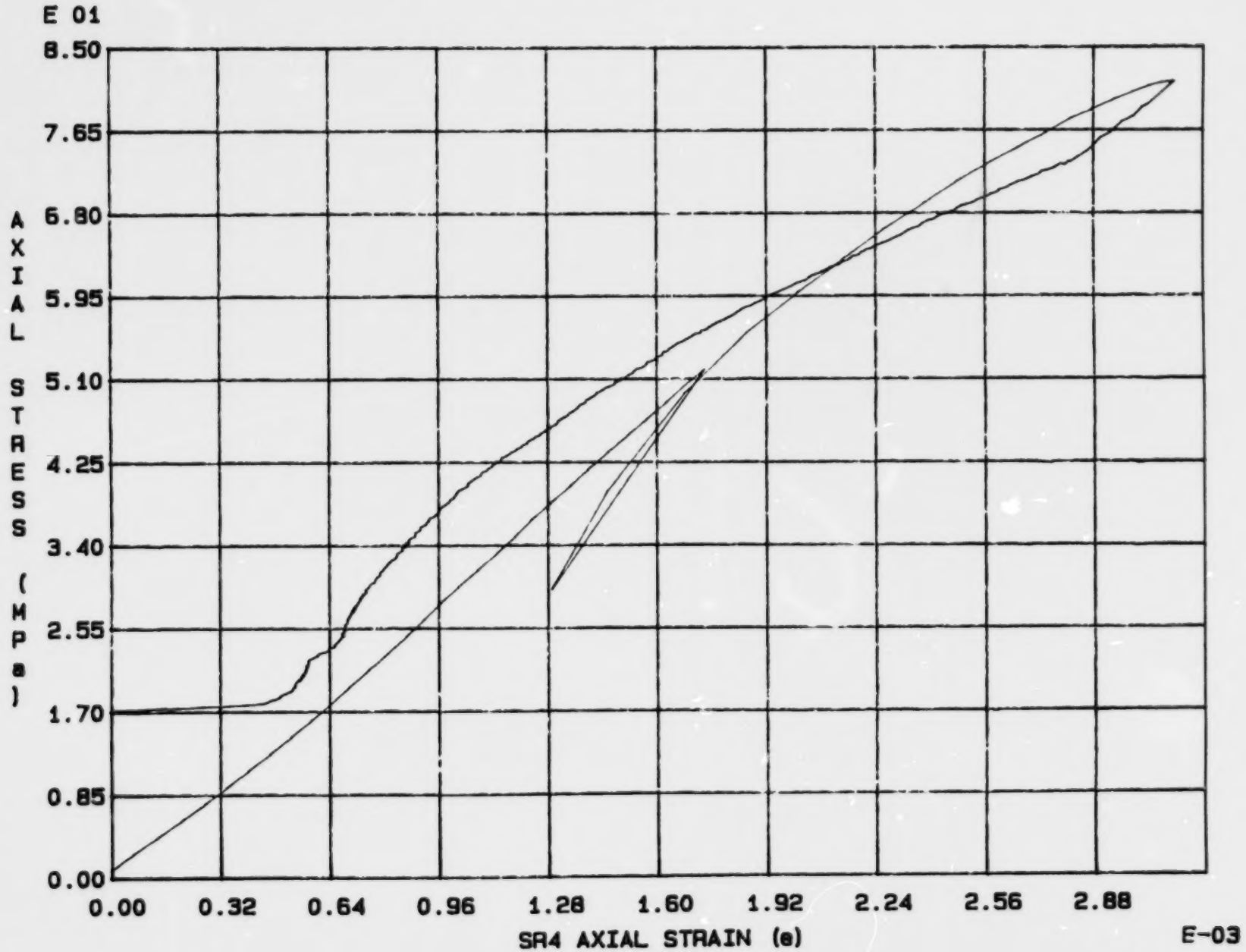

Fig. 2 - 37 Specimen M39U

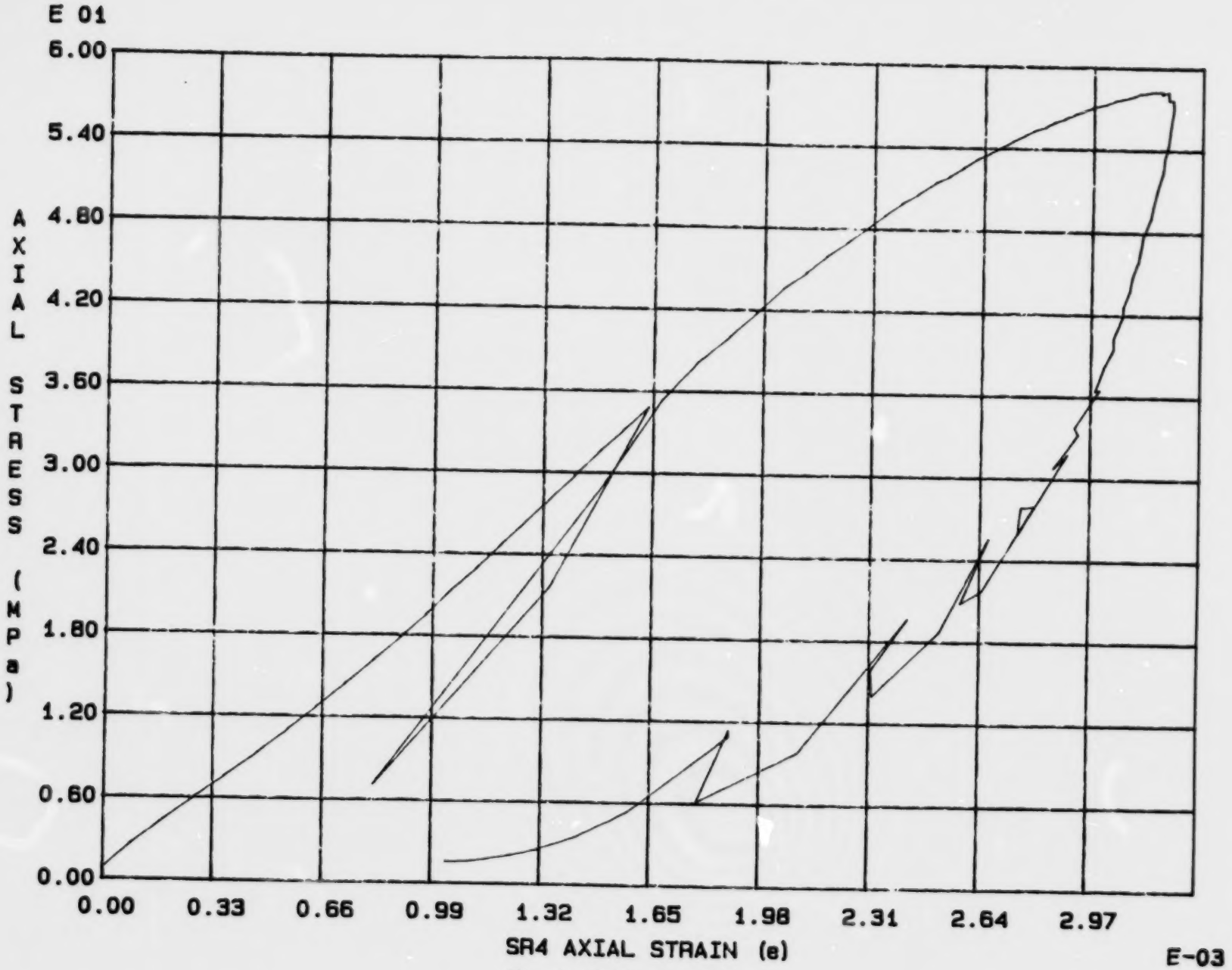

Fig. 2 - 38 Specimen M40U

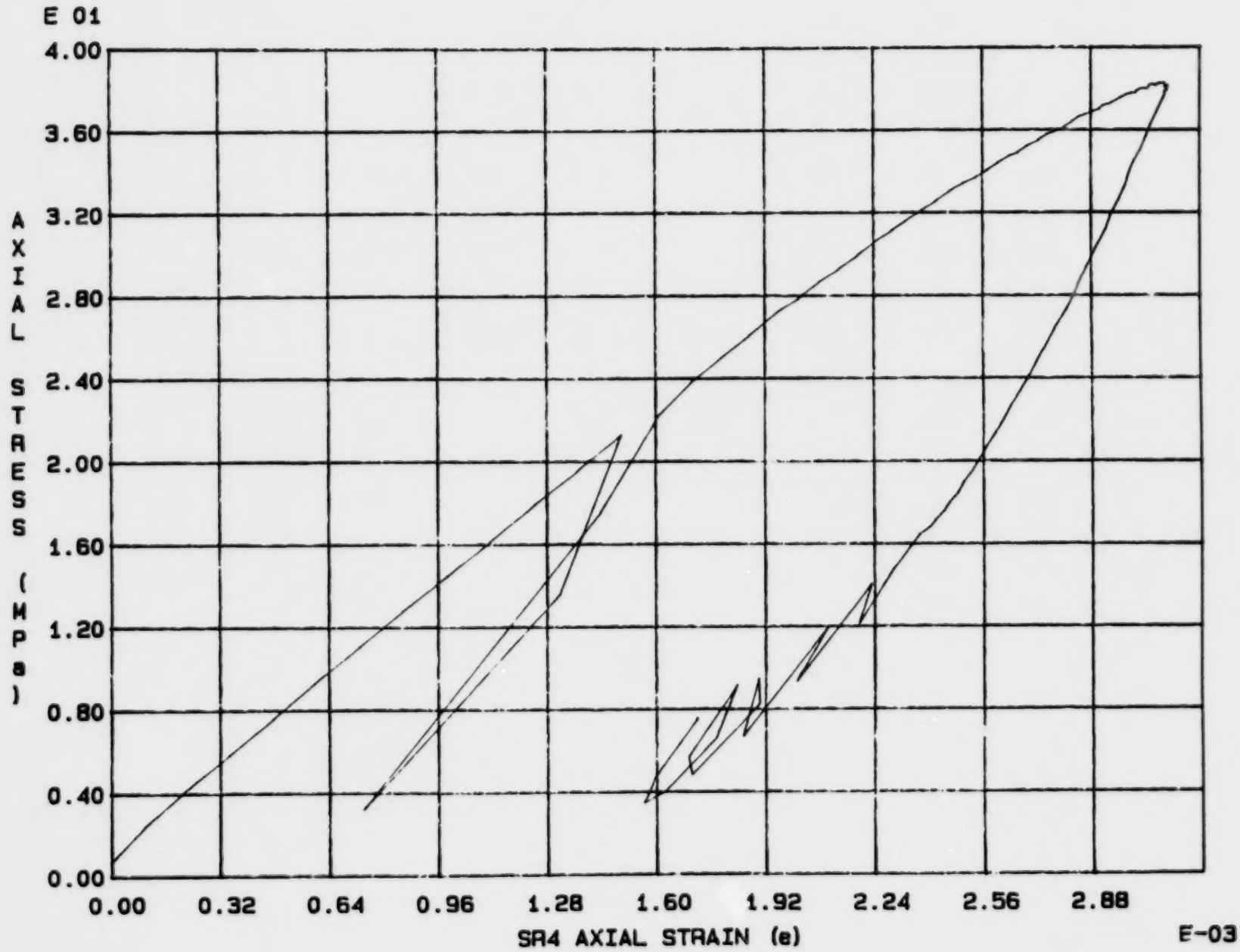

Fig. 2 - 39 Specimen M41U

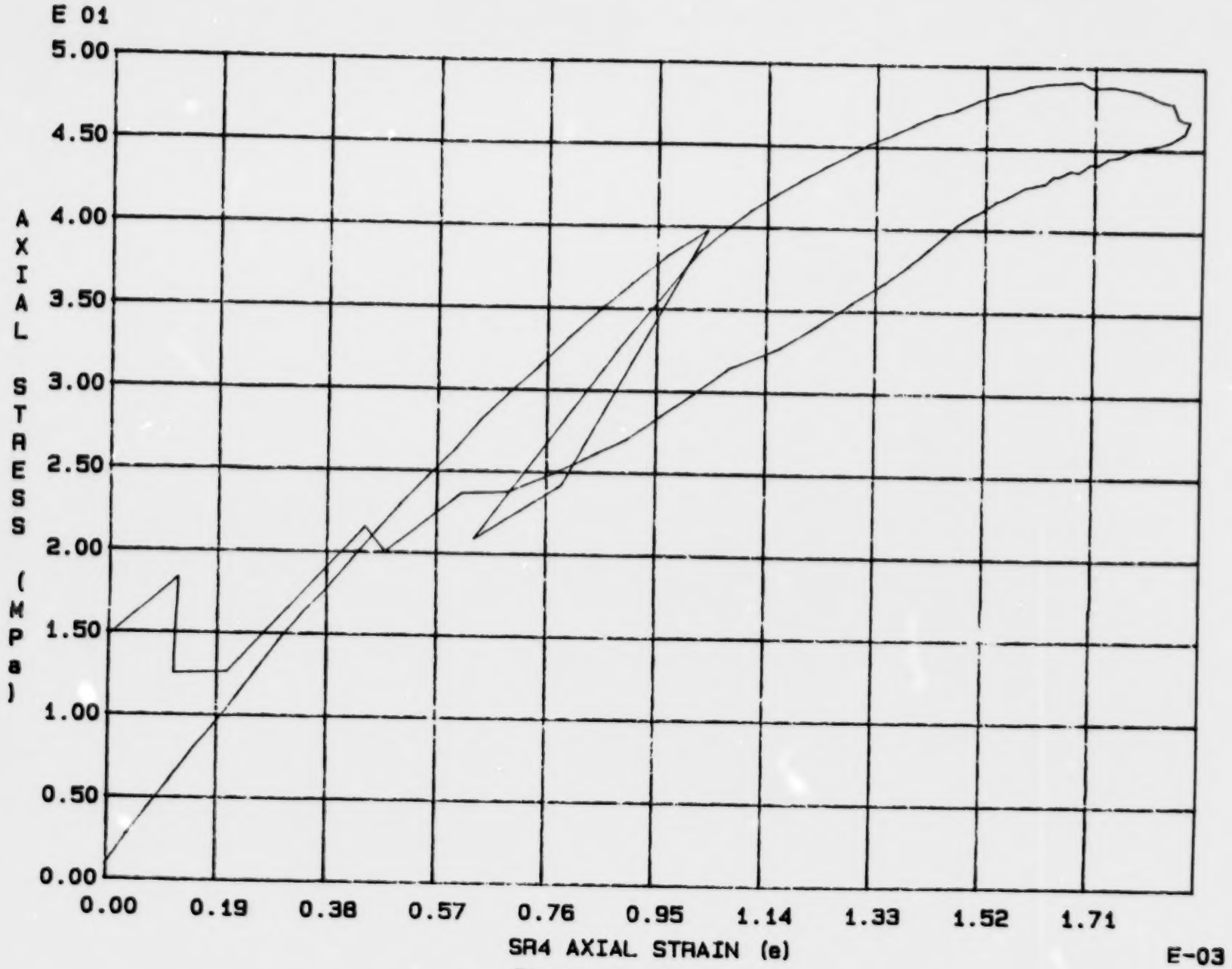

Fig. 2 - 40 Specimen M42U

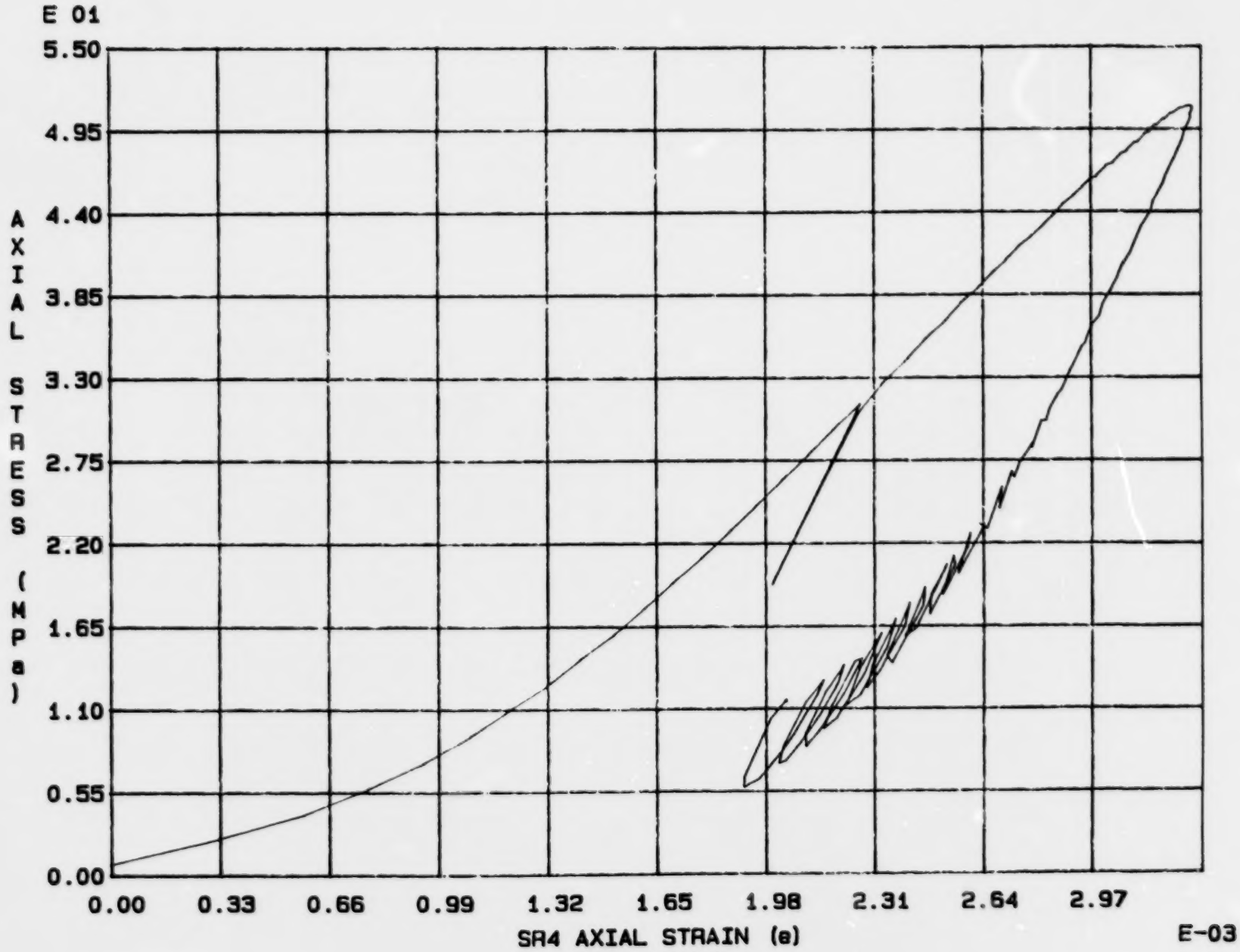

Fig. 2 - 41 Specimen M43U

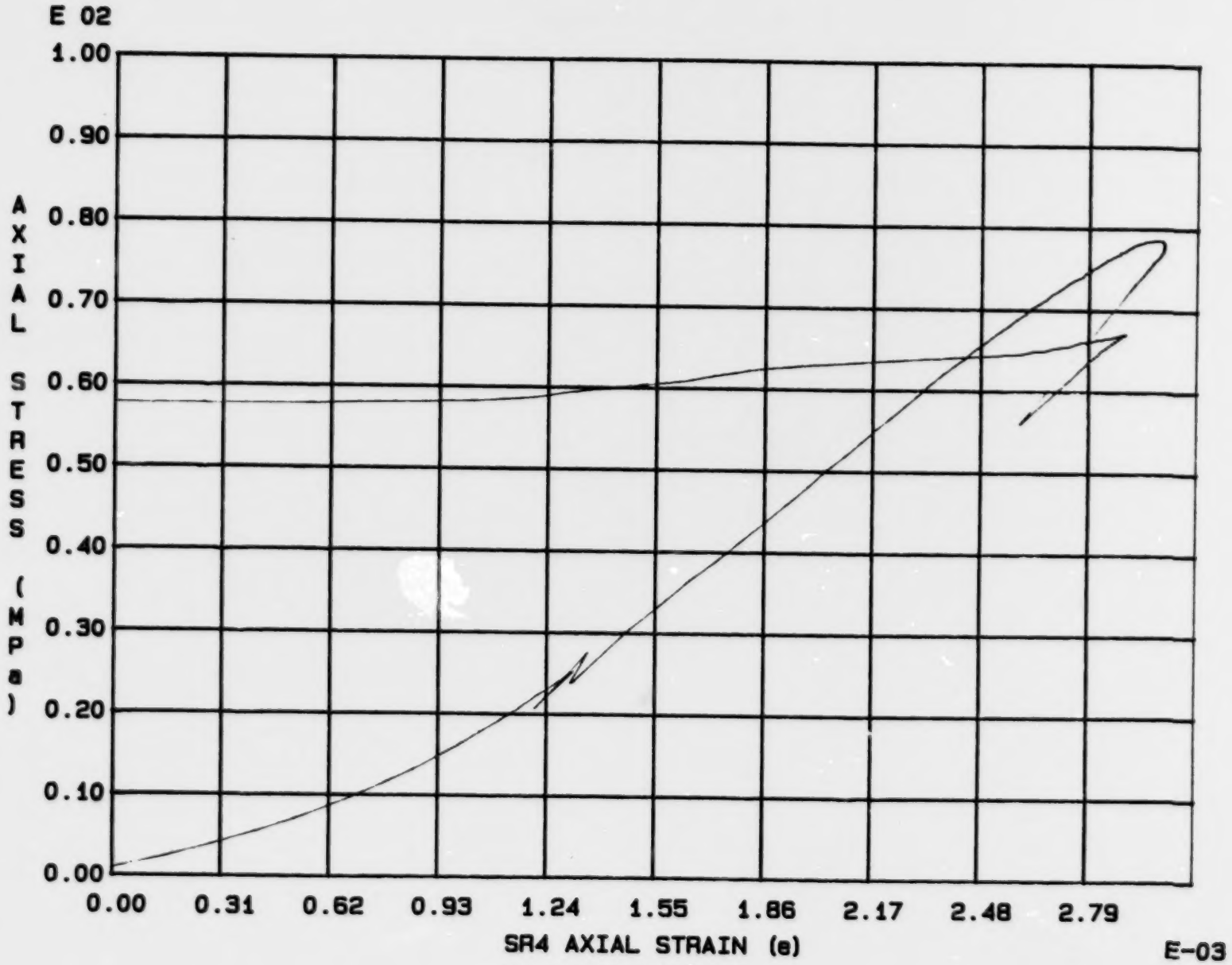

Fig. 2 - 42 Specimen M81U

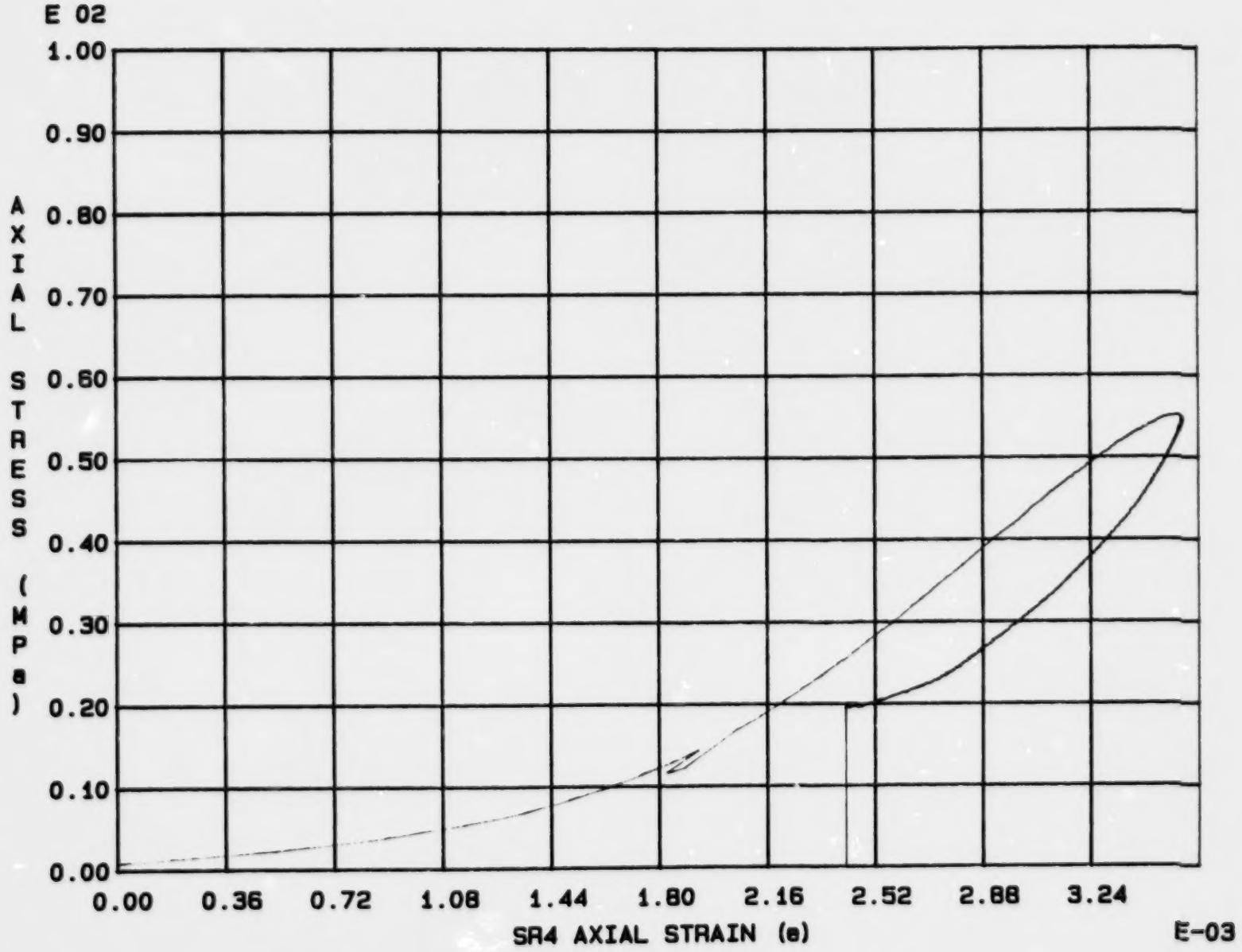

Fig. 2 - 43 Specimen M82U

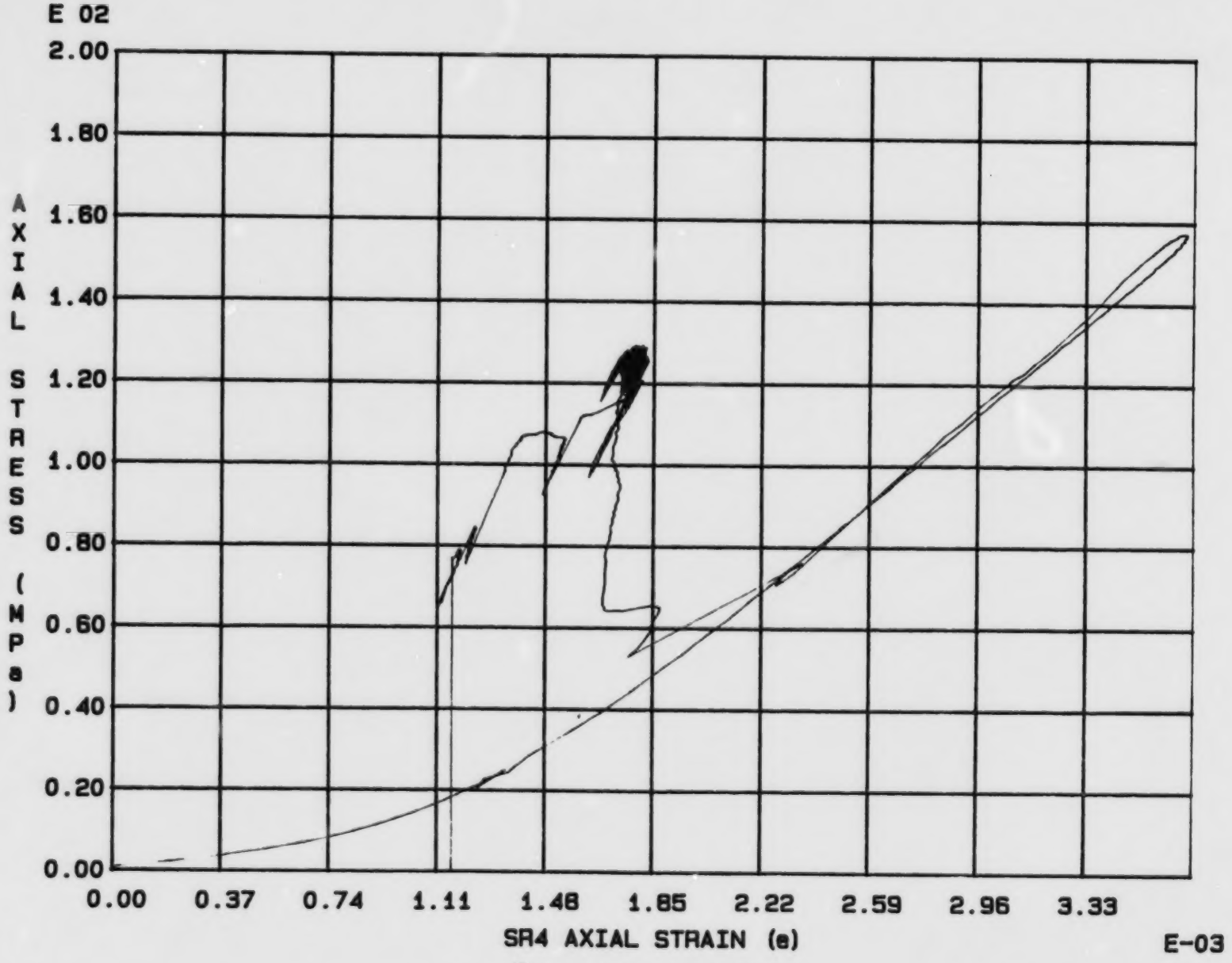

Fig. 2 - 44 Specimen M83U

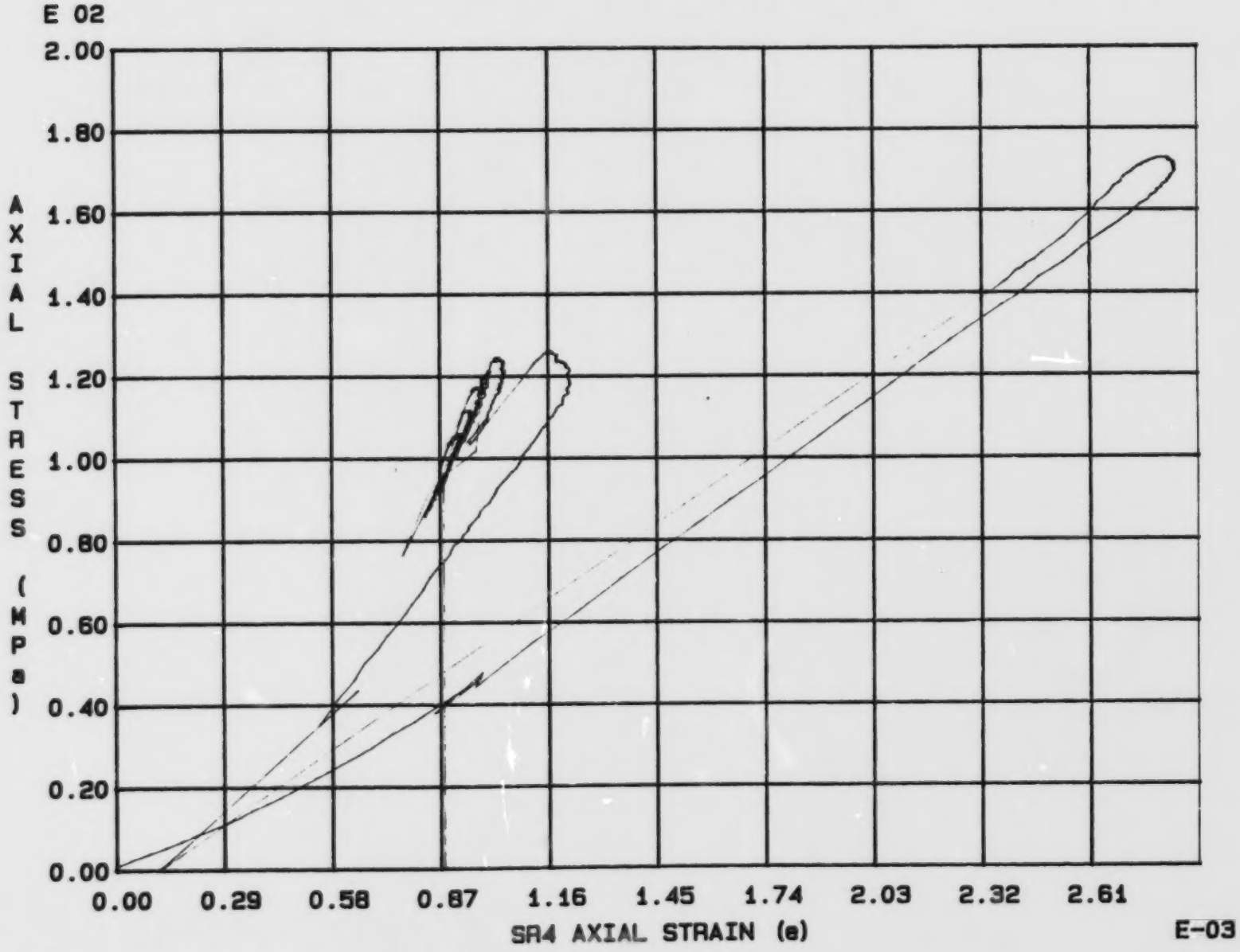

Fig. 2 - 45 Specimen M84U

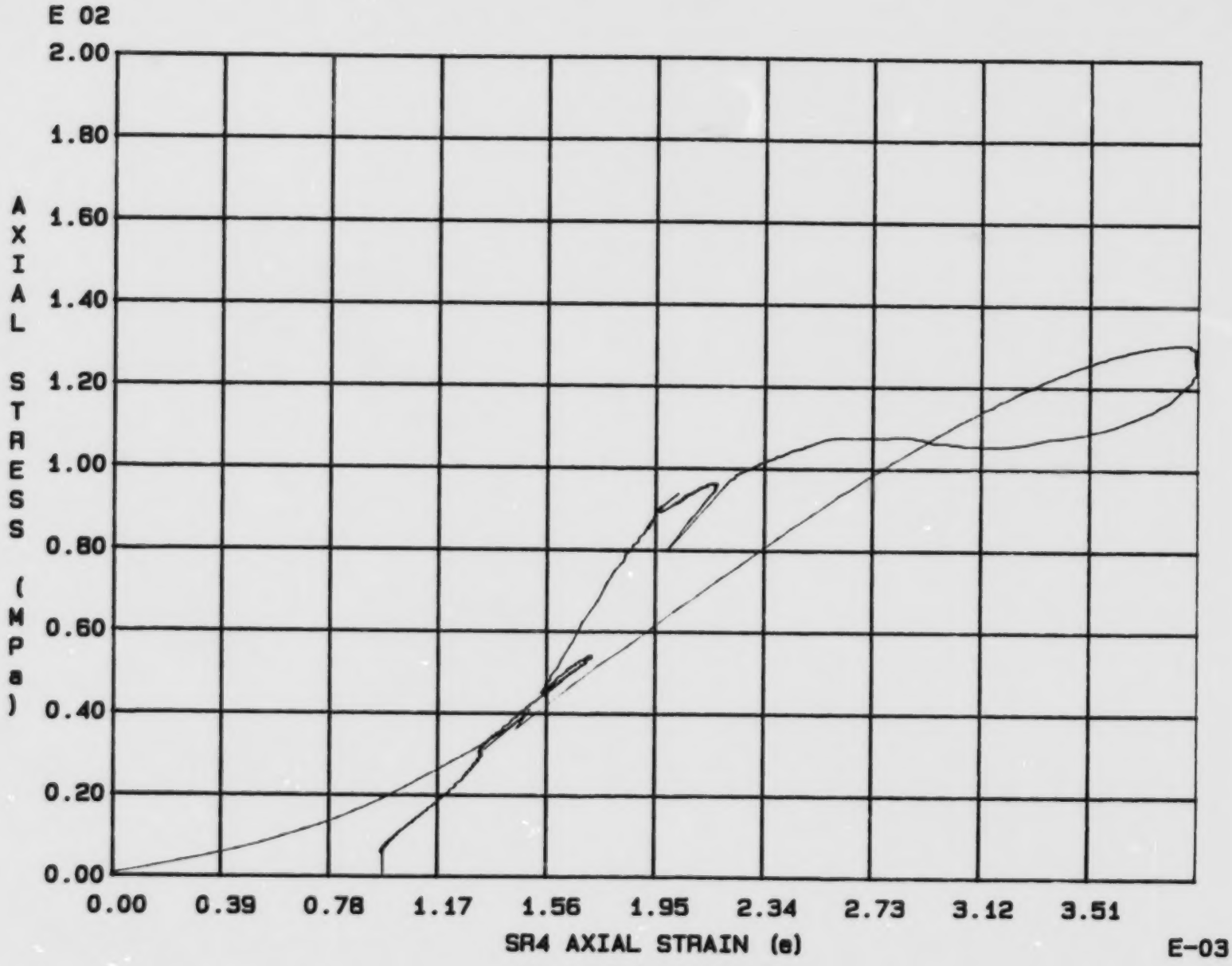

Fig. 2 - 46 Specimen M85U

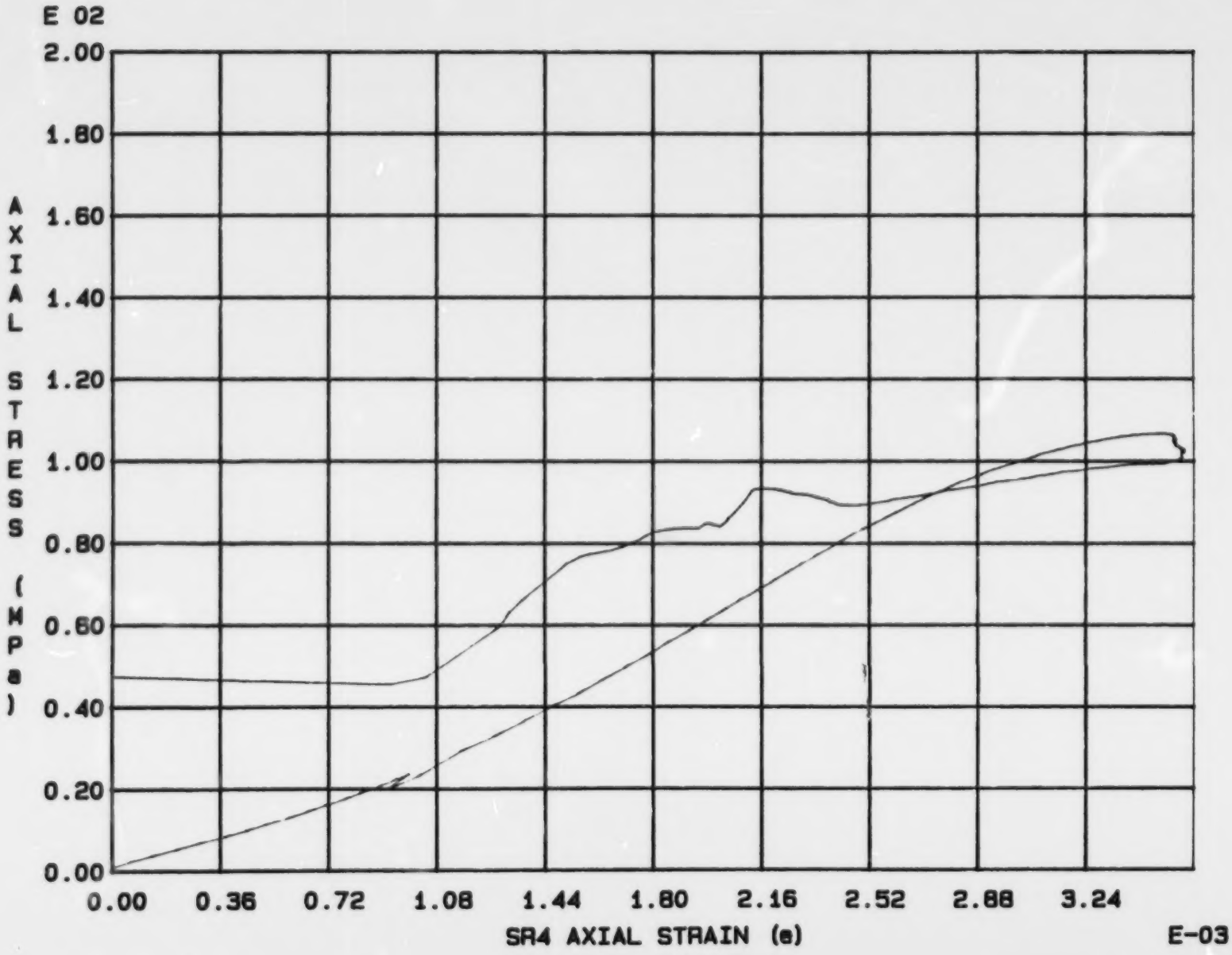

Fig. 2 - 47 Specimen M86U

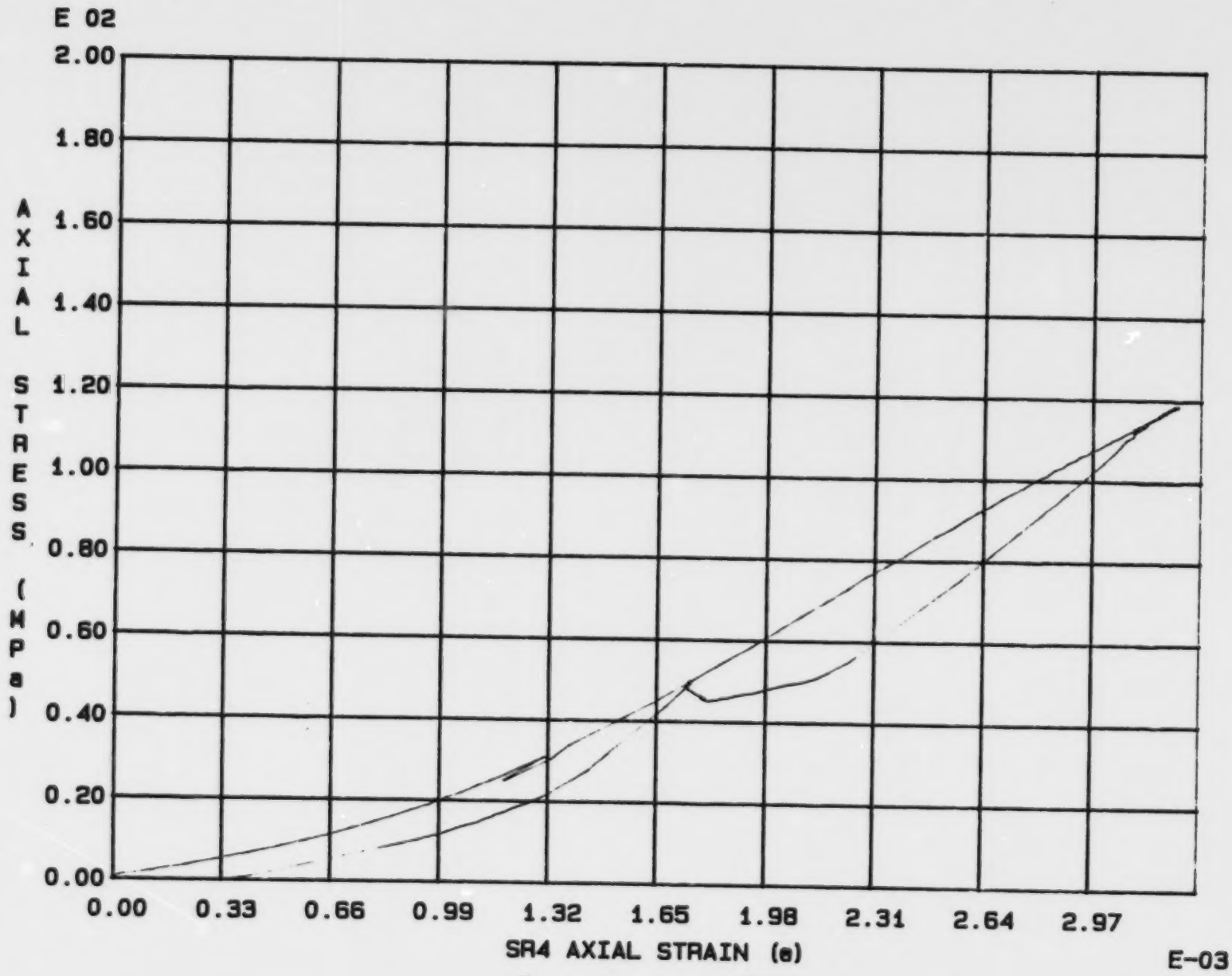

Fig. 2 - 48 Specimen M87U

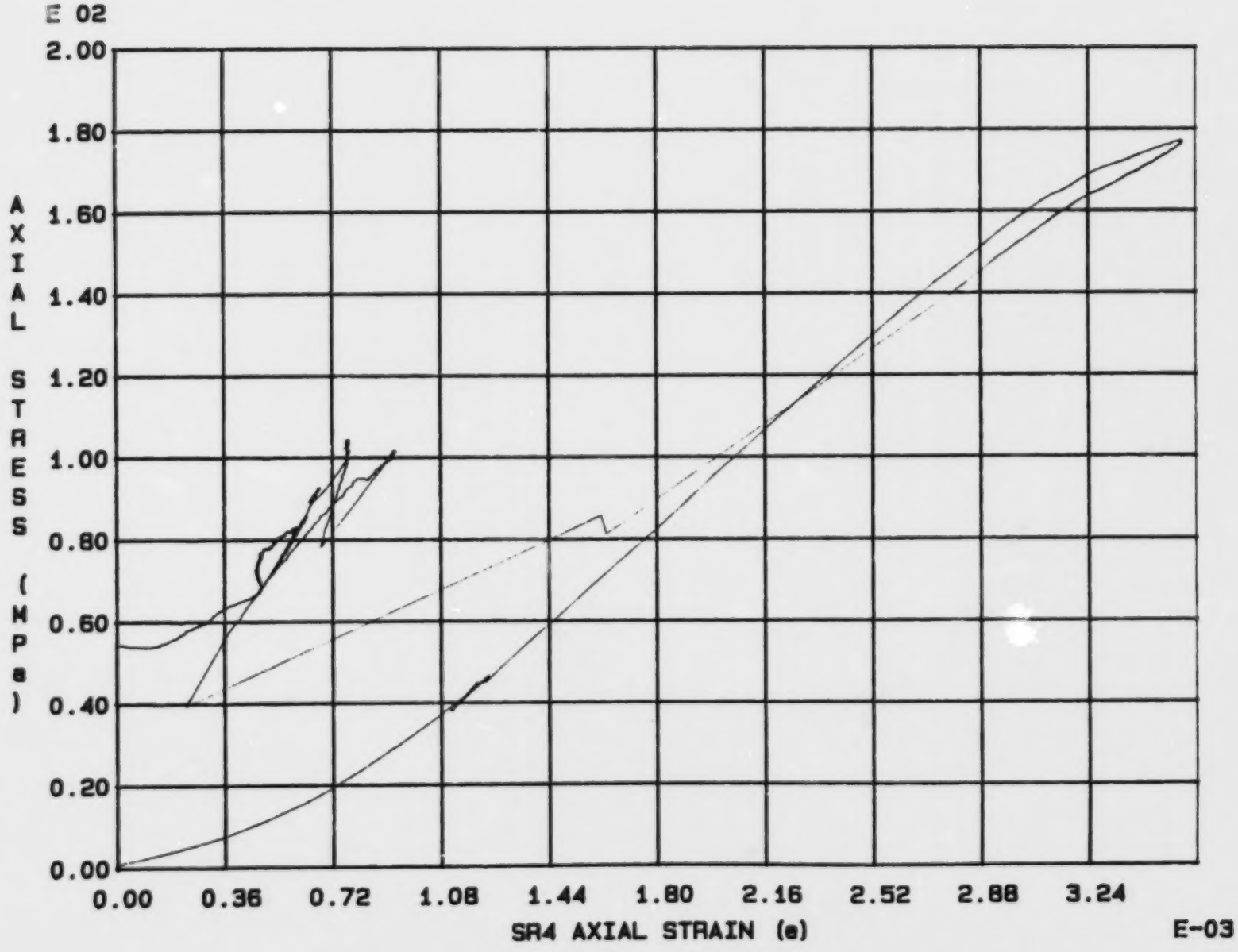

Fig. 2 - 49 Specimen M88U

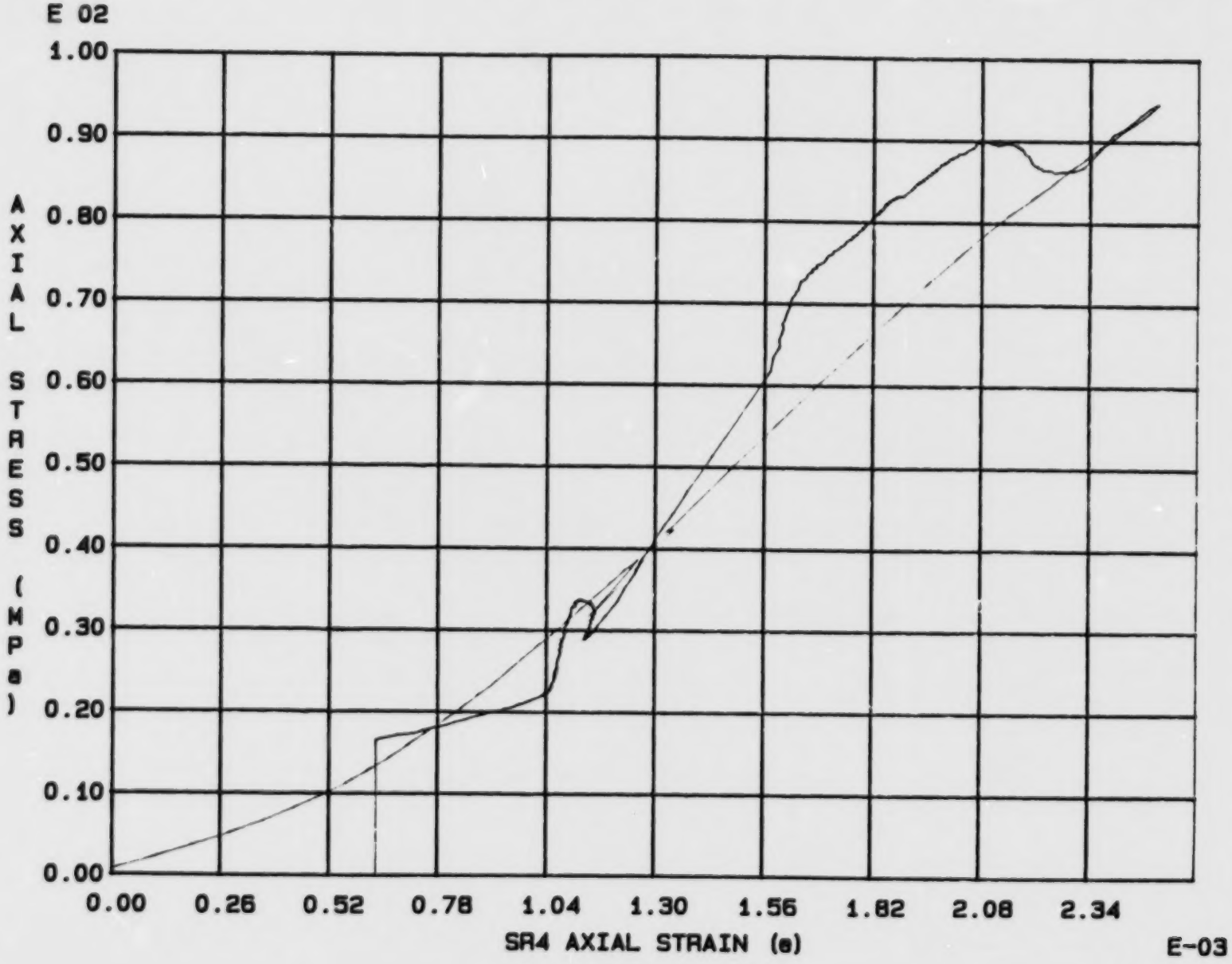

Fig. 2 - 50 Specimen M89U

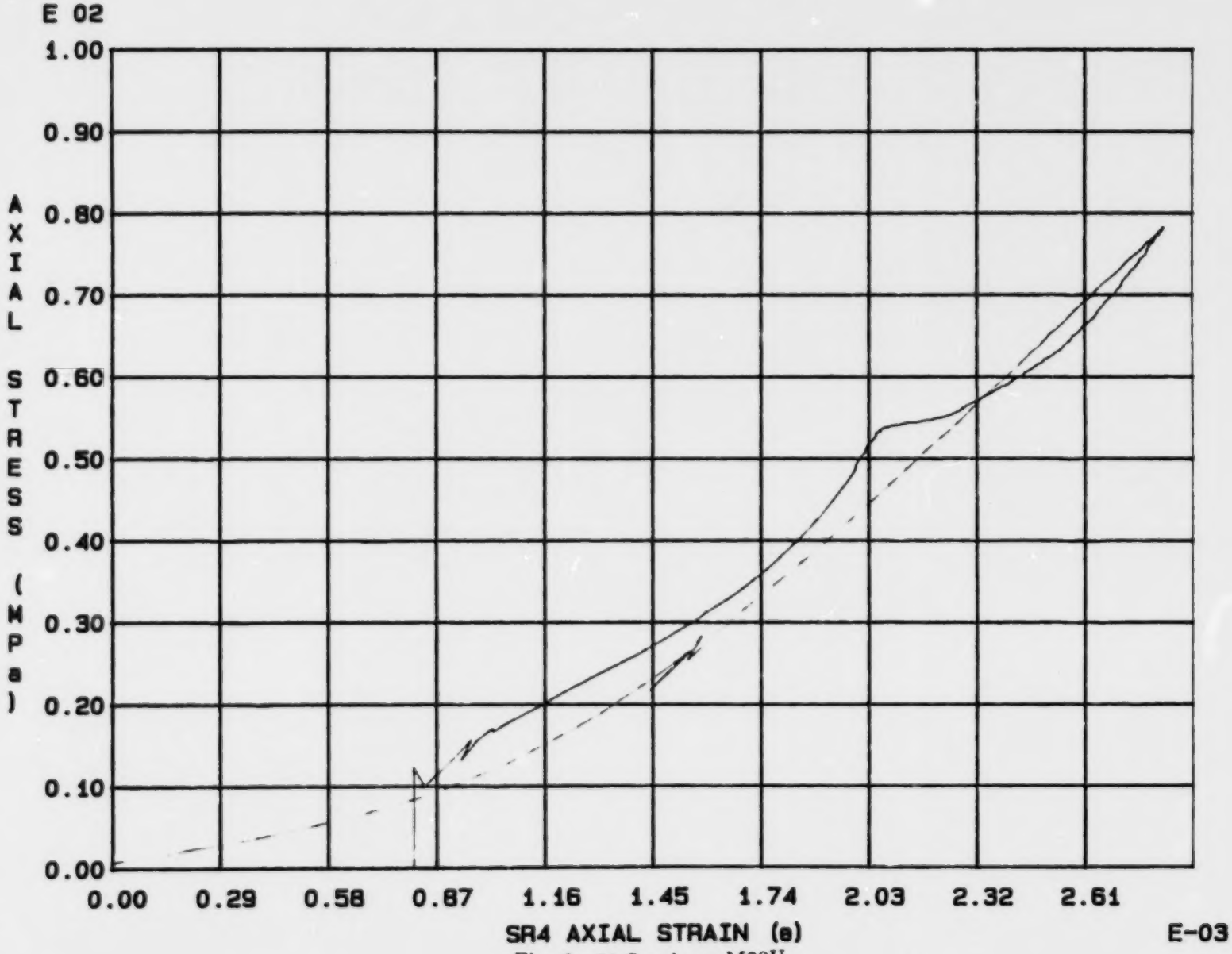

Fig. 2 - 51 Specimen M90U

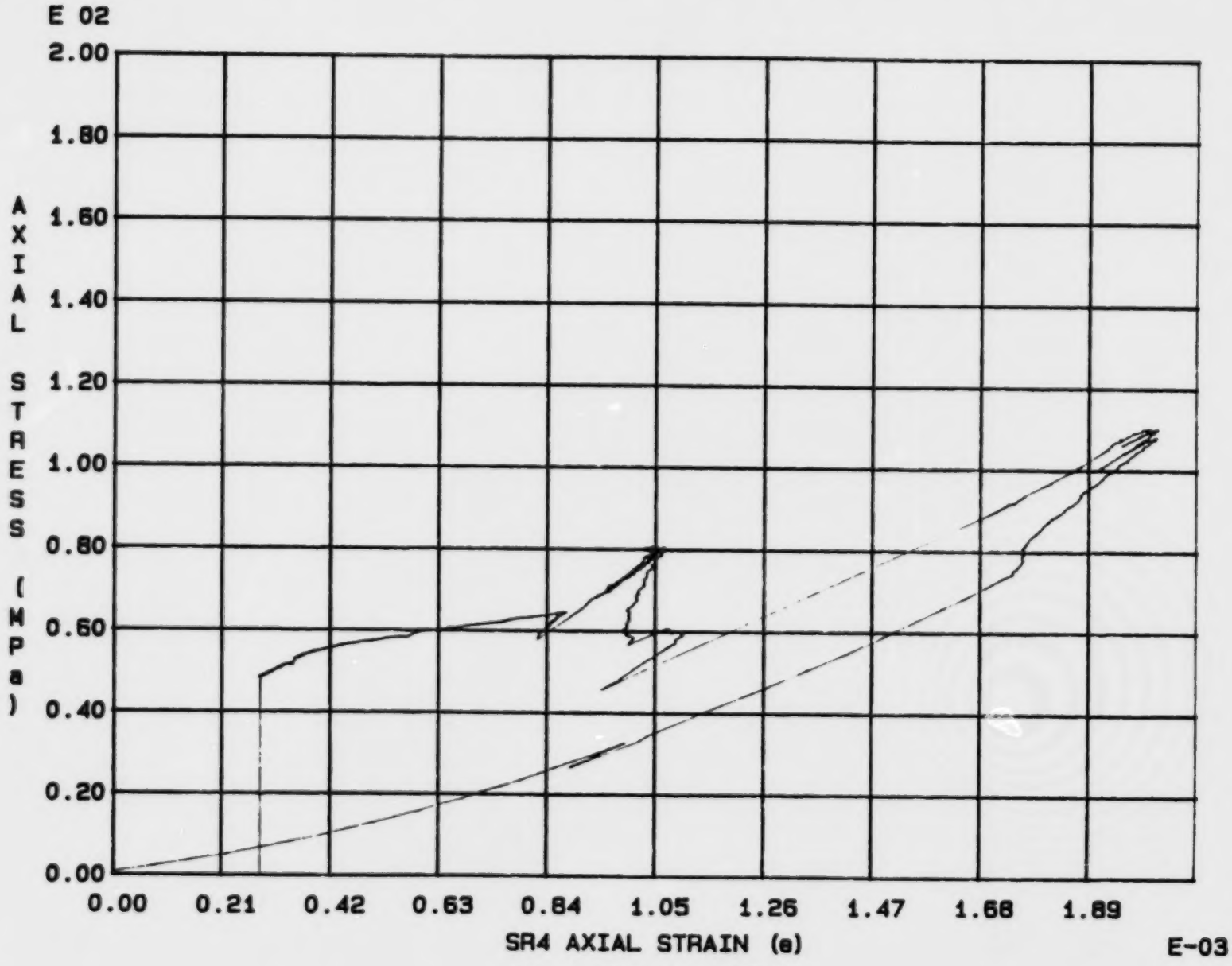

Fig. 2 - 52 Specimen M91U

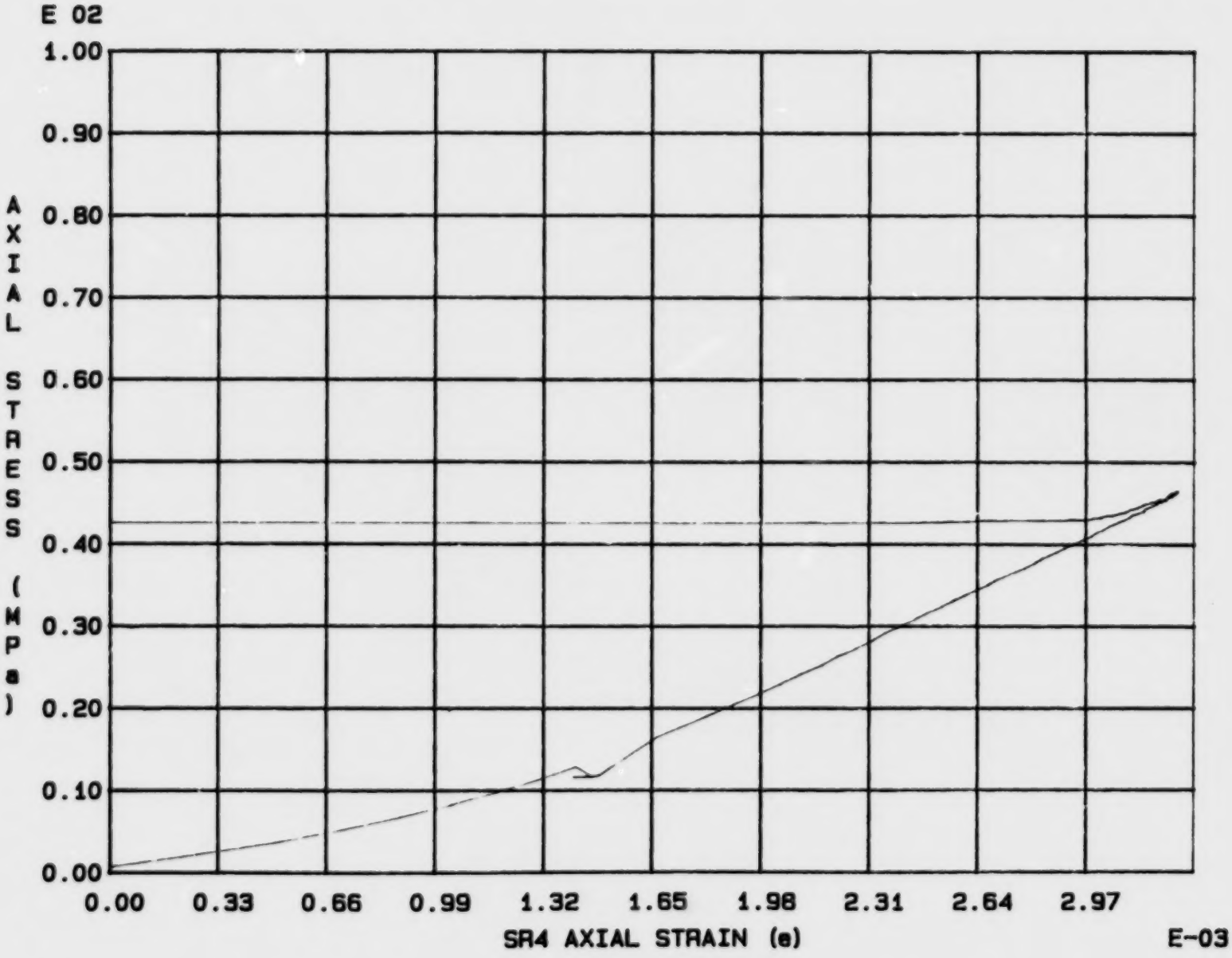

Fig. 2 - 53 Specimen M92U

Appendix 3.

Stress-strain curves of uniaxial tests using circumferential extensometer

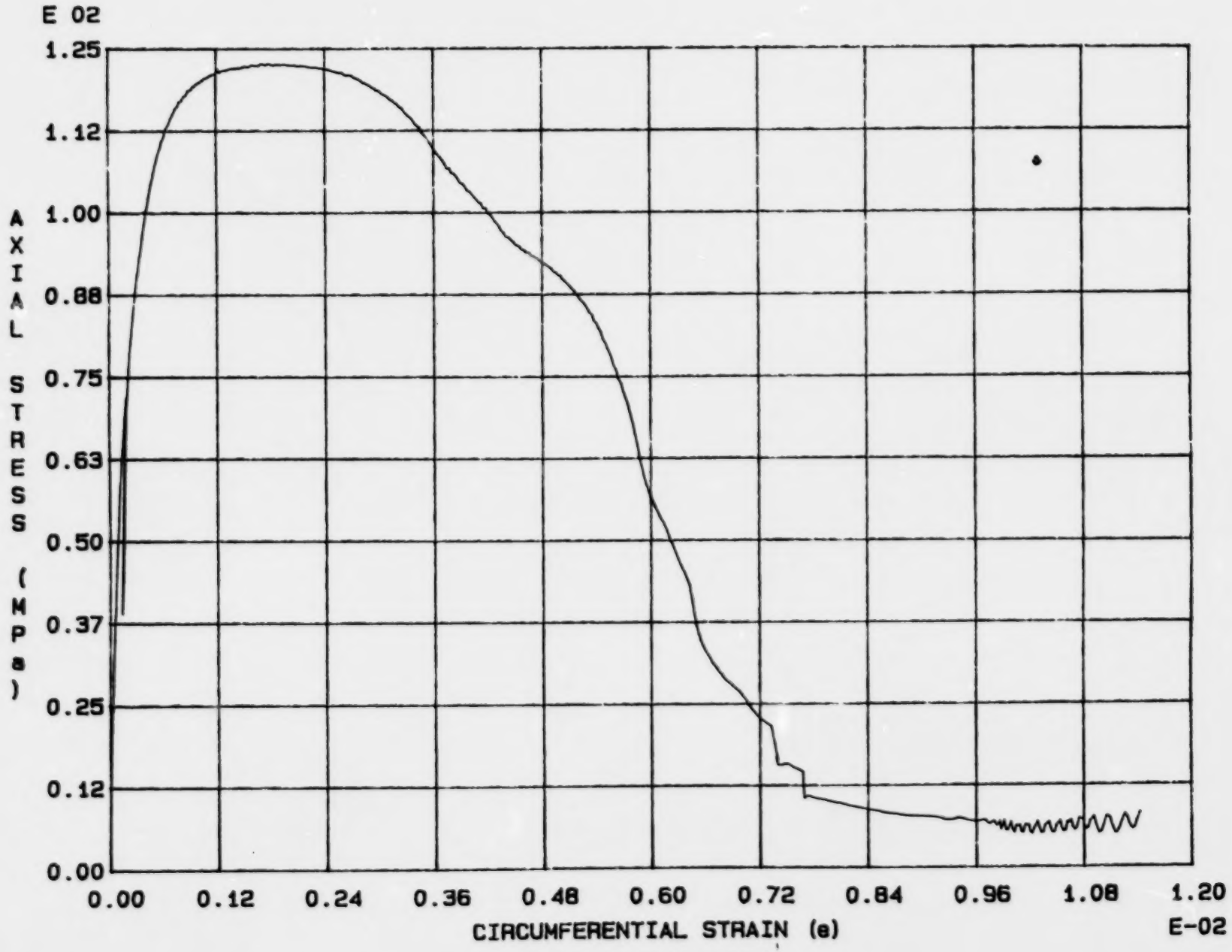

Fig. 3 - 1 Specimen M3U

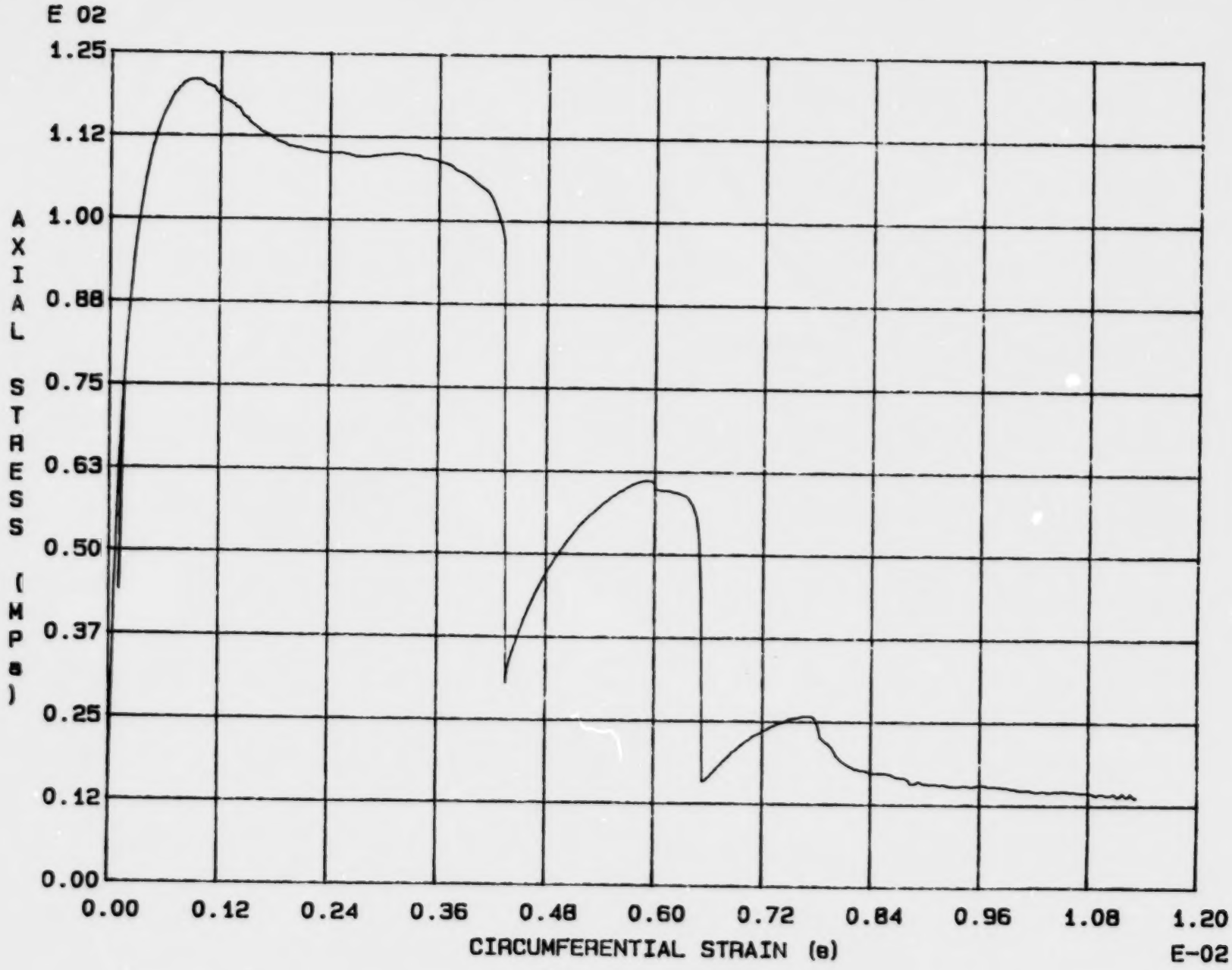

Fig. 3 - 2 Specimen M4U

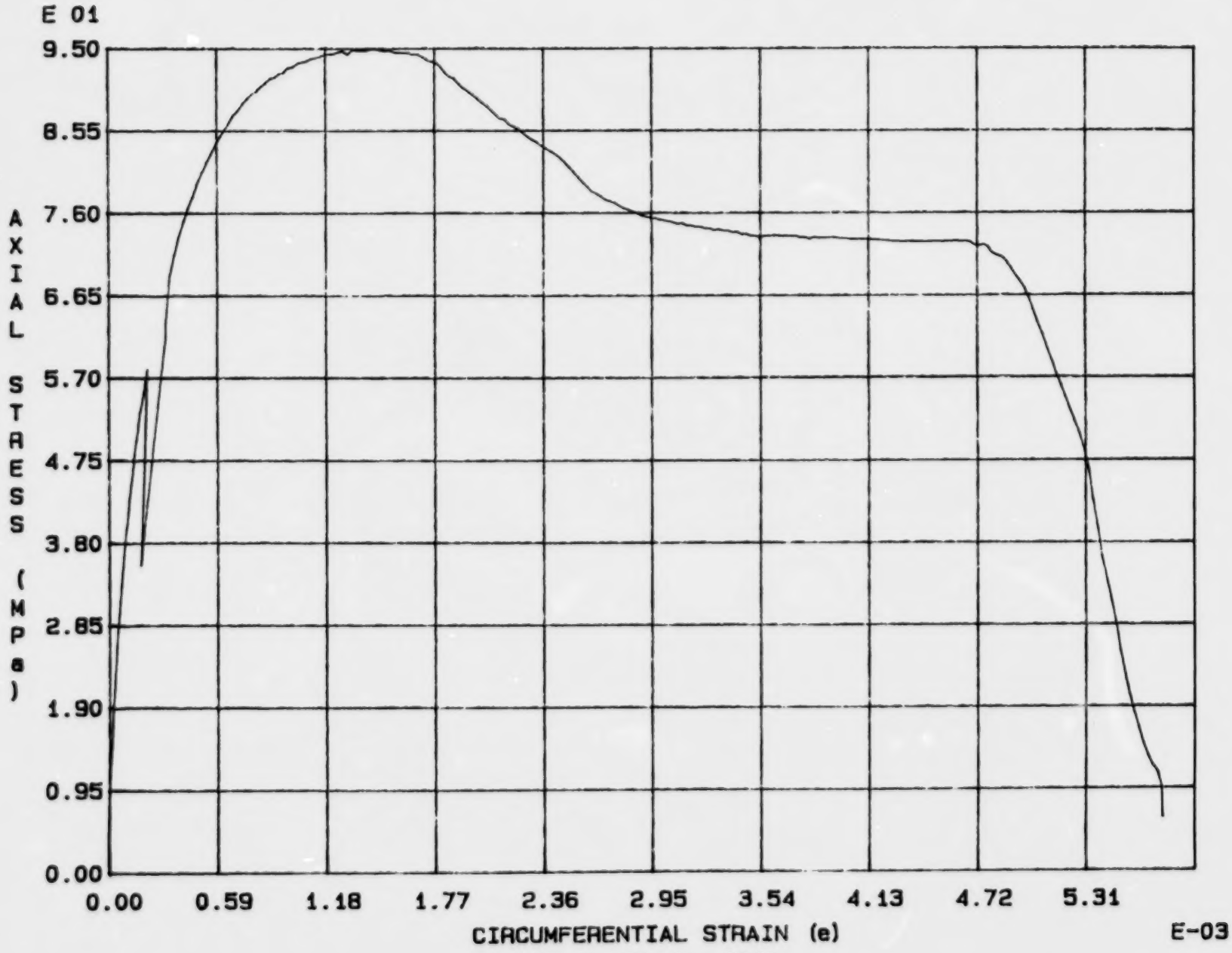

Fig. 3 - 3 Specimen M5U

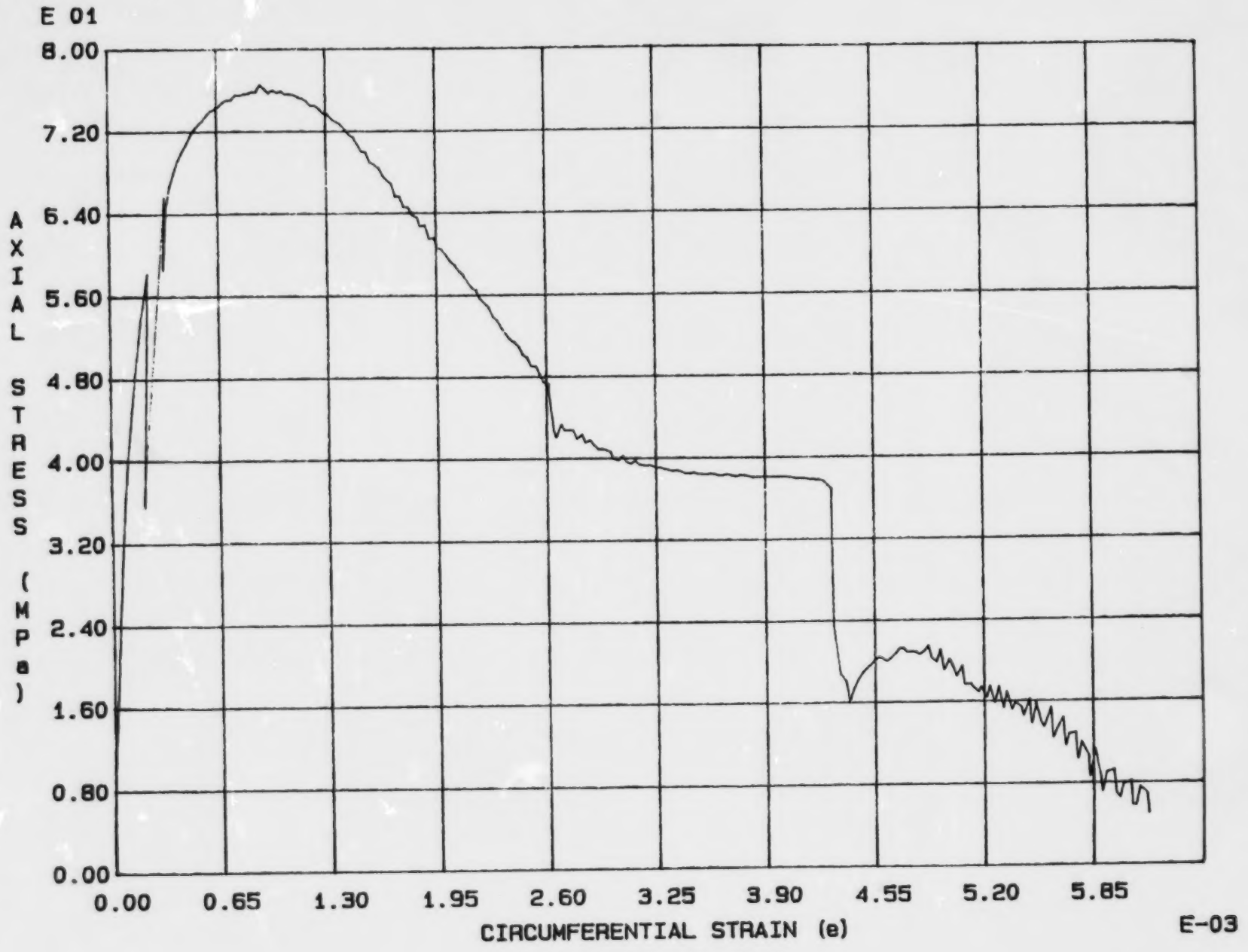

Fig. 3 - 4 Specimen M6U

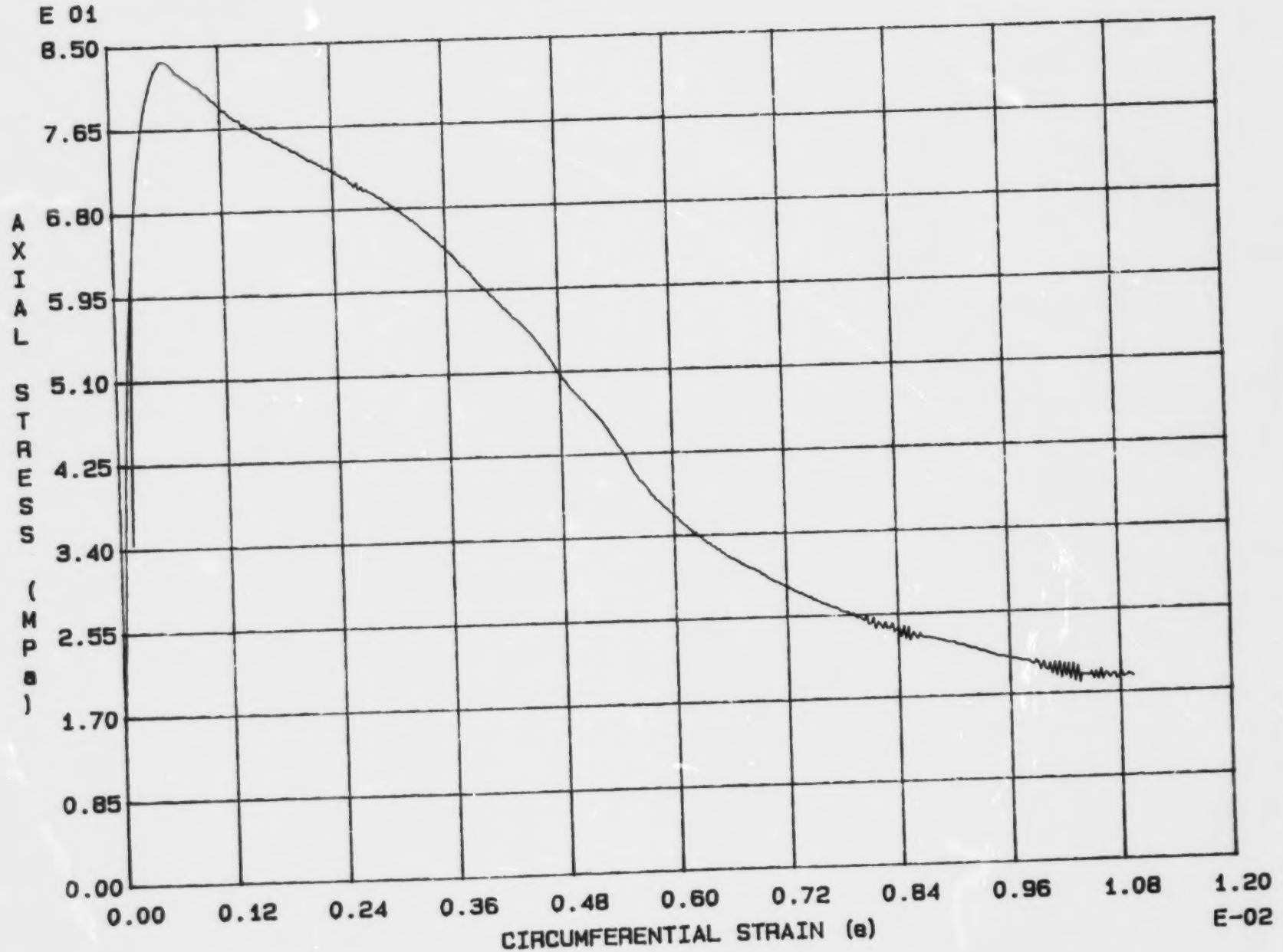

Fig. 3 - 5 Specimen M7U

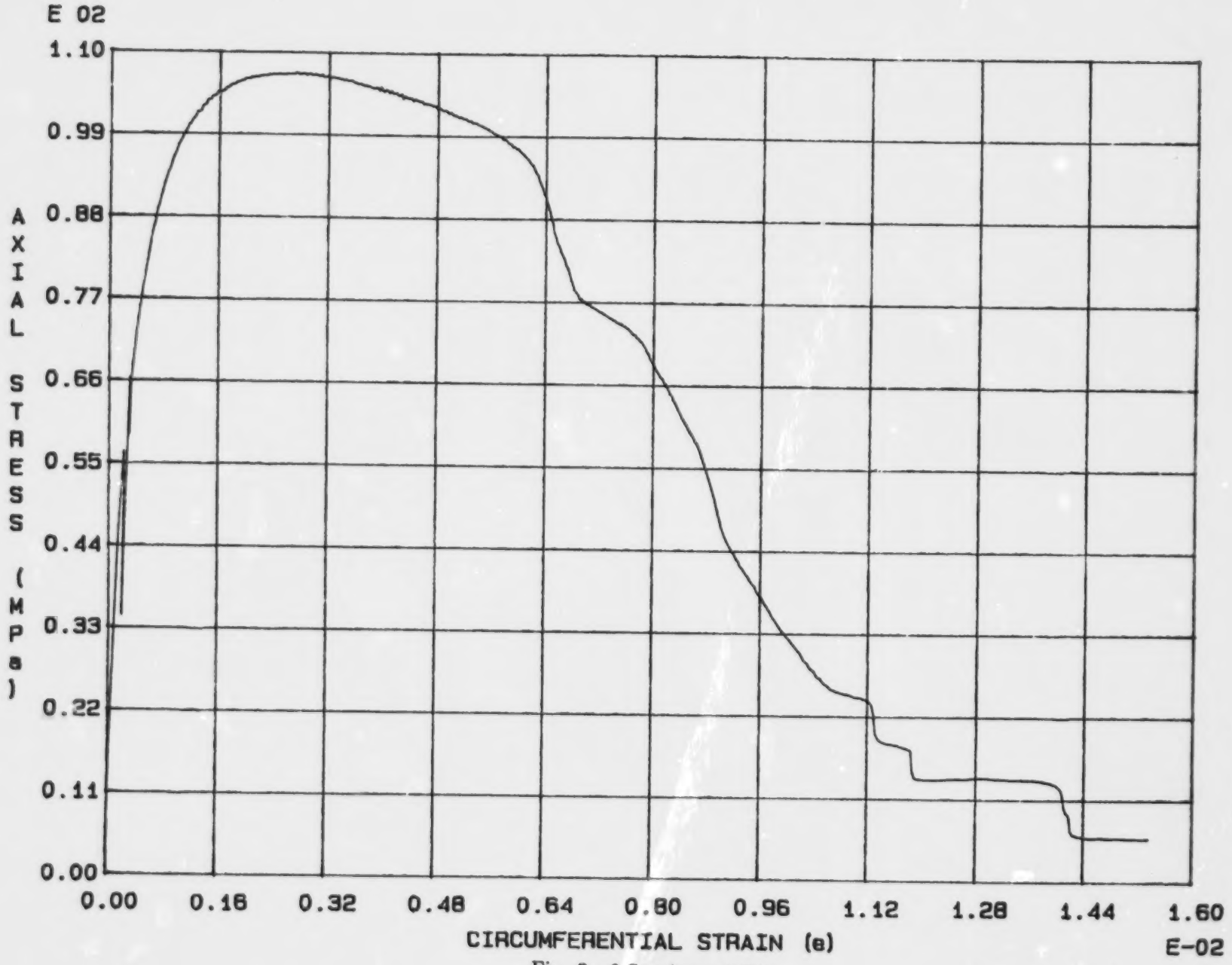

Fig. 3 - 6 Specimen M8U

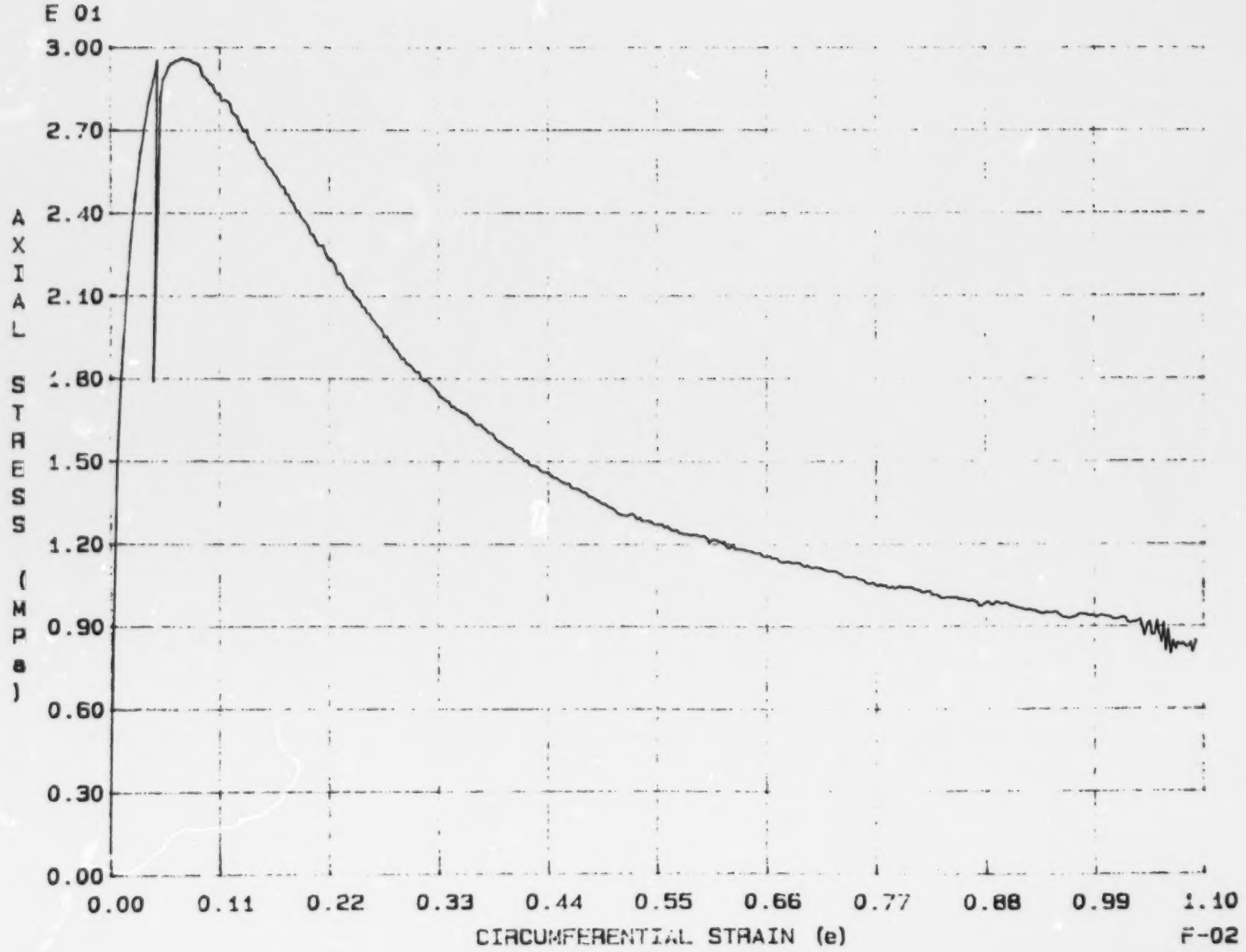

Fig. 3 - 7 Specimen M9U

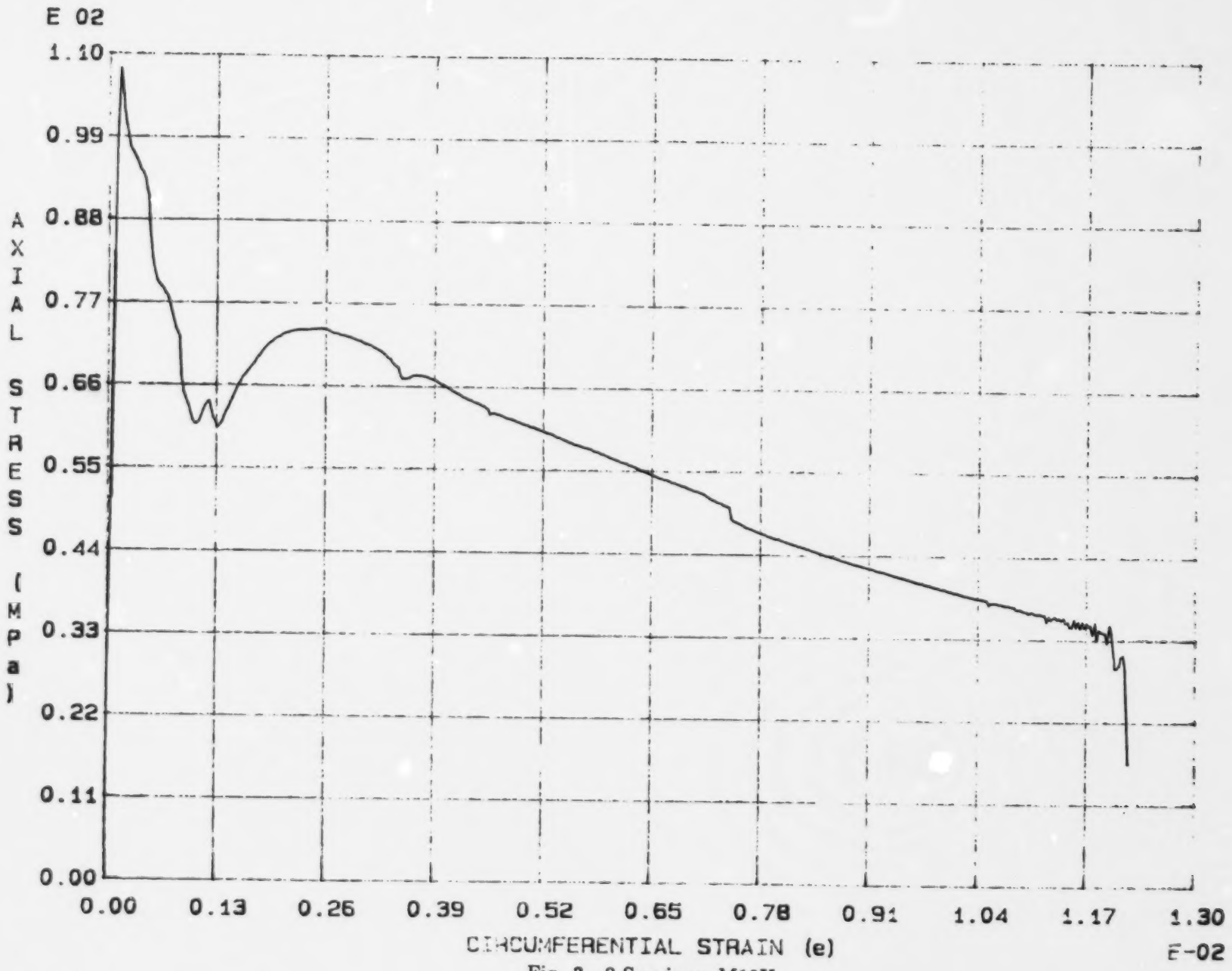

Fig. 3 - 8 Specimen M10U

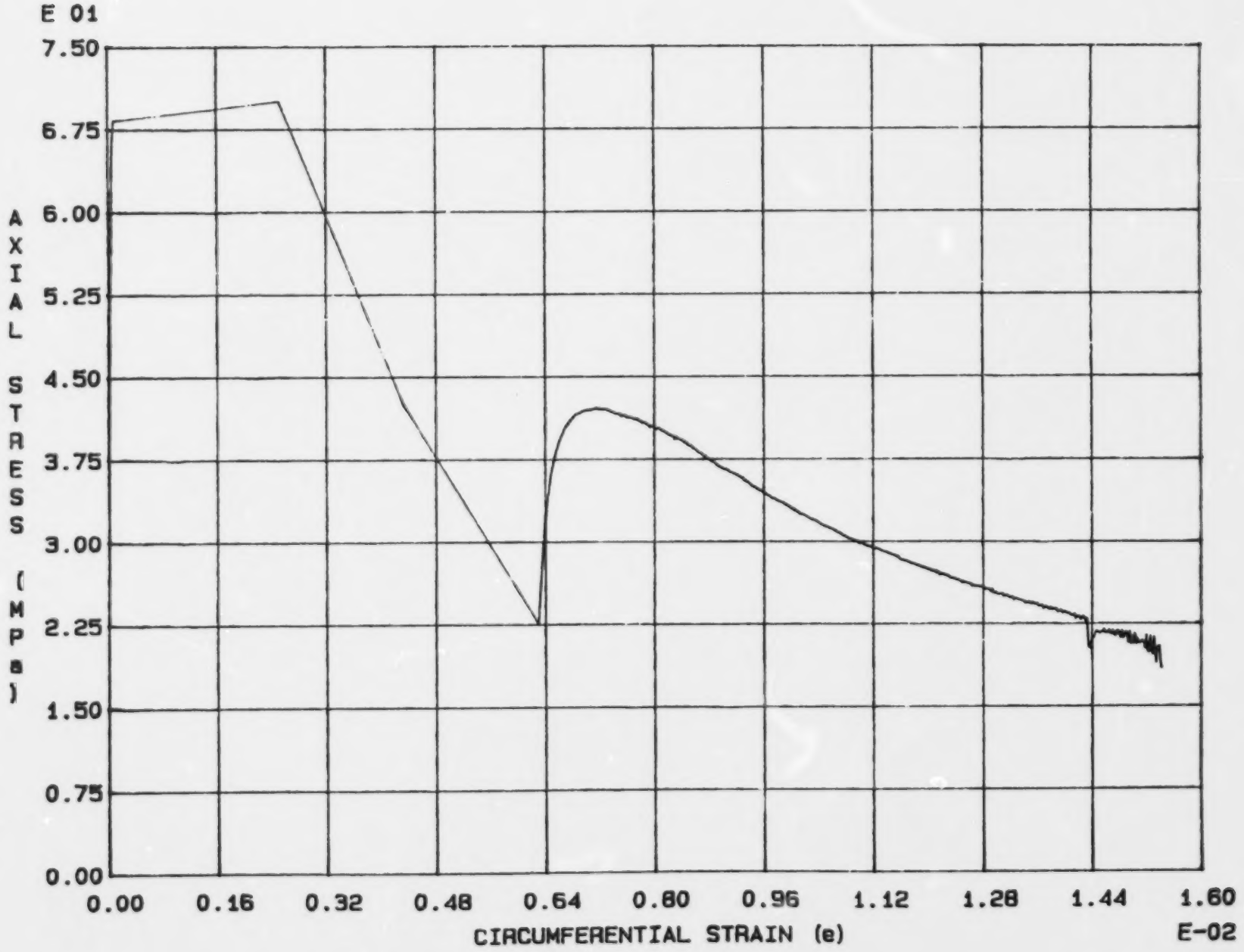

Fig. 3 - 9 Specimen M11U

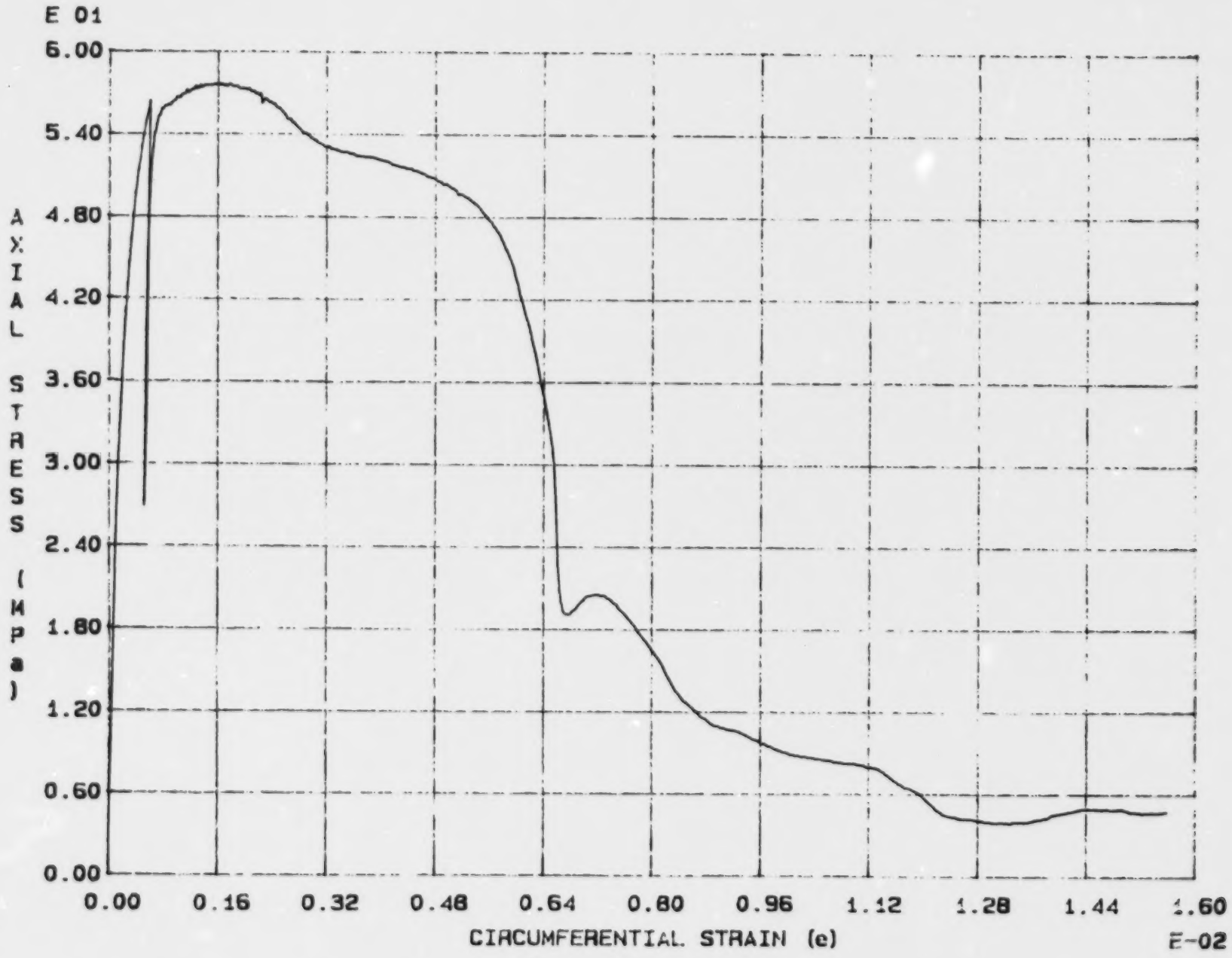

Fig. 3 - 10 Specimen M12U

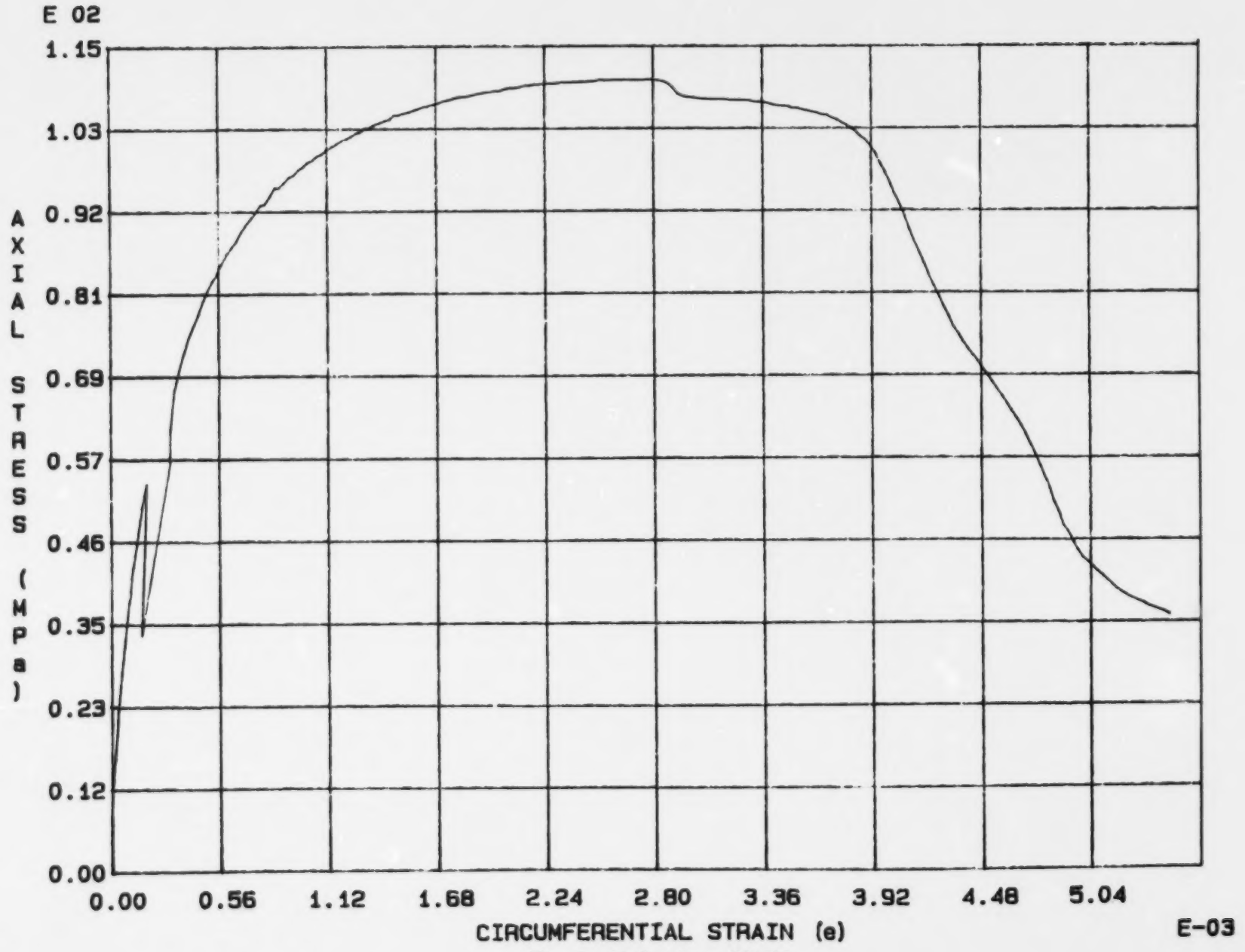

Fig. 3 - 11 Specimen M13U

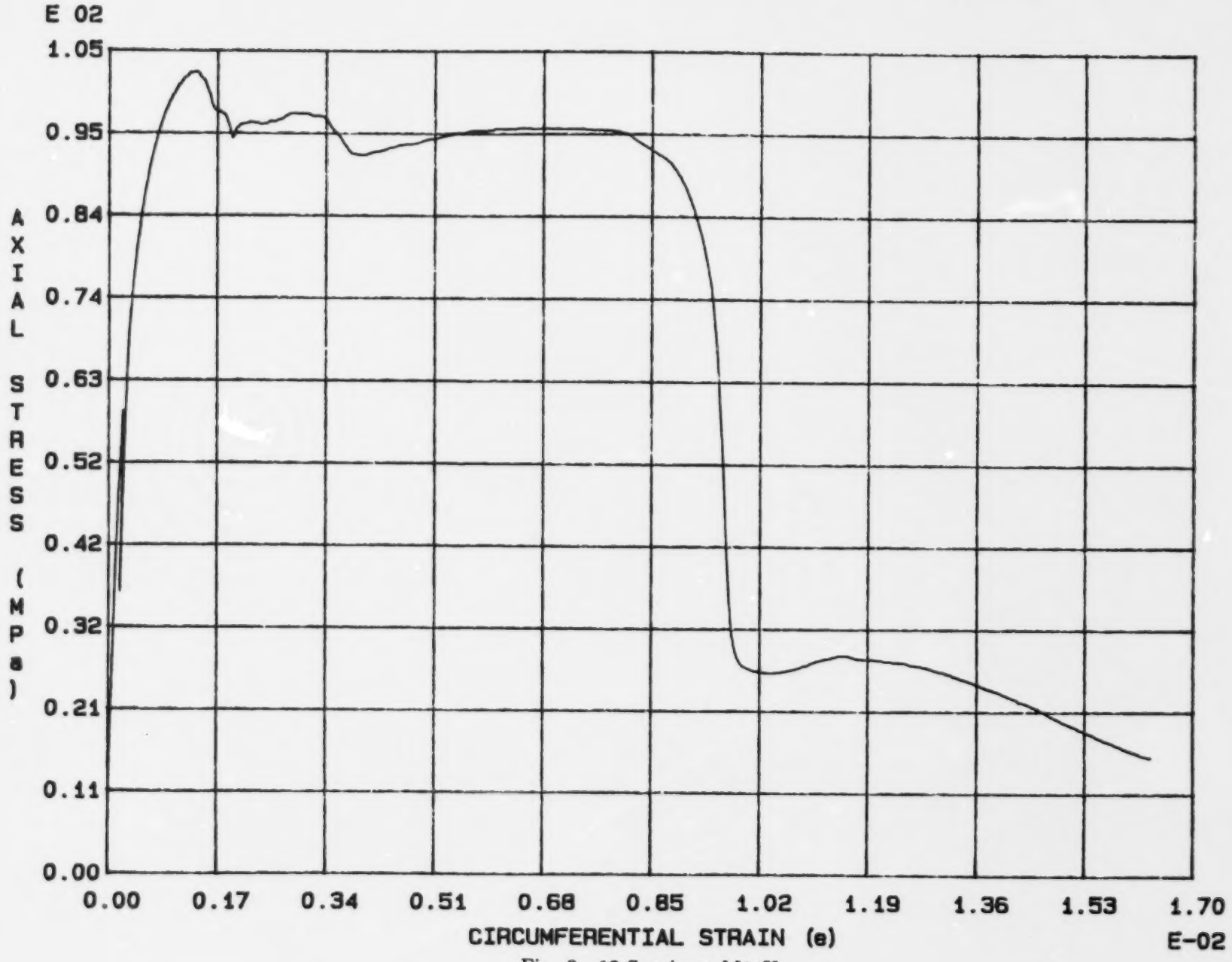

Fig. 3 - 12 Specimen M14U

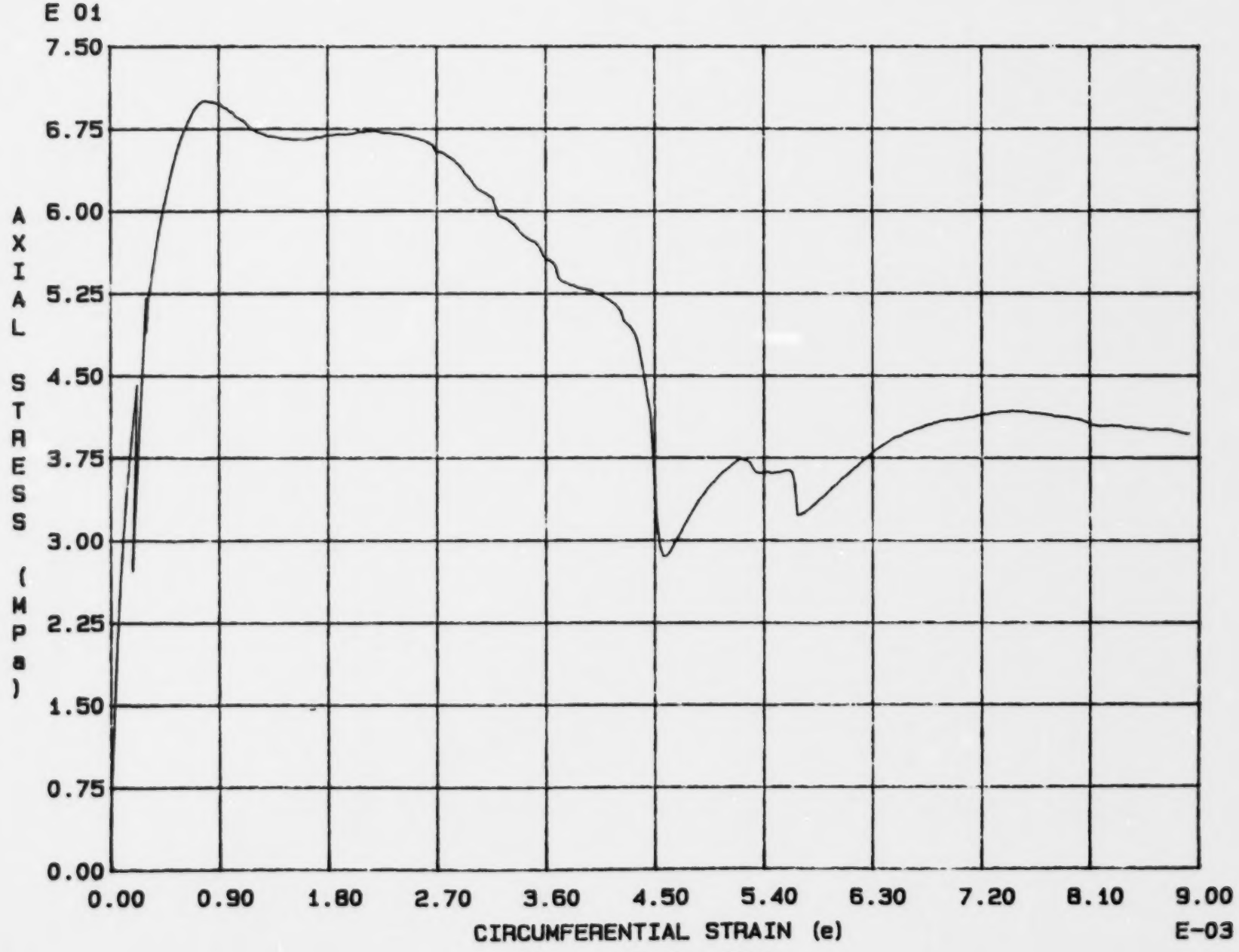

Fig. 3 - 13 Specimen M15U

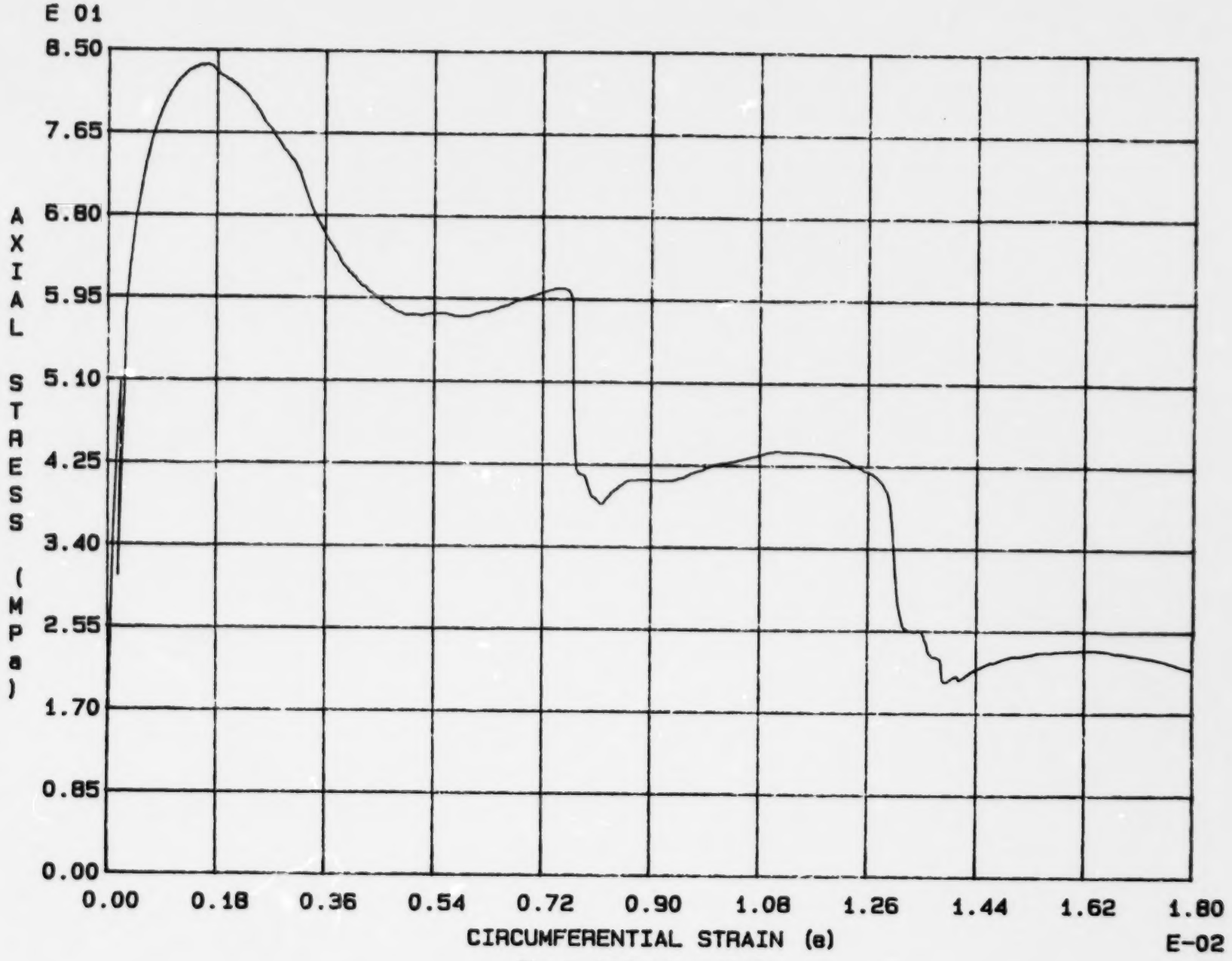

Fig. 3 - 14 Specimen M16U

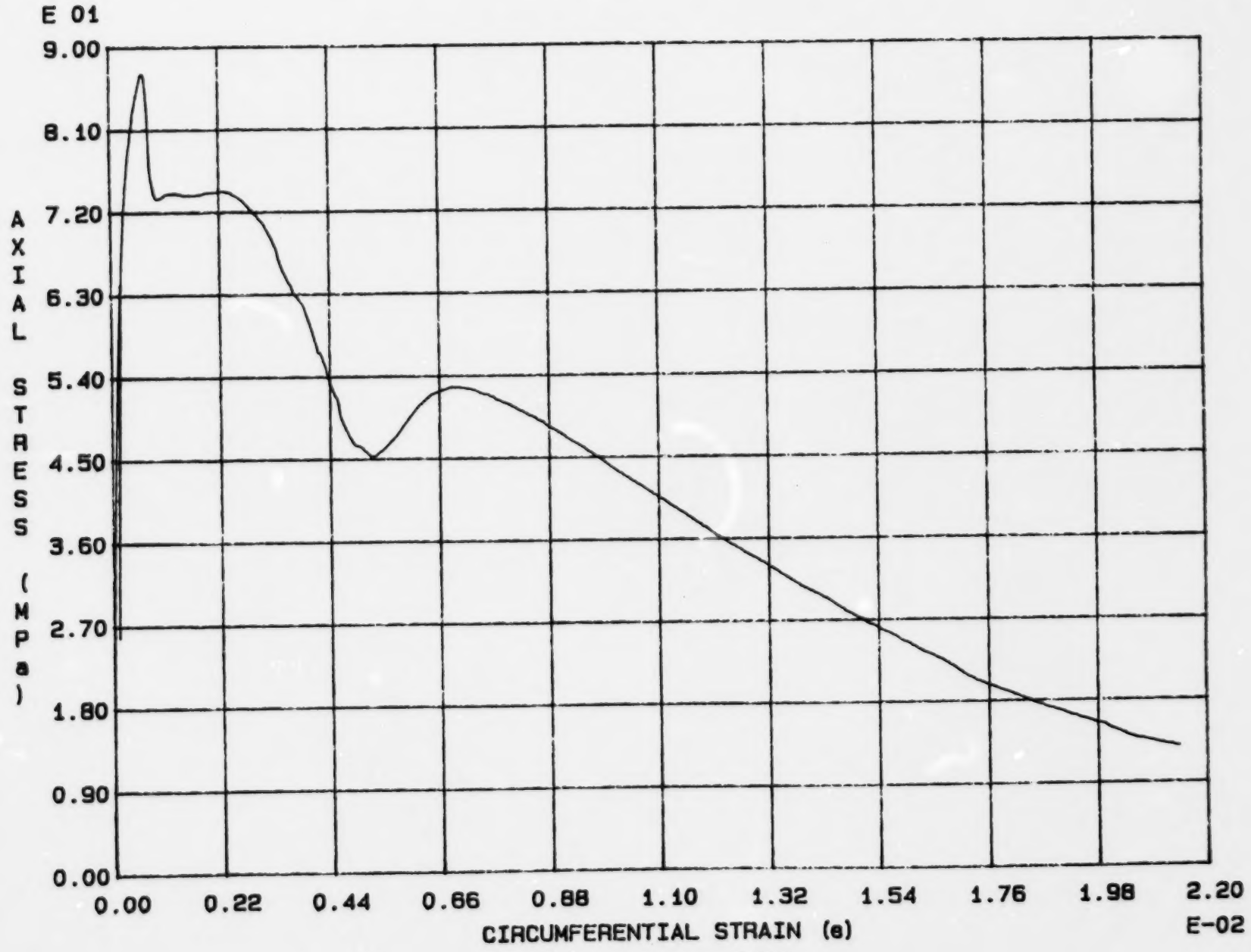

Fig. 3 - 15 Specimen M17U

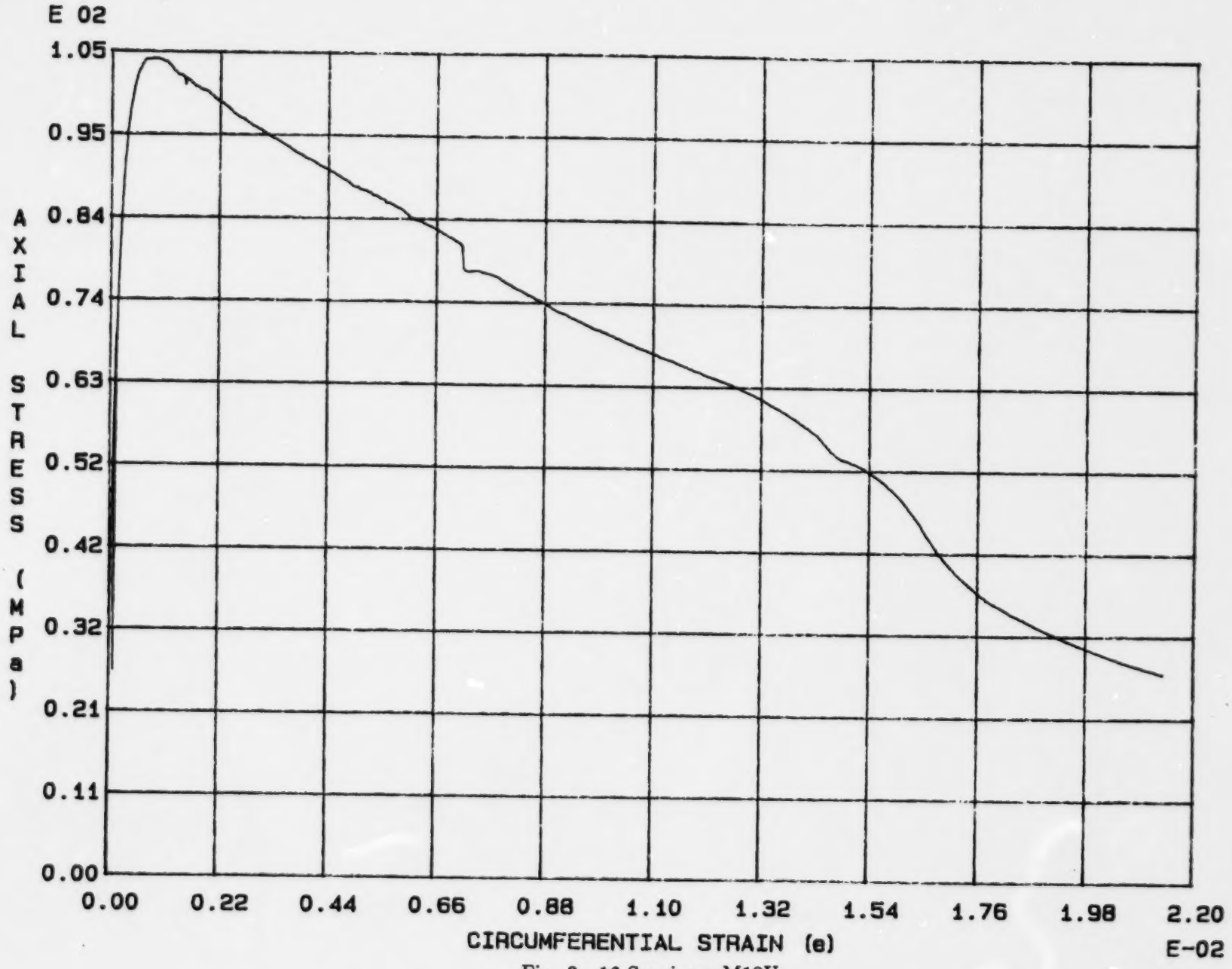

Fig. 3 - 16 Specimen M18U

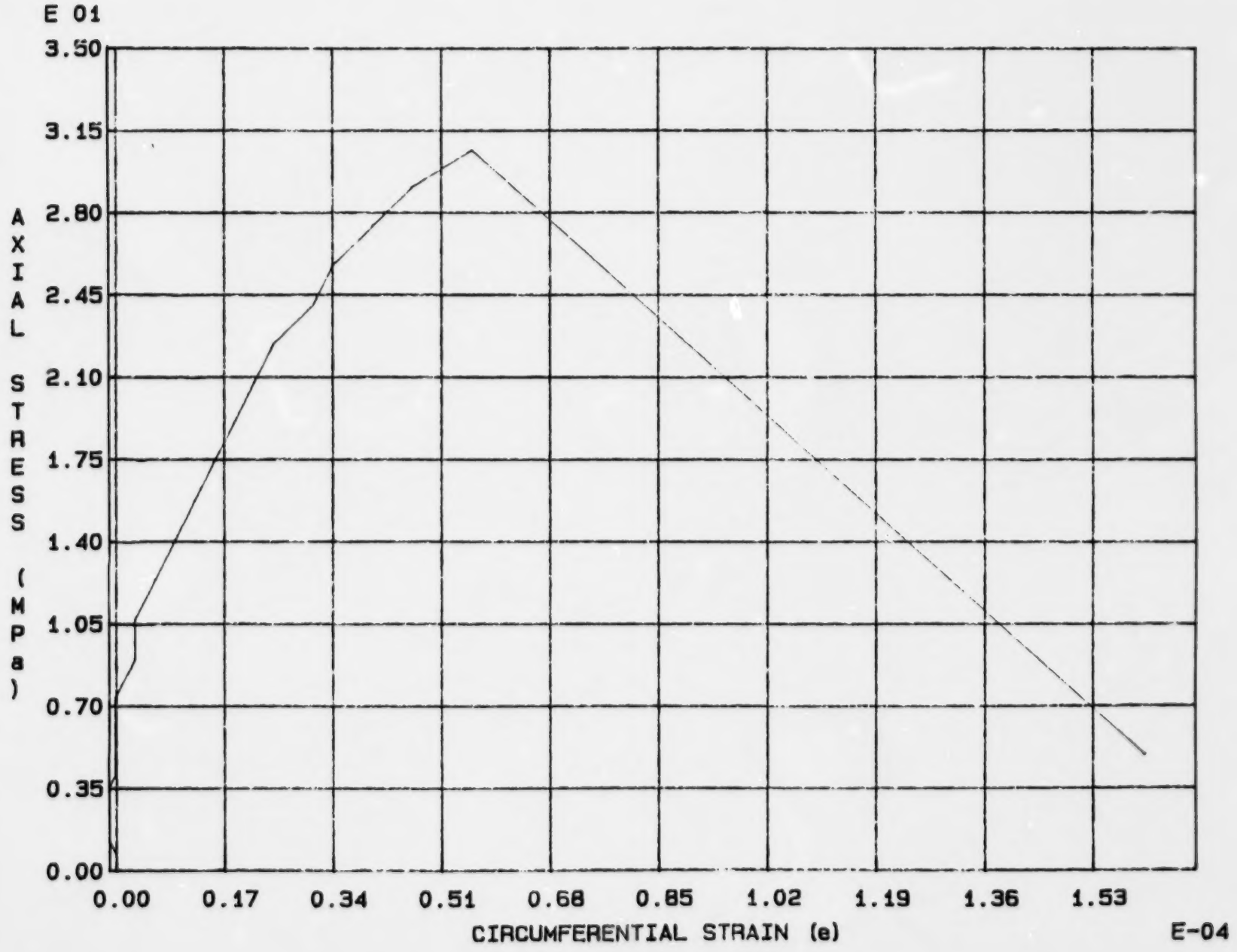

Fig. 3 - 17 Specimen M19U

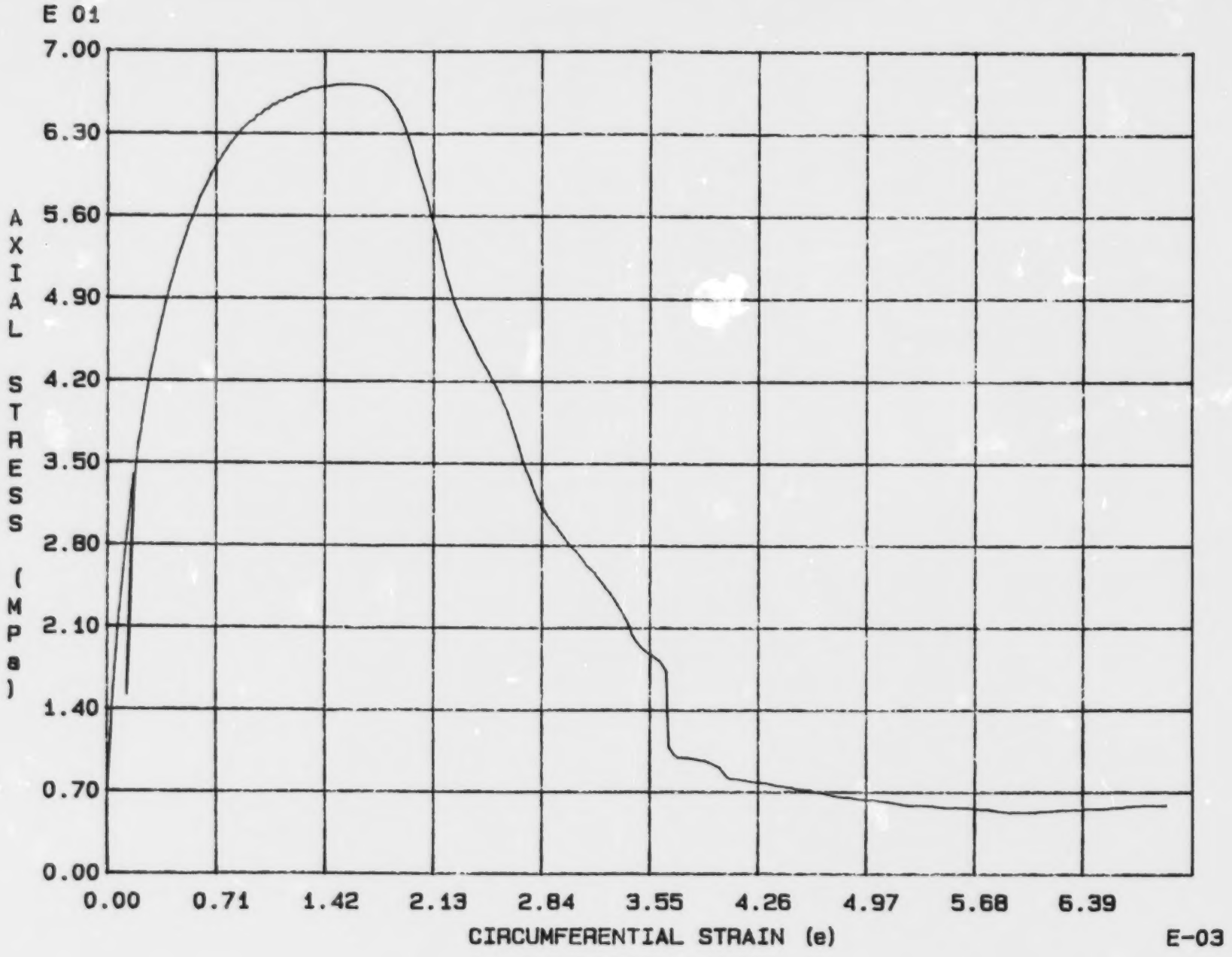

Fig. 3 - 18 Specimen M20U

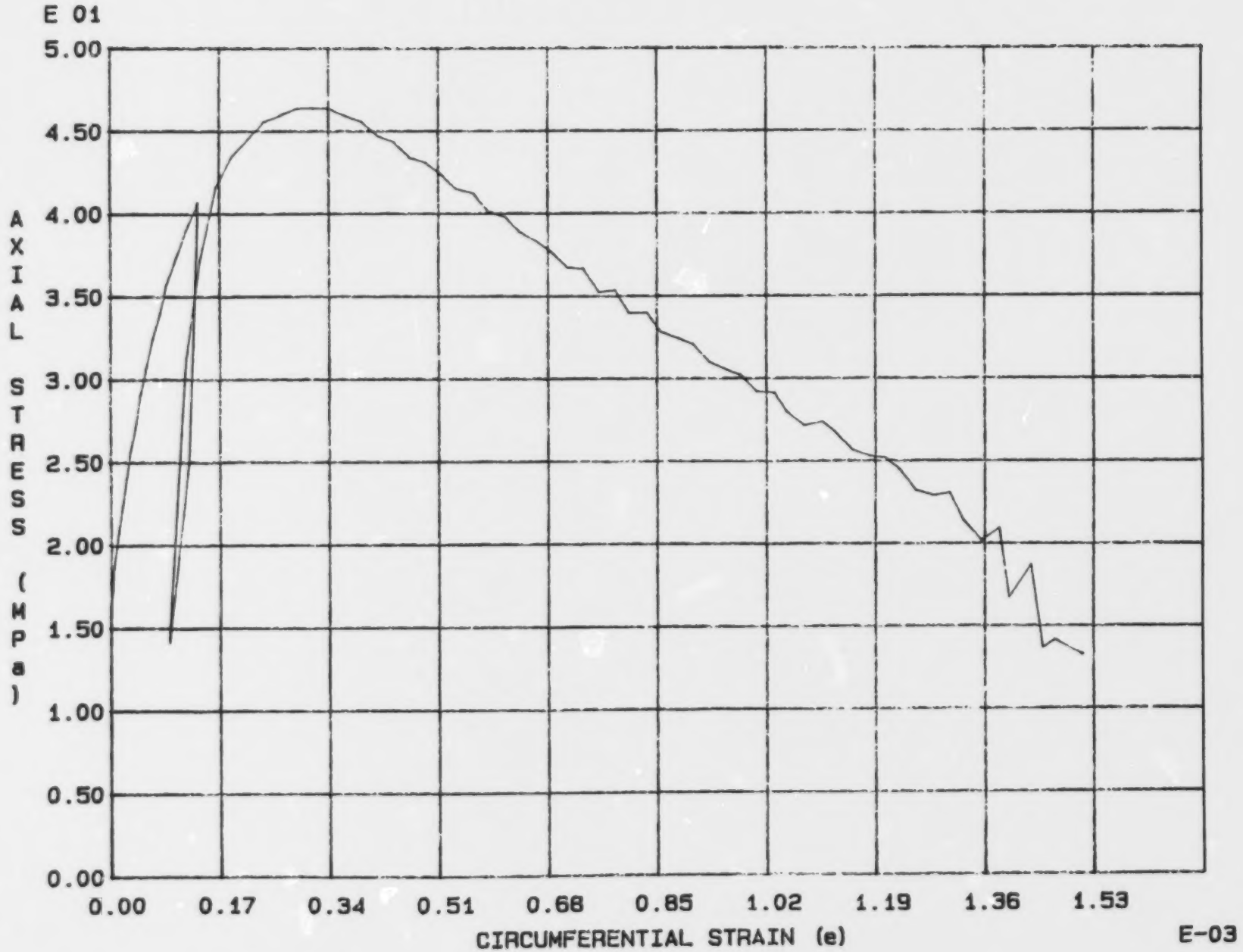

Fig. 3 - 19 Specimen M21U

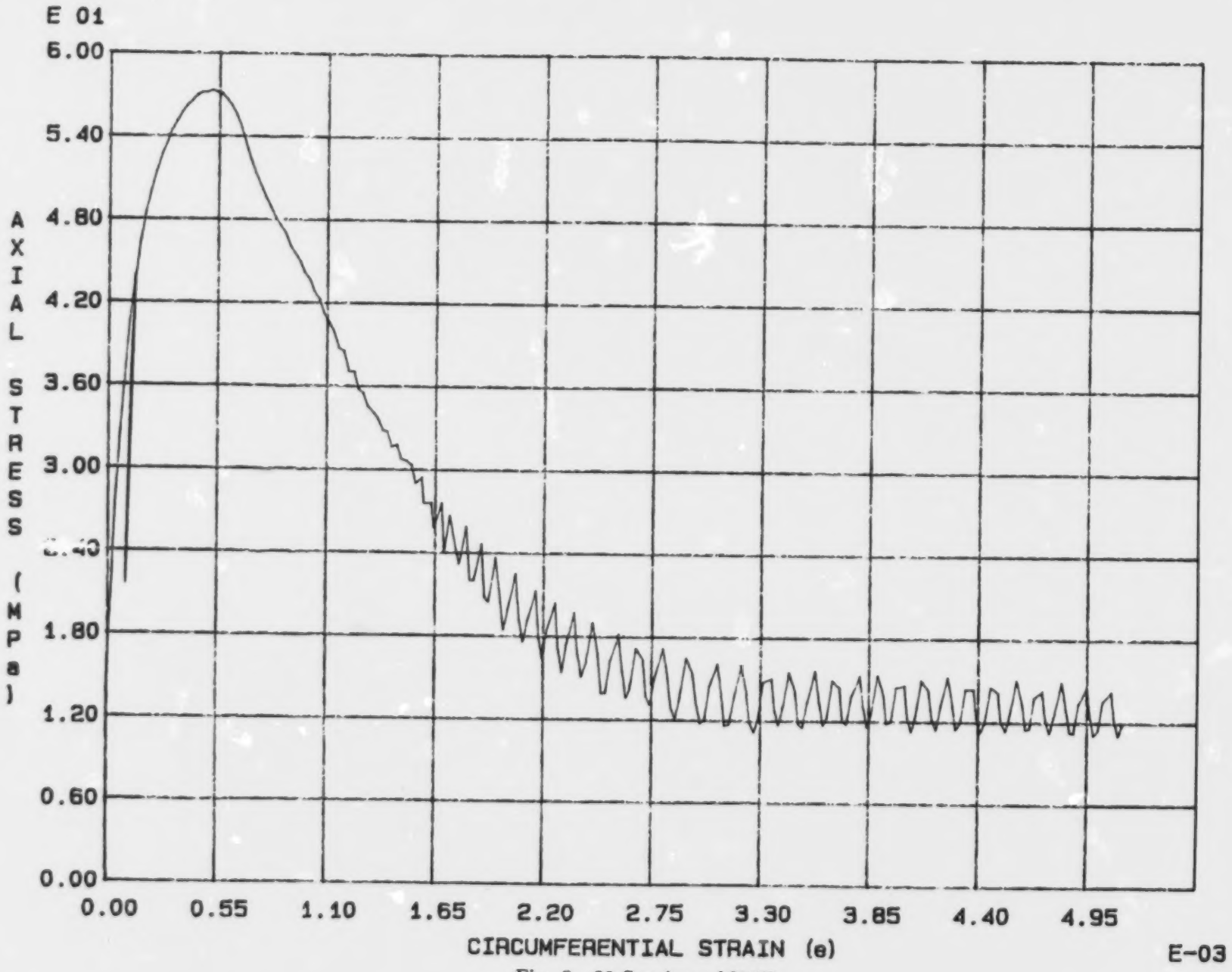

Fig. 3 - 20 Specimen M22U

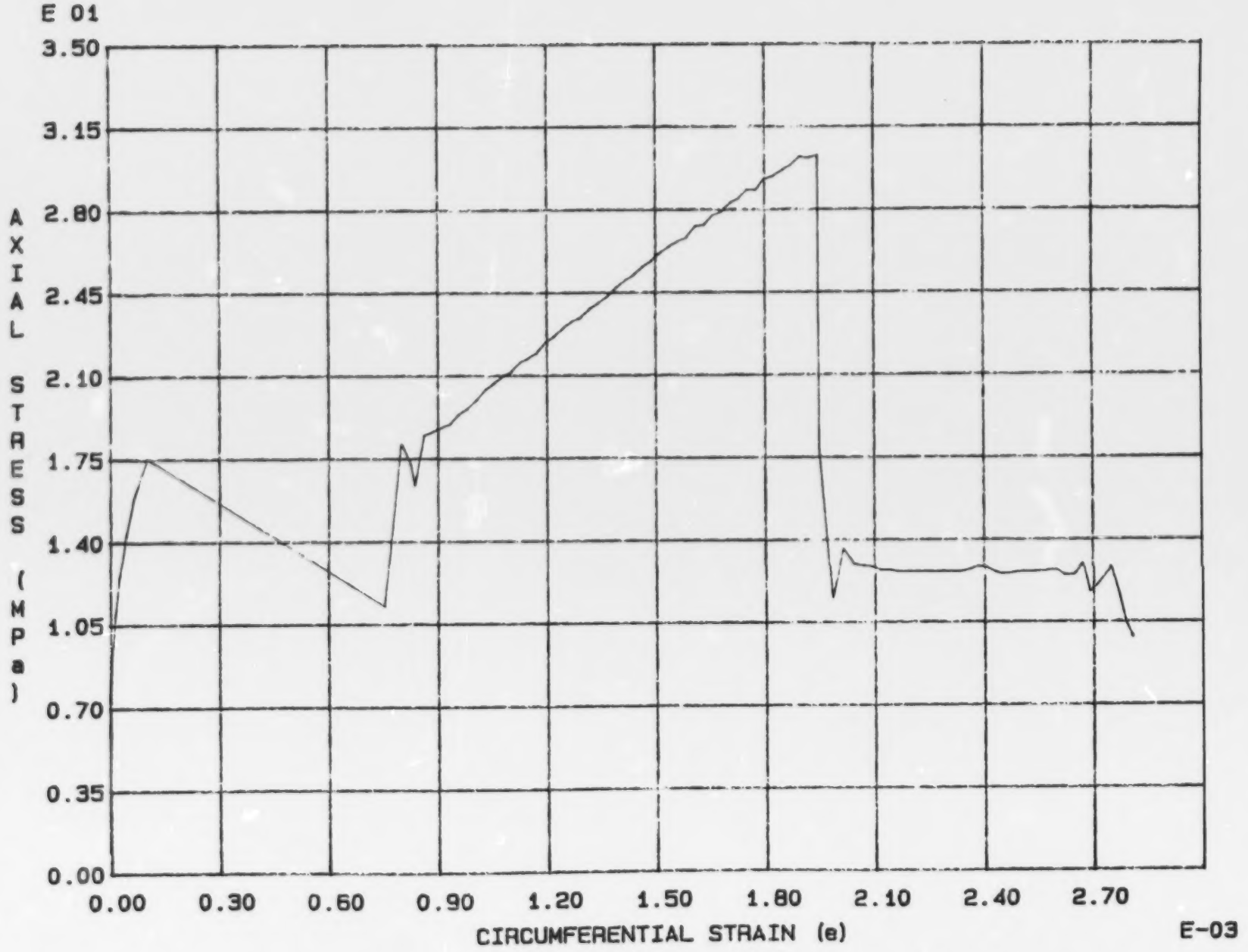

Fig. 3 - 21 Specimen M23U

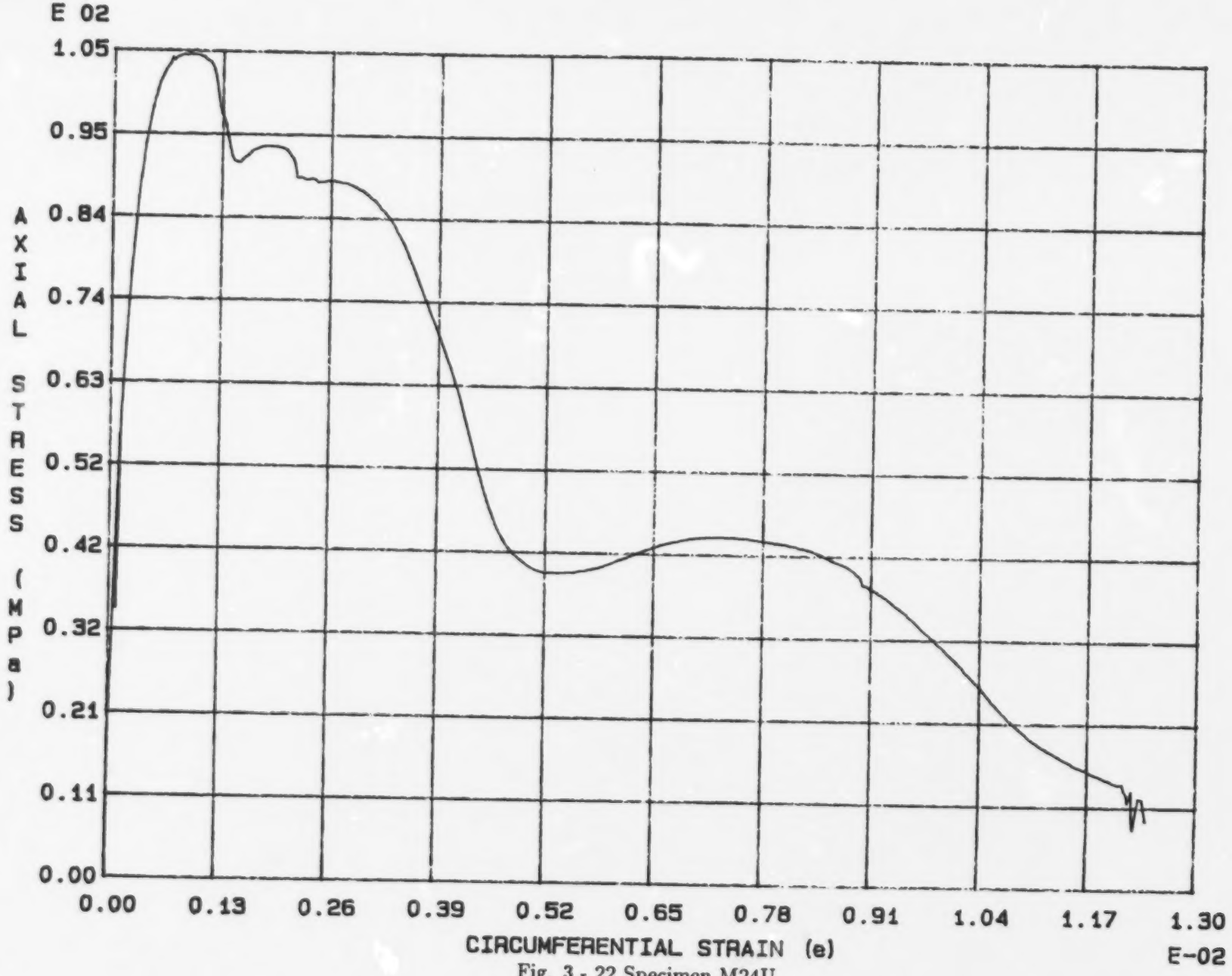

Fig. 3 - 22 Specimen M24U

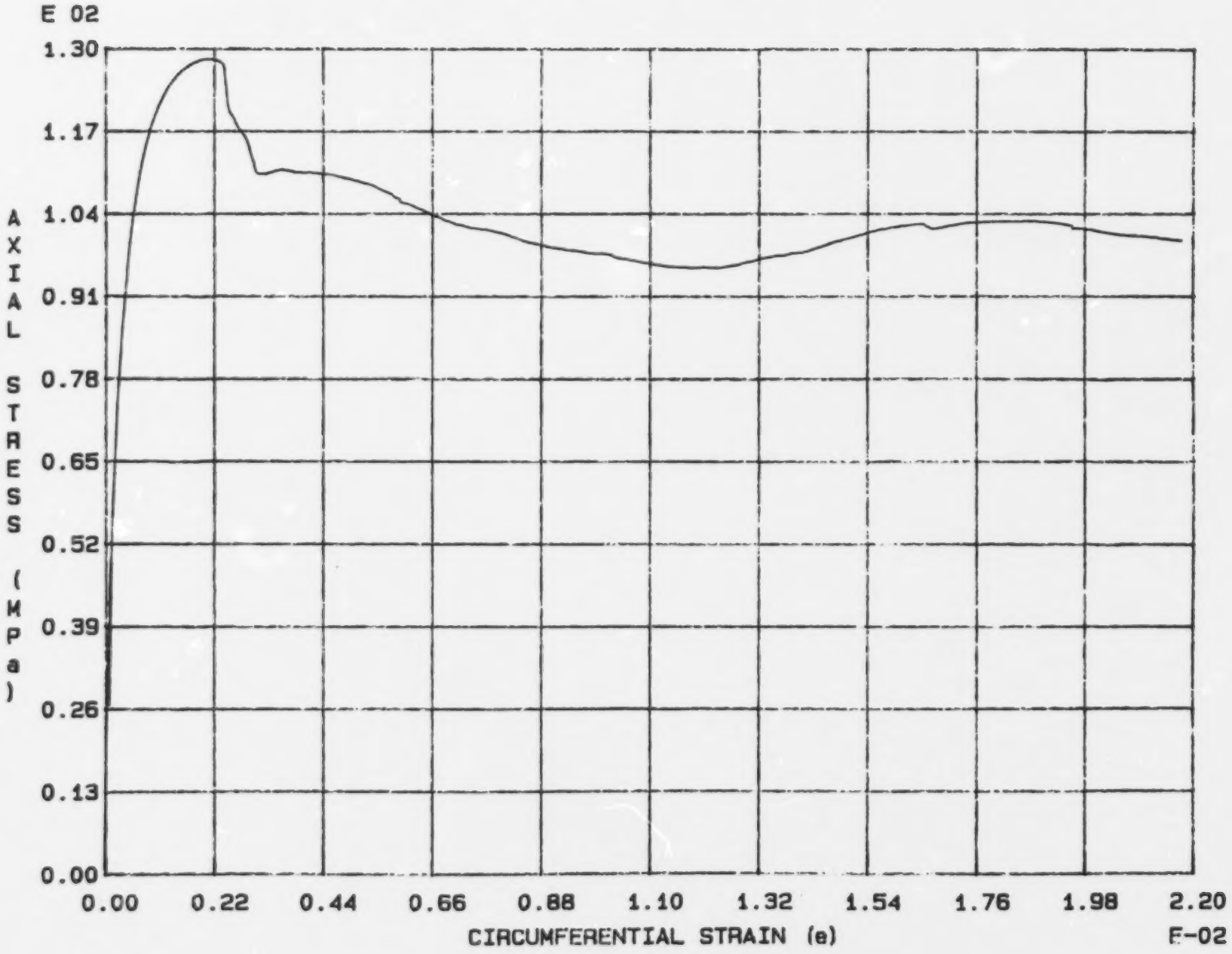

Fig. 3 - 23 Specimen M25U

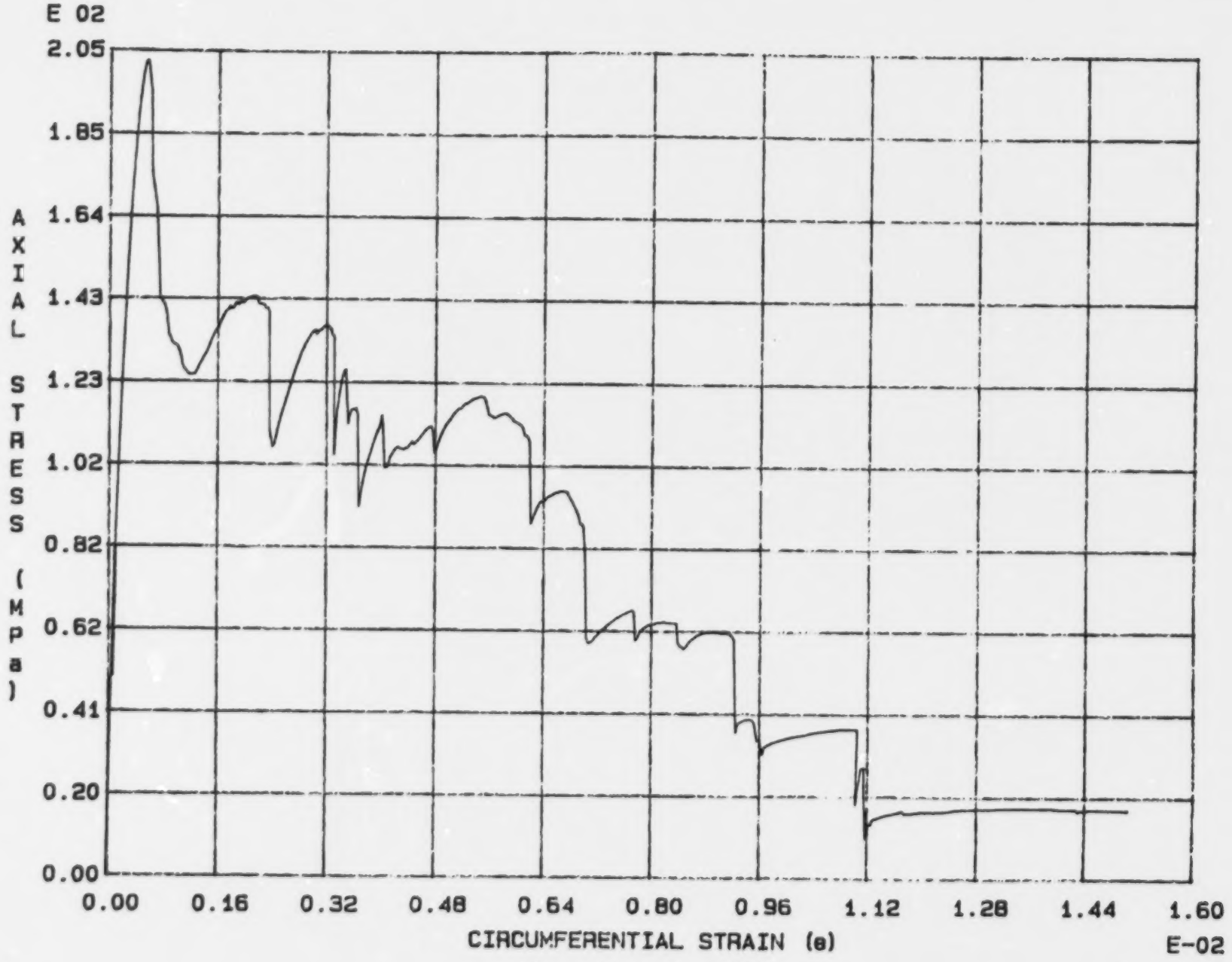

Fig. 3 - 24 Specimen M26U

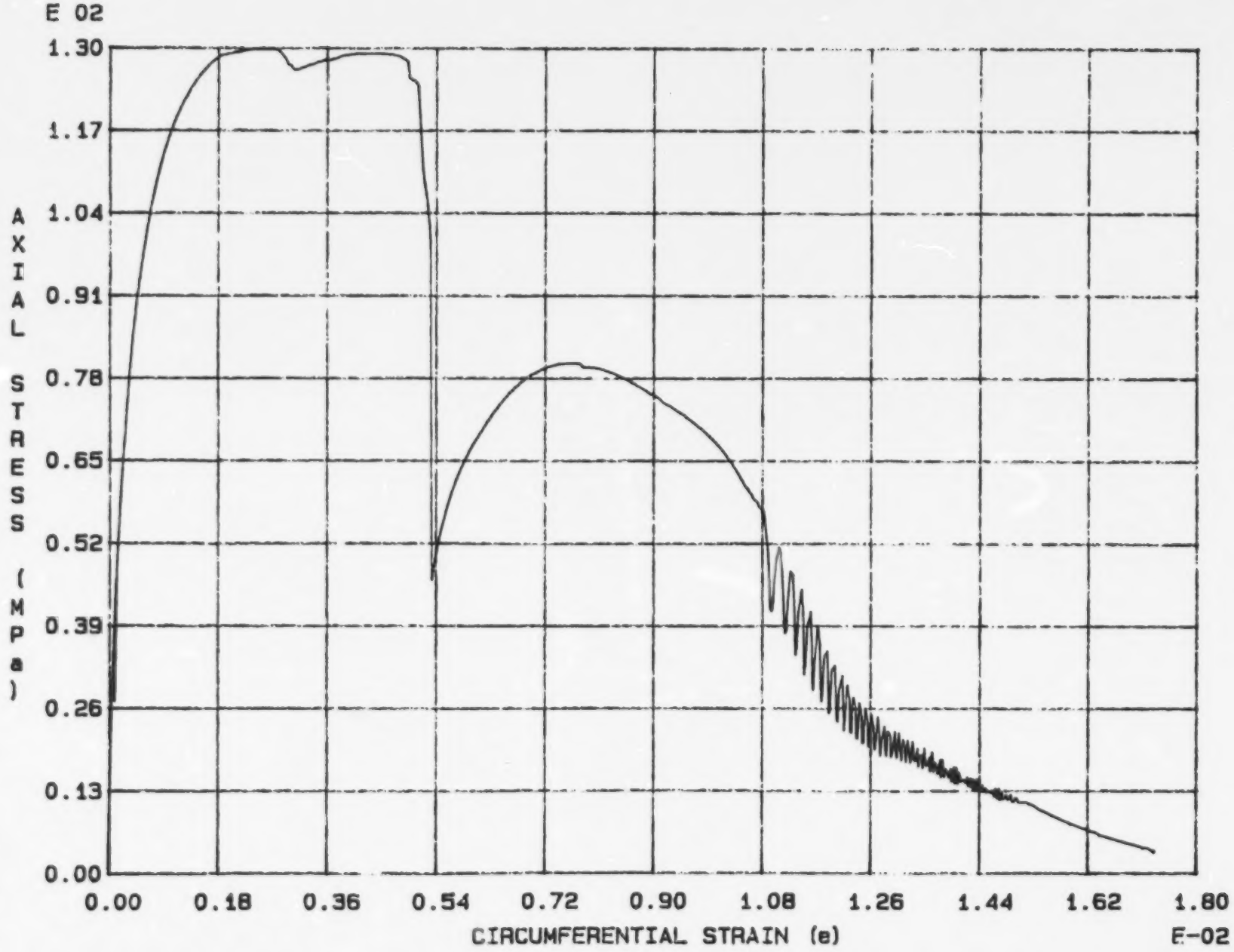

Fig. 3 - 25 Specimen M27U

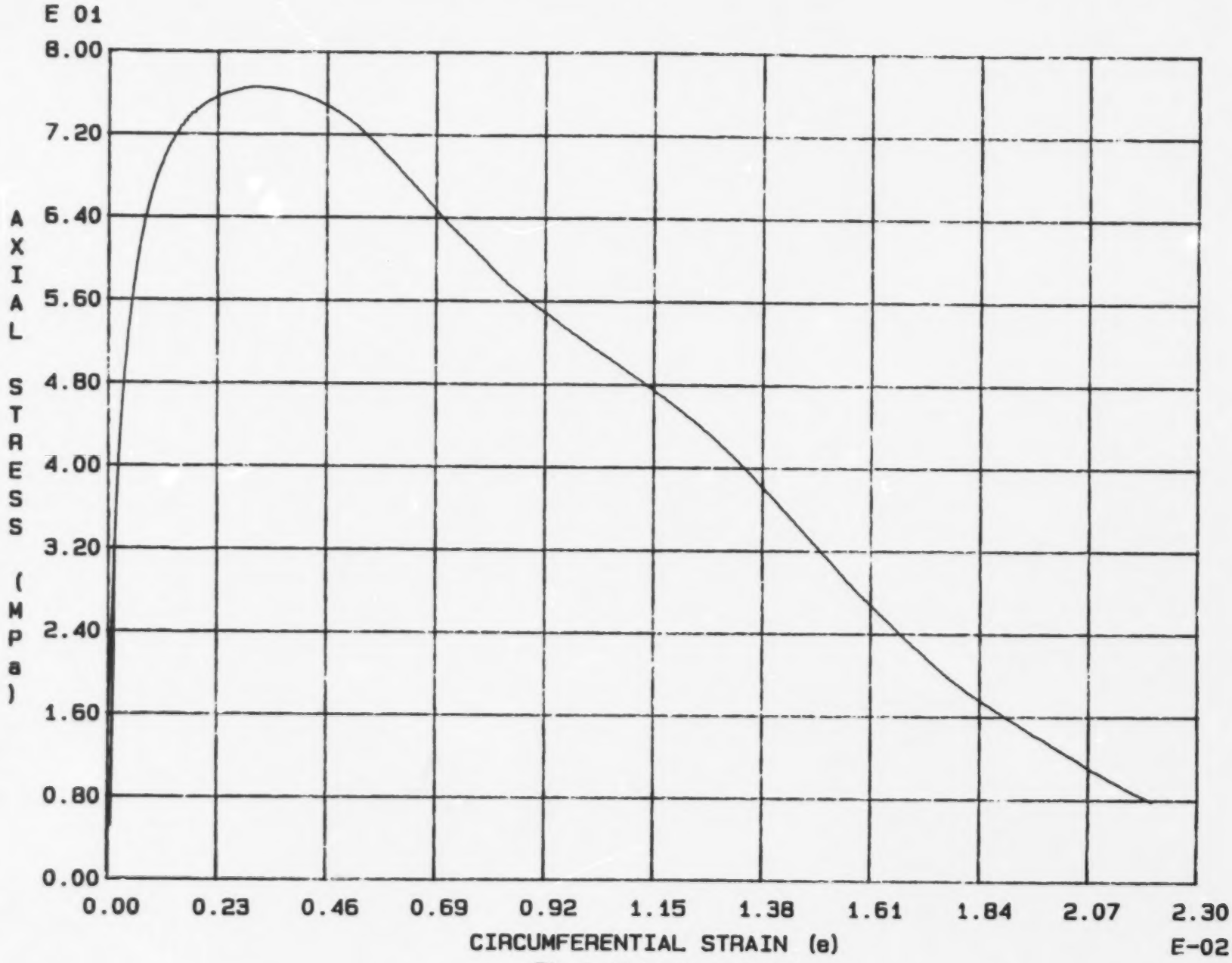

Fig. 3 - 26 Specimen M28U

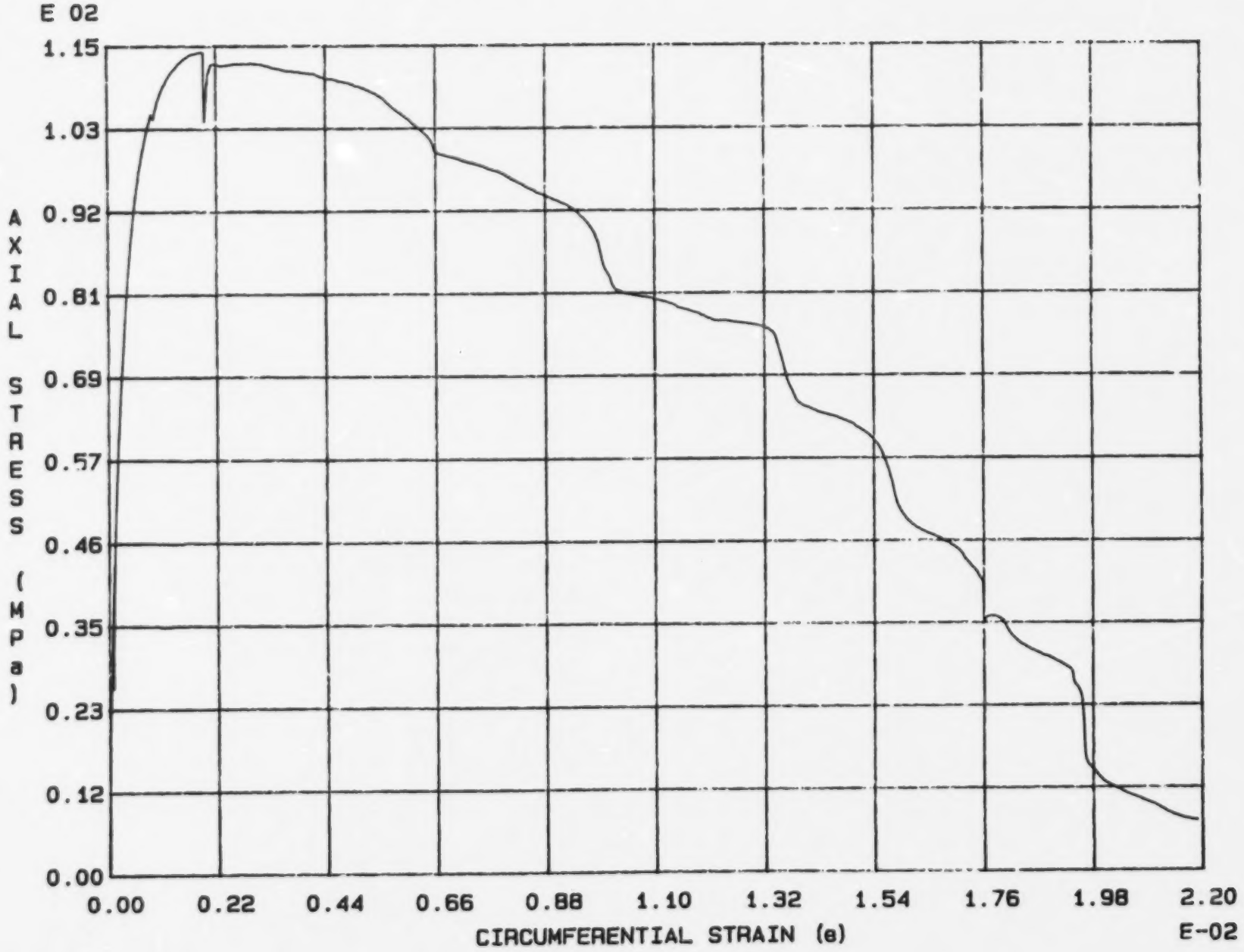

Fig. 3 - 27 Specimen M29U

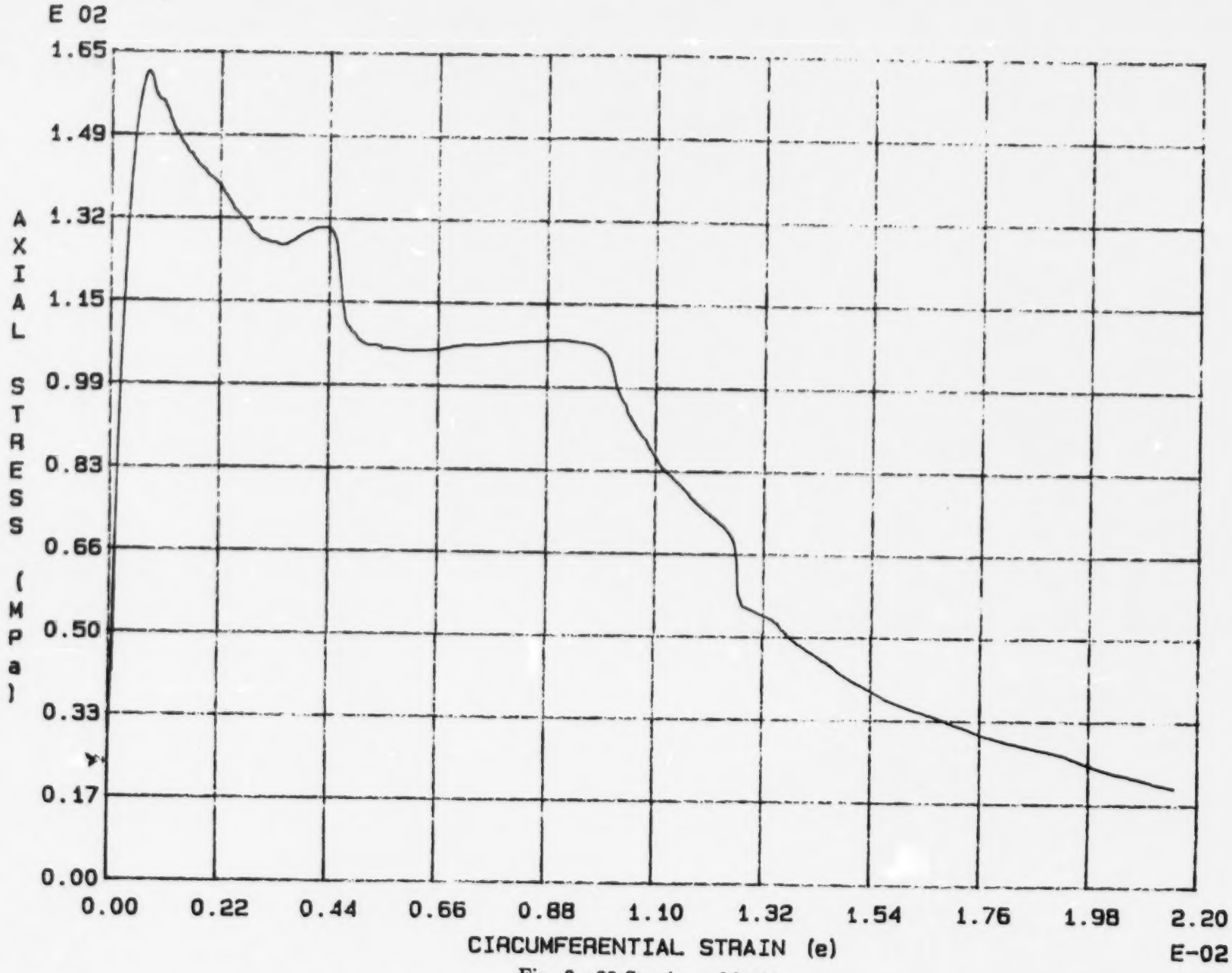

Fig. 3 - 28 Specimen M30U

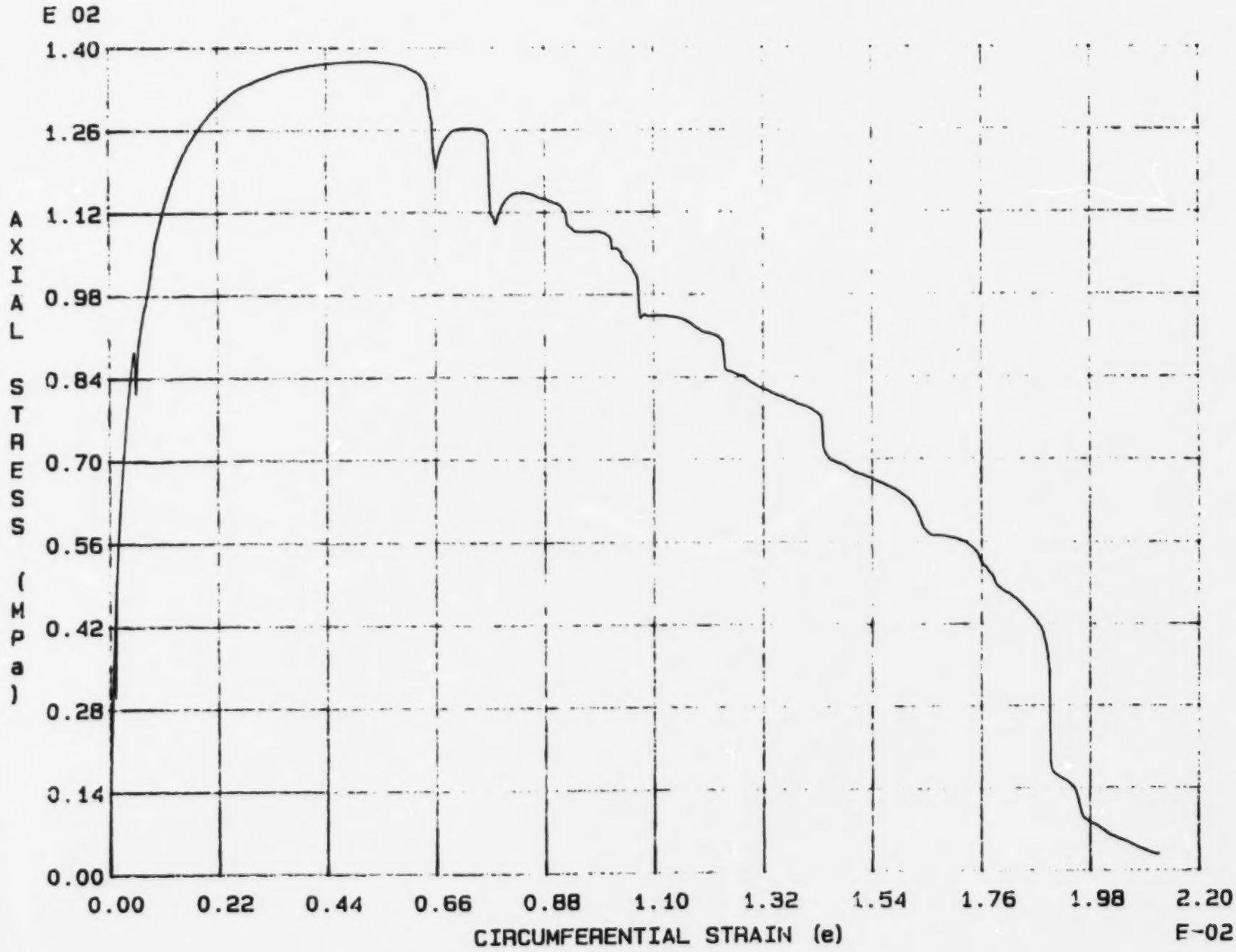

Fig. 3 - 29 Specimen M31U

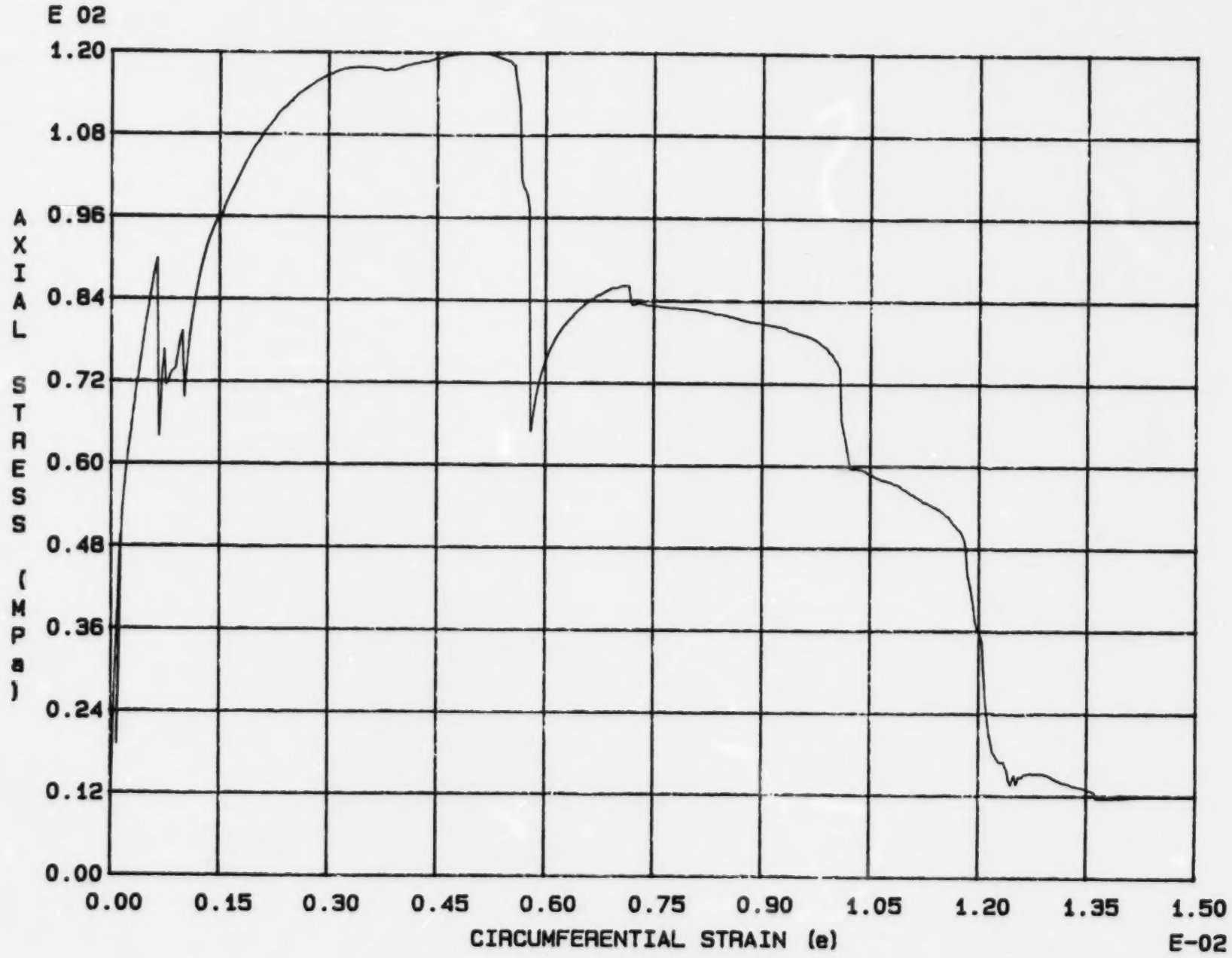

Fig. 3 - 30 Specimen M32U

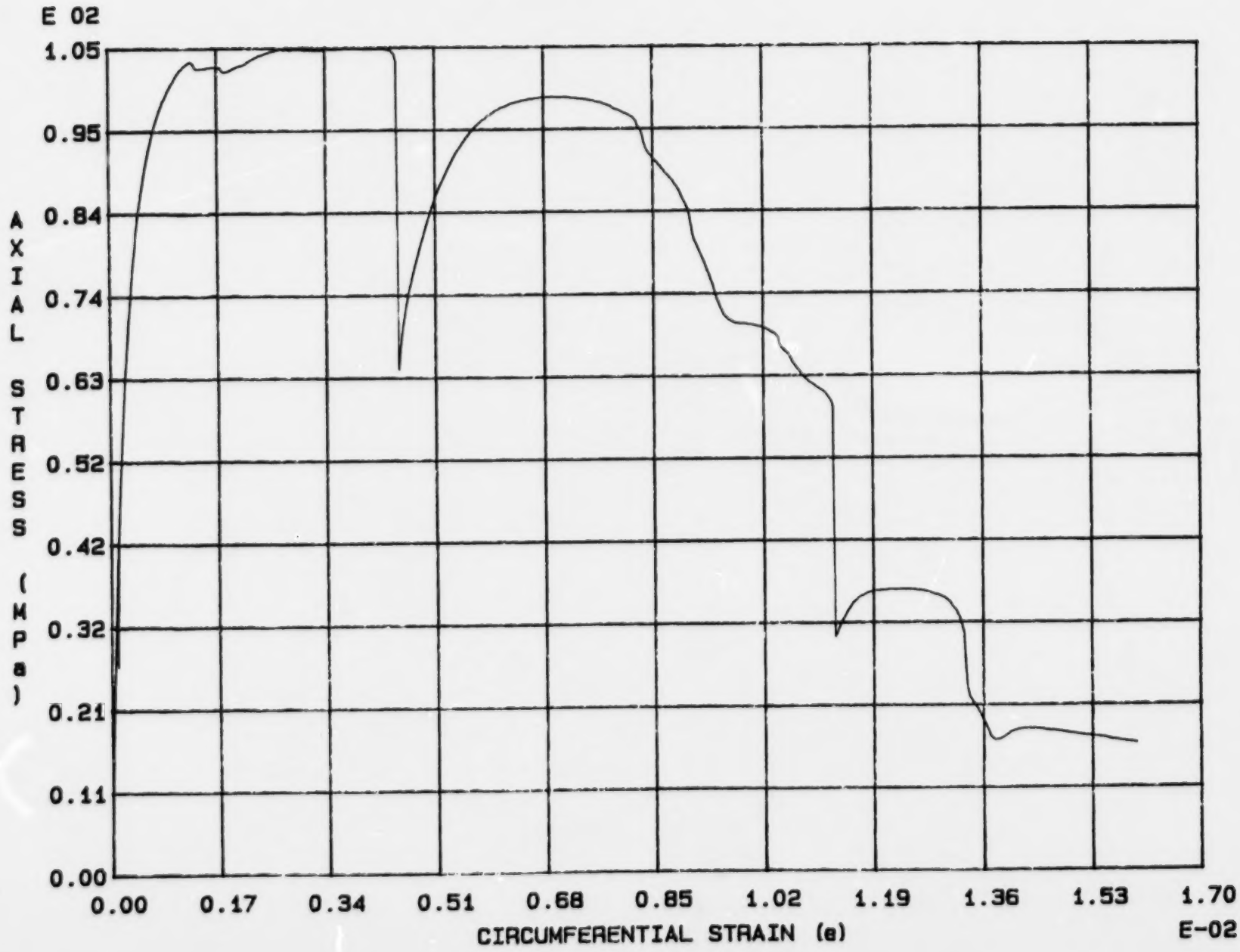

Fig. 3 - 31 Specimen M33U

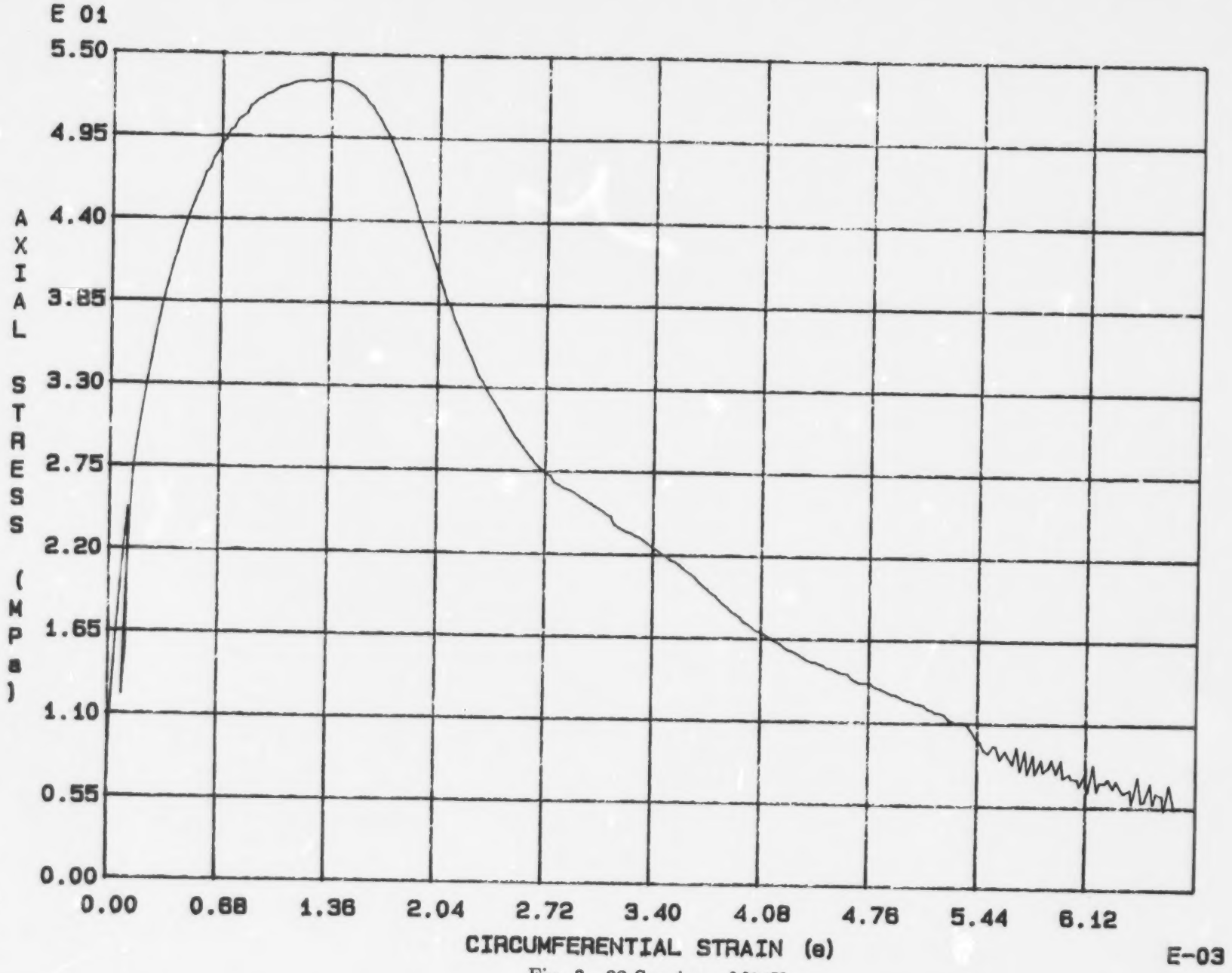

Fig. 3 - 32 Specimen M34U

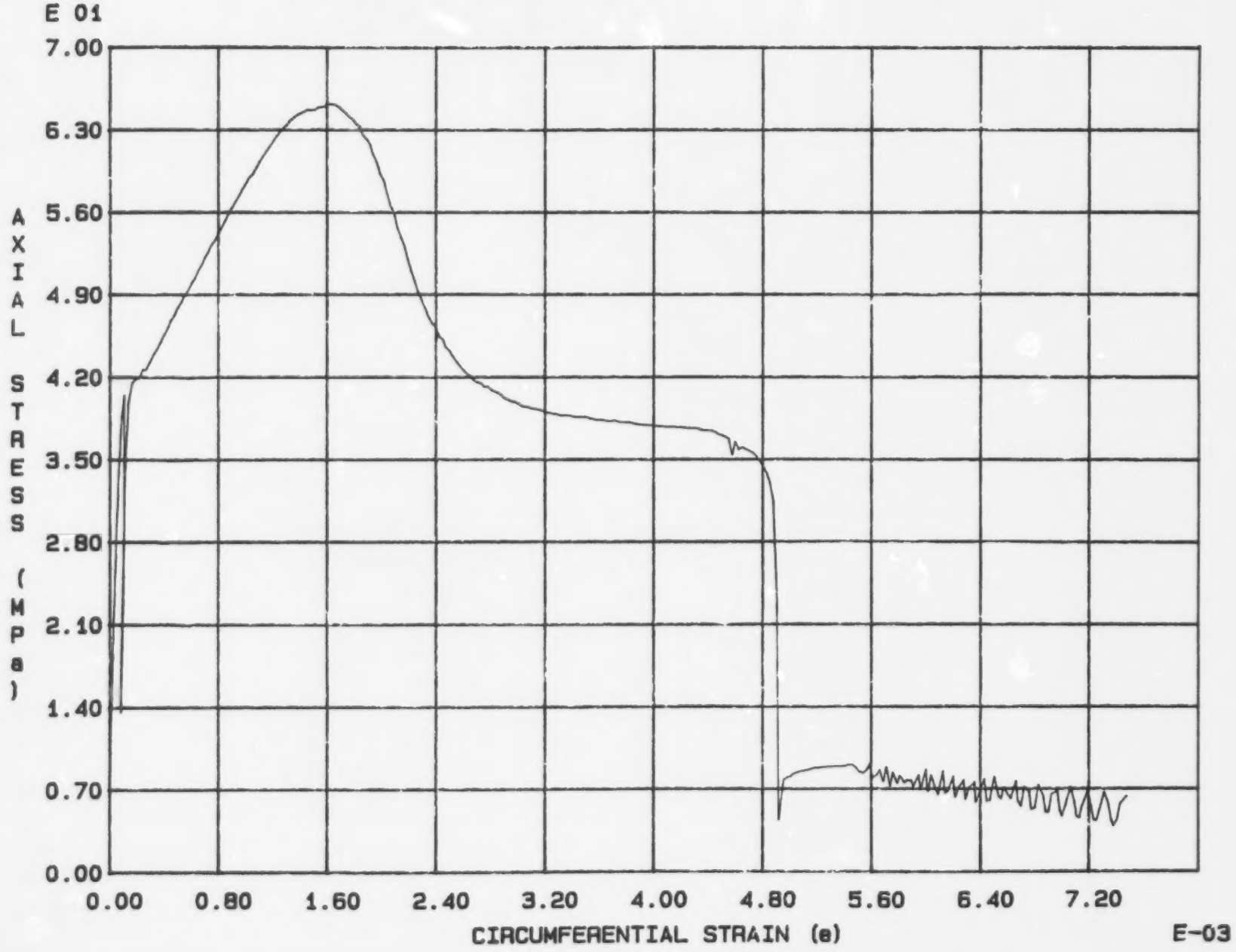

Fig. 3 - 33 Specimen M35U

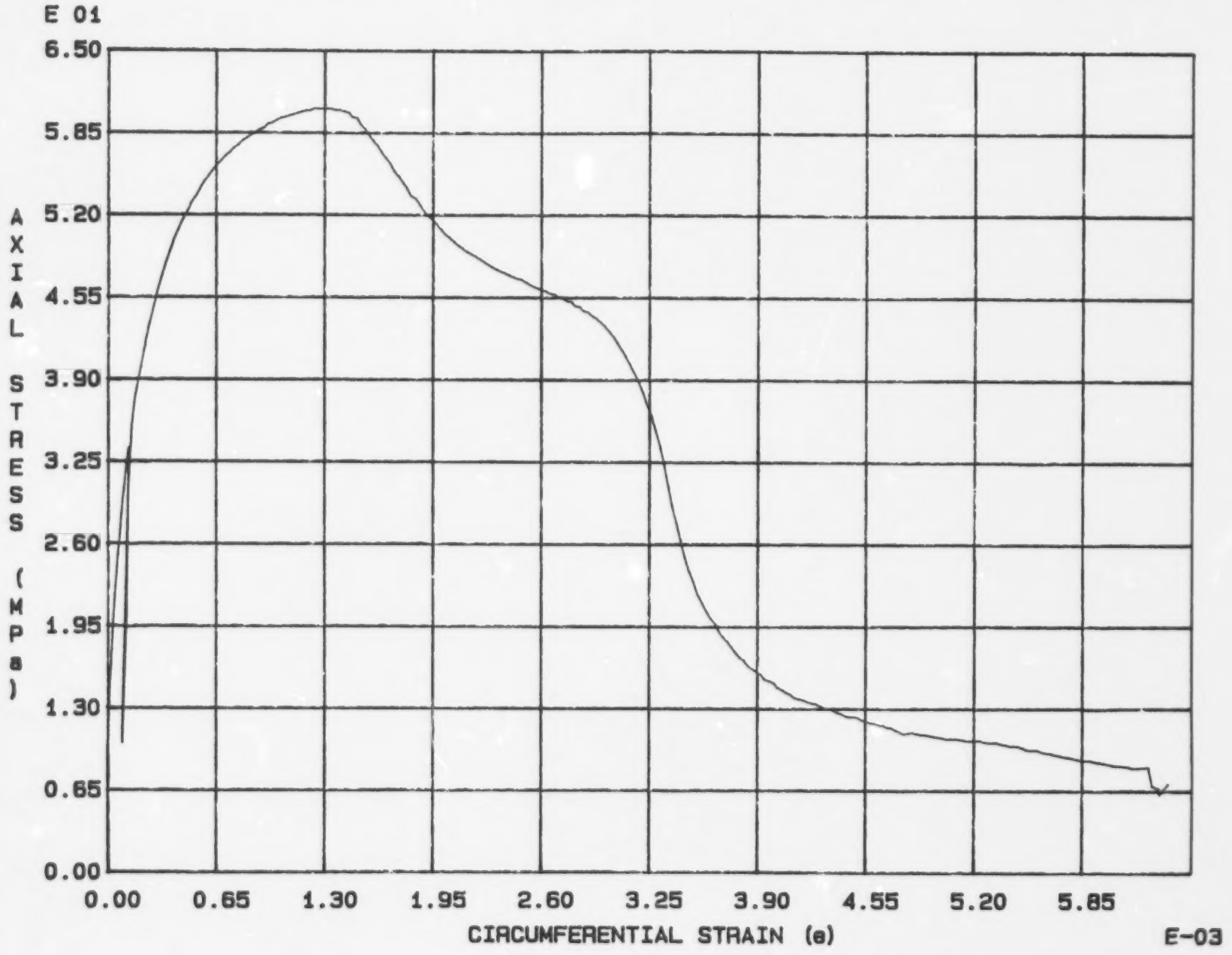

Fig. 3 - 34 Specimen M36U

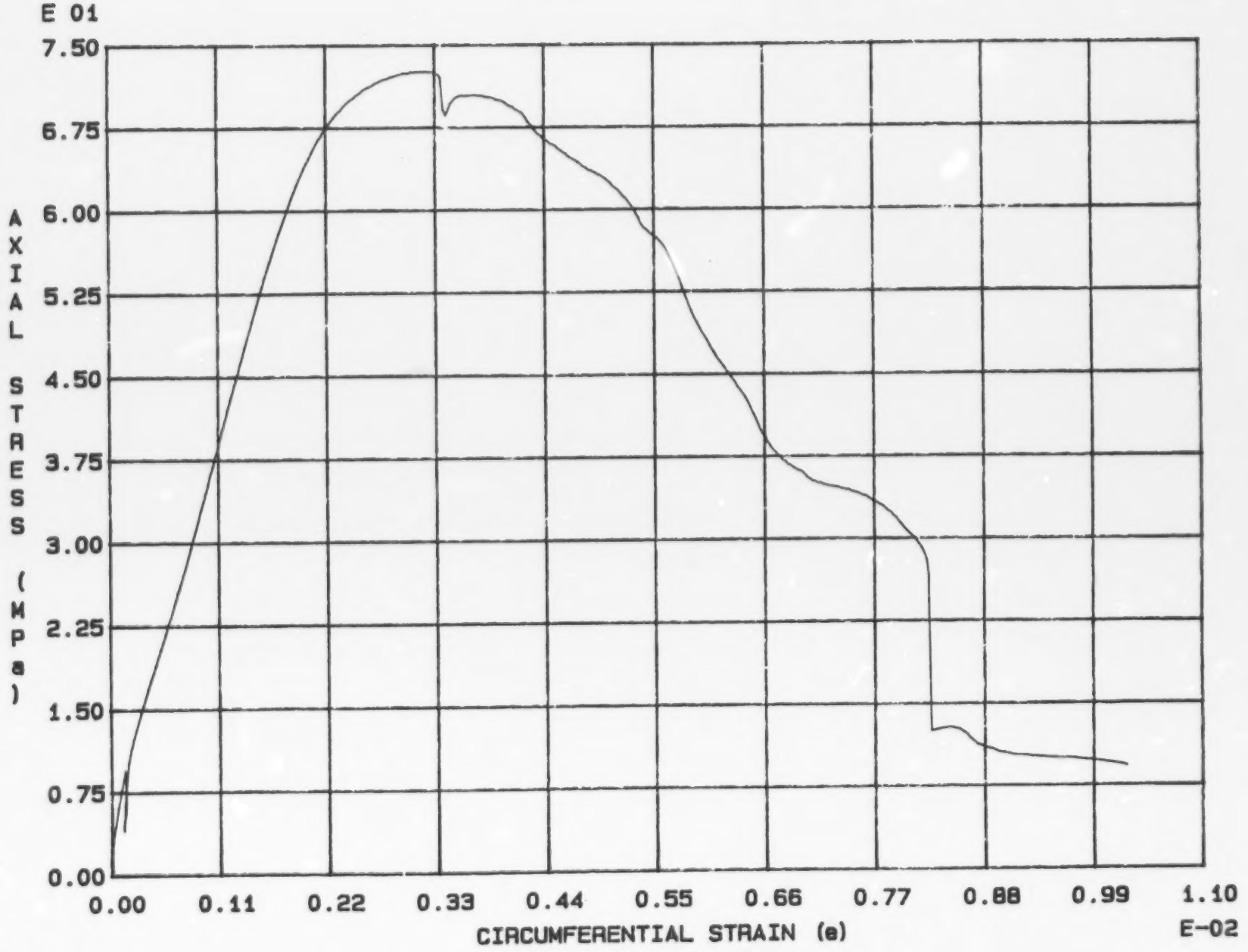

Fig. 3 - 35 Specimen M37U

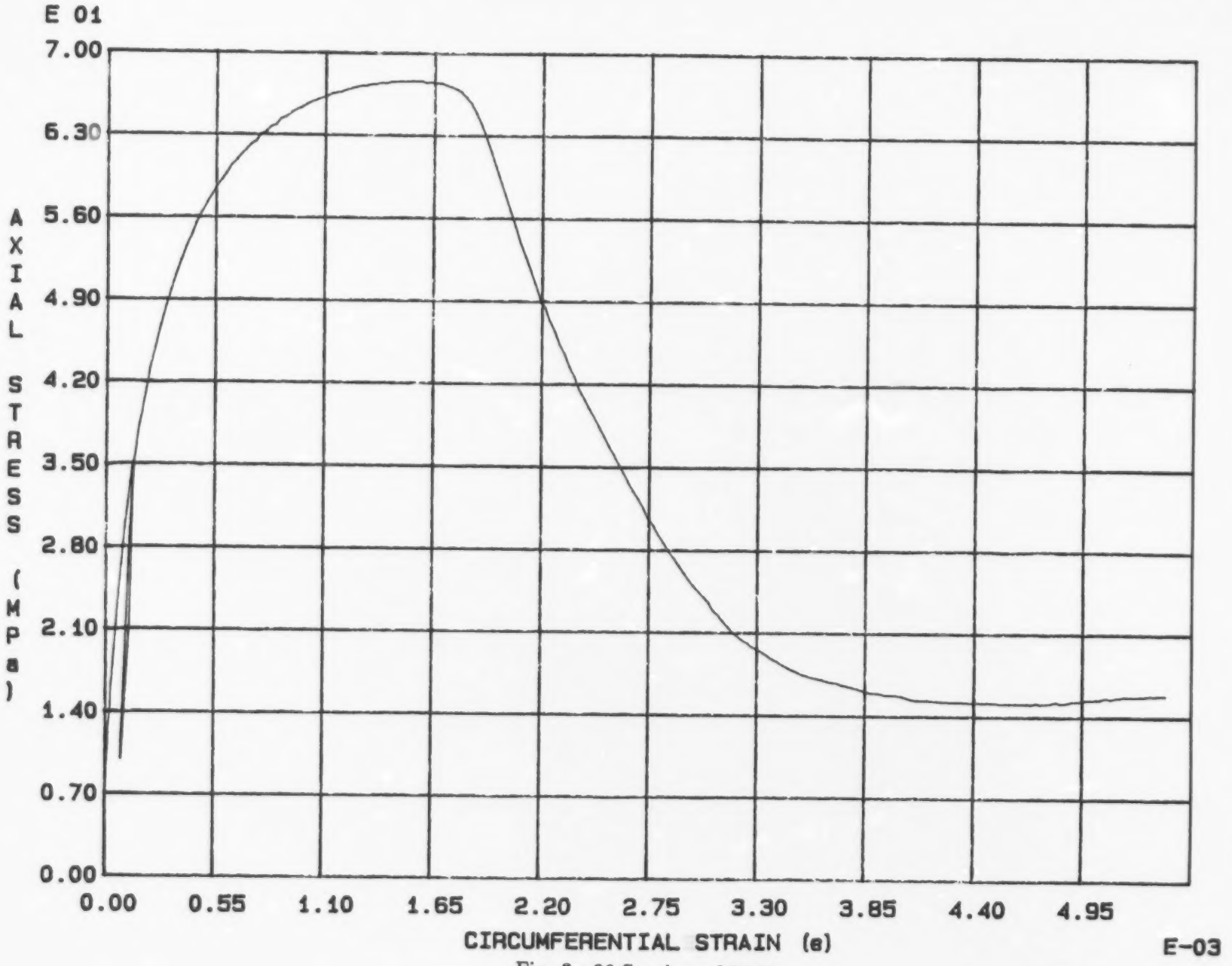

Fig. 3 - 36 Specimen M38U

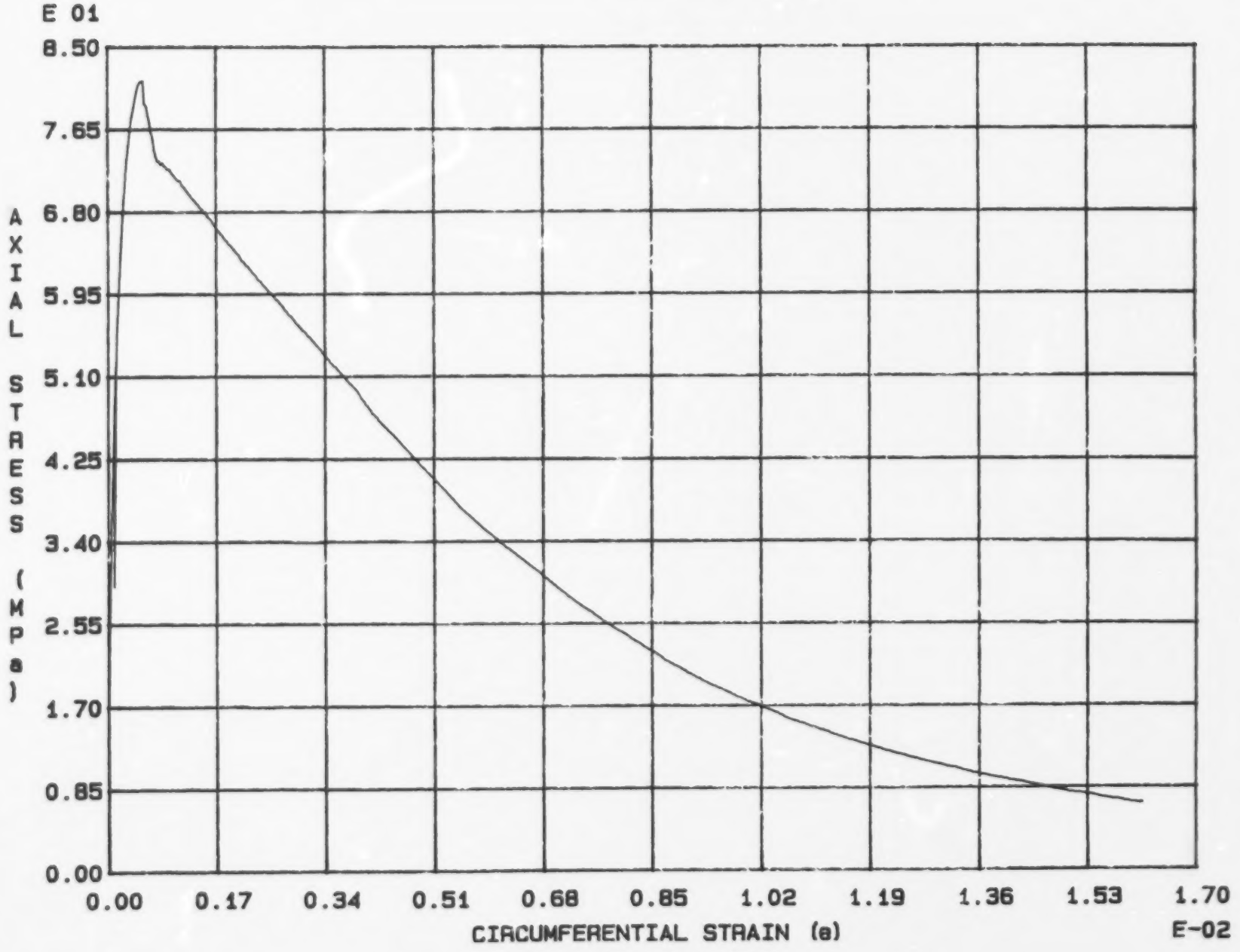

Fig. 3 - 37 Specimen M39U

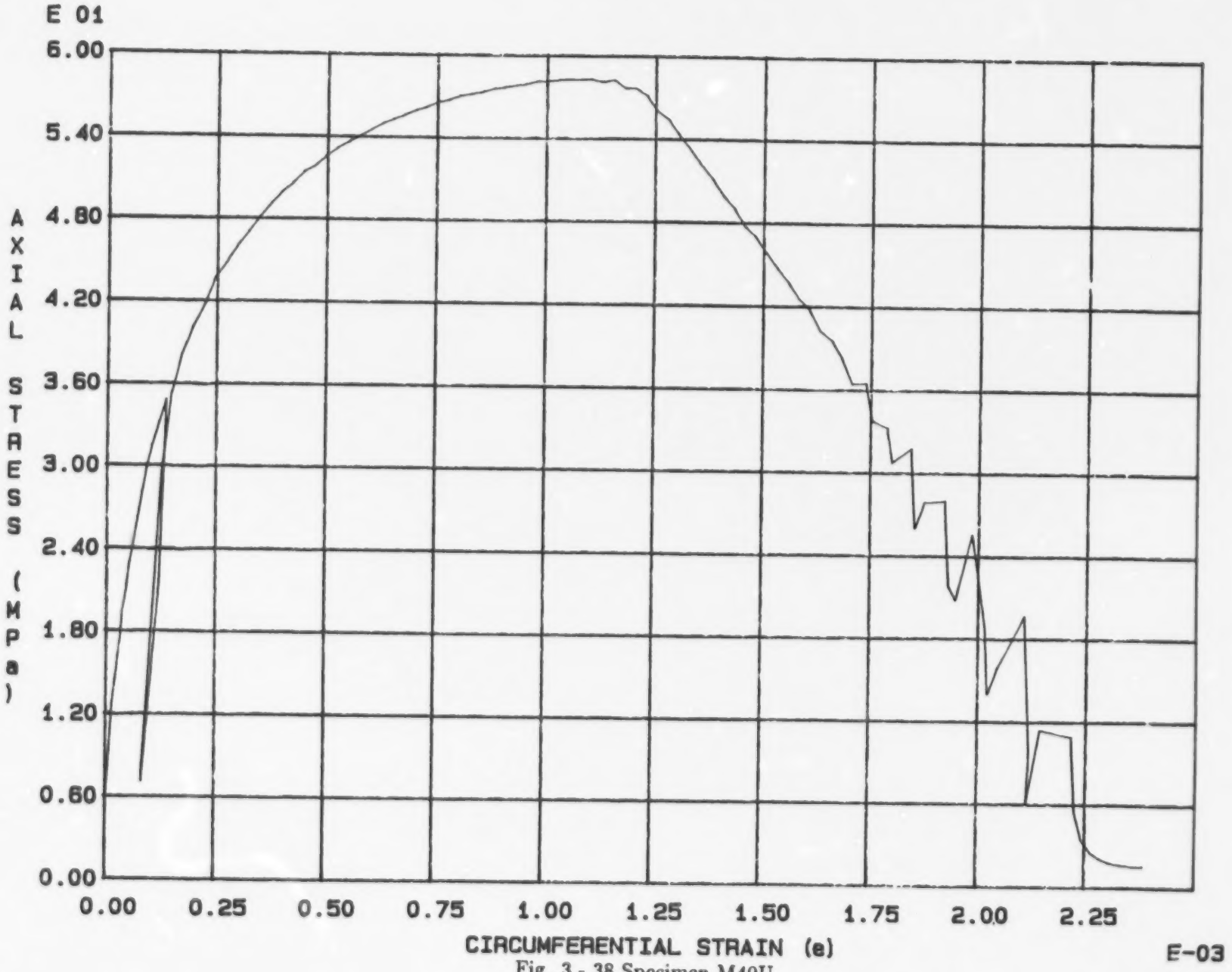

Fig. 3 - 38 Specimen M40U

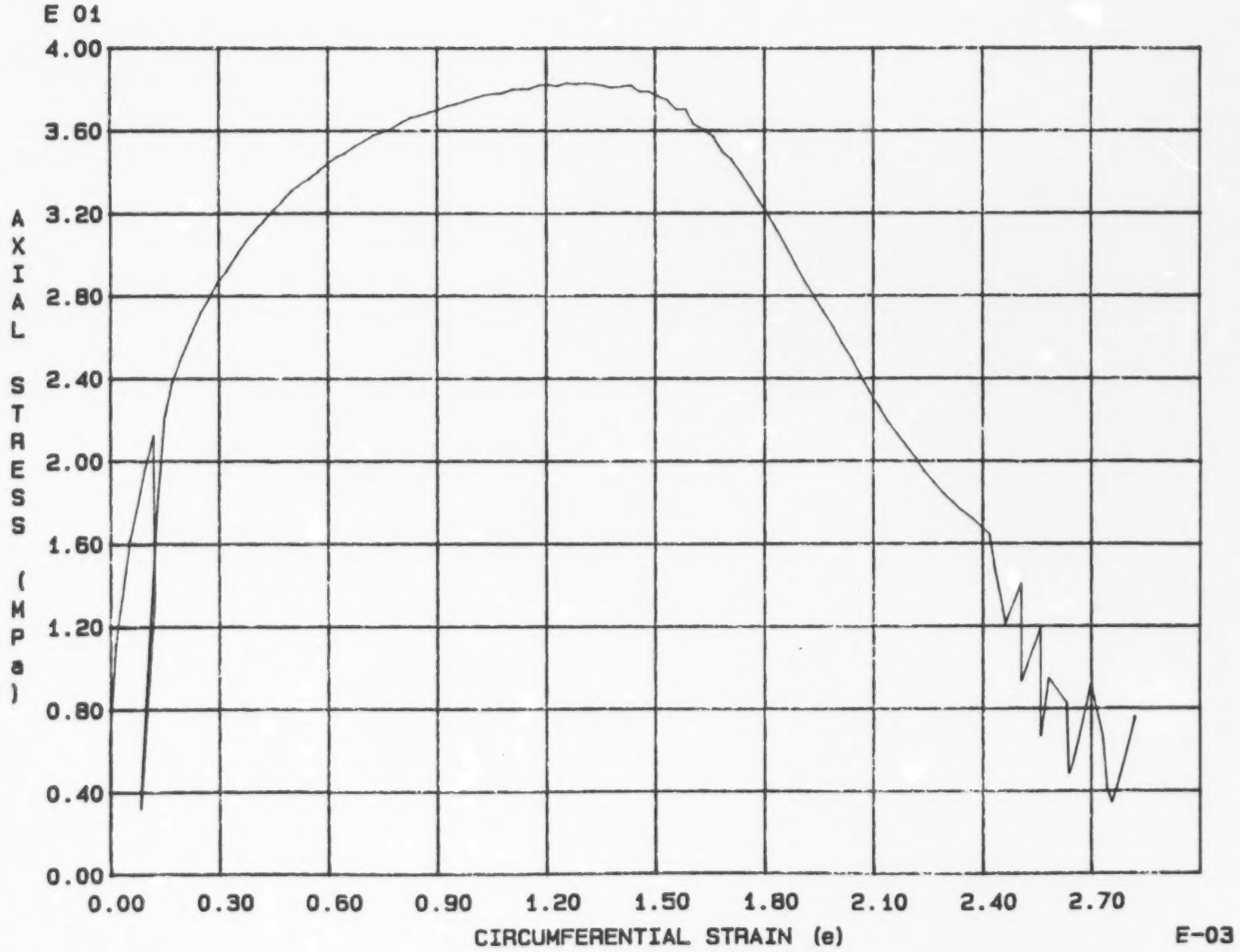

Fig. 3 - 39 Specimen M41U

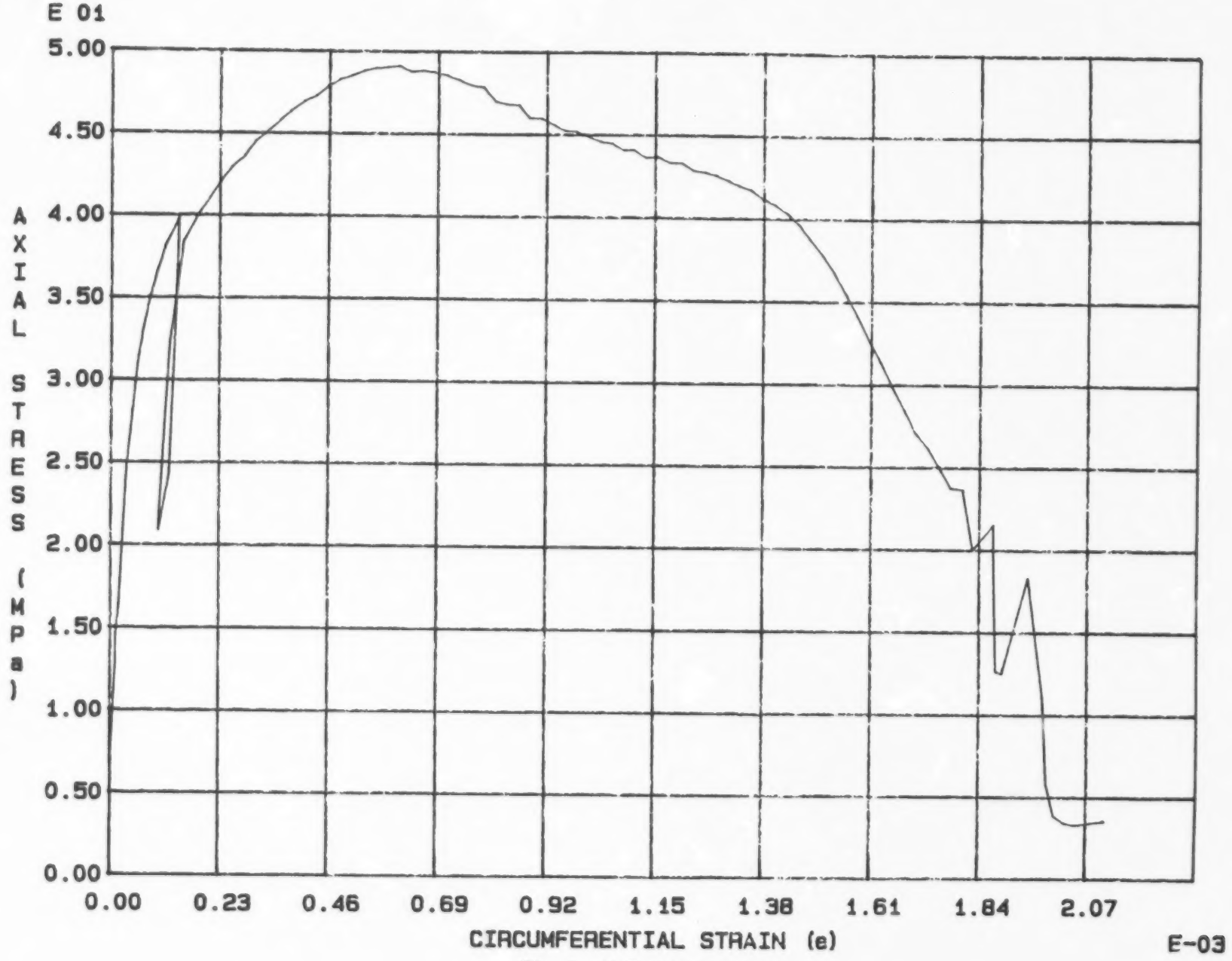

Fig. 3 - 40 Specimen M42U

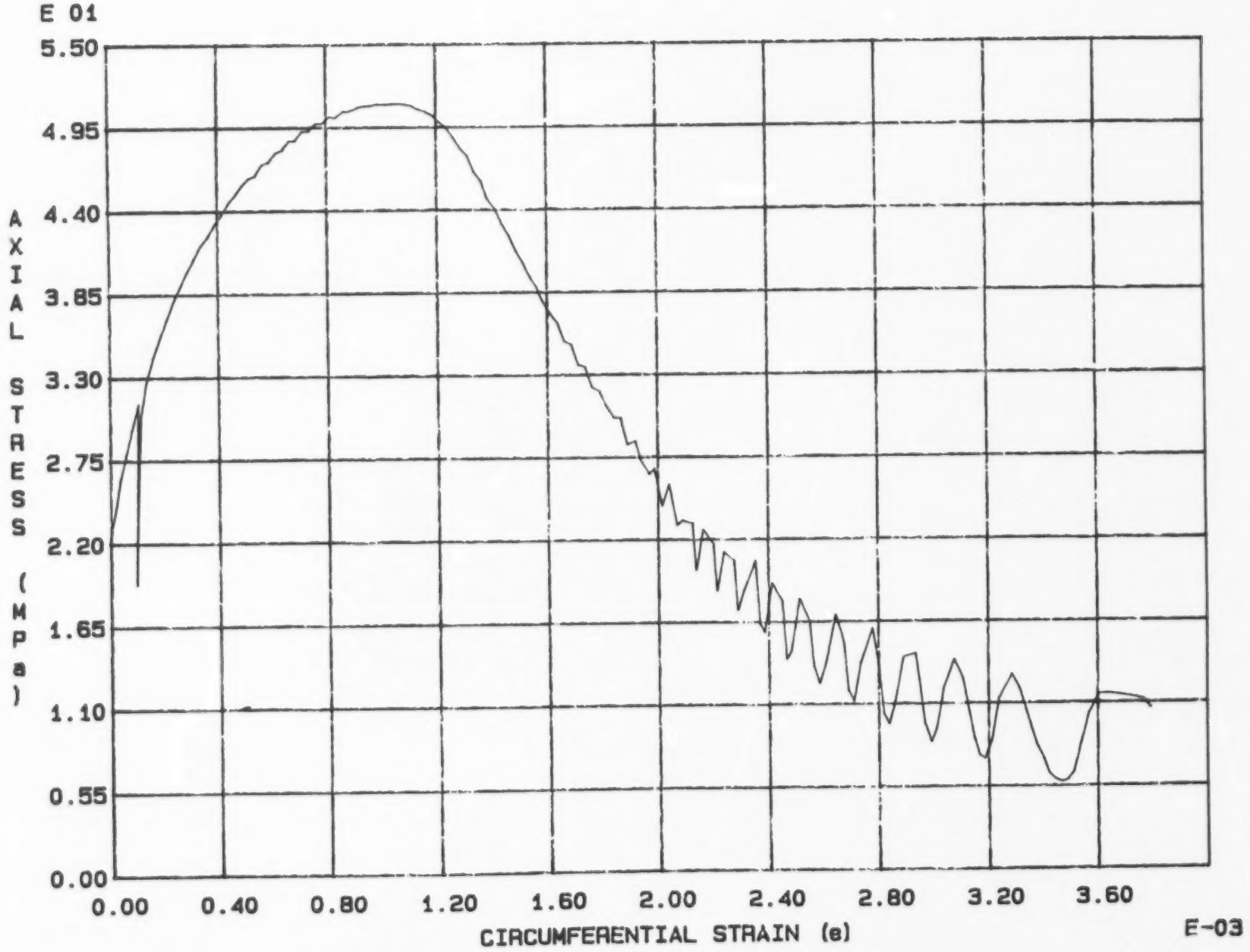

Fig. 3 - 41 Specimen M43U

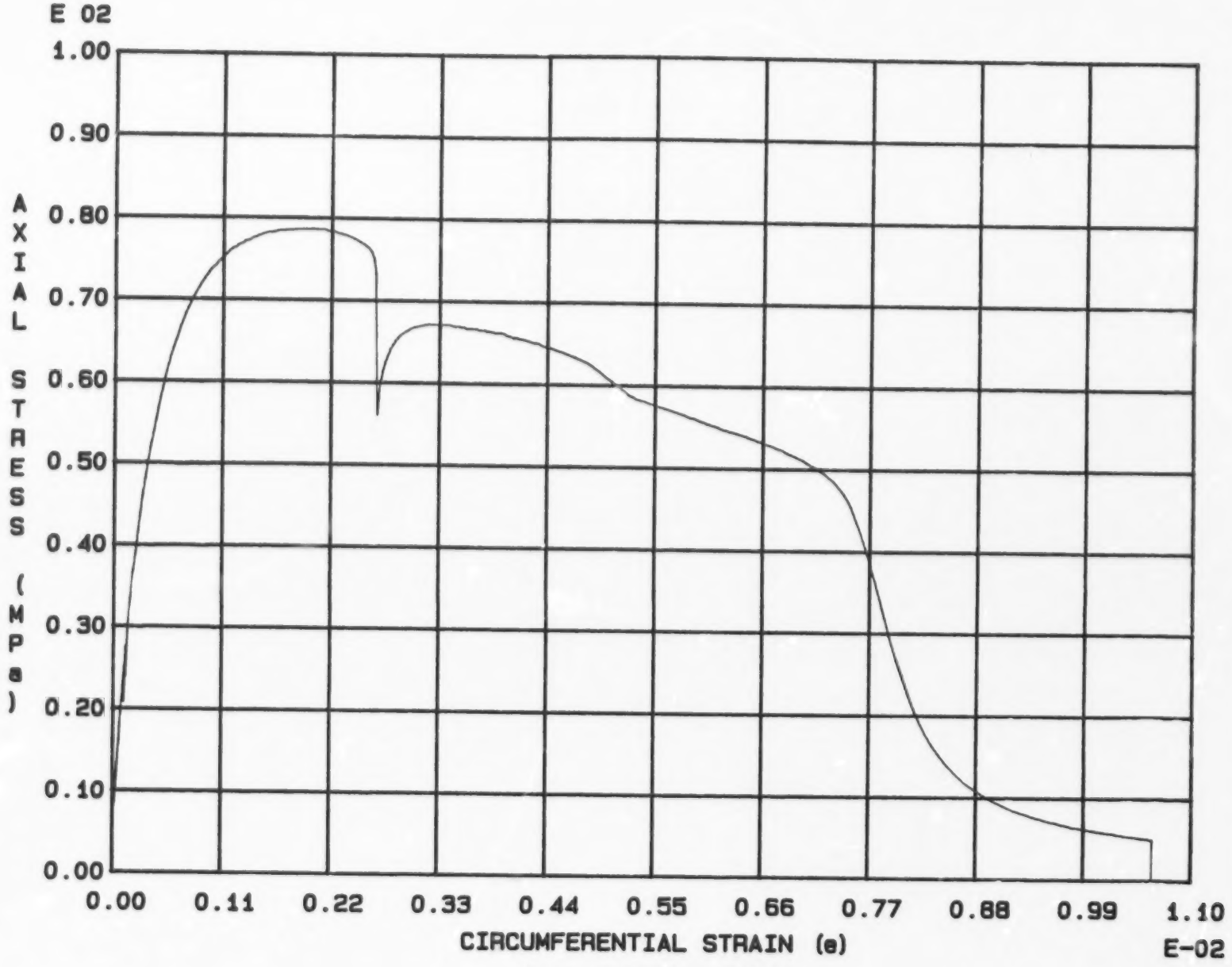

Fig. 3 - 42 Specimen M81U

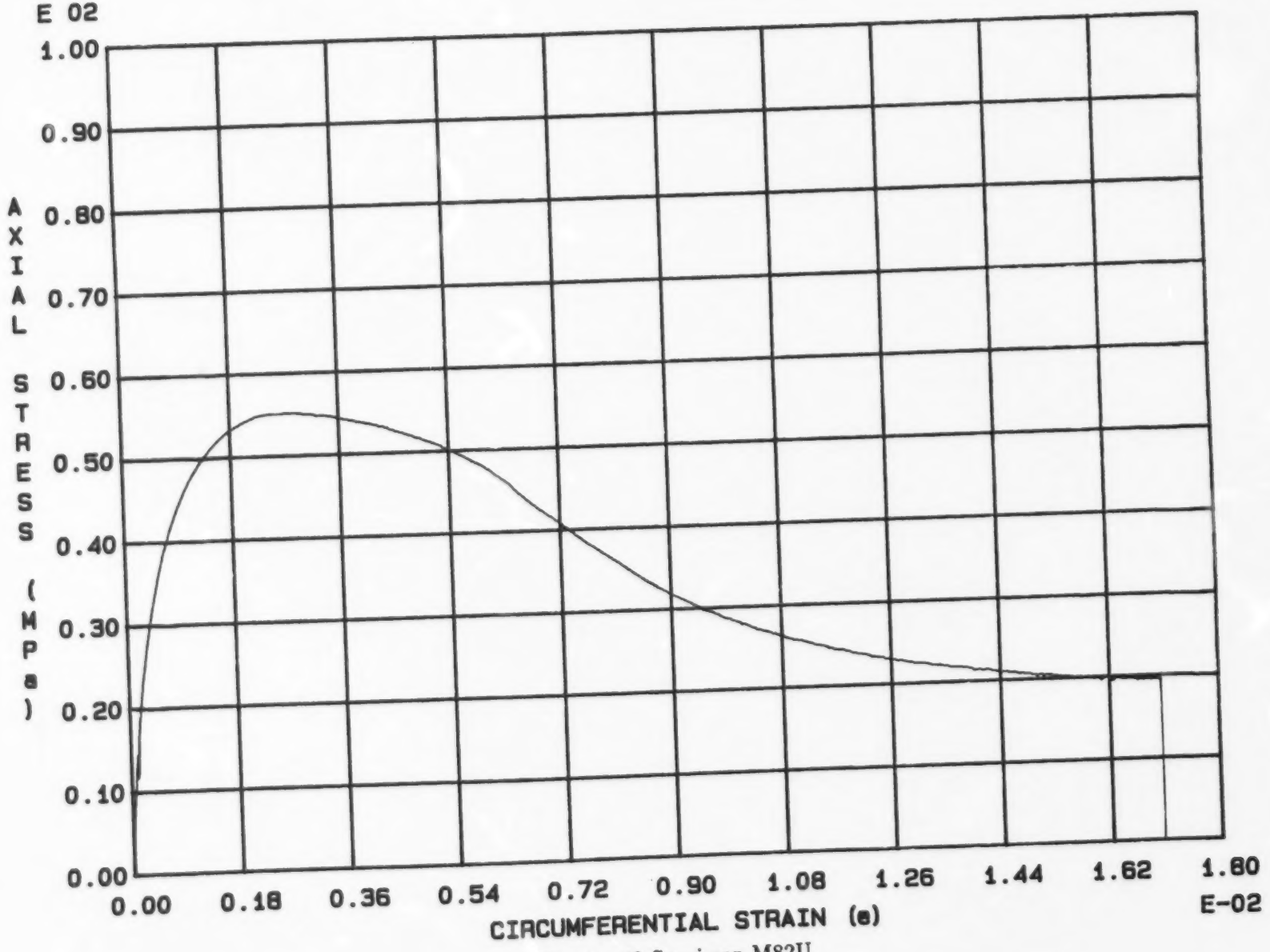

Fig. 3 - 43 Specimen M82U

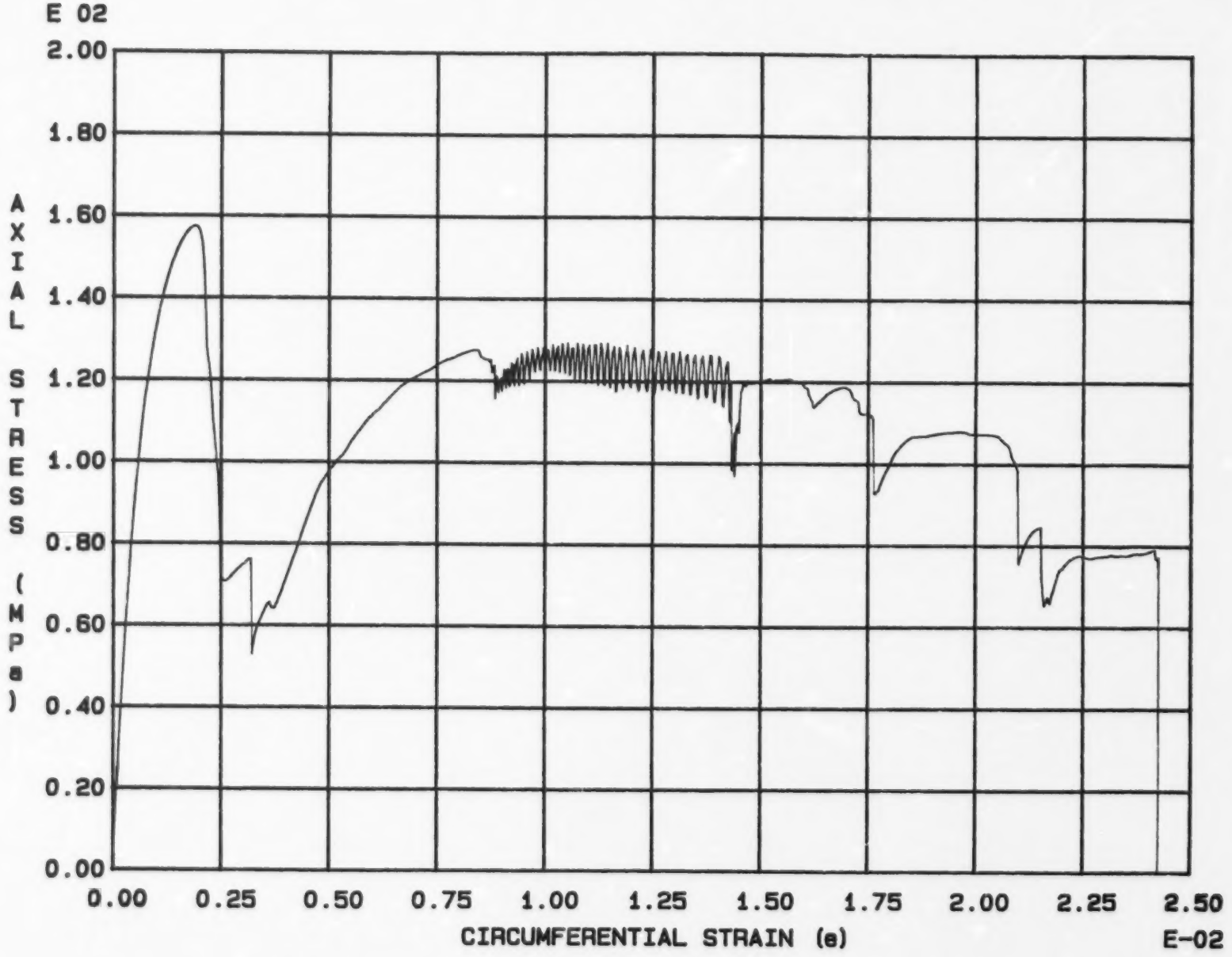

Fig. 3 - 44 Specimen M83U

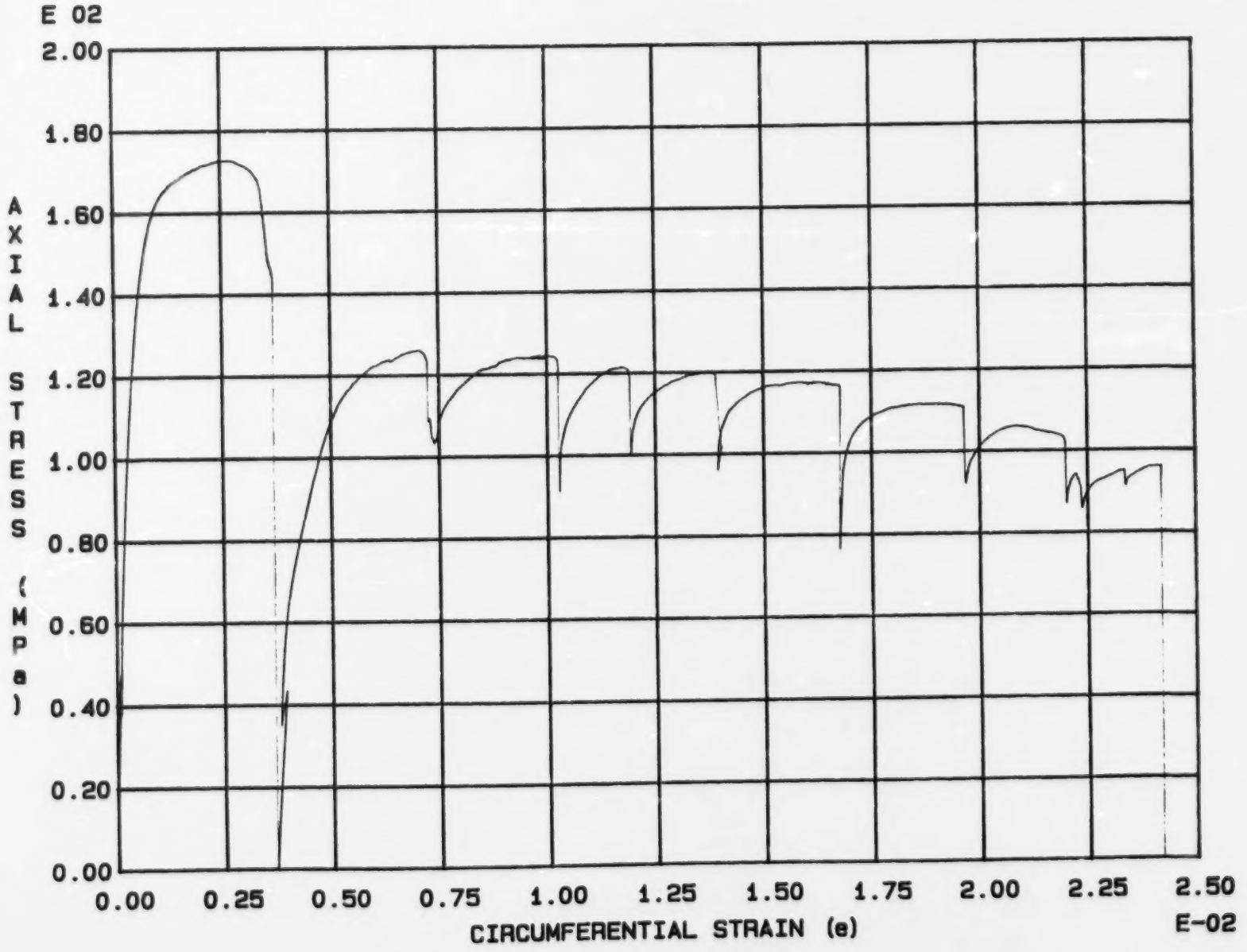

Fig. 3 - 45 Specimen M84U

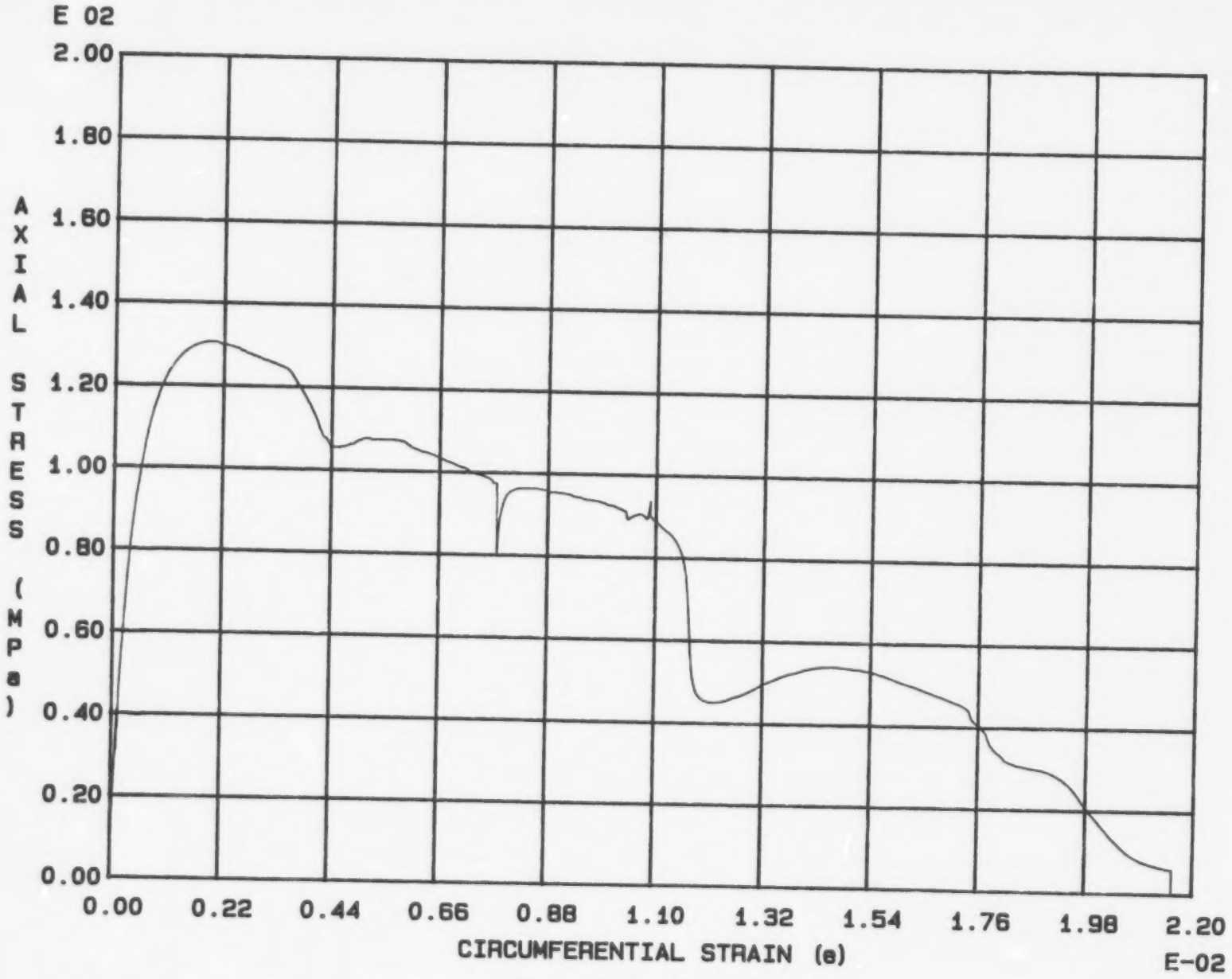

Fig. 3 - 46 Specimen M85U

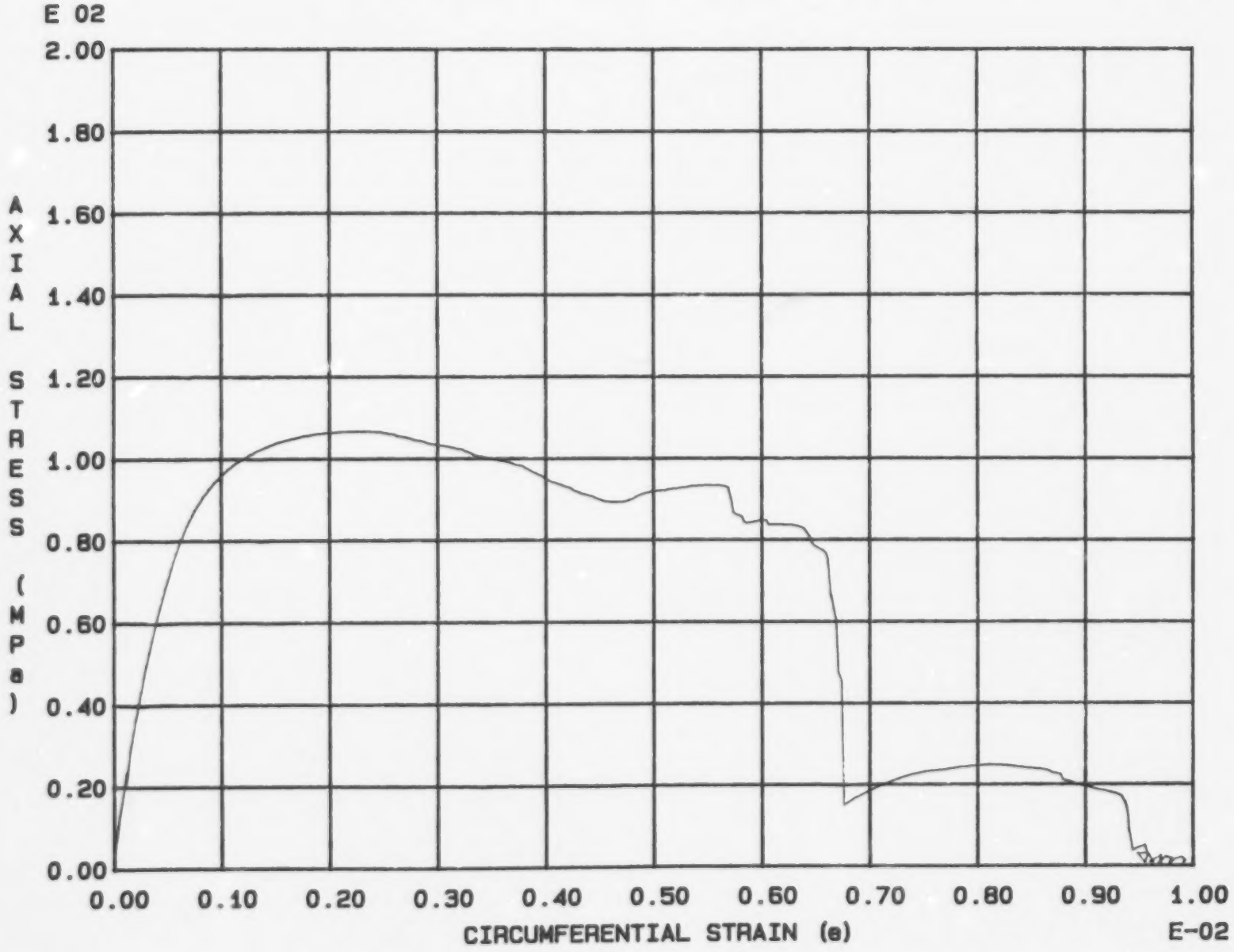

Fig. 3 - 47 Specimen M86U

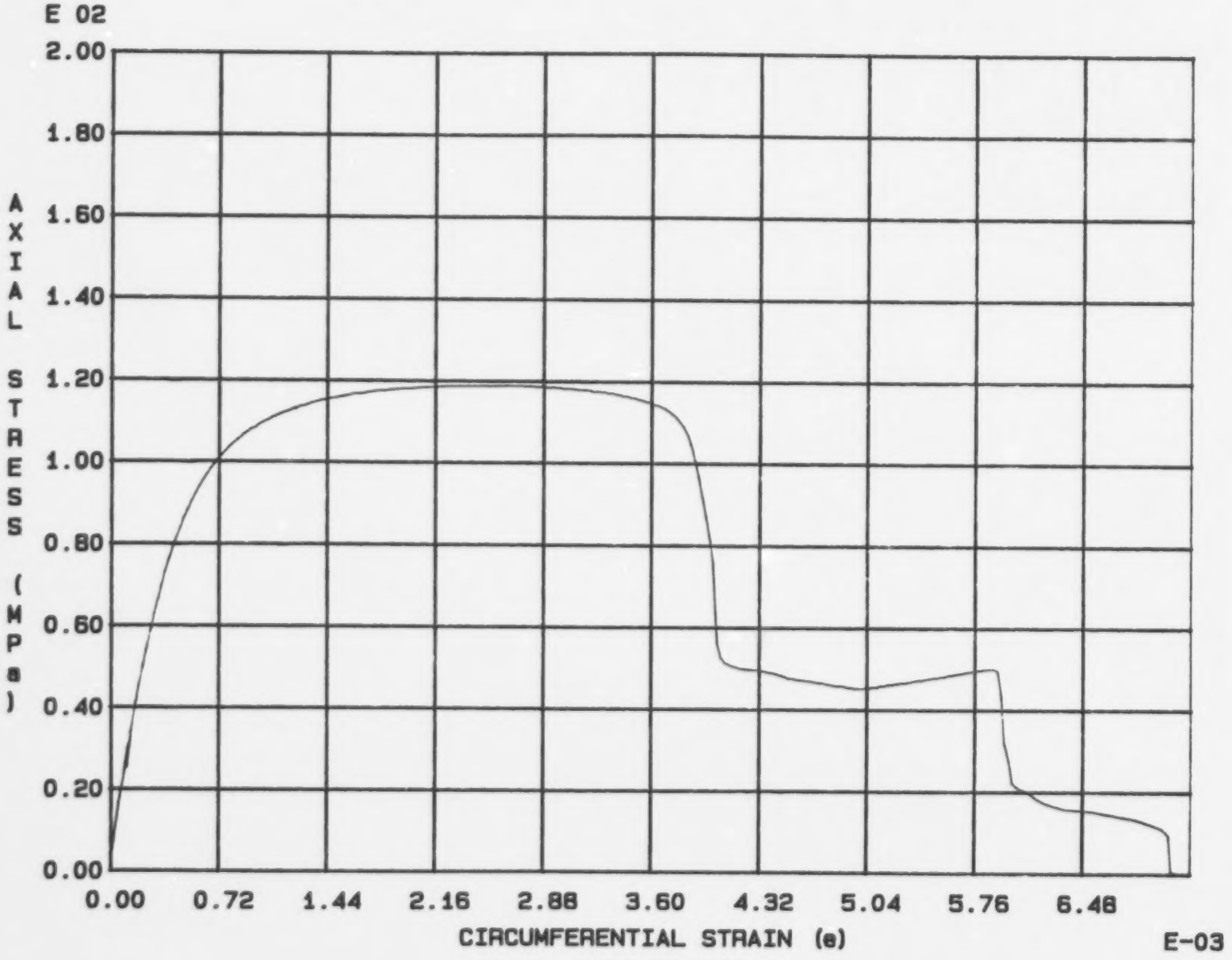

Fig. 3 - 48 Specimen M87U

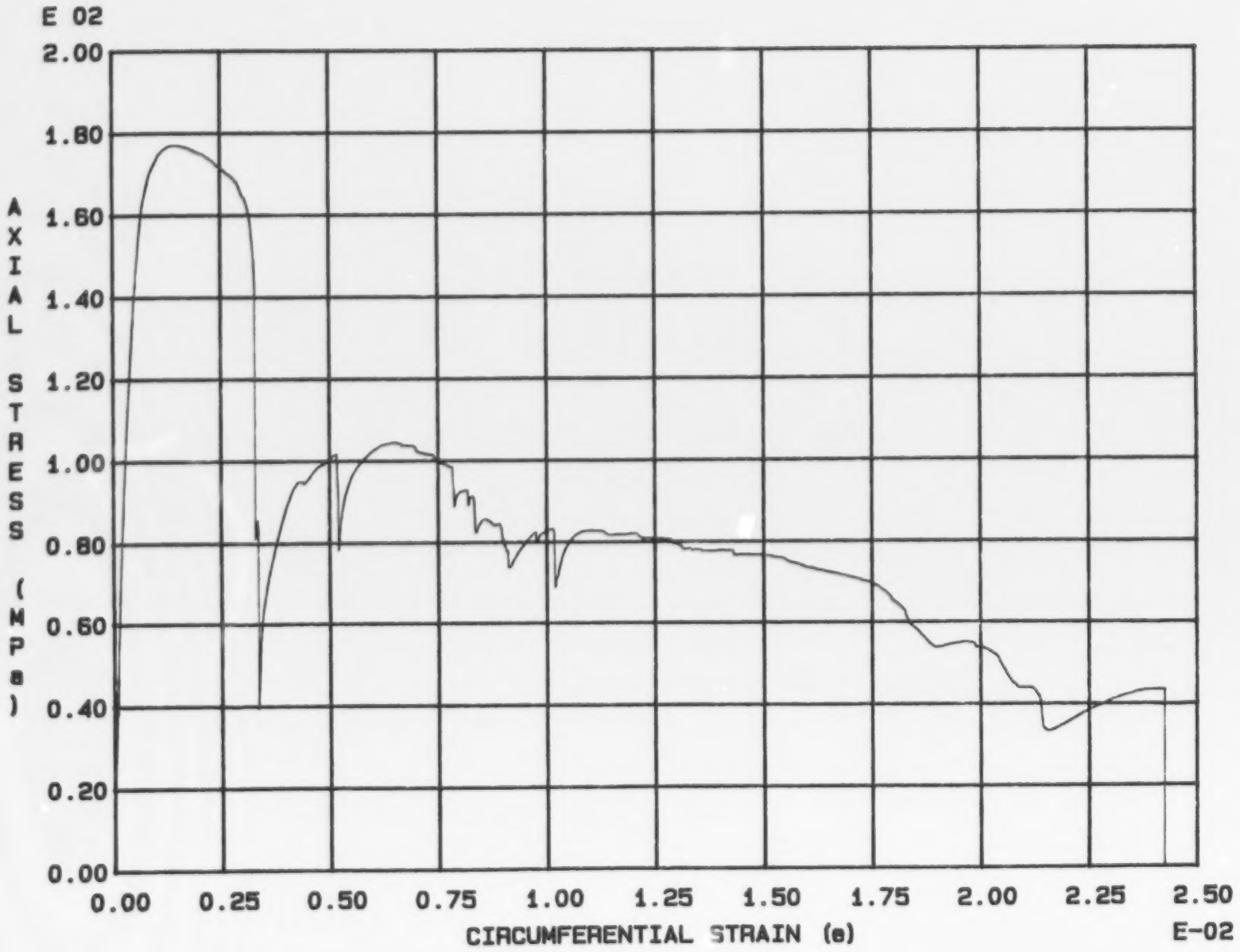

Fig. 3 - 49 Specimen M88U

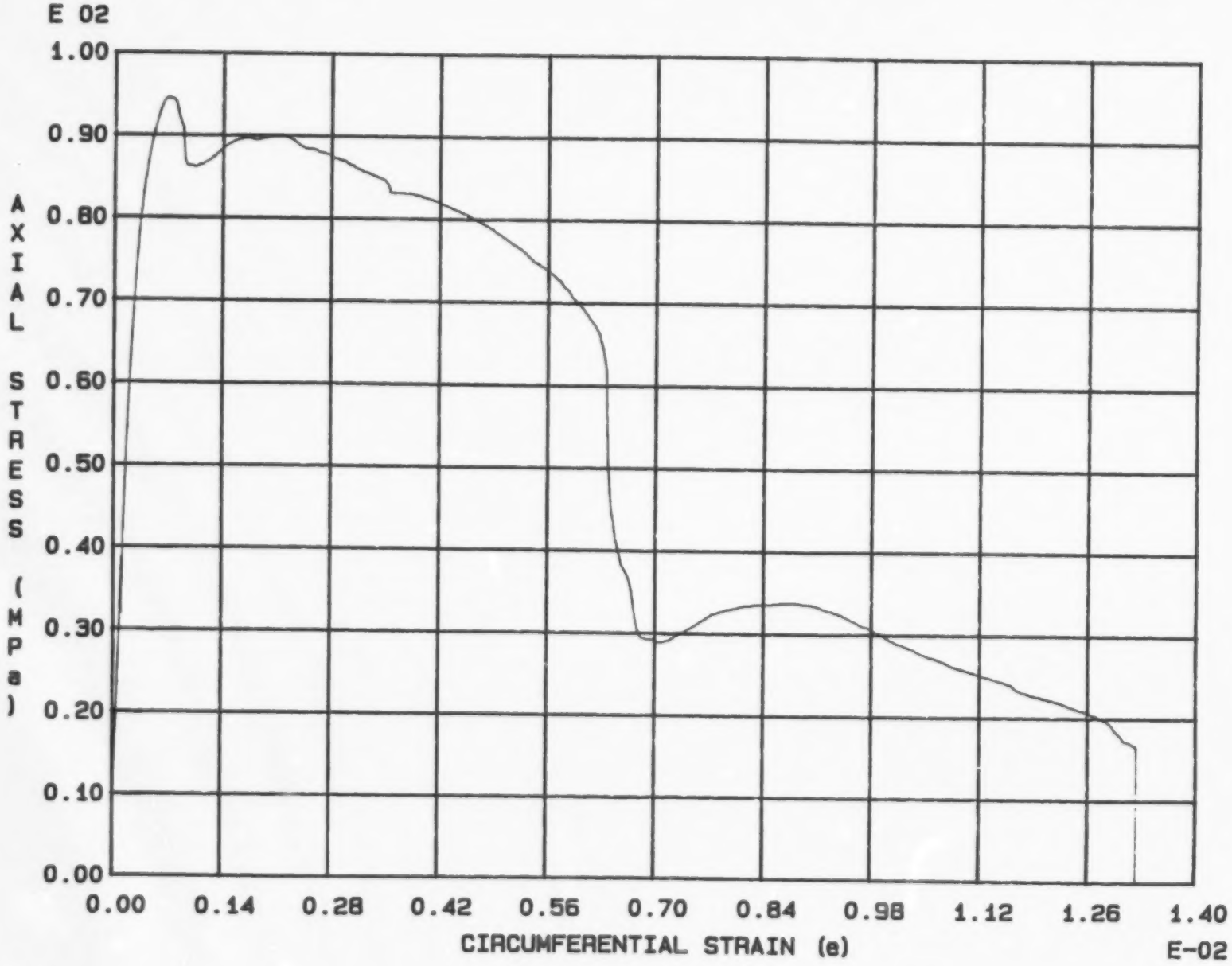

Fig. 3 - 50 Specimen M89U

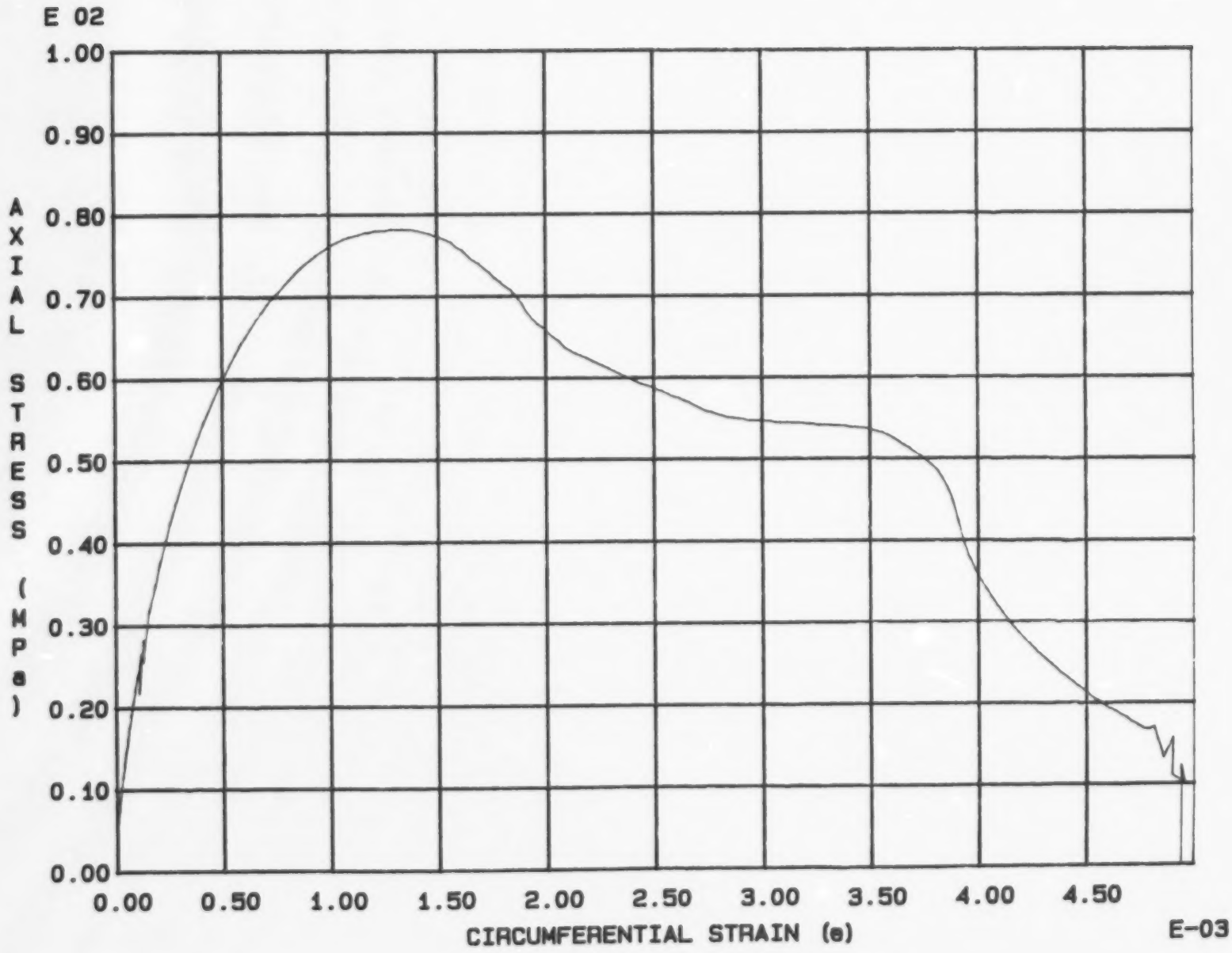

Fig. 3 - 51 Specimen M90U

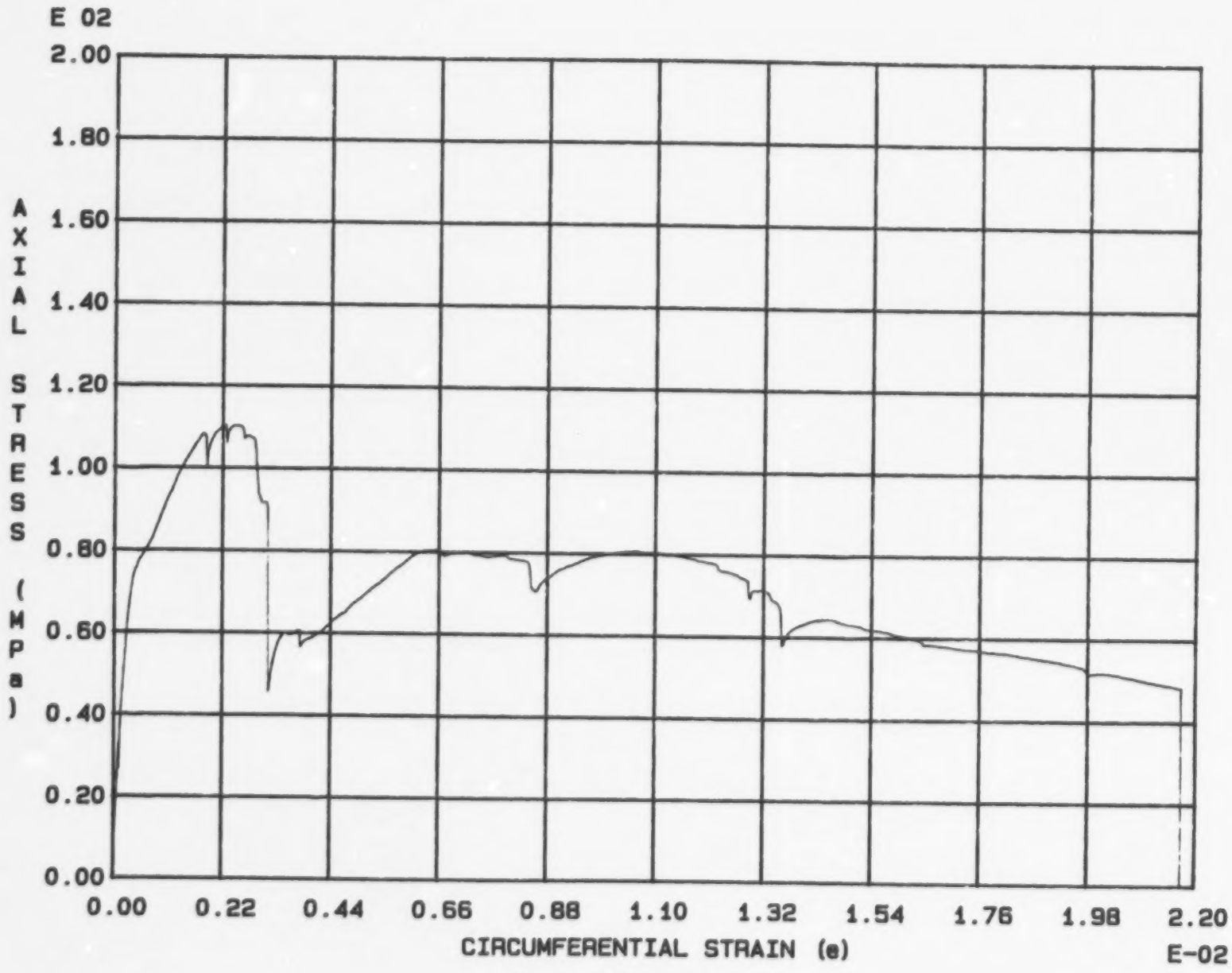

Fig. 3 - 52 Specimen M91U

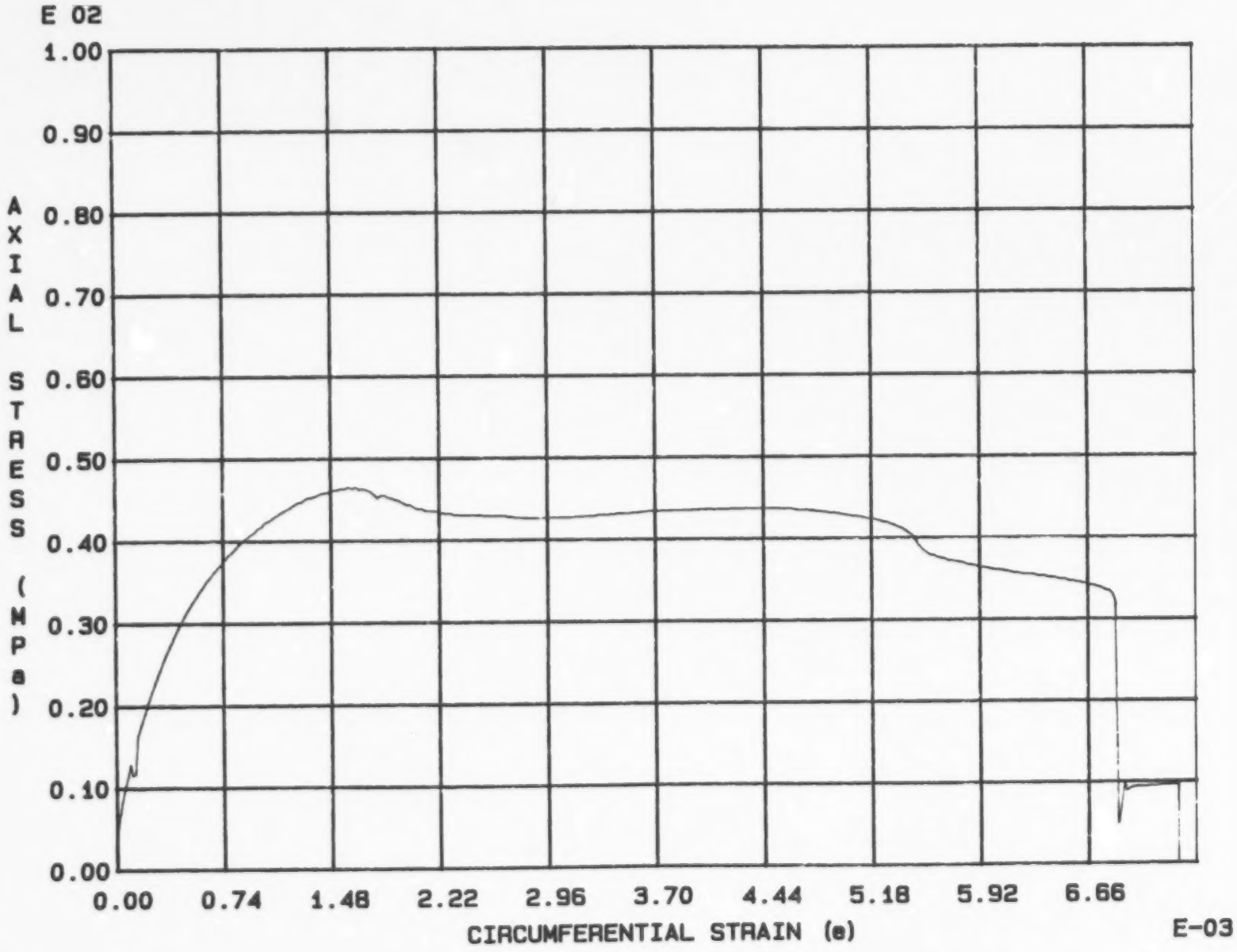

Fig. 3 - 53 Specimen M92U

Appendix 4.

Stress-strain curves of uniaxial tests using circumferential strain gauges

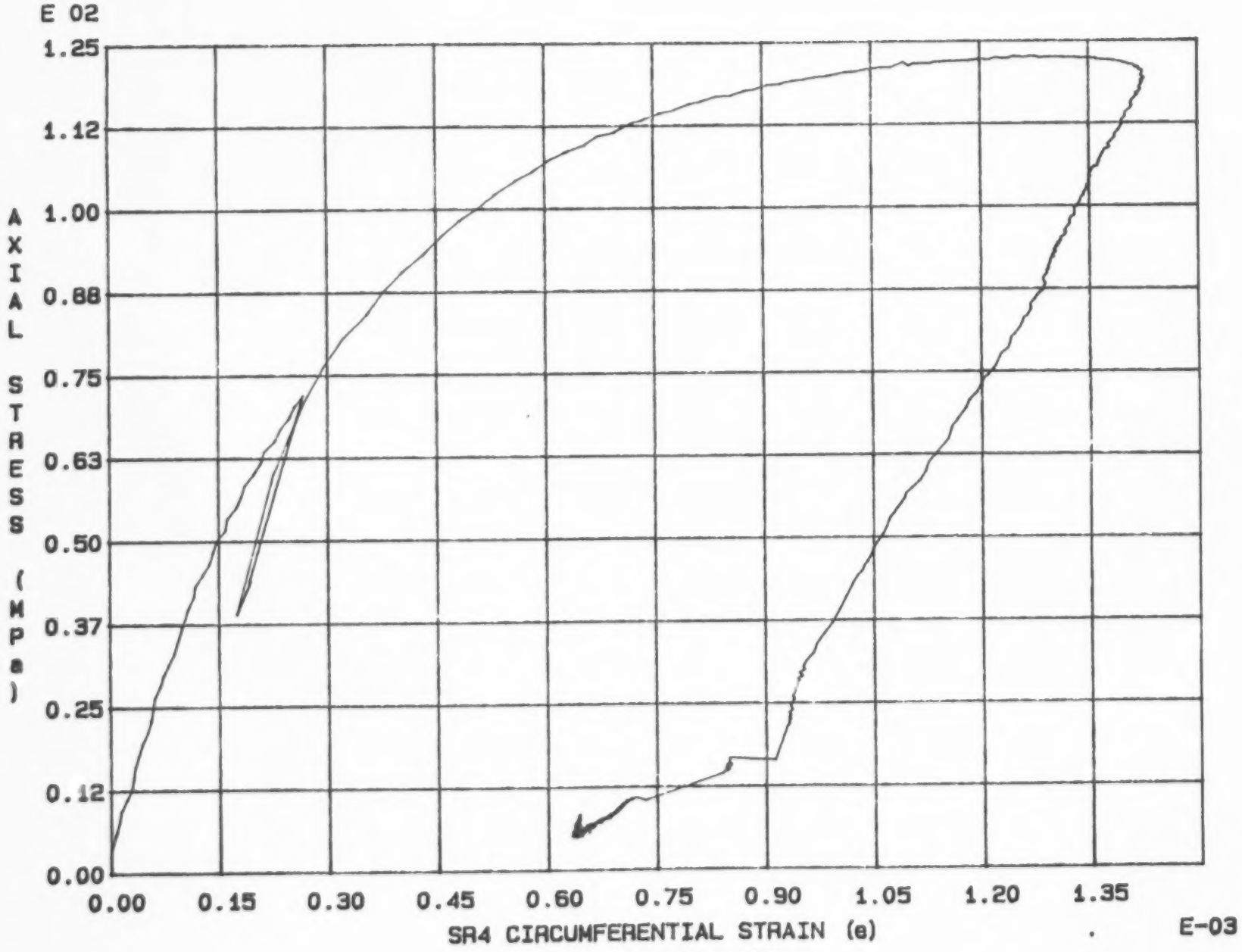

Fig. 4 - 1 Specimen M3U

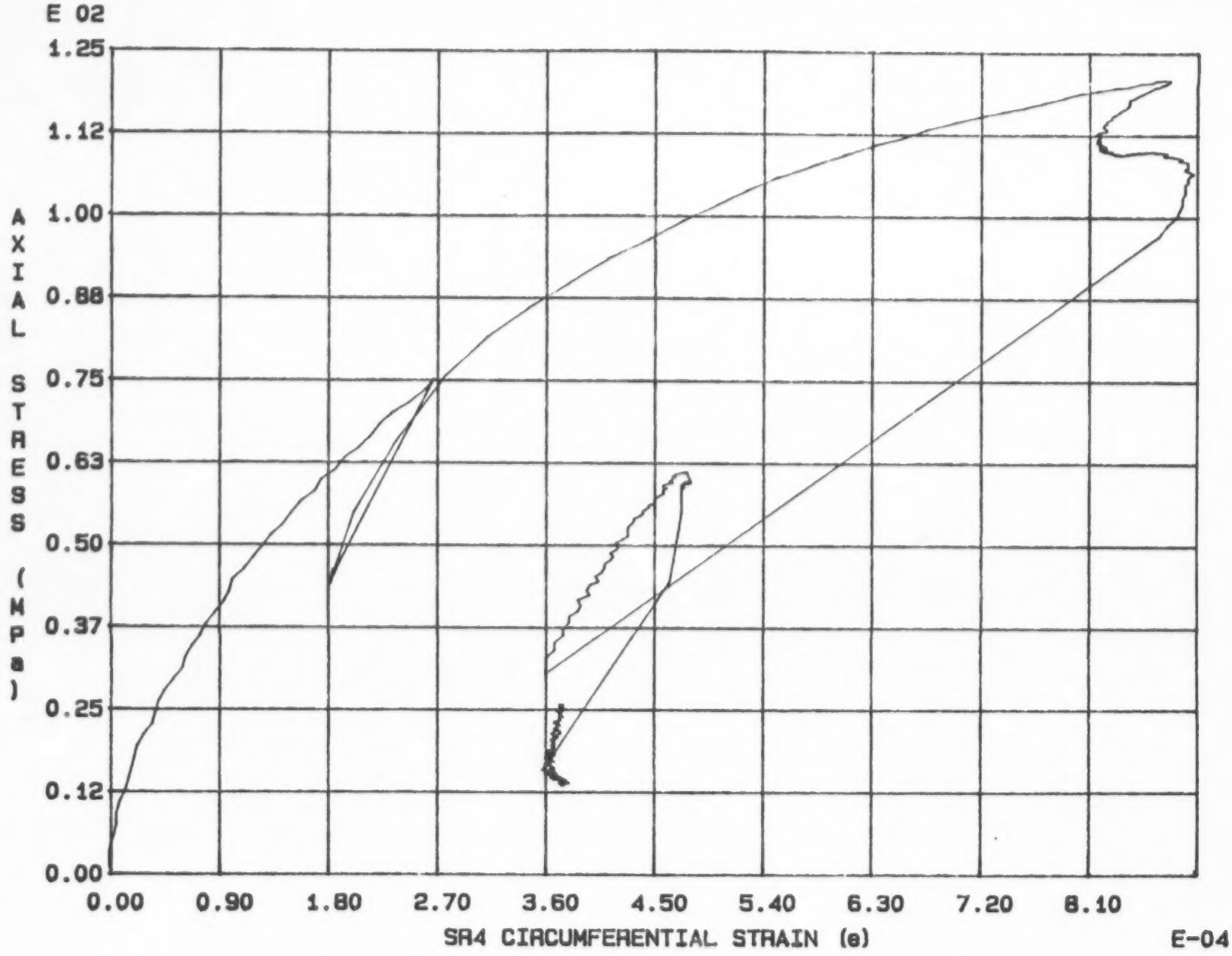

Fig. 4 - 2 Specimen M4U

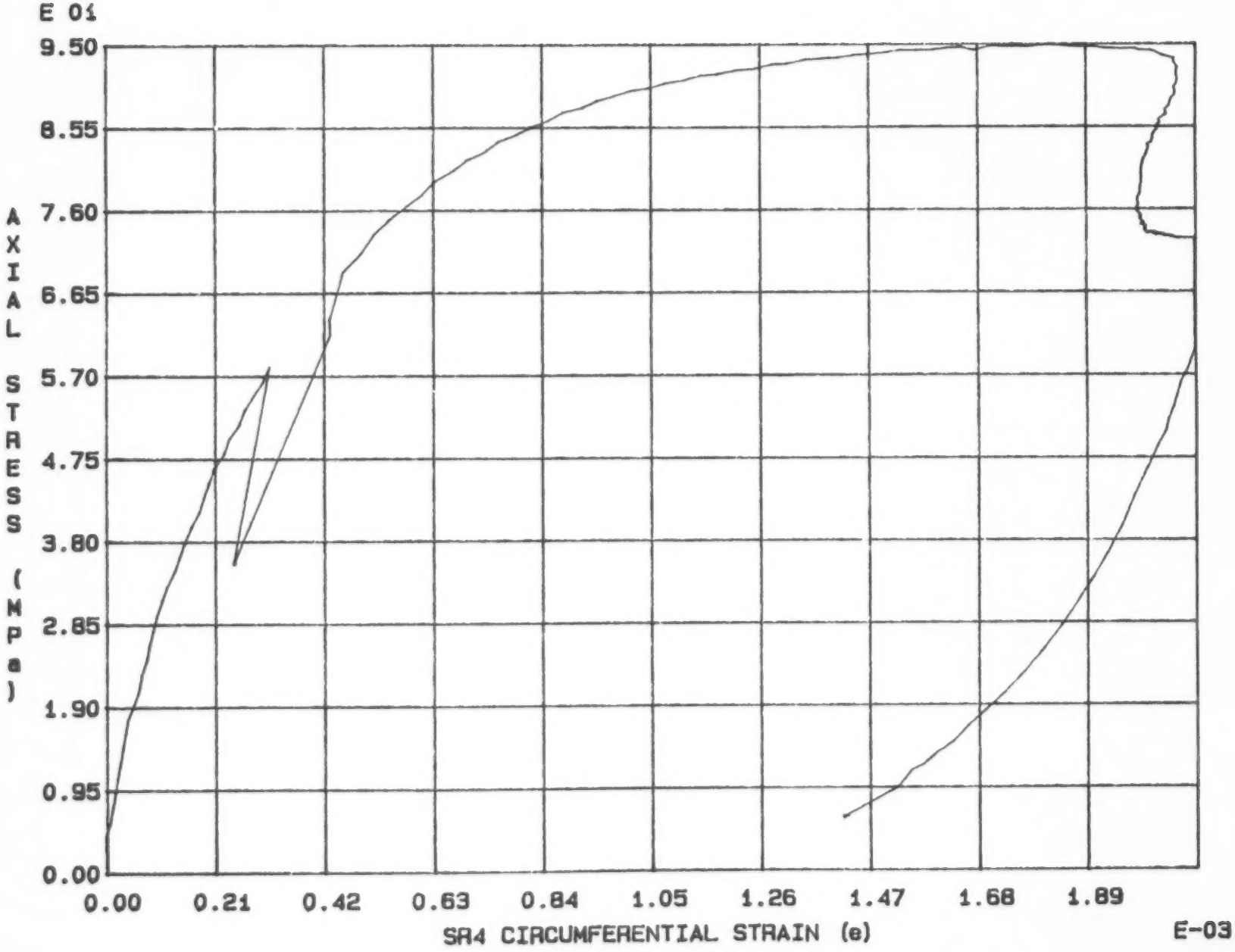

Fig. 4 - 3 Specimen M5U

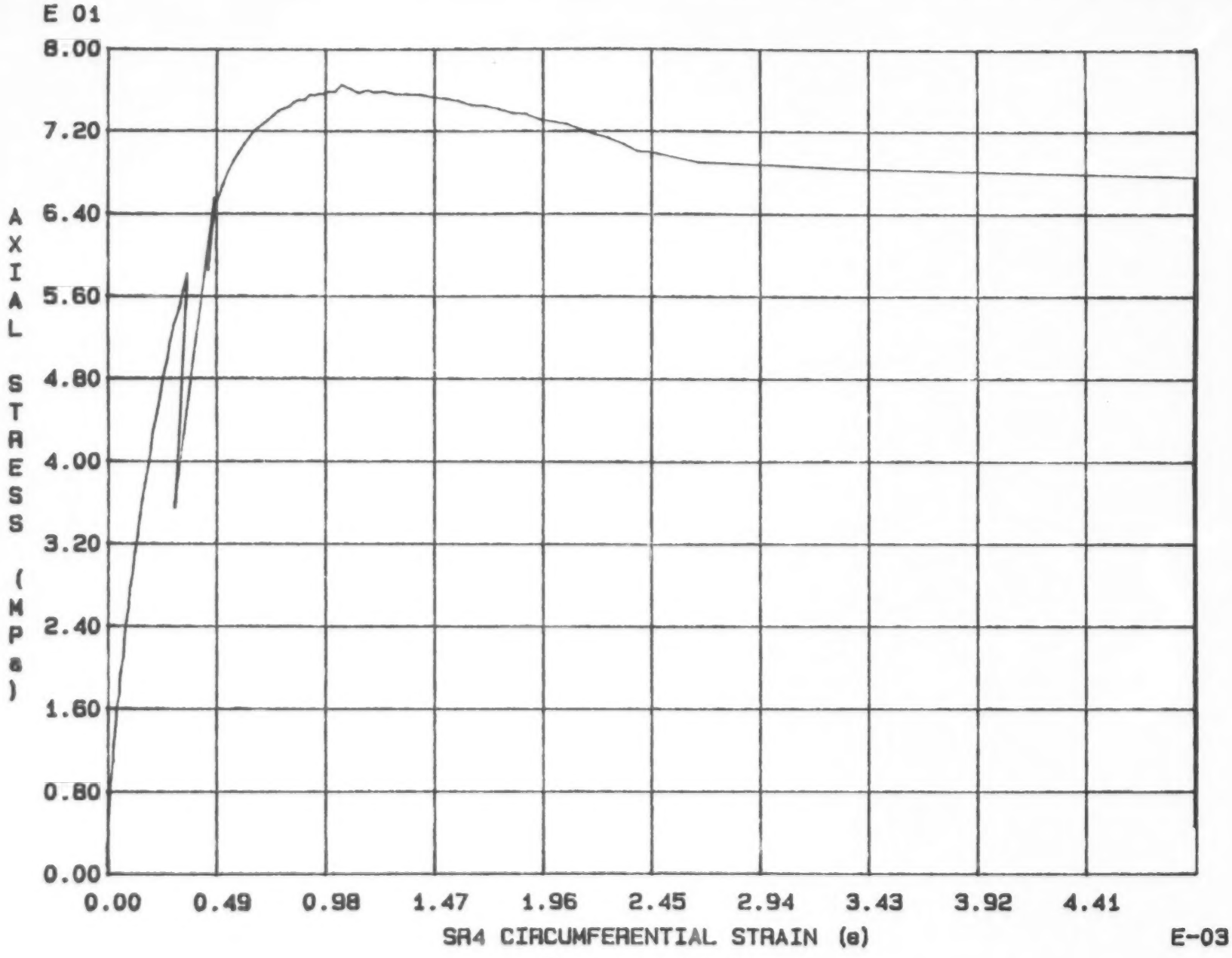

Fig. 4 - 4 Specimen M6U

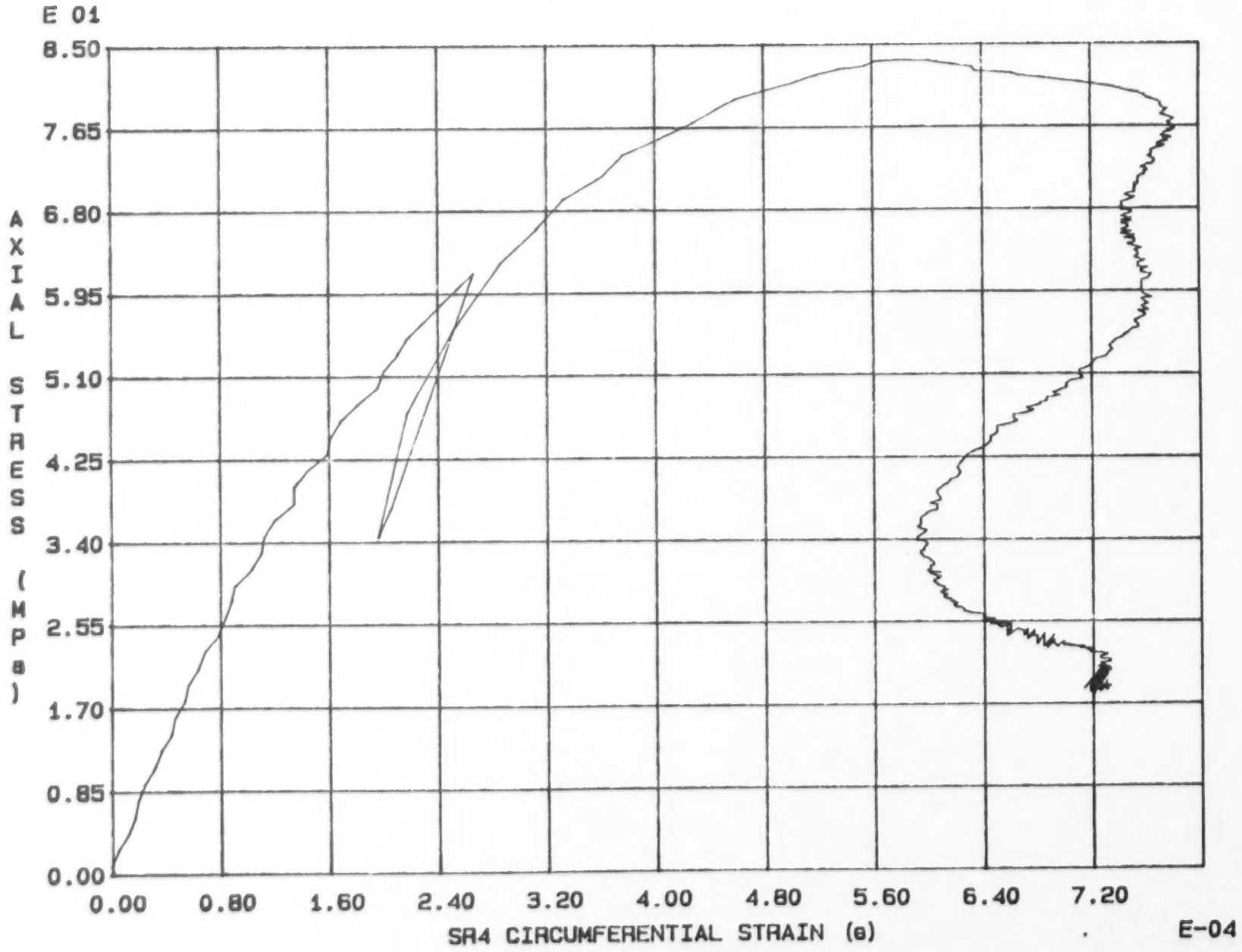

Fig. 4 - 5 Specimen M7U

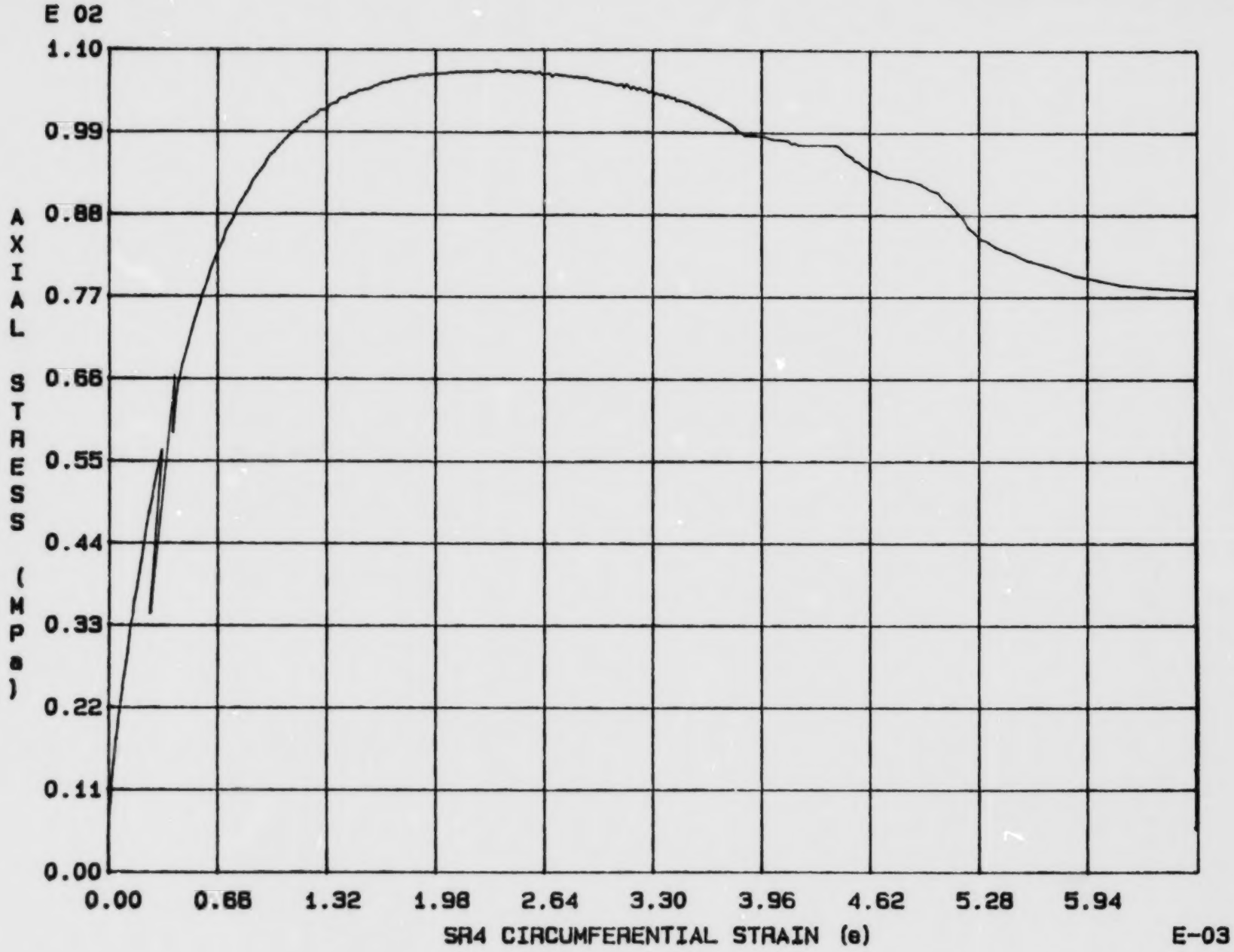

Fig. 4 - 6 Specimen M8U

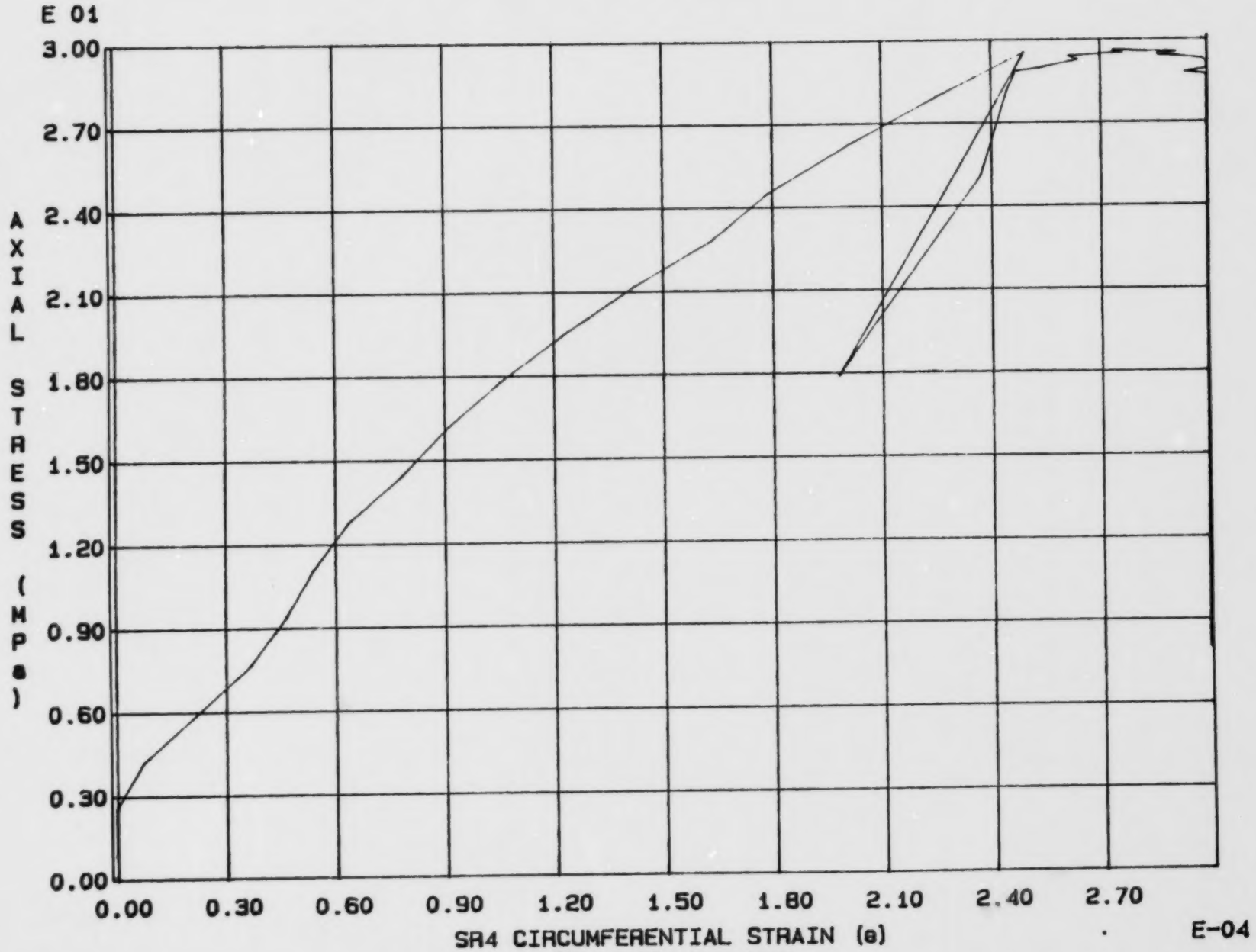

Fig. 4 - 7 Specimen M9U

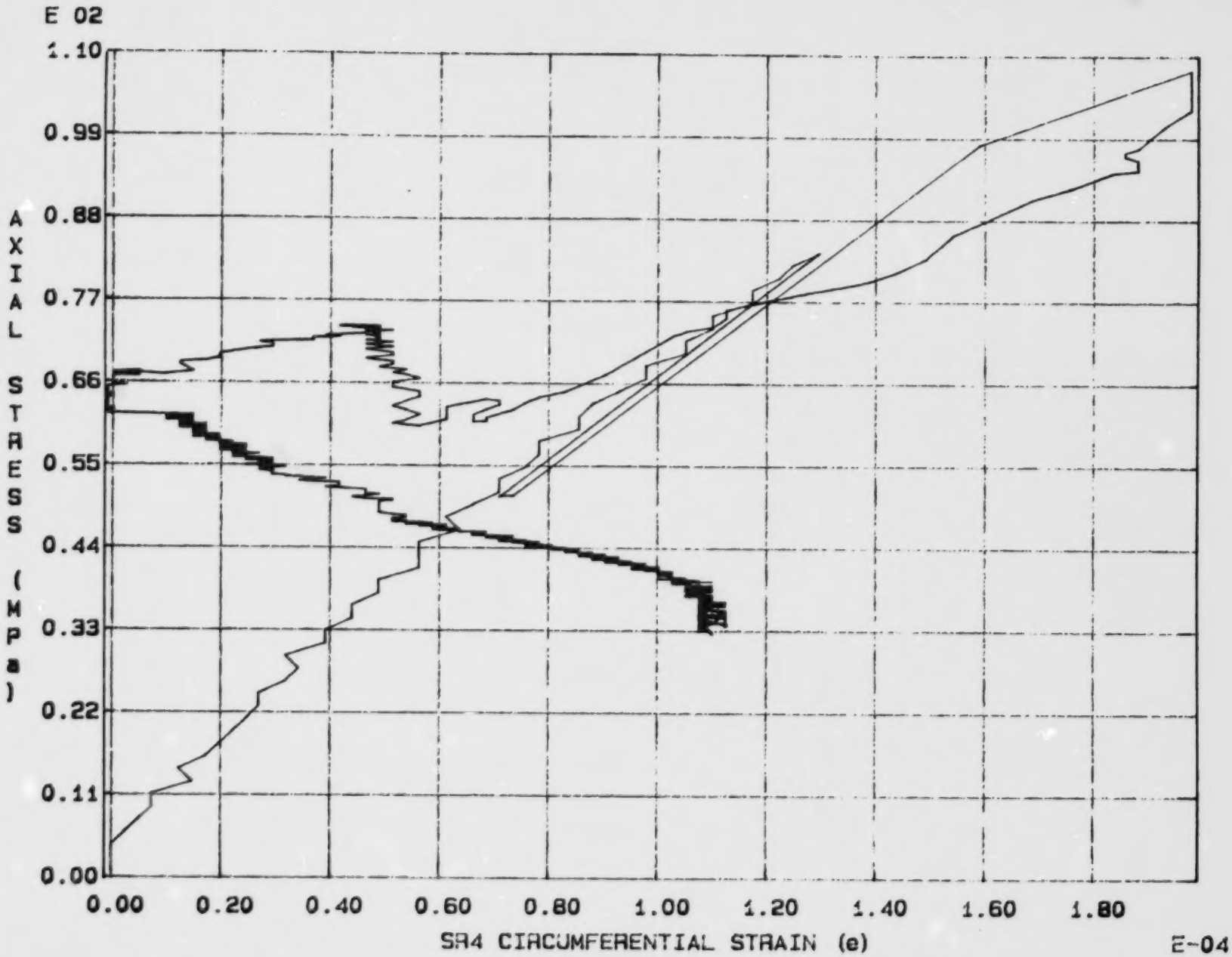

Fig. 4 - 8 Specimen M10U

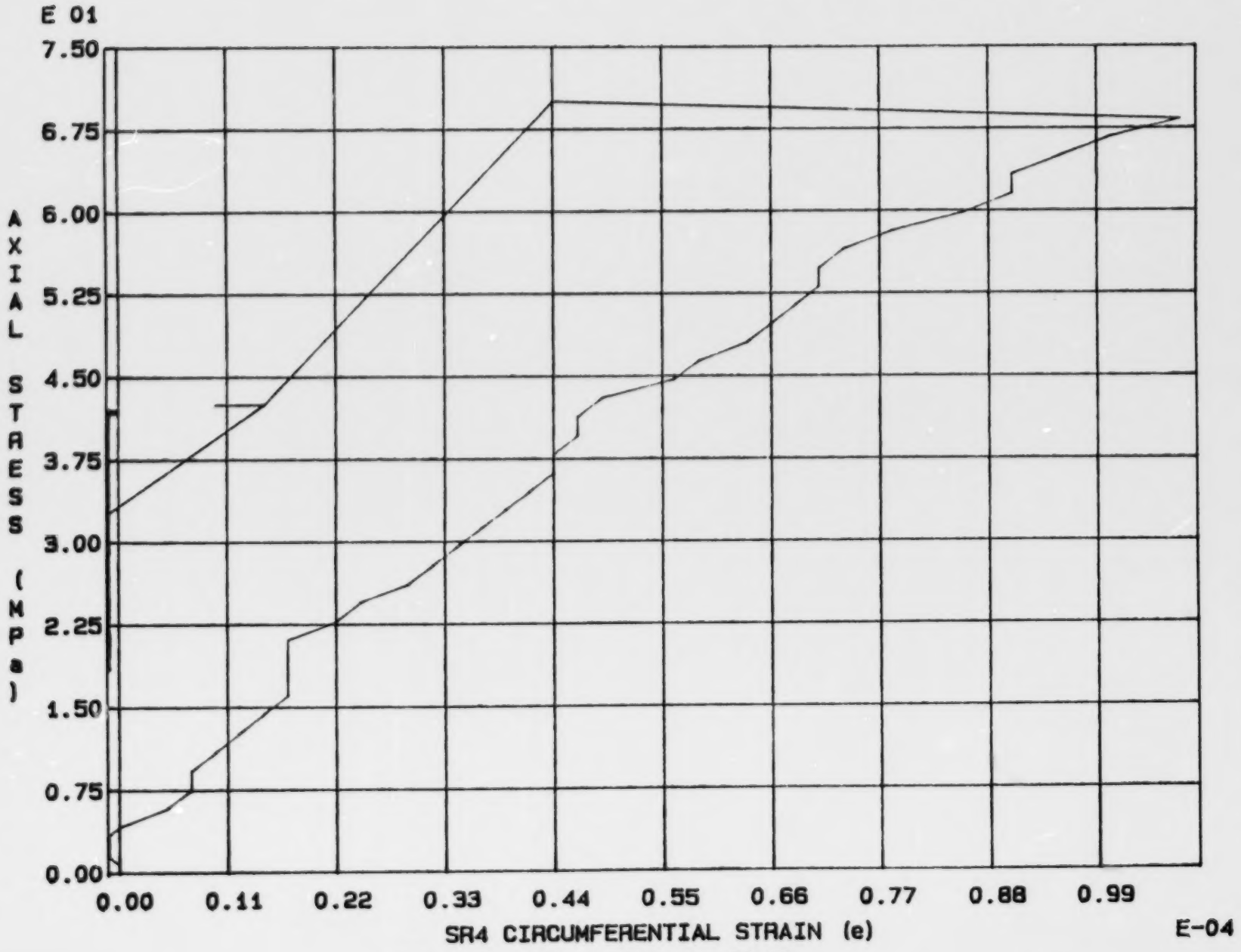

Fig. 4 - 9 Specimen M11U

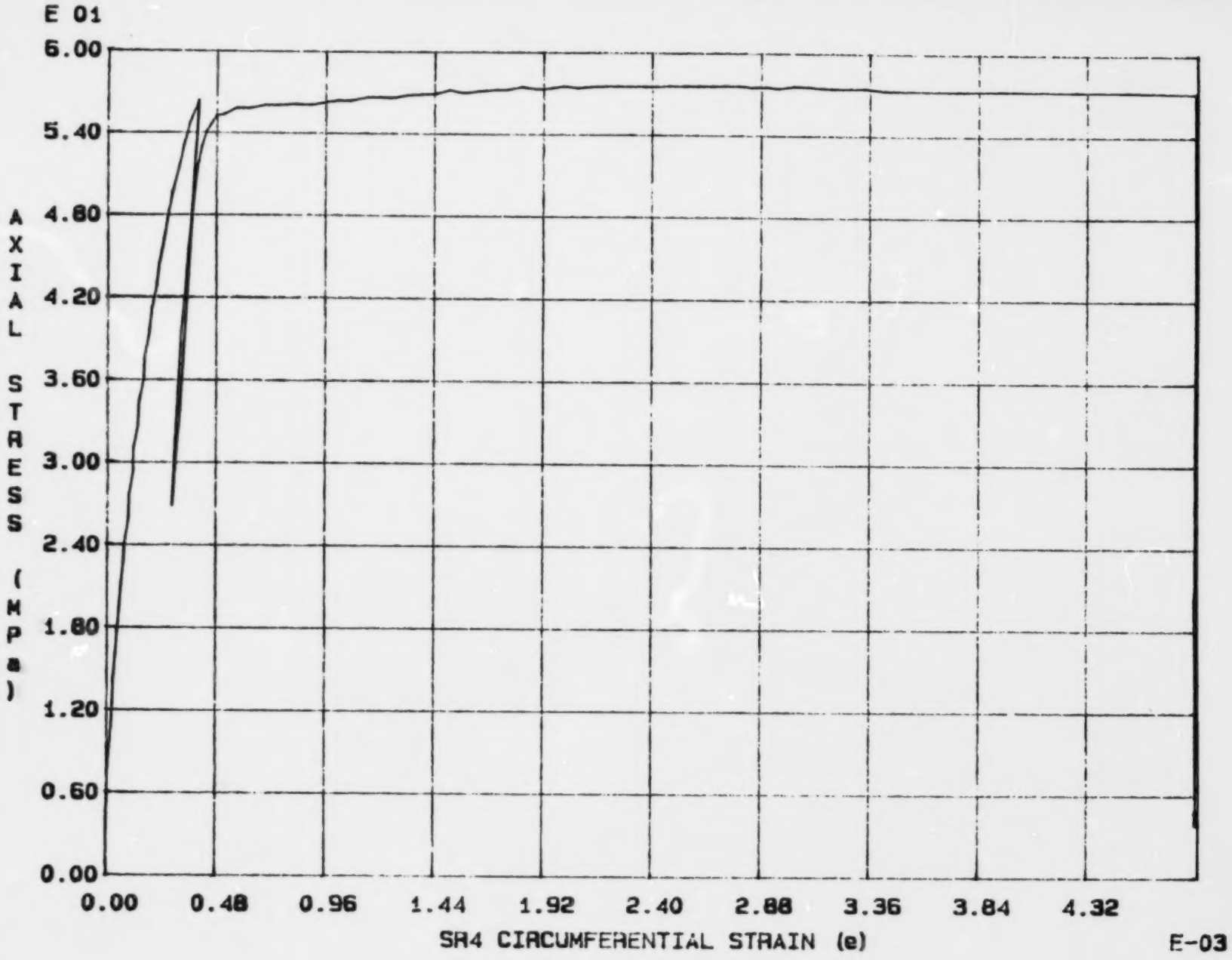

Fig. 4 - 10 Specimen M12U

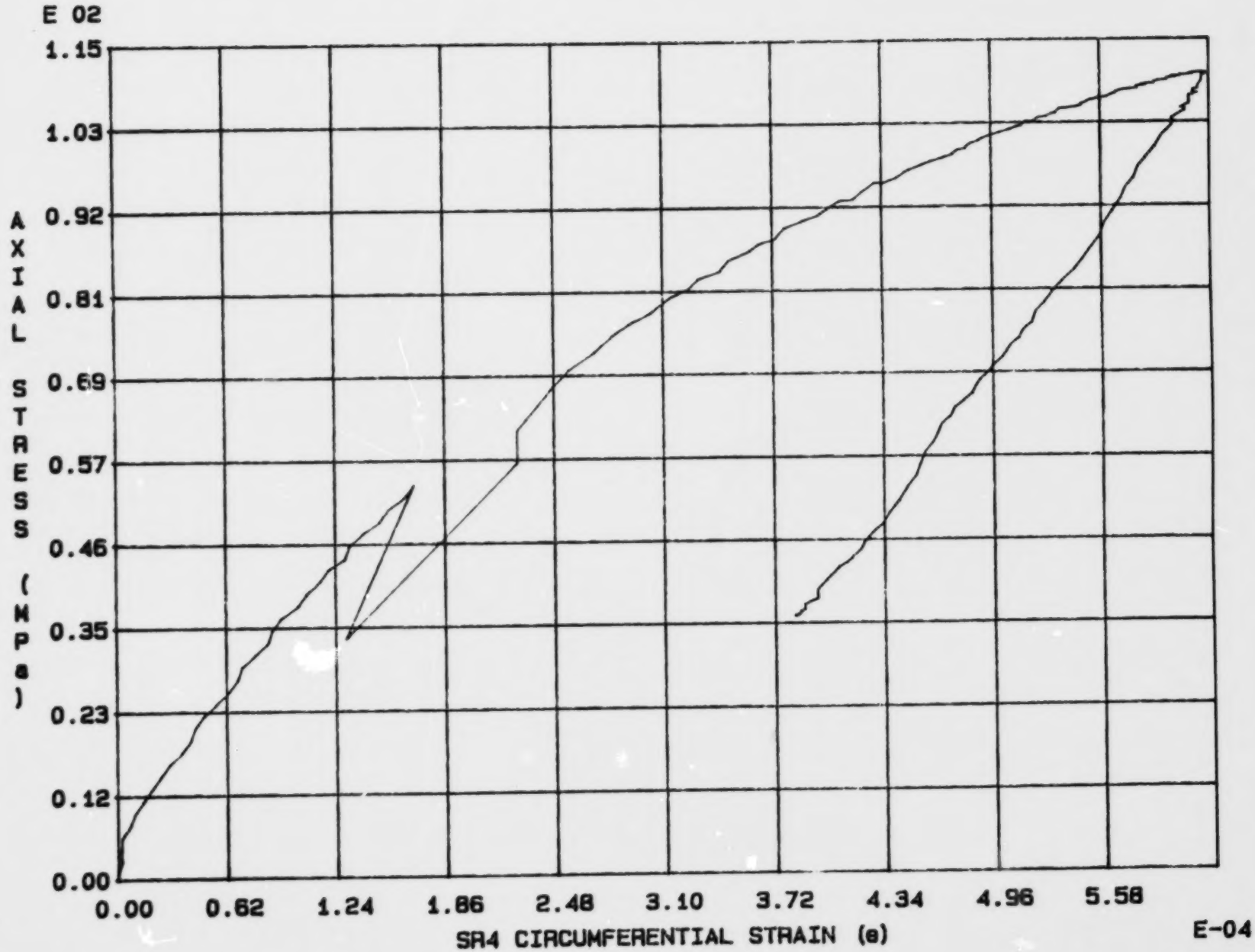

Fig. 4 - 11 Specimen M13U

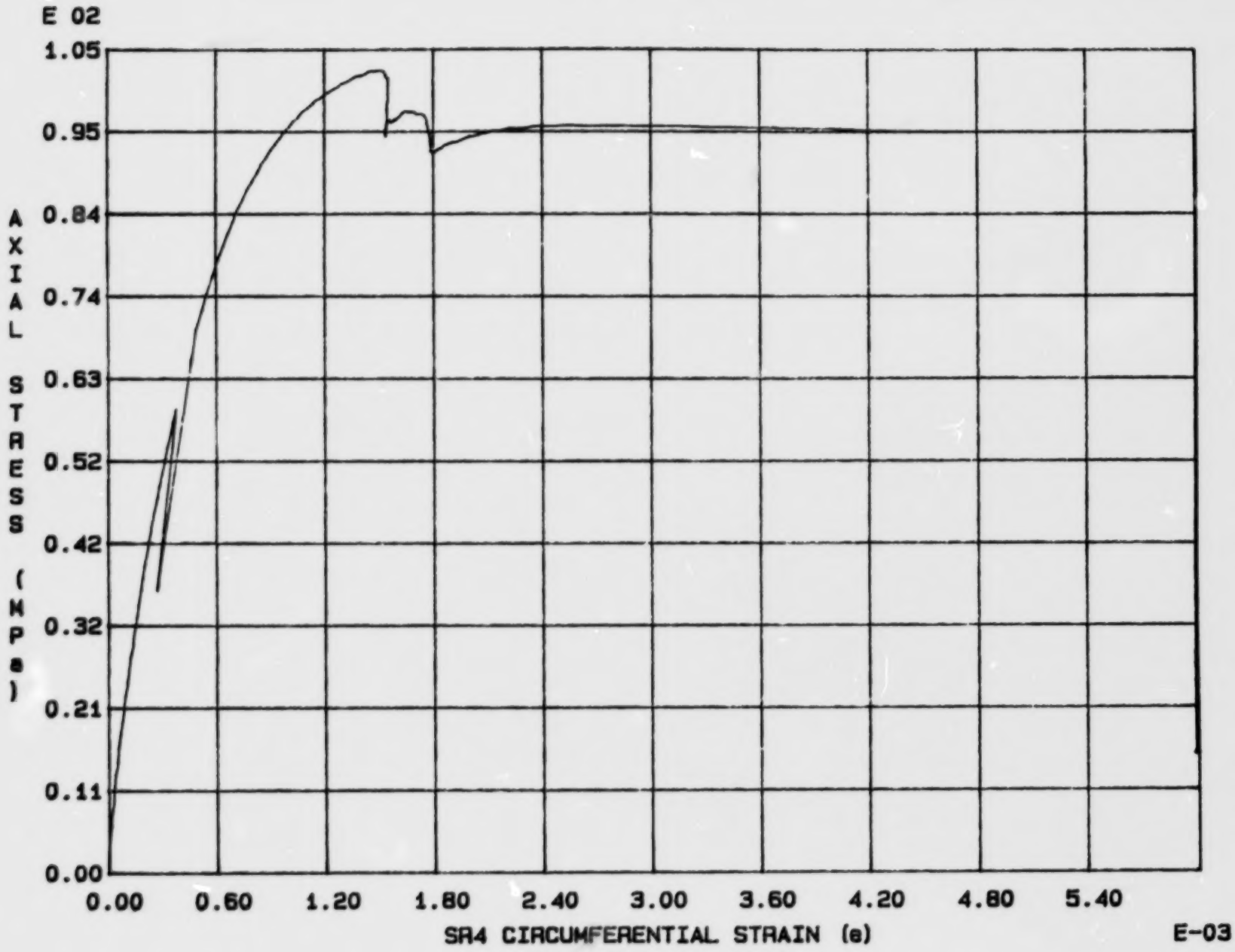

Fig. 4 - 12 Specimen M14U

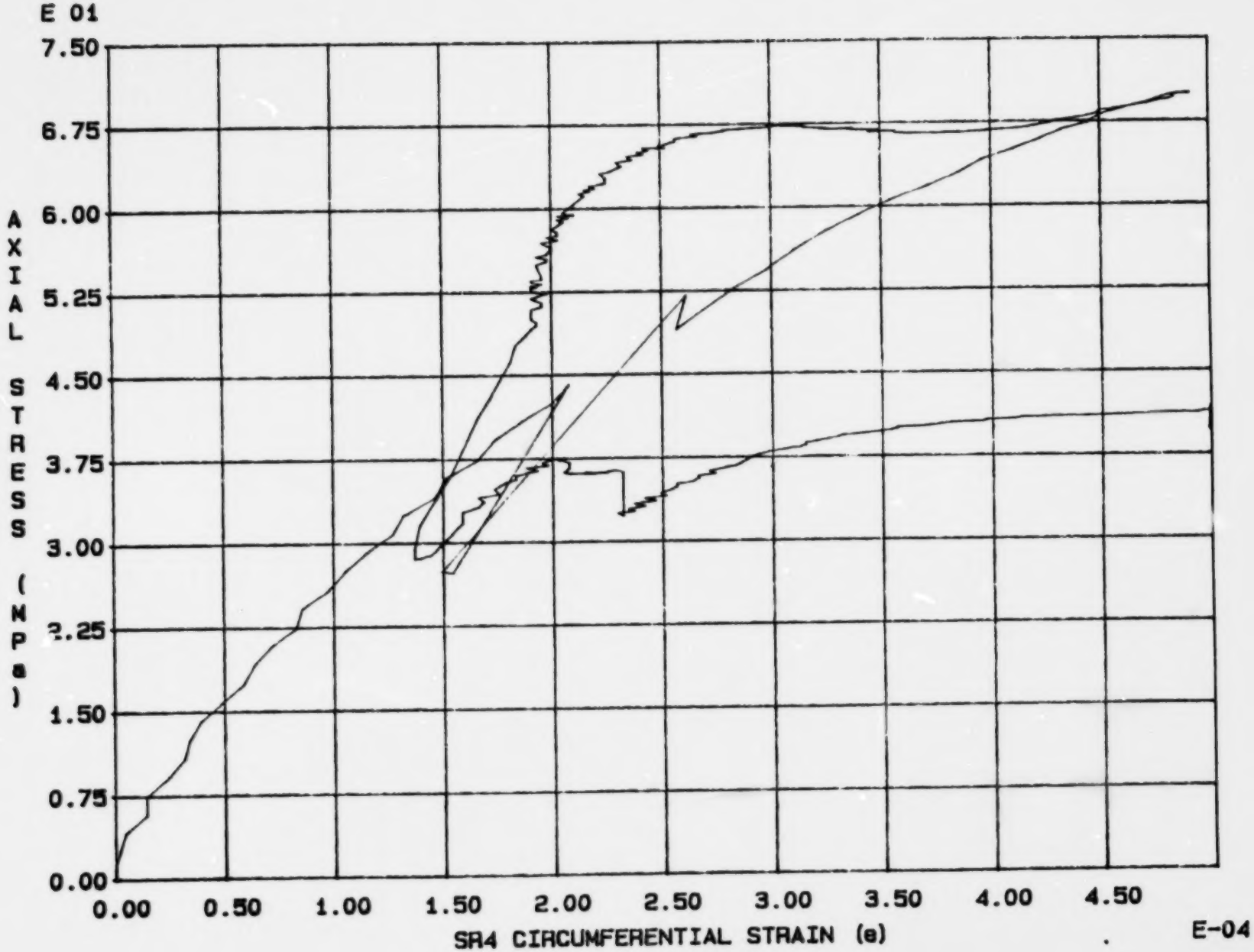

Fig. 4 - 13 Specimen M15U

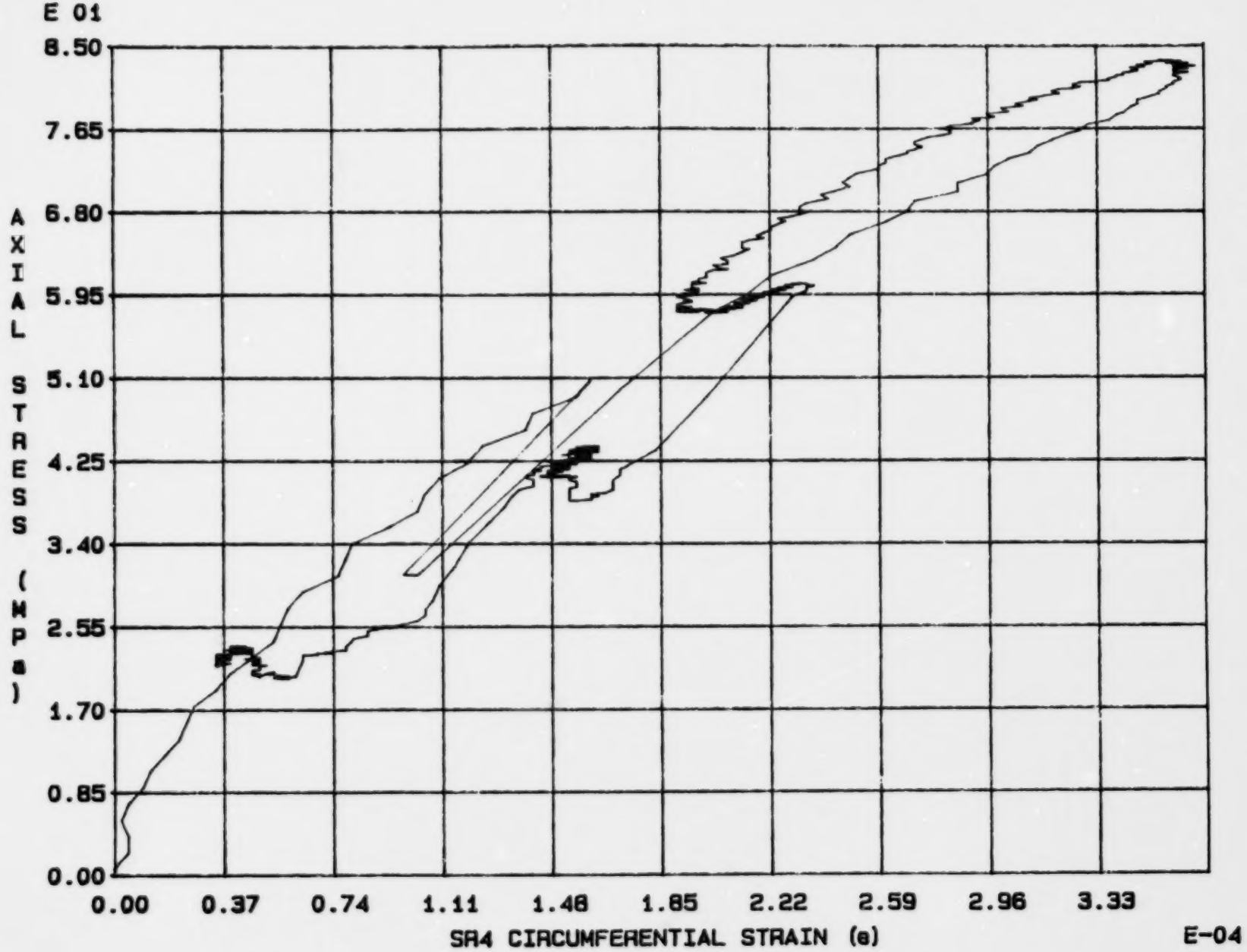

Fig. 4 - 14 Specimen M16U

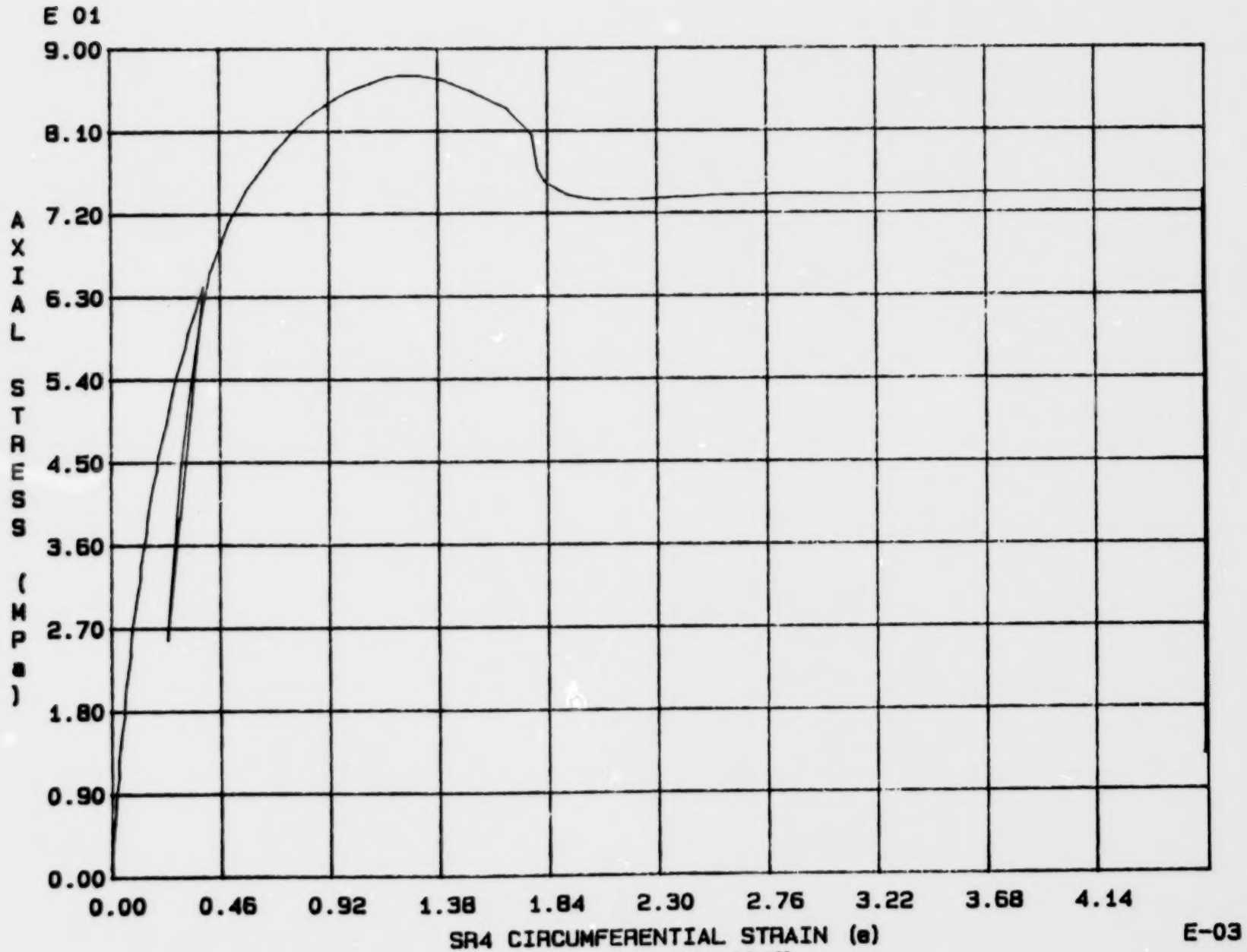

Fig. 4 - 15 Specimen M17U

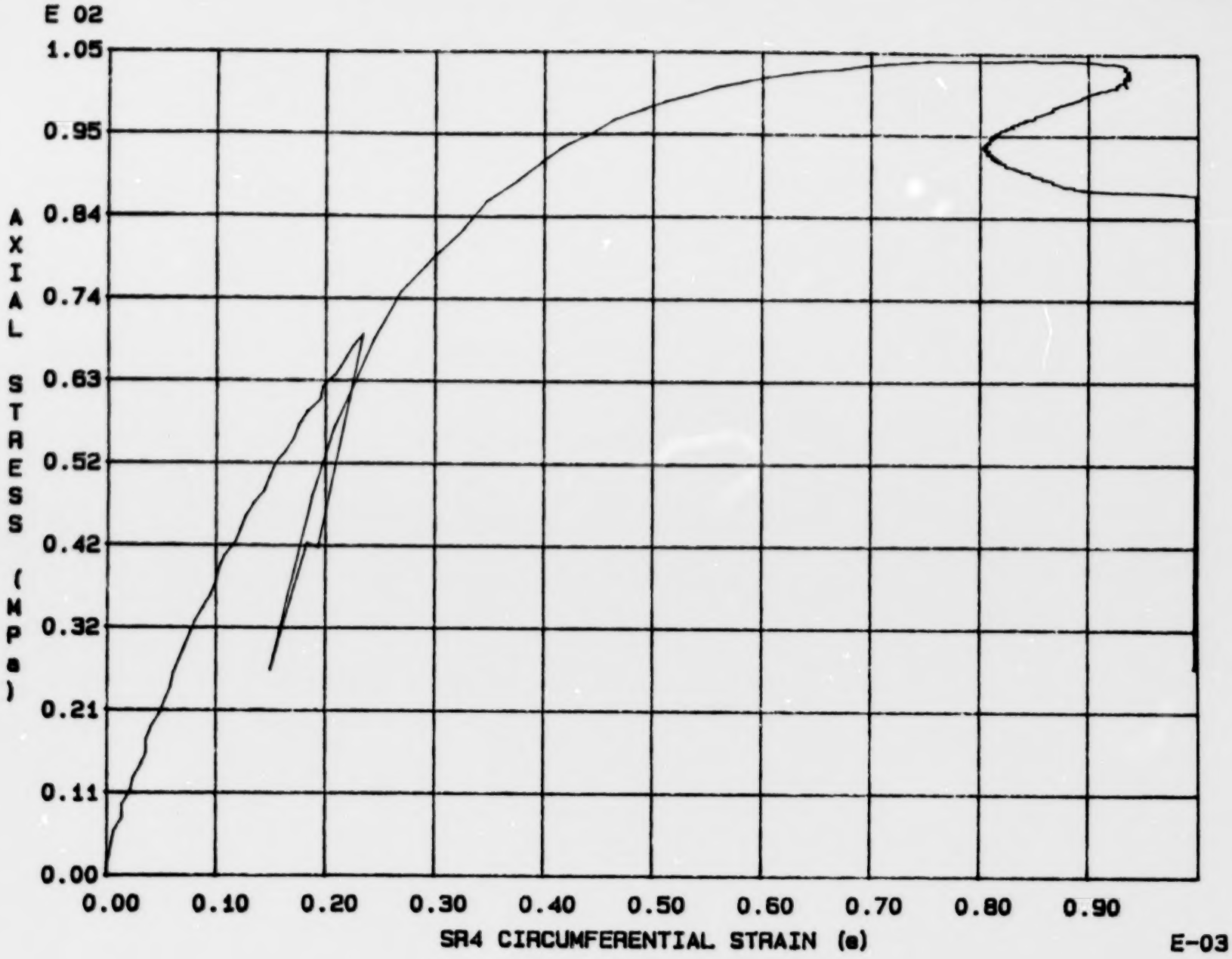

Fig. 4 - 16 Specimen M18U

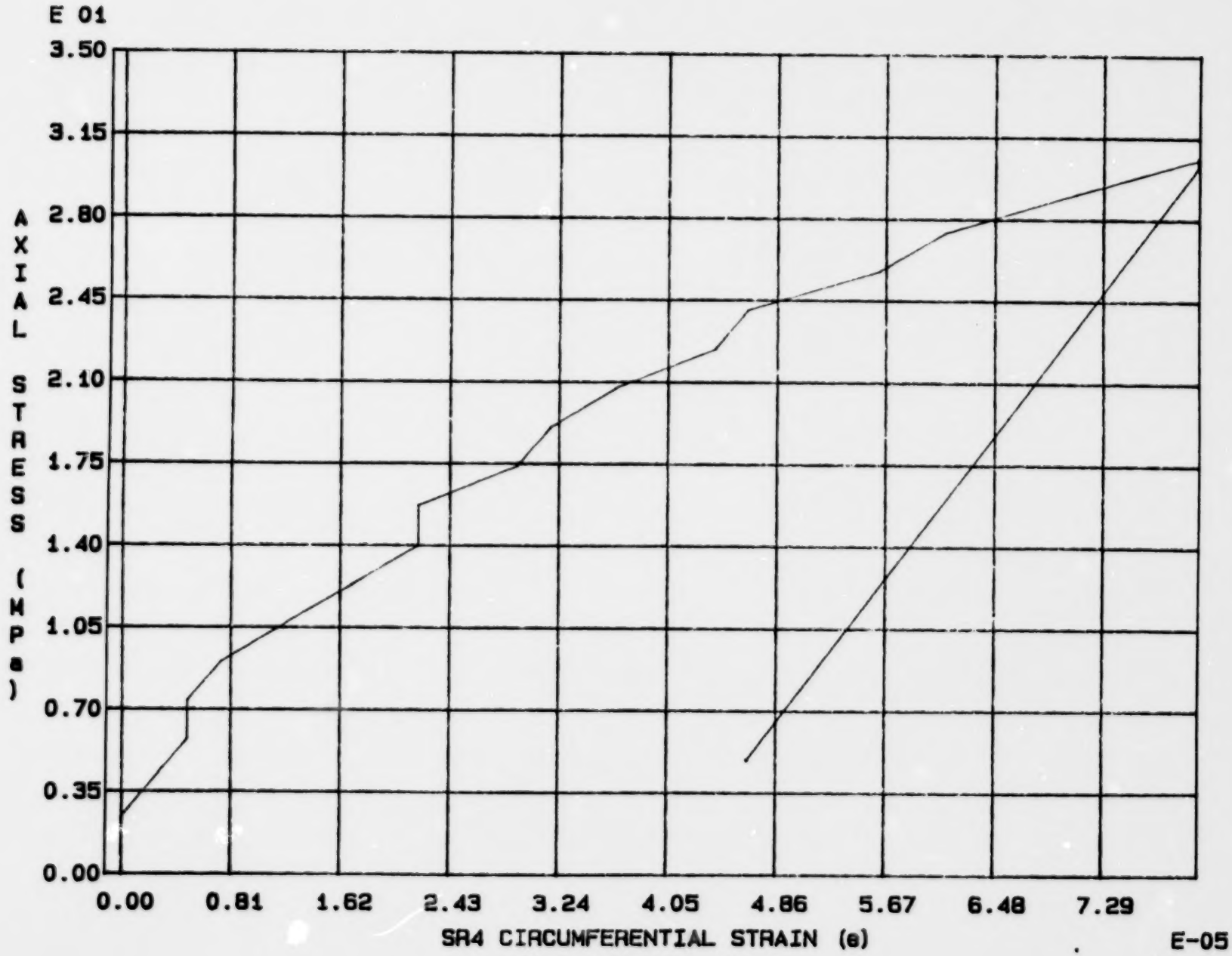

Fig. 4 - 17 Specimen M19U

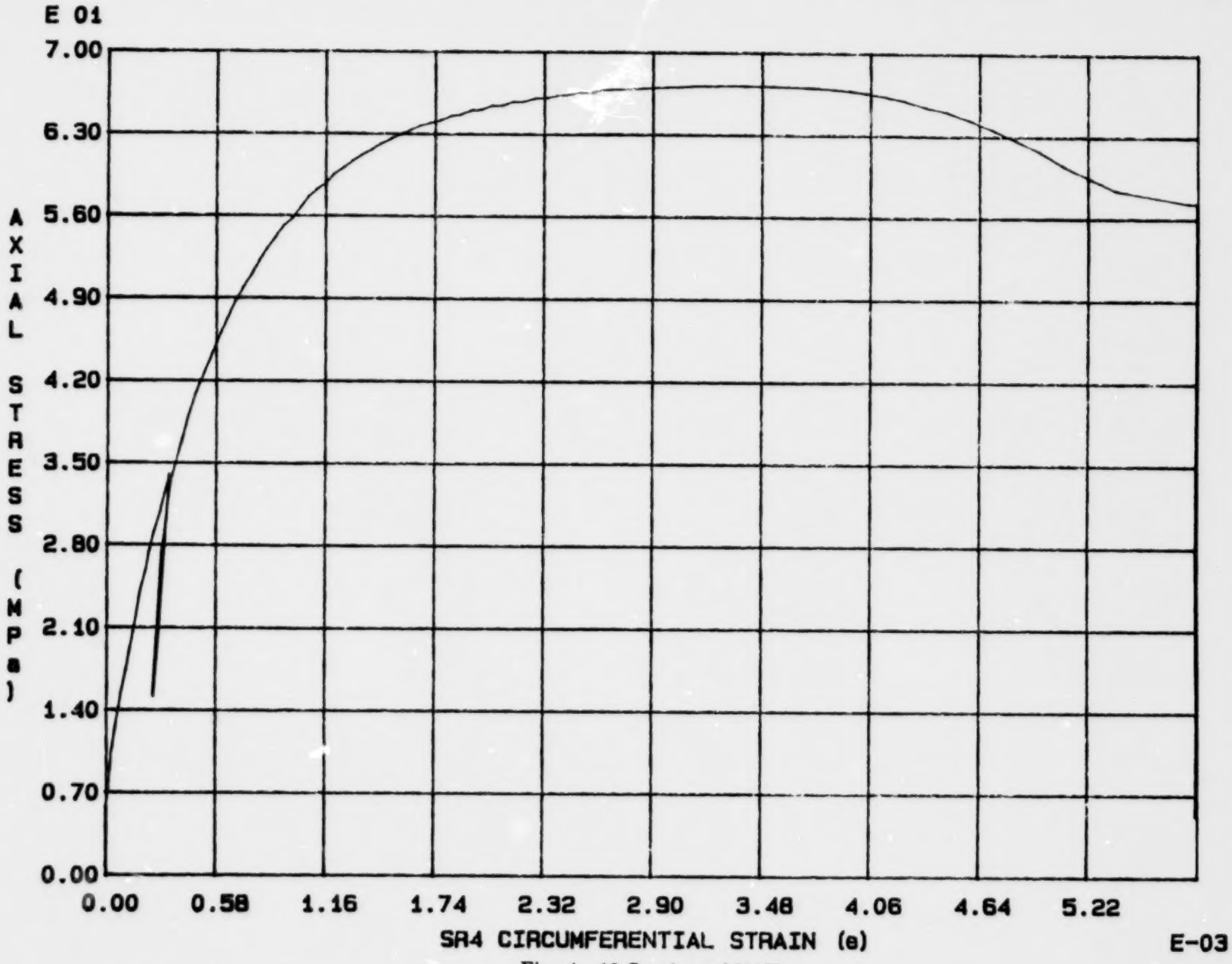

Fig. 4 - 18 Specimen M20U

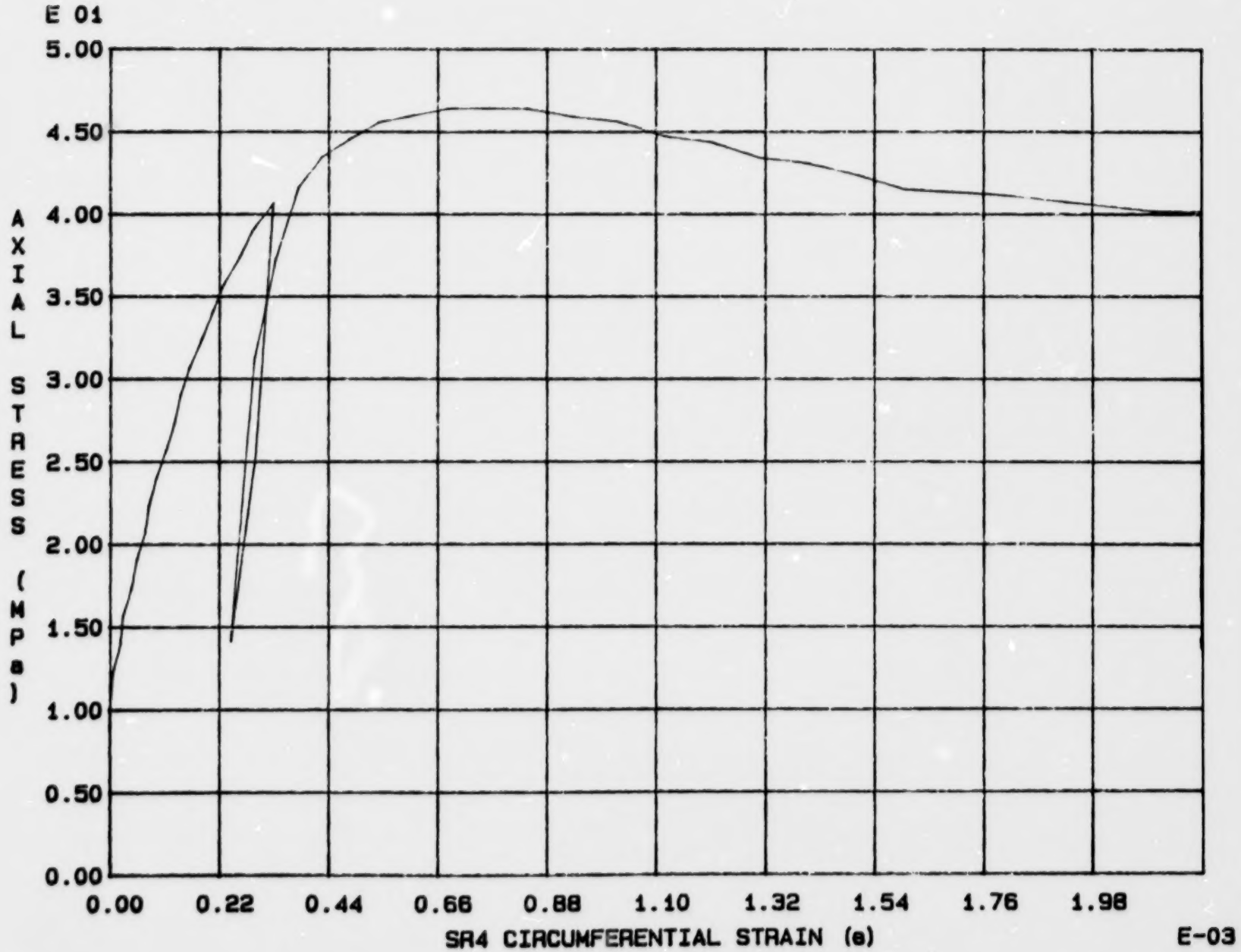

Fig. 4 - 19 Specimen M21U

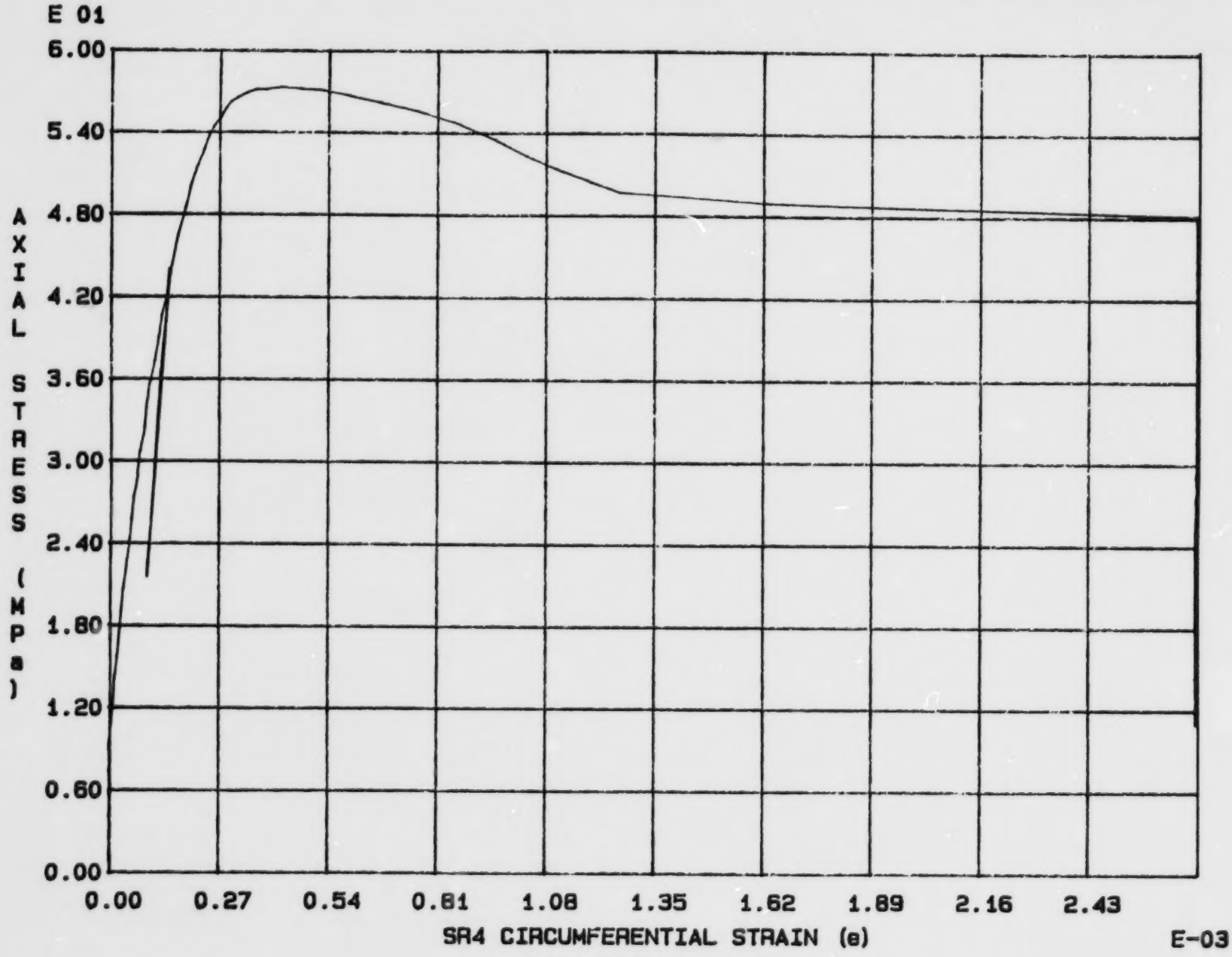

Fig. 4 - 20 Specimen M22U

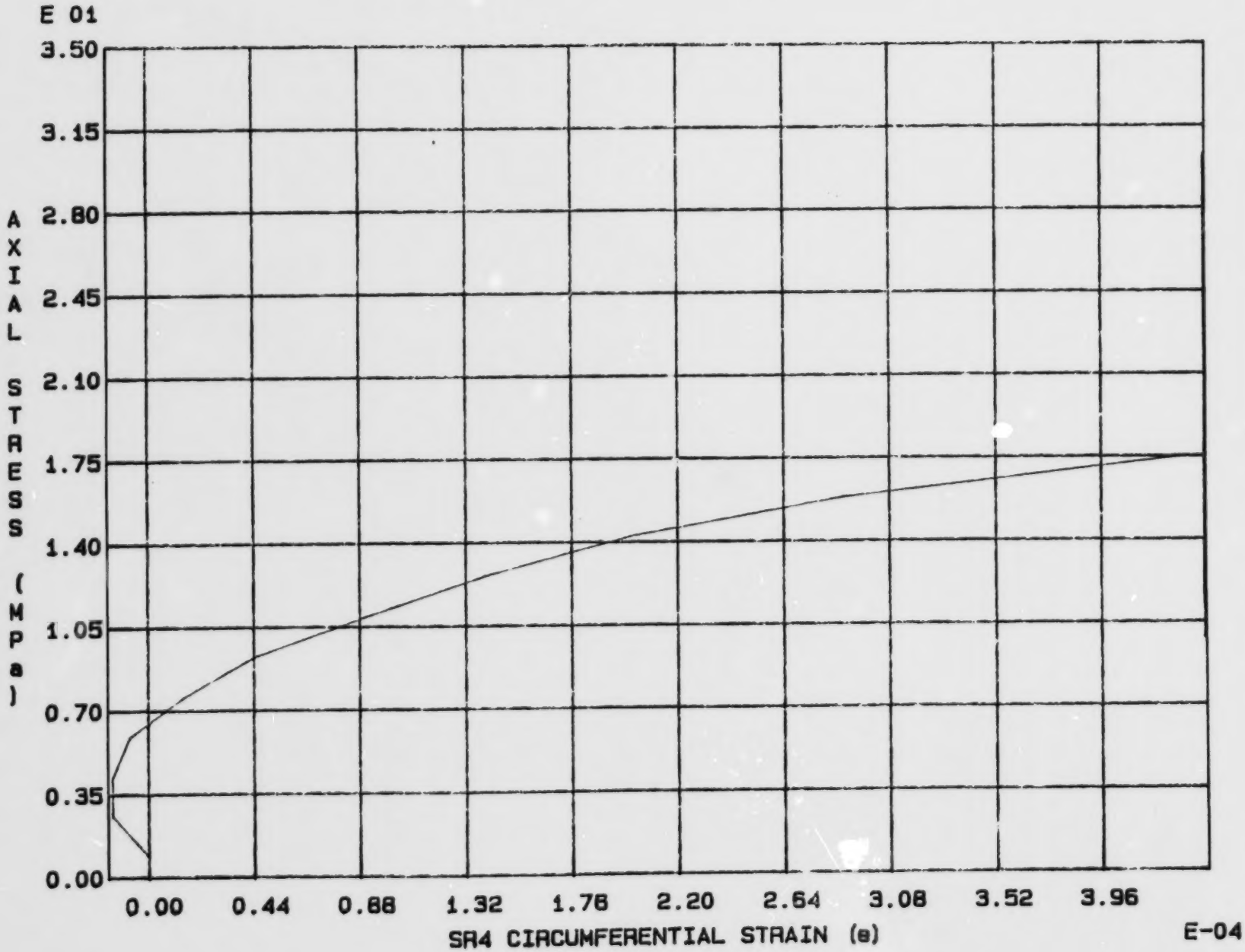

Fig. 4 - 21 Specimen M23U

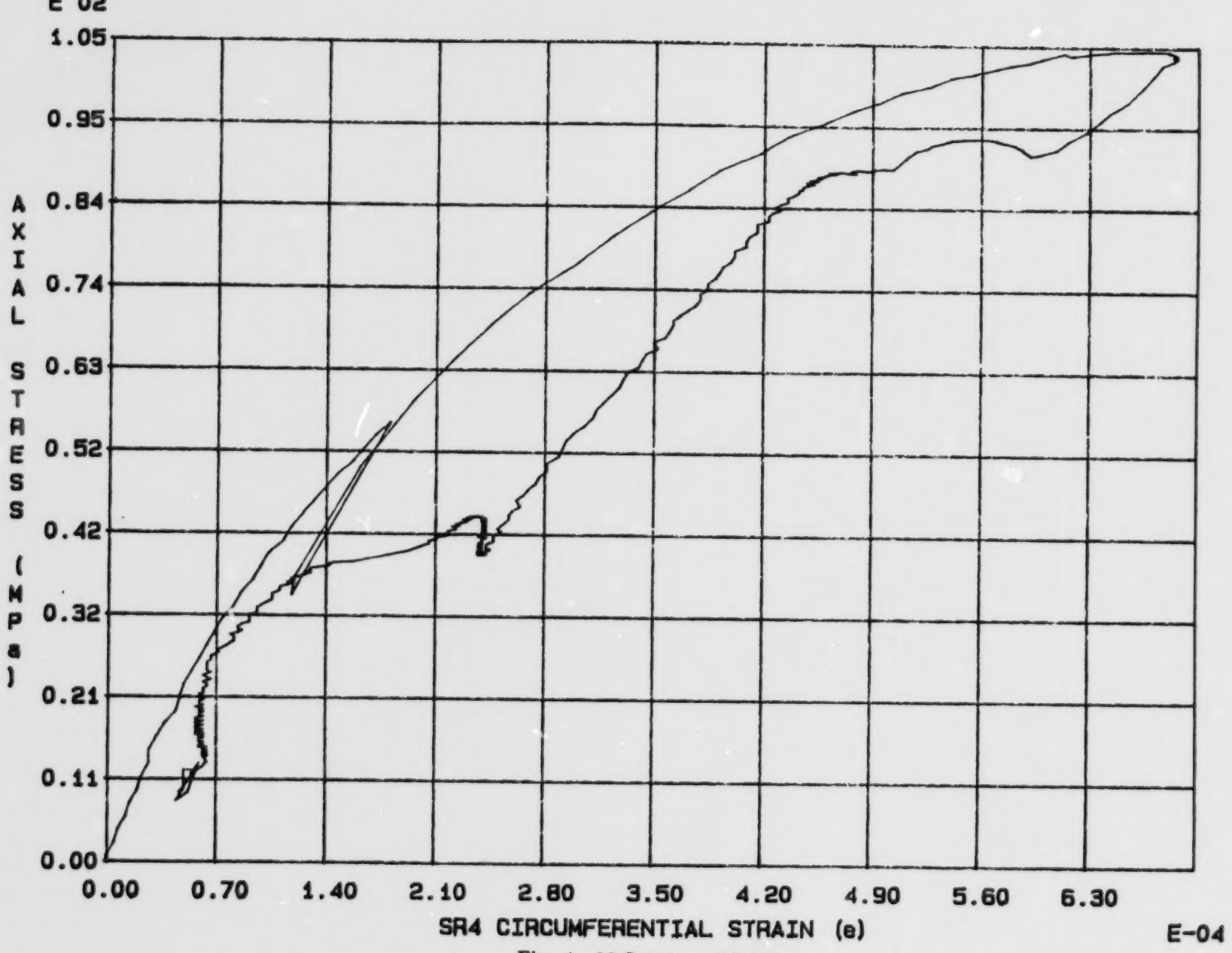

Fig. 4 - 22 Specimen M24U

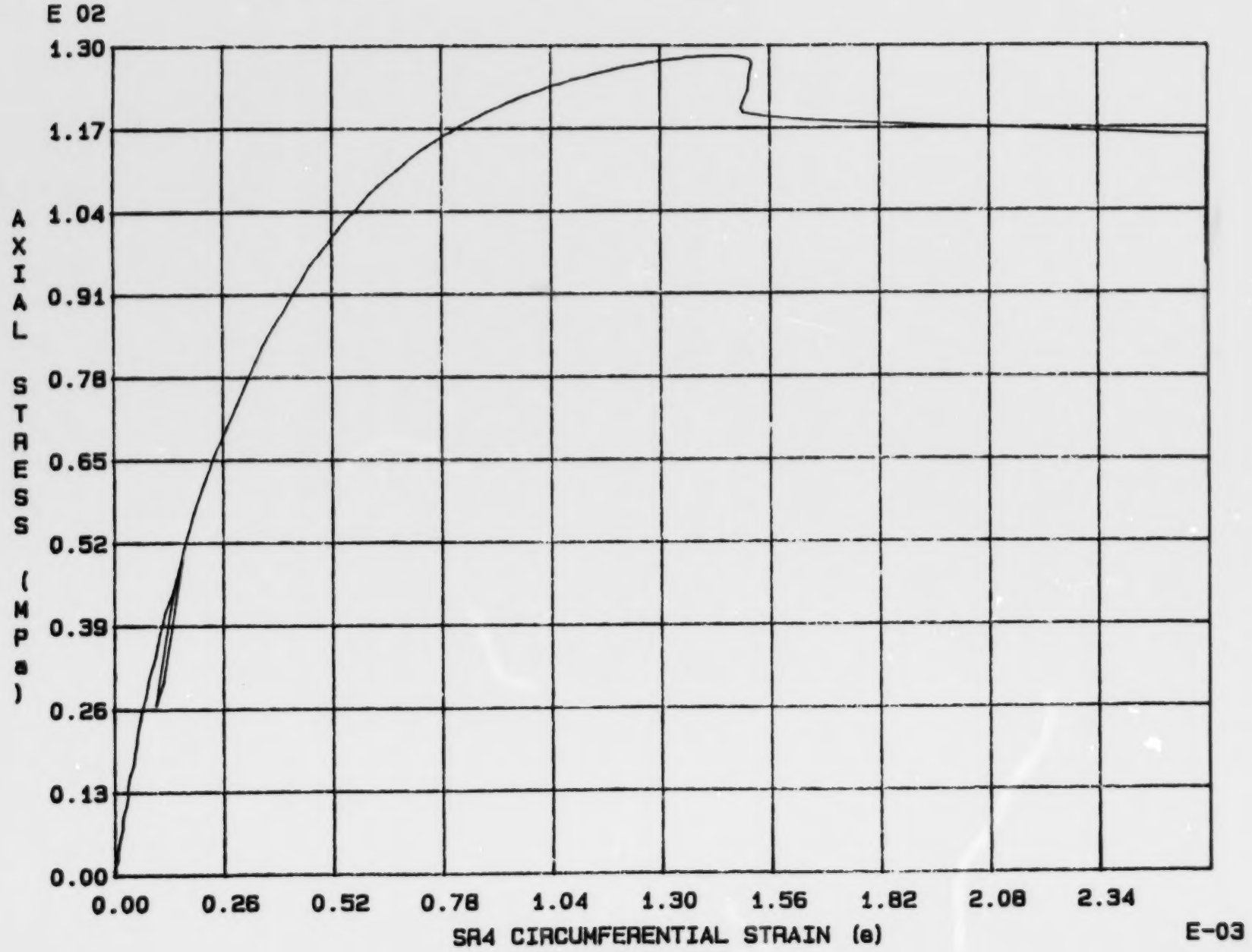

Fig. 4 - 23 Specimen M25U

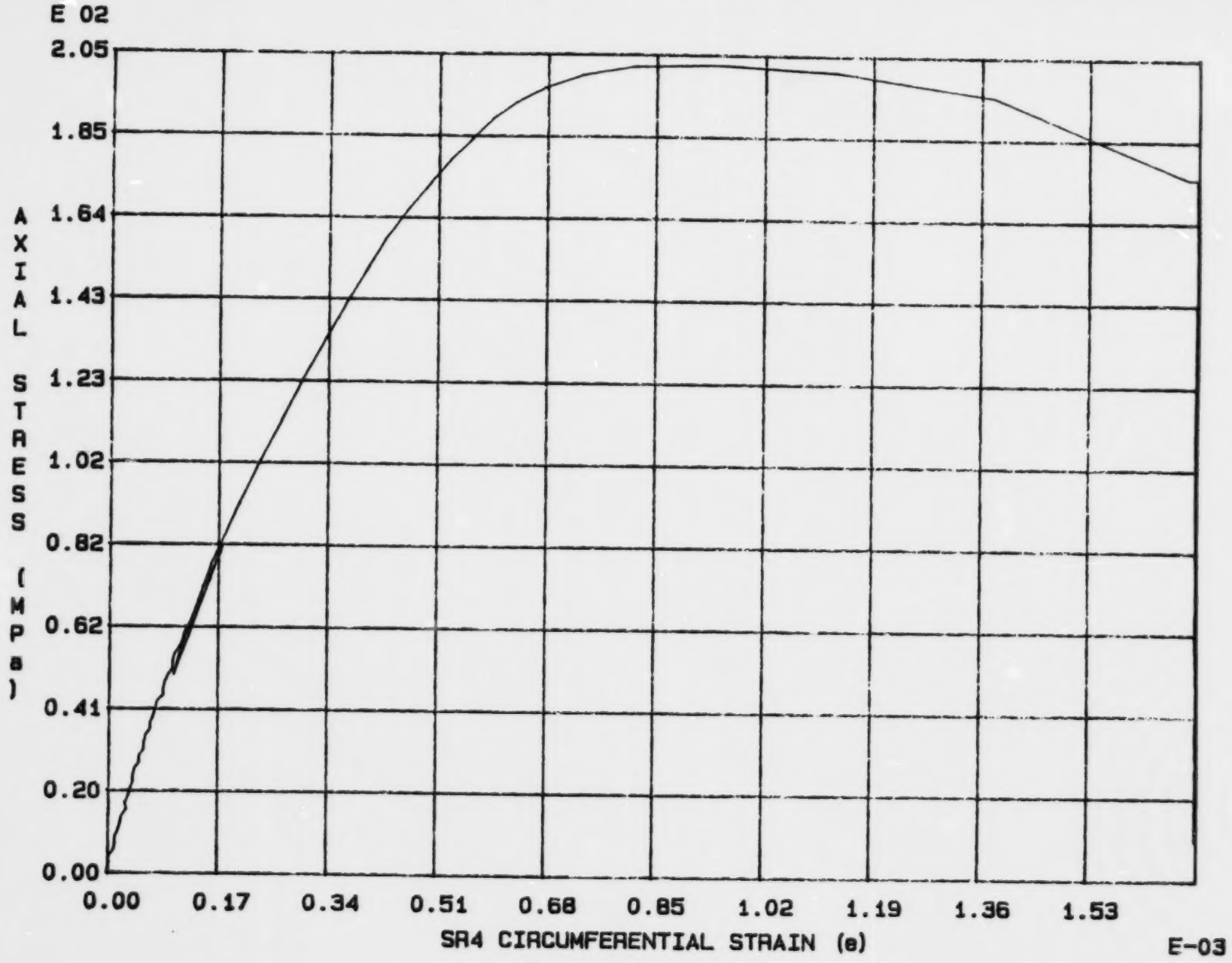

Fig. 4 - 24 Specimen M26U

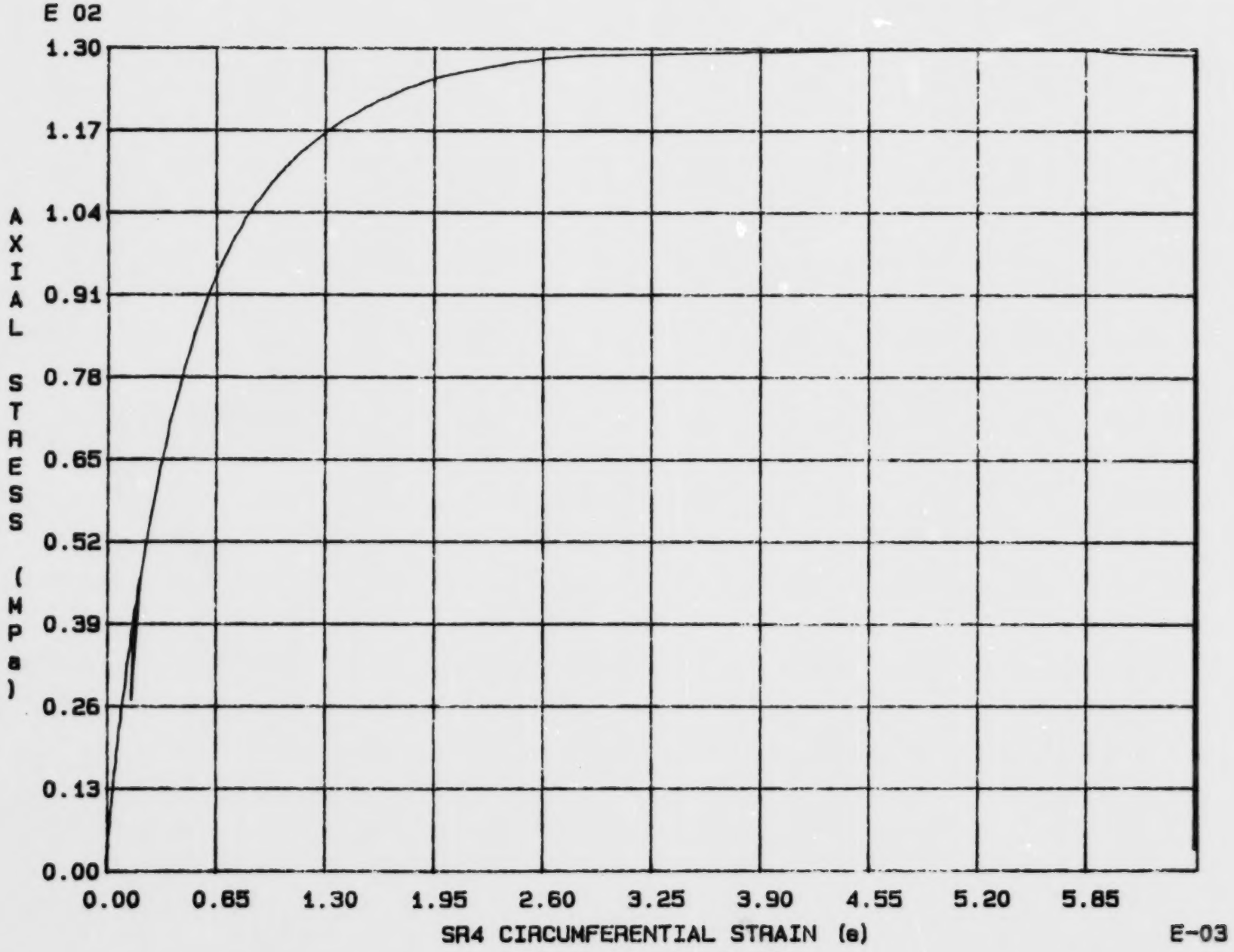

Fig. 4 - 25 Specimen M27U

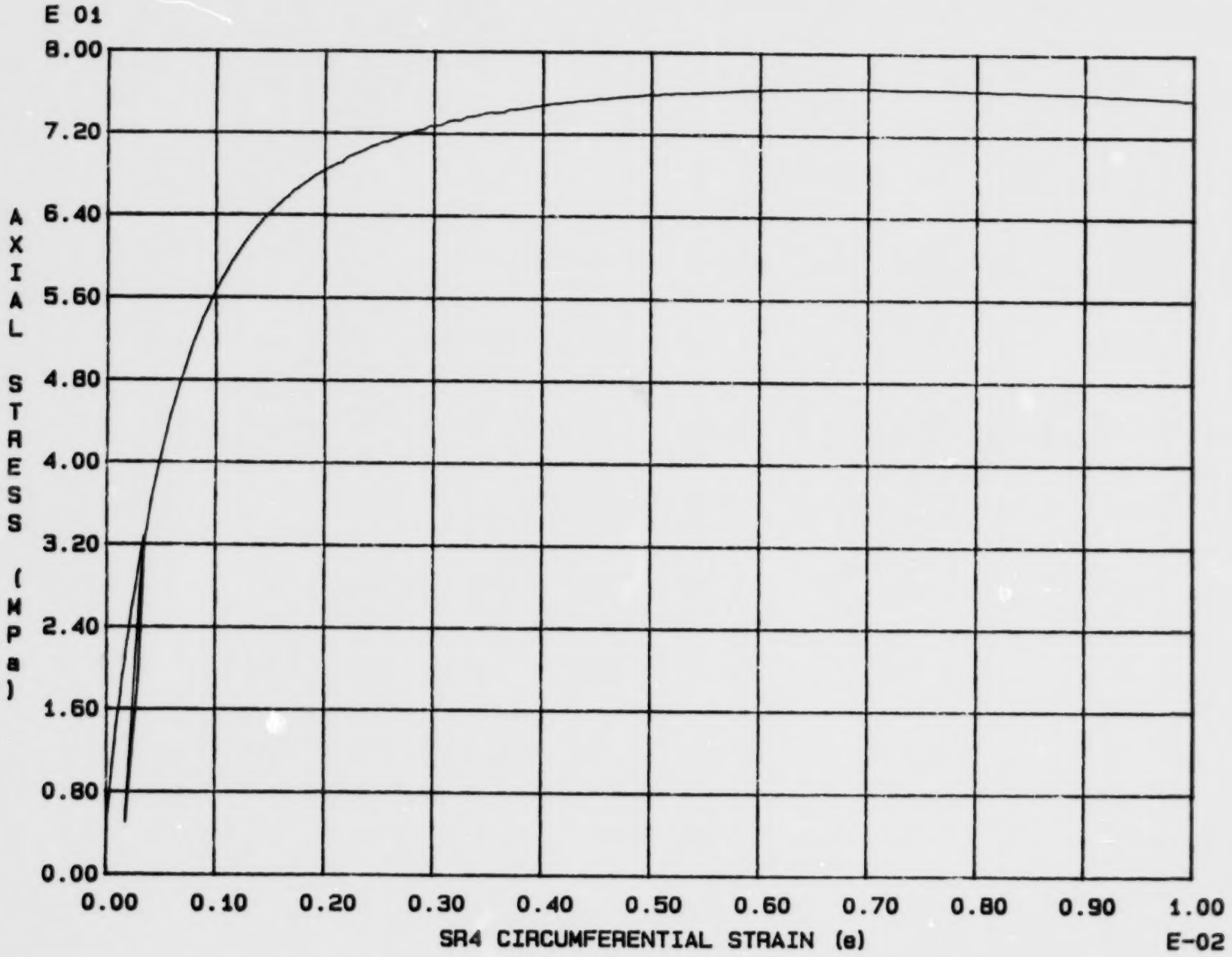

Fig. 4 - 26 Specimen M28U

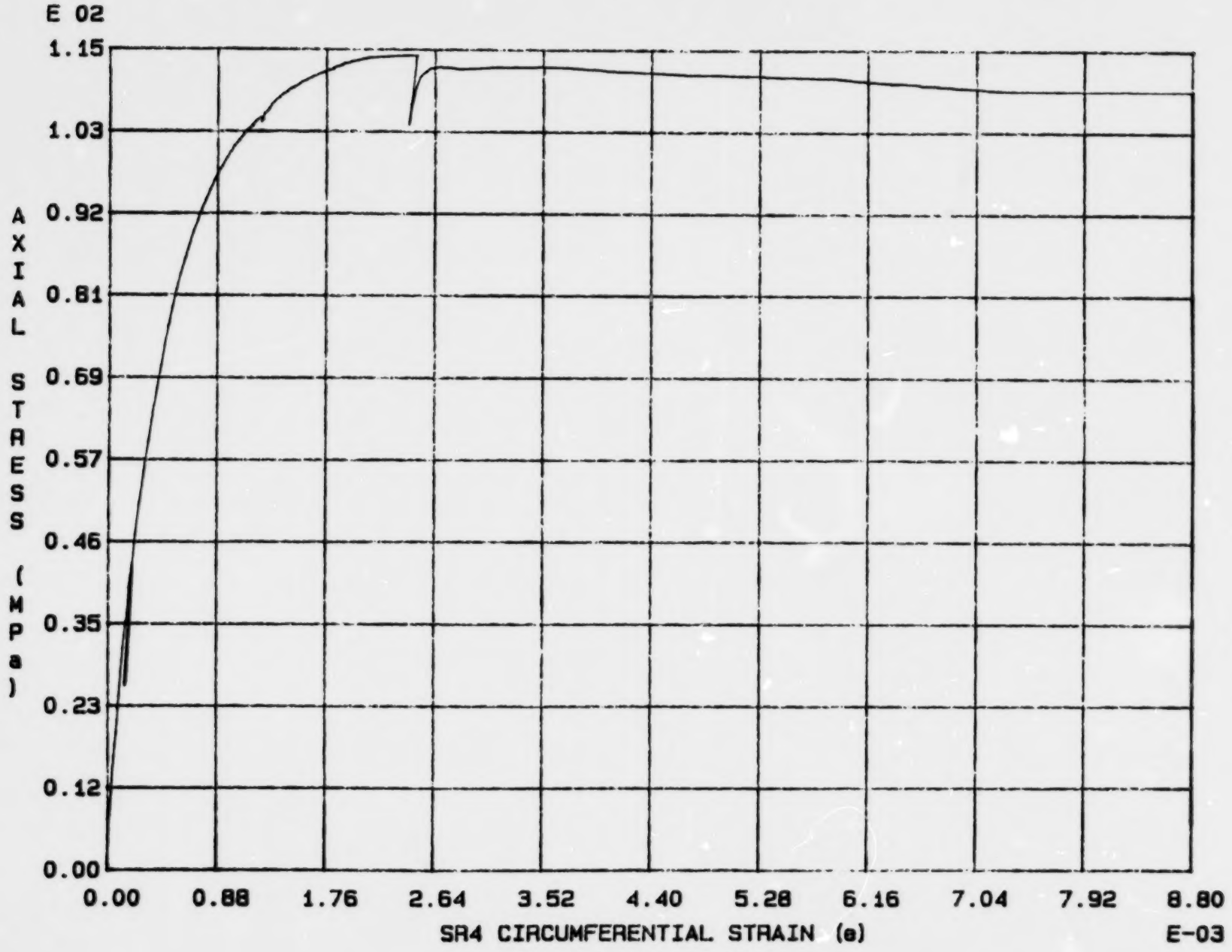

Fig. 4 - 27 Specimen M29U

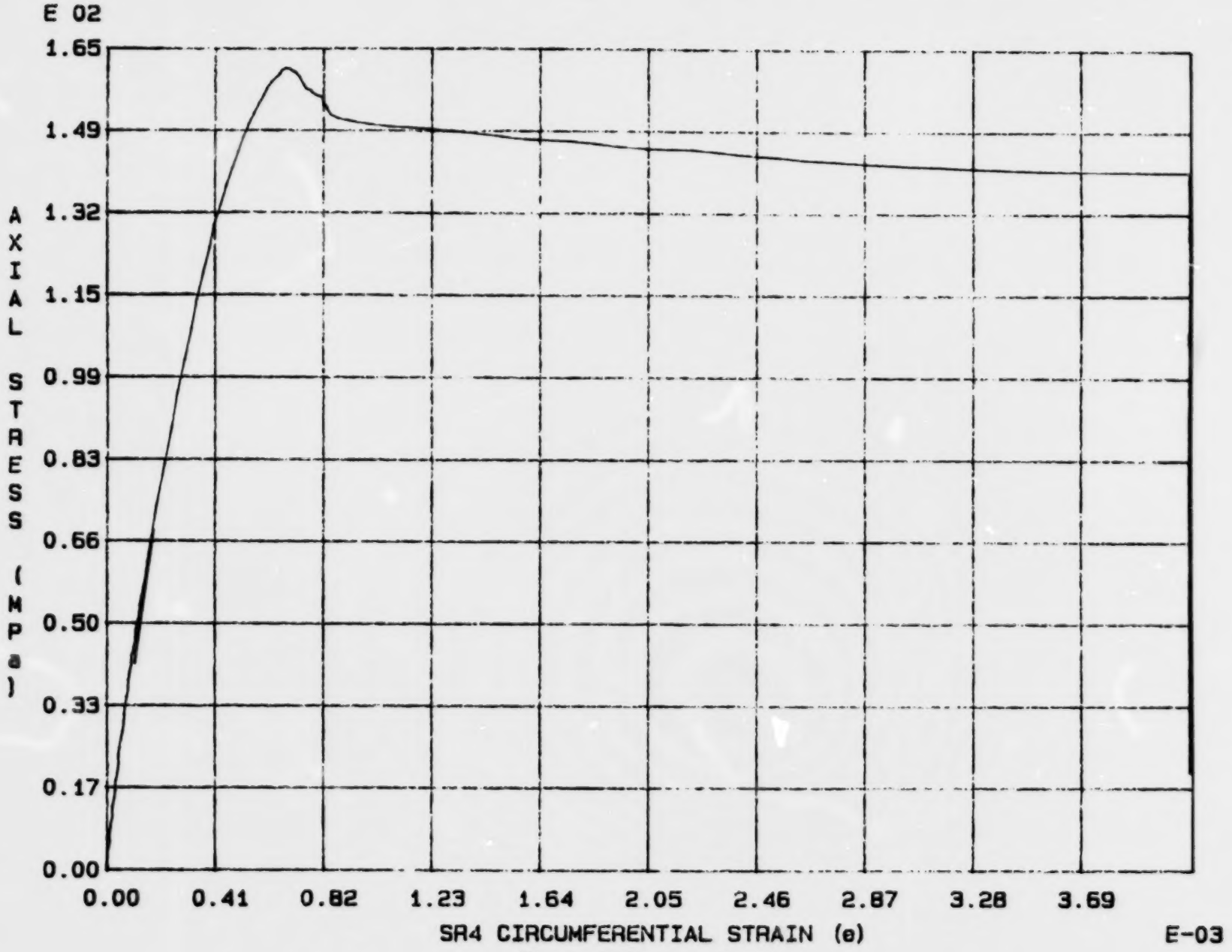

Fig. 4 - 28 Specimen M30U

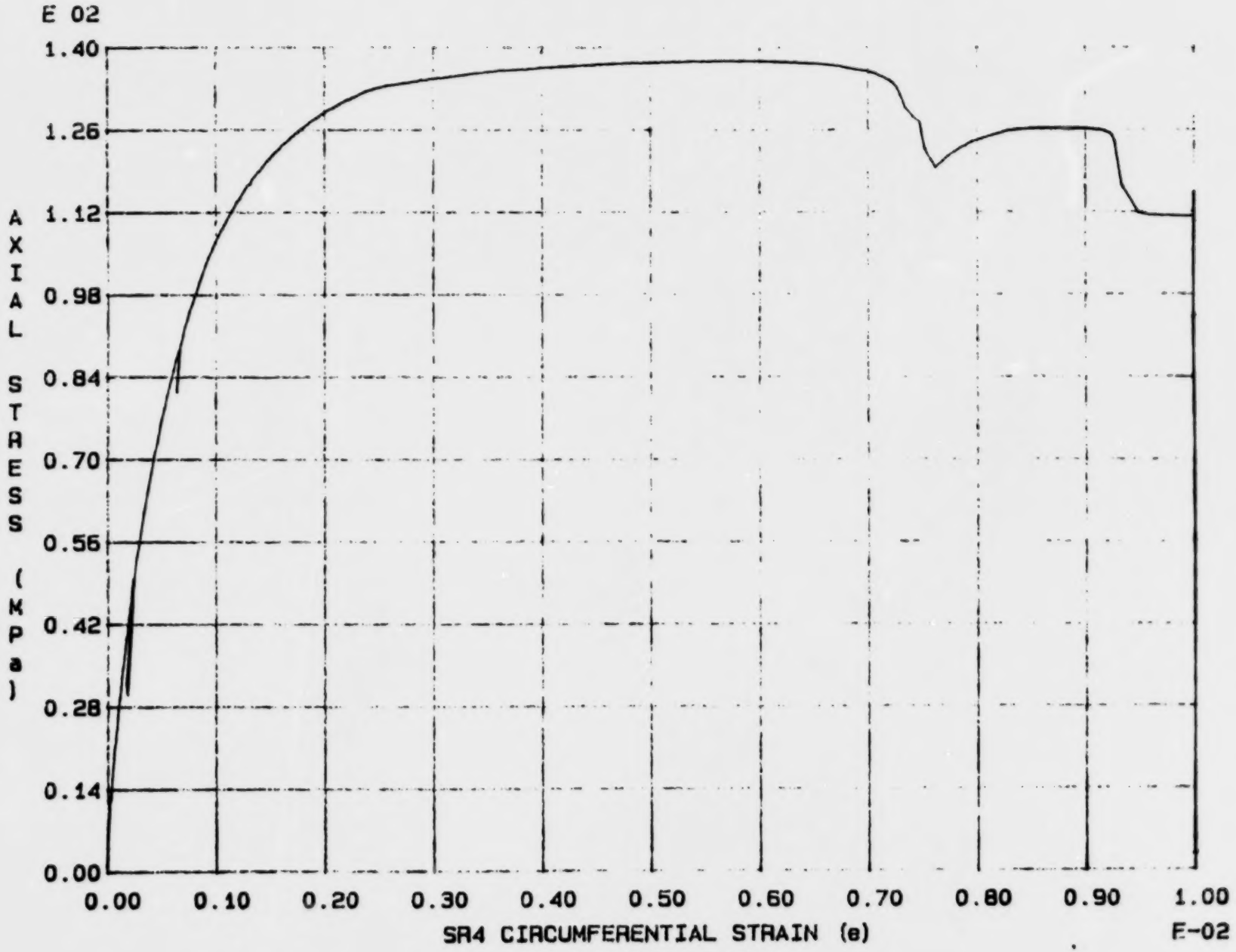

Fig. 4 - 29 Specimen M31U

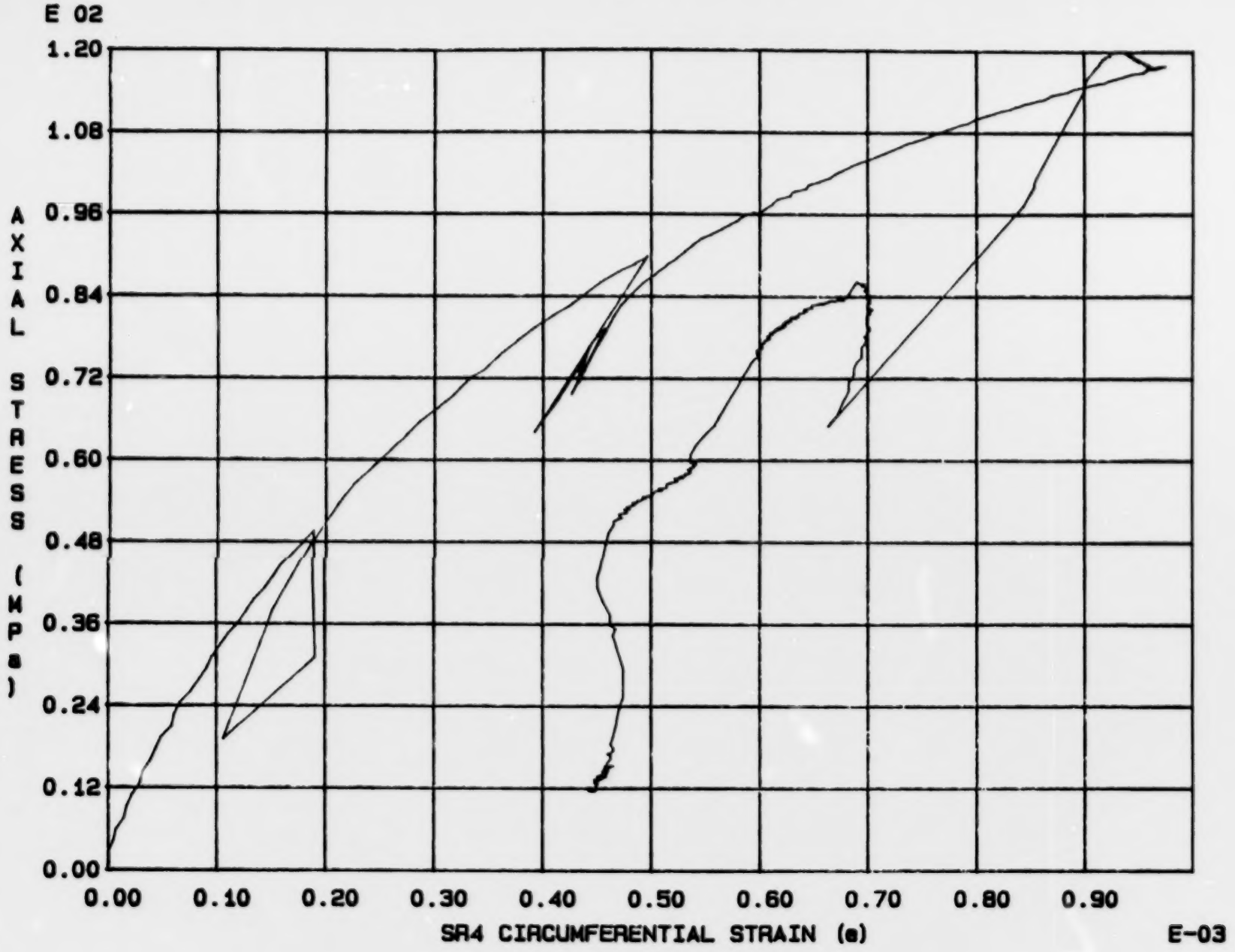

Fig. 4 - 30 Specimen M32U

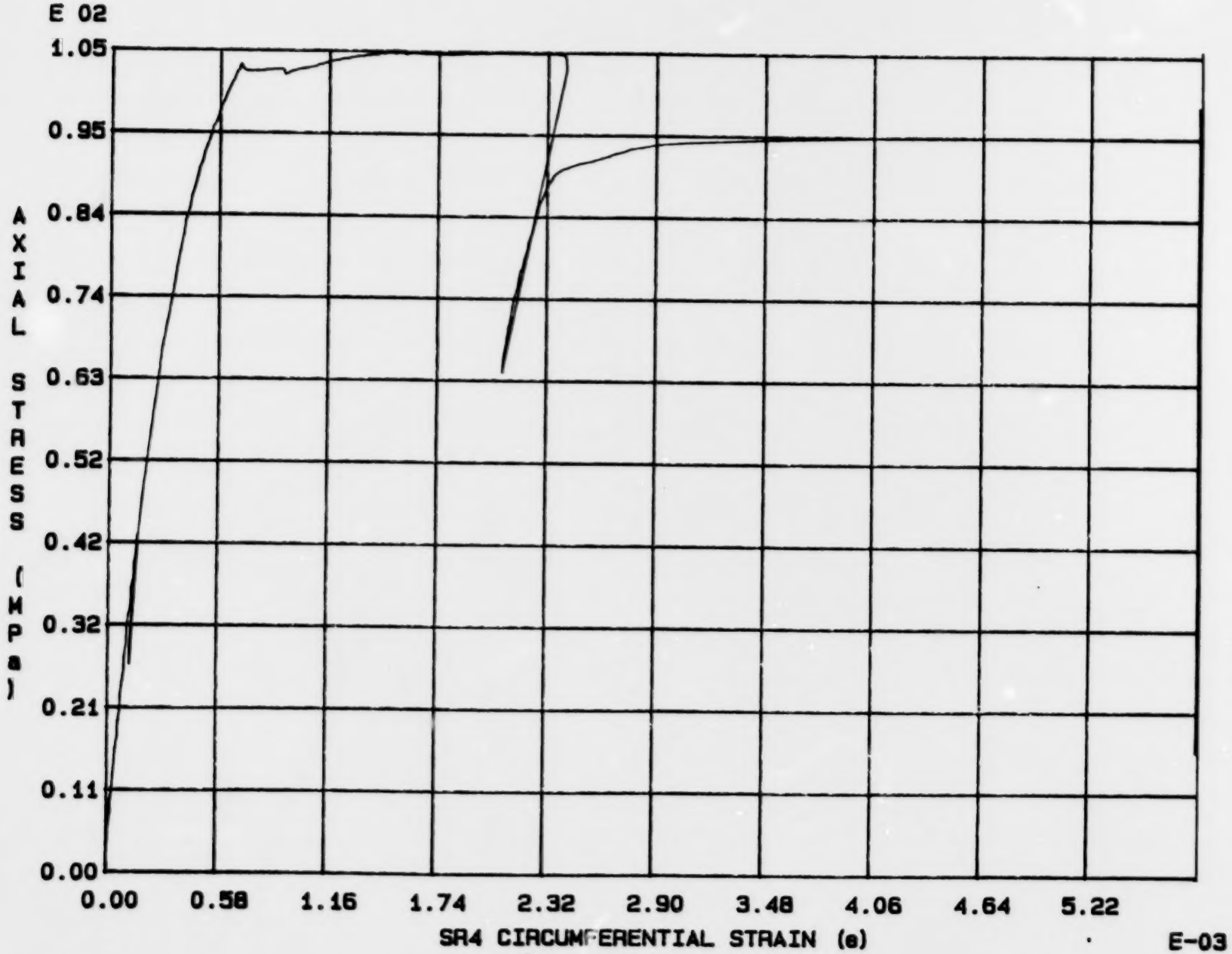

Fig. 4 - 31 Specimen M33U

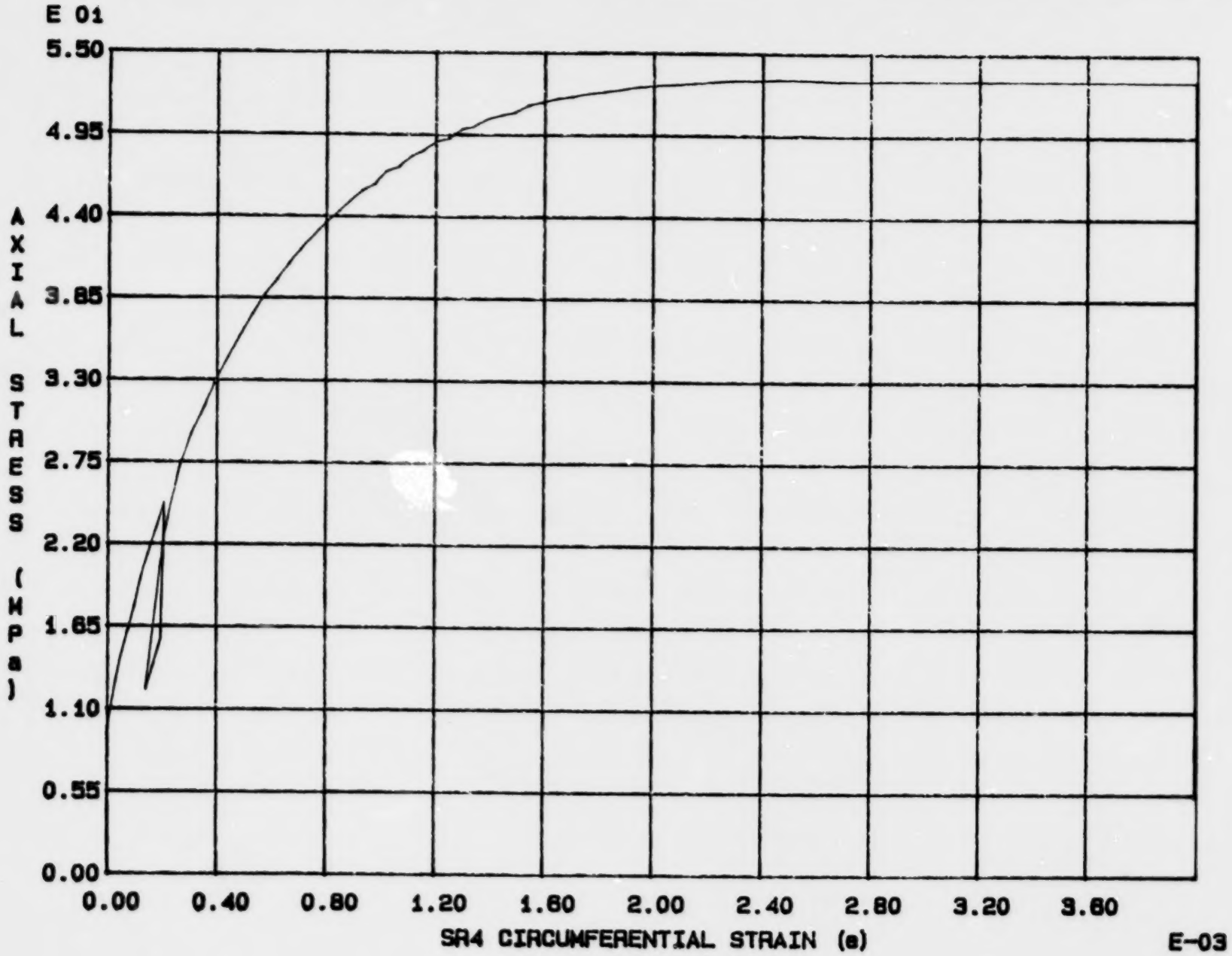

Fig. 4 - 32 Specimen M34U

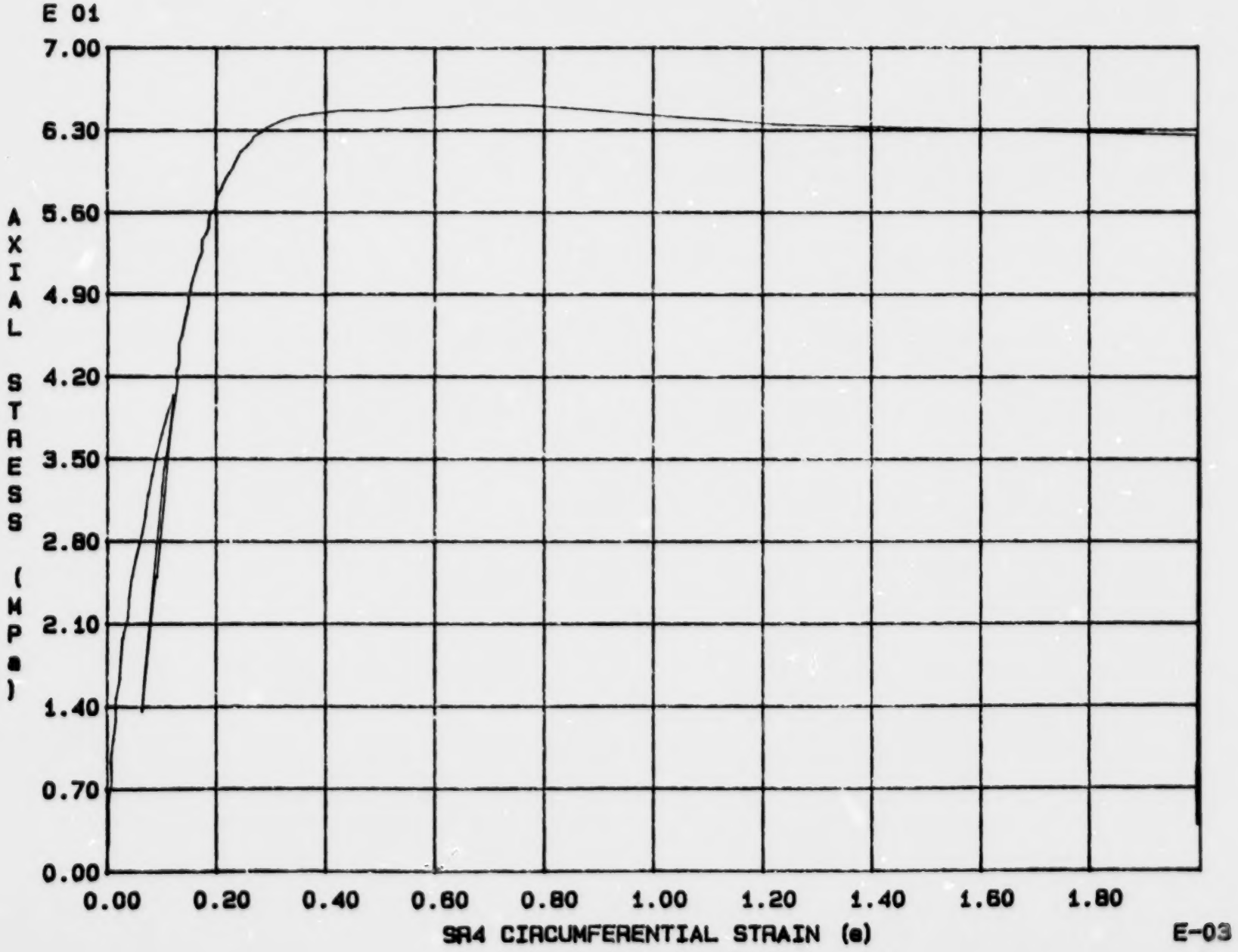

Fig. 4 - 33 Specimen M35U

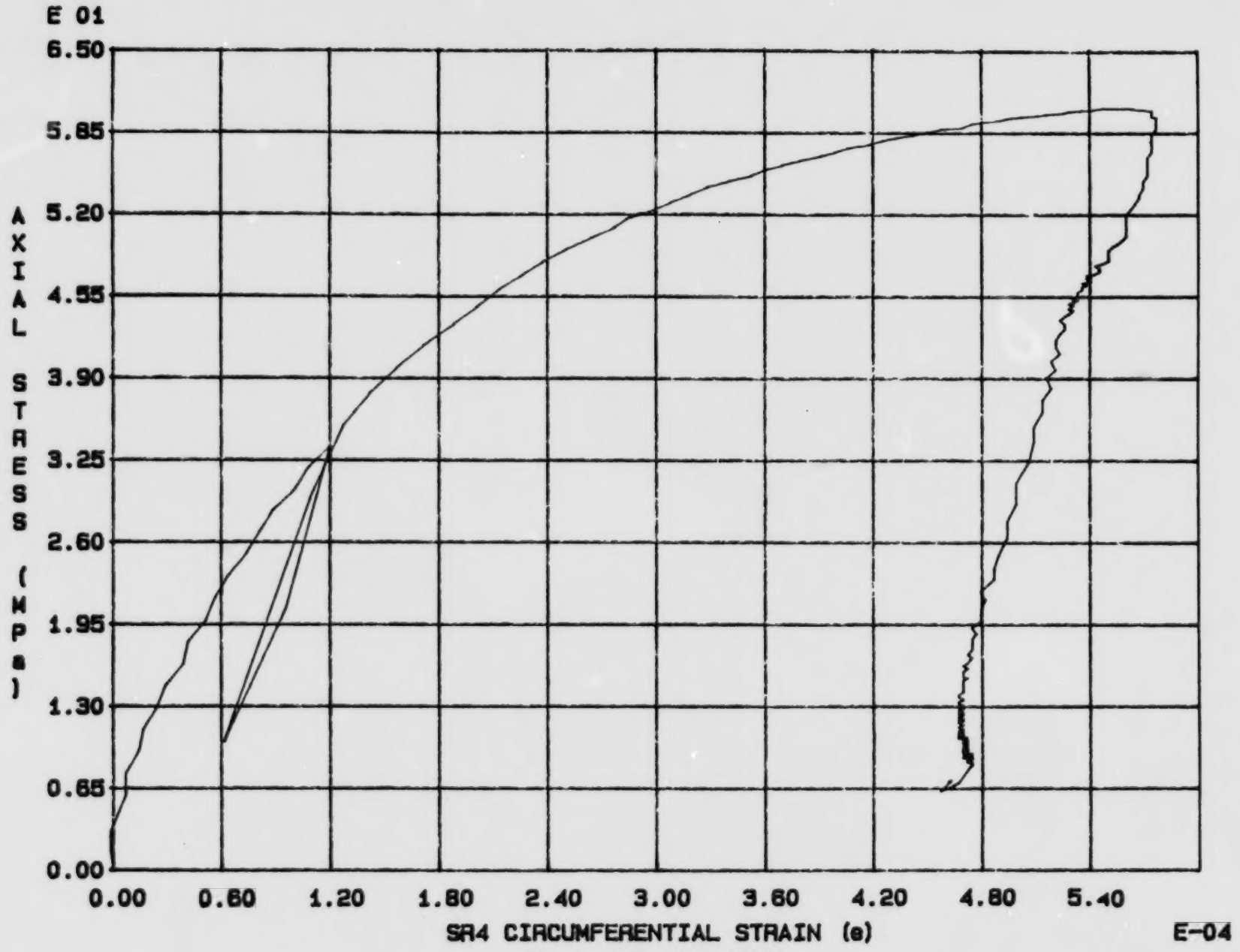

Fig. 4 - 34 Specimen M36U

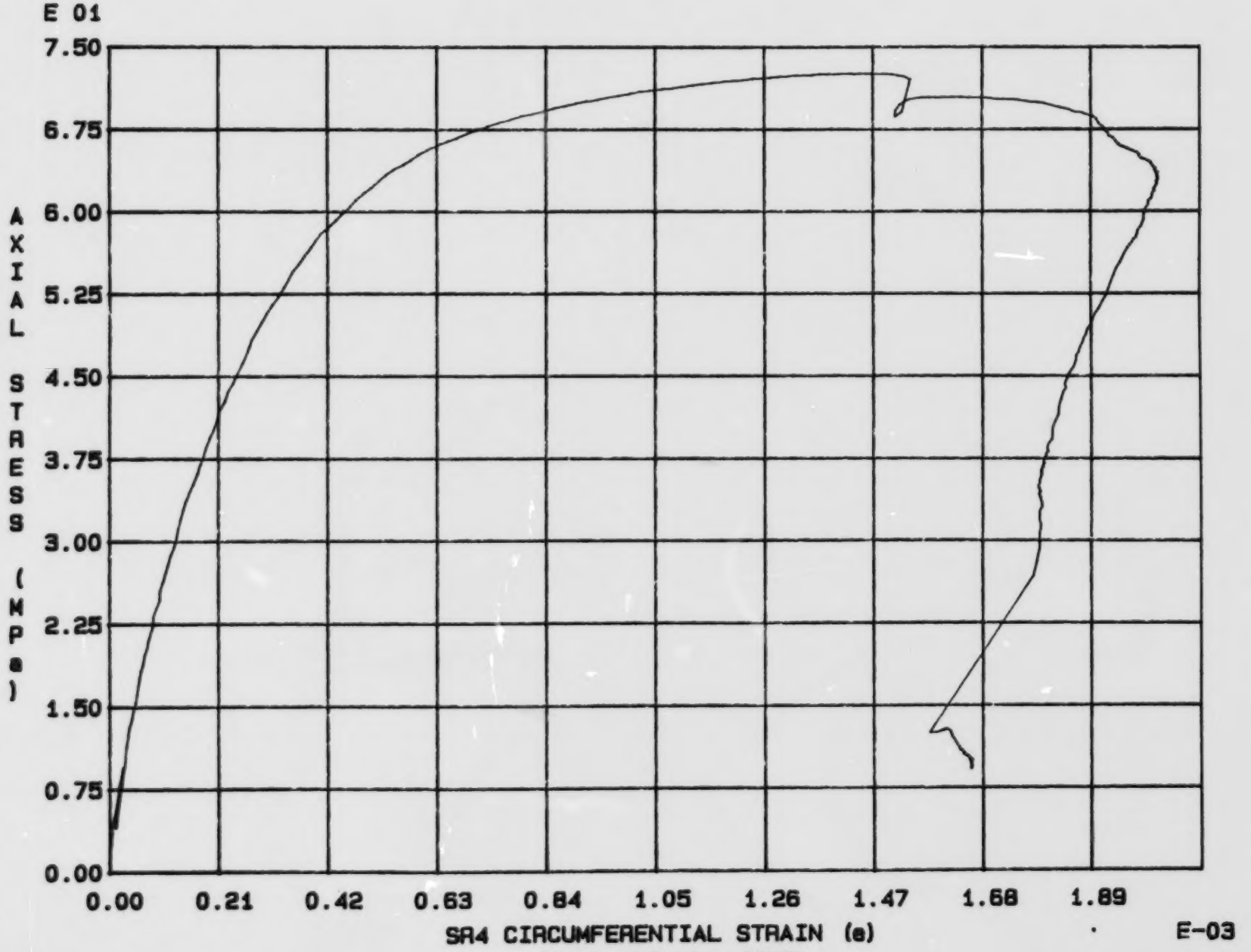

Fig. 4 - 35 Specimen M37U

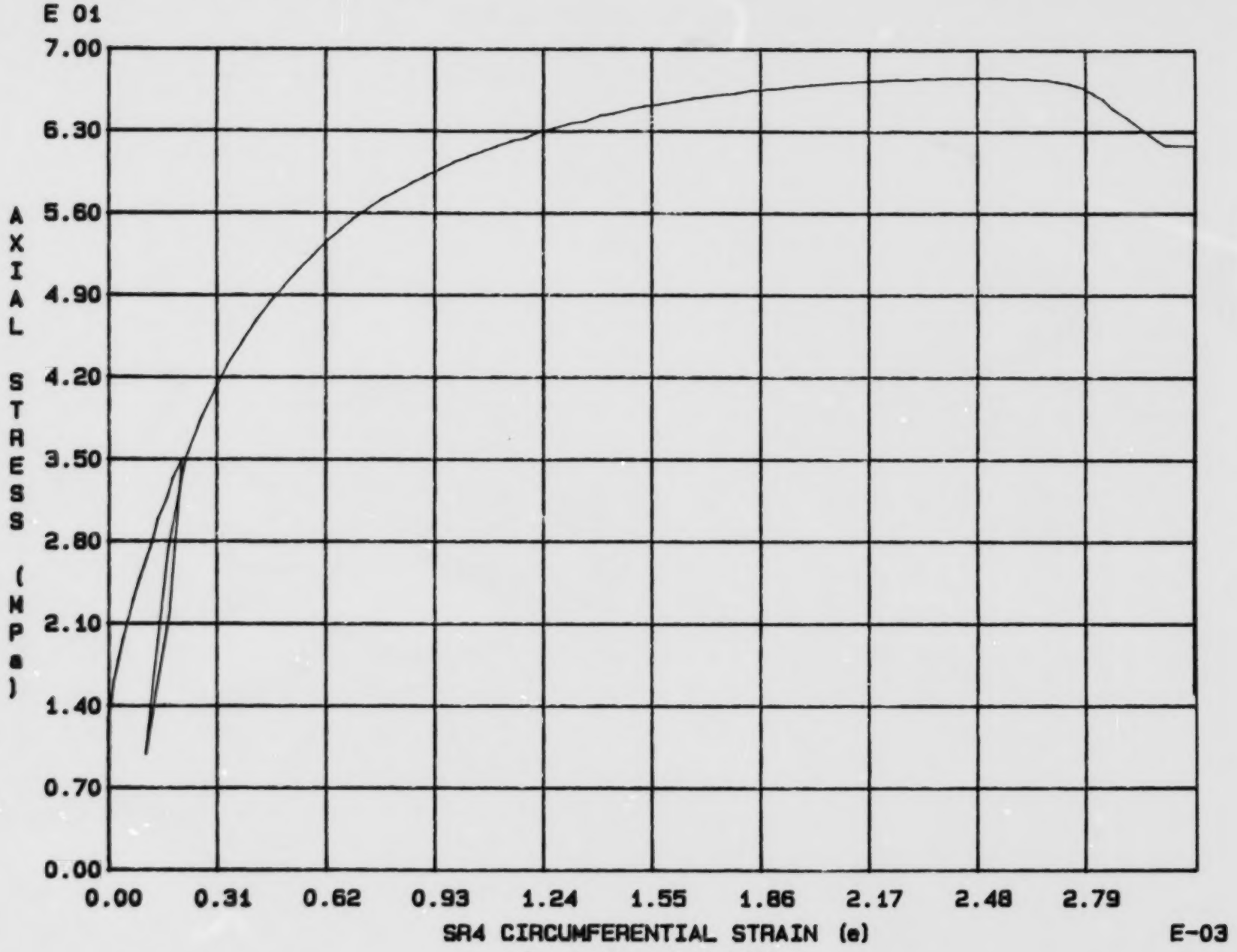

Fig. 4 - 36 Specimen M38U

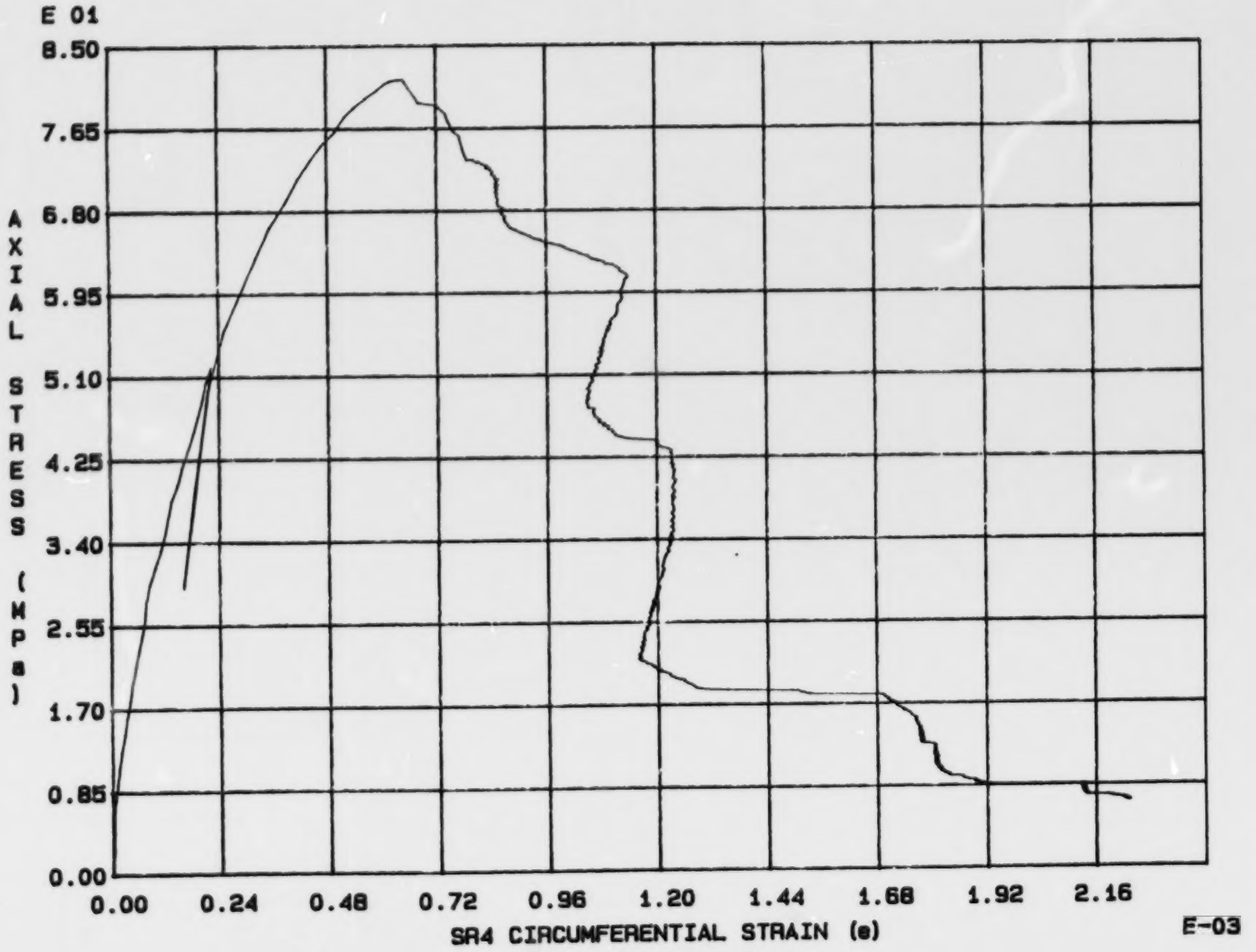

Fig. 4 - 37 Specimen M39U

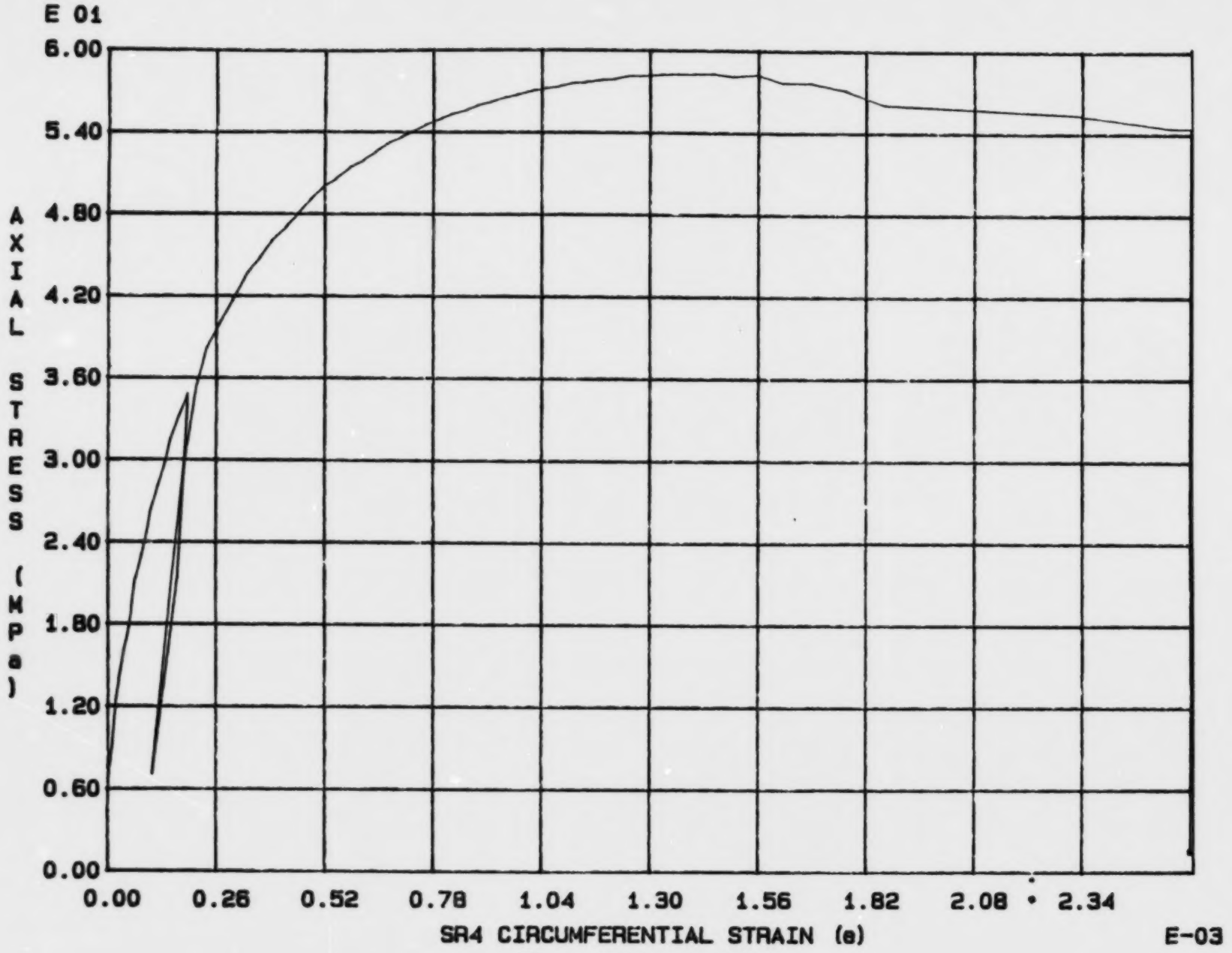

Fig. 4 - 38 Specimen M40U

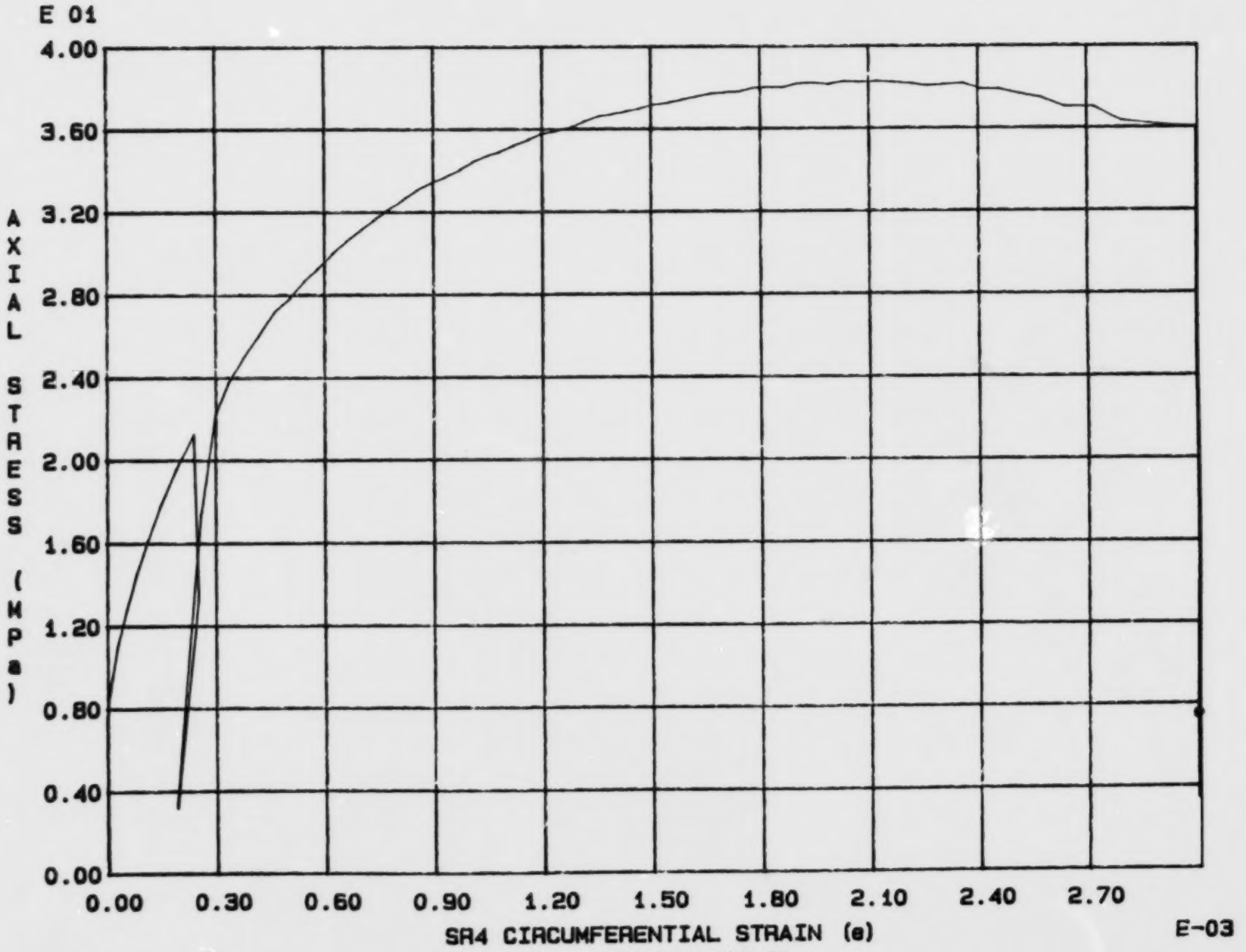

Fig. 4 - 39 Specimen M41U

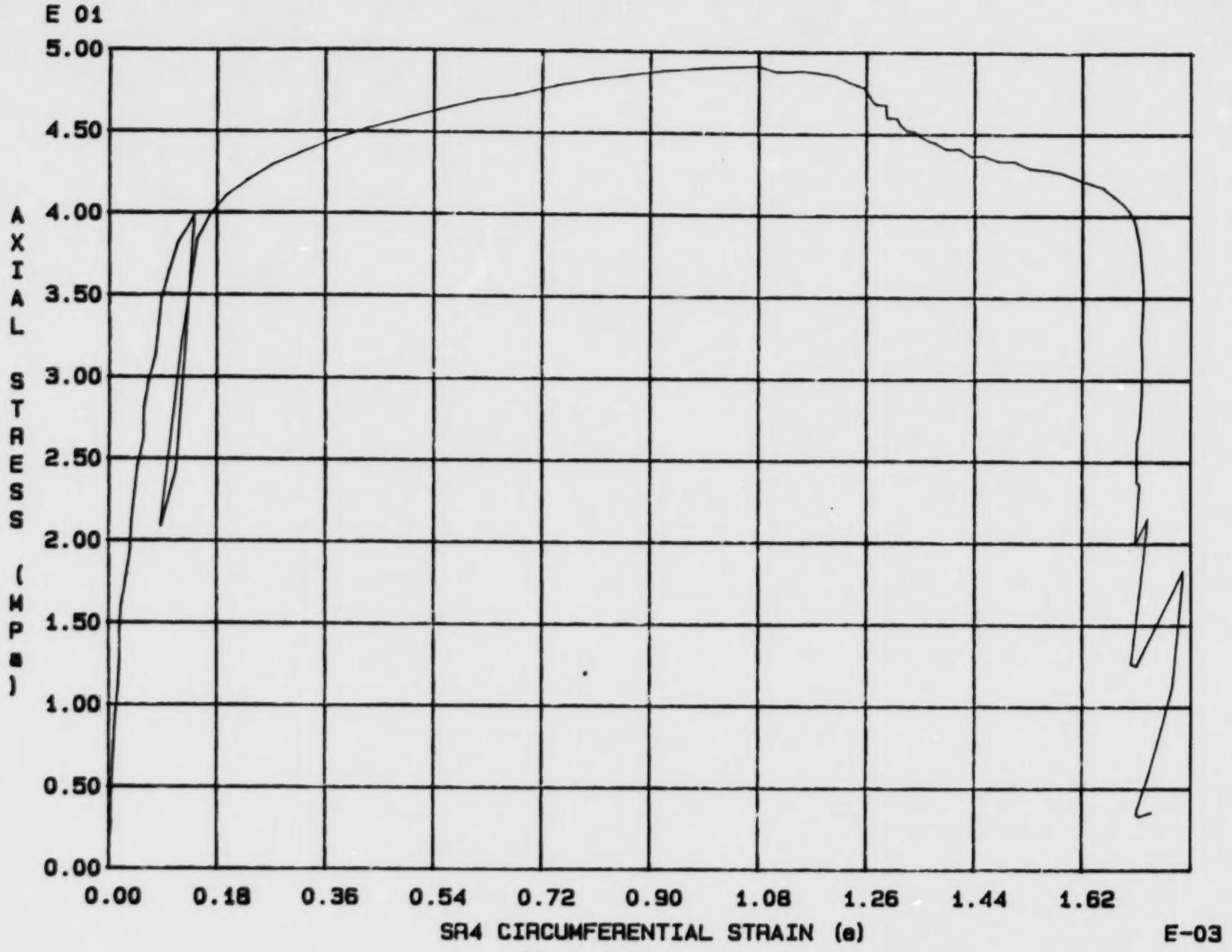

Fig. 4 - 40 Specimen M42U

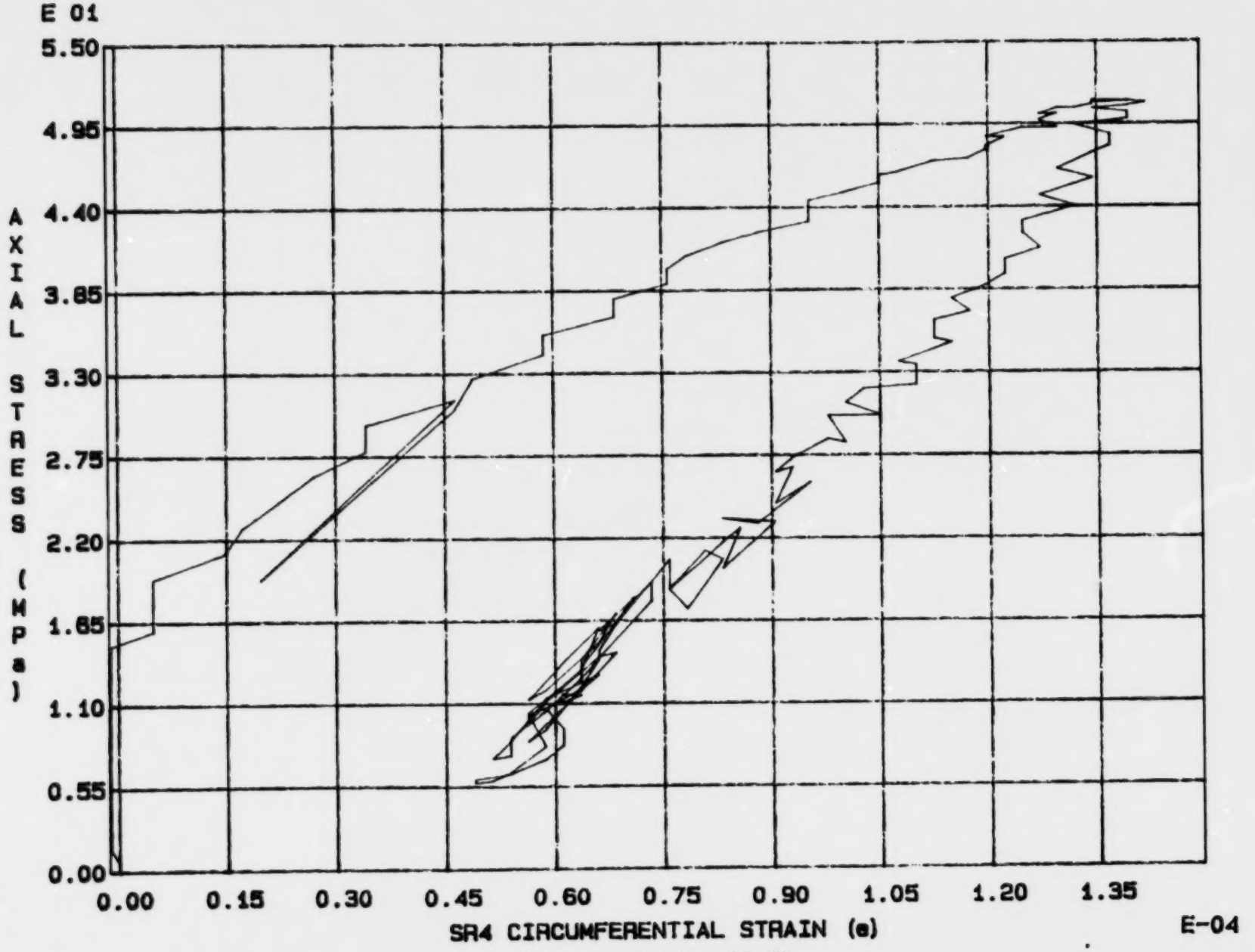

Fig. 4 - 41 Specimen M43U

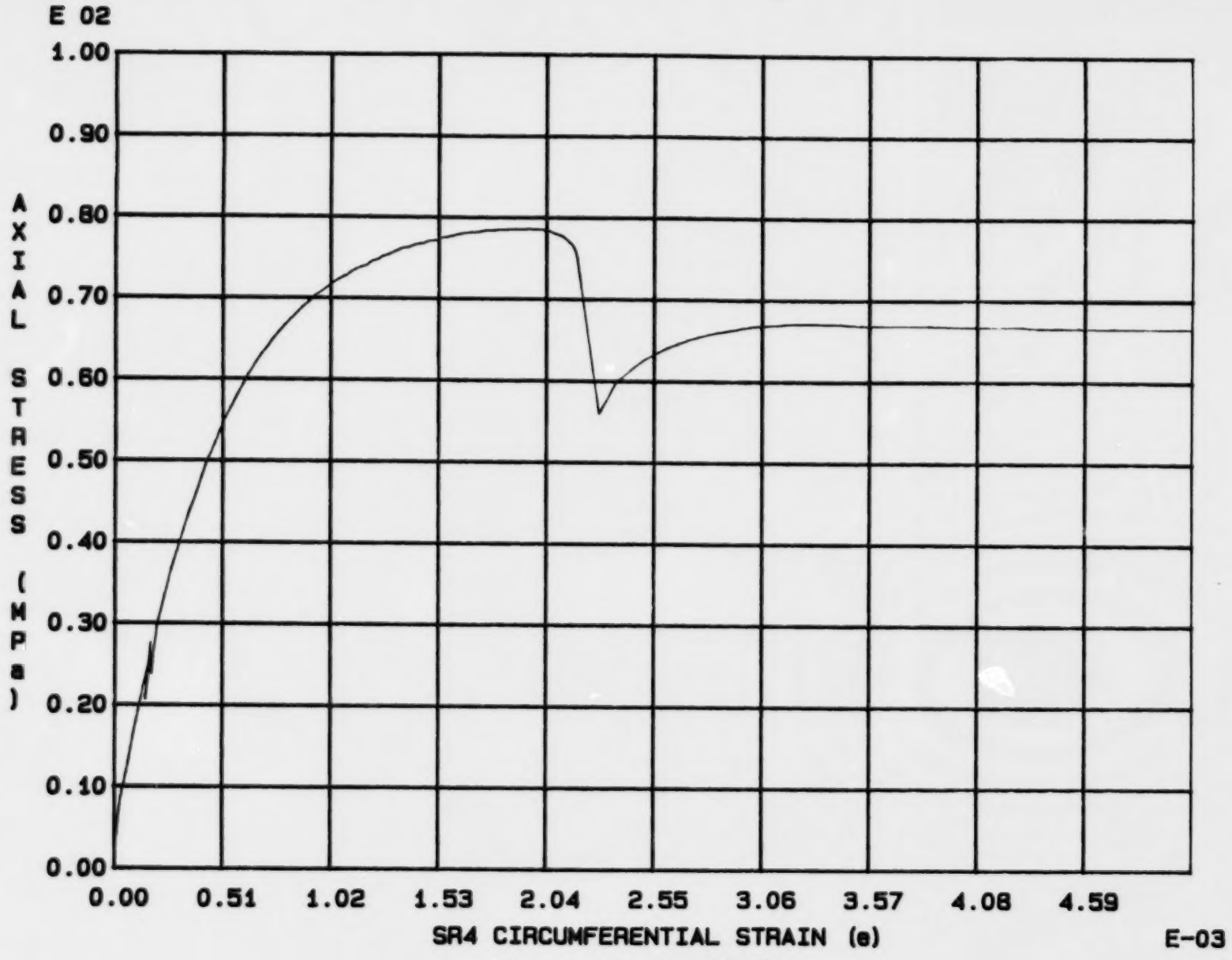

Fig. 4 - 42 Specimen M81U

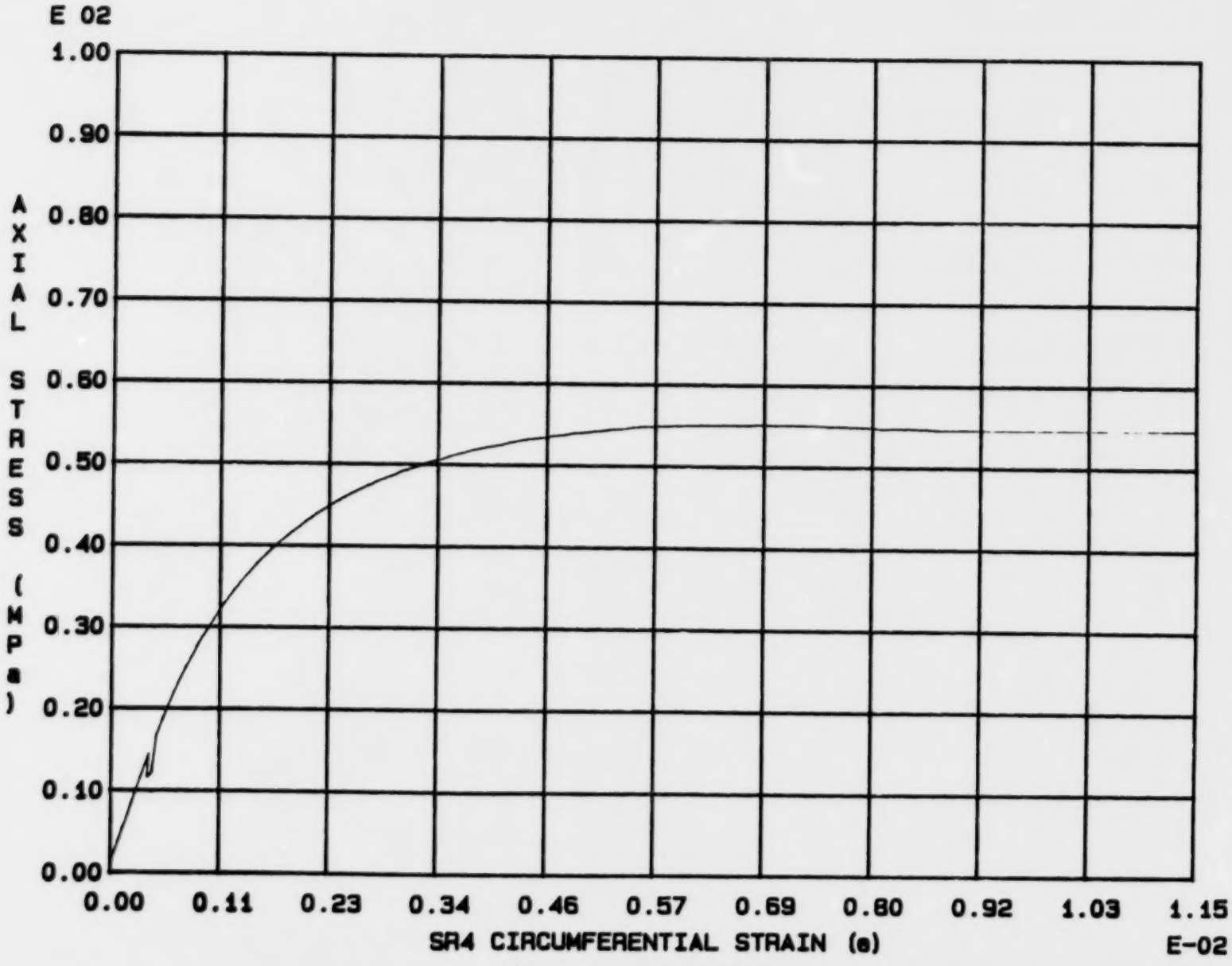

Fig. 4 - 43 Specimen M82U

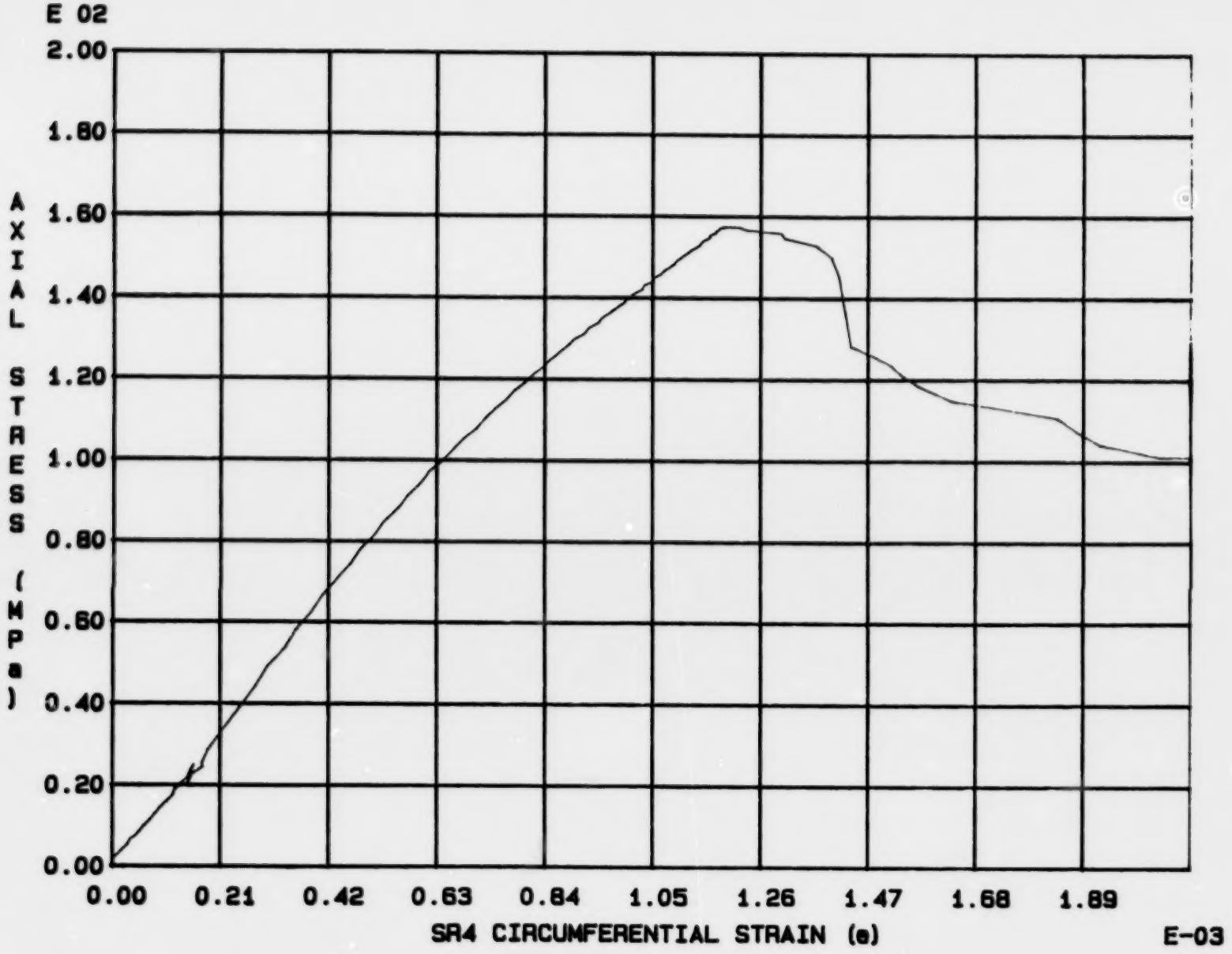

Fig. 4 - 44 Specimen M83U

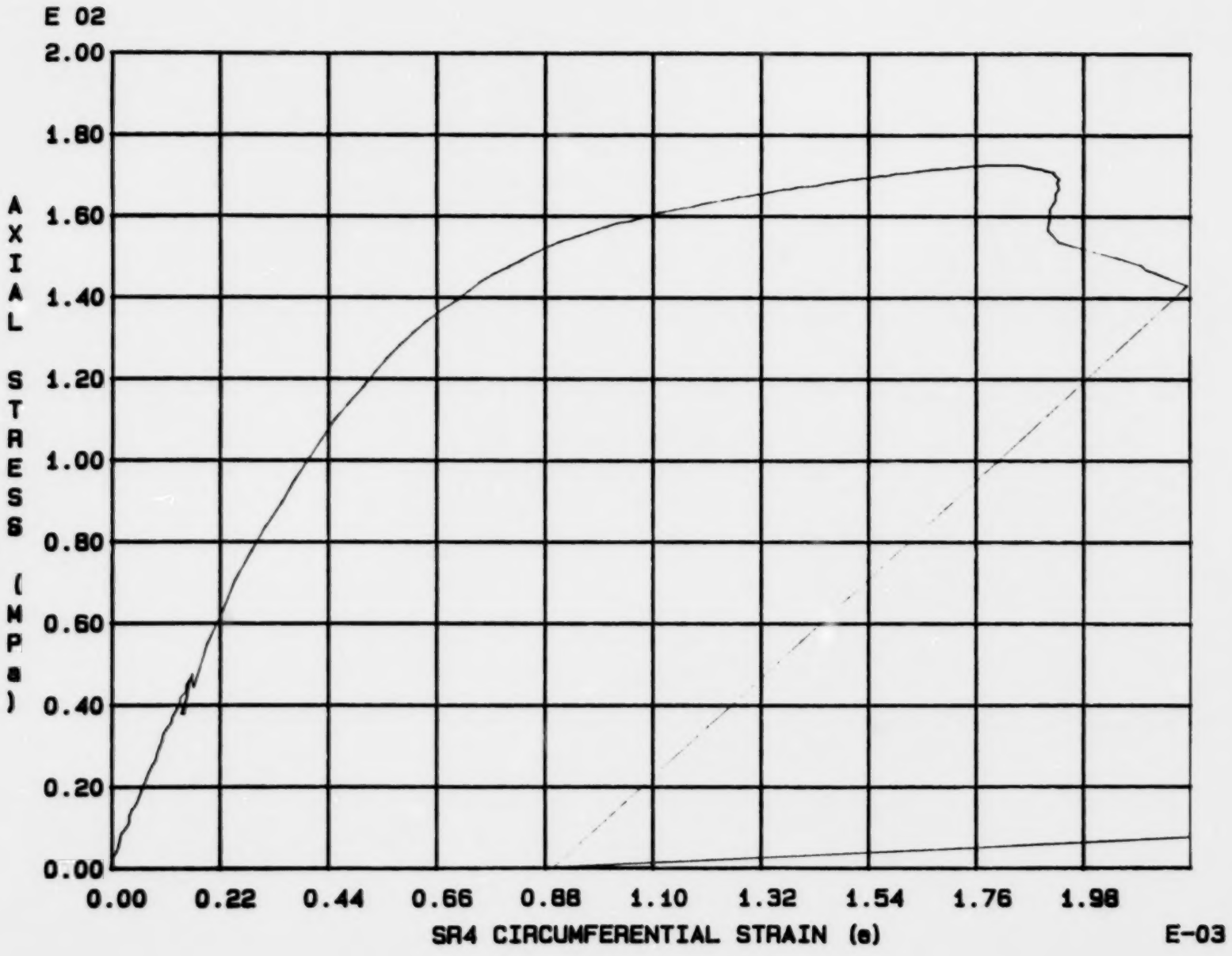

Fig. 4 - 45 Specimen M84U

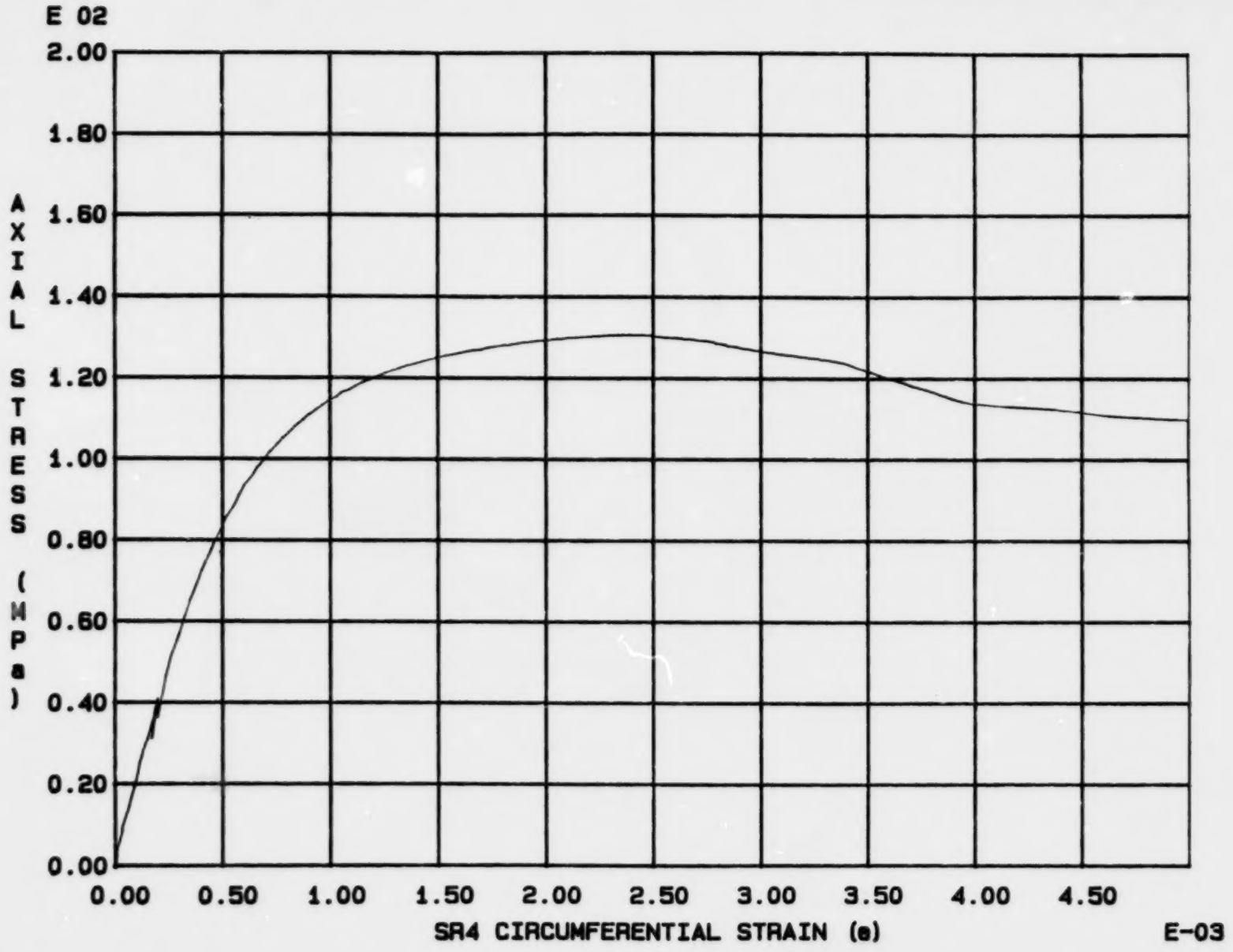

Fig. 4 - 46 Specimen M85U

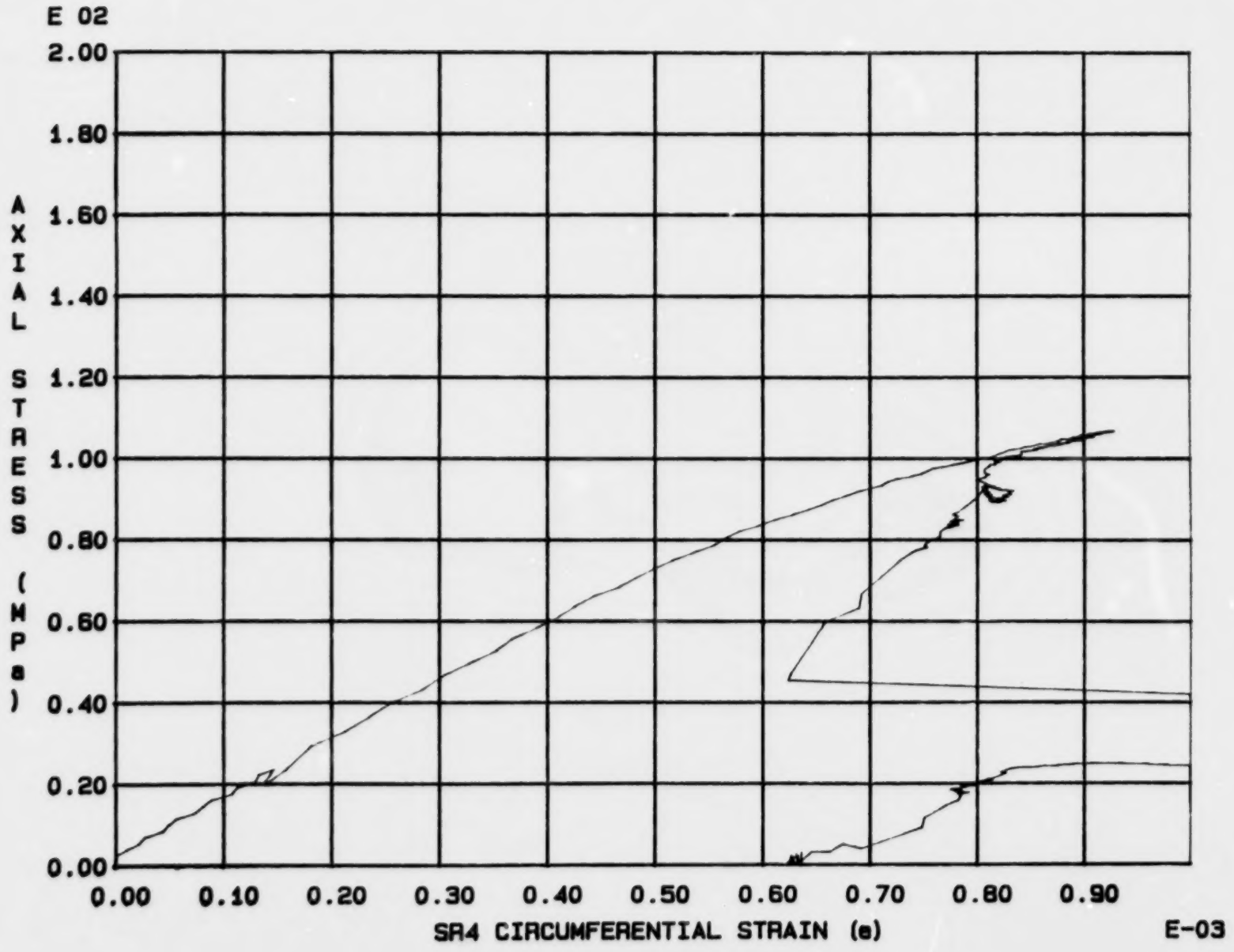

Fig. 4 - 47 Specimen M86U

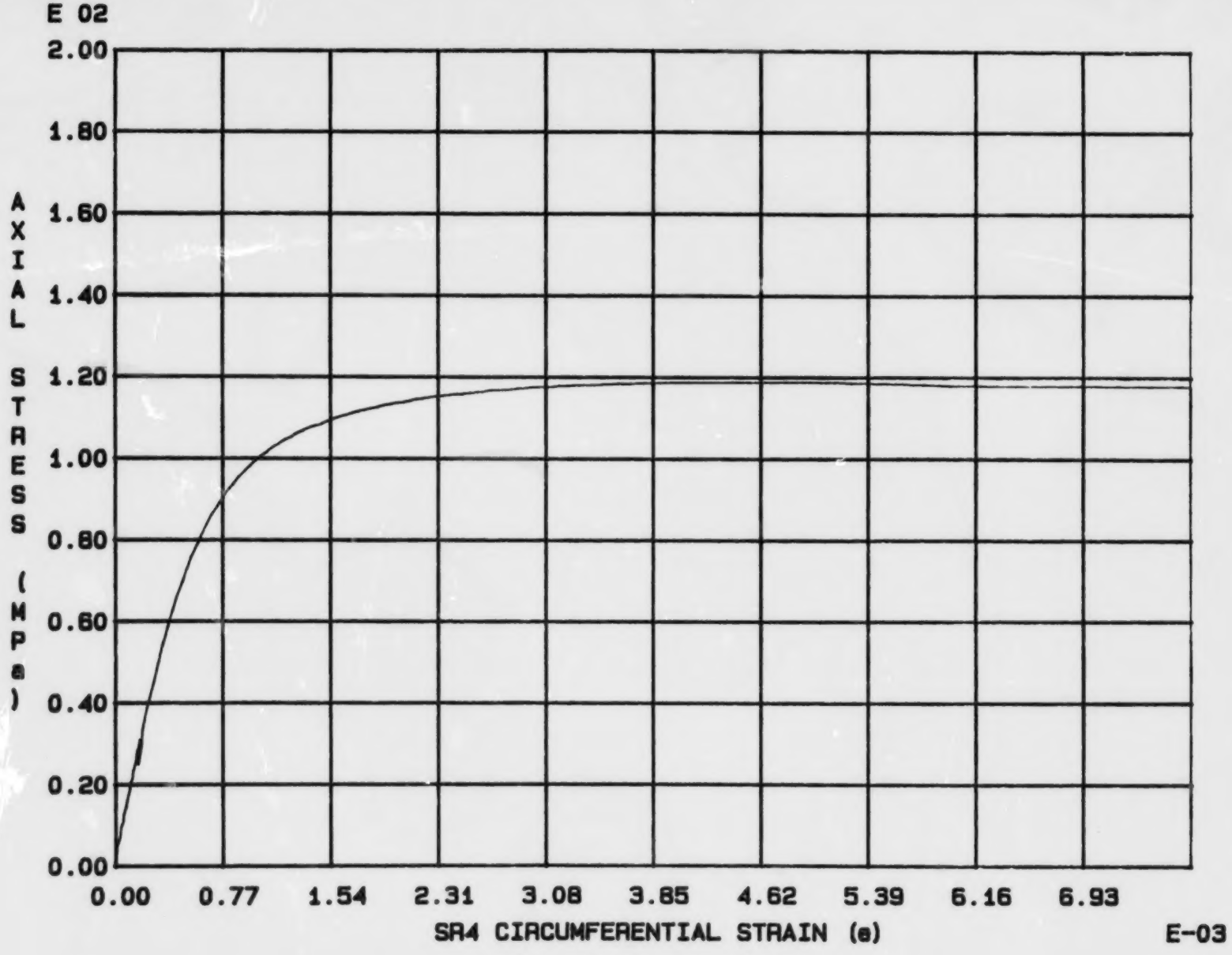

Fig. 4 - 48 Specimen M87U

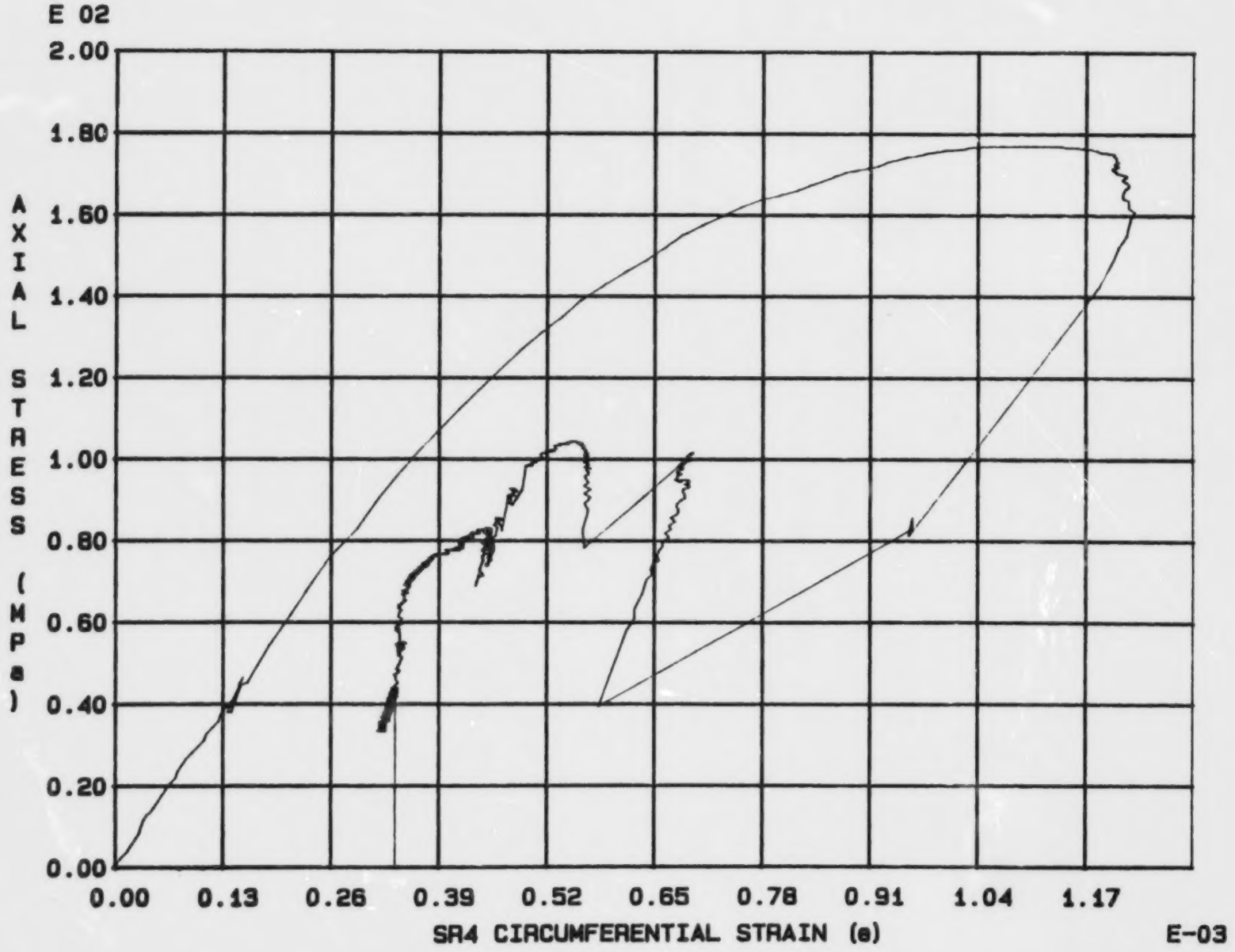

Fig. 4 - 49 Specimen M88U

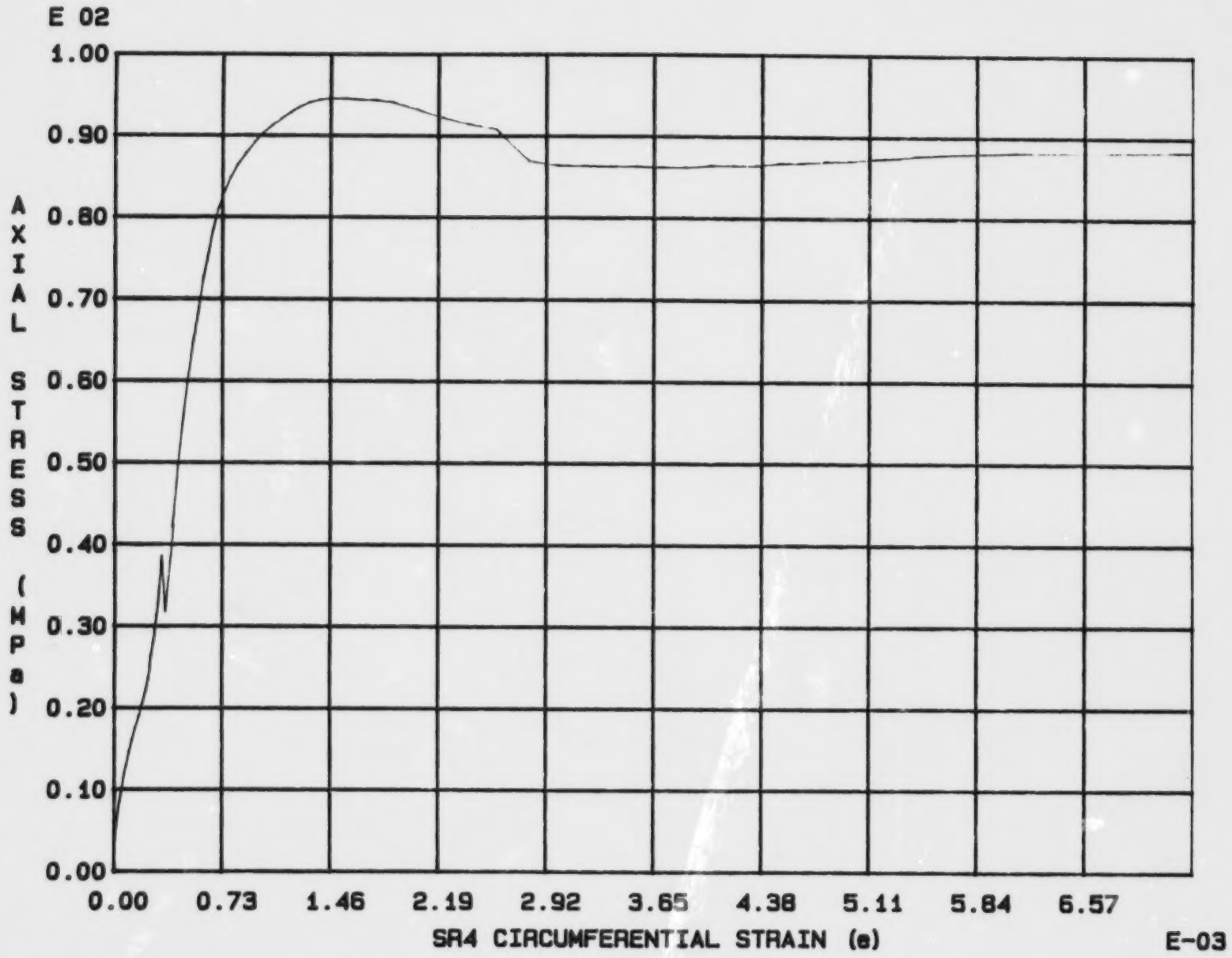

Fig. 4 - 50 Specimen M89U

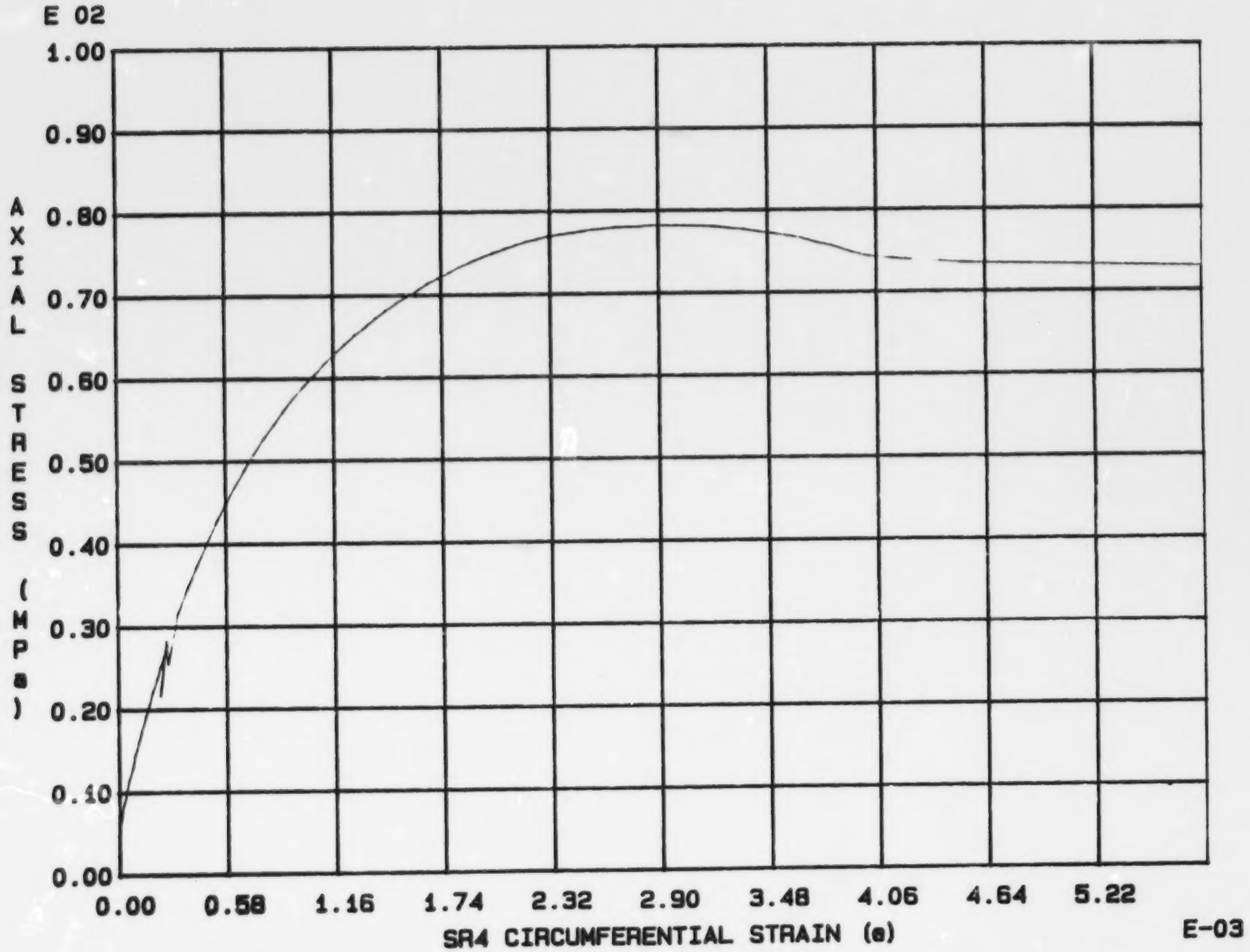

Fig. 4 - 51 Specimen M90U

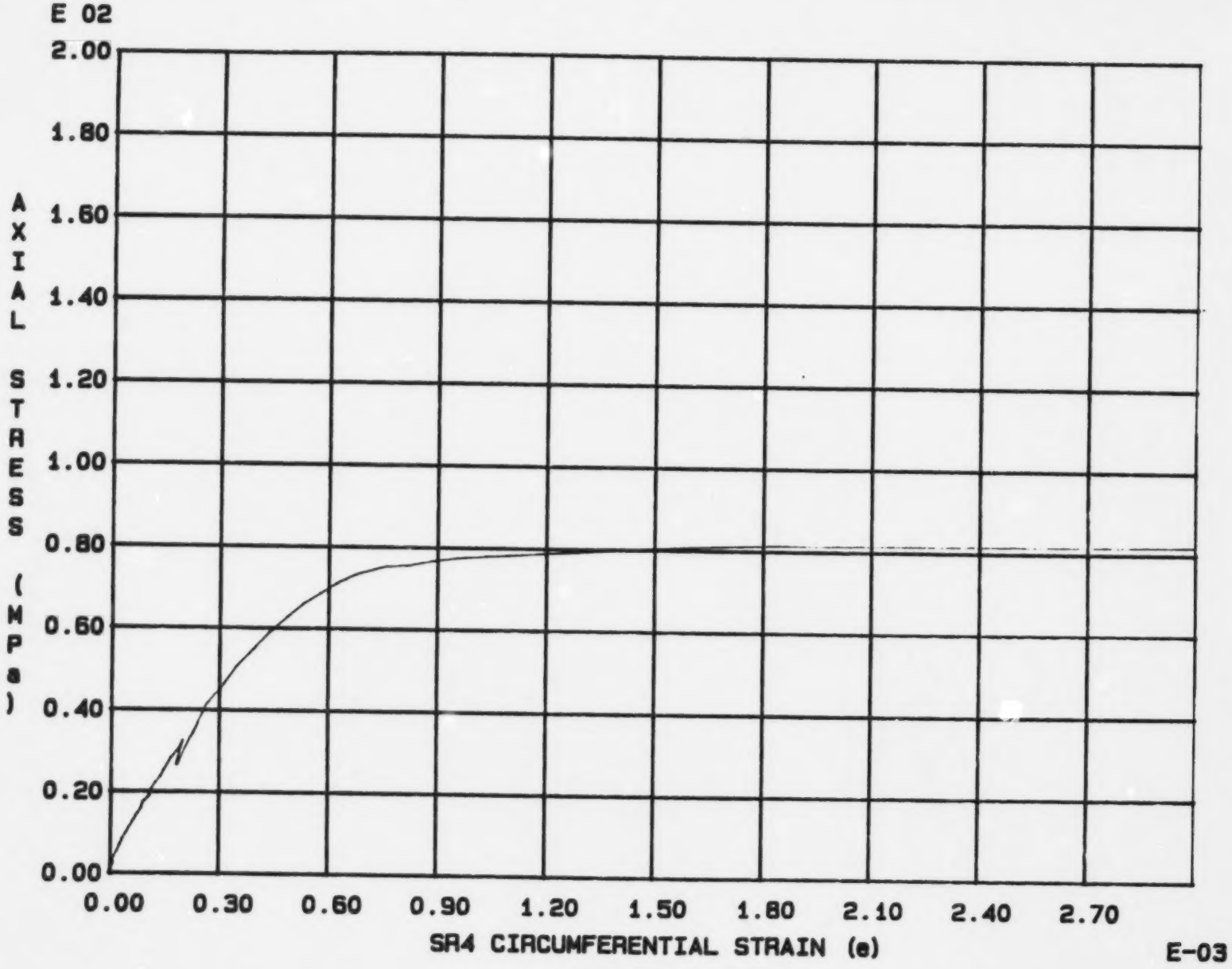

Fig. 4 - 52 Specimen M91U

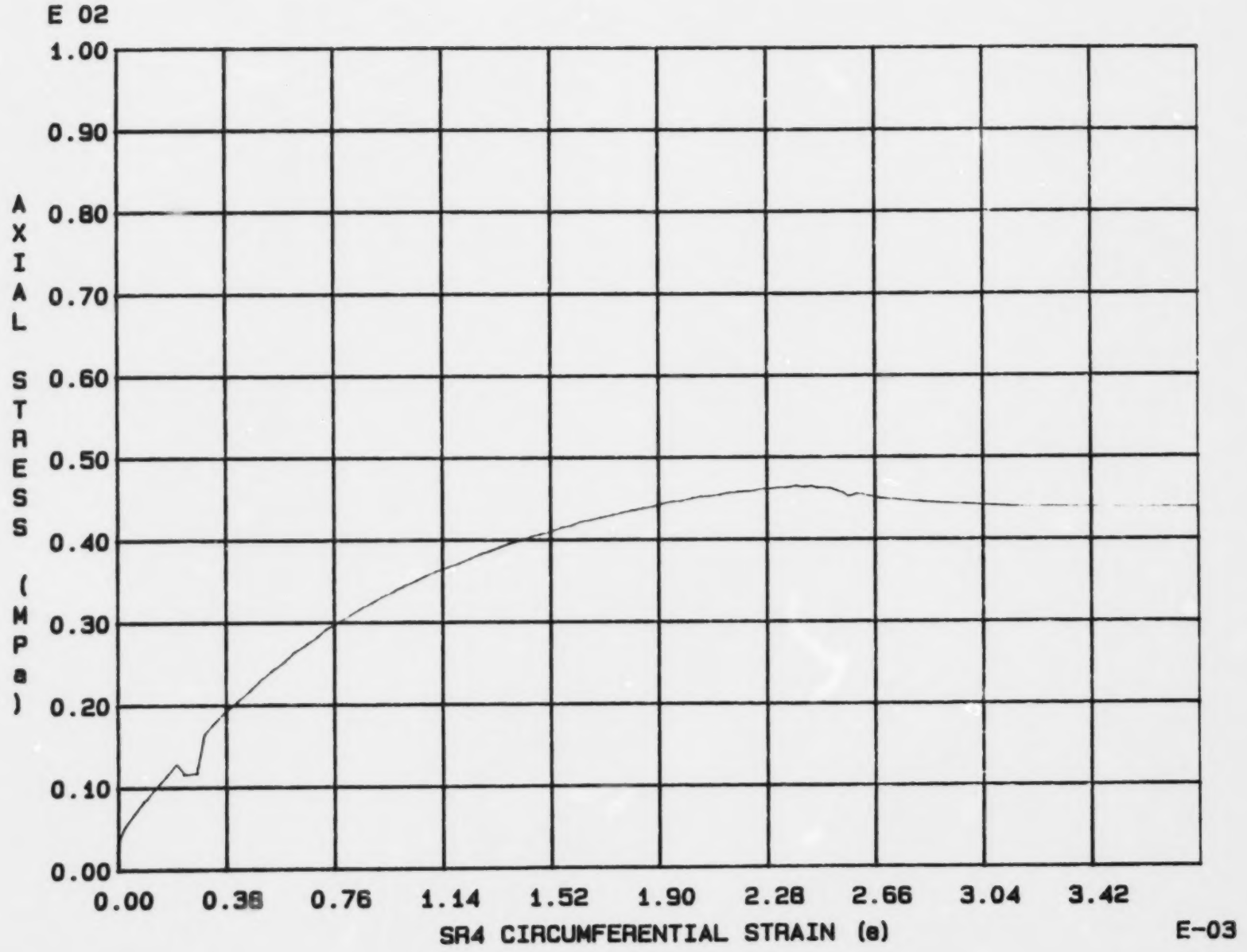

Fig. 4 - 53 Specimen M92U

Appendix 5.

Stress-strain curves of triaxial tests using axial LVDT #1

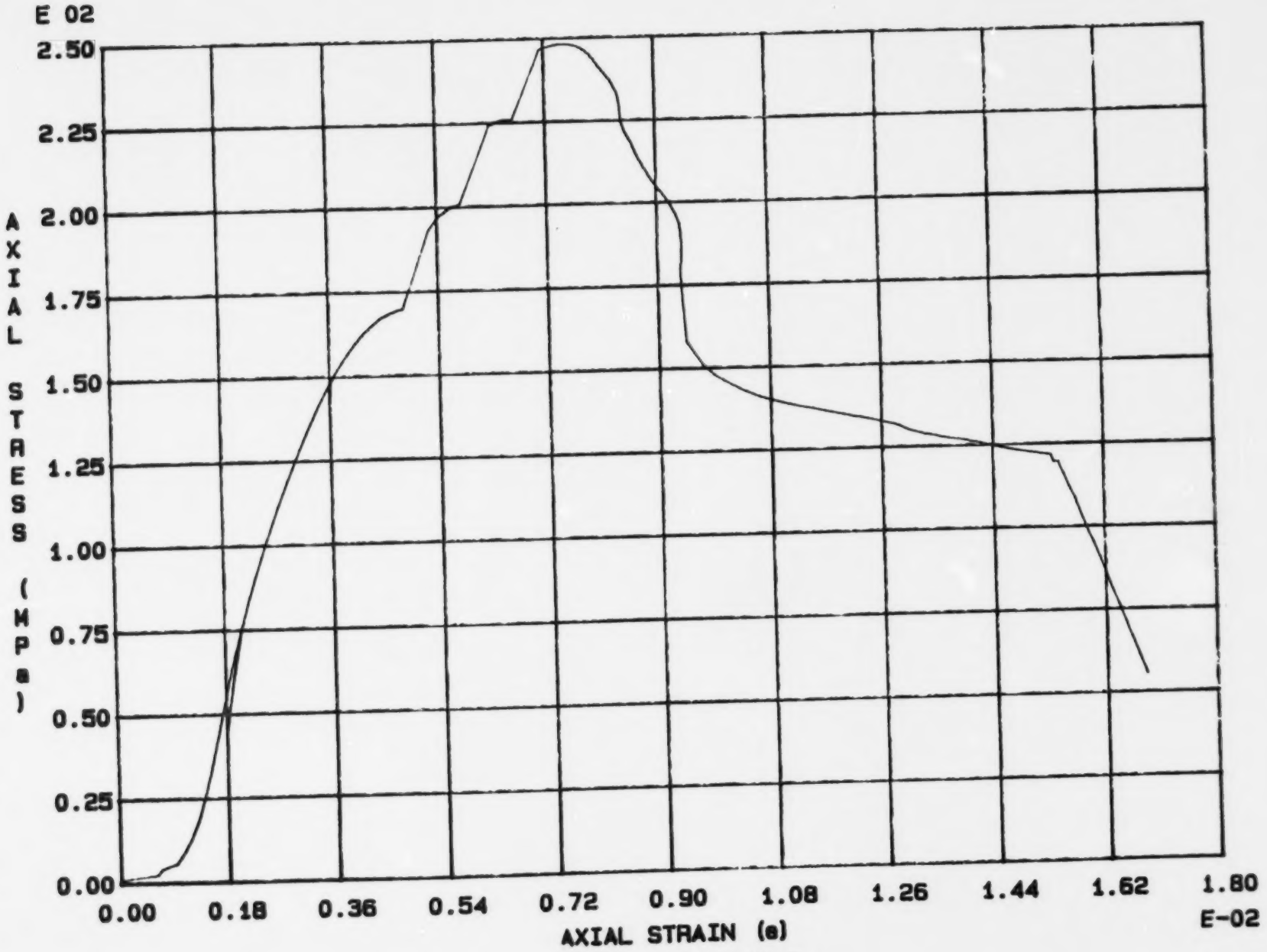

Fig. 5 - 1 Specimen M44T

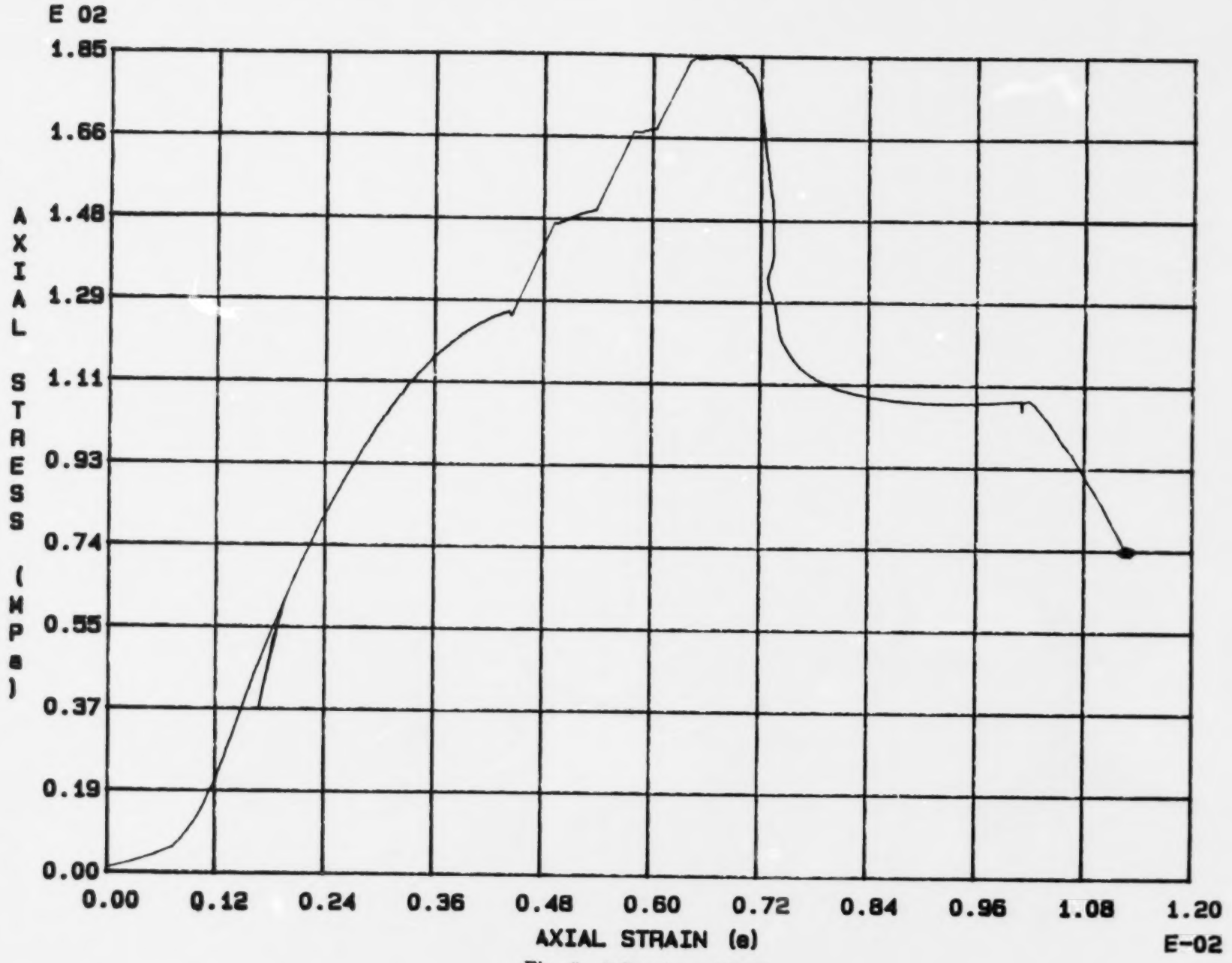

Fig. 5 - 2 Specimen M45T

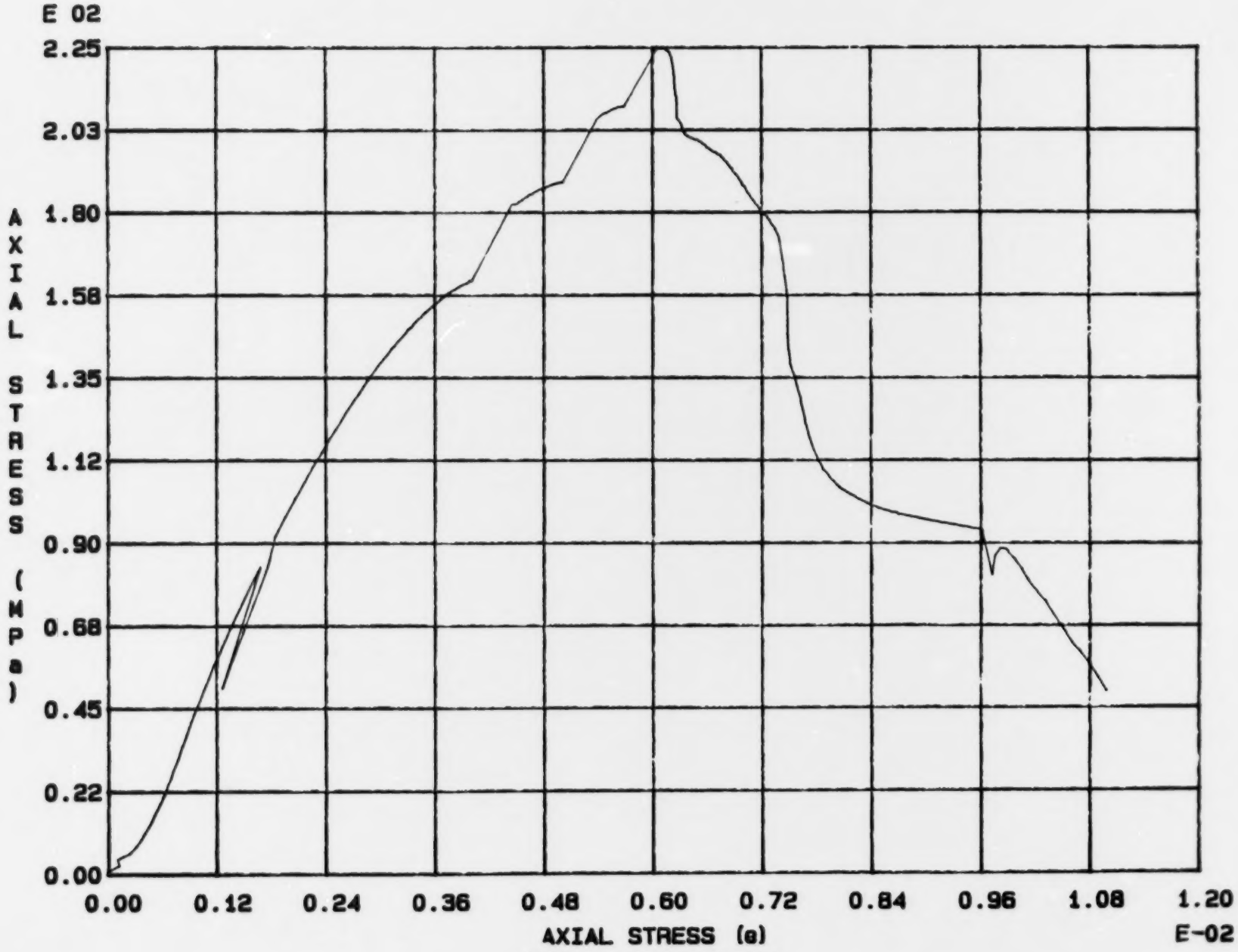

Fig. 5 - 3 Specimen M46T

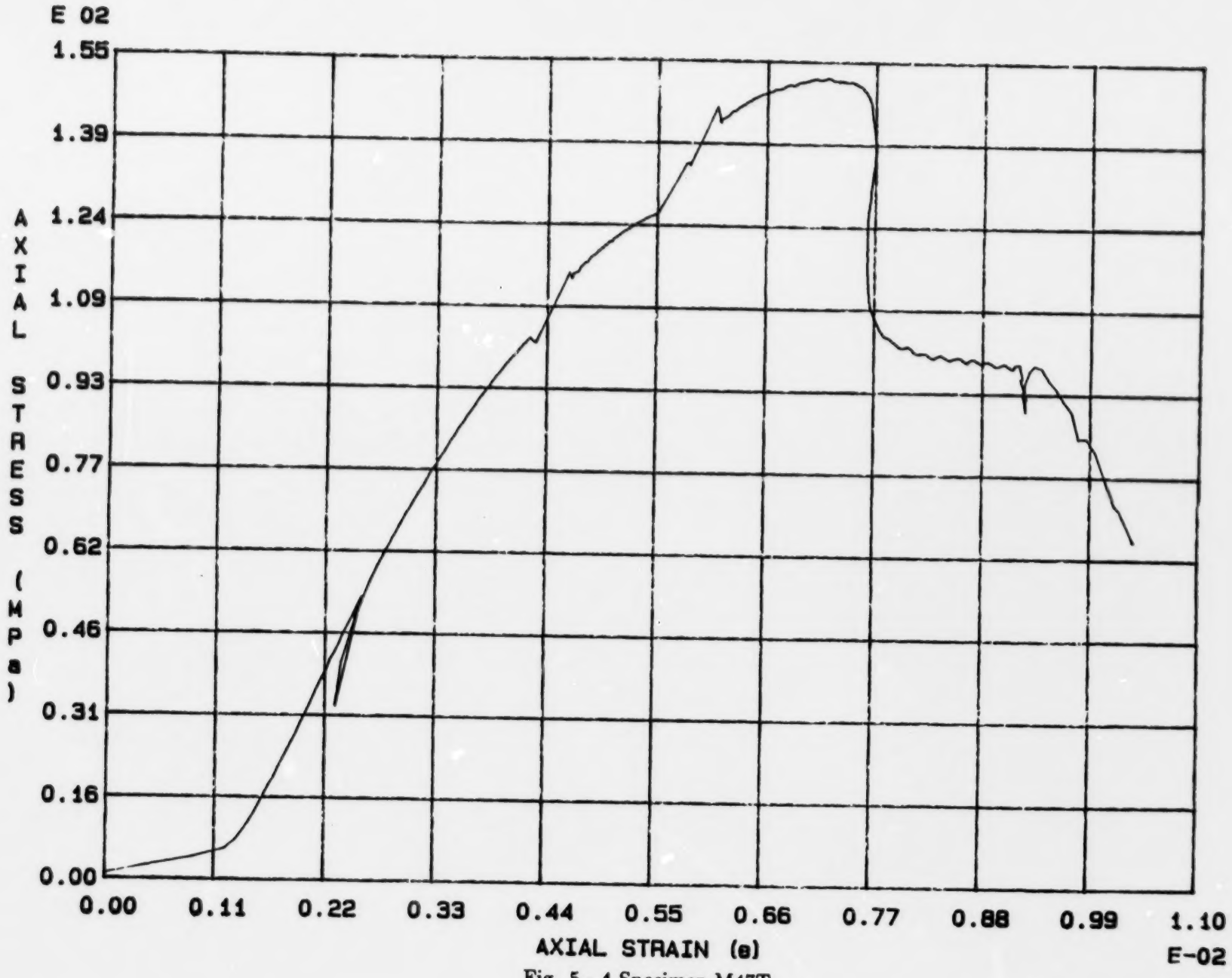

Fig. 5 - 4 Specimen M47T

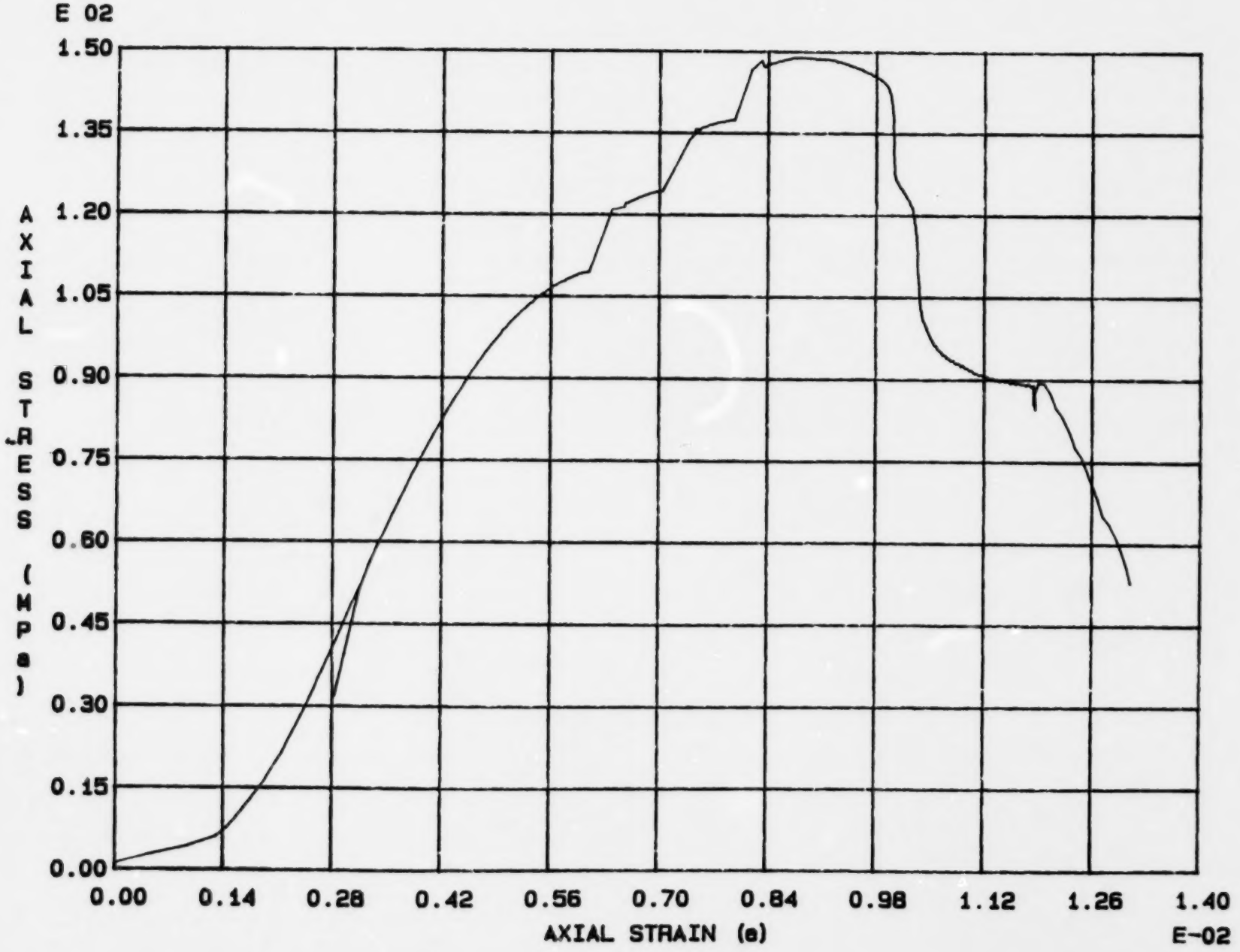

Fig. 5 - 5 Specimen M48T

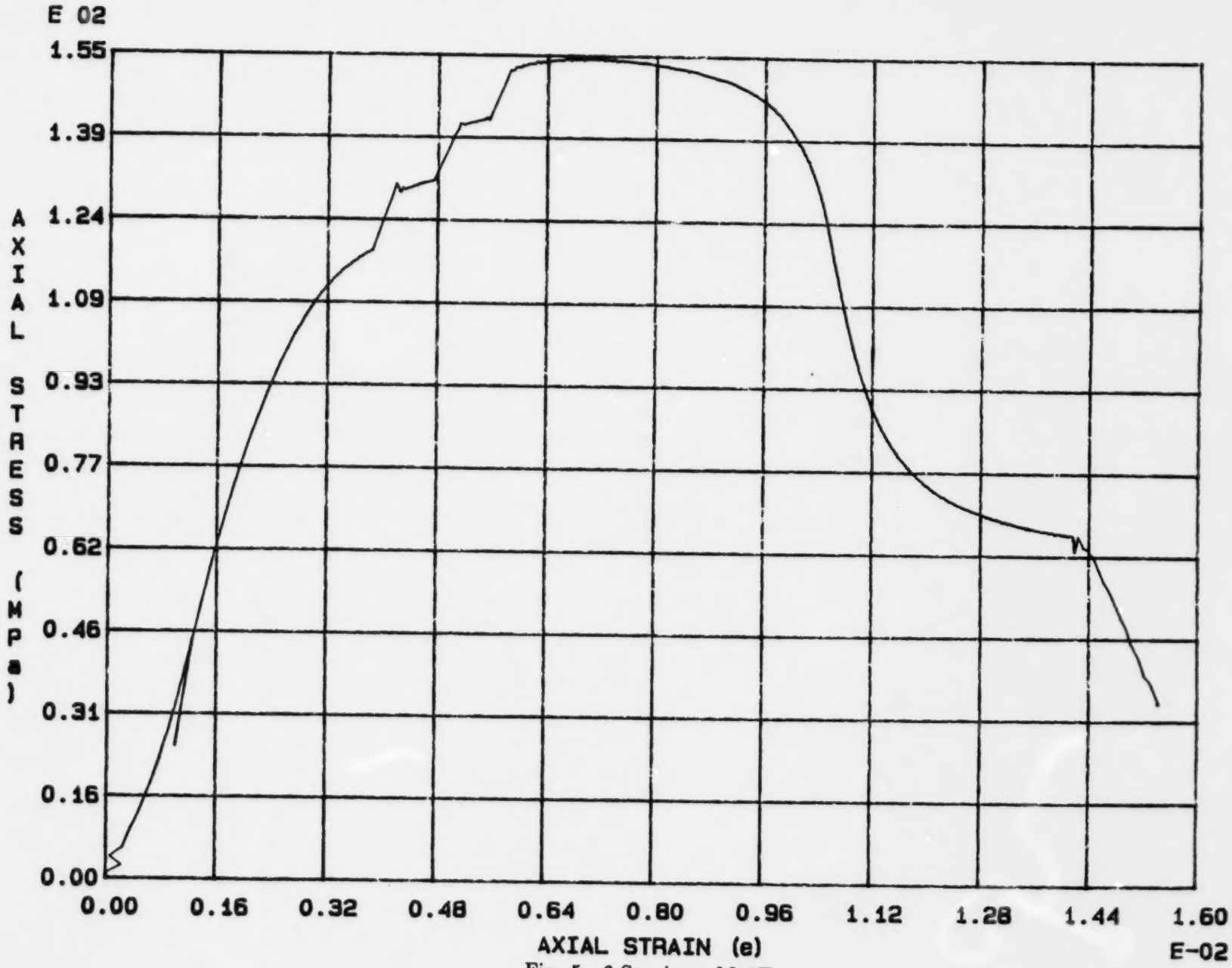

Fig. 5 - 6 Specimen M49T

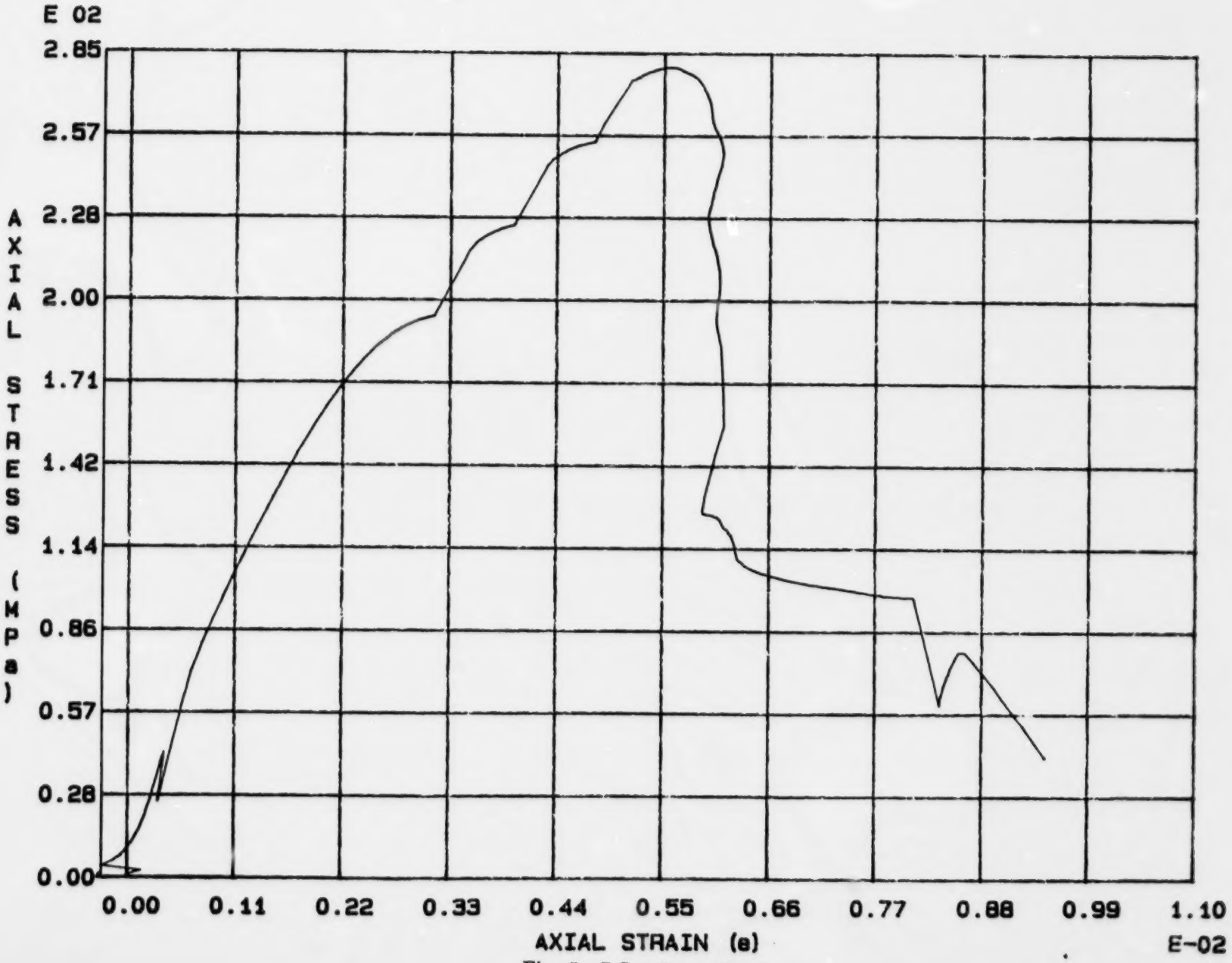

Fig. 5 - 7 Specimen M50T

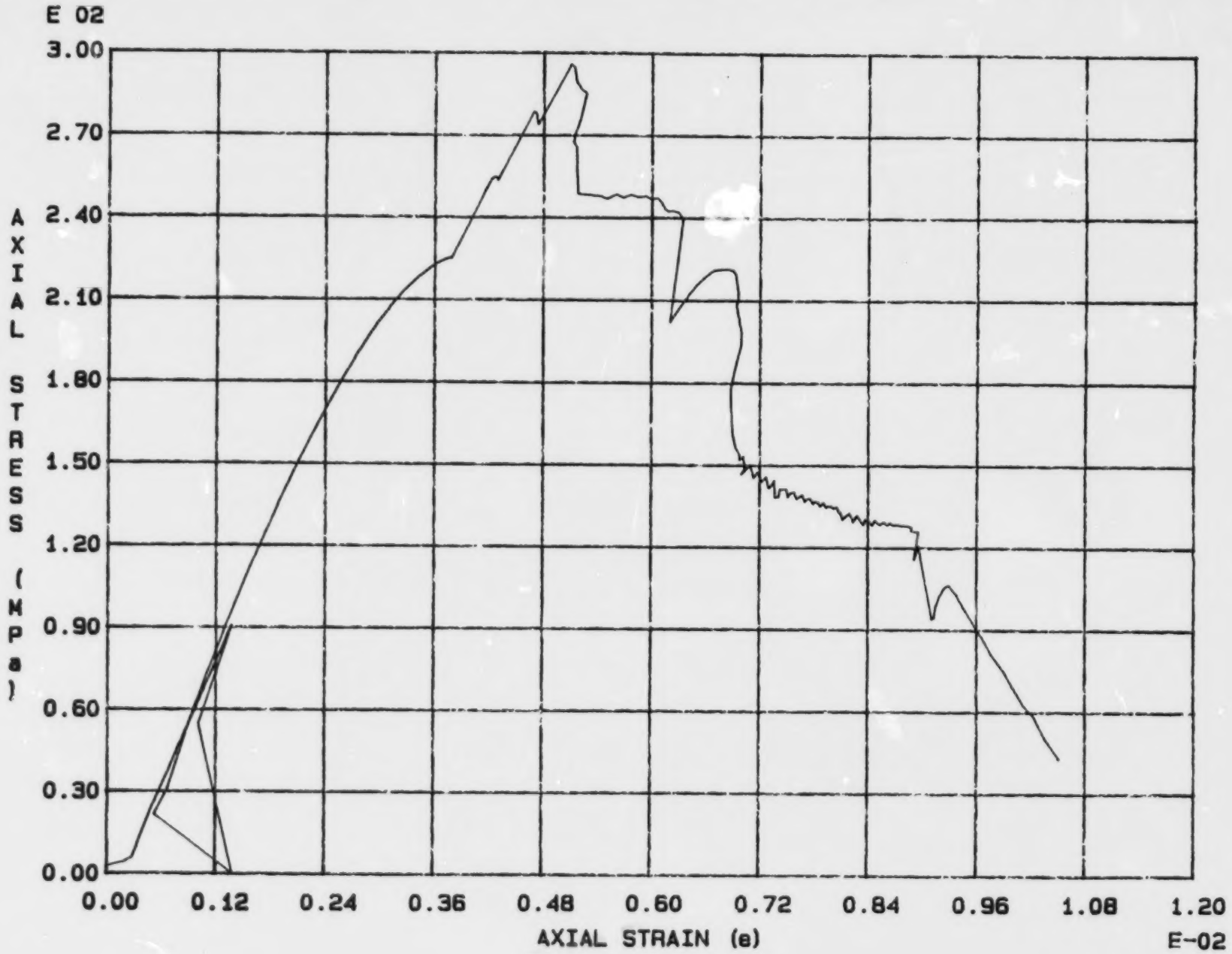

Fig. 5 - 8 Specimen M51T

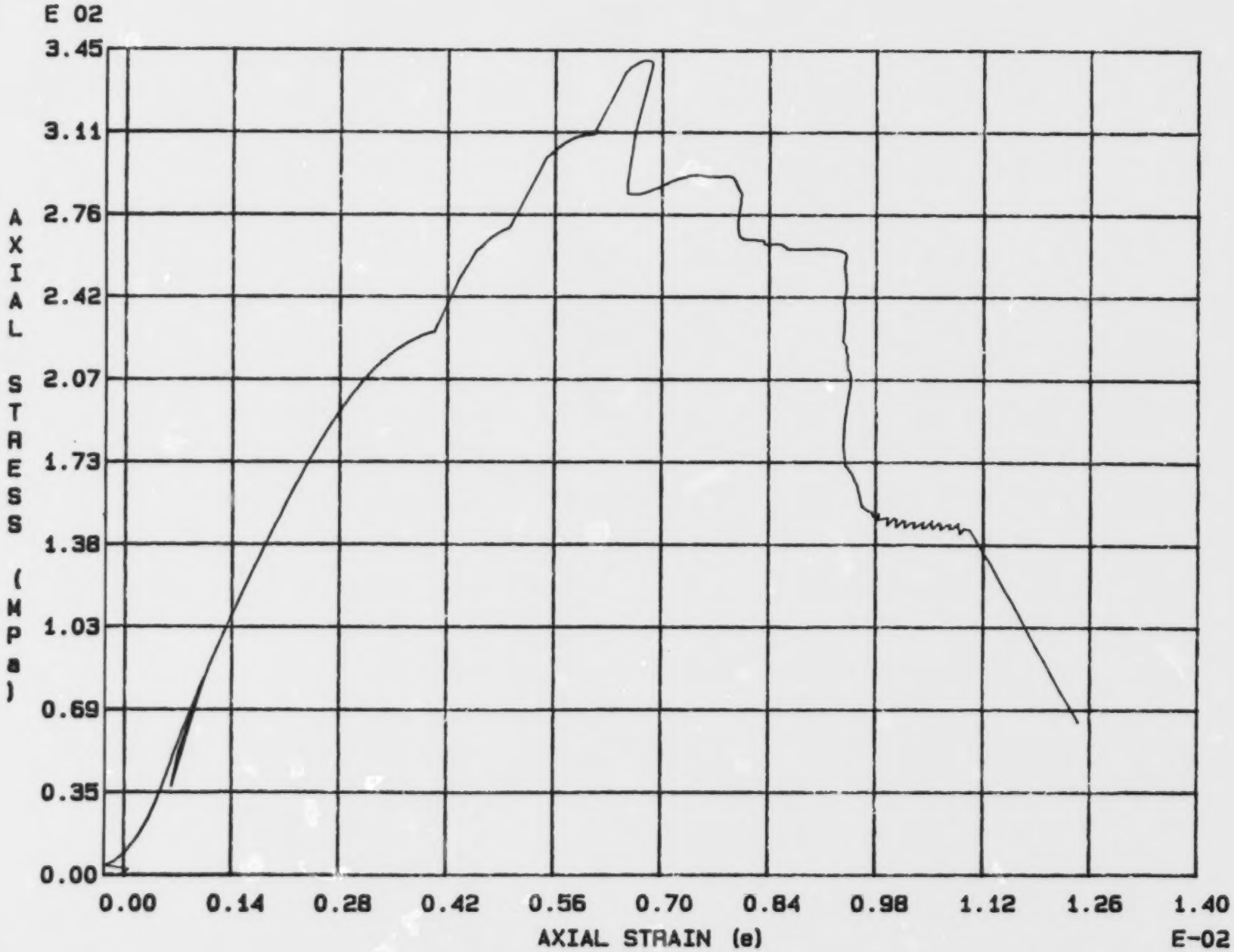

Fig. 5 - 9 Specimen M52T

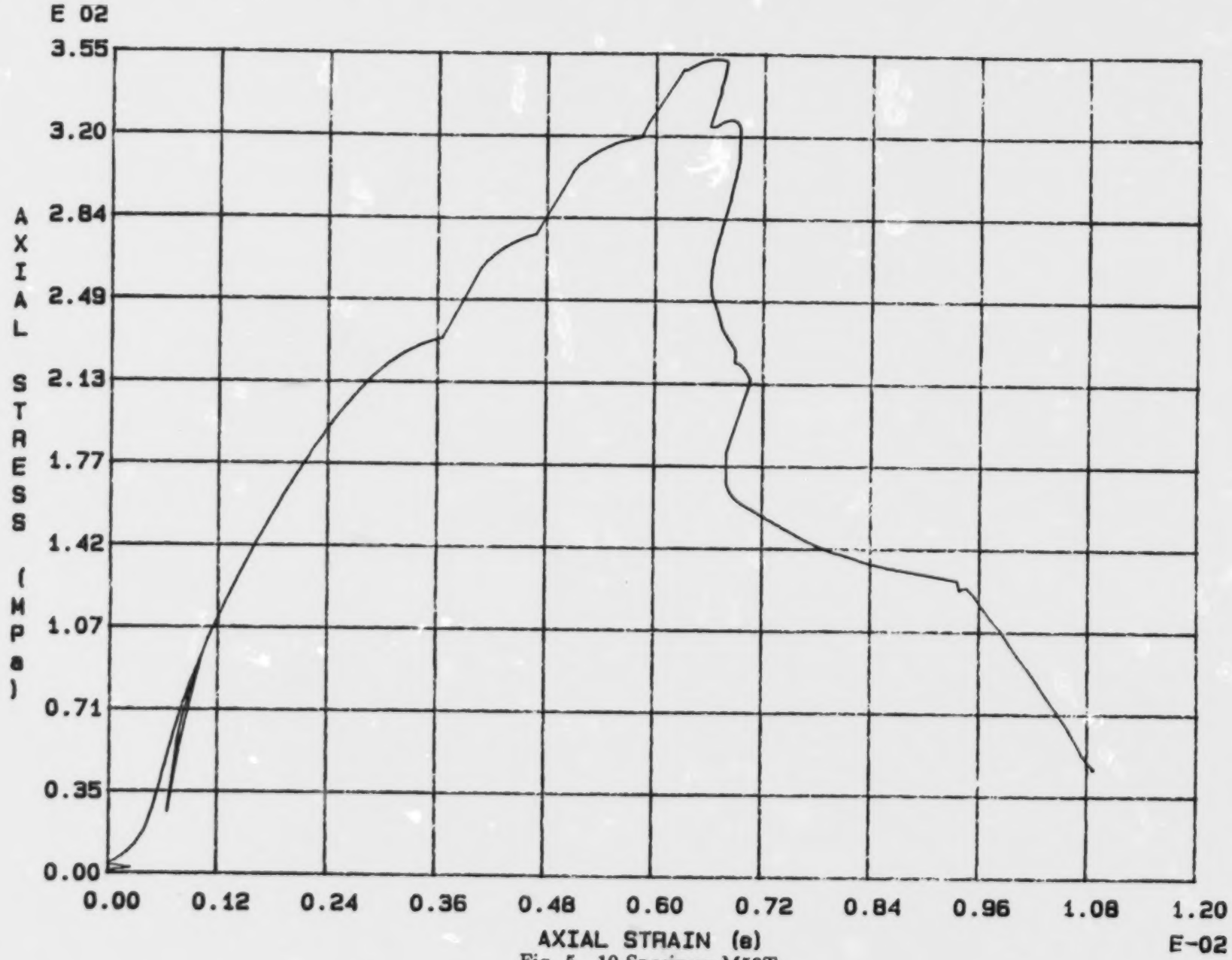

Fig. 5 - 10 Specimen M53T

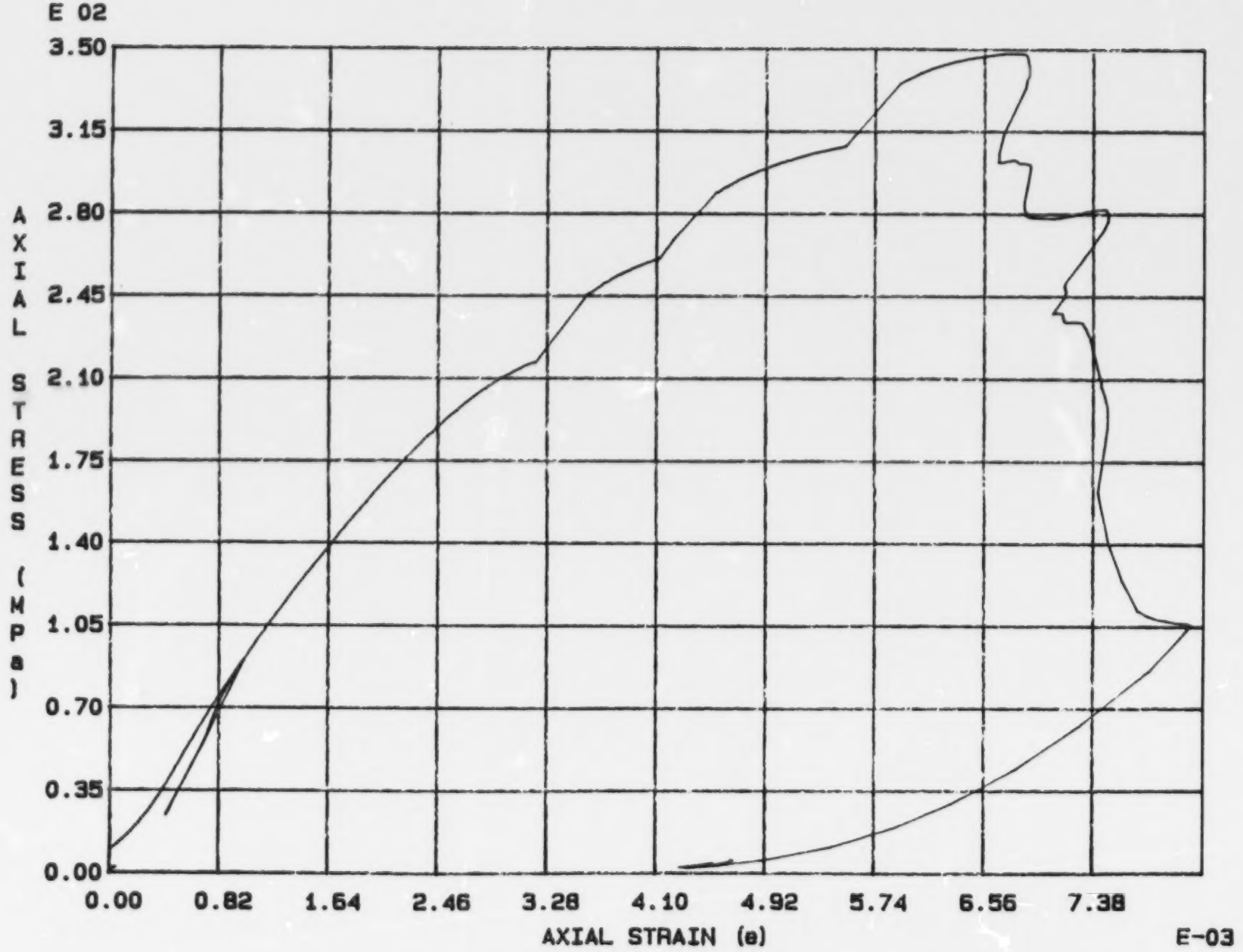

Fig. 5 - 11 Specimen M54T

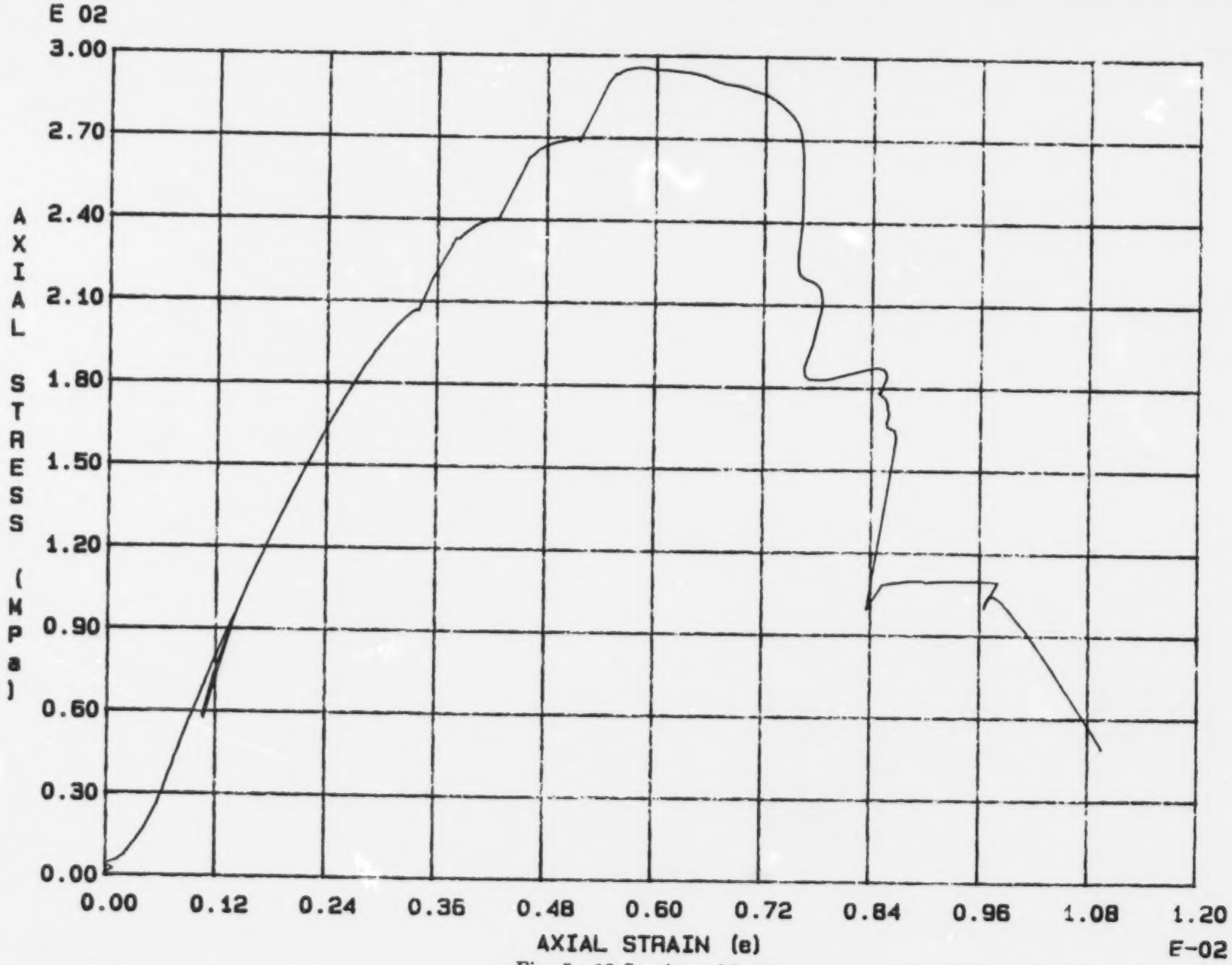

Fig. 5 - 12 Specimen M55T

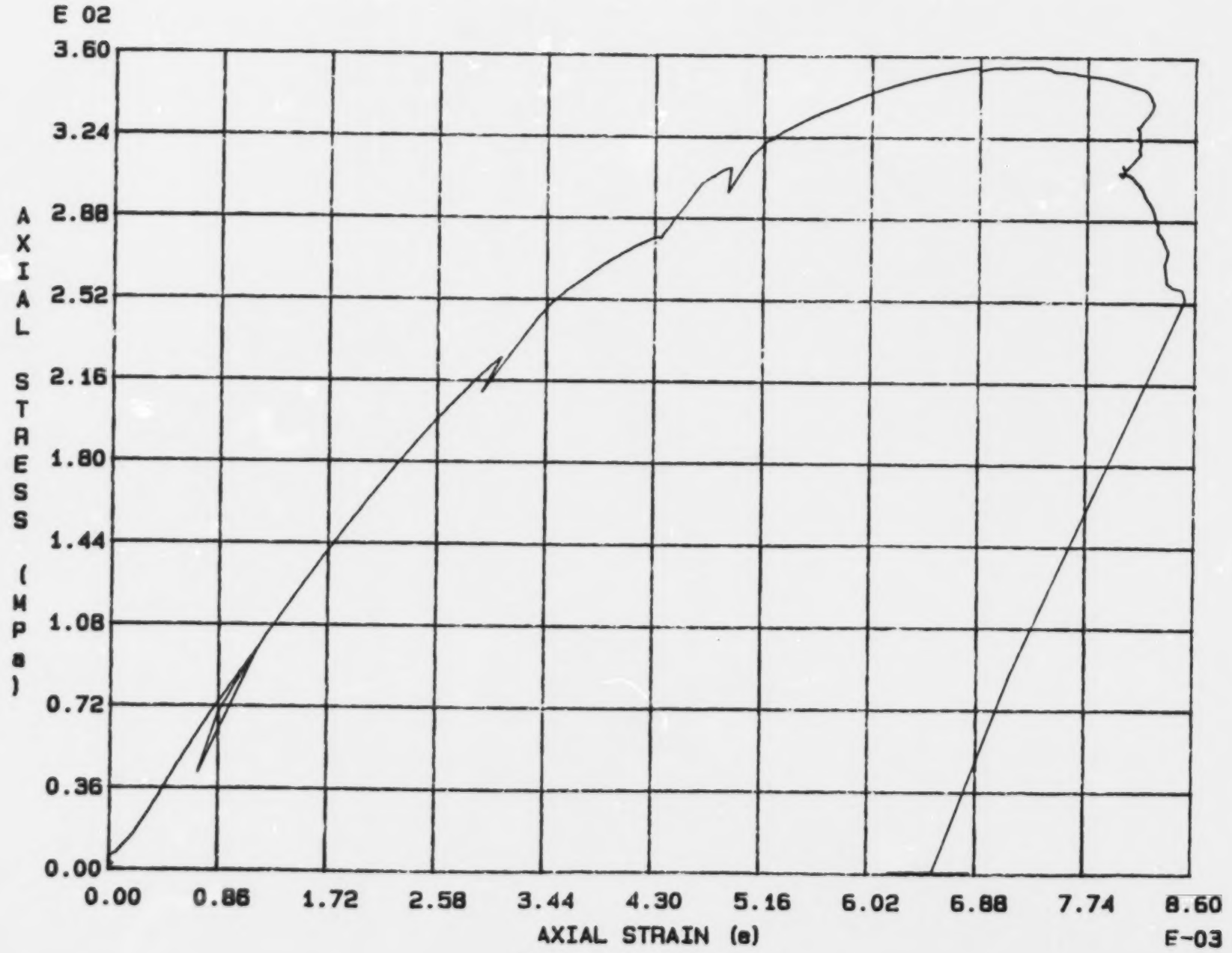

Fig. 5 - 13 Specimen M56T

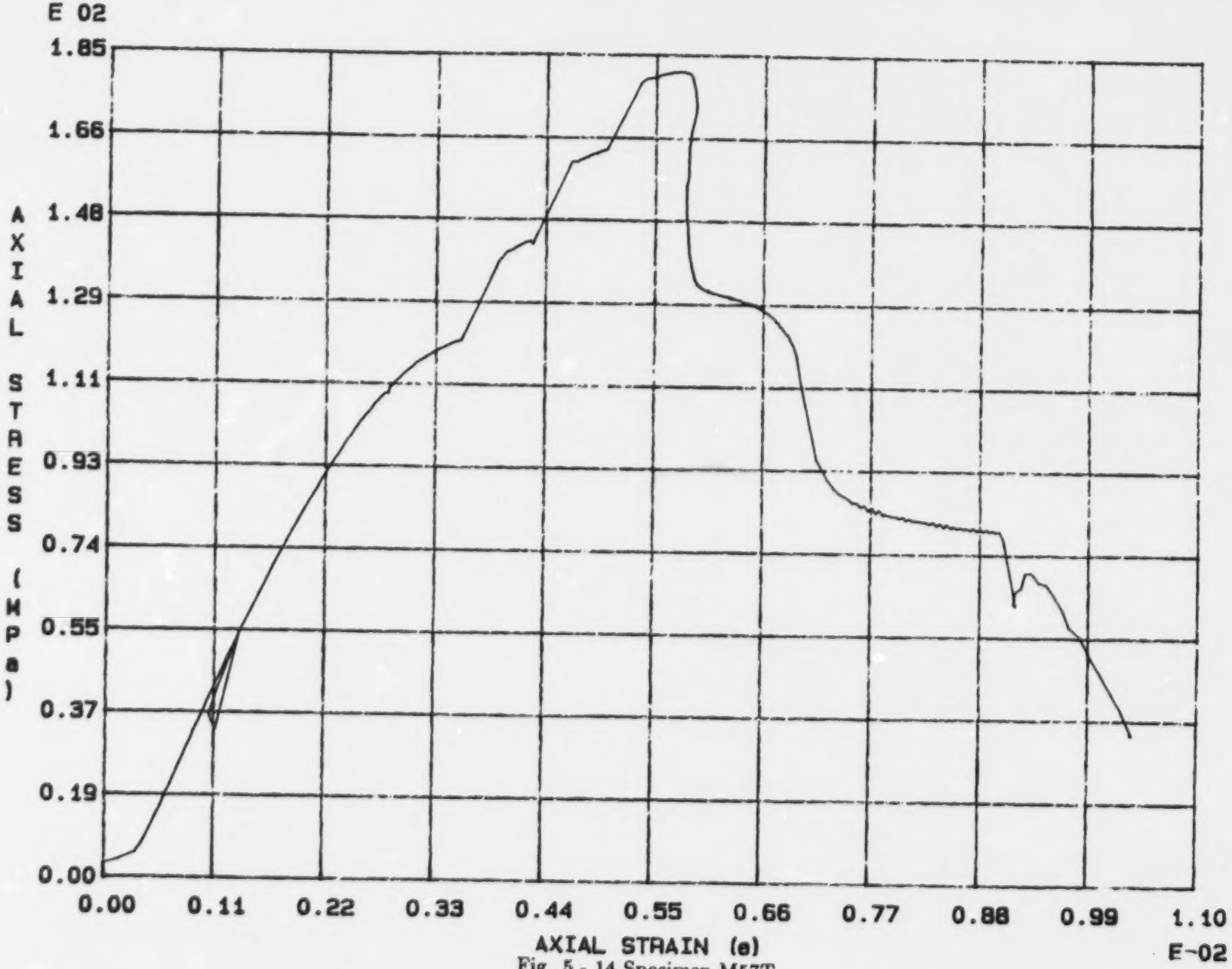

Fig. 5 - 14 Specimen M57T

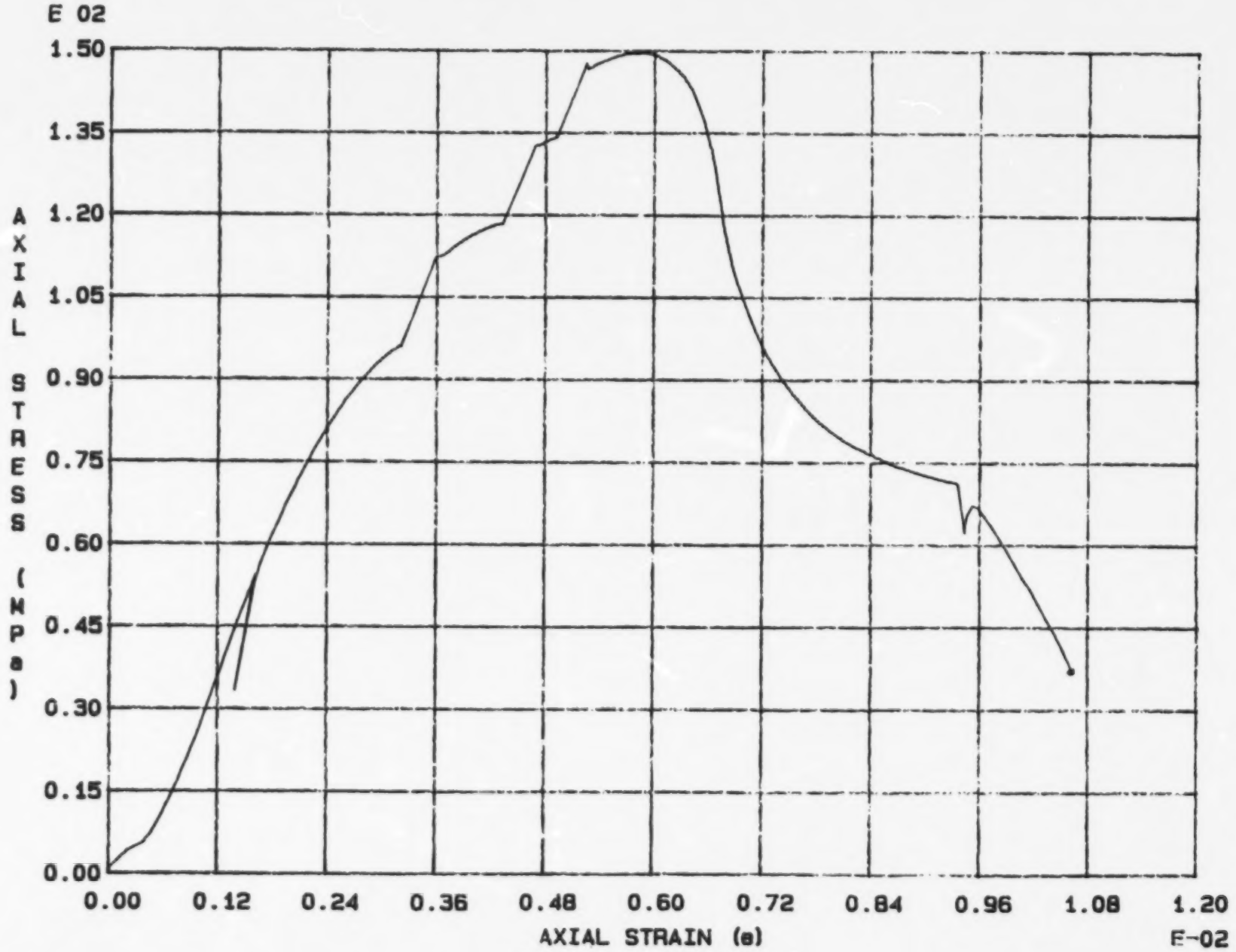

Fig. 5 - 15 Specimen M58T

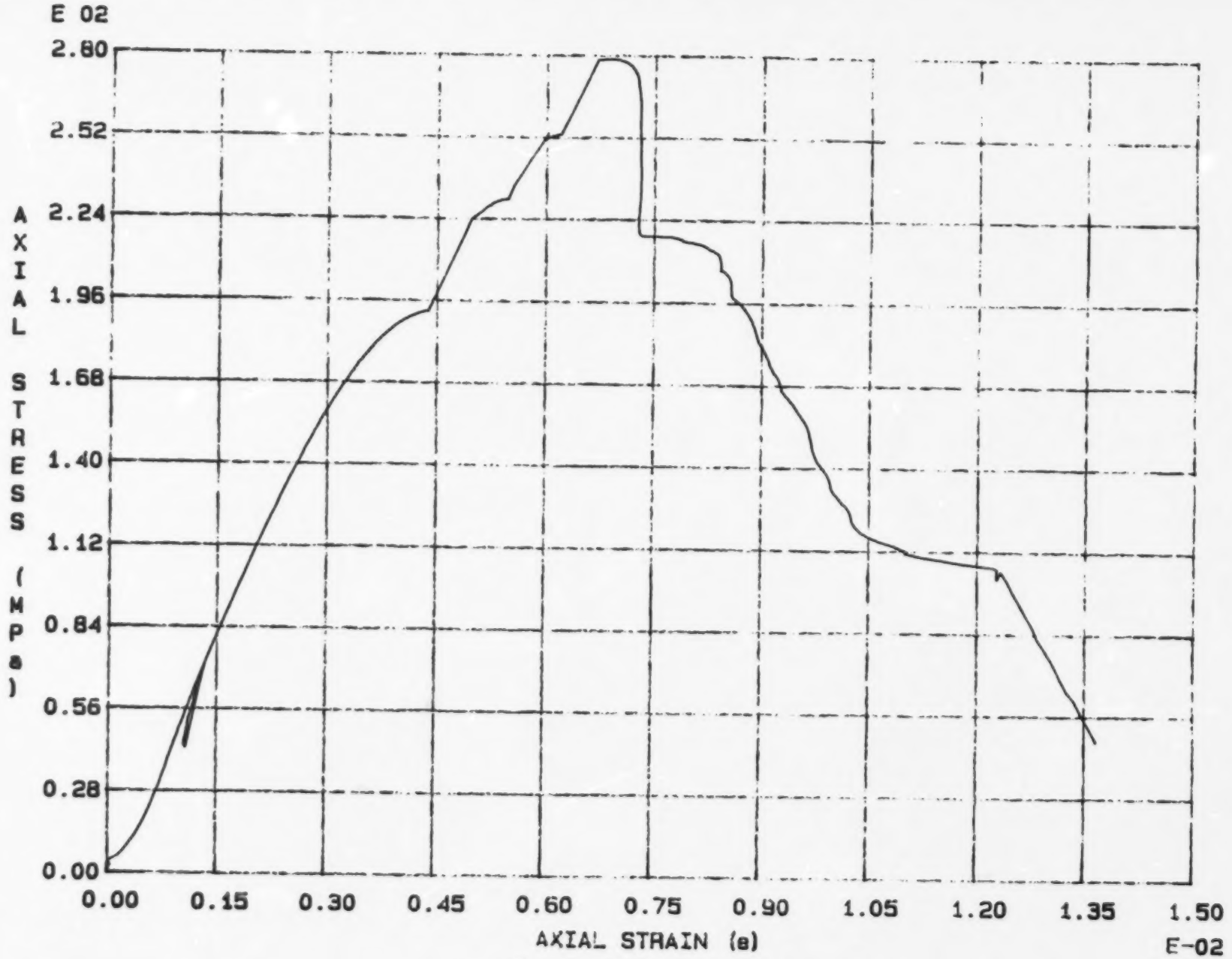

Fig. 5 - 16 Specimen M59T

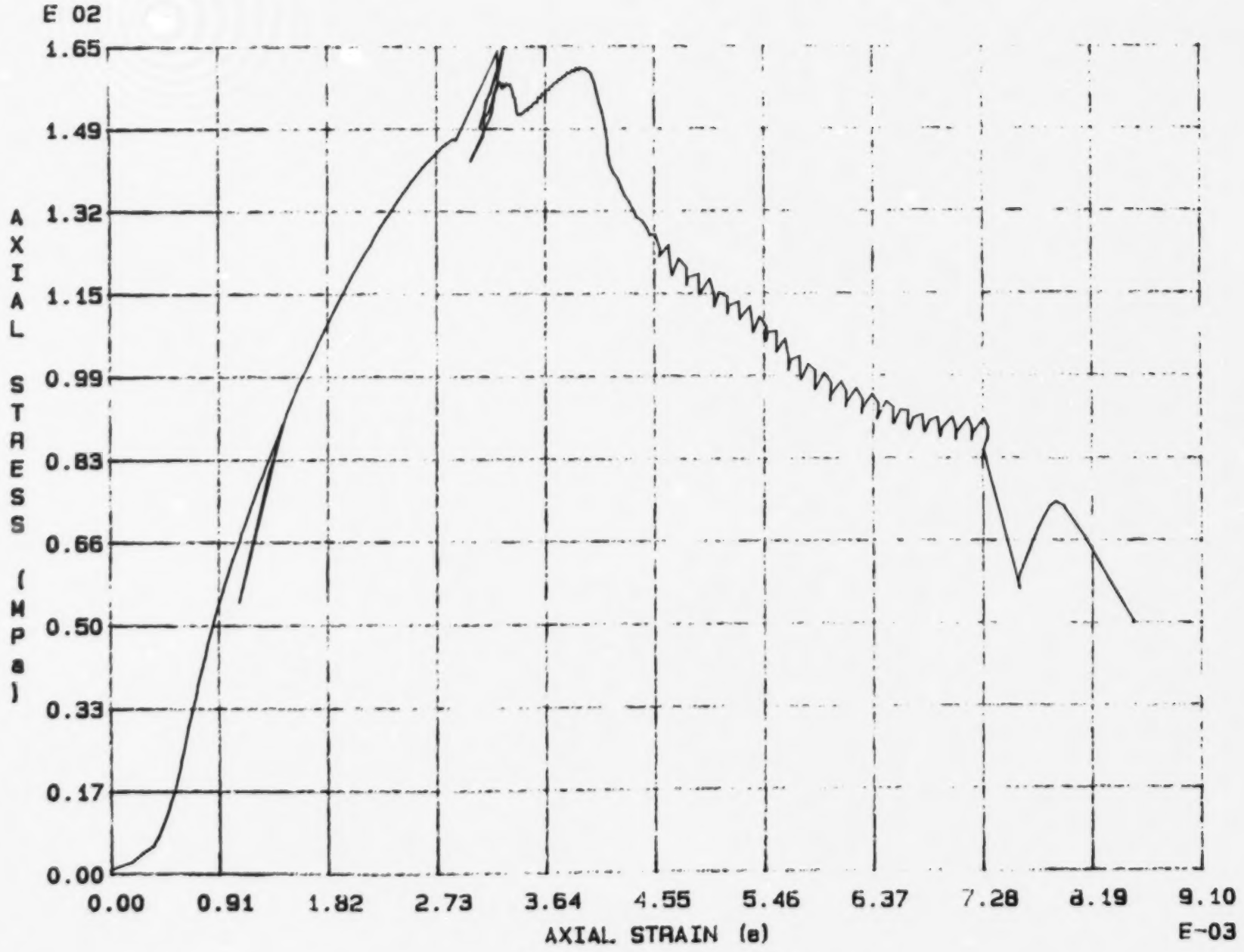

Fig. 5 - 17 Specimen M60T

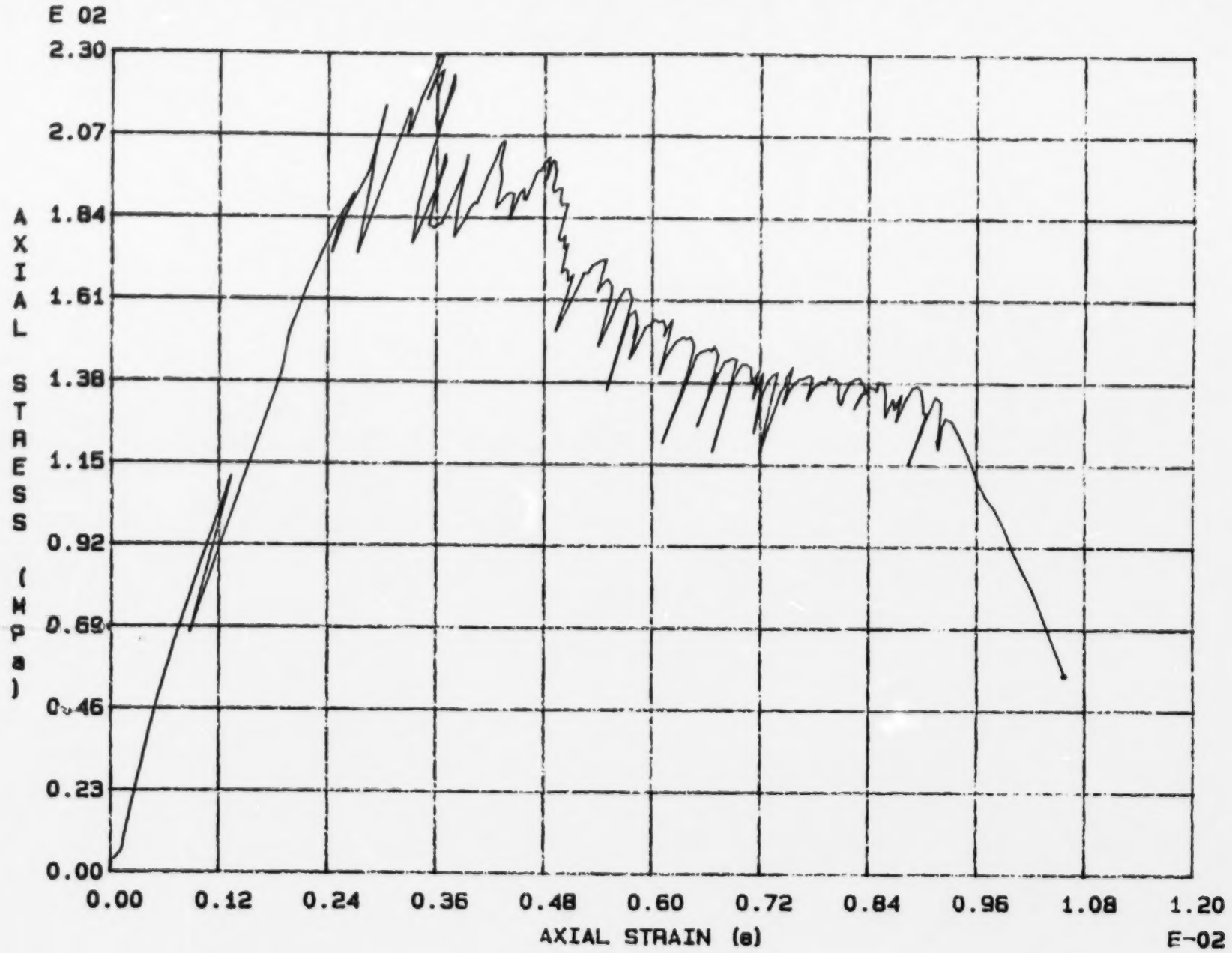

Fig. 5 - 18 Specimen M61T

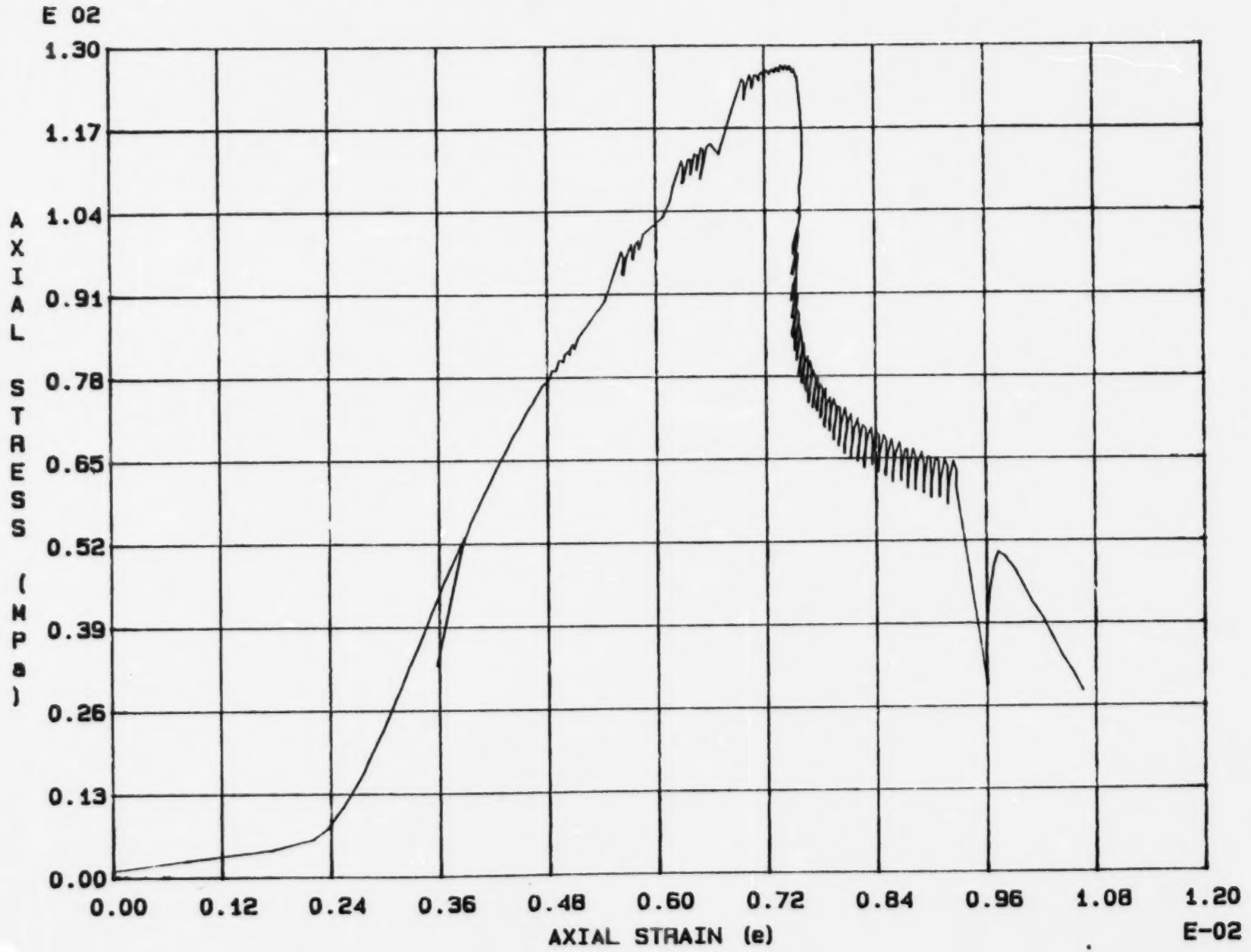

Fig. 5 - 19 Specimen M62T

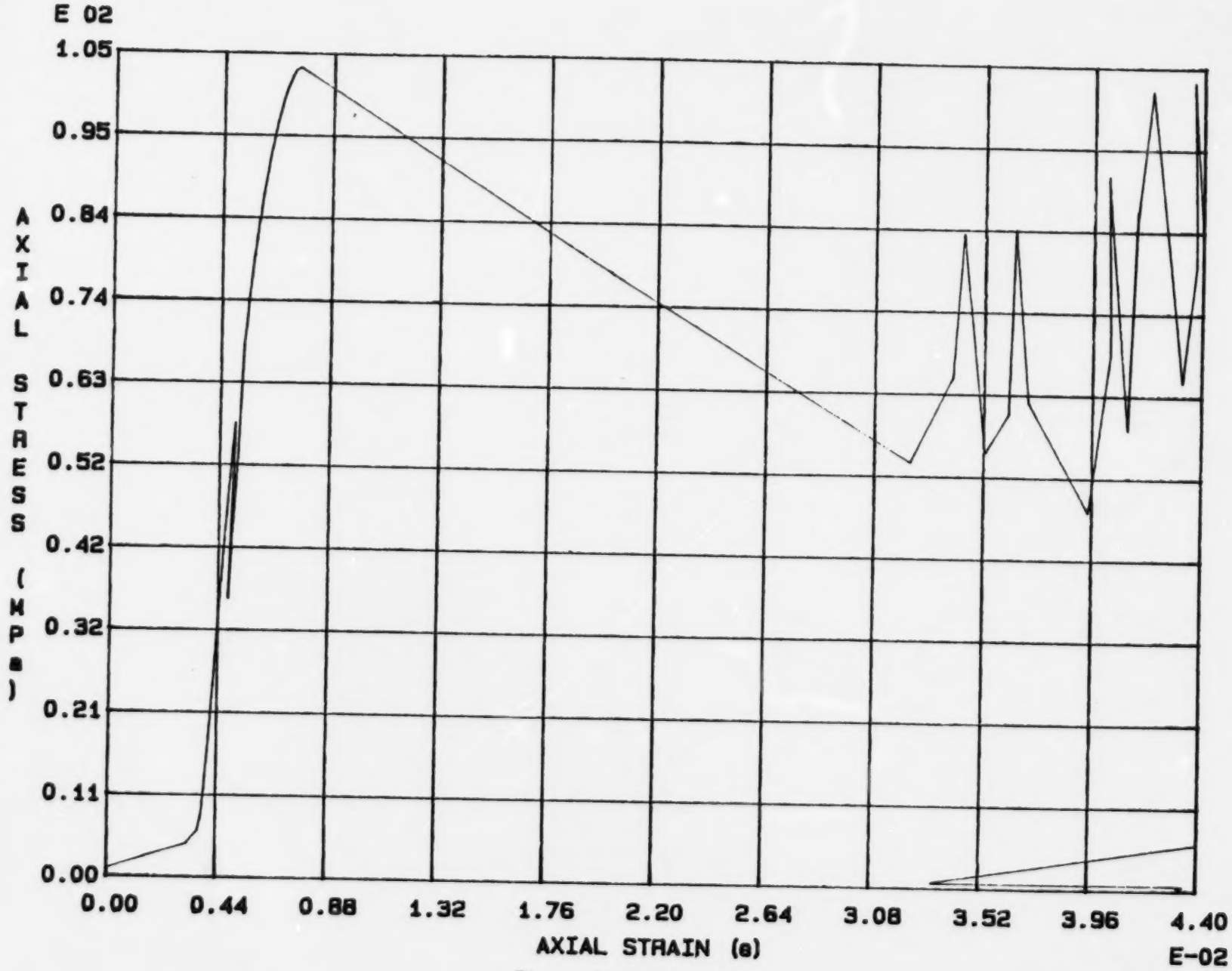

Fig. 5 - 20 Specimen M63T

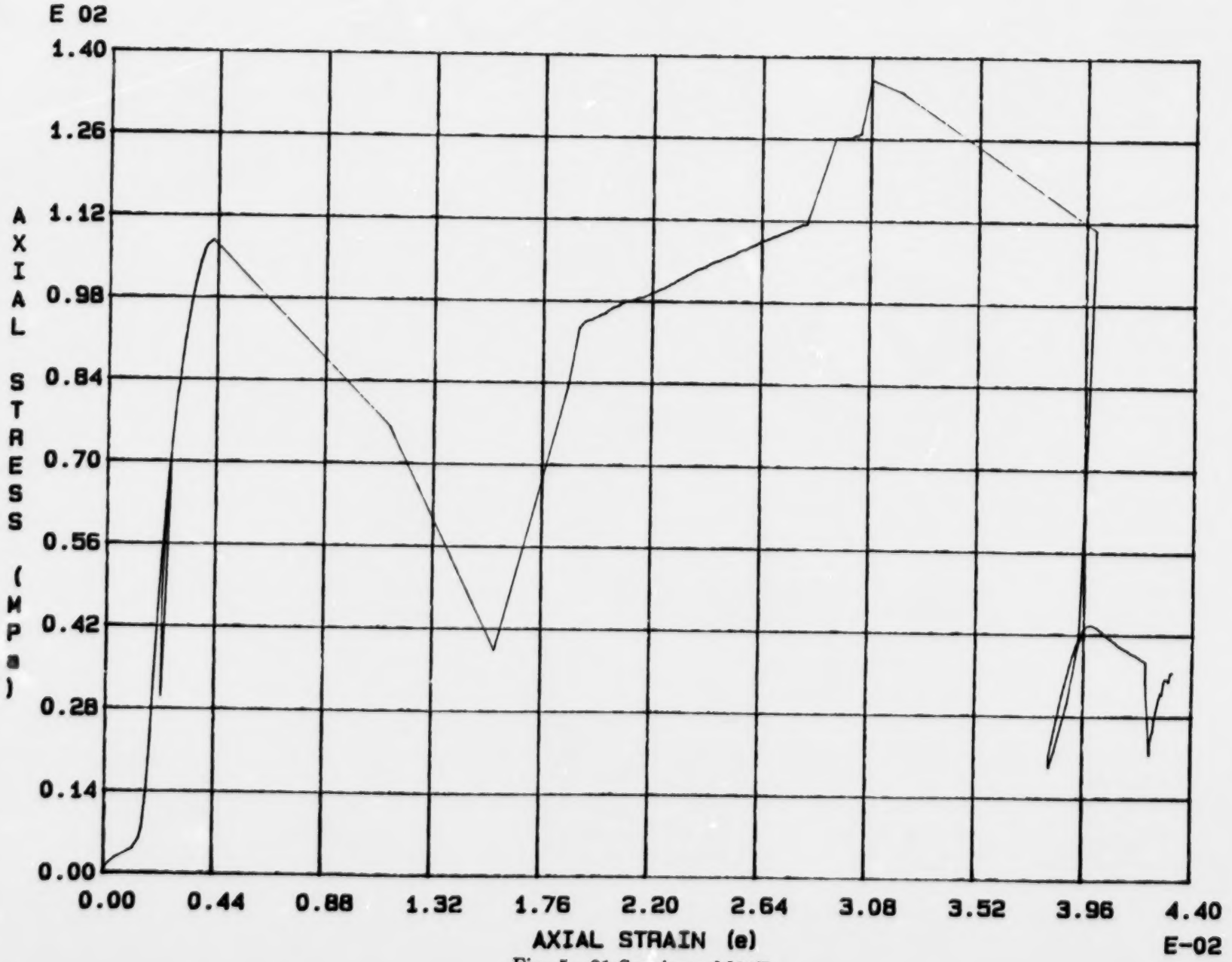

Fig. 5 - 21 Specimen M64T

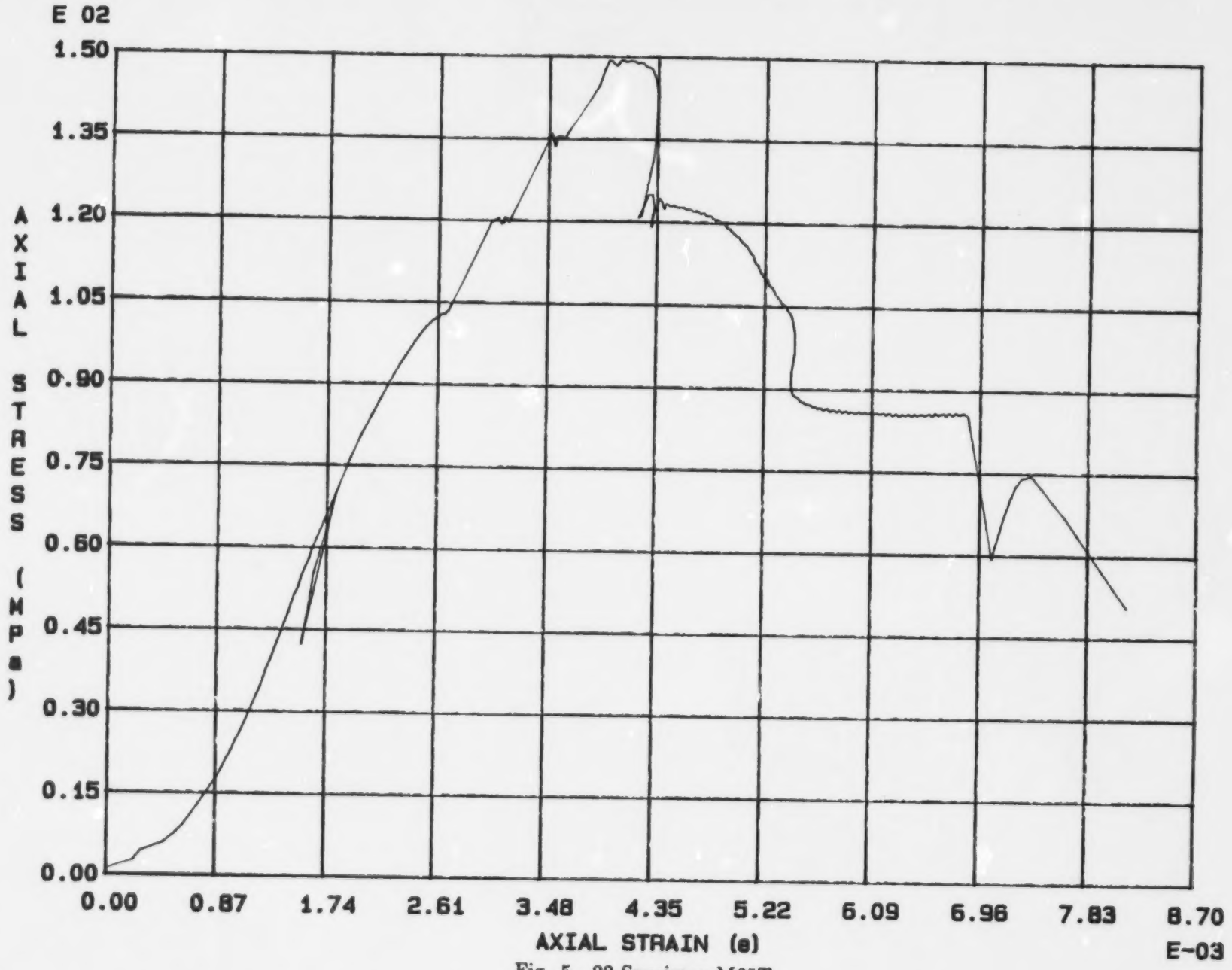

Fig. 5 - 22 Specimen M65T

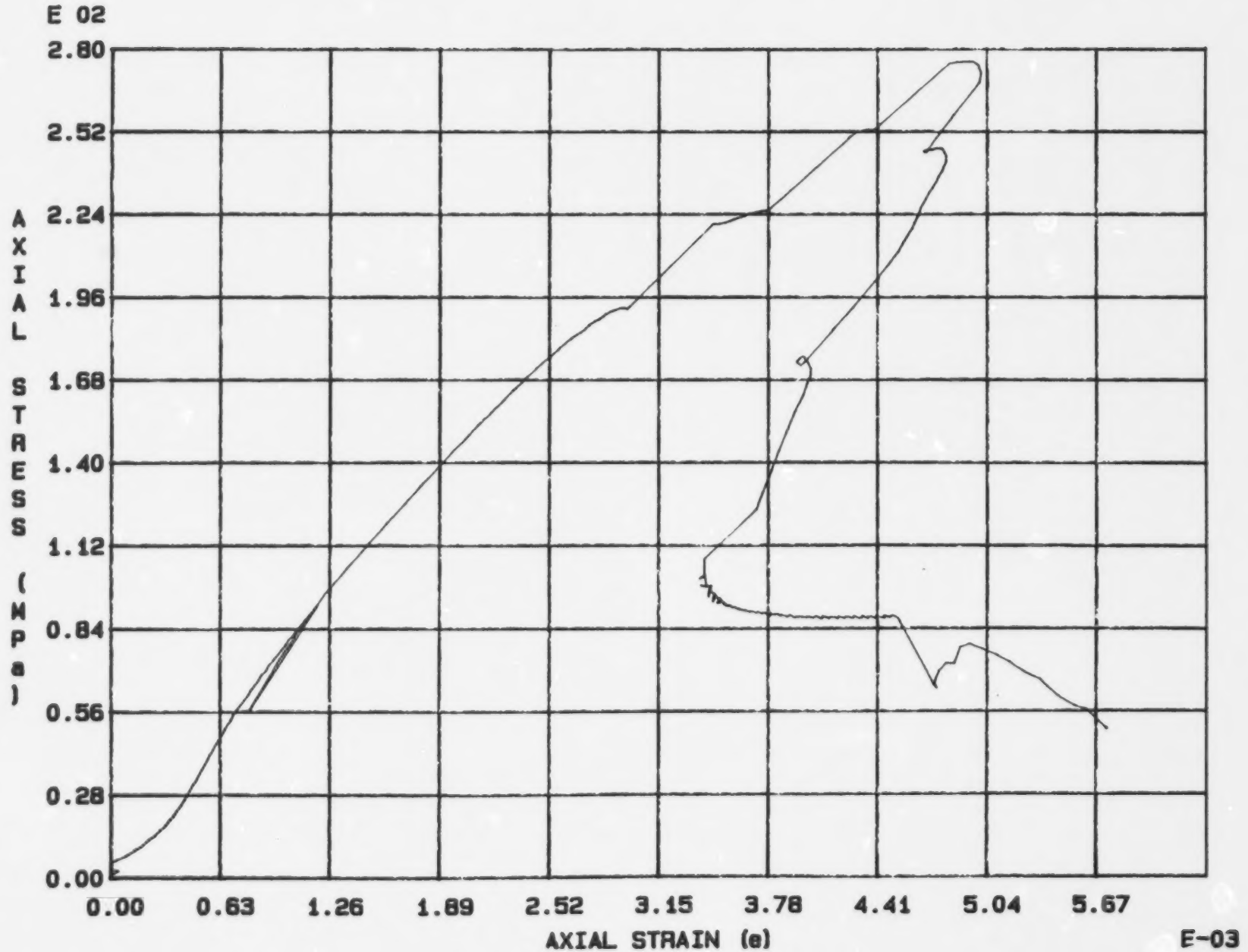

Fig. 5 - 23 Specimen M66T

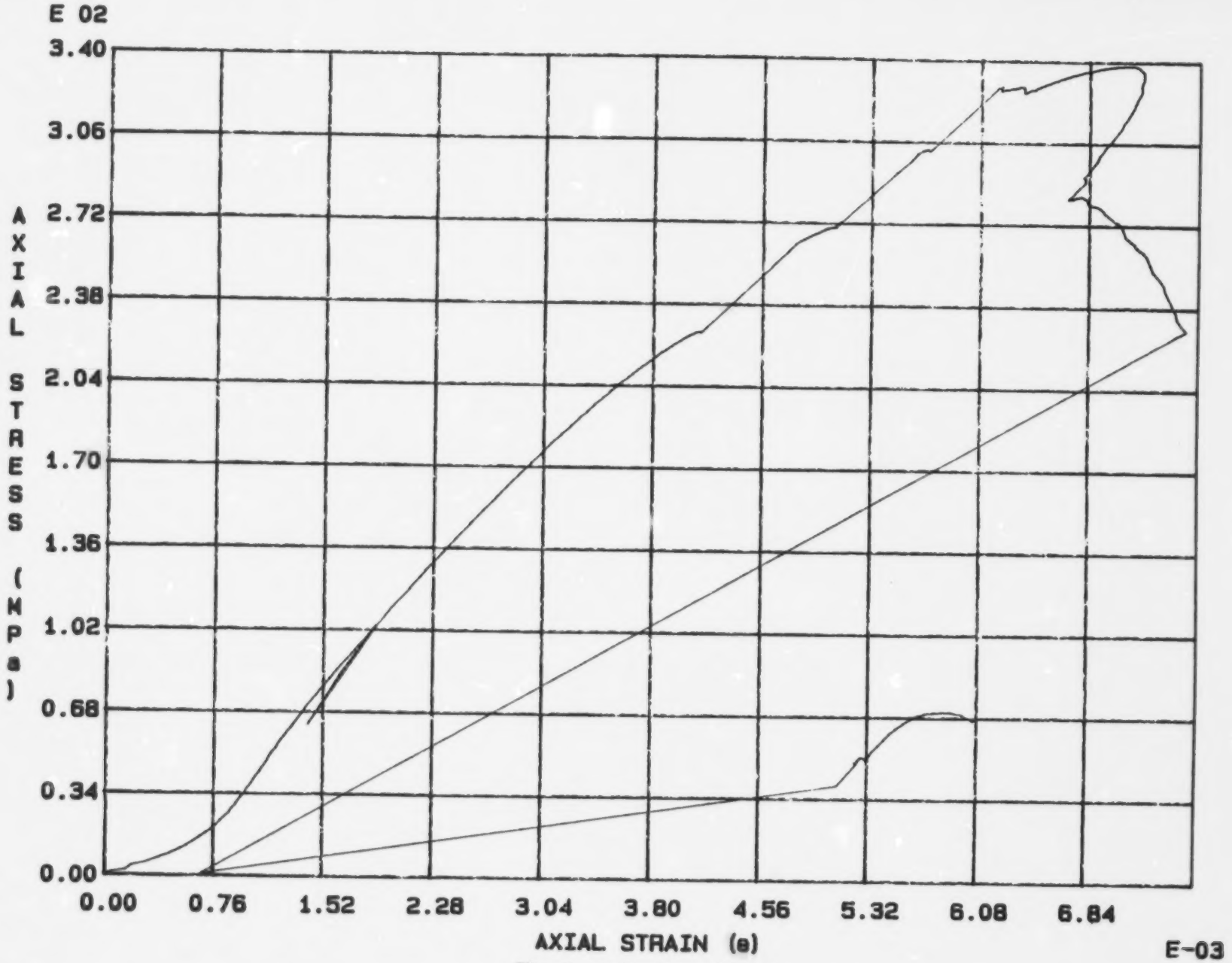

Fig. 5 - 24 Specimen M67T

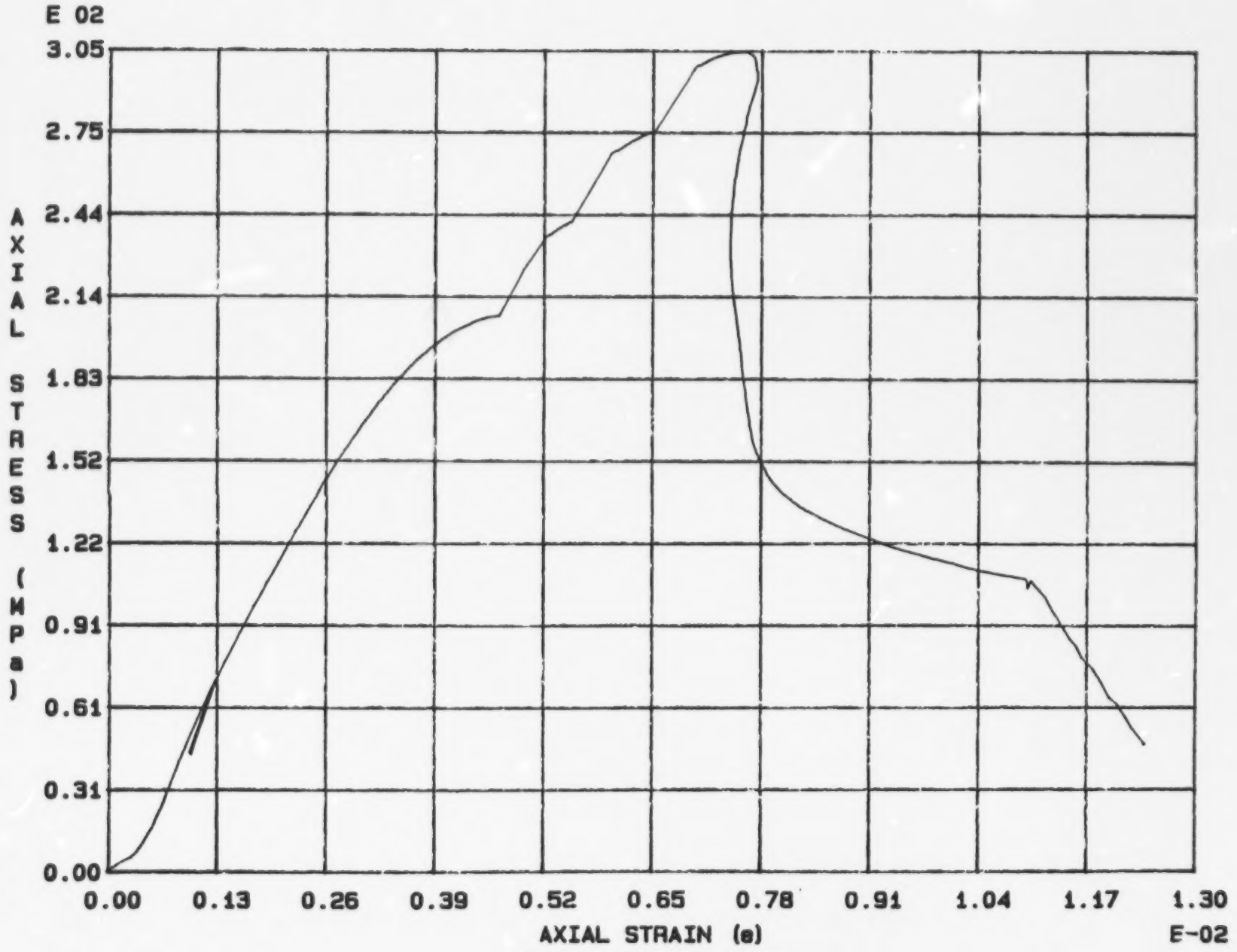

Fig. 5 - 25 Specimen M68T

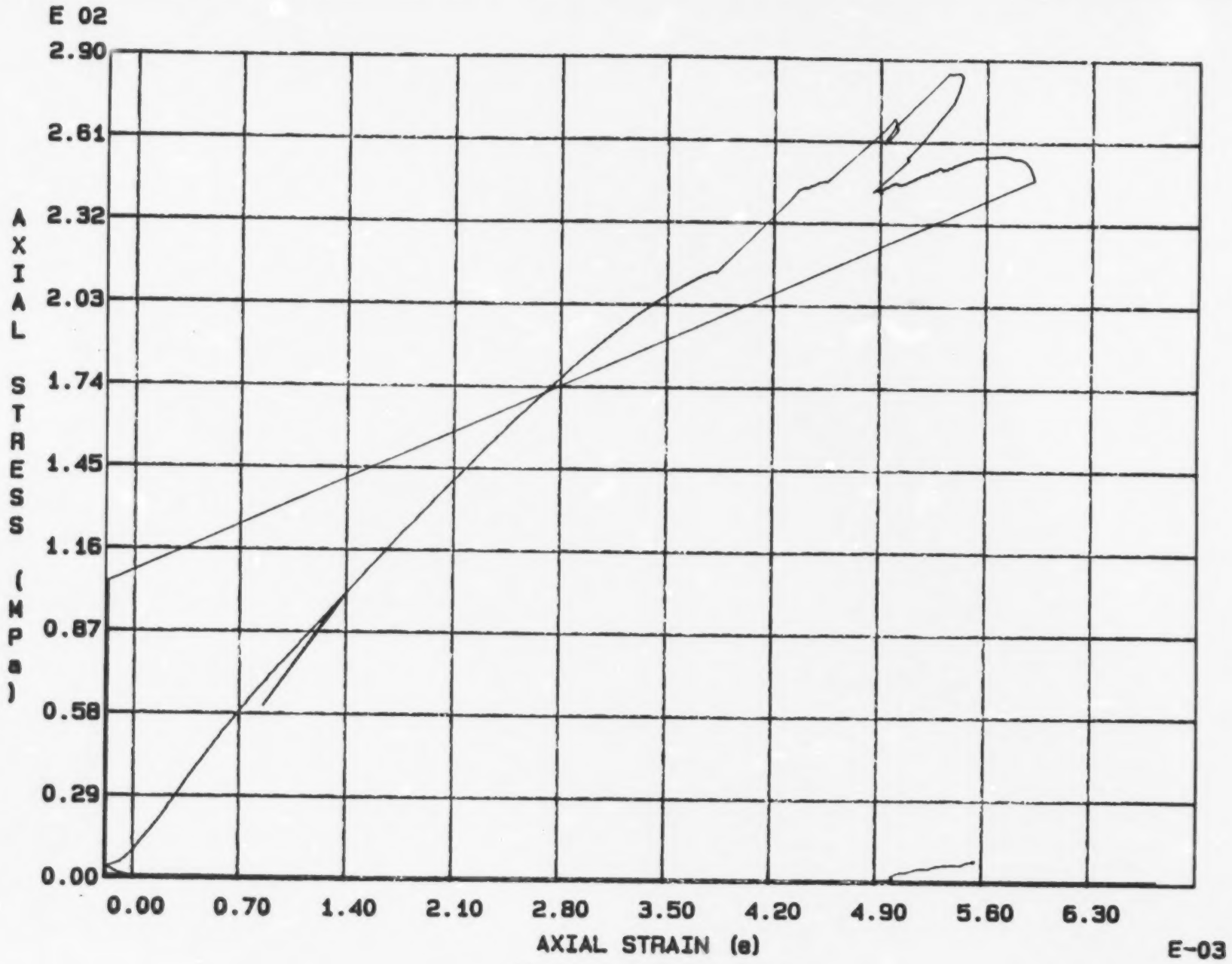

Fig. 5 - 26 Specimen M69T

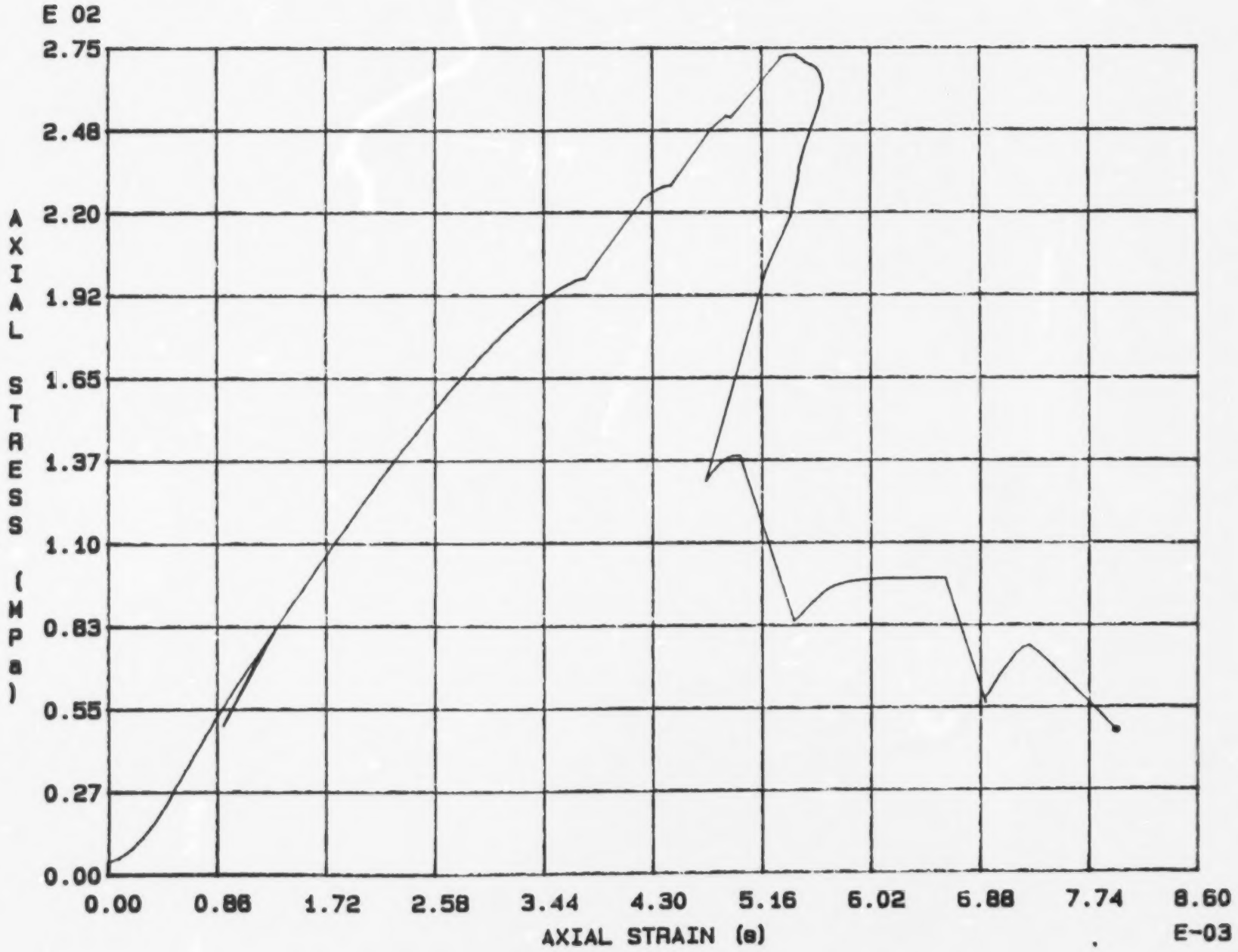

Fig. 5 - 27 Specimen M70T

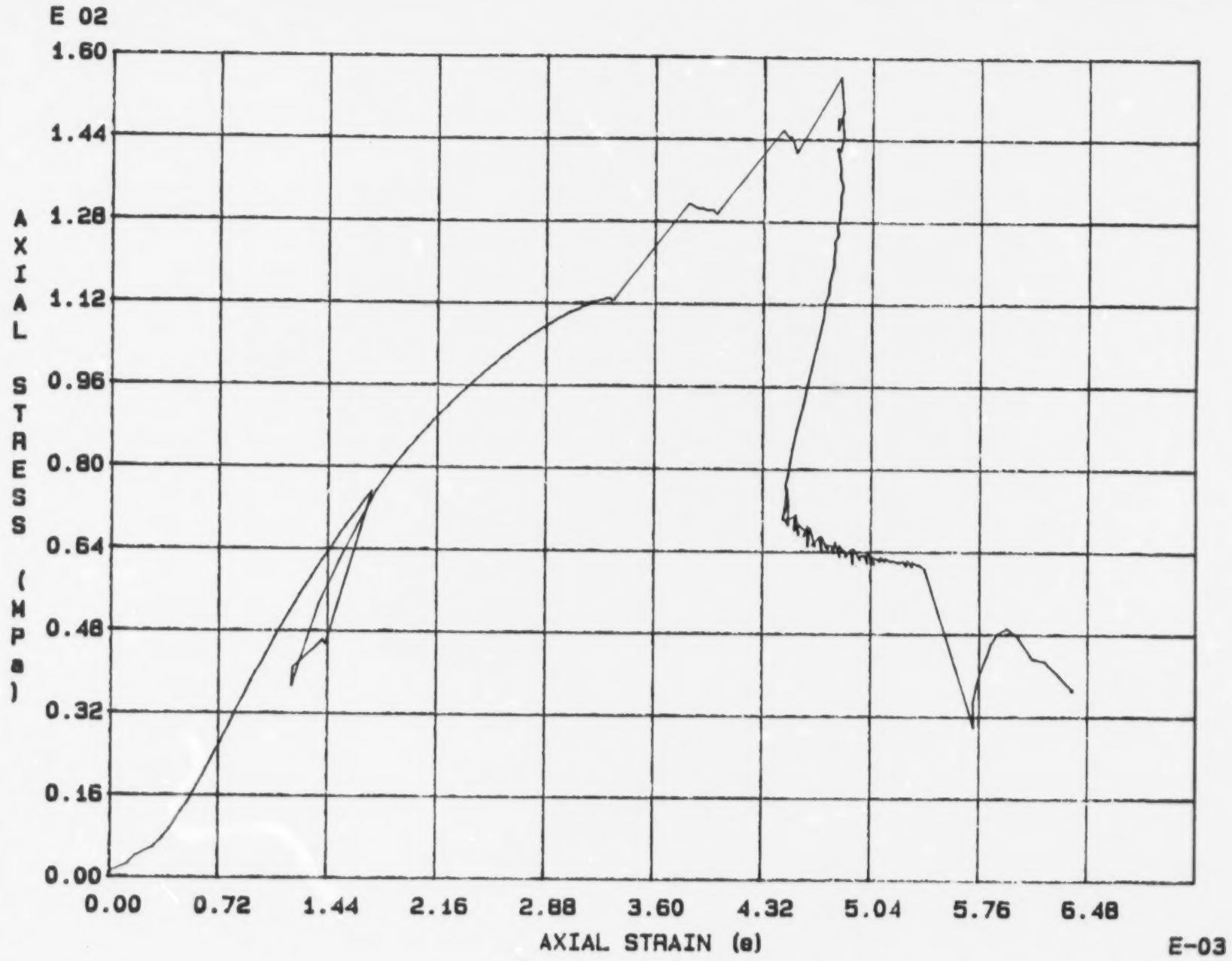

Fig. 5 - 28 Specimen M71T

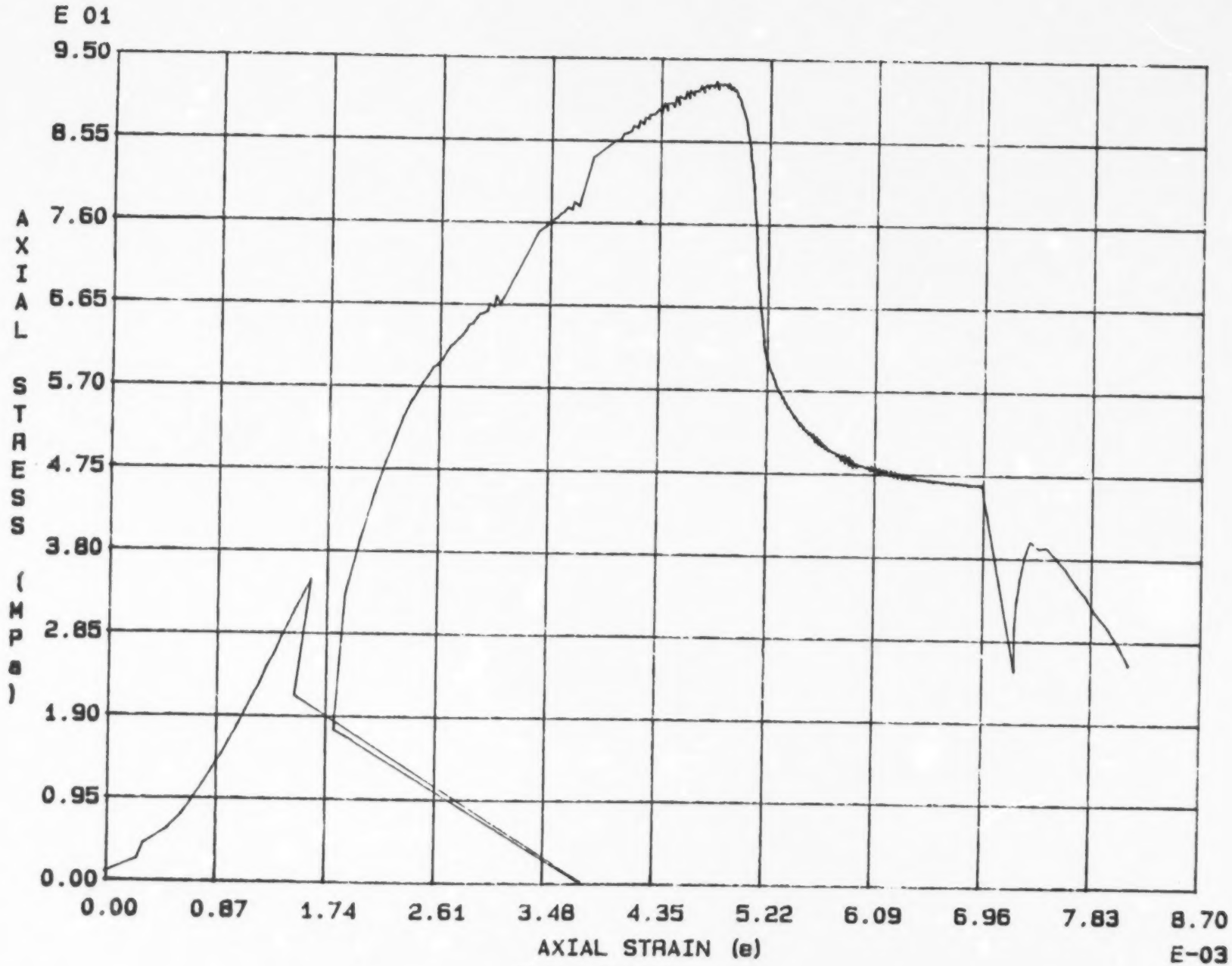

Fig. 5 - 29 Specimen M72T

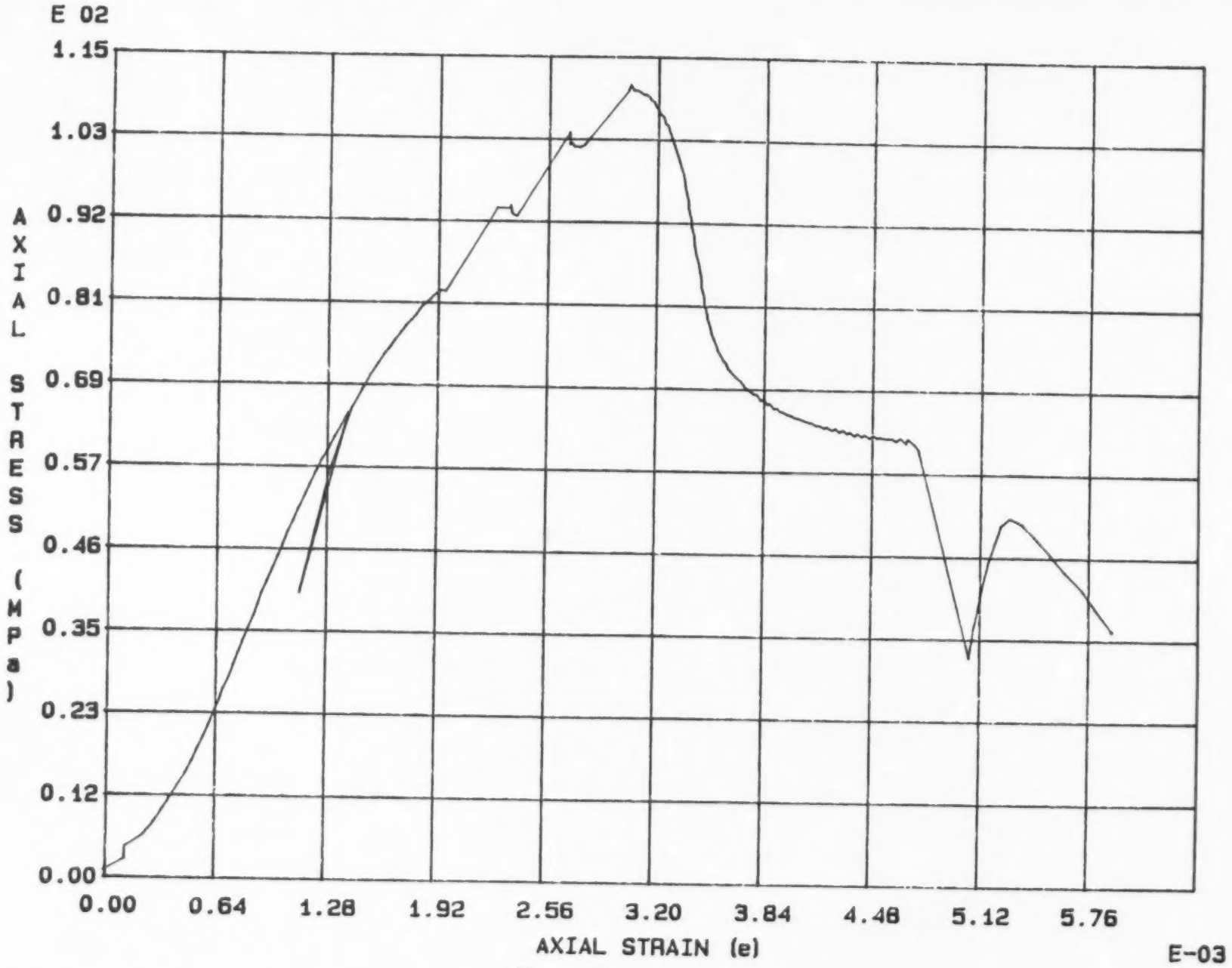

Fig. 5 - 30 Specimen M73T

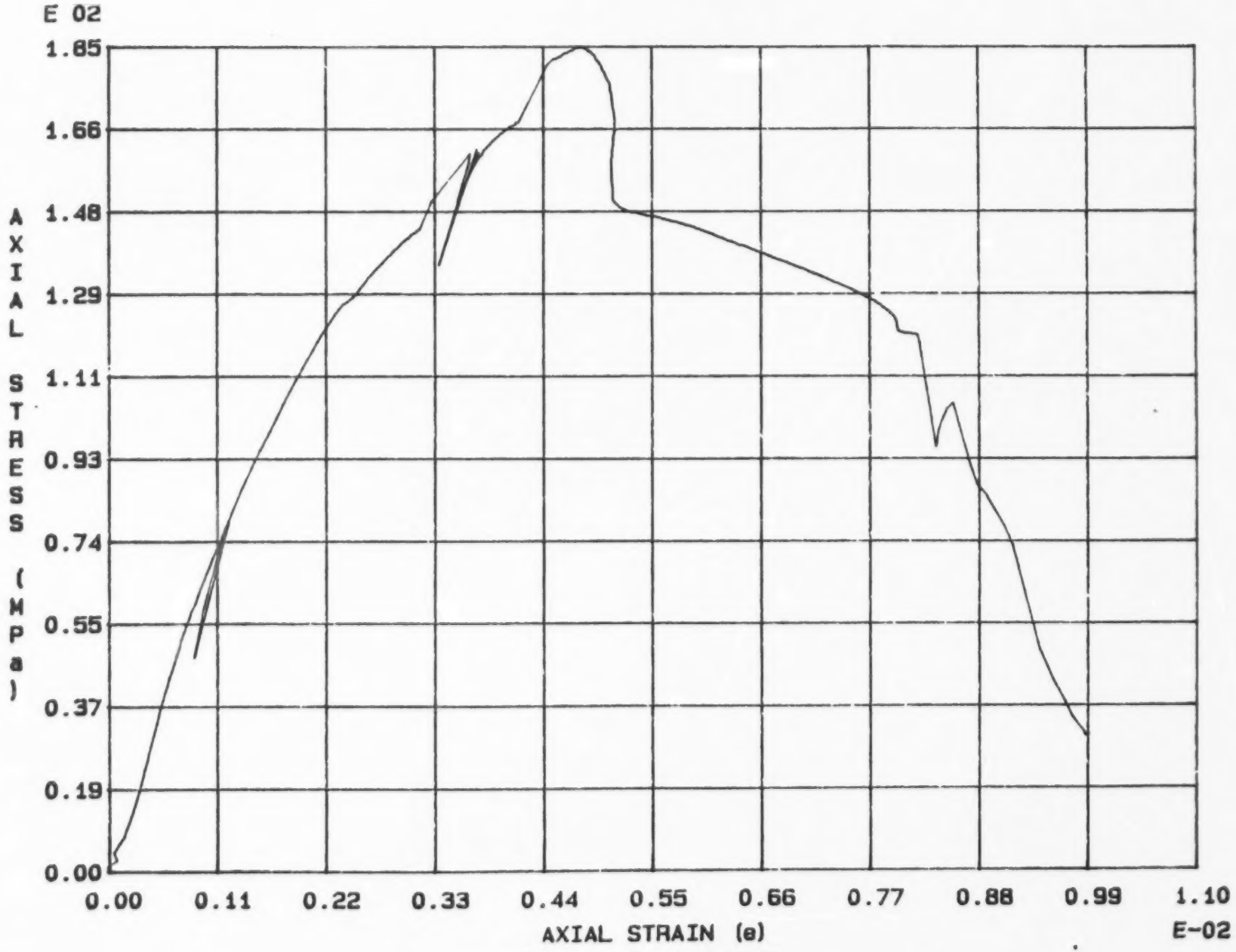

Fig. 5 - 31 Specimen M74T

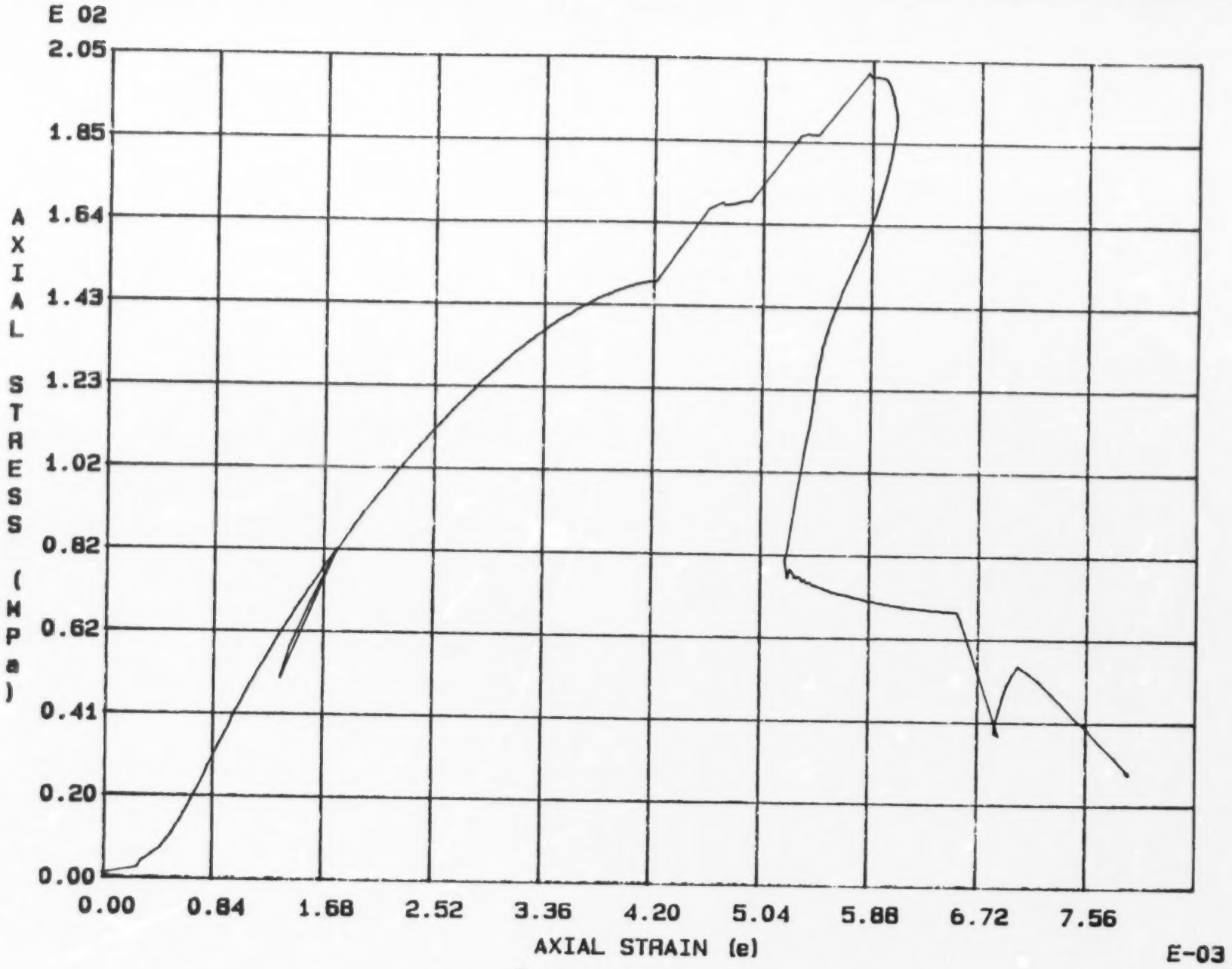

Fig. 5 - 32 Specimen M75T

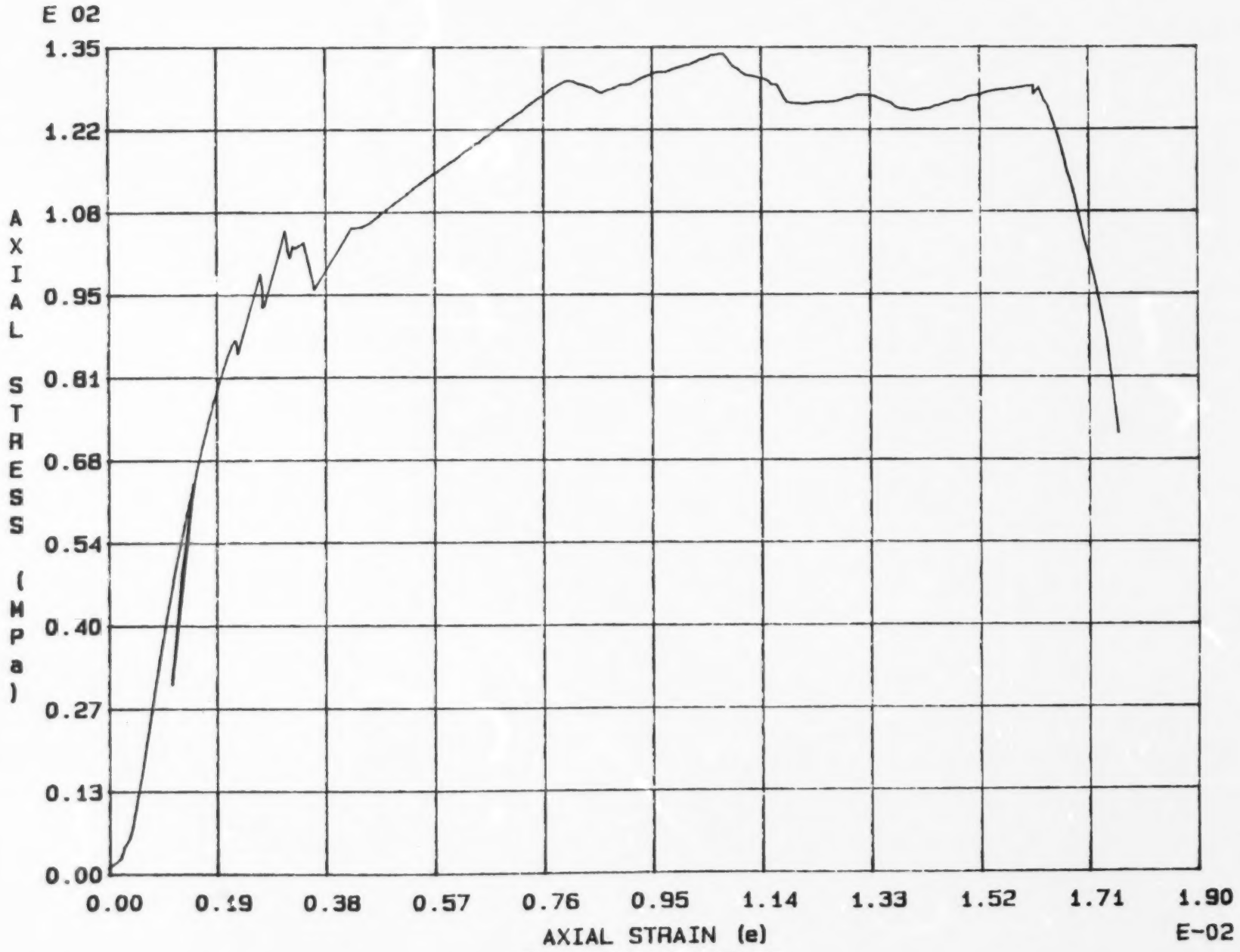

Fig. 5 - 33 Specimen M76T

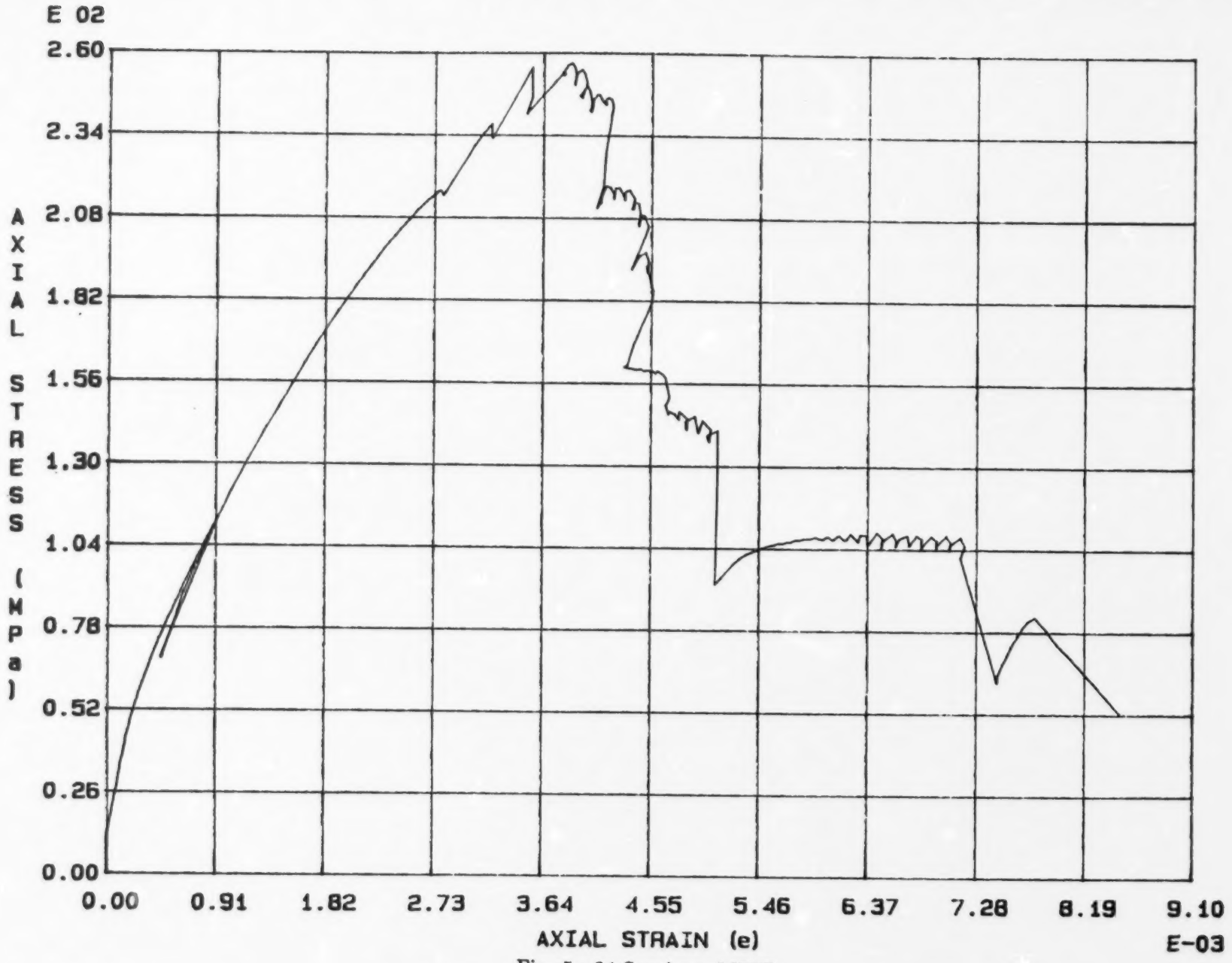

Fig. 5 - 34 Specimen M77T

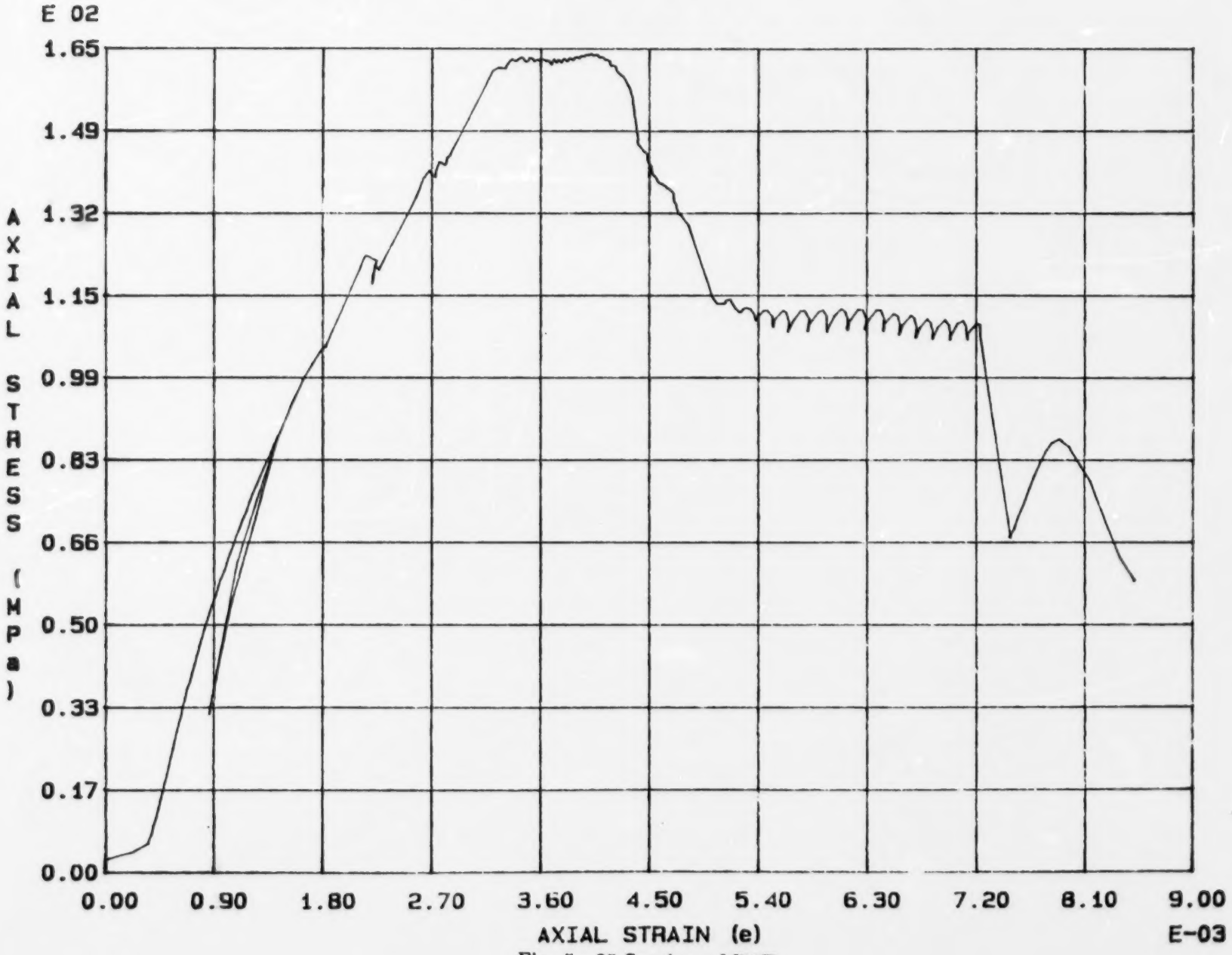

Fig. 5 - 35 Specimen M78T

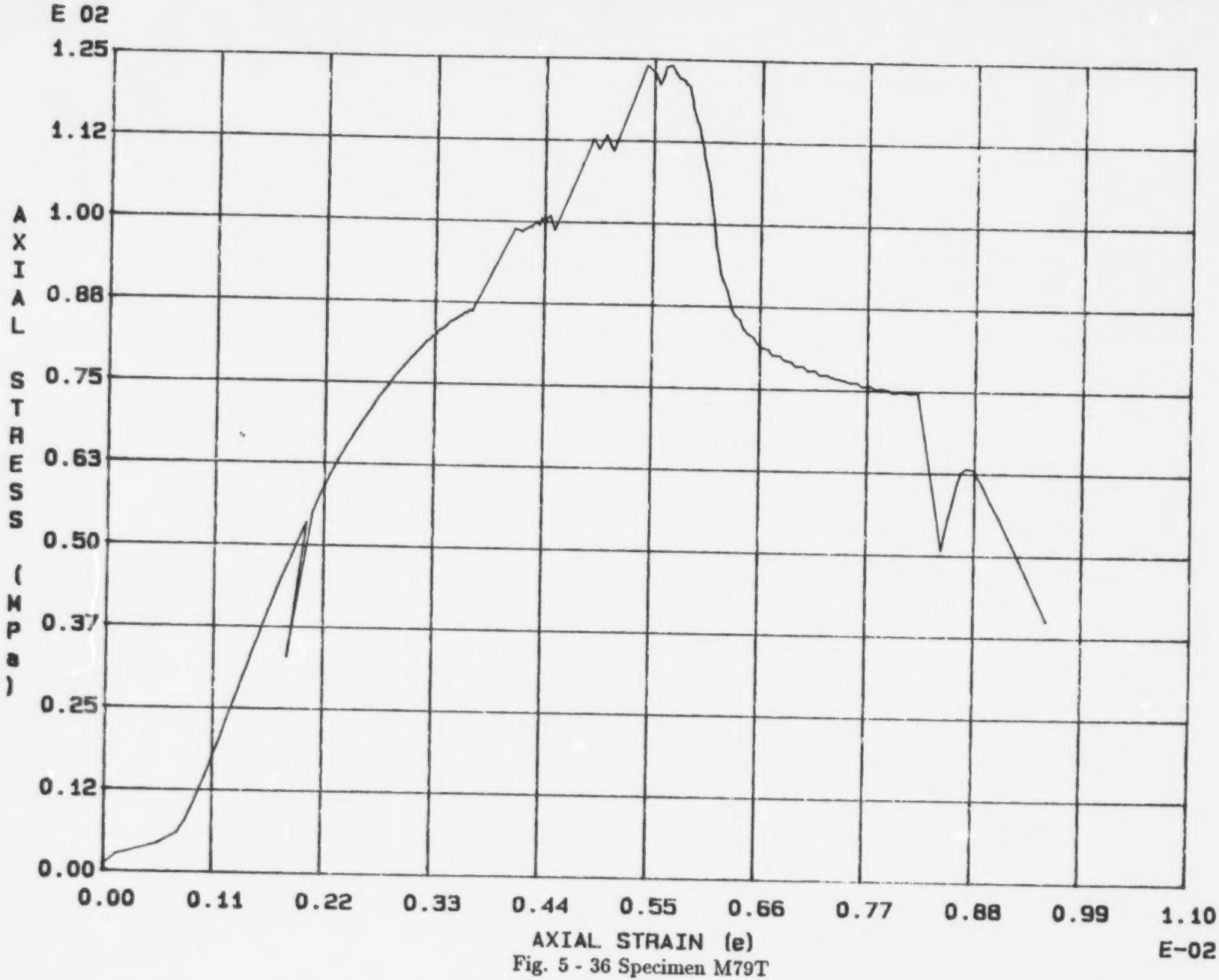

Fig. 5 - 36 Specimen M79T

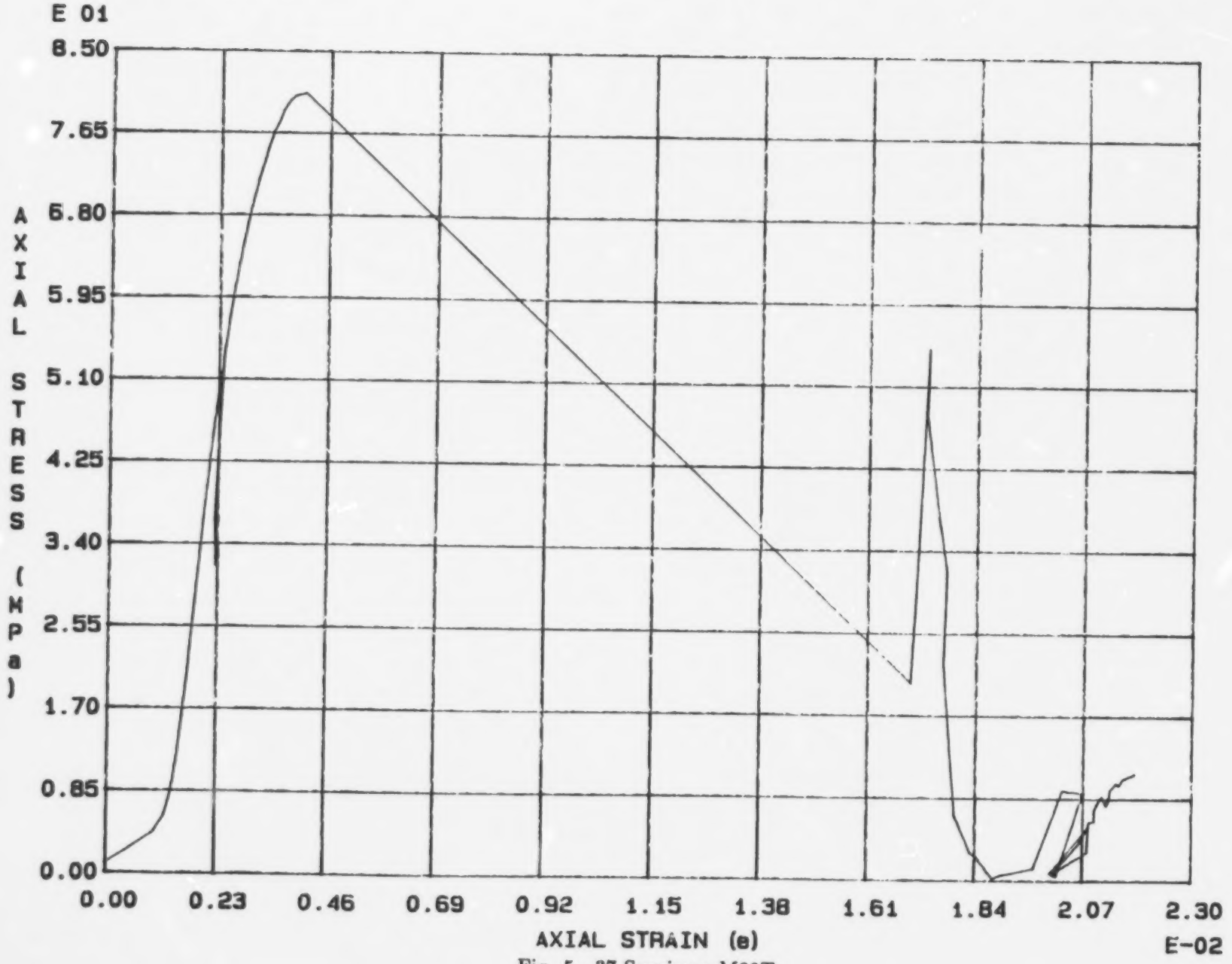

Fig. 5 - 37 Specimen M80T

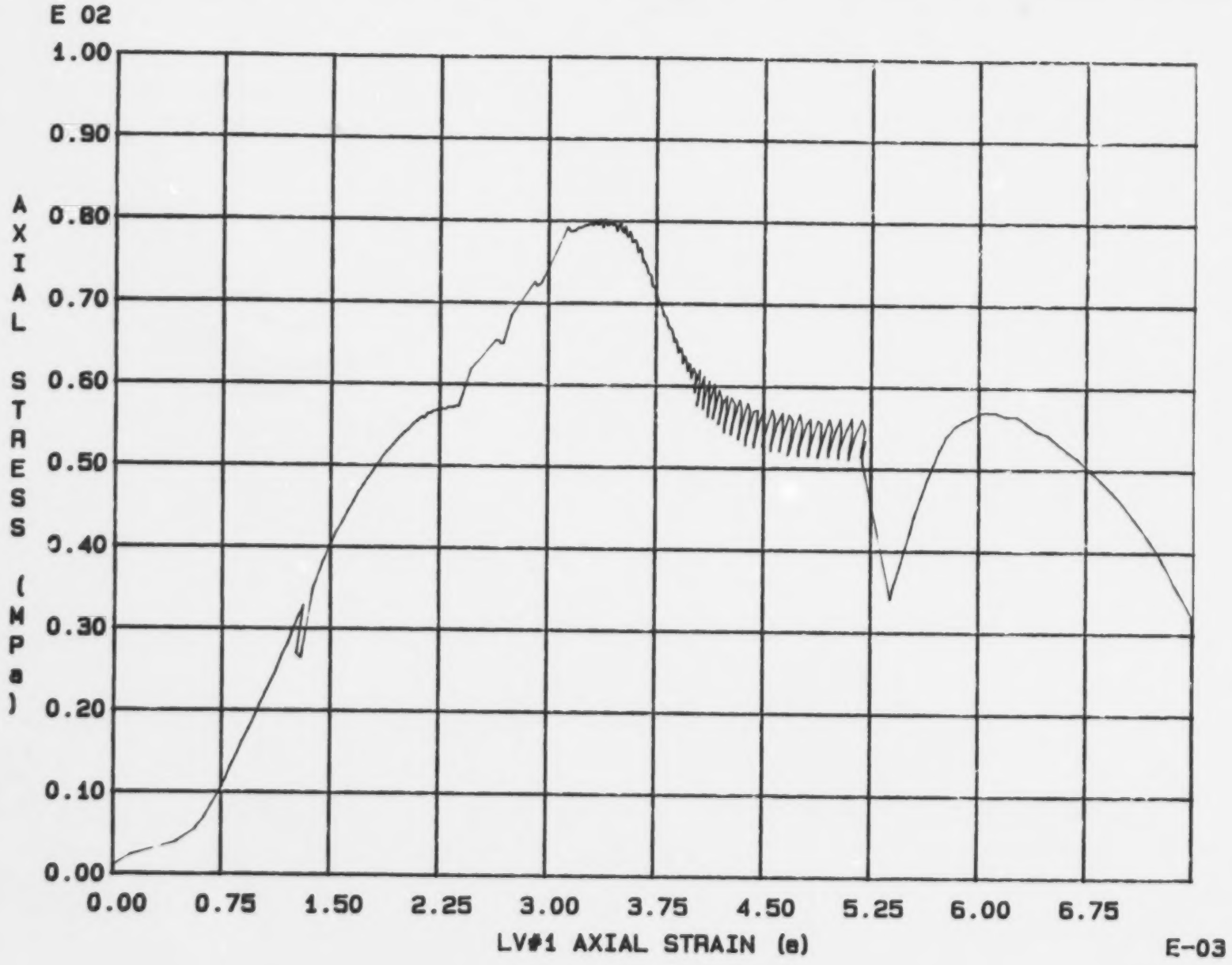

Fig. 5 - 38 Specimen M93T

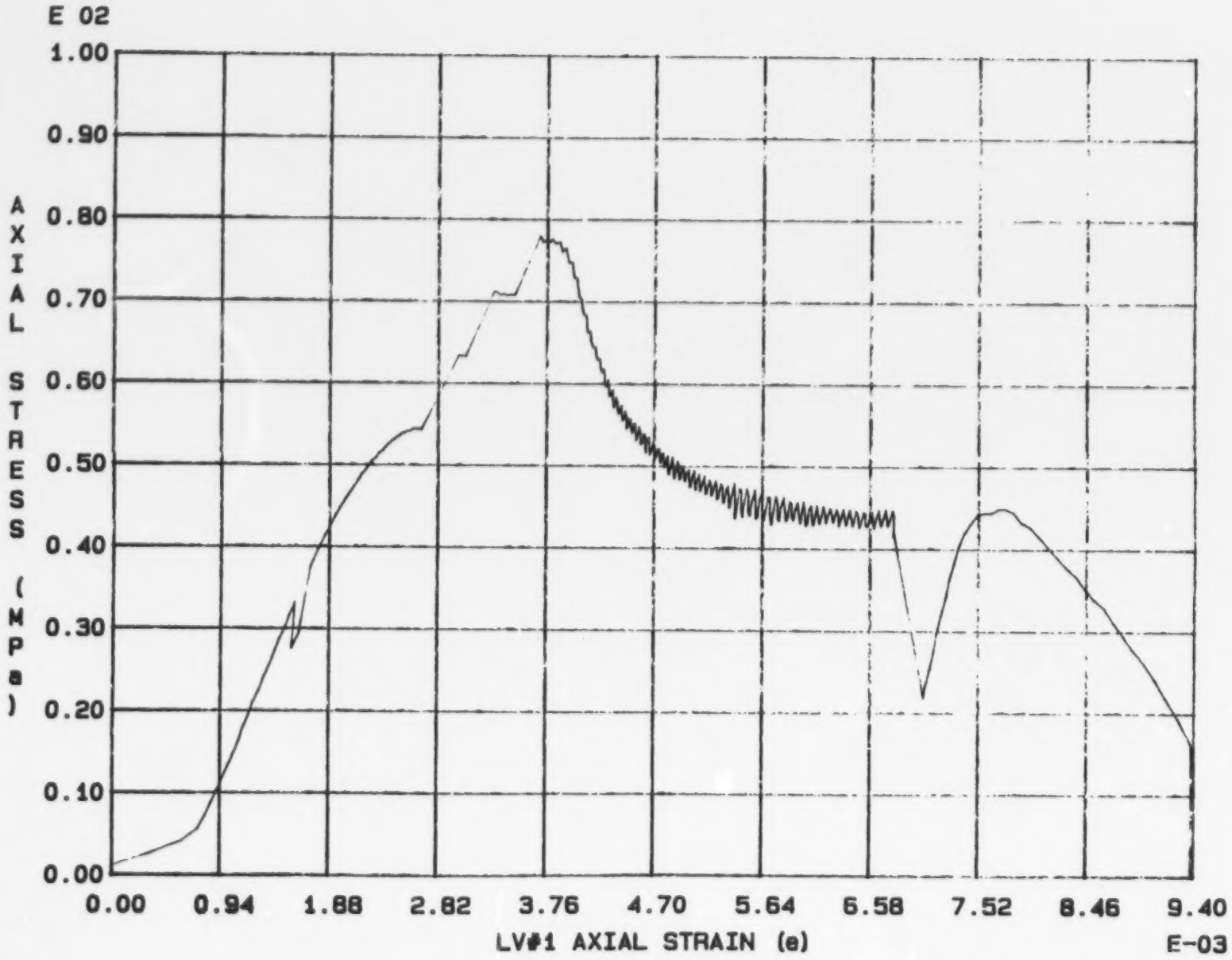

Fig. 5 - 39 Specimen M94T

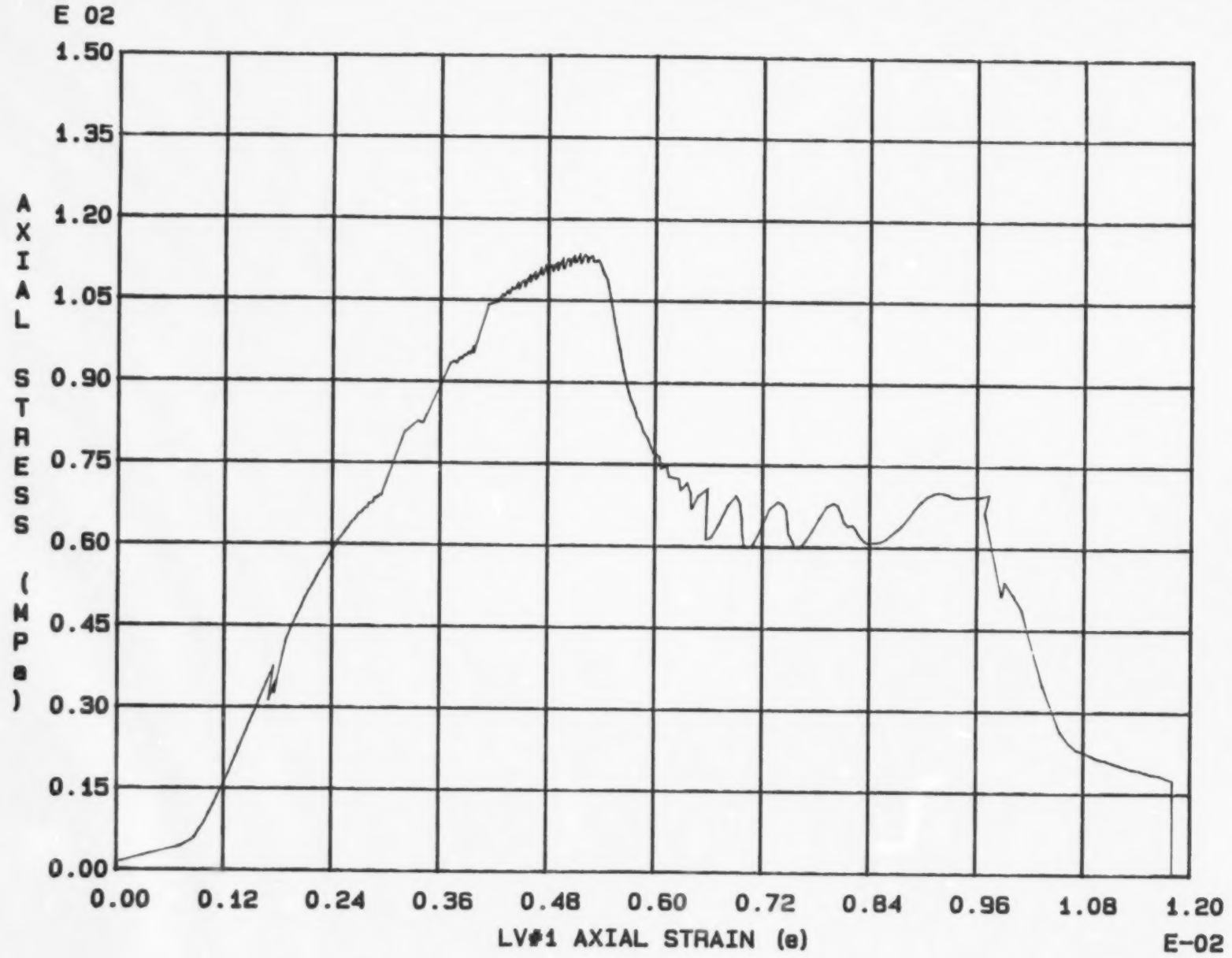

Fig. 5 - 40 Specimen M95T

Appendix 6.

Stress-strain curves of triaxial tests using circumferential extensometer

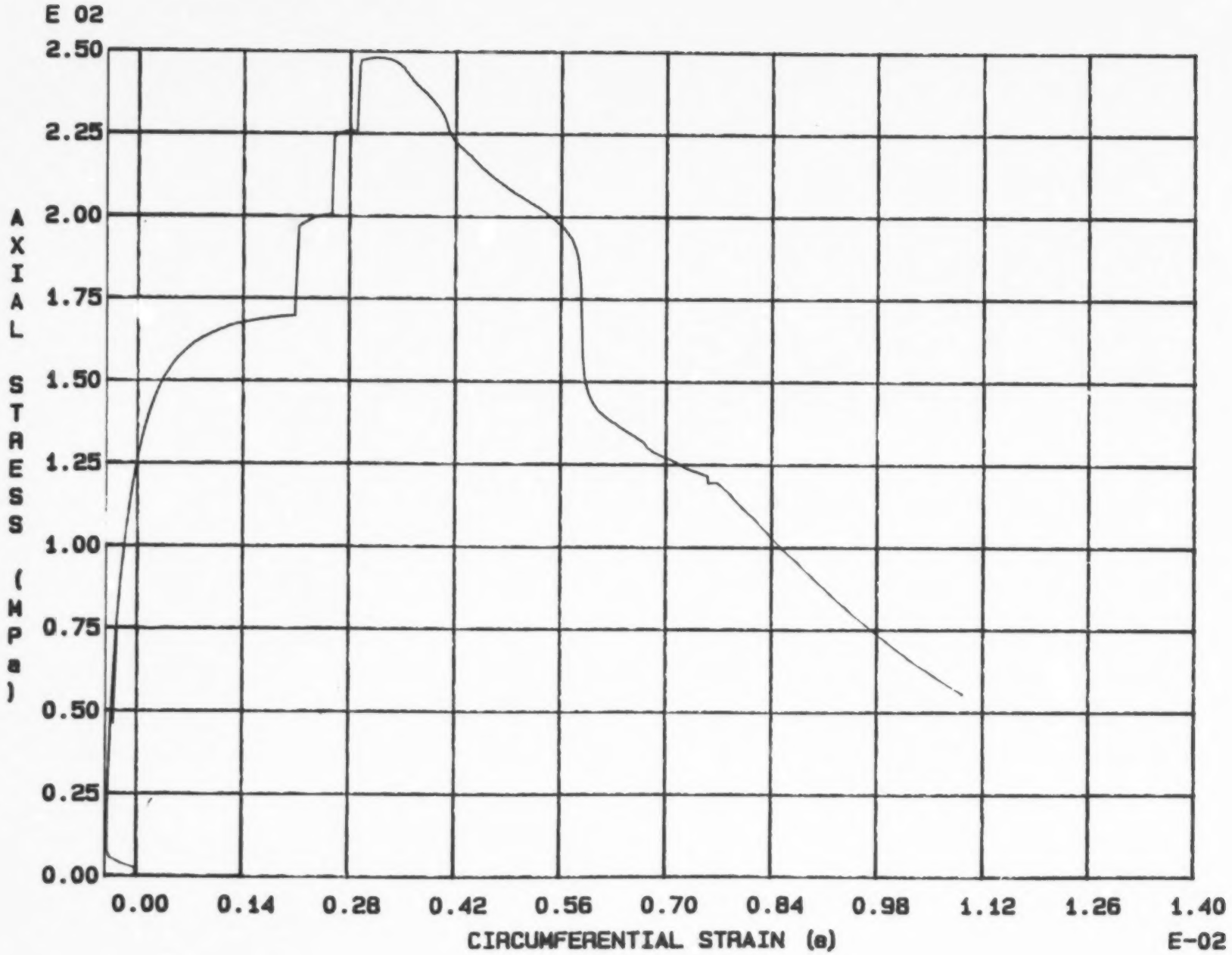

Fig. 6 - 1 Specimen M44T

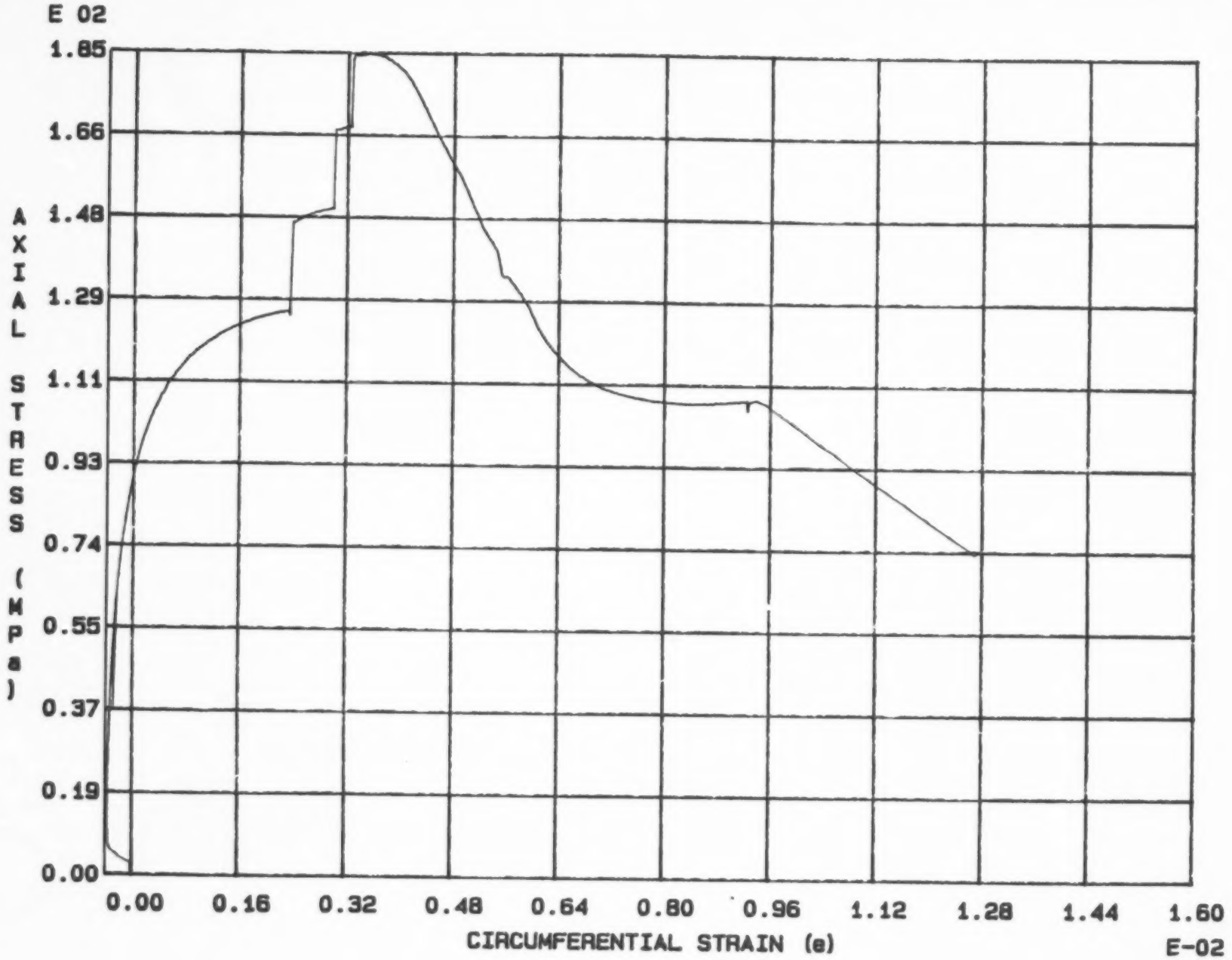

Fig. 6 - 2 Specimen M45T

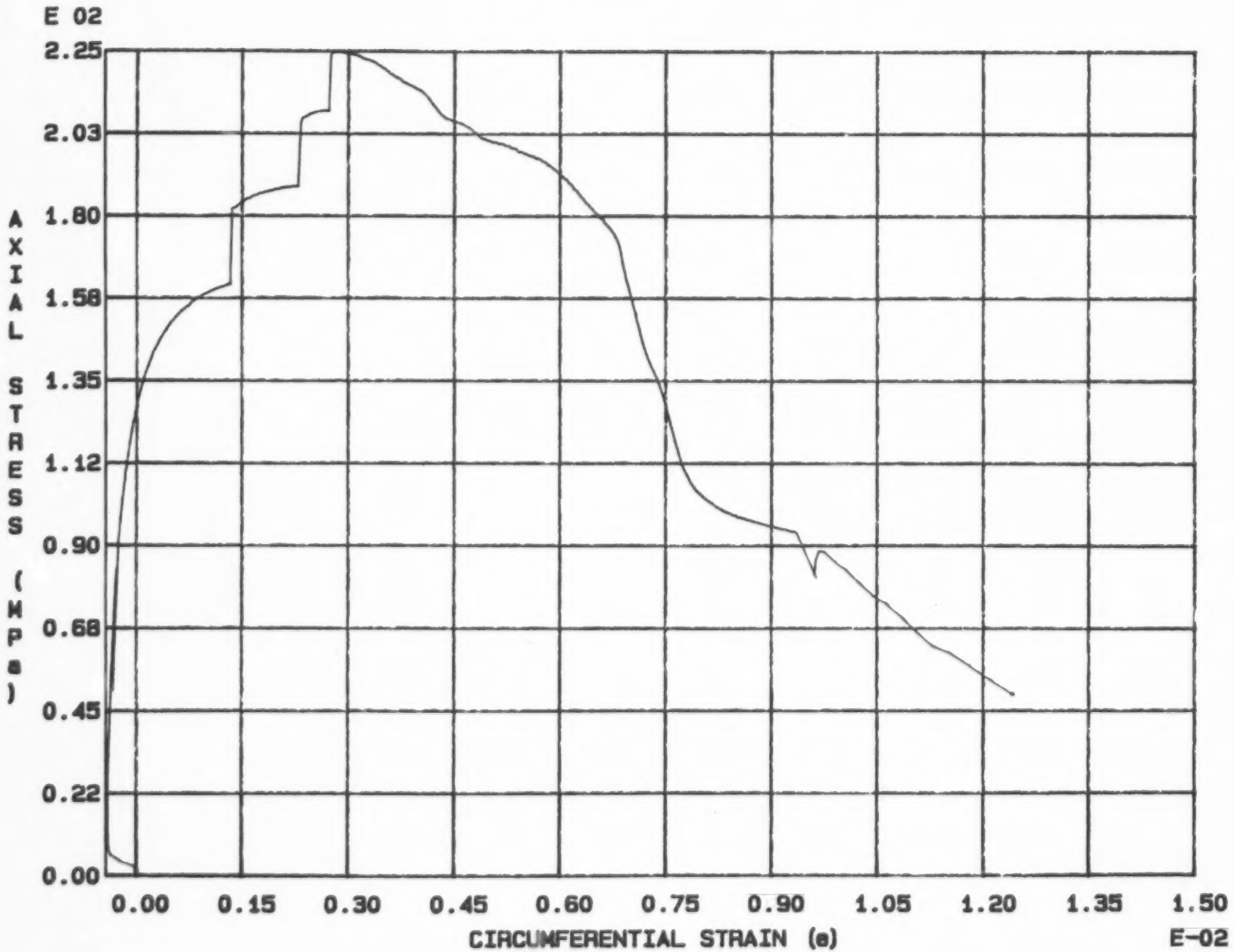

Fig. 6 - 3 Specimen M46T

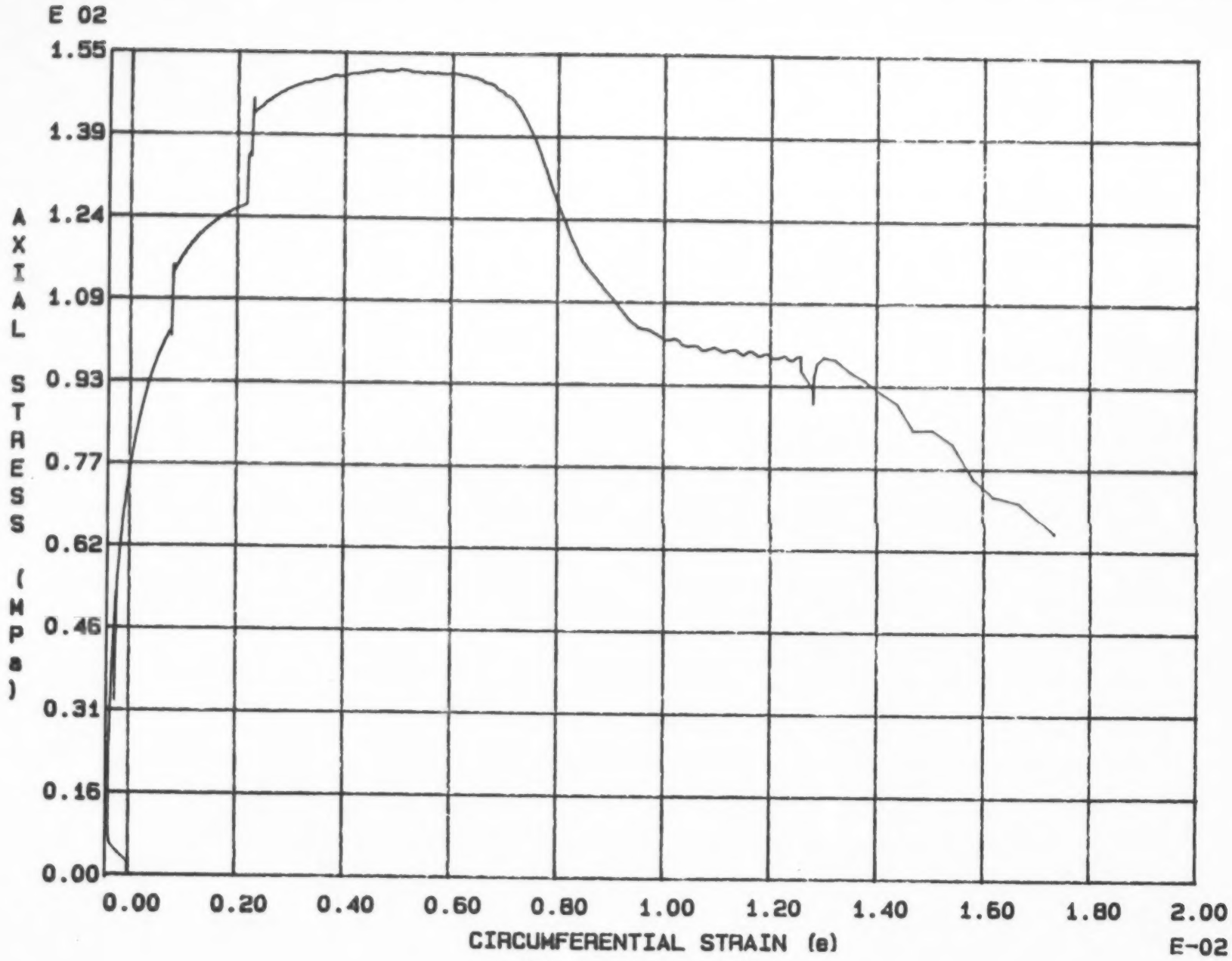

Fig. 6 - 4 Specimen M47T

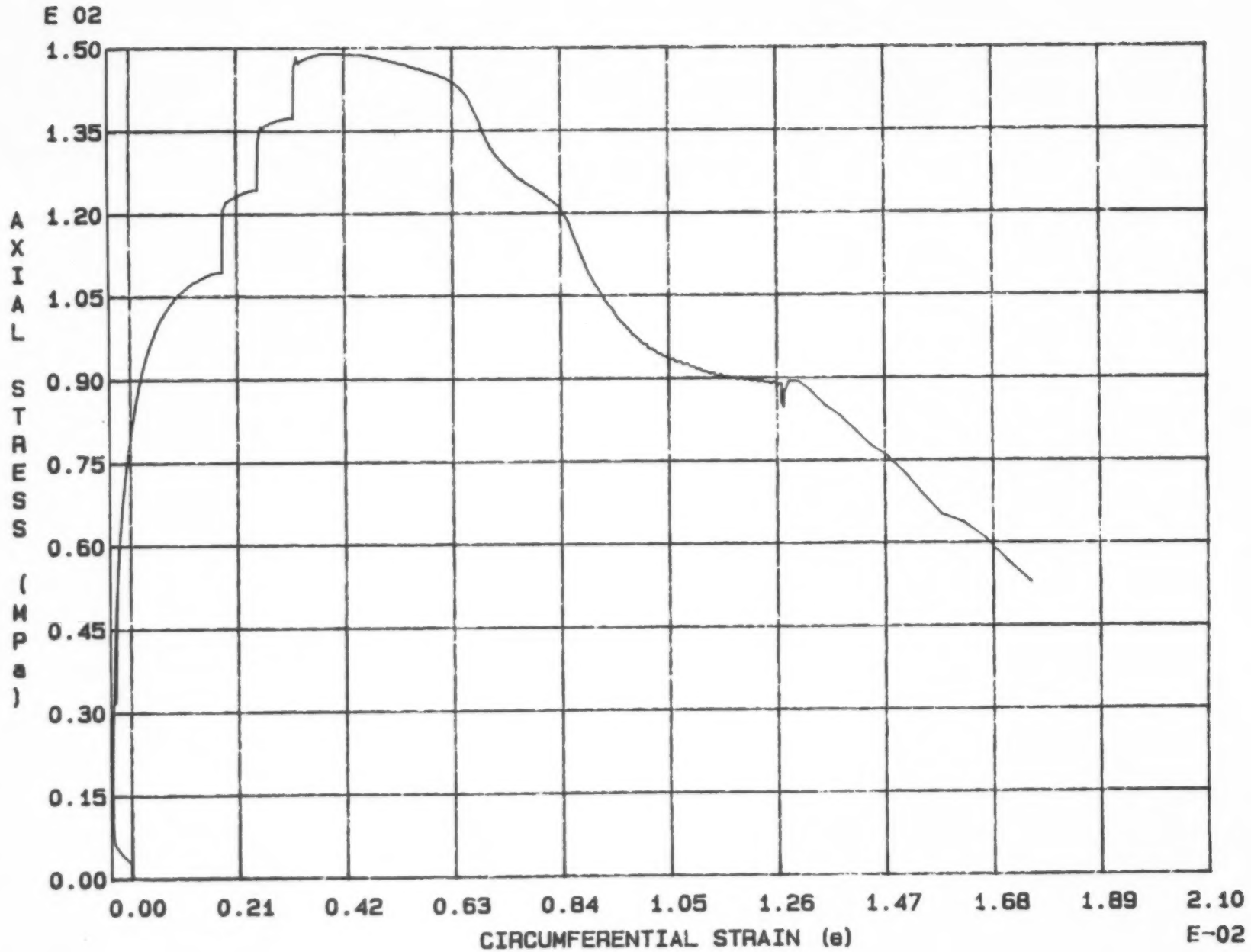

Fig. 6 - 5 Specimen M48T

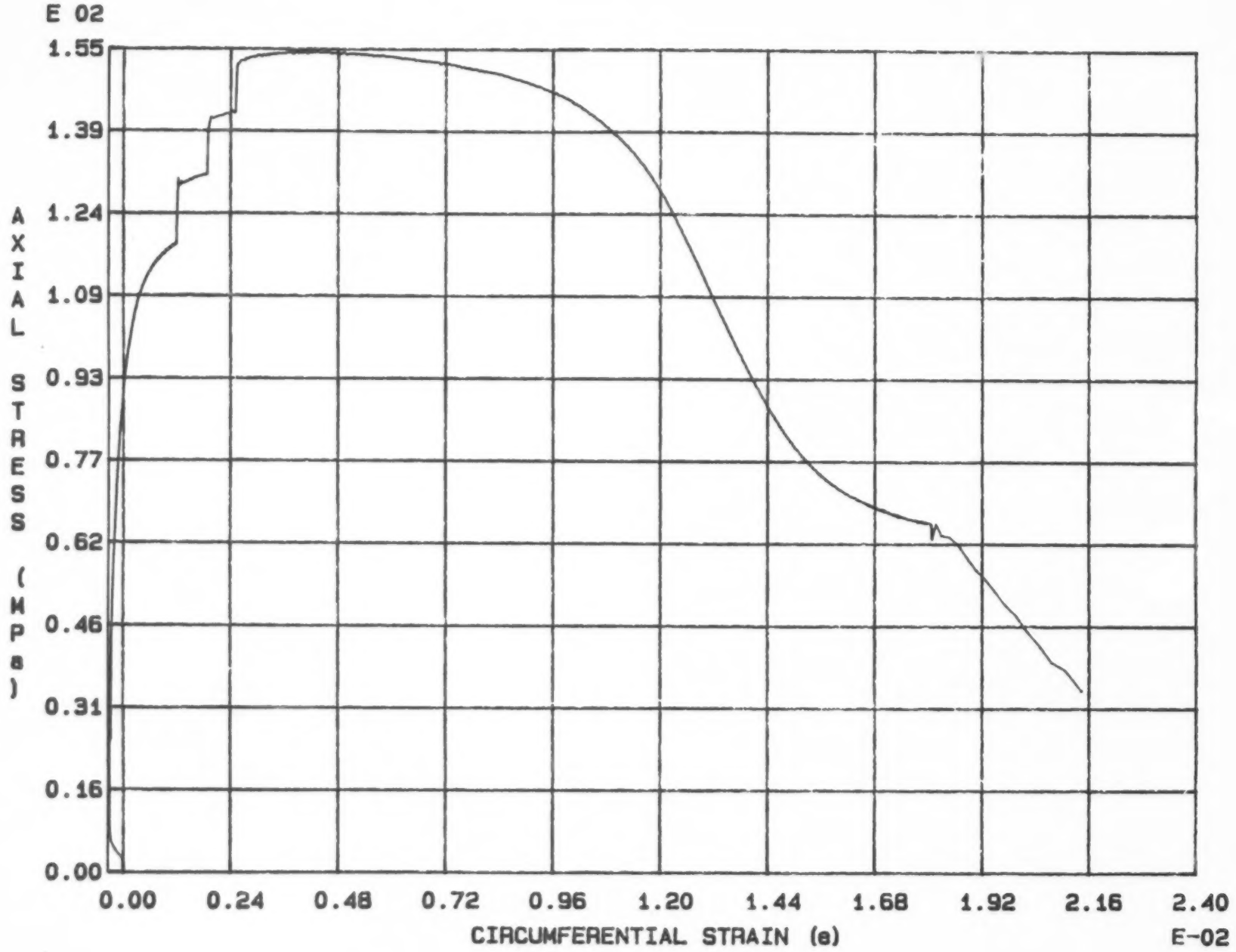

Fig. 6 - 6 Specimen M49T

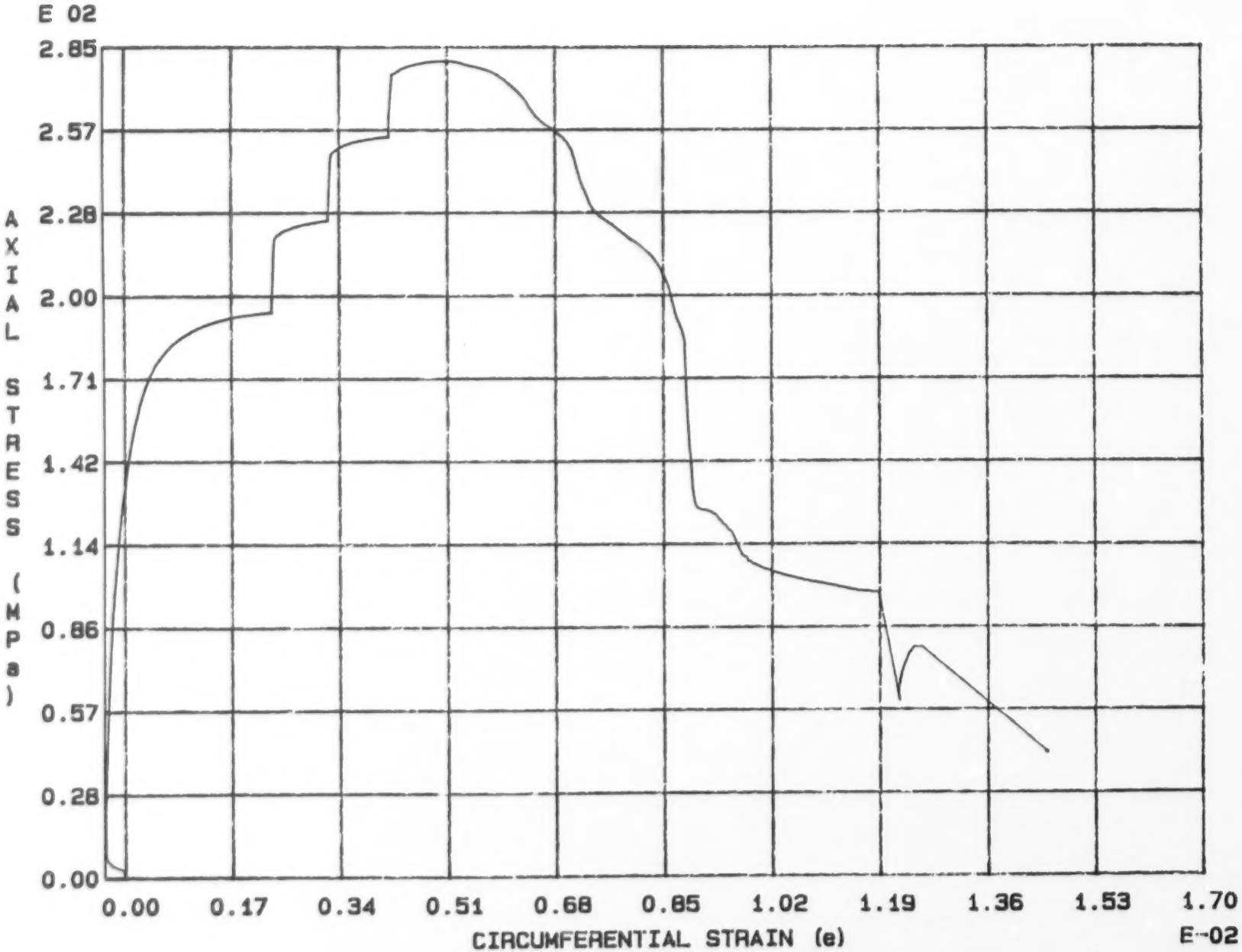

Fig. 6 - 7 Specimen M50T

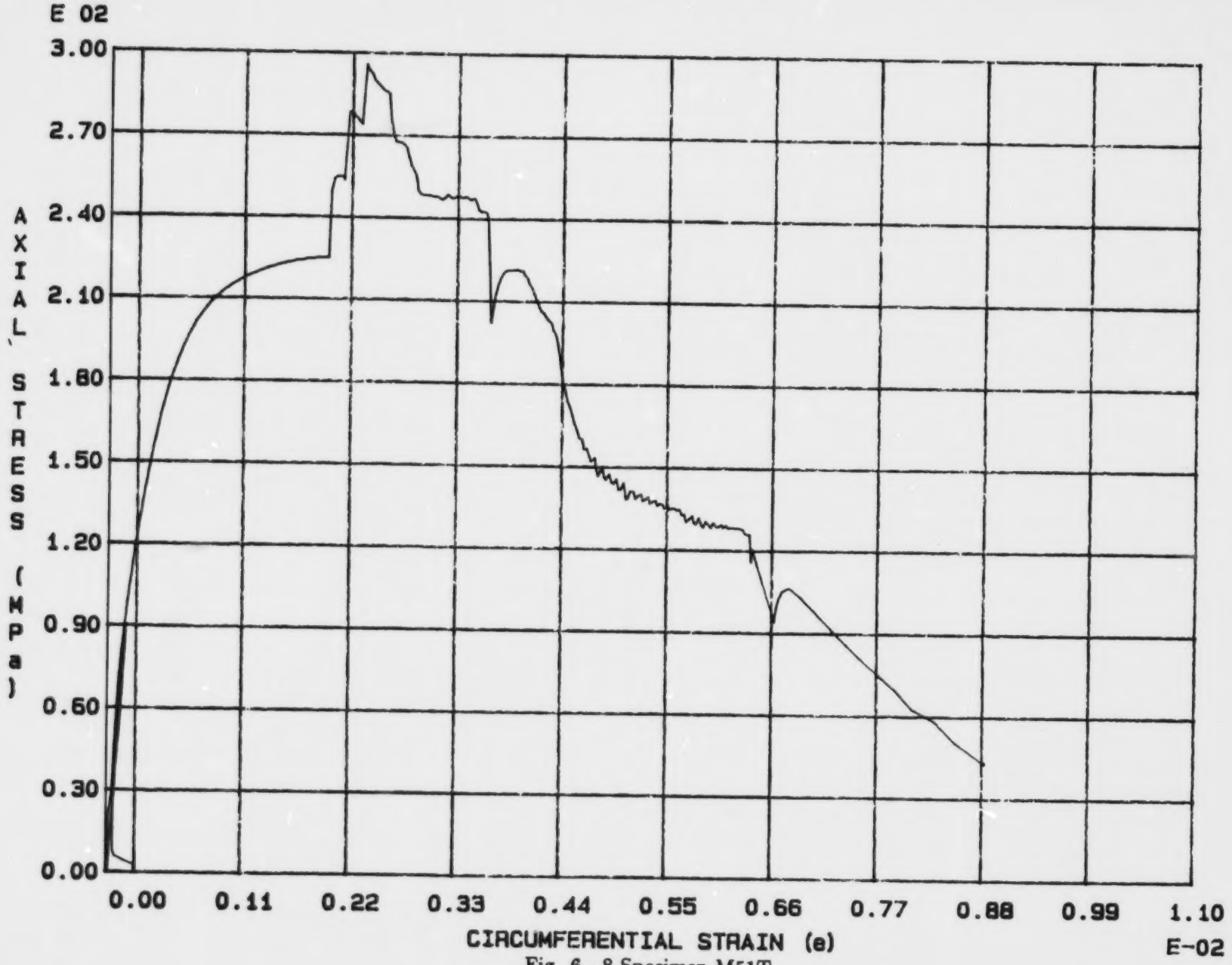

Fig. 6 - 8 Specimen M51T

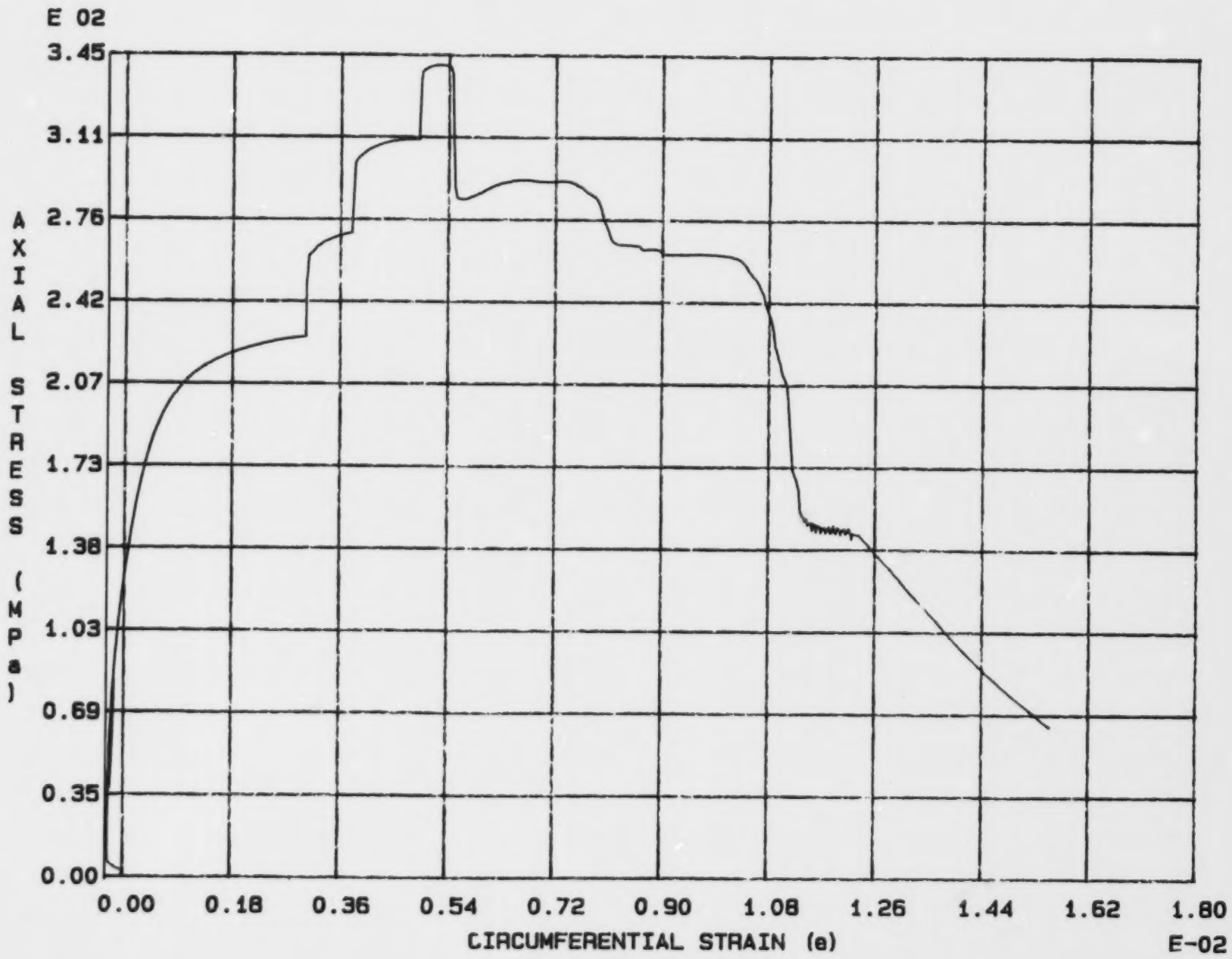

Fig. 6 - 9 Specimen M52T

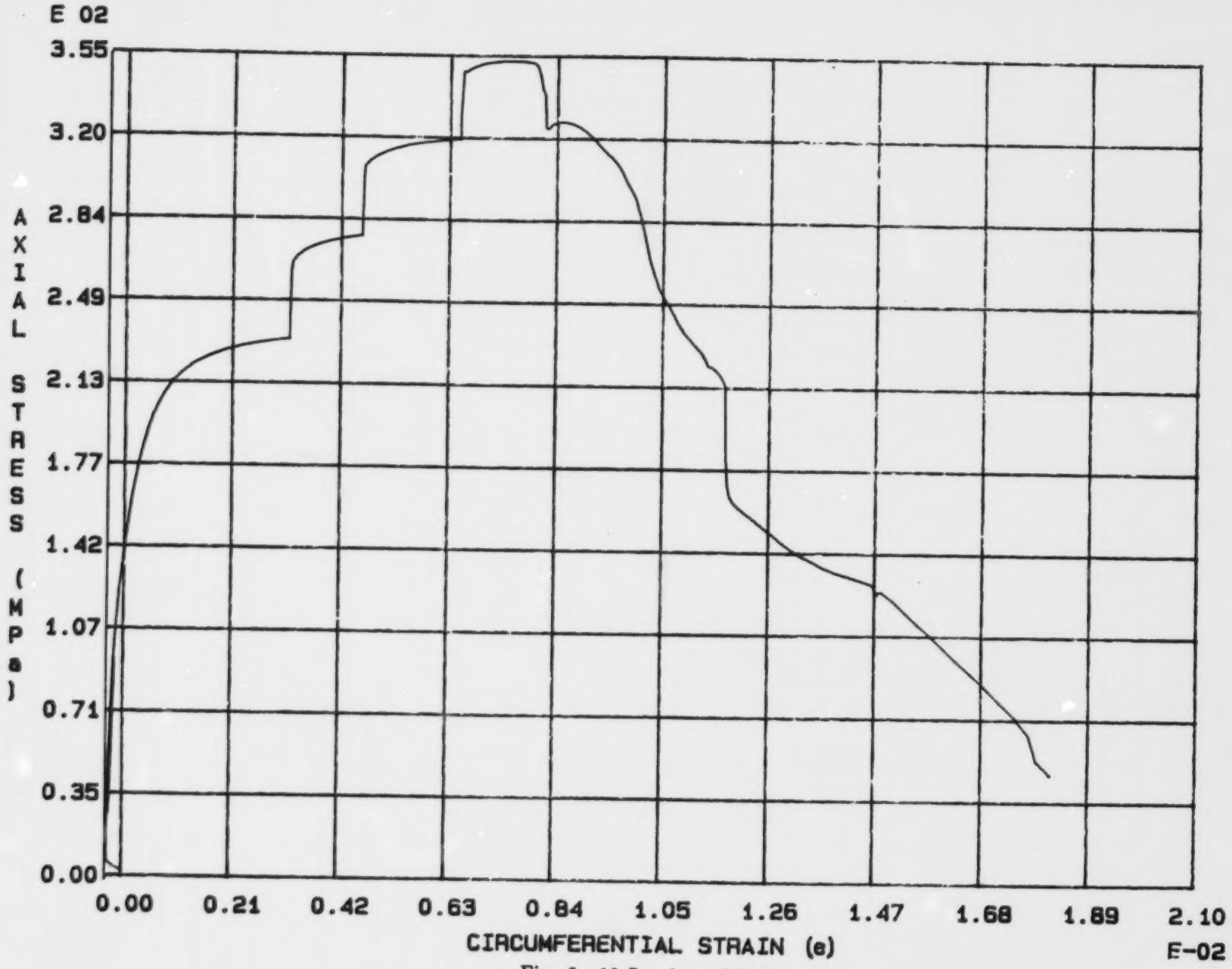

Fig. 6 - 10 Specimen M53T

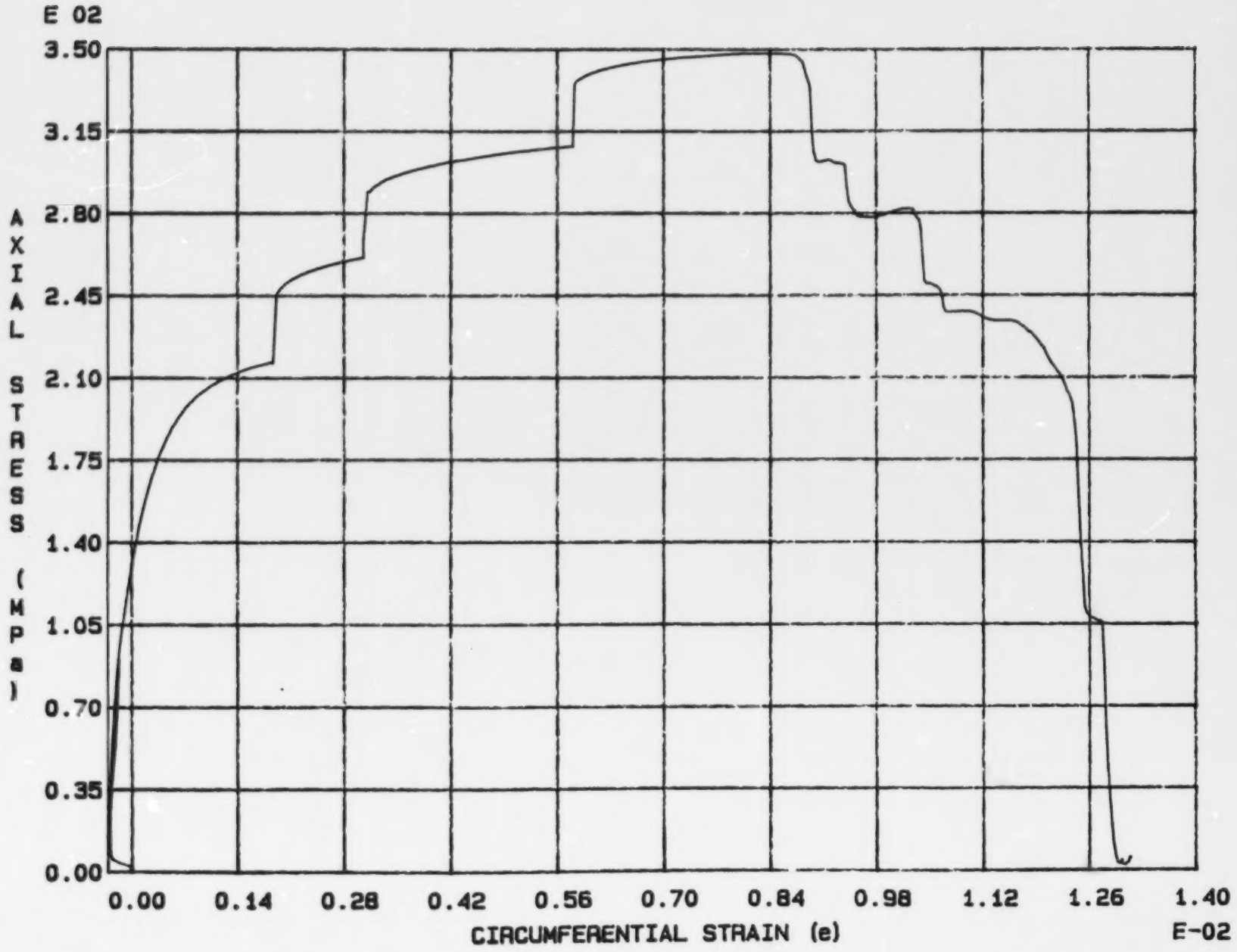

Fig. 6 - 11 Specimen M54T

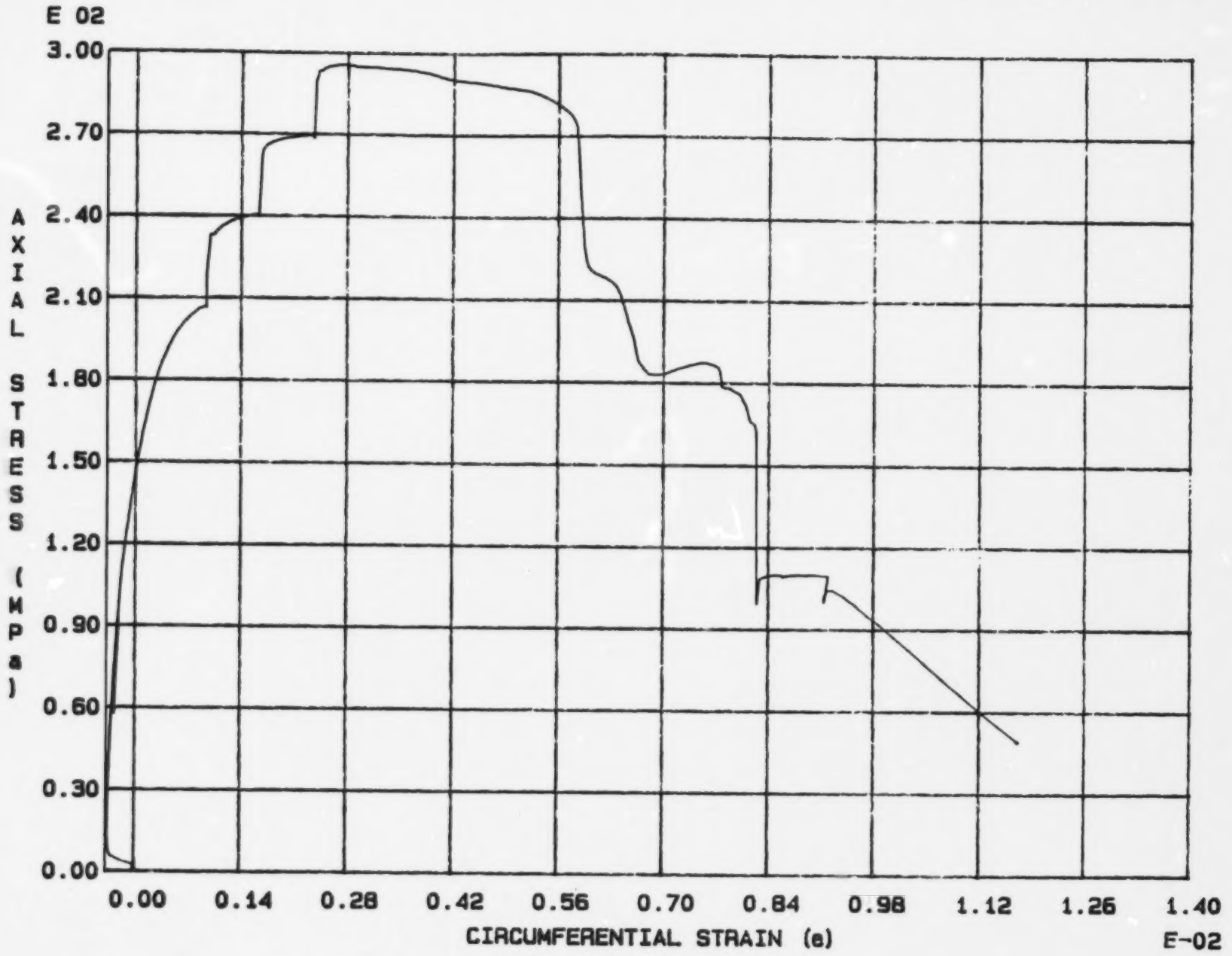

Fig. 6 - 12 Specimen M55T

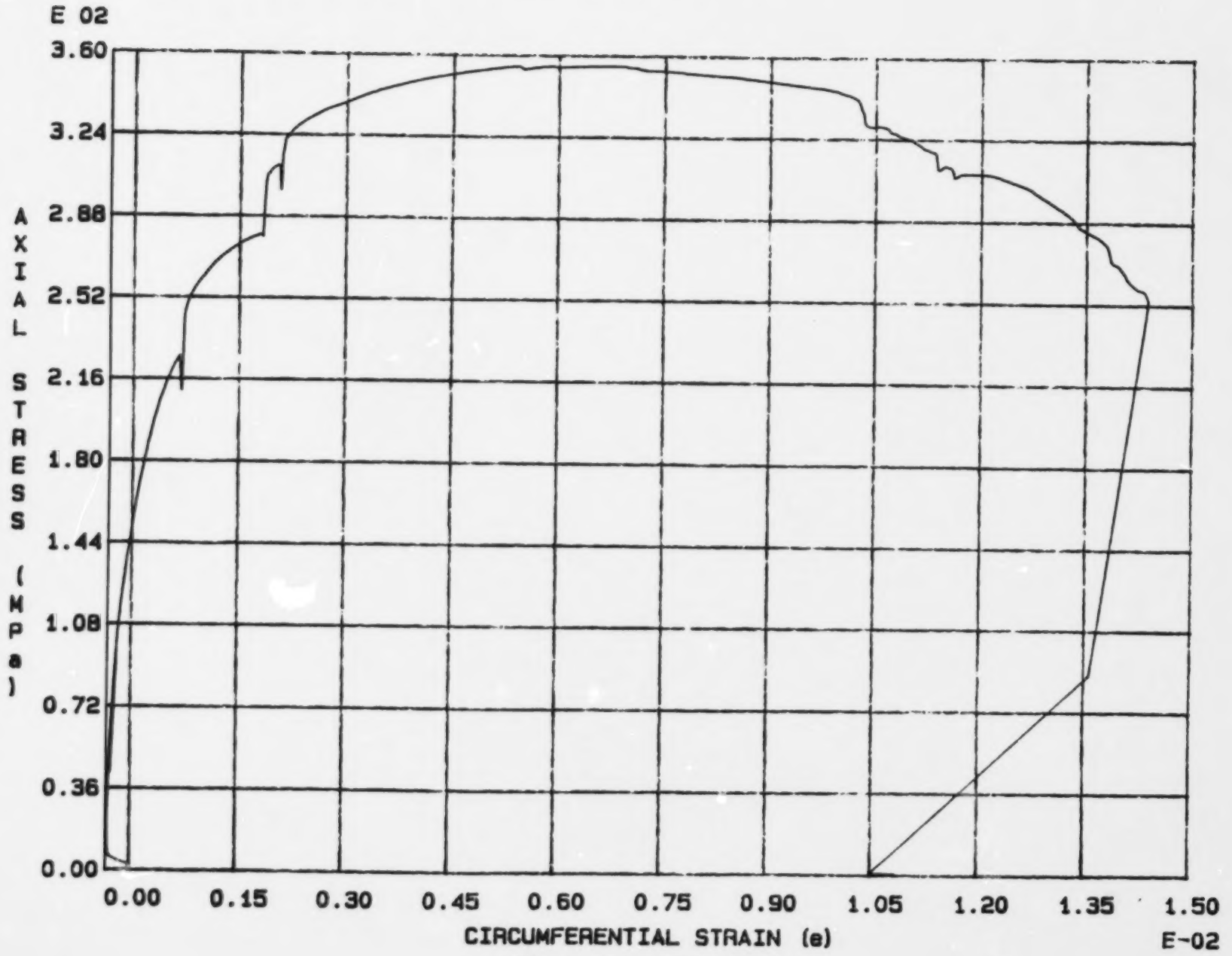

Fig. 6 - 13 Specimen M56T

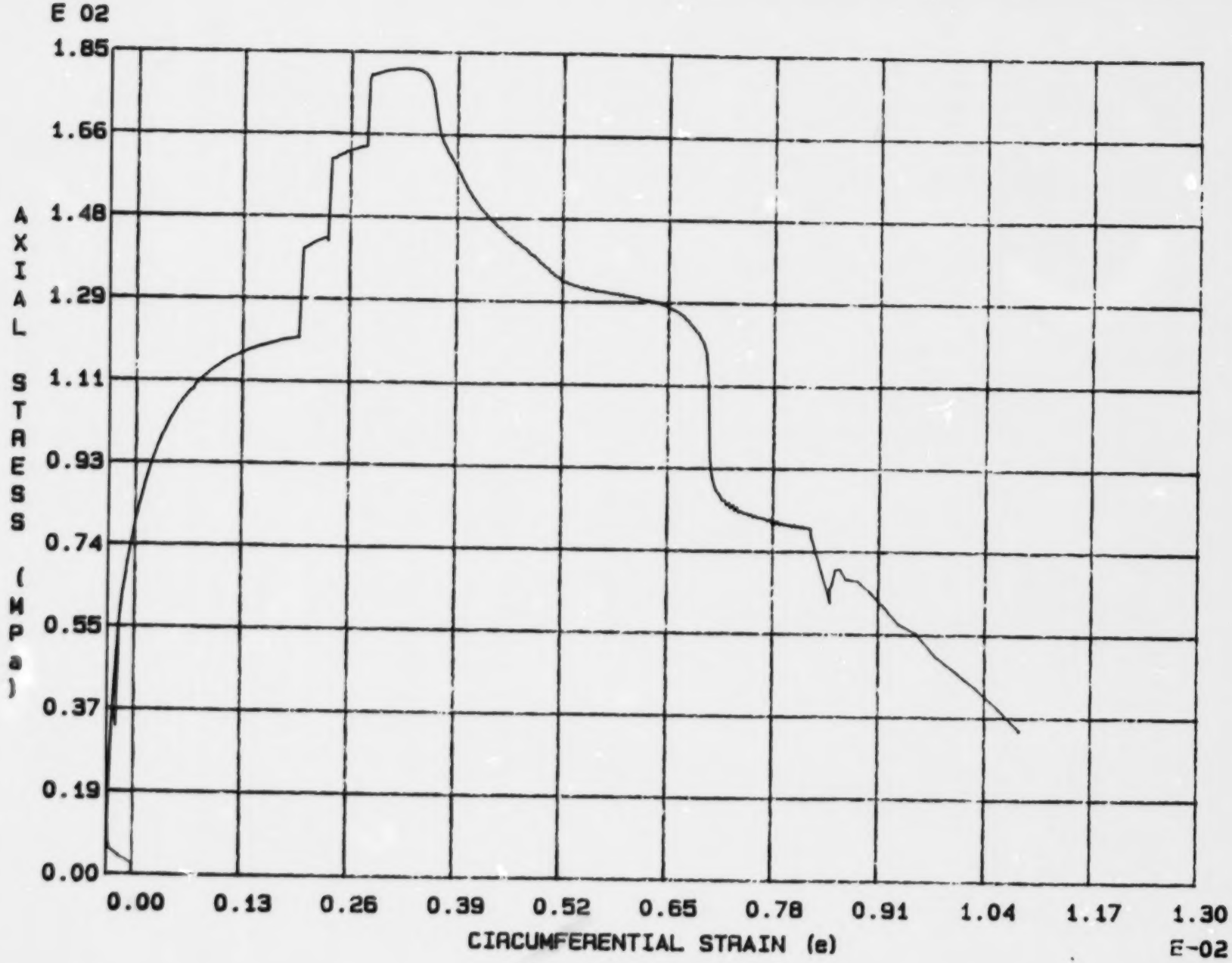

Fig. 6 - 14 Specimen M57T

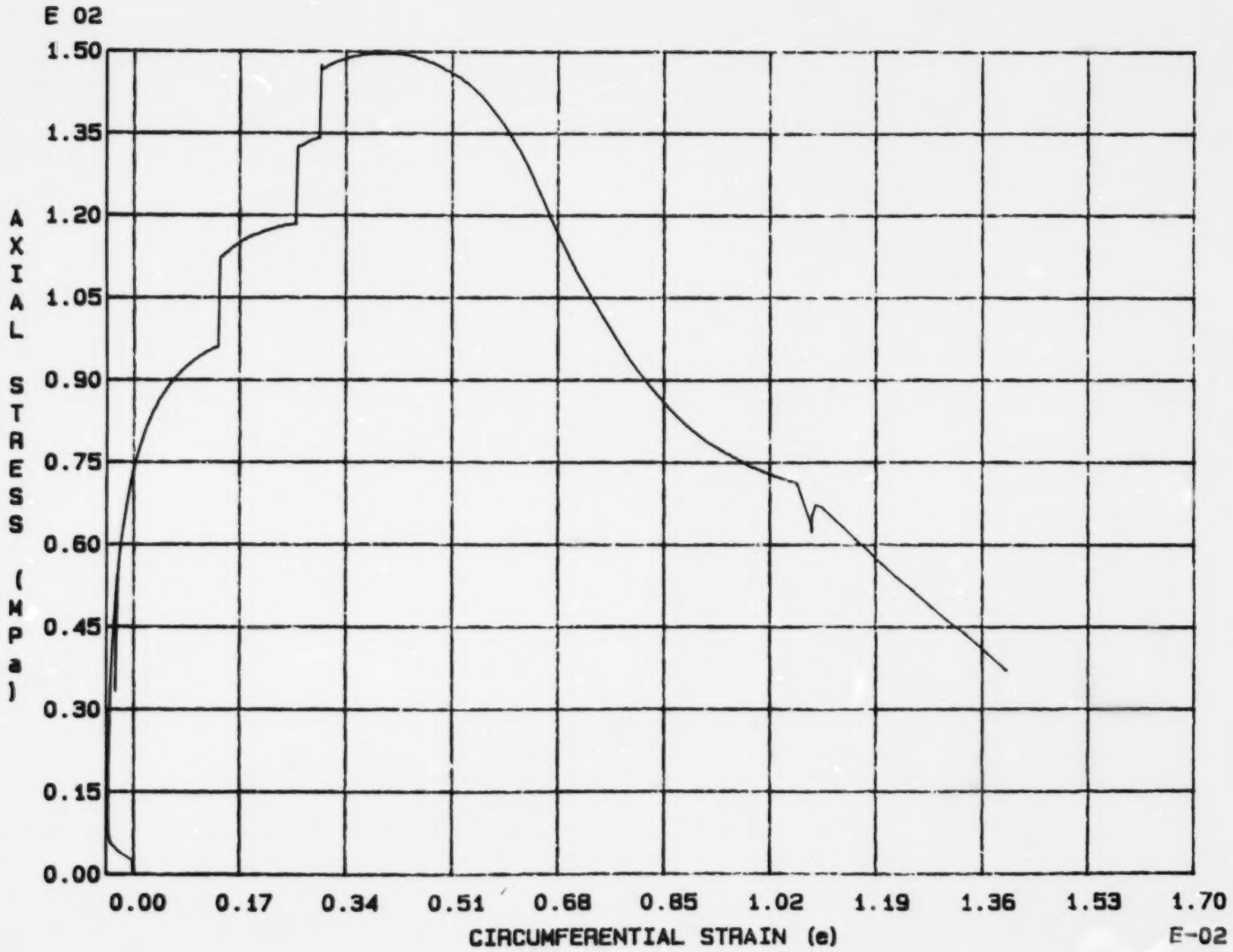

Fig. 6 - 15 Specimen M58T

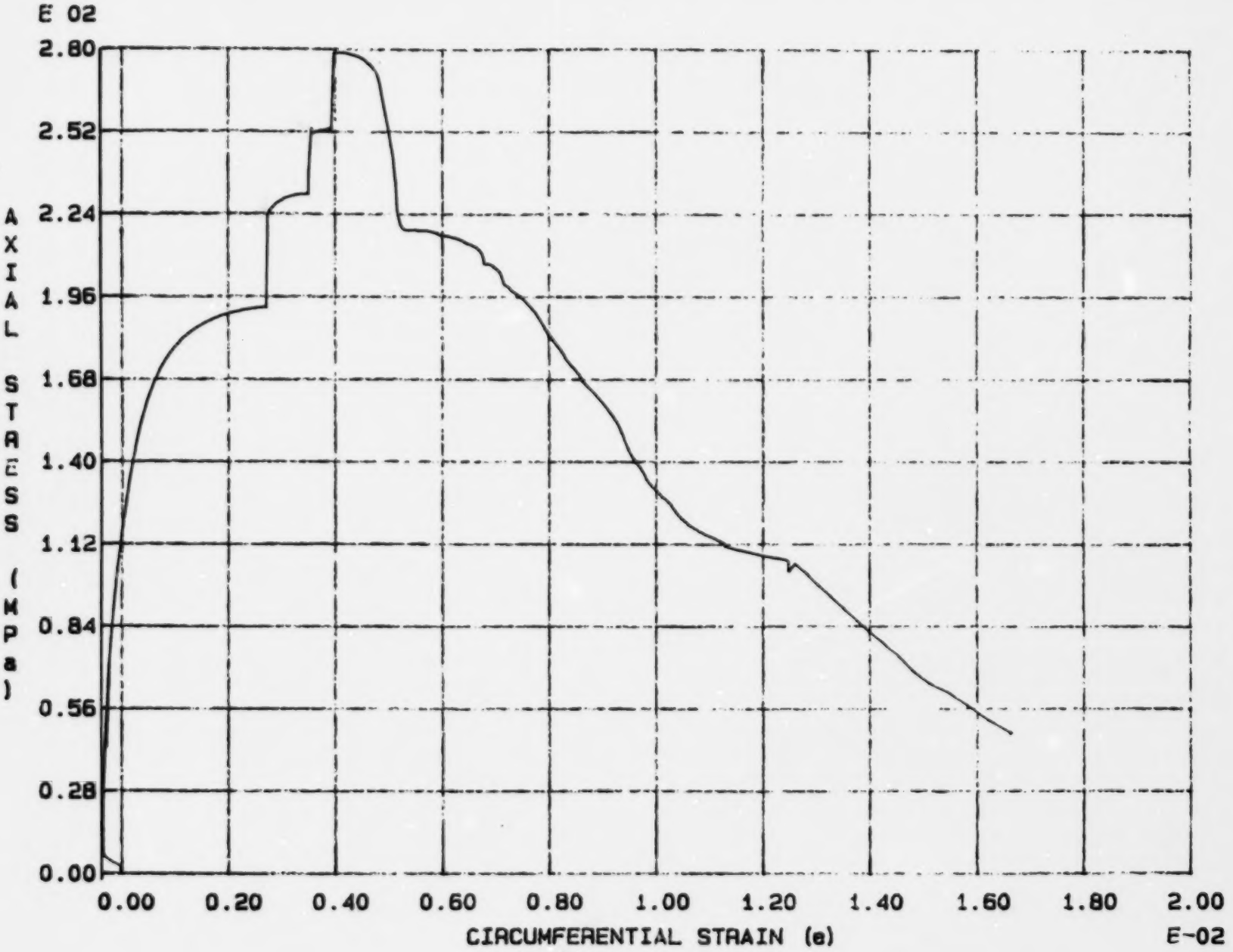

Fig. 6 - 16 Specimen M59T

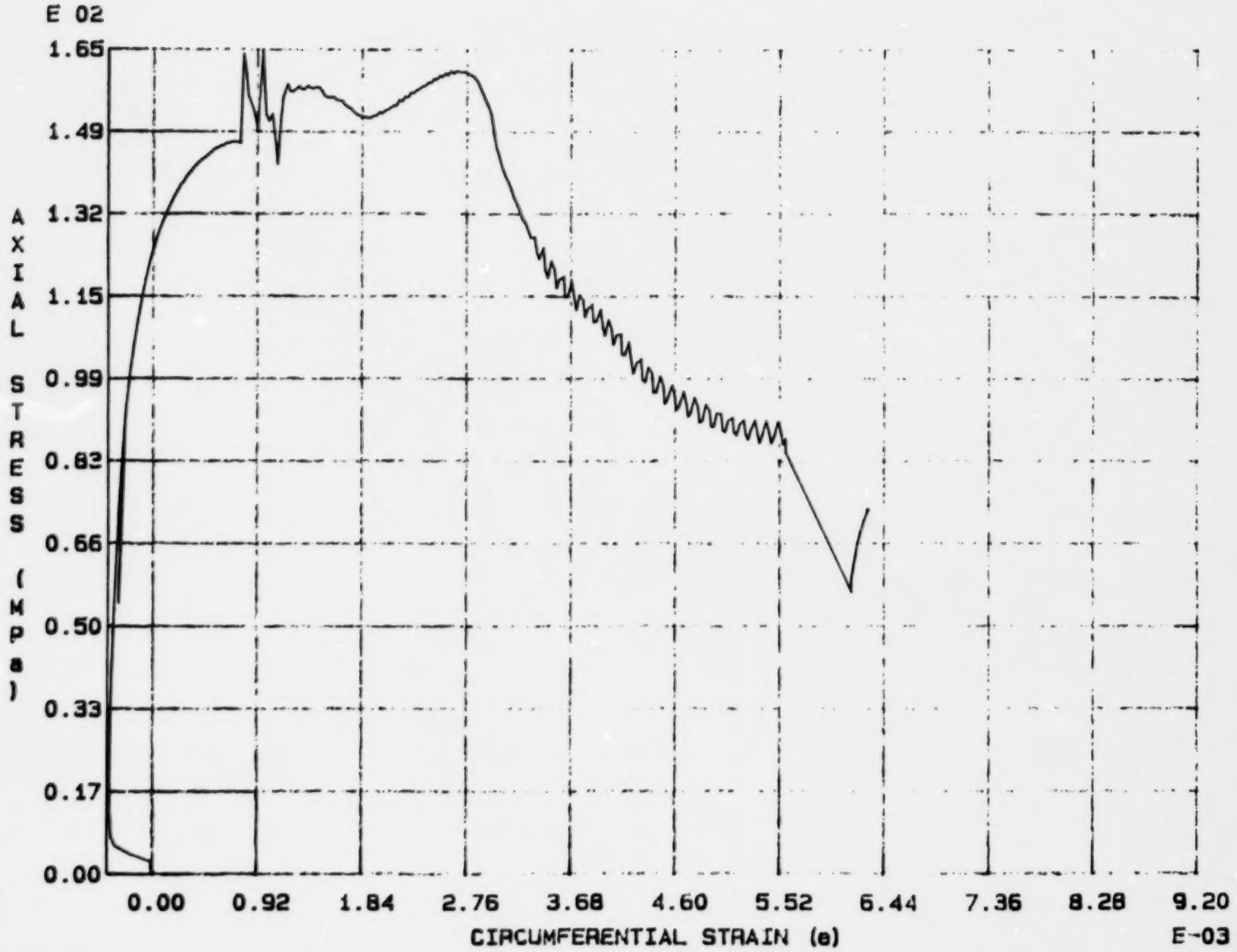

Fig. 6 - 17 Specimen M60T

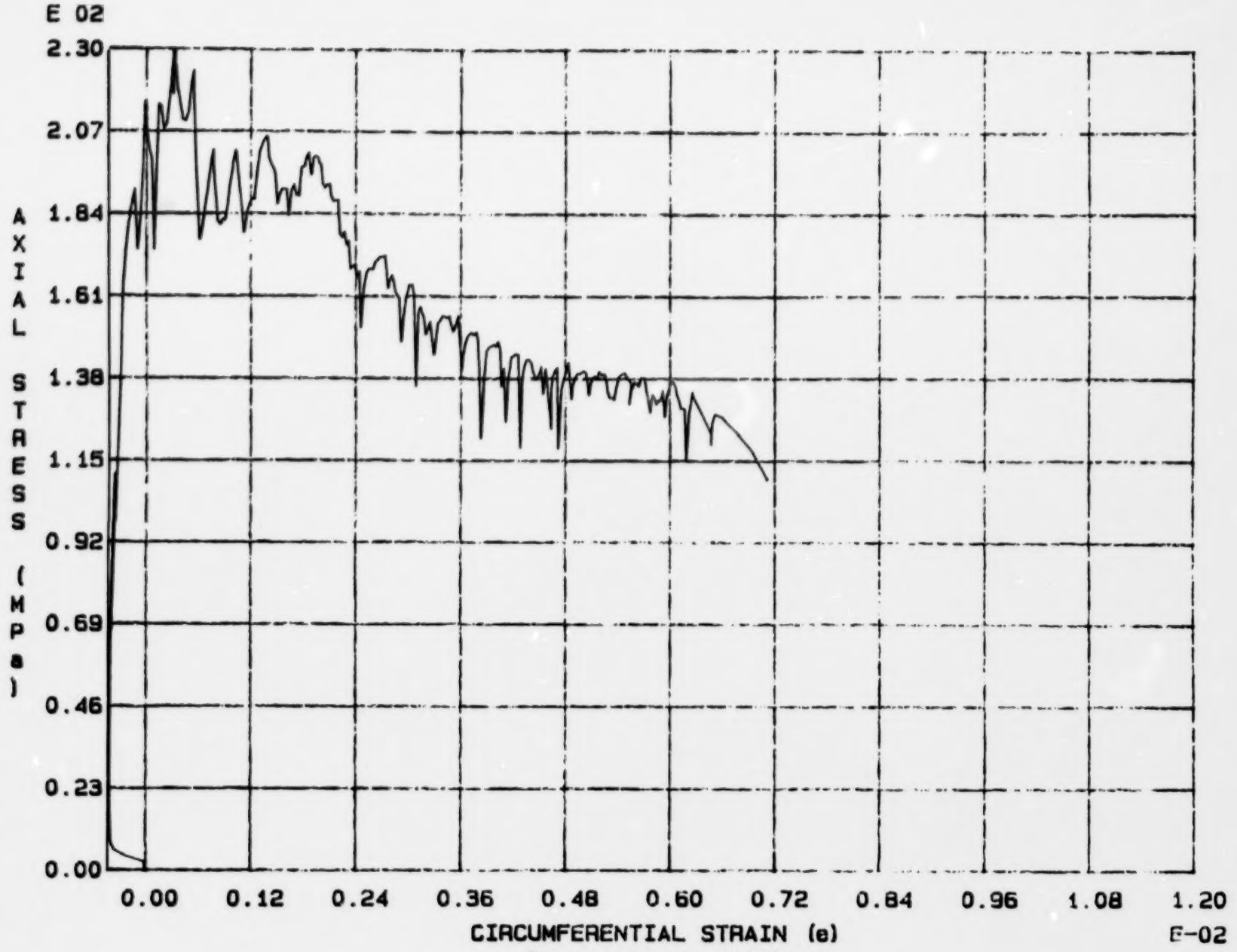

Fig. 6 - 18 Specimen M61T

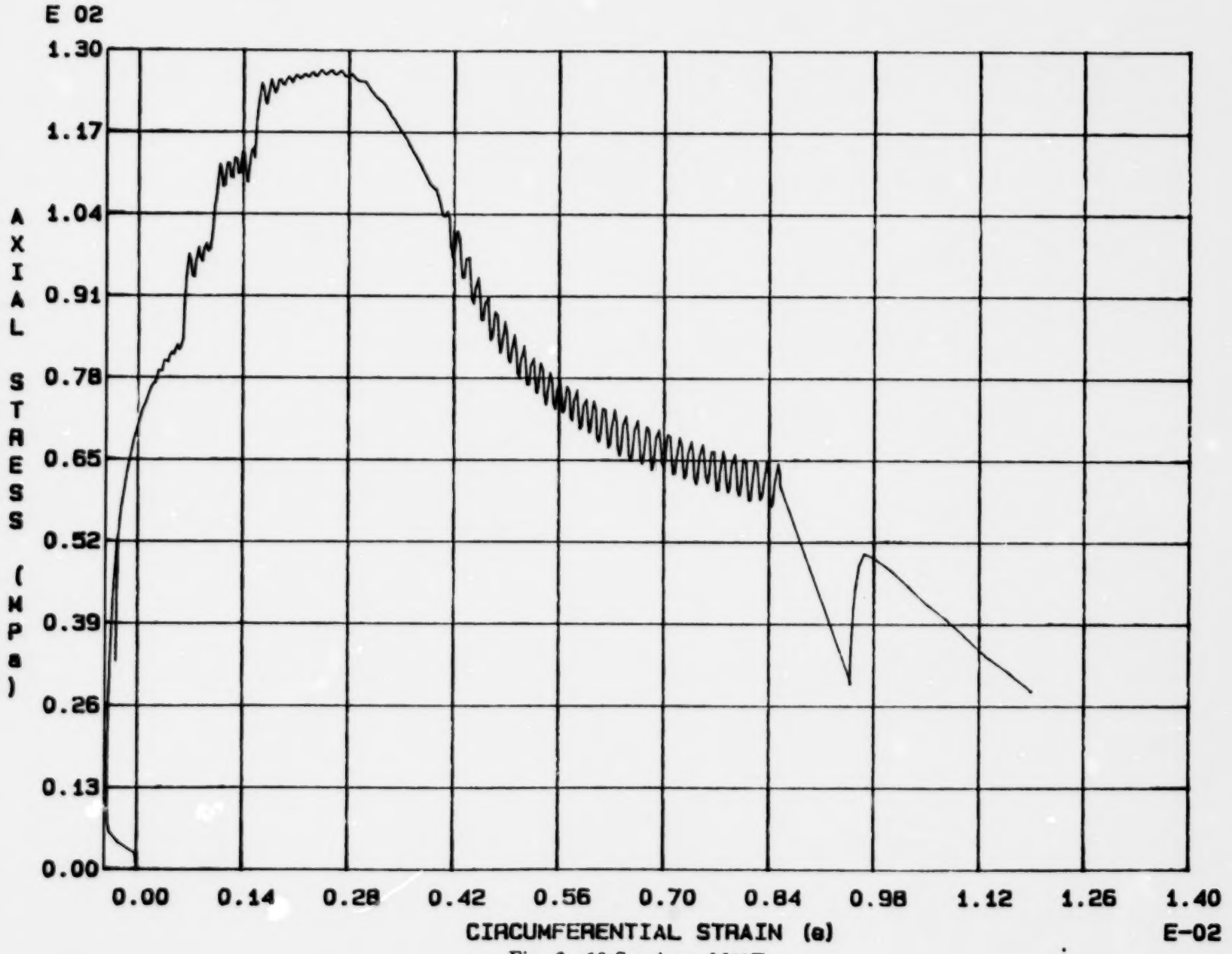

Fig. 6 - 19 Specimen M62T

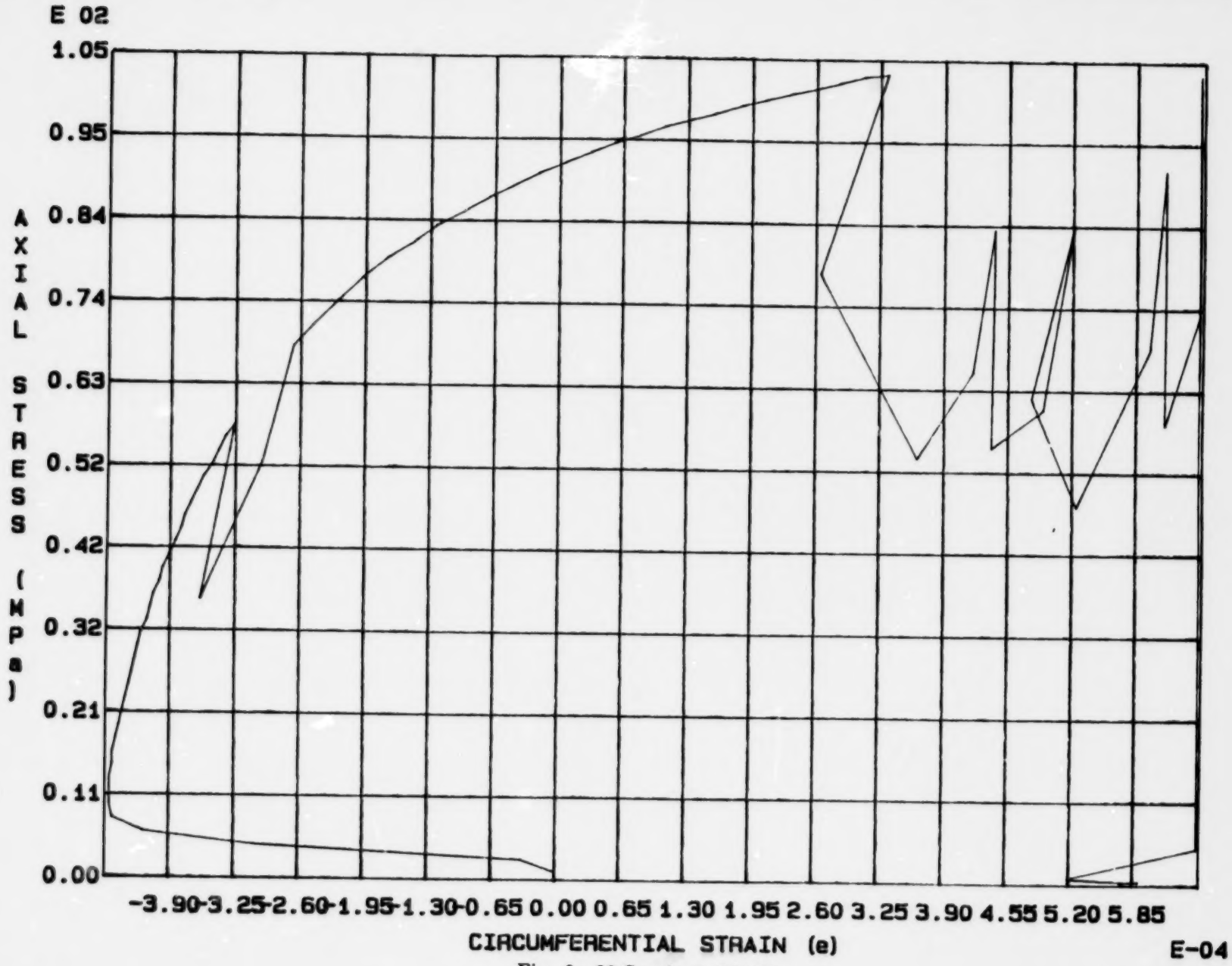

Fig. 6 - 20 Specimen M63T

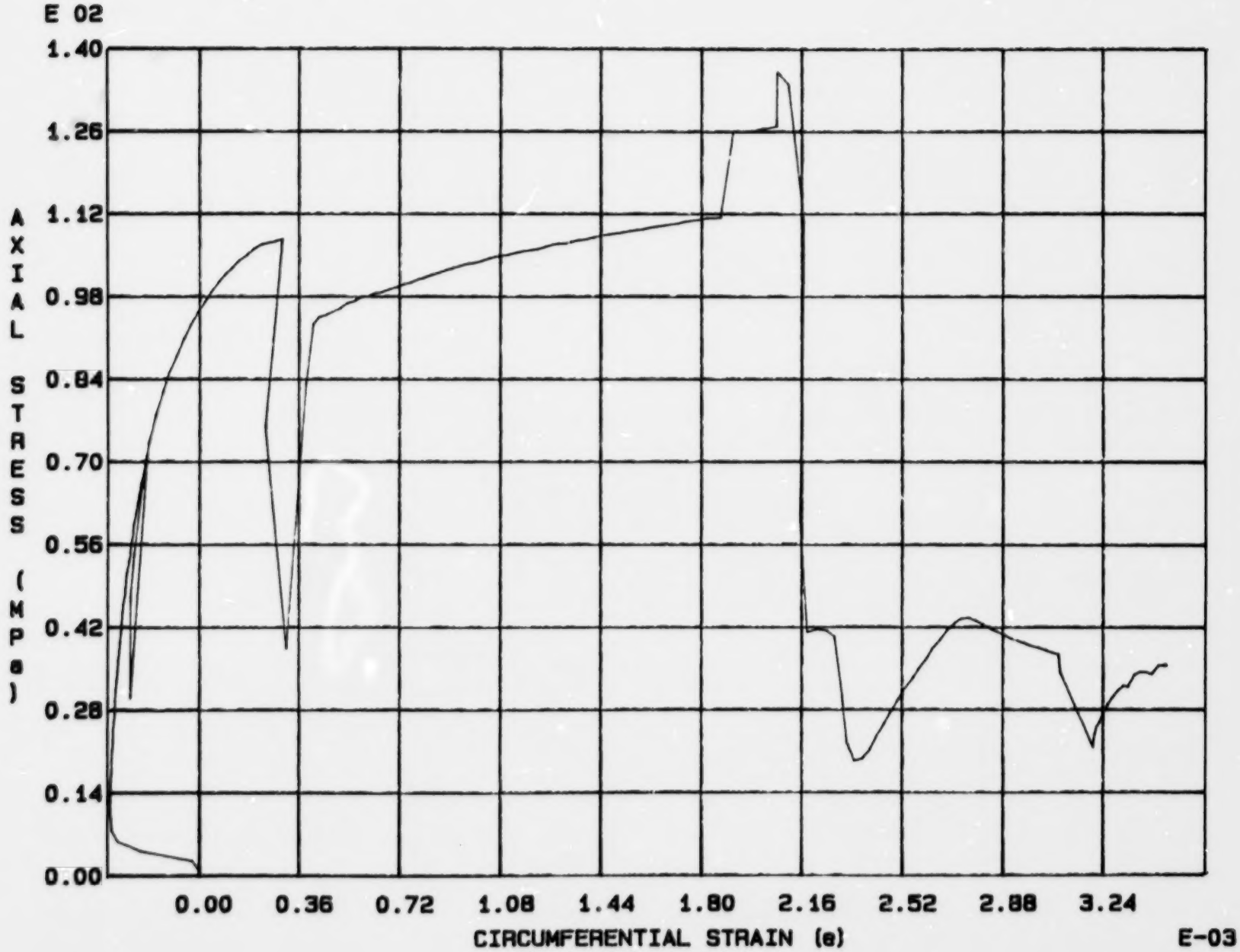

Fig. 6 - 21 Specimen M64T

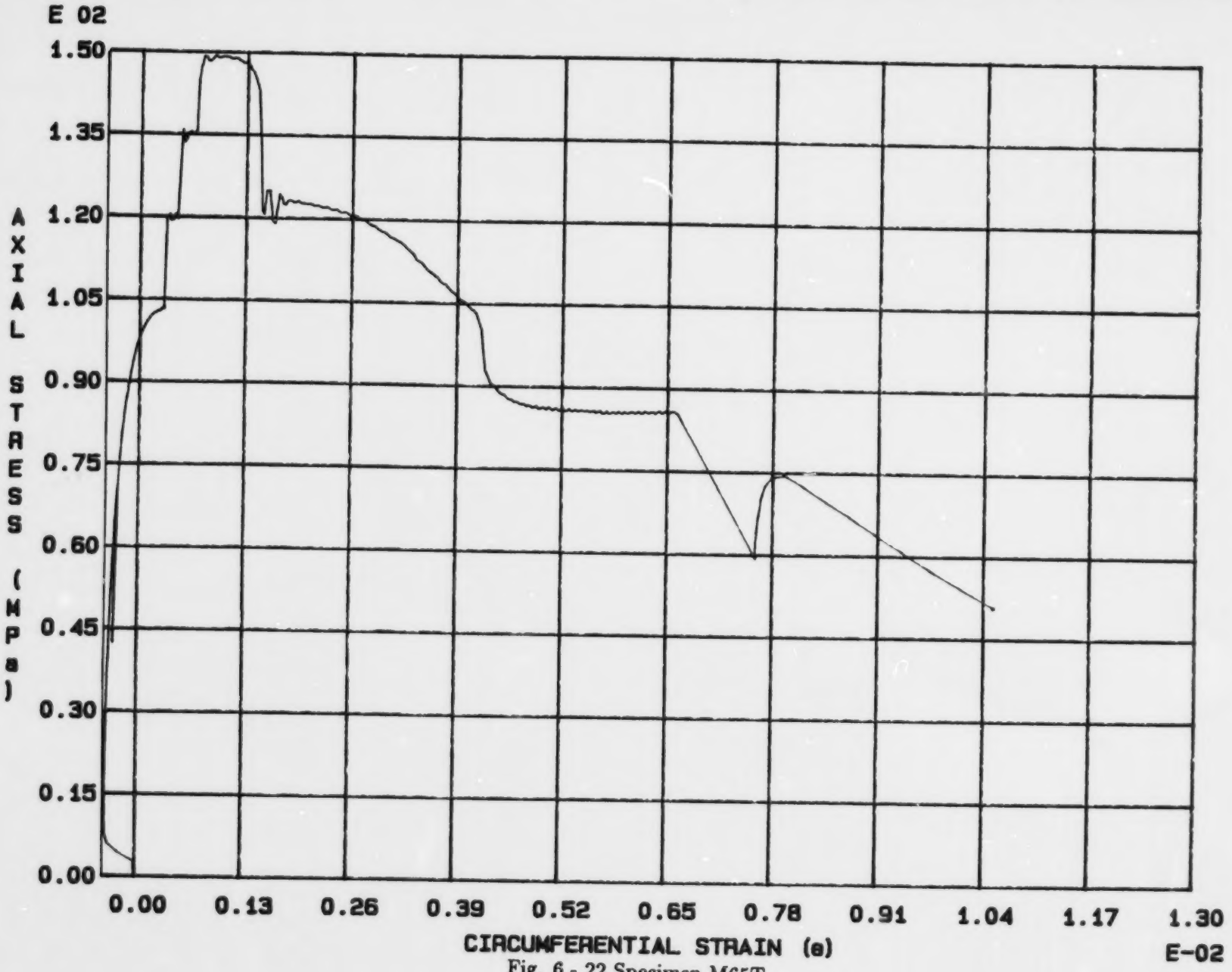

Fig. 6 - 22 Specimen M65T

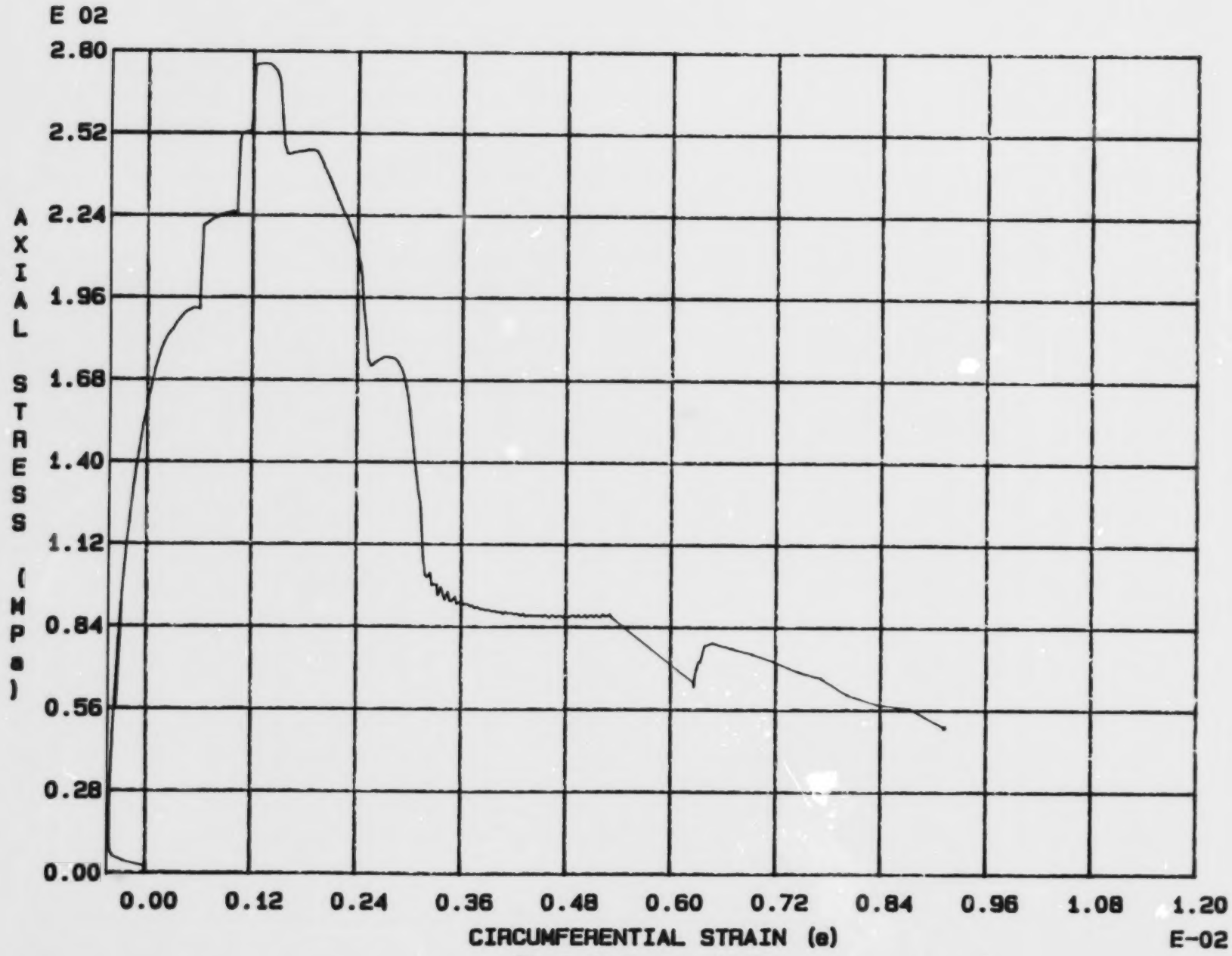

Fig. 6 - 23 Specimen M66T

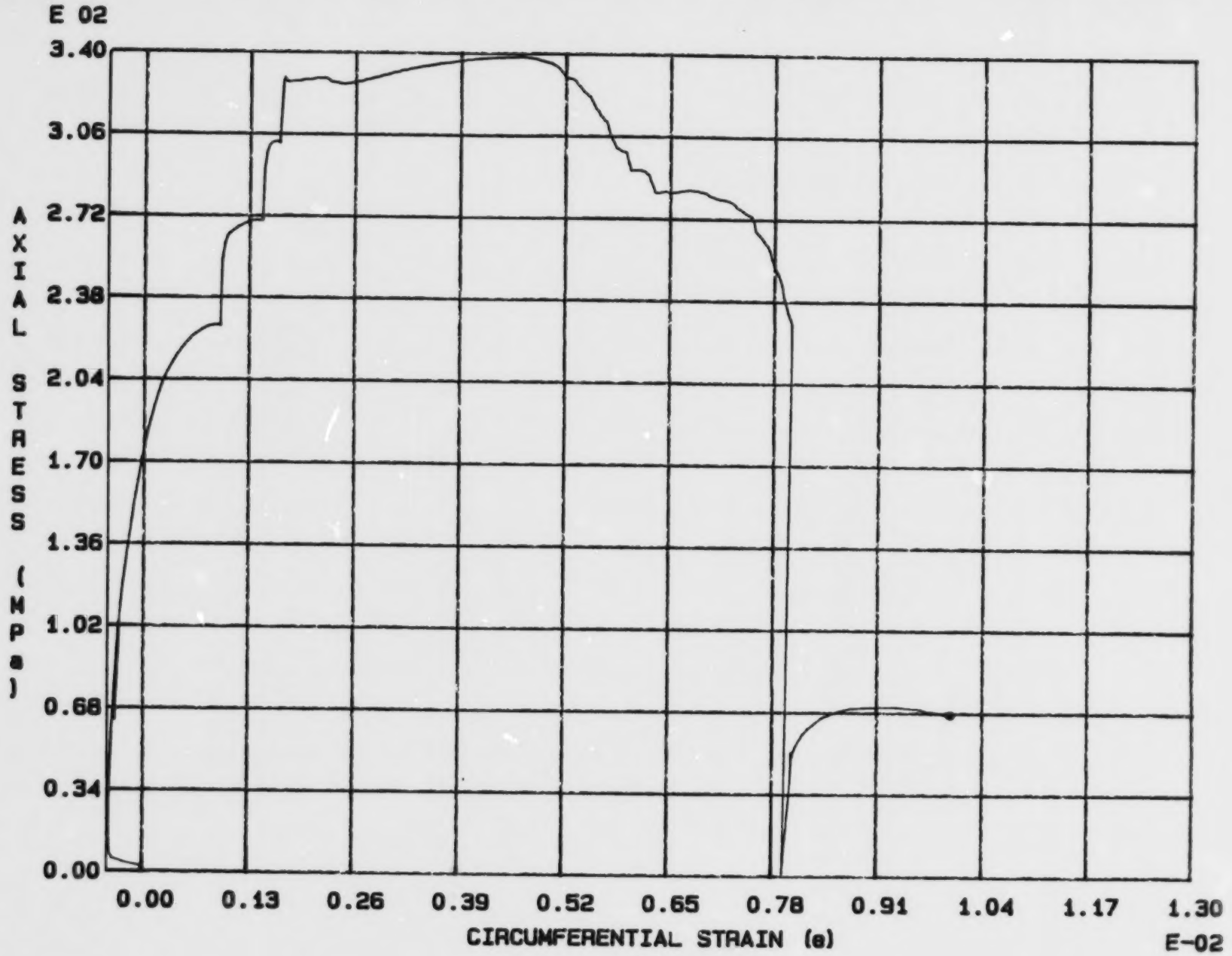

Fig. 6 - 24 Specimen M67T

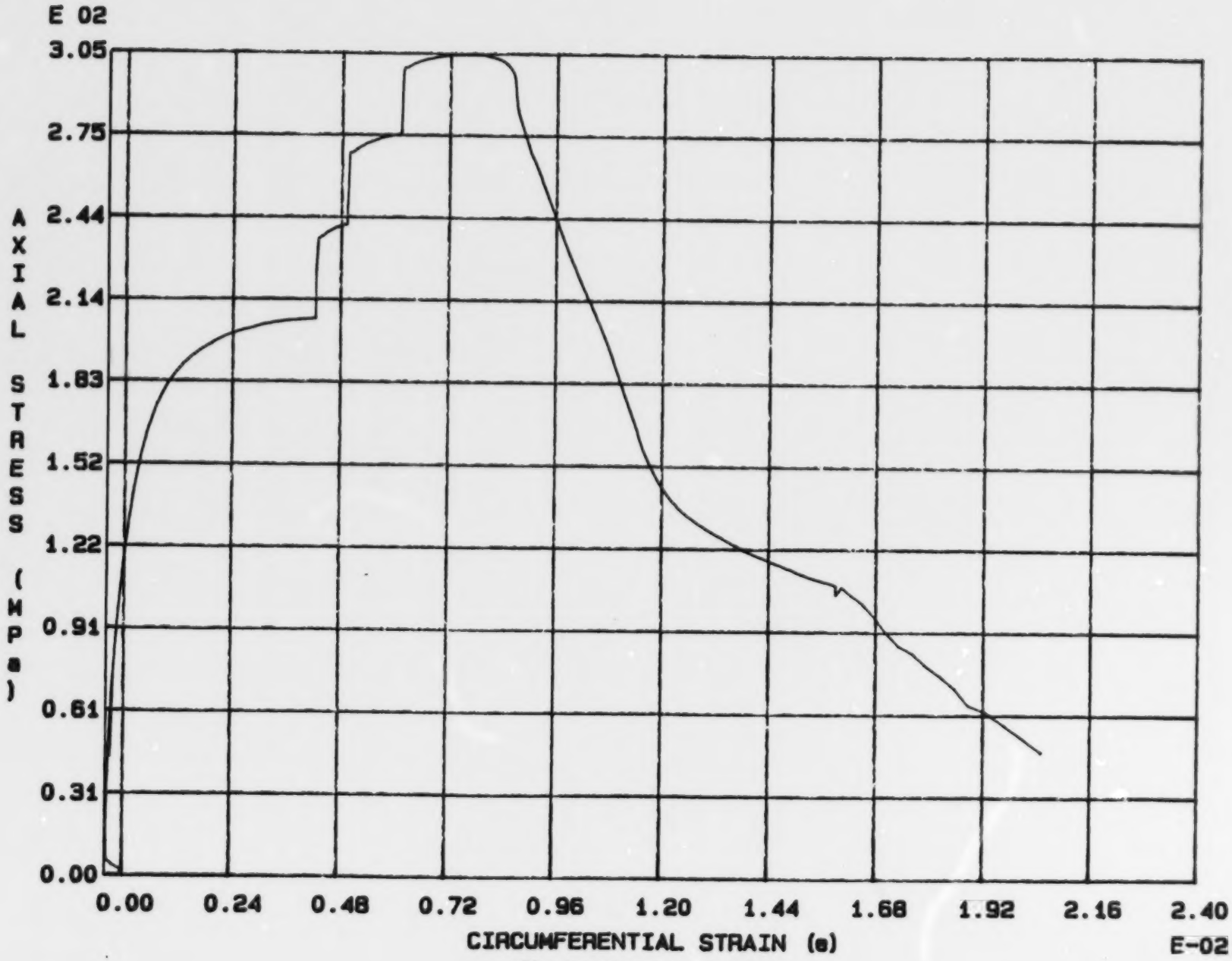

Fig. 6 - 25 Specimen M68T

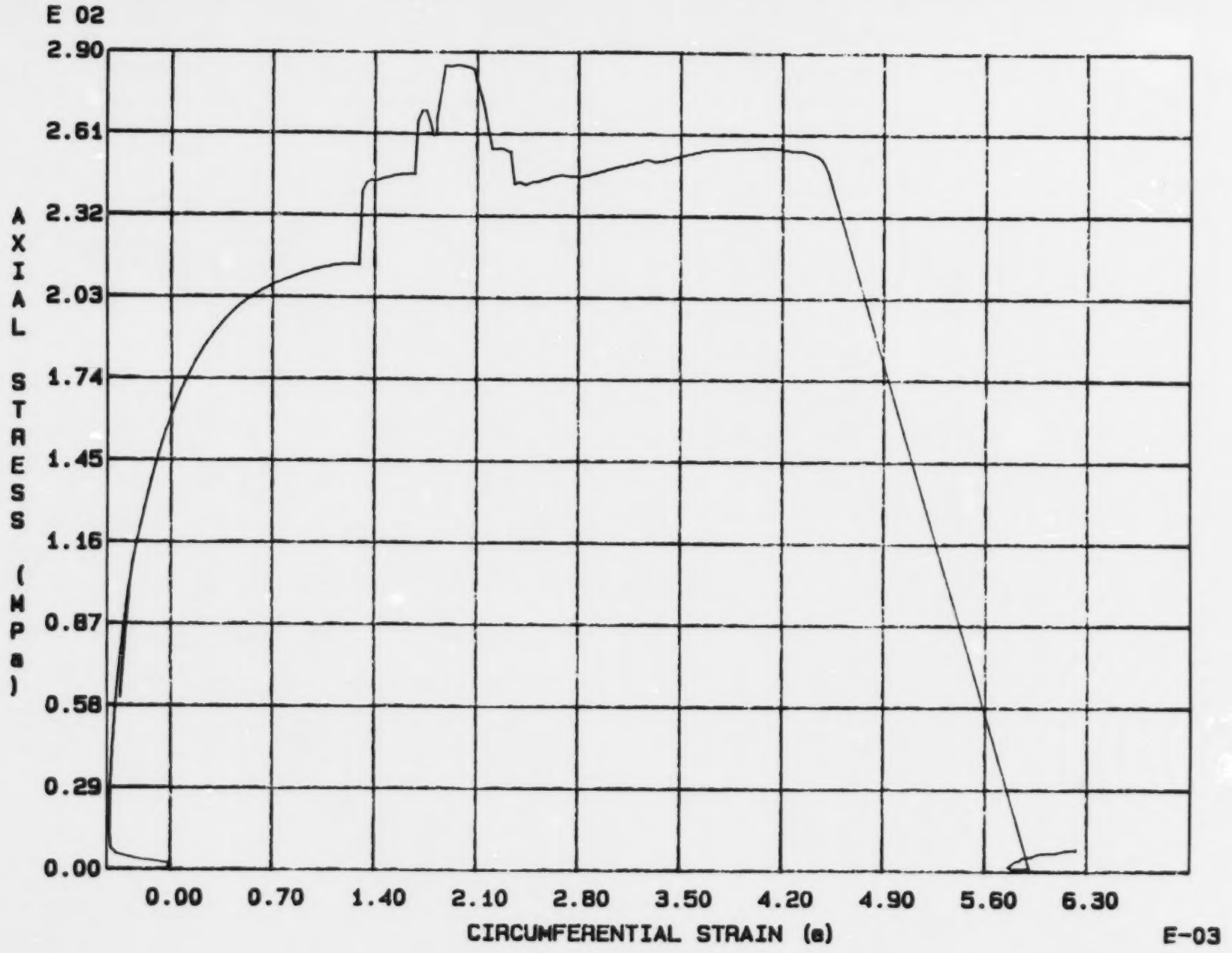

Fig. 6 - 26 Specimen M69T

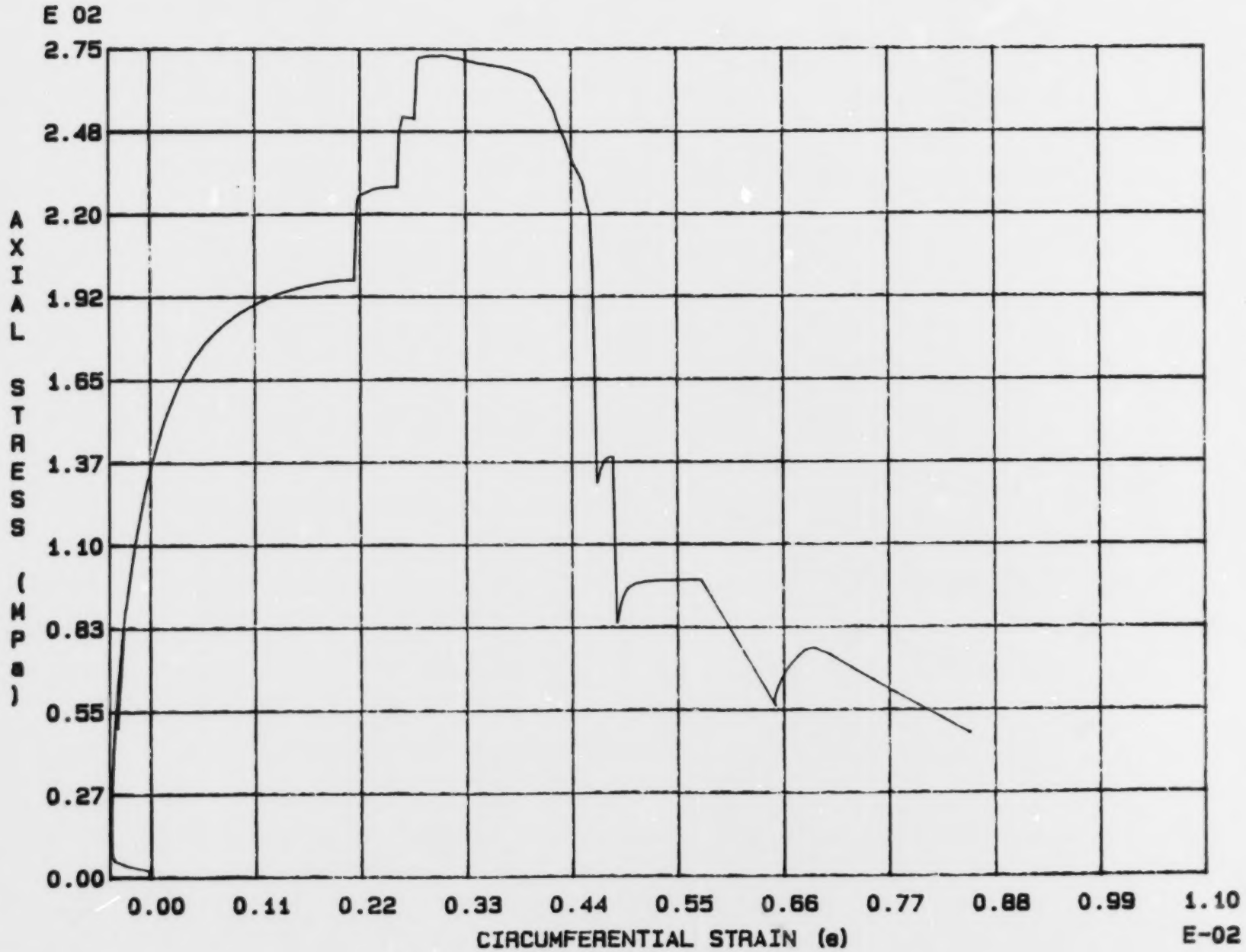

Fig. 6 - 27 Specimen M70T

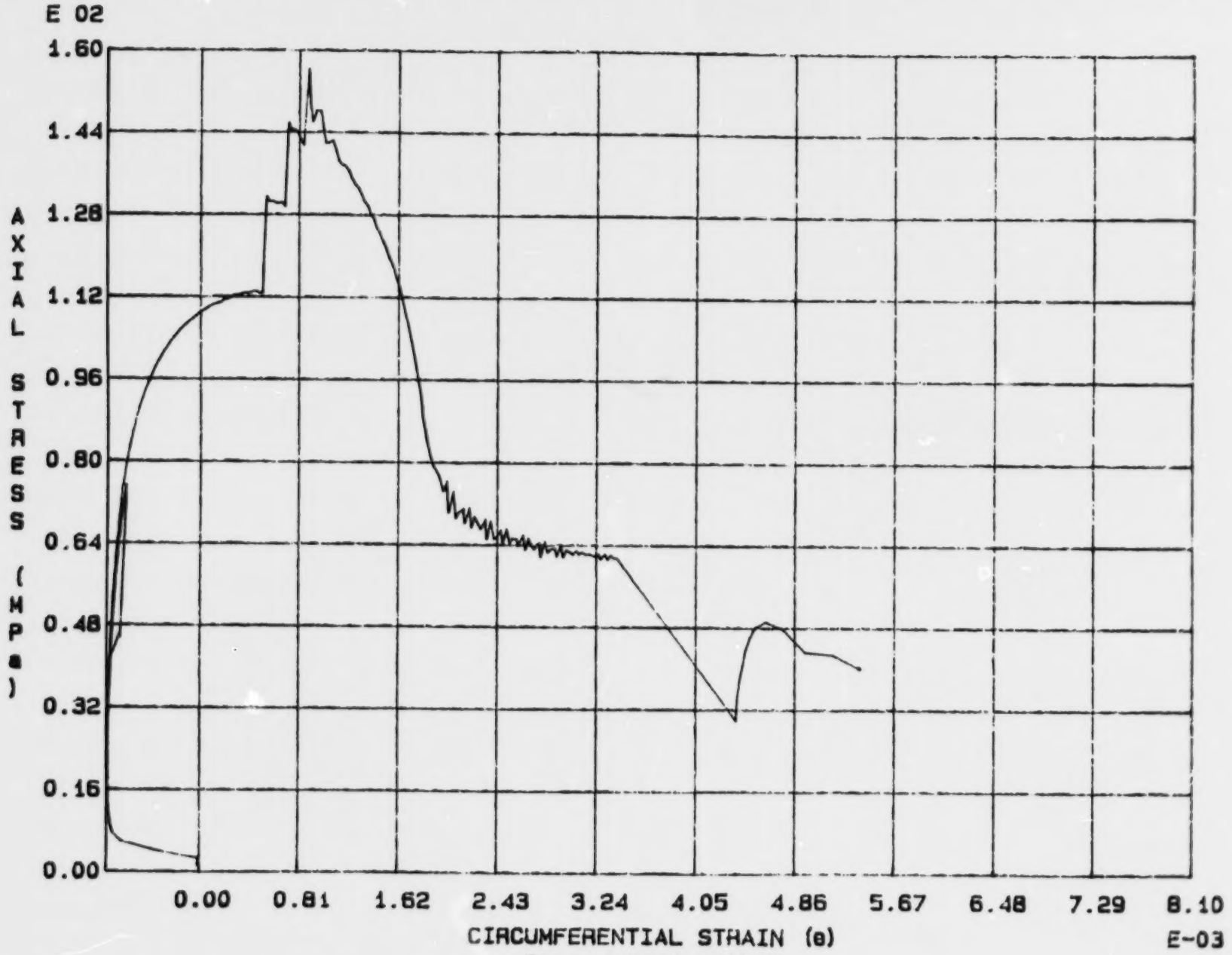

Fig. 6 - 28 Specimen M71T

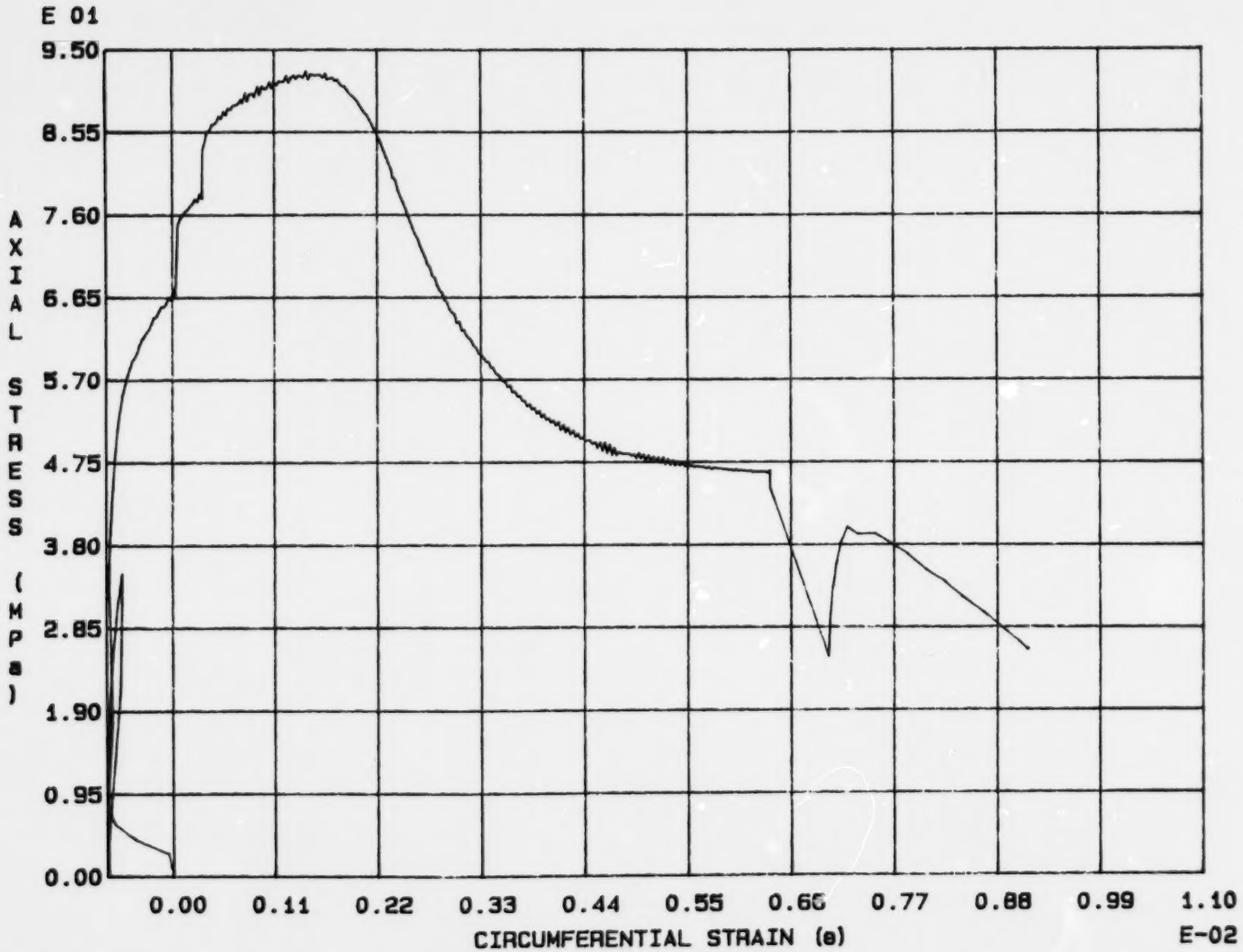

Fig. 6 - 29 Specimen M72T

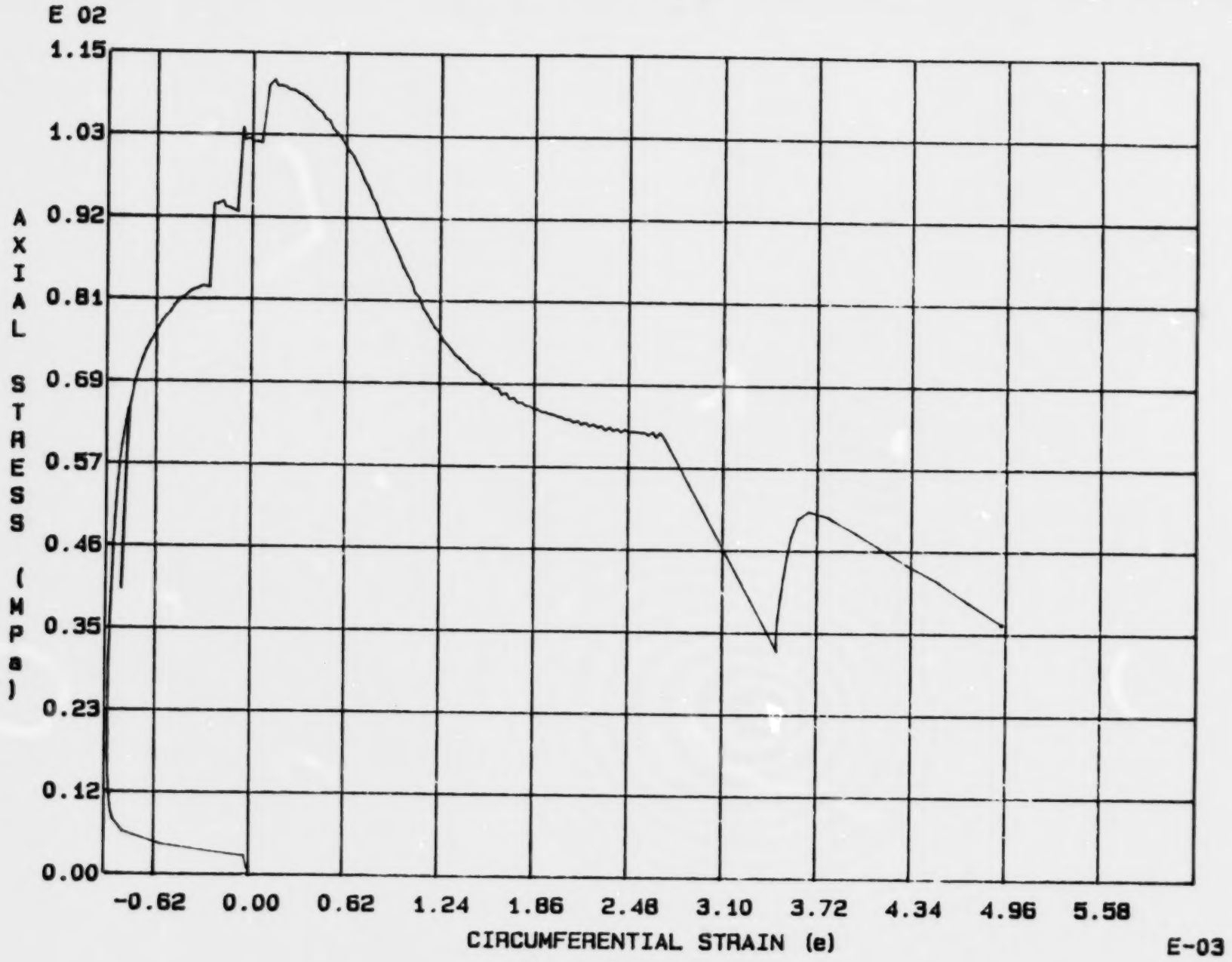

Fig. 6 - 30 Specimen M73T

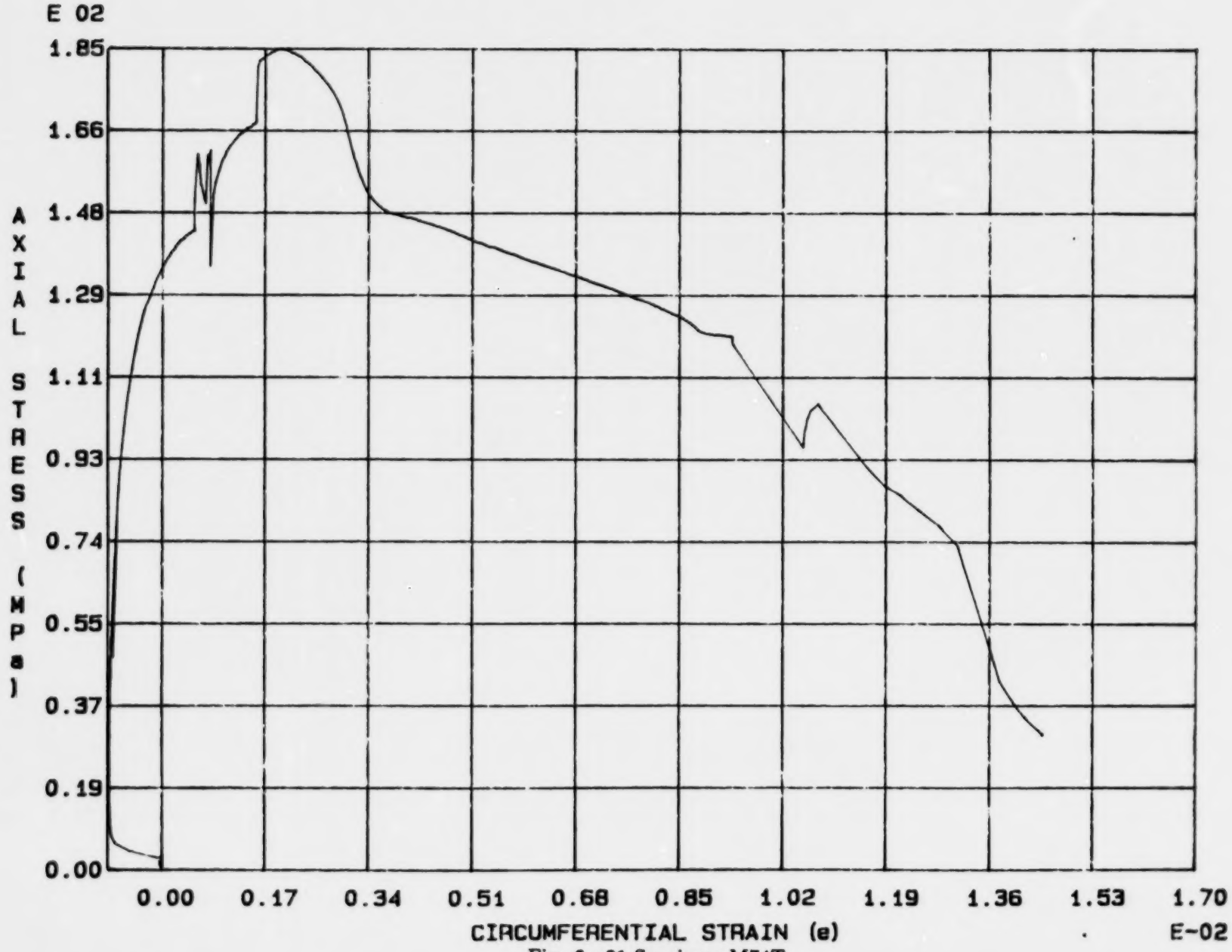

Fig. 6 - 31 Specimen M74T

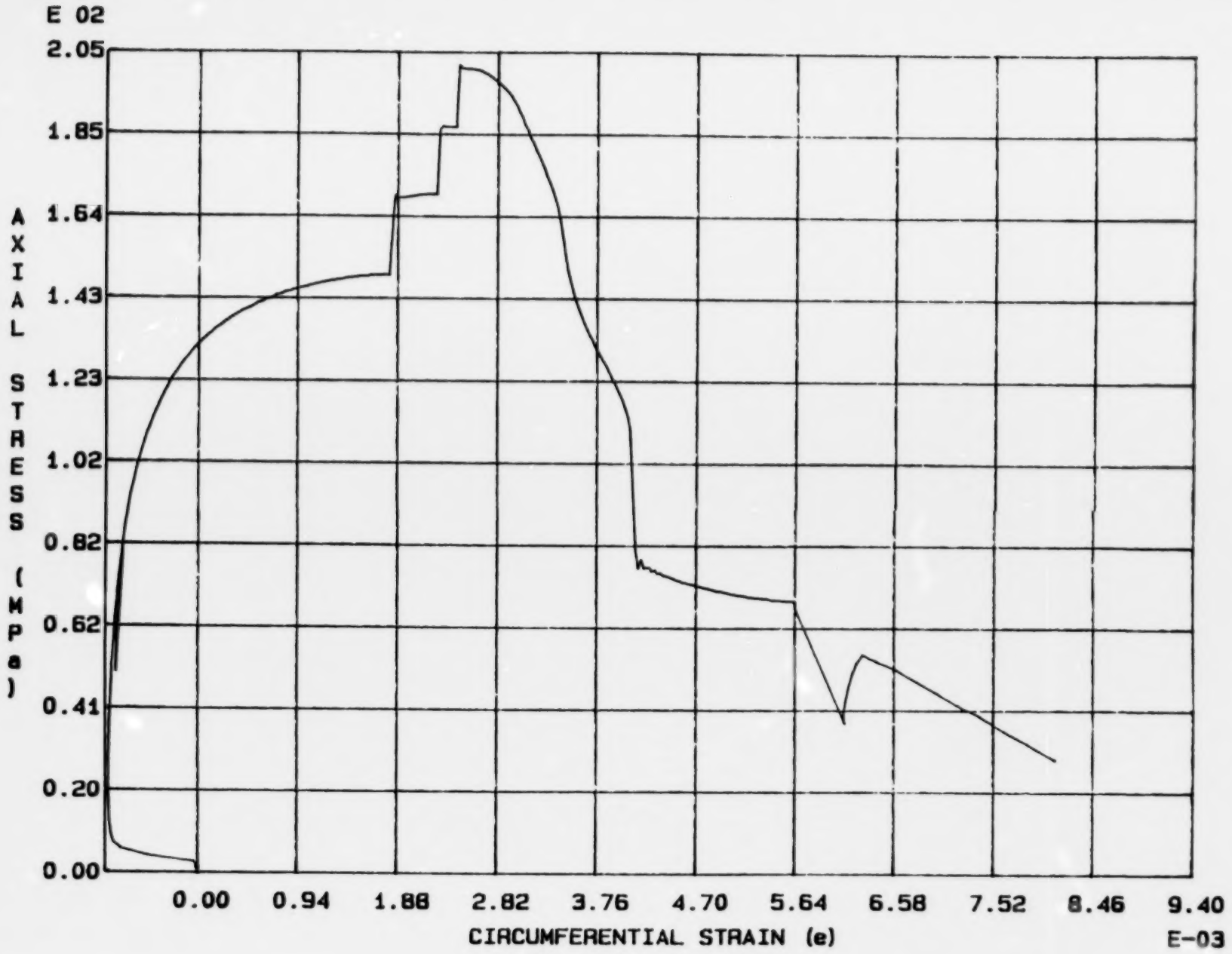

Fig. 6 - 32 Specimen M75T

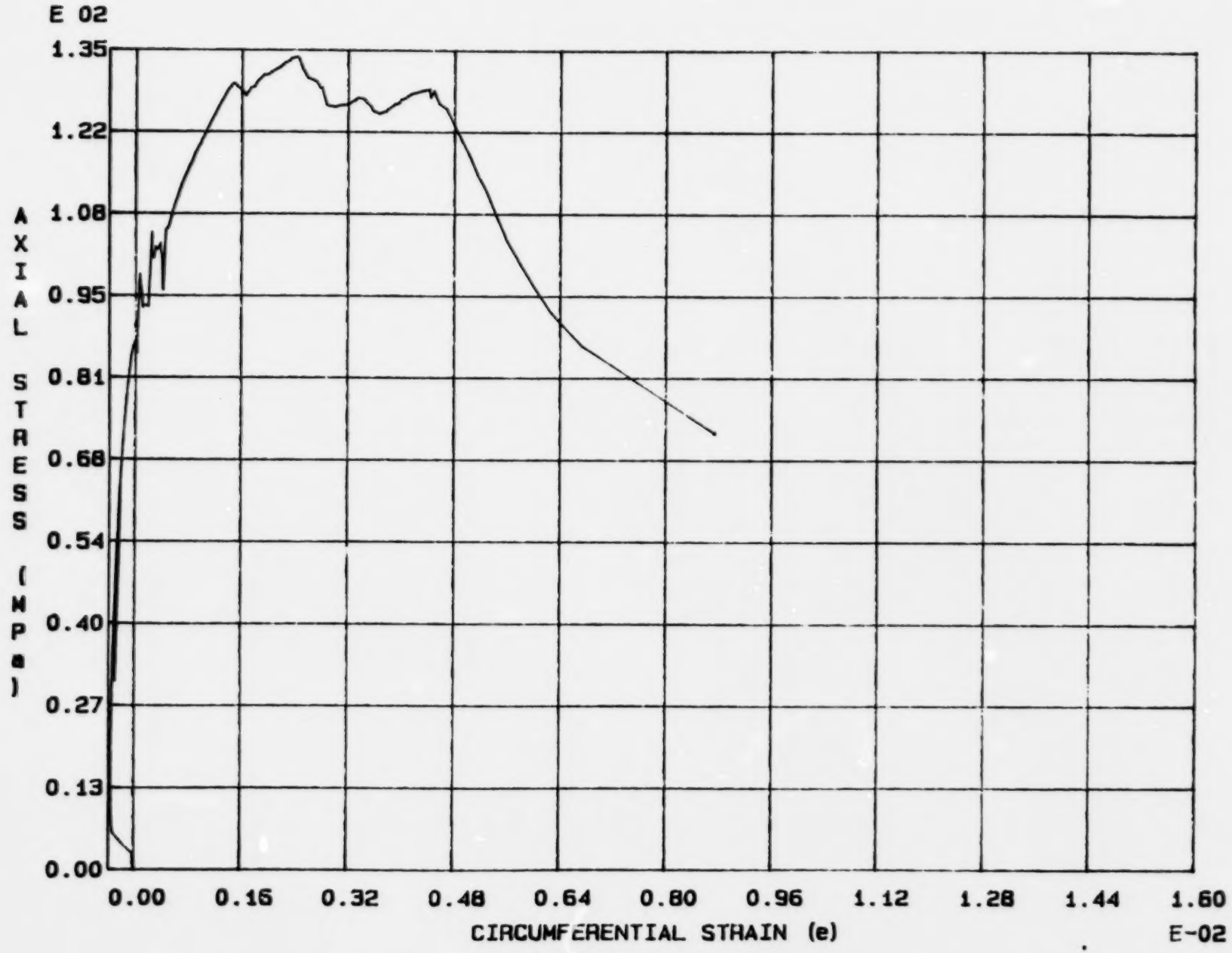

Fig. 6 - 33 Specimen M76T

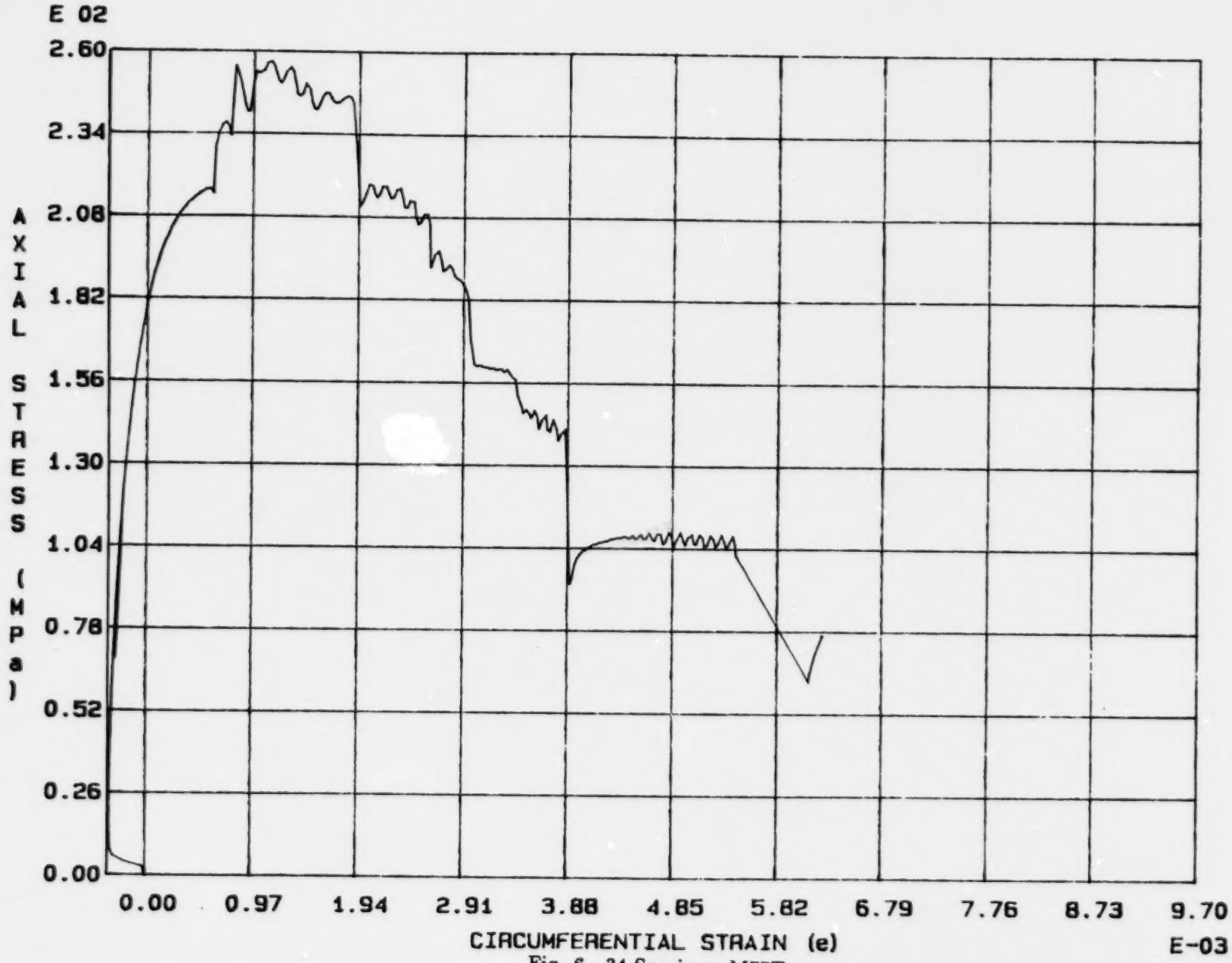

Fig. 6 - 34 Specimen M77T

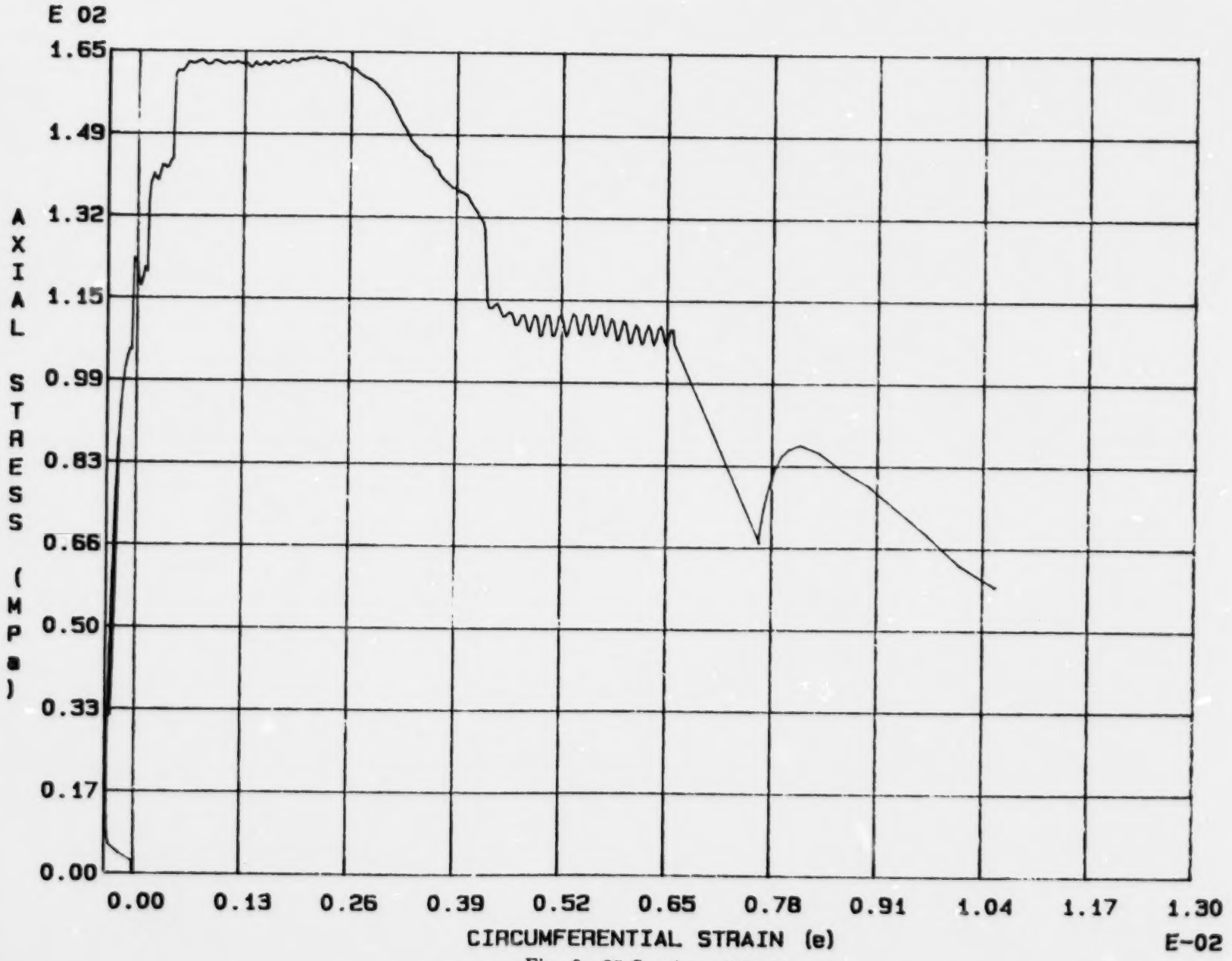

Fig. 6 - 35 Specimen M78T

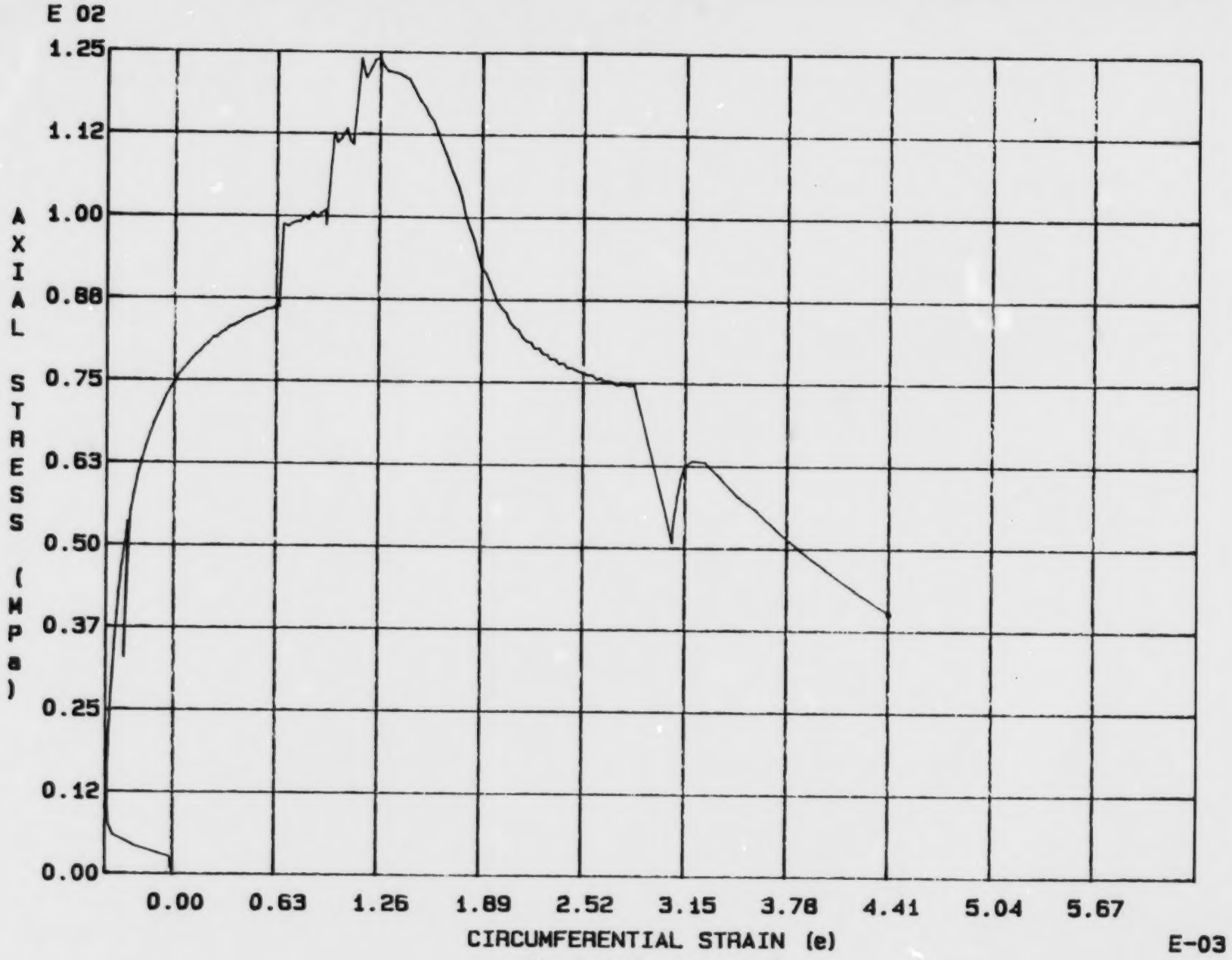

Fig. 6 - 36 Specimen M79T

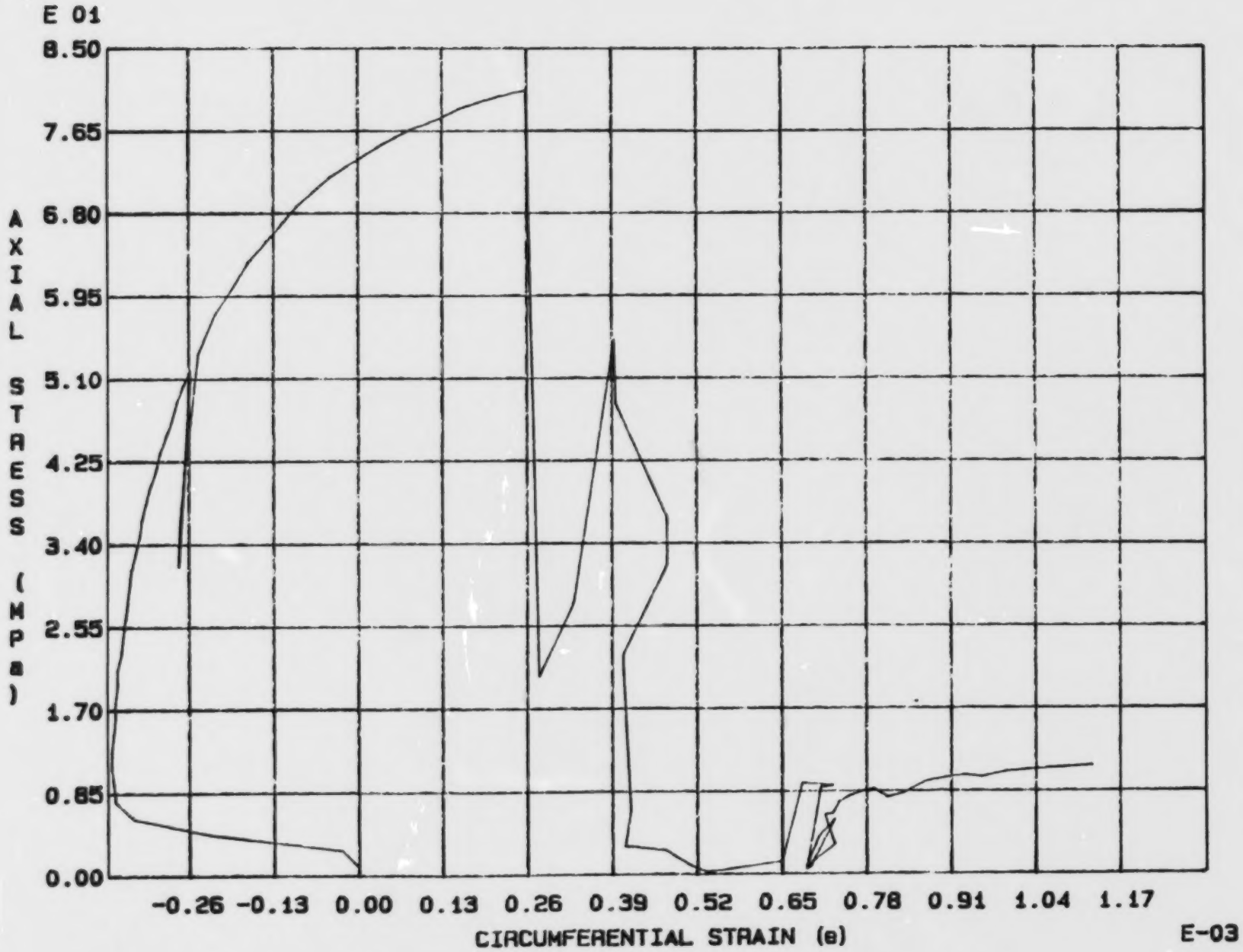

Fig. 6 - 37 Specimen M80T

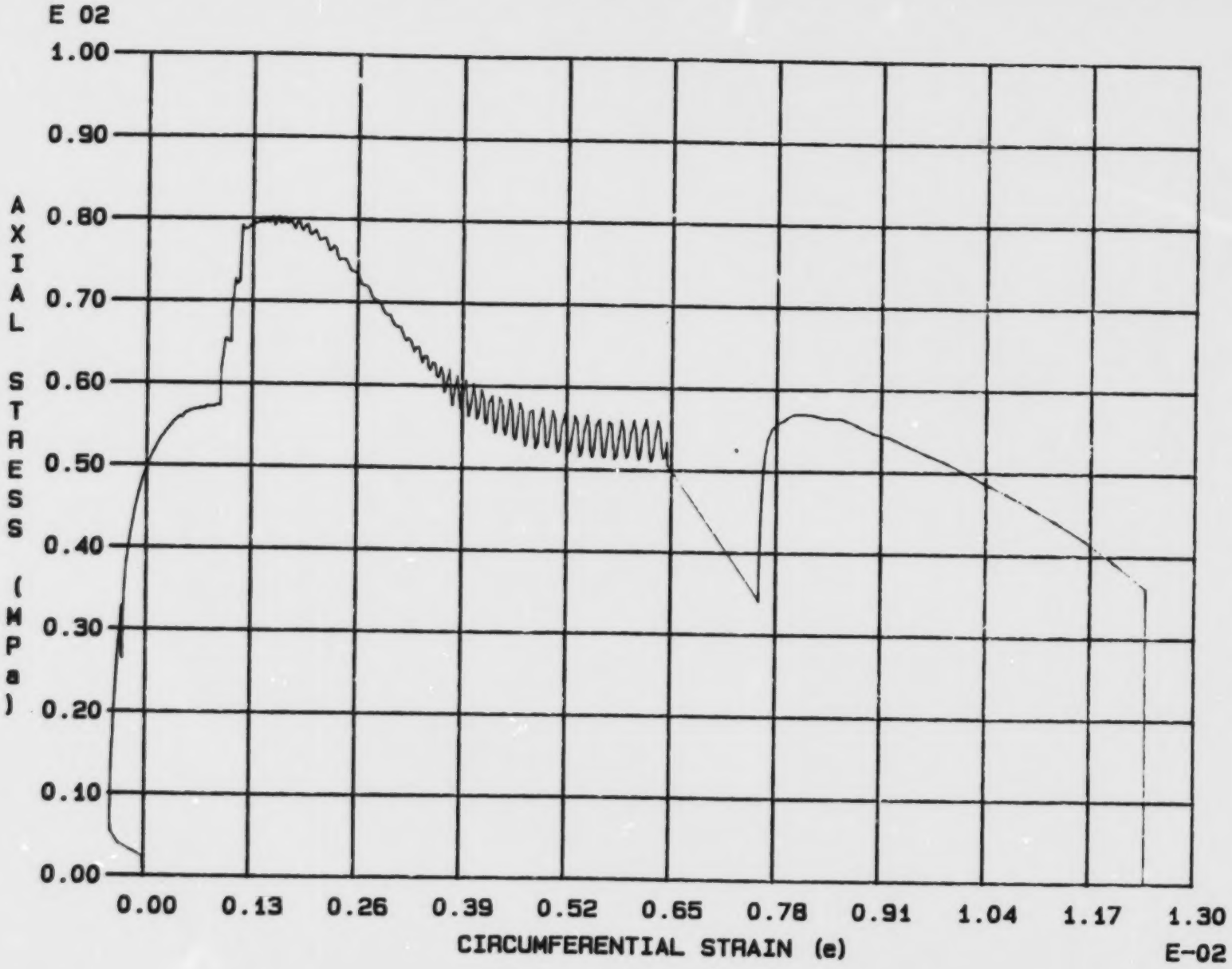

Fig. 6 - 38 Specimen M93T

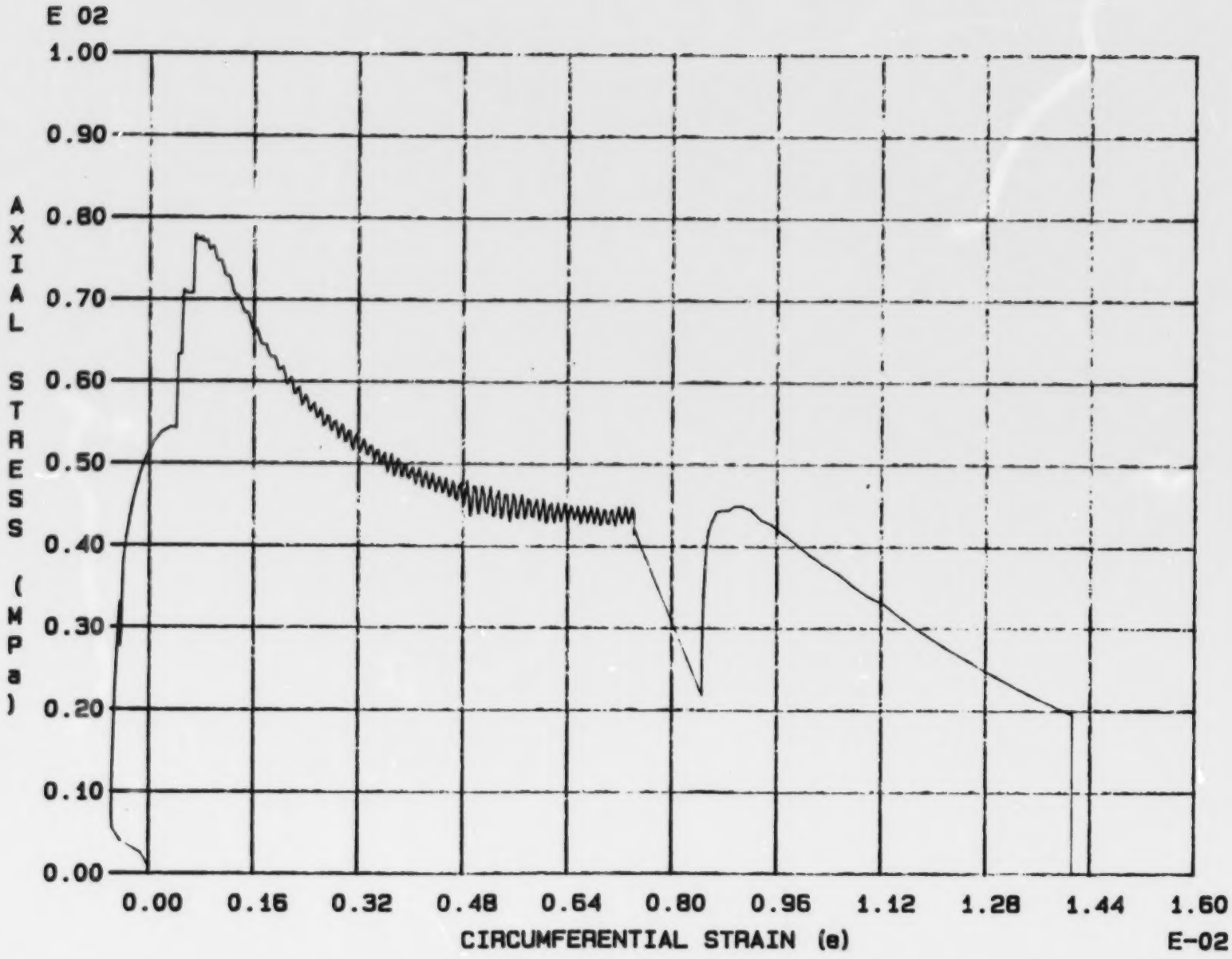

Fig. 6 - 39 Specimen M94T

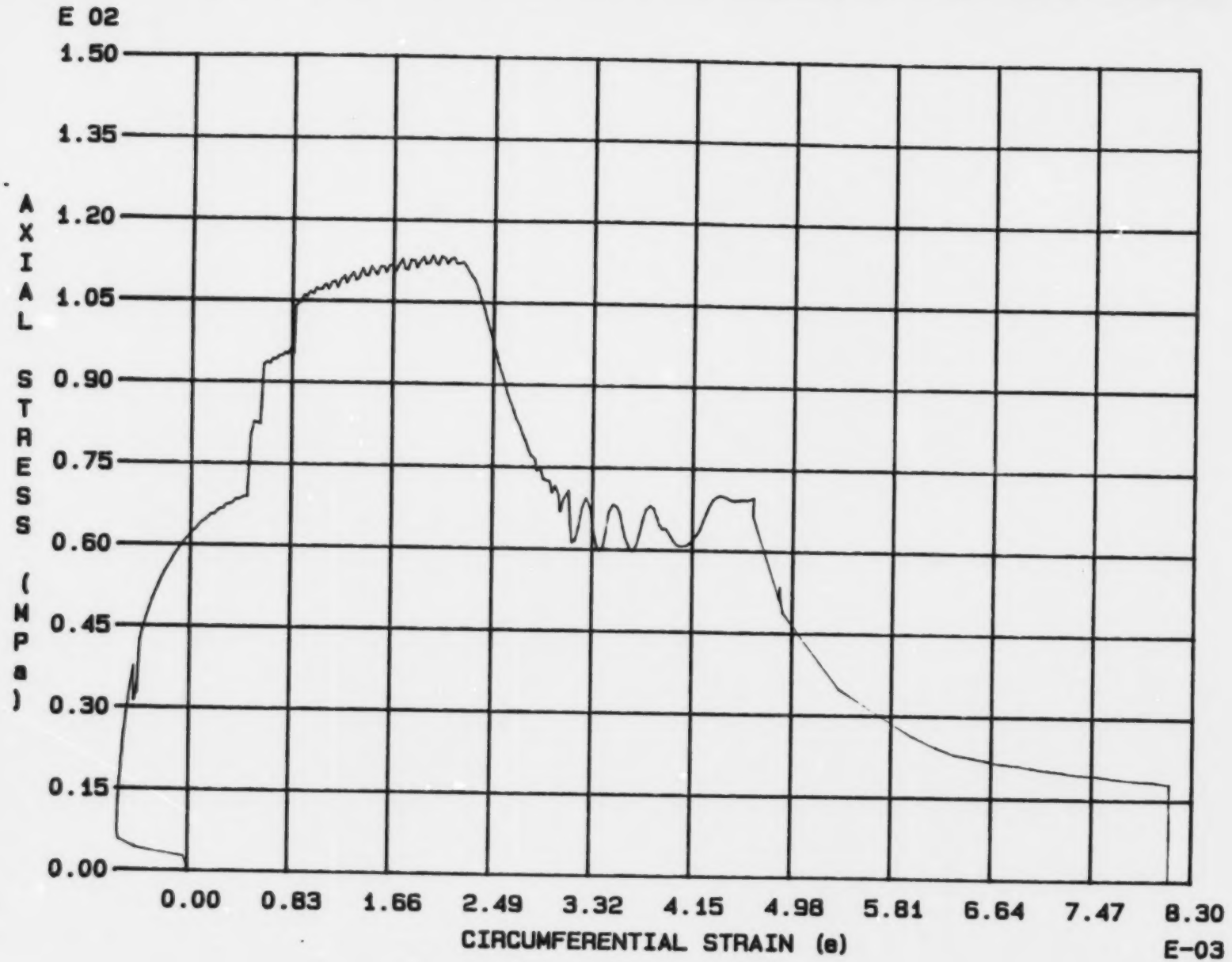

Fig. 6 - 40 Specimen M95T

Appendix 7.

Post-failure strength-confining pressure curves

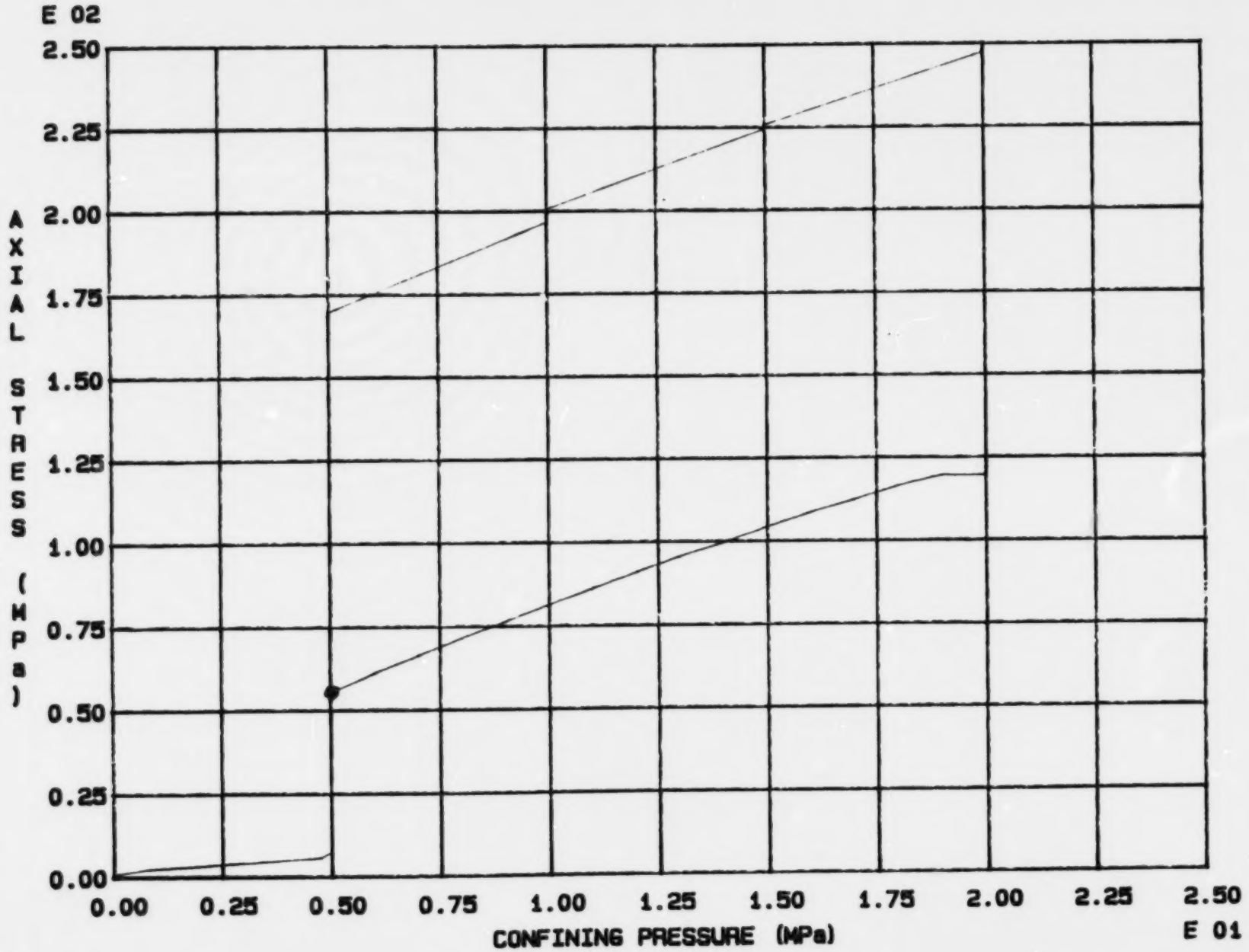

Fig. 7 - 1 Specimen M44T

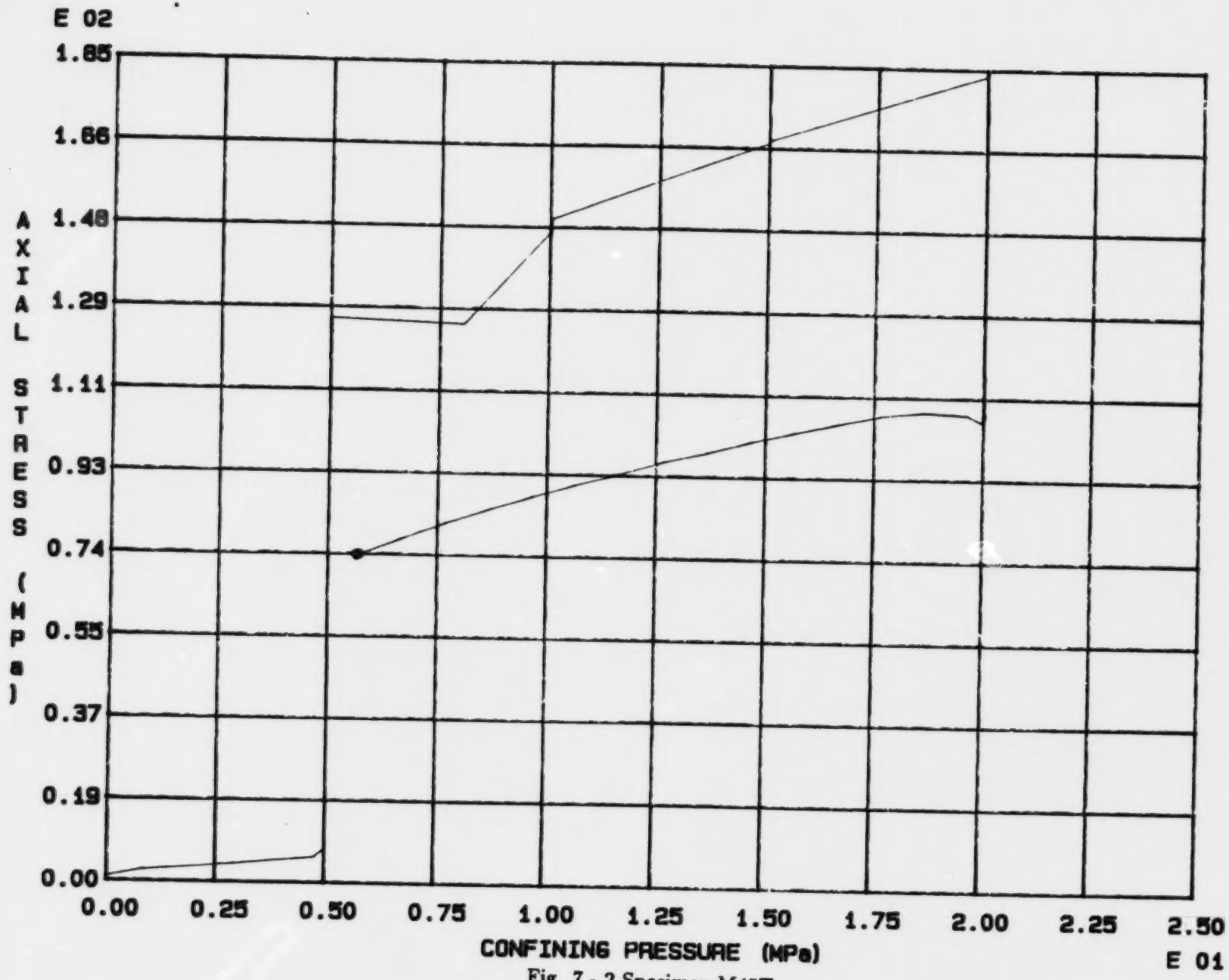

Fig. 7 - 2 Specimen M45T

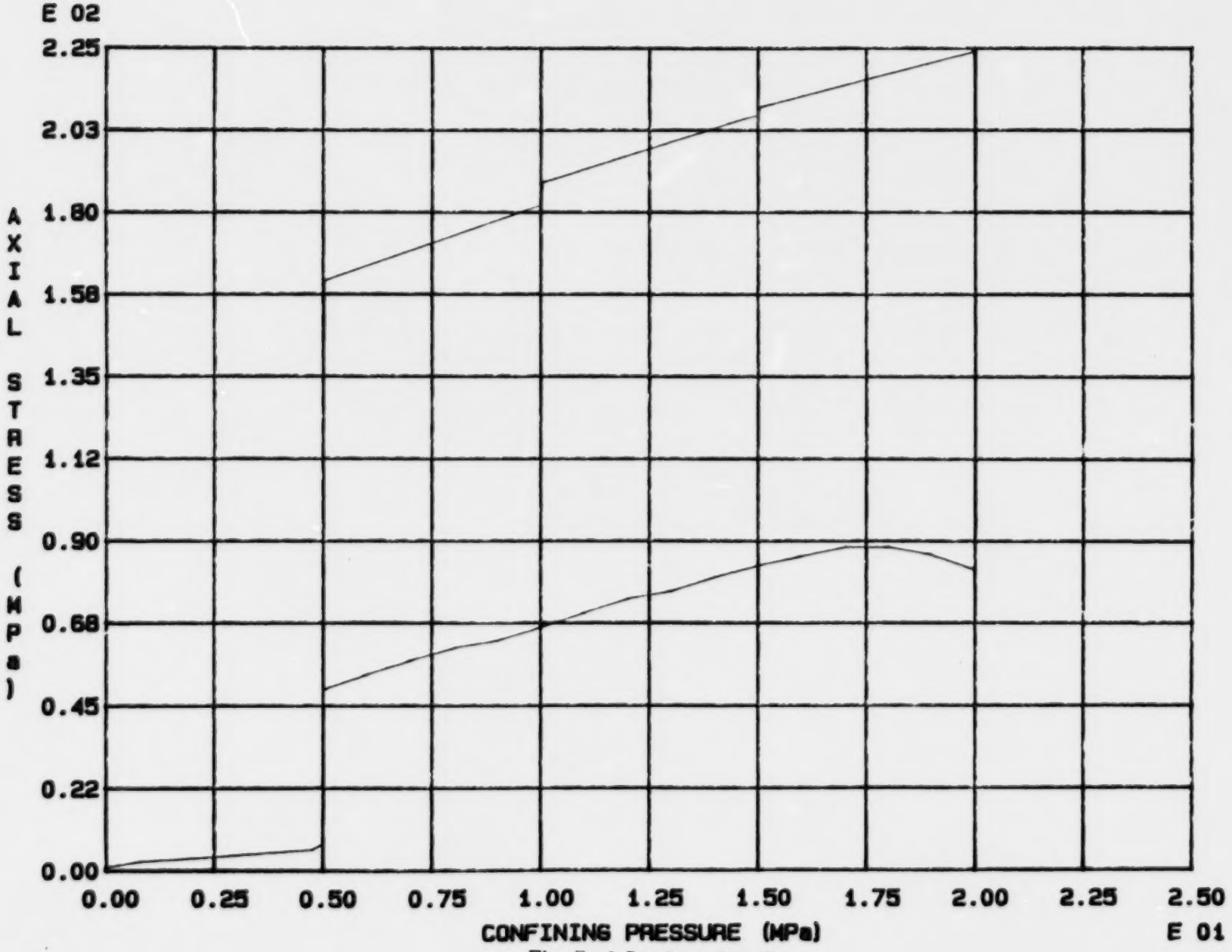

Fig. 7 - 3 Specimen M46T

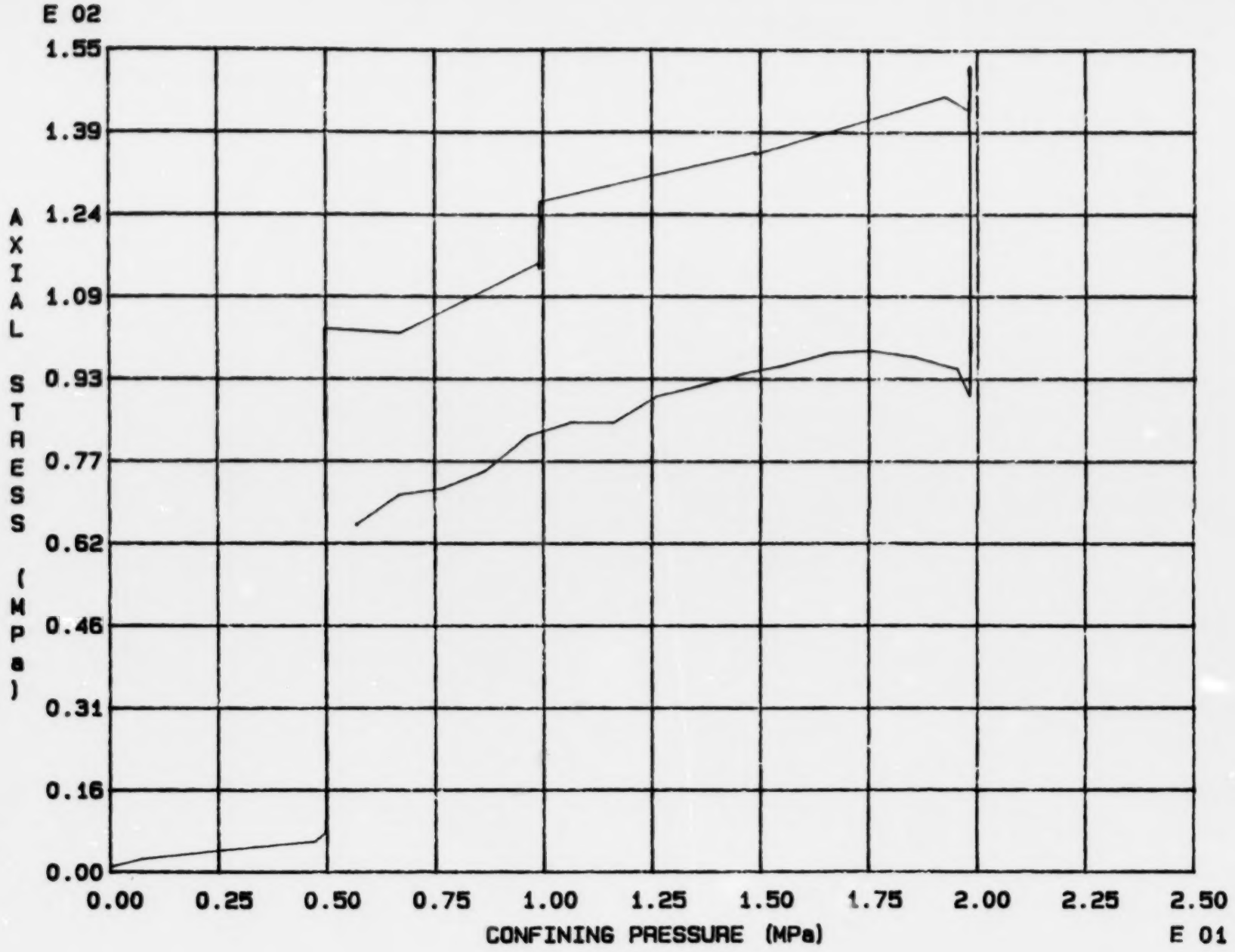

Fig. 7 - 4 Specimen M47T

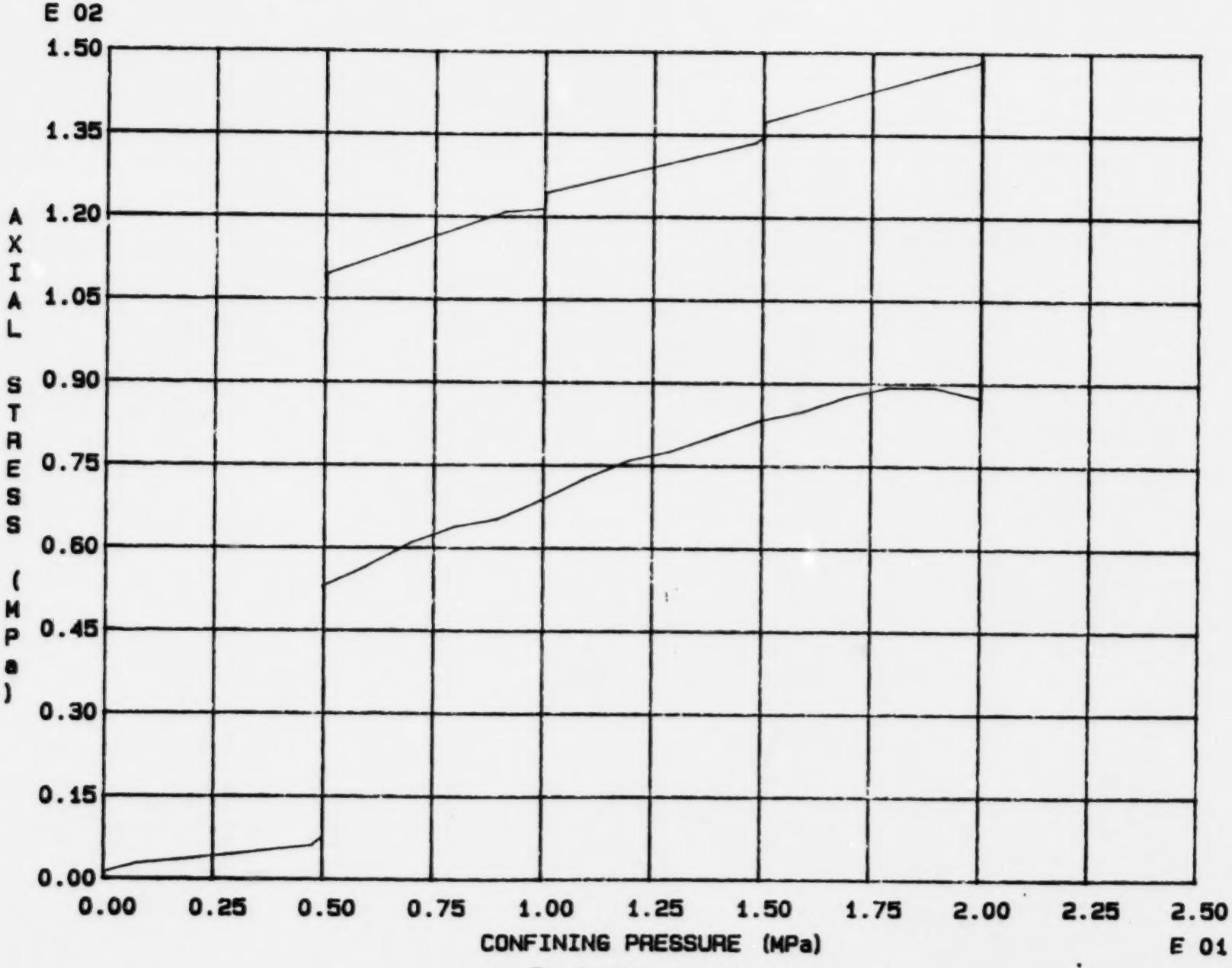

Fig. 7 - 5 Specimen M48T

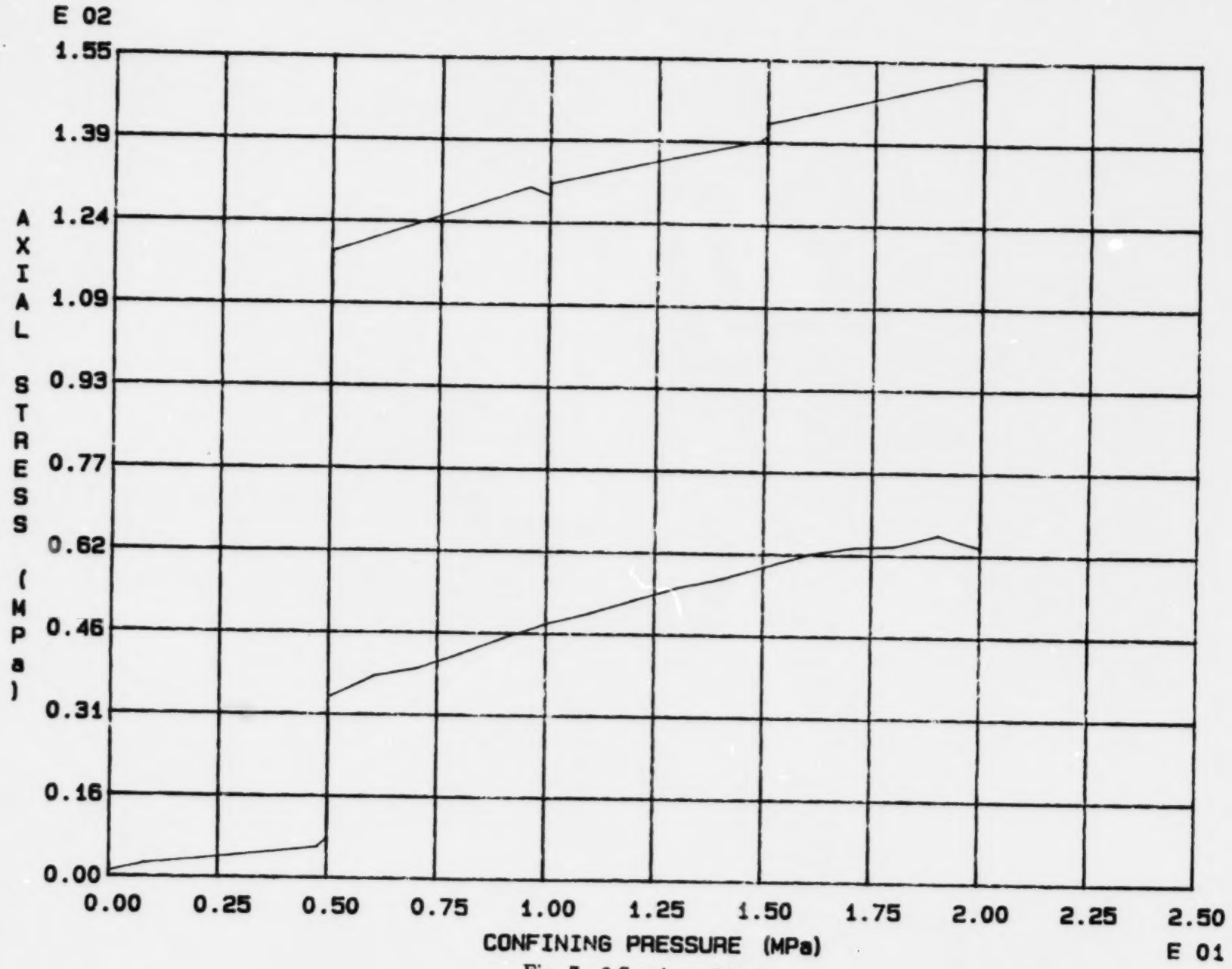

Fig. 7 - 6 Specimen M49T

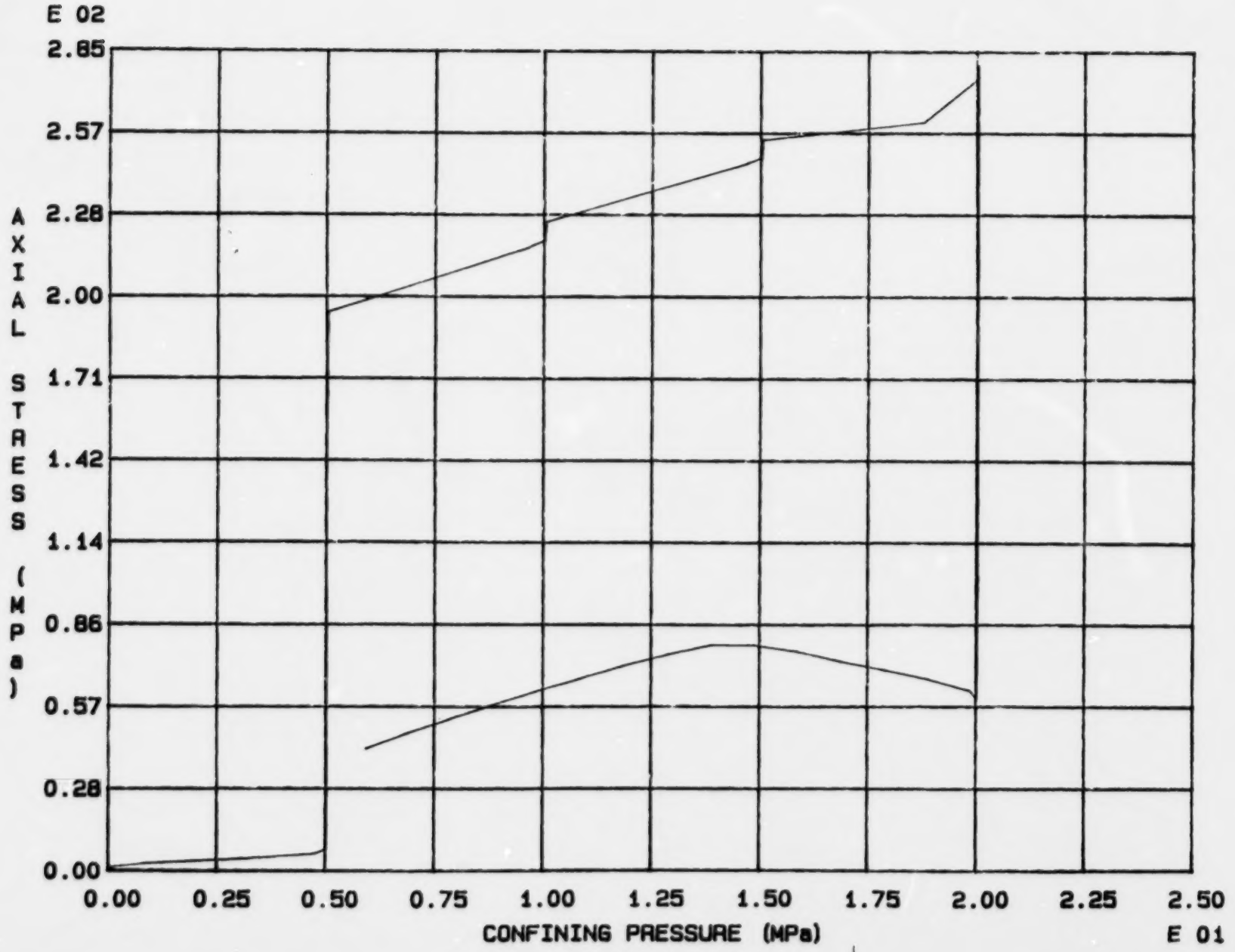

Fig. 7 - 7 Specimen M50T

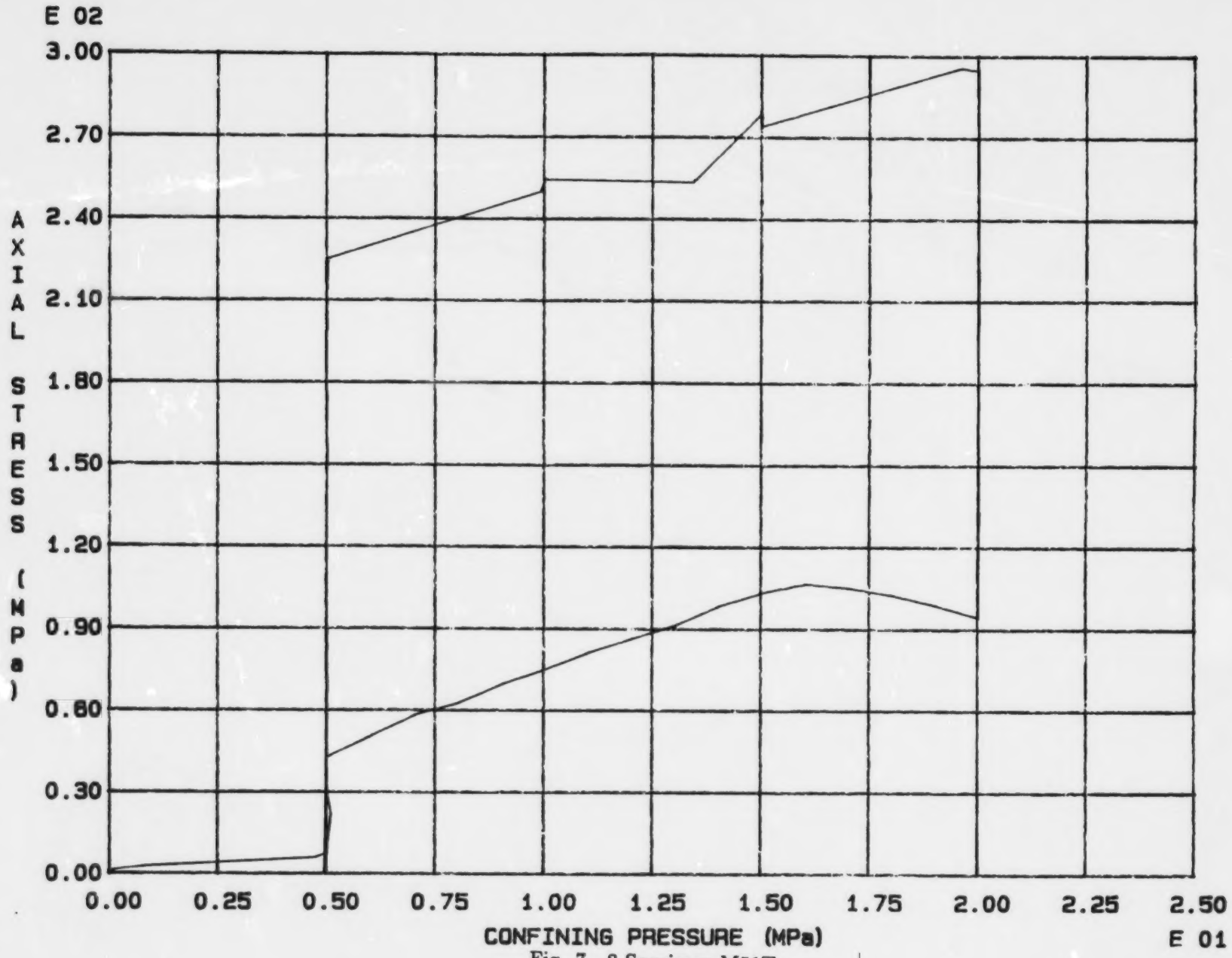

Fig. 7 - 8 Specimen M51T

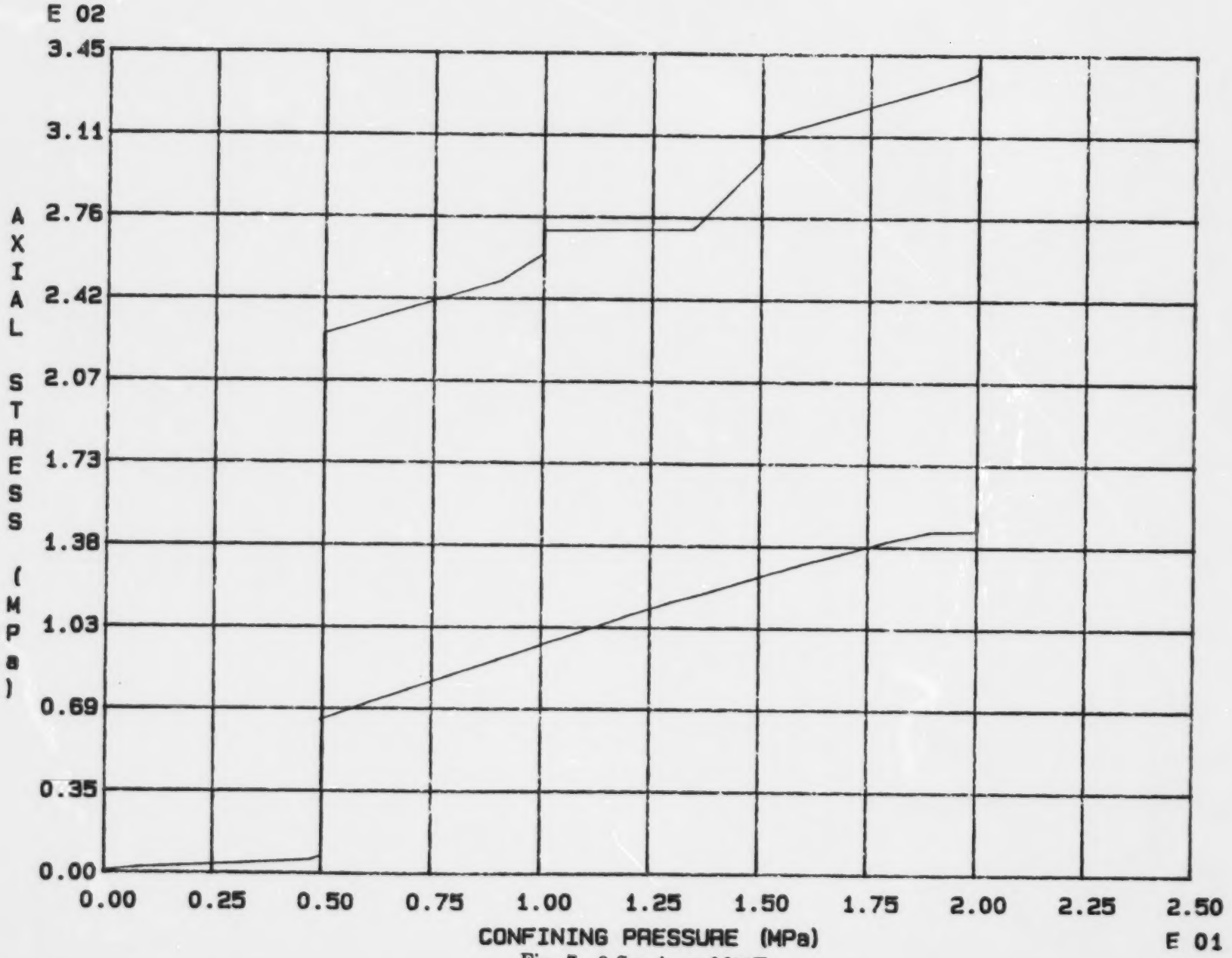

Fig. 7 - 9 Specimen M52T

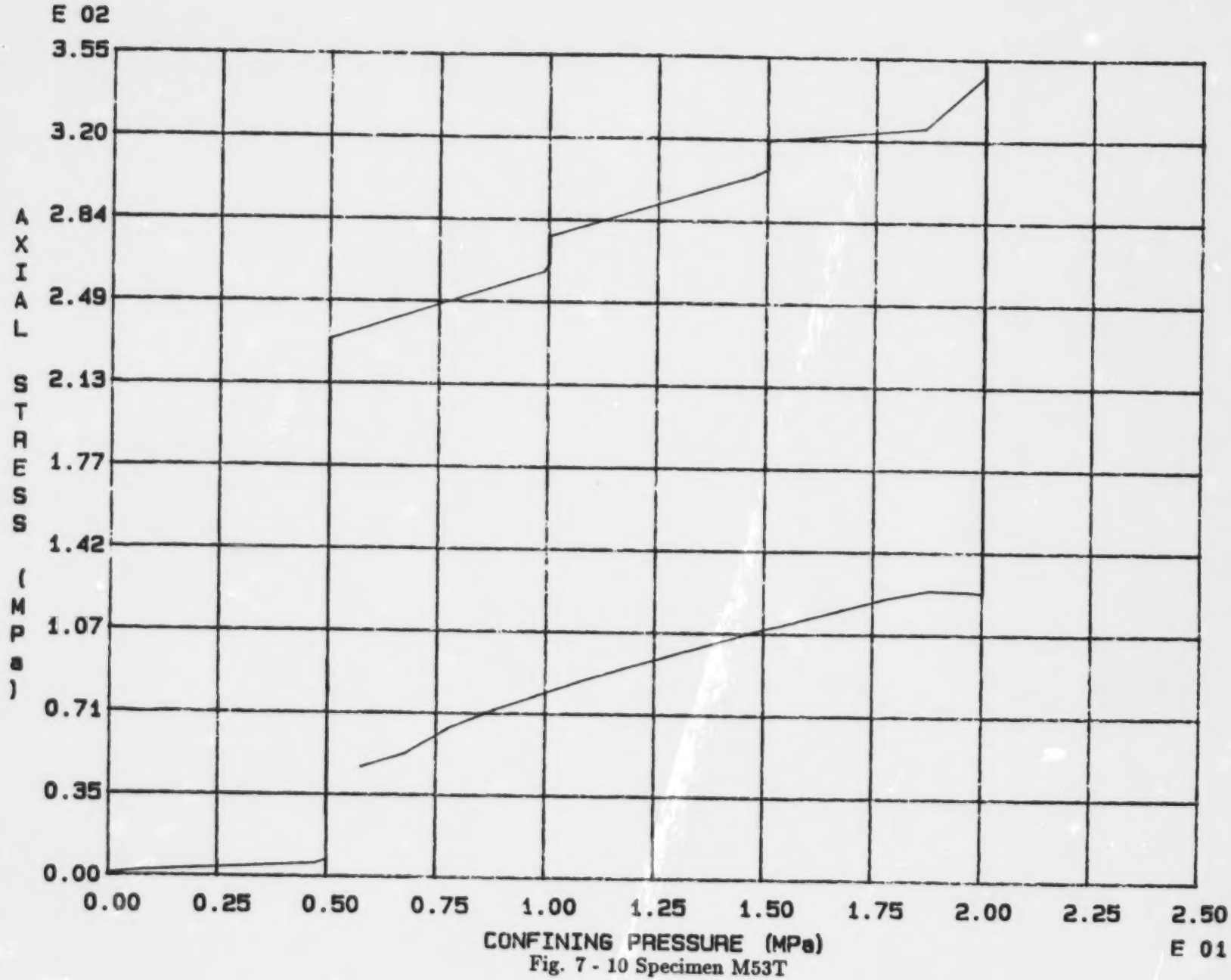

Fig. 7 - 10 Specimen M53T

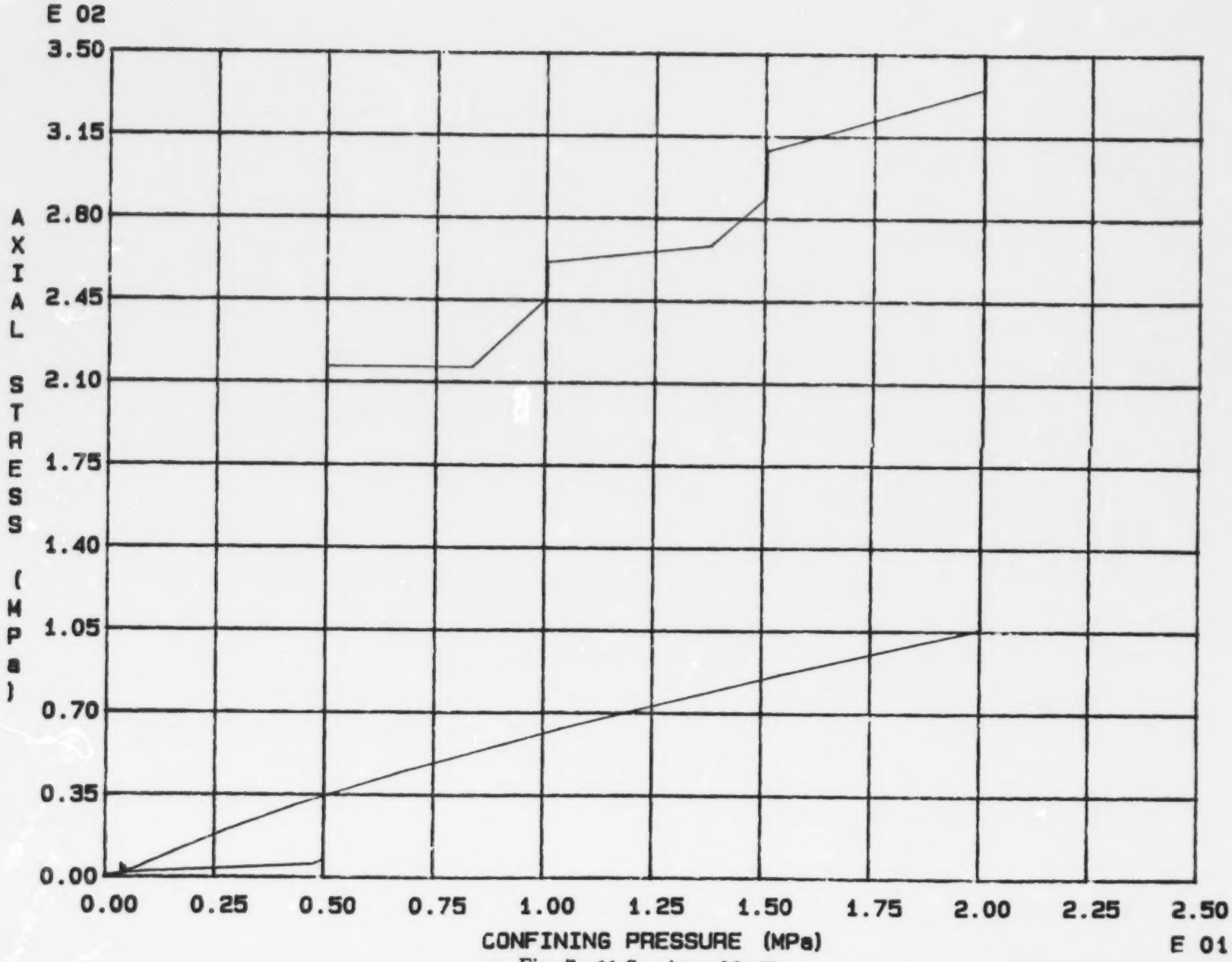

Fig. 7 - 11 Specimen M54T

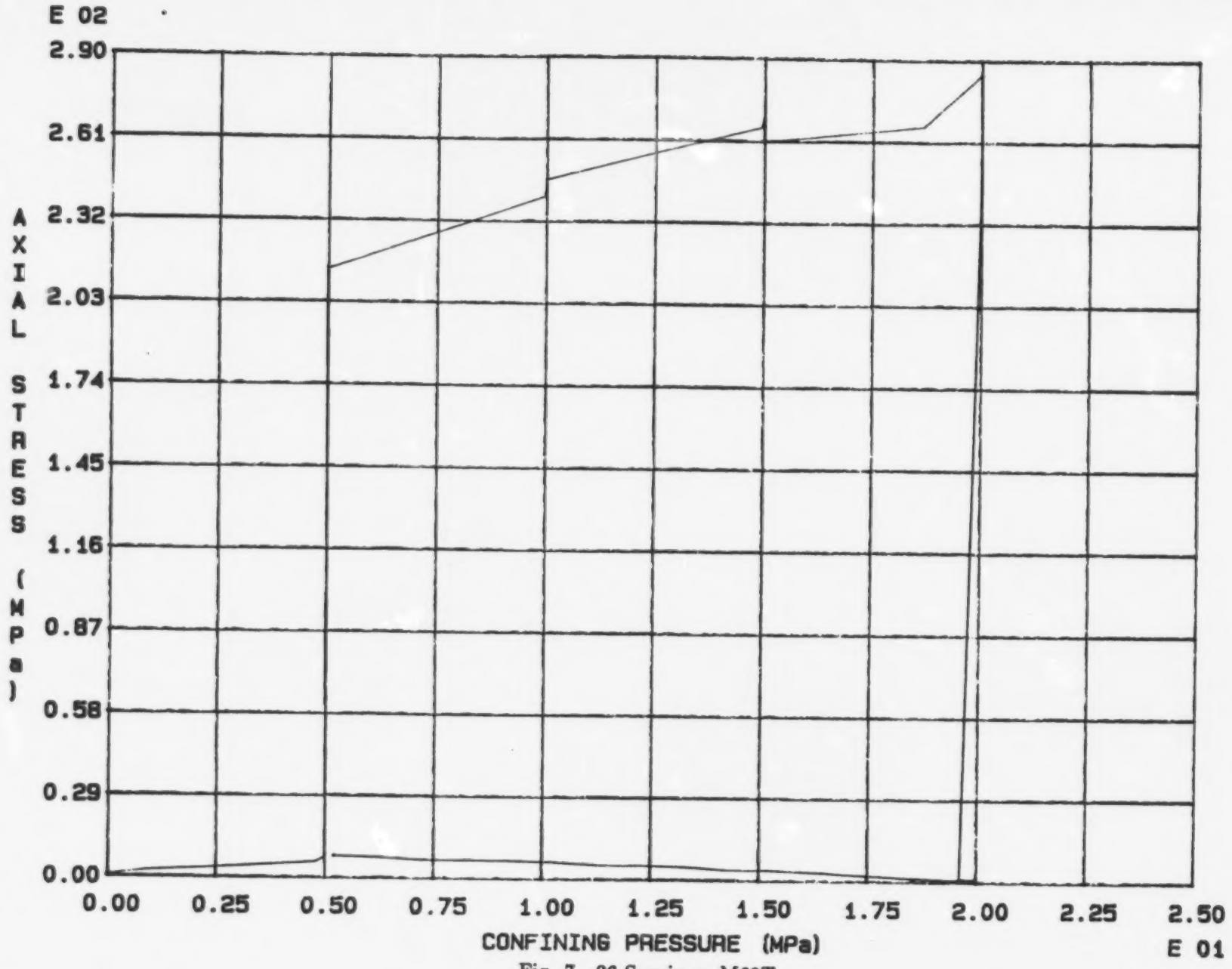

Fig. 7 - 26 Specimen M69T

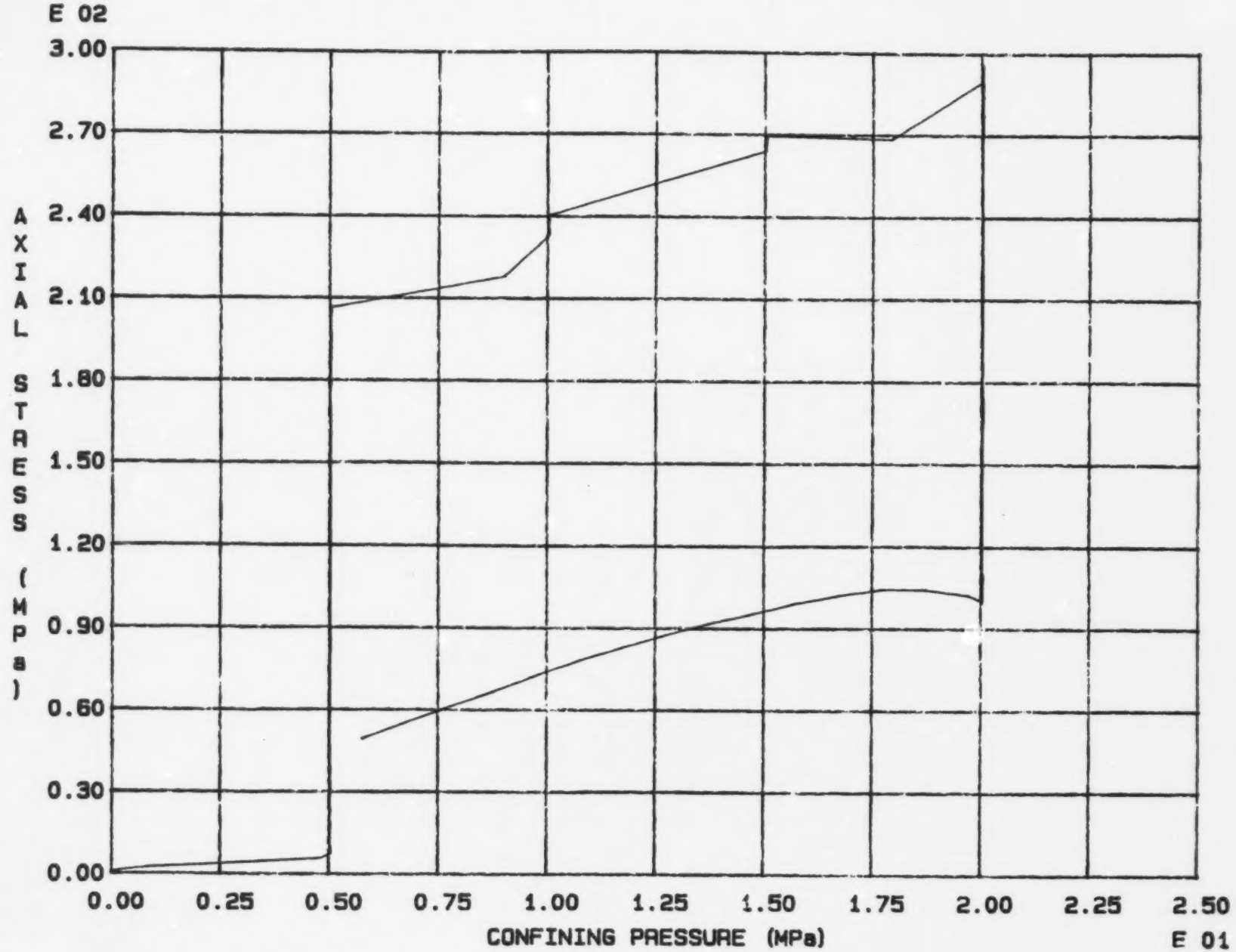

Fig. 7 - 12 Specimen M55T

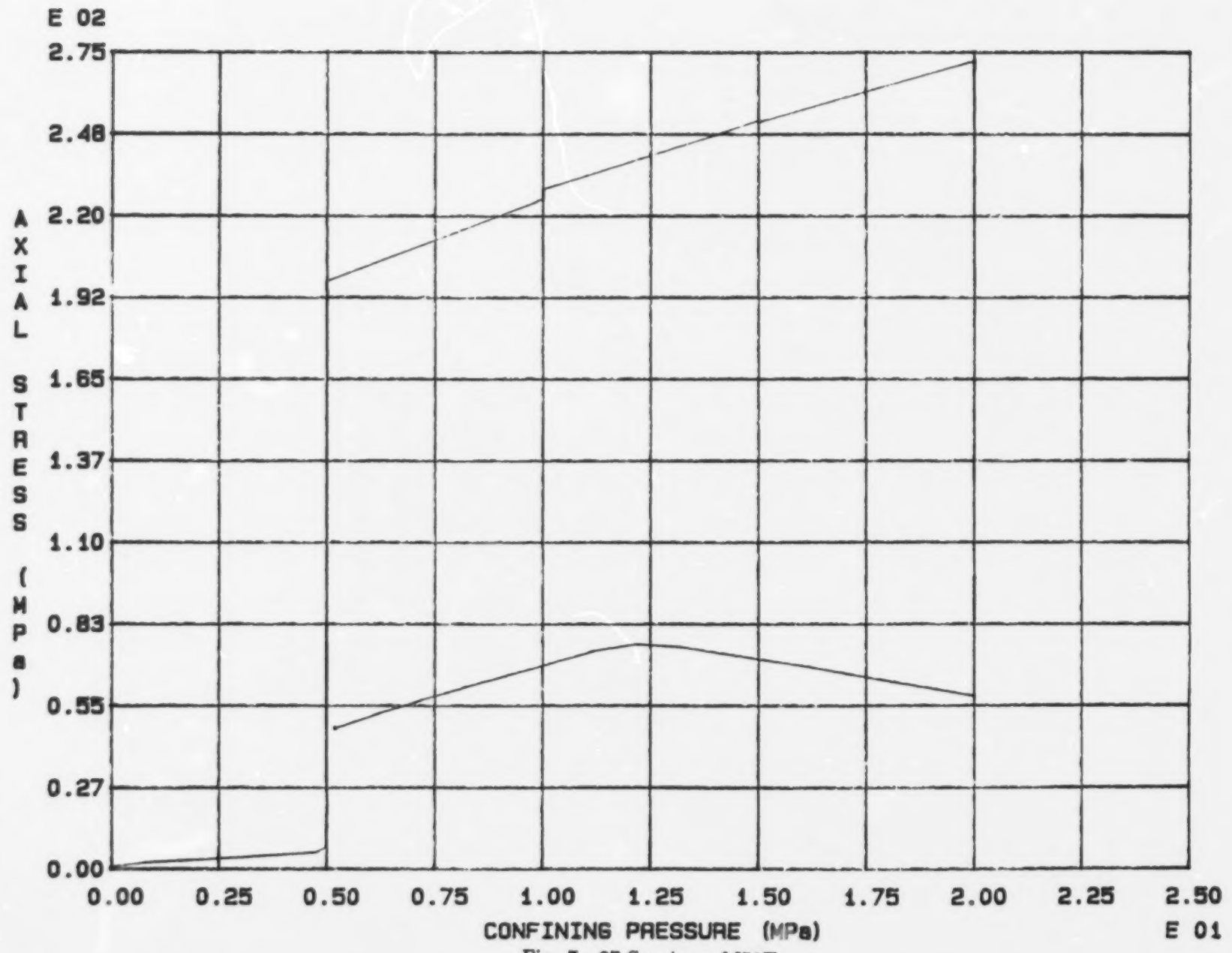

Fig. 7 - 27 Specimen M70T

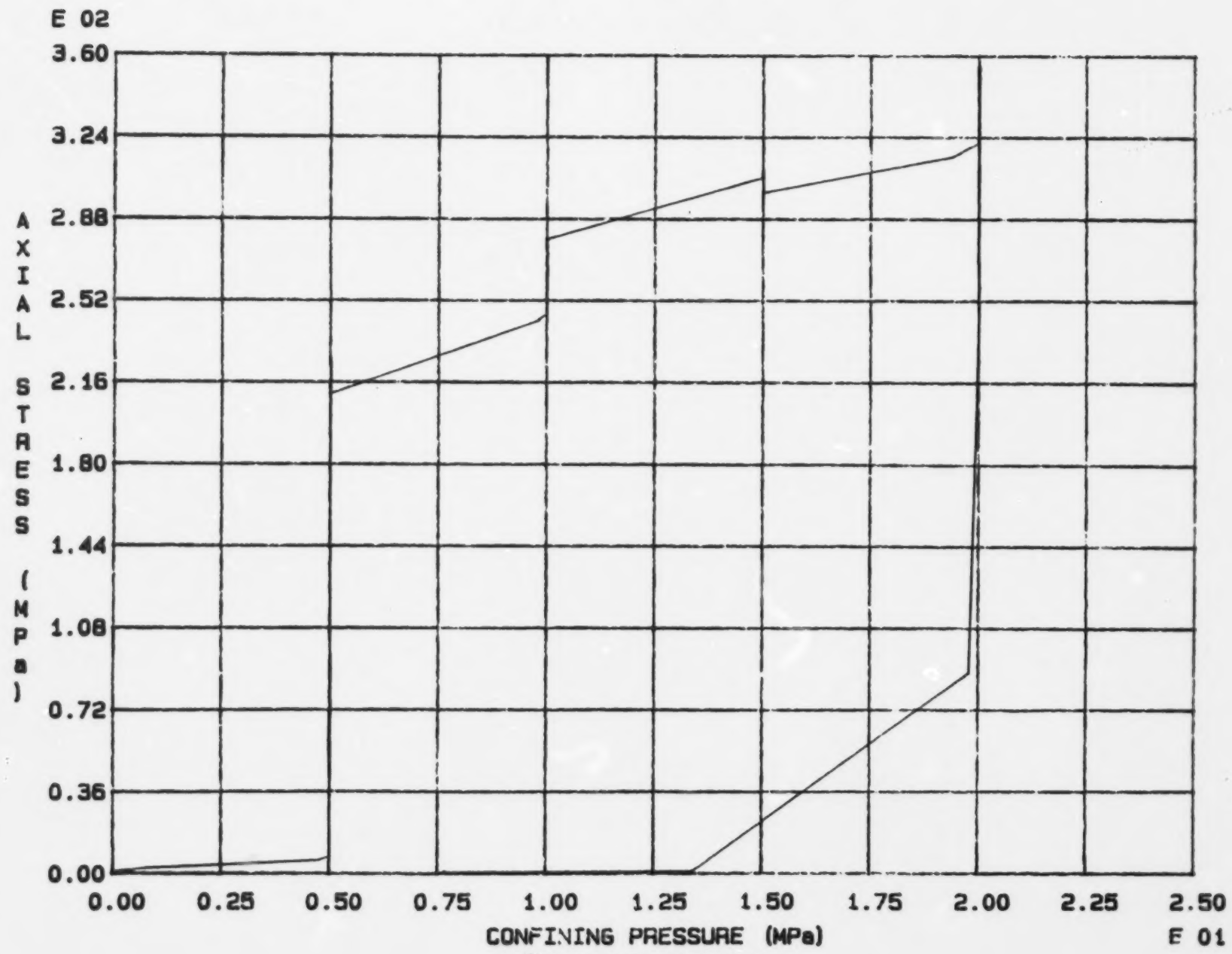

Fig. 7 - 13 Specimen M56T

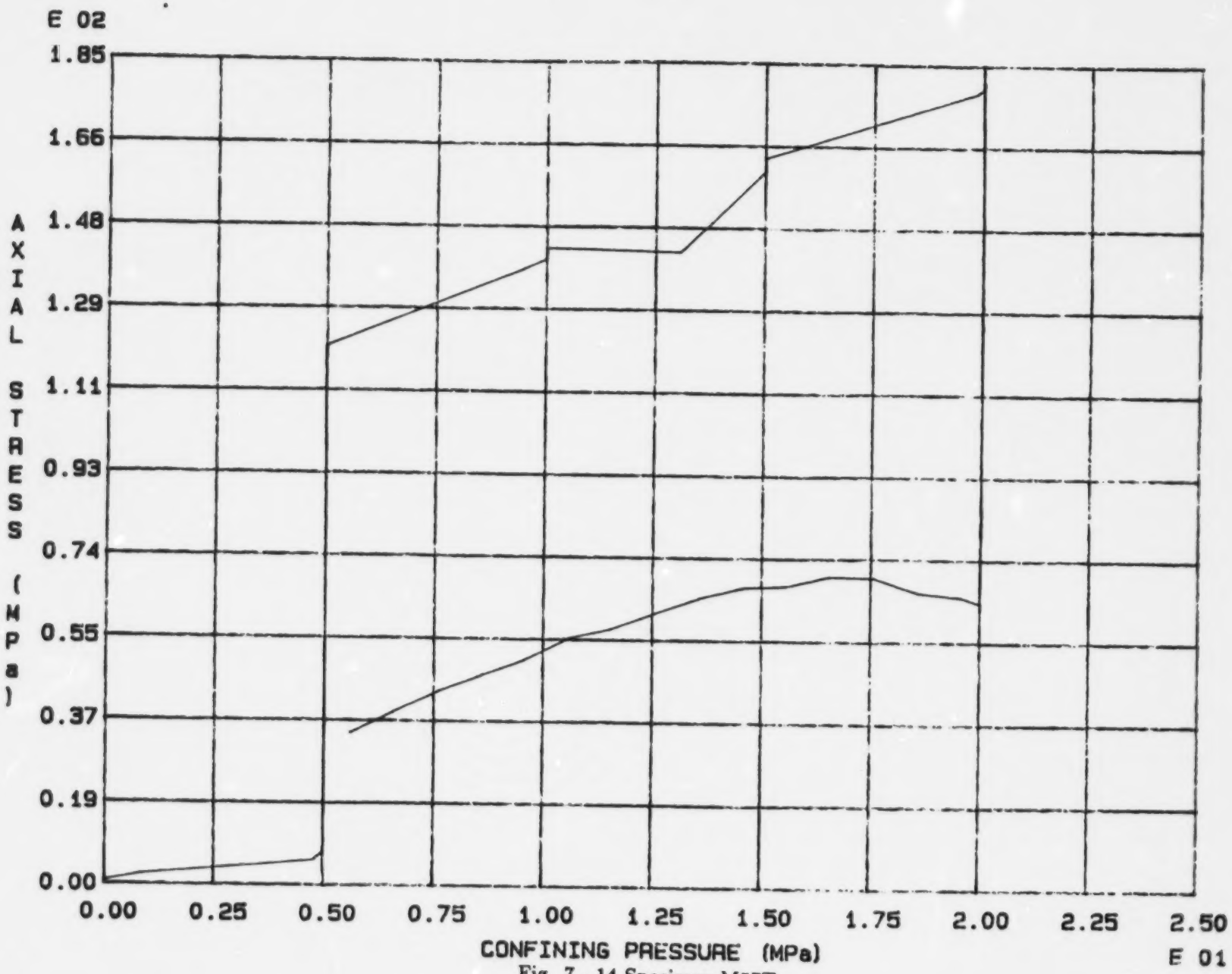

Fig. 7 - 14 Specimen M57T

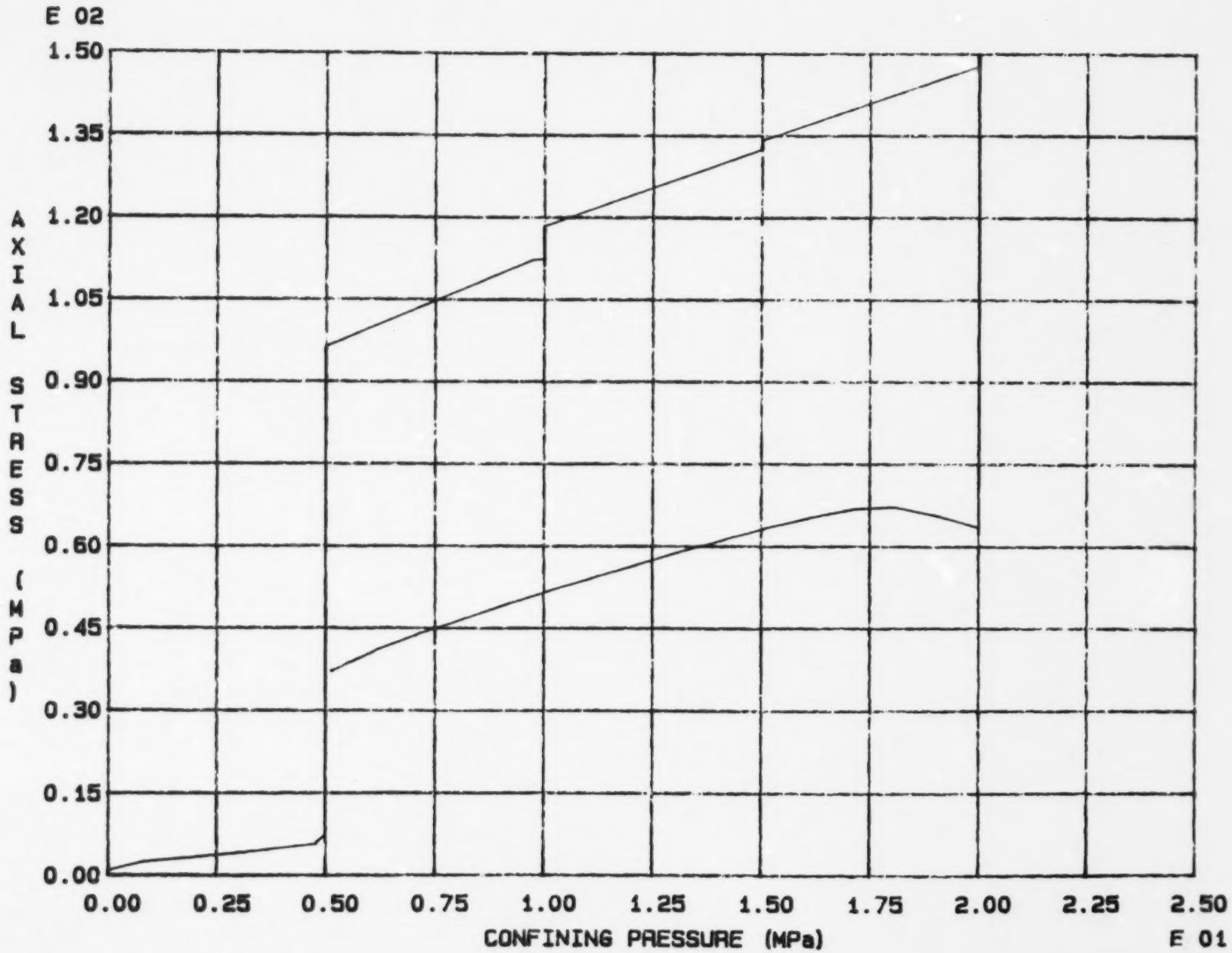

Fig. 7 - 15 Specimen M58T

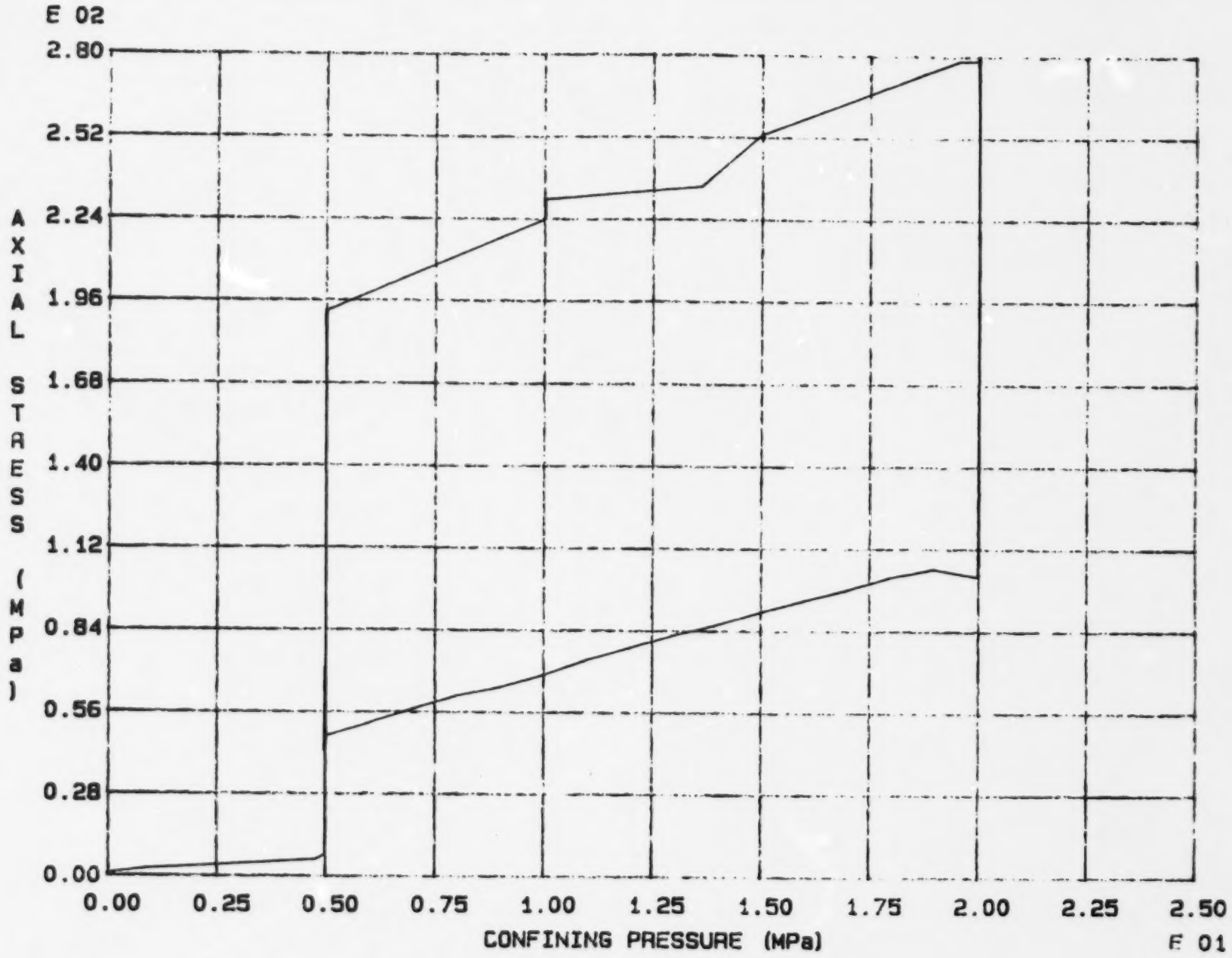

Fig. 7 - 16 Specimen M59T

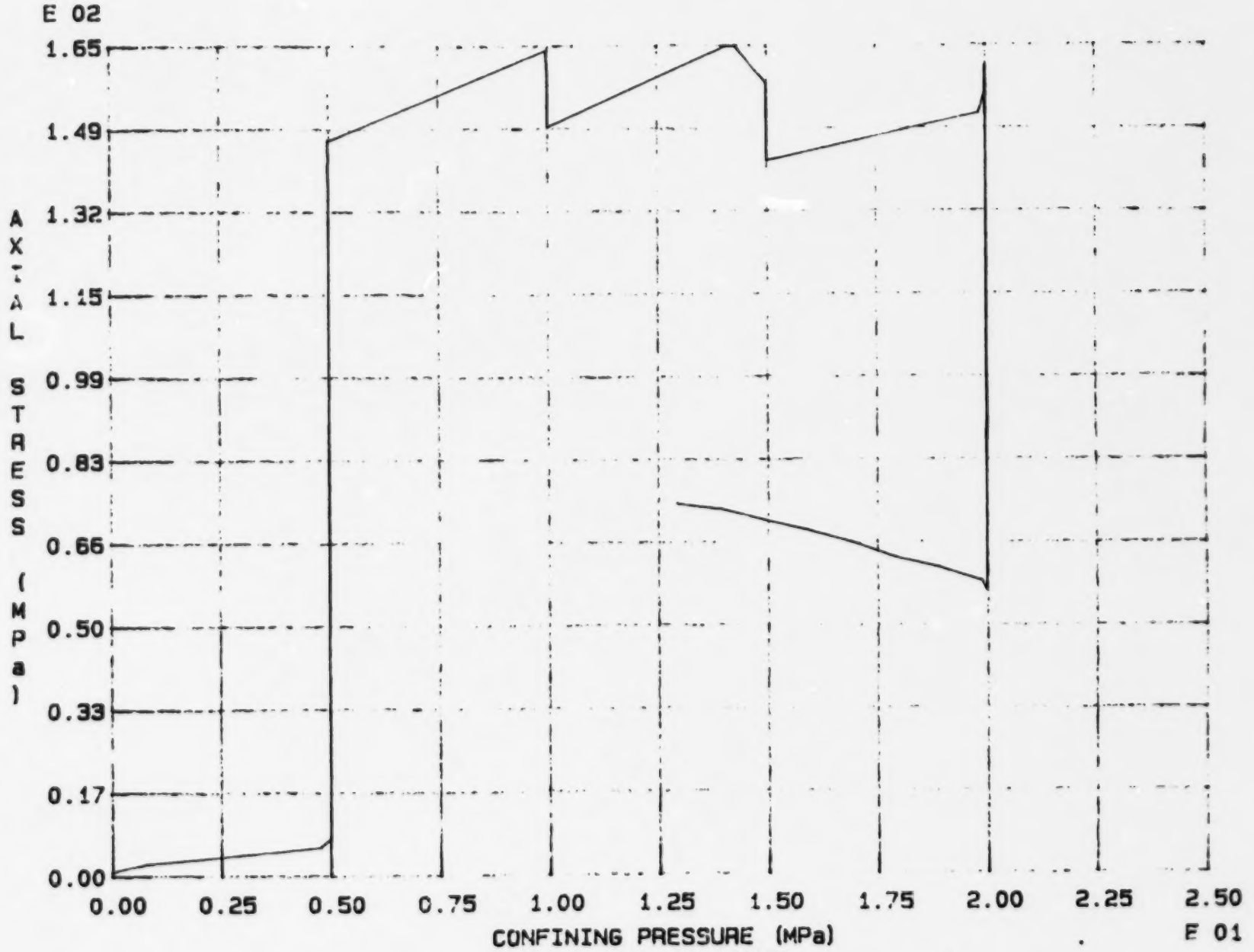

Fig. 7 - 17 Specimen M60T

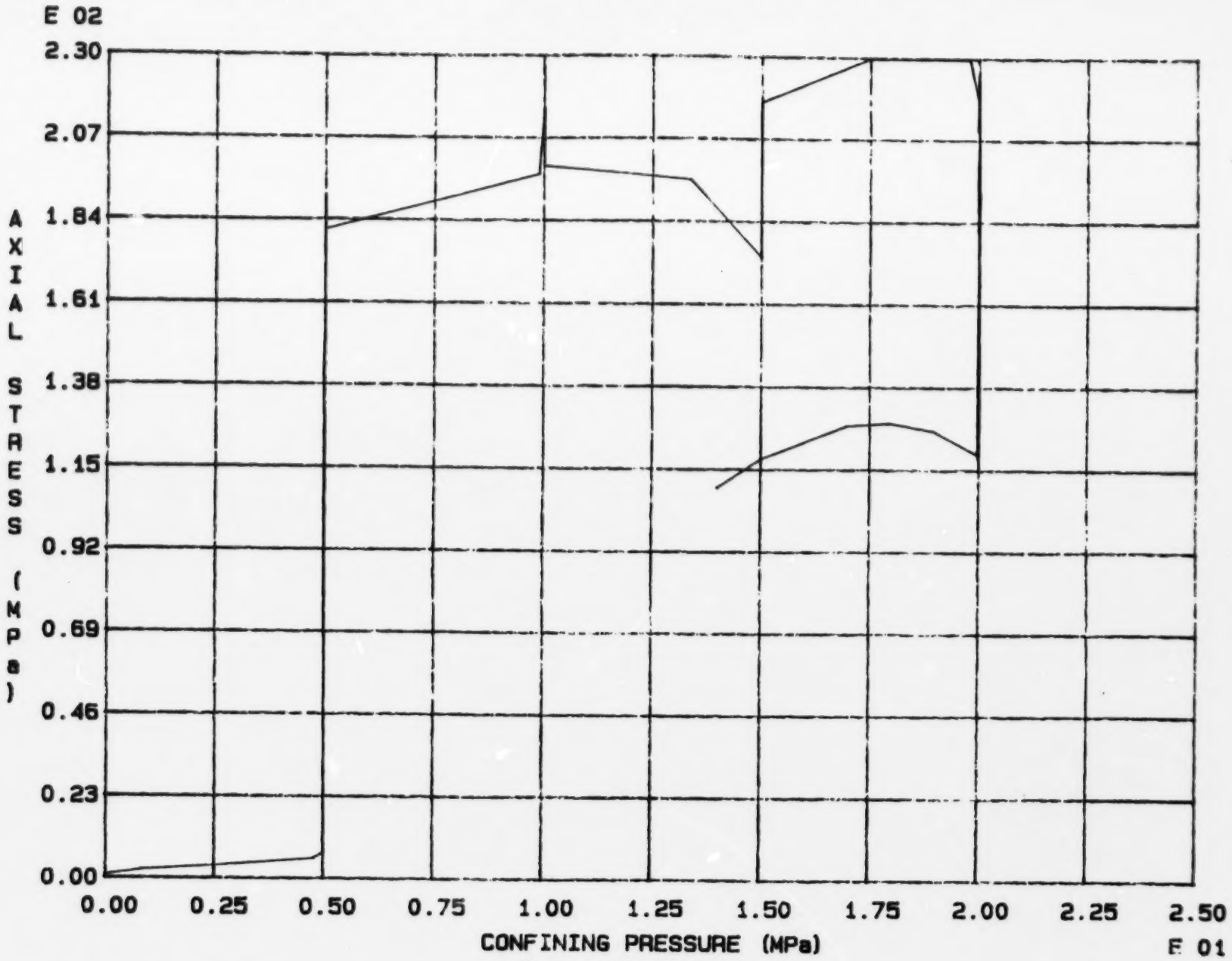

Fig. 7 - 18 Specimen M61T

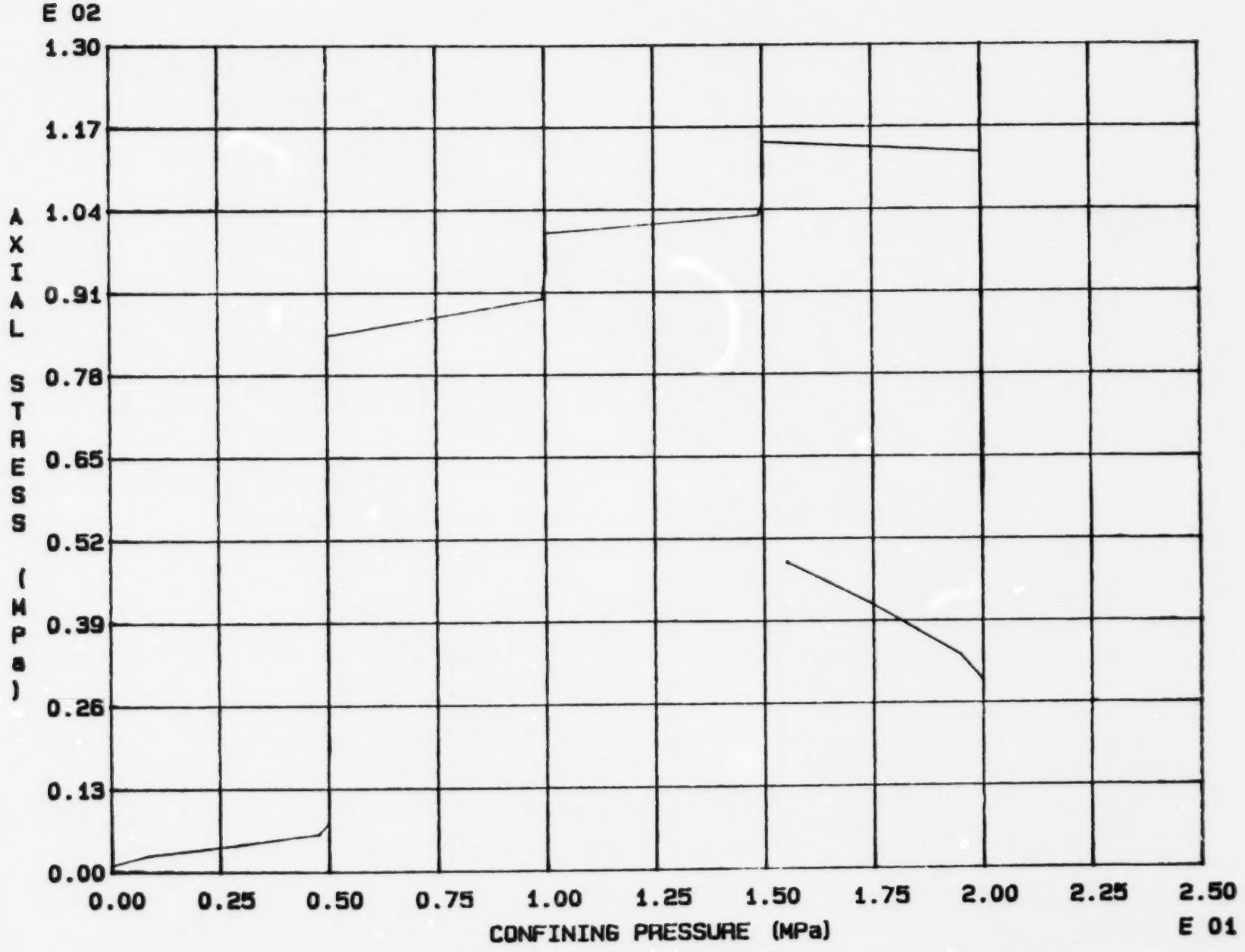

Fig. 7 - 19 Specimen M62T

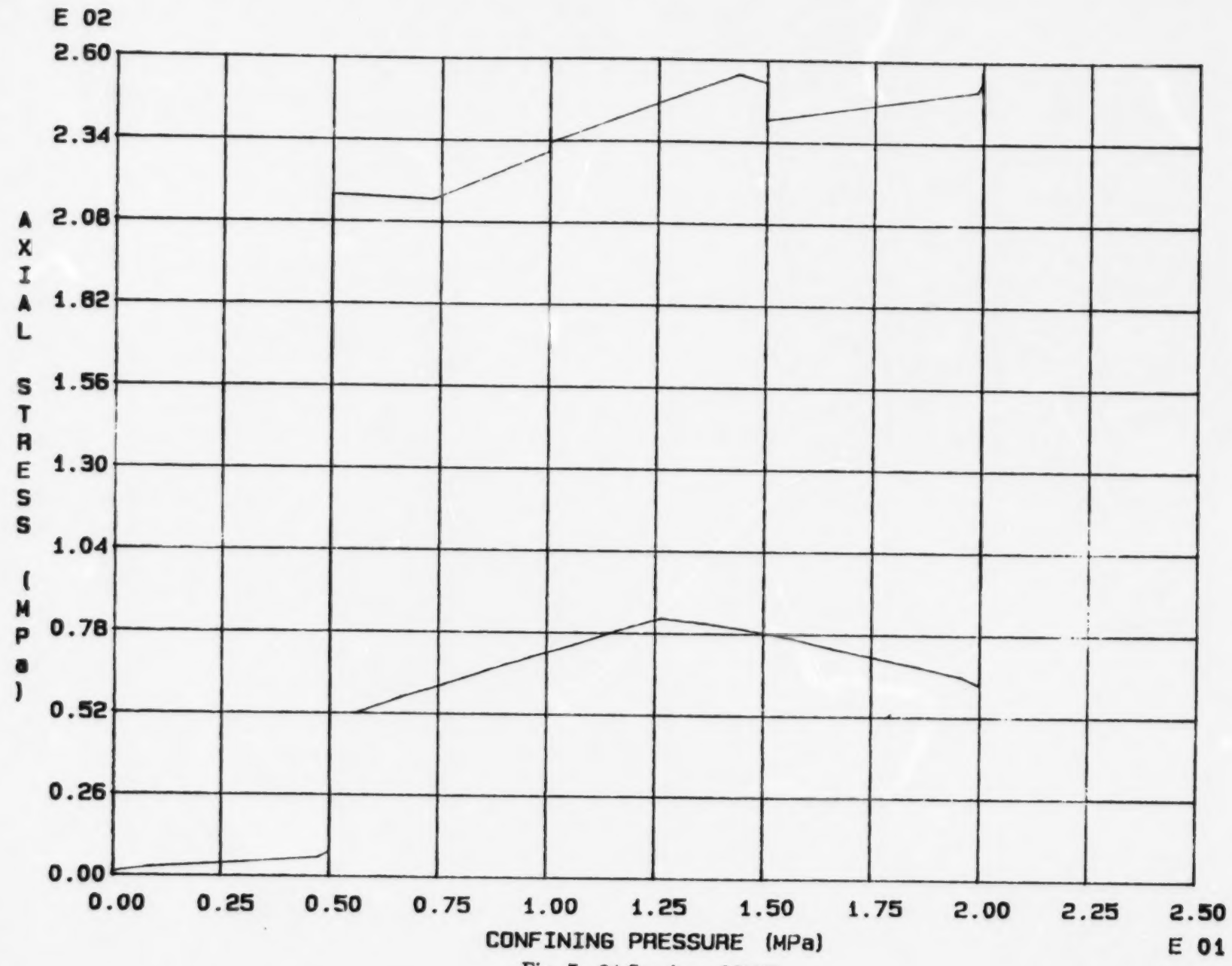

Fig. 7 - 34 Specimen M77T

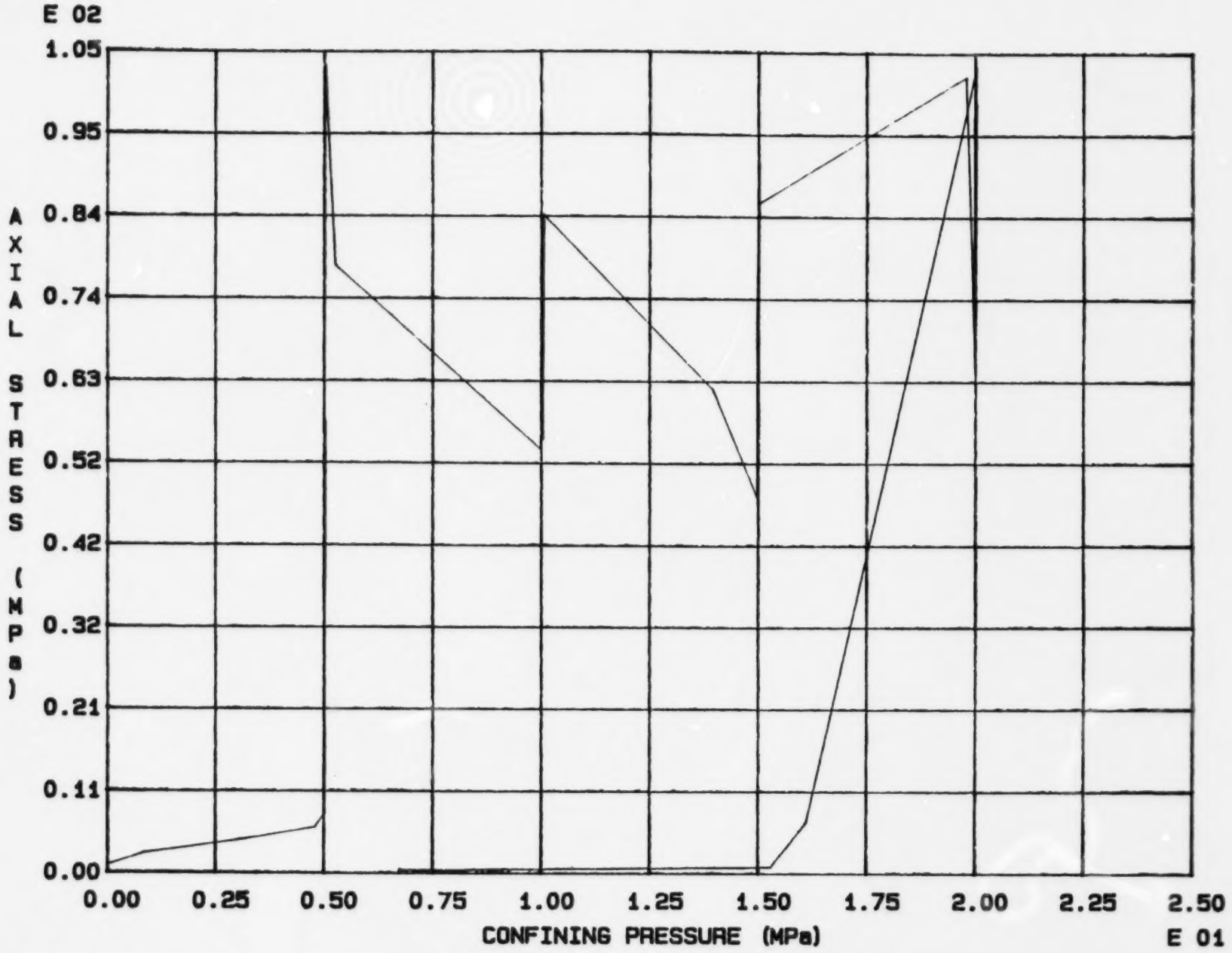

Fig. 7 - 20 Specimen M63T

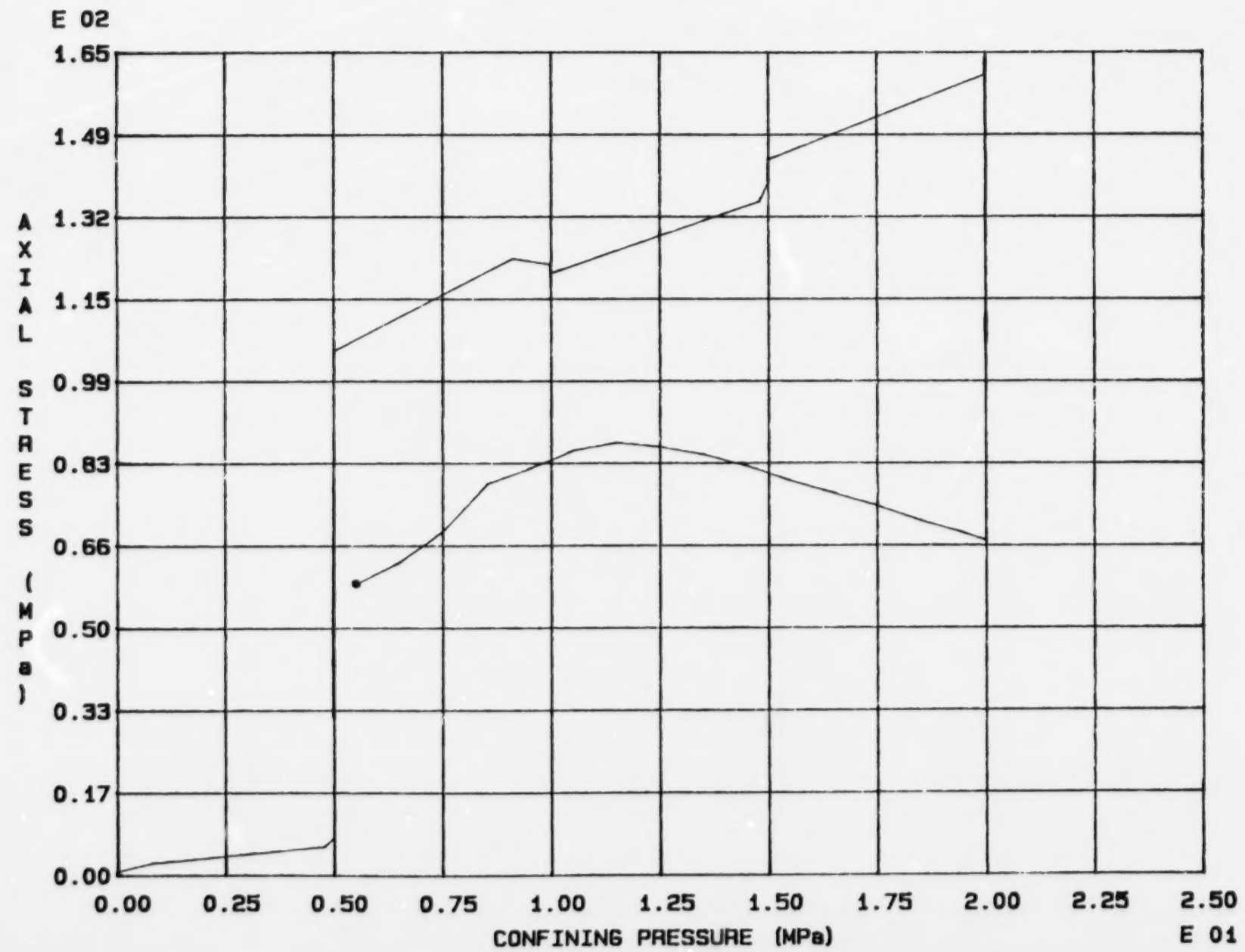

Fig. 7 - 35 Specimen M78T

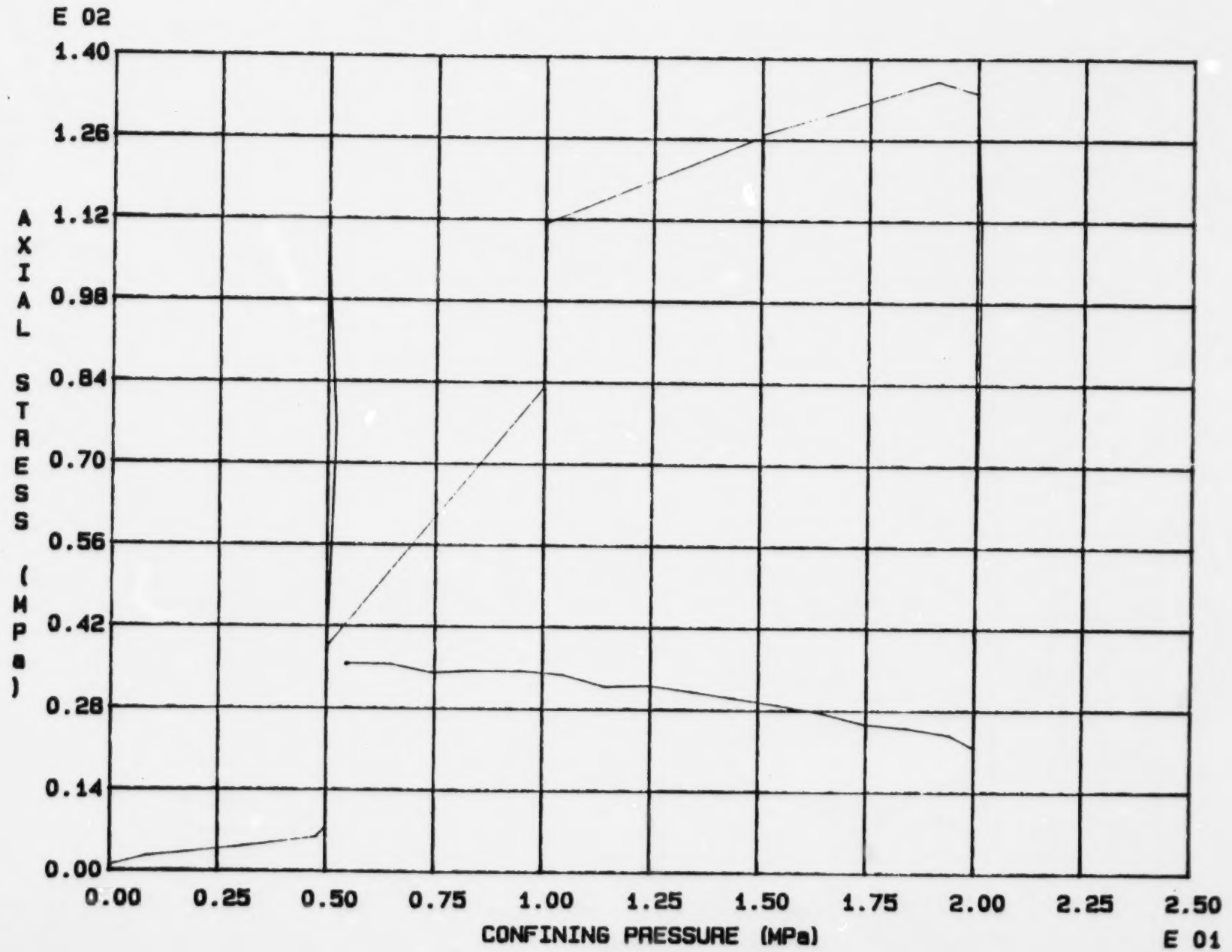

Fig. 7 - 21 Specimen M64T

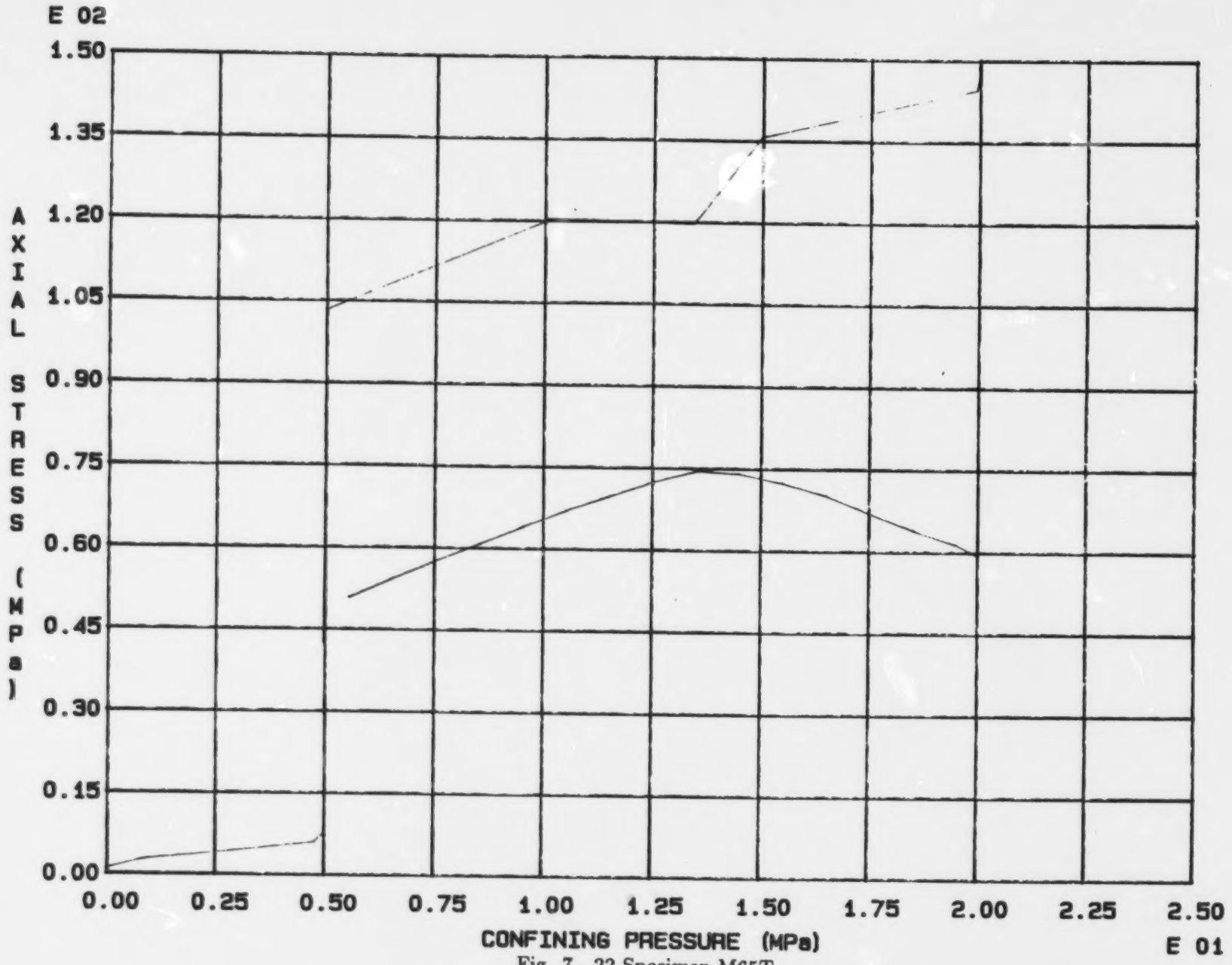

Fig. 7 - 22 Specimen M65T

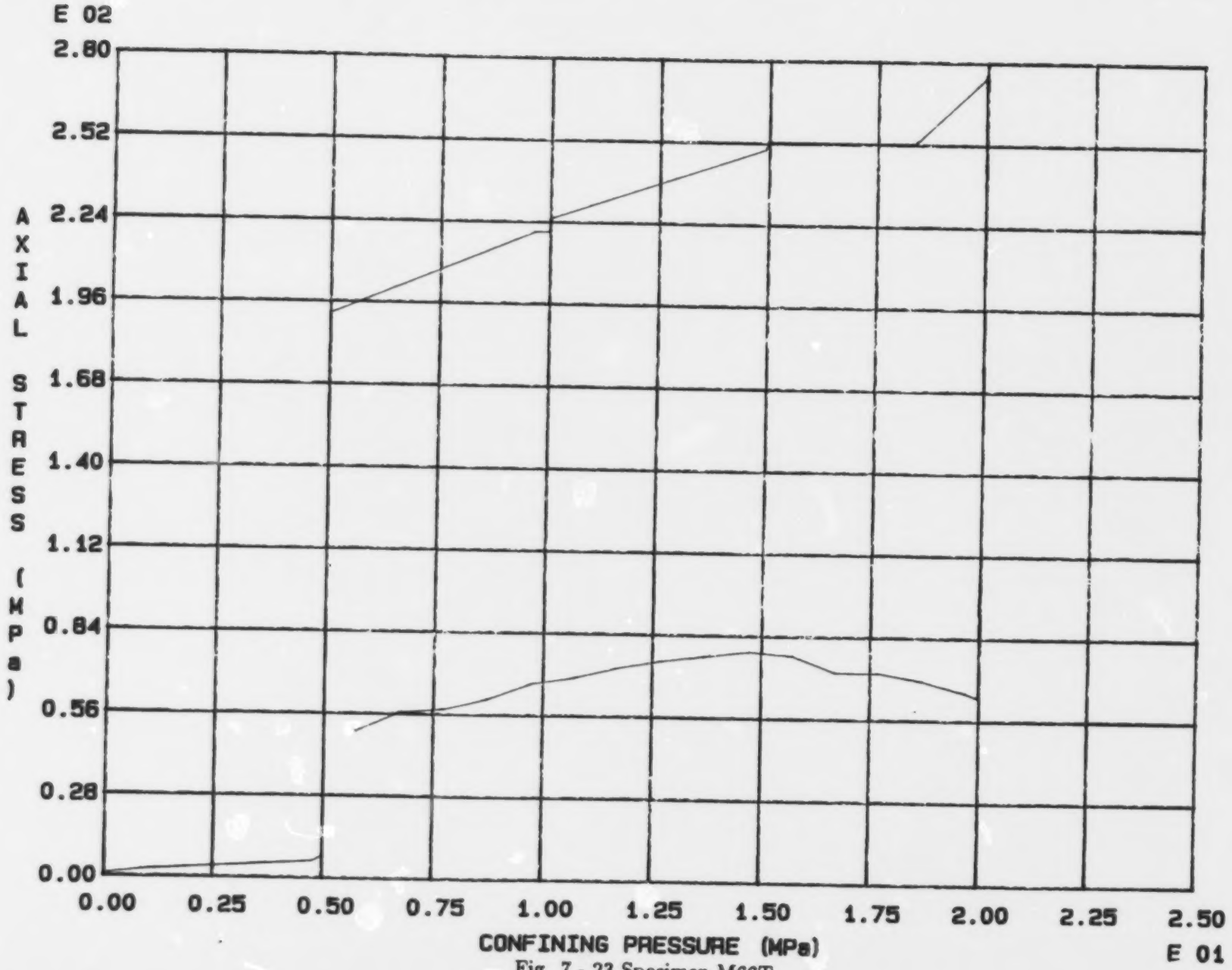

Fig. 7 - 23 Specimen M66T

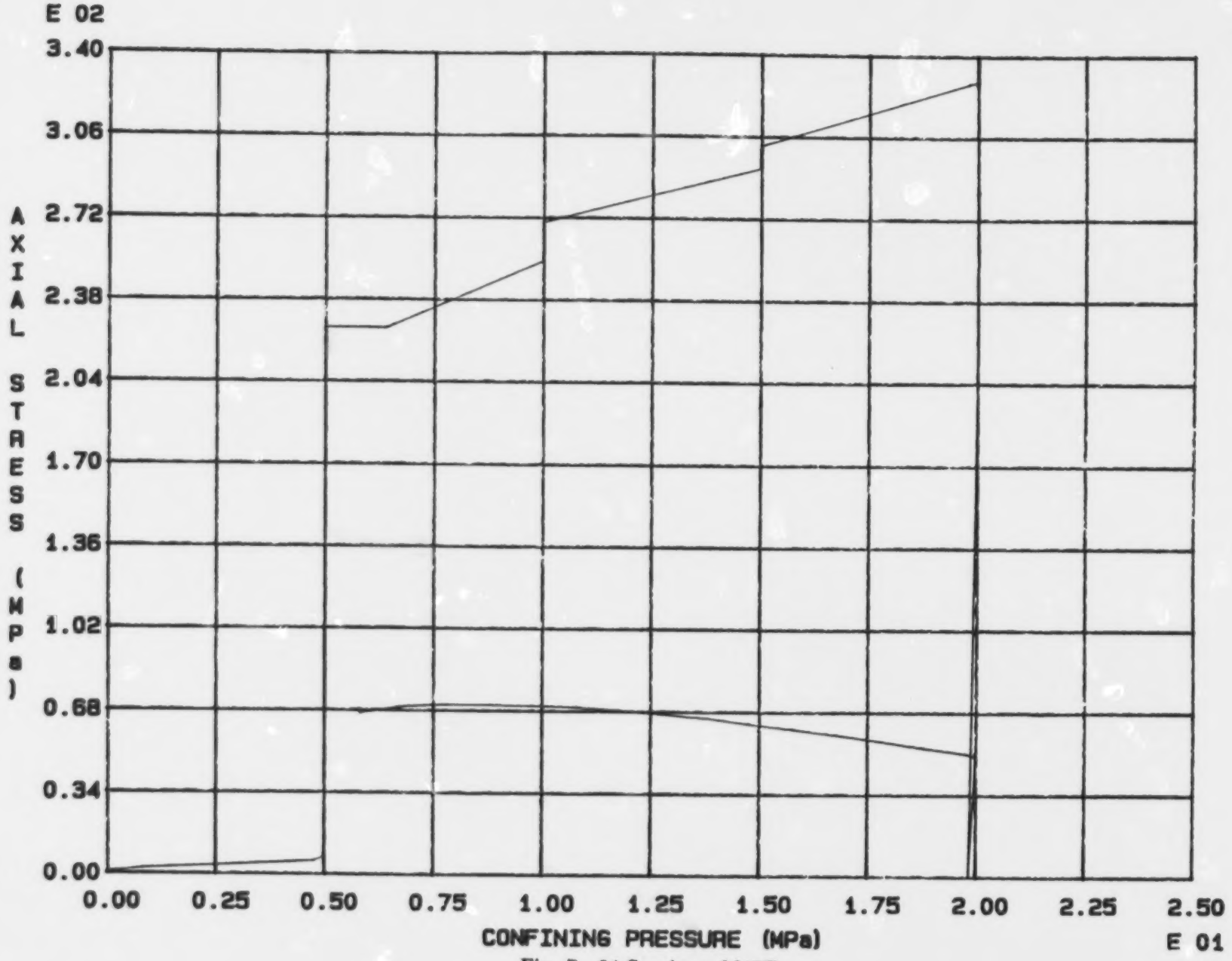

Fig. 7 - 24 Specimen M67T

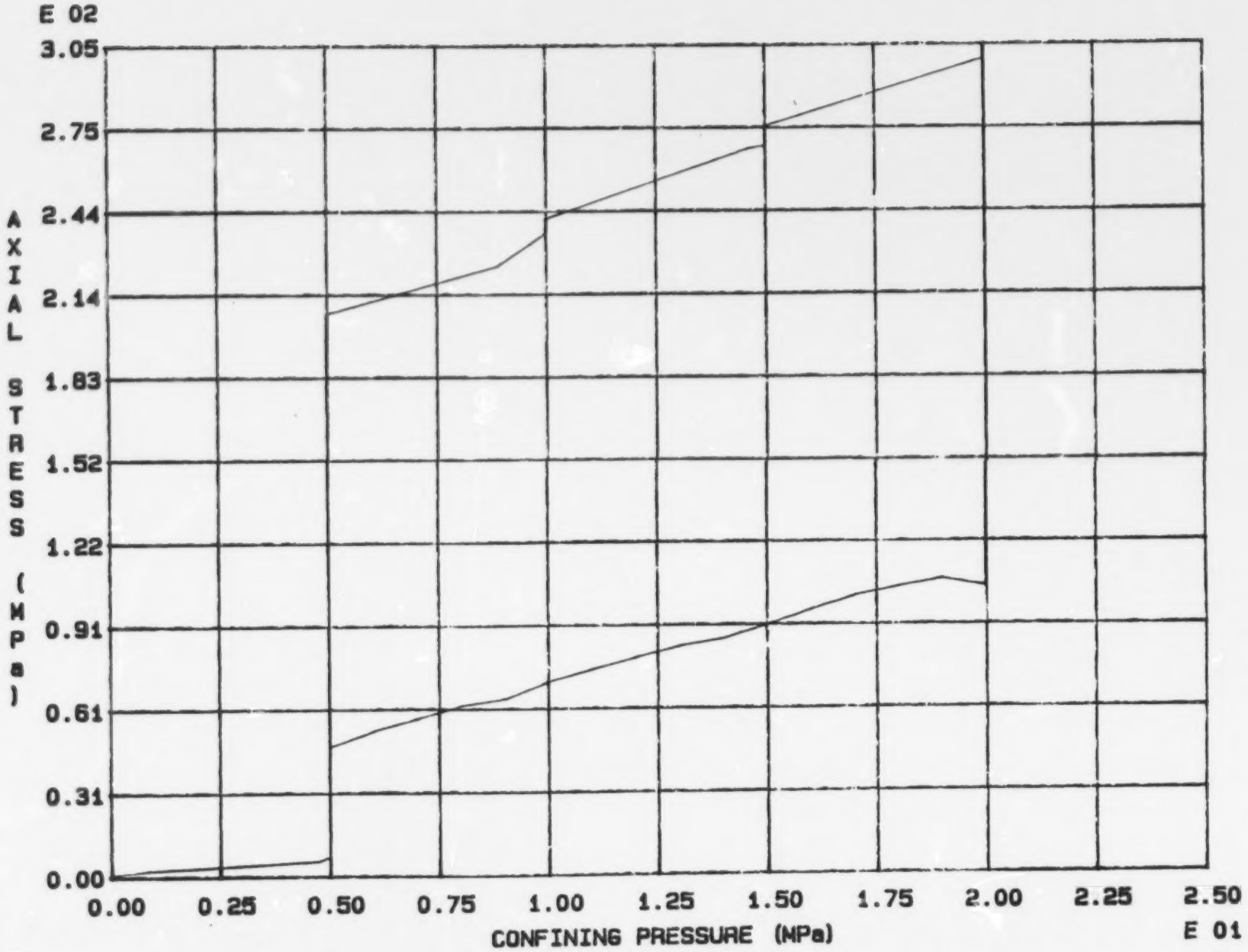

Fig. 7 - 25 Specimen M68T

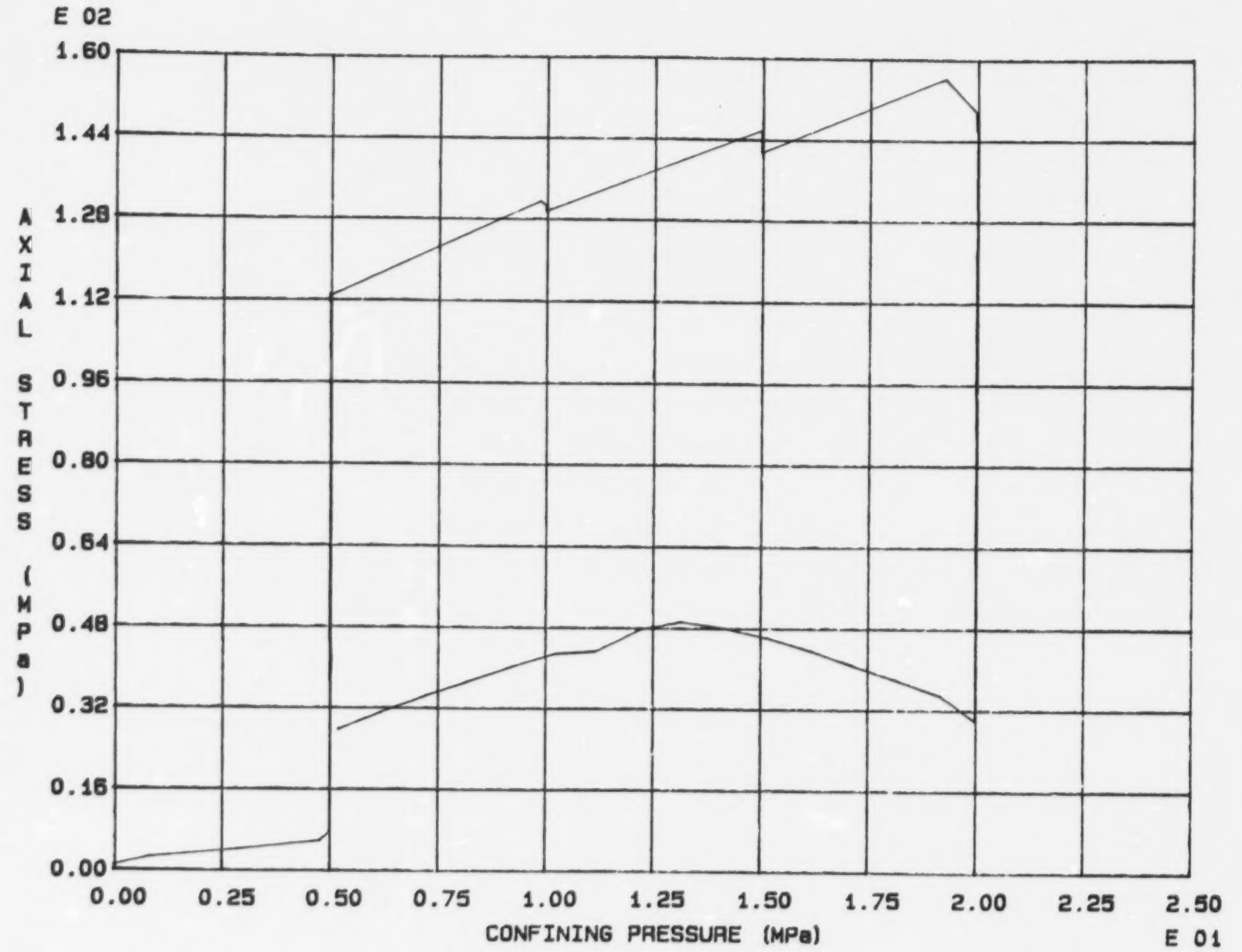

Fig. 7 - 28 Specimen M71T

MOHR ENVELOPE

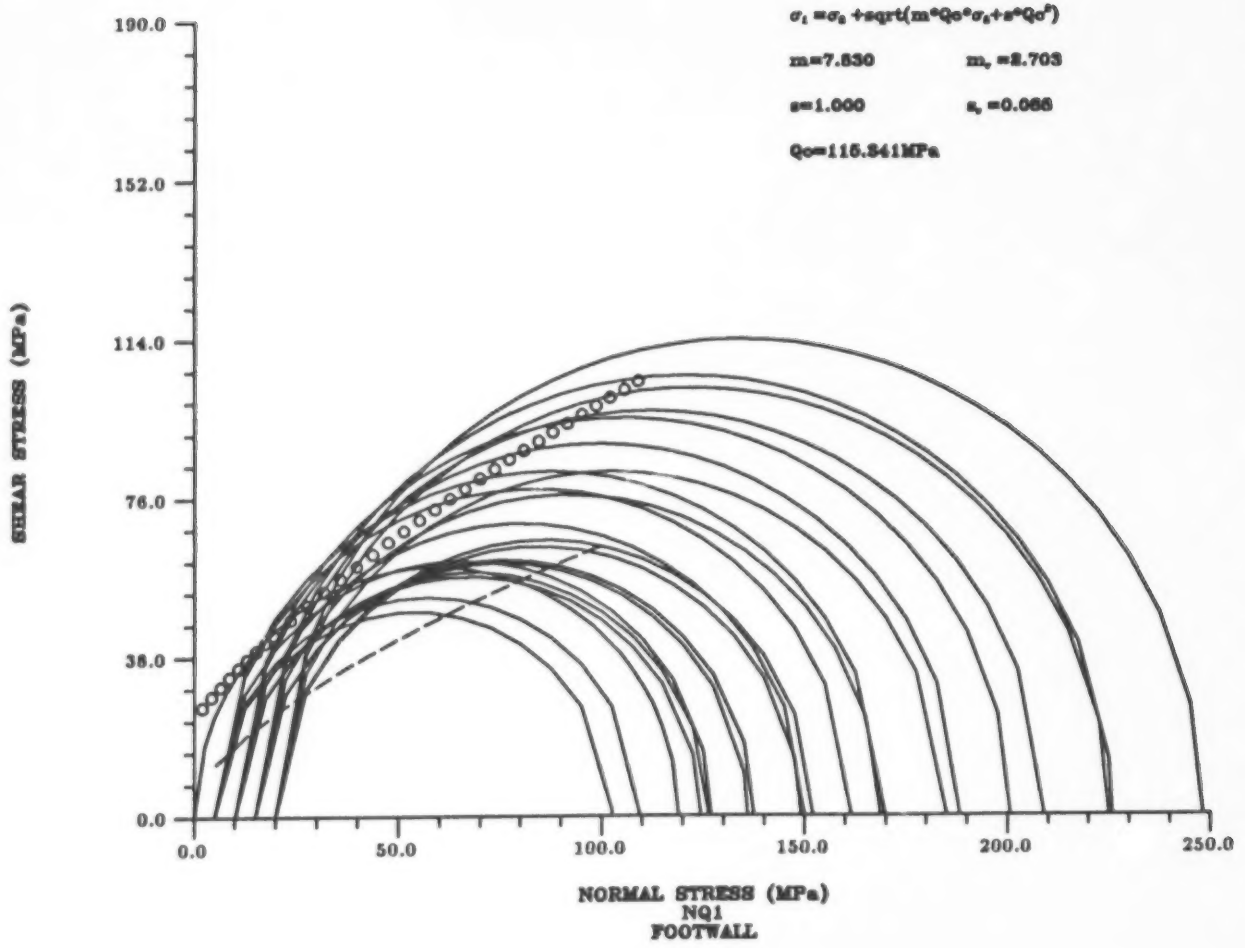

Fig. 8 - 1

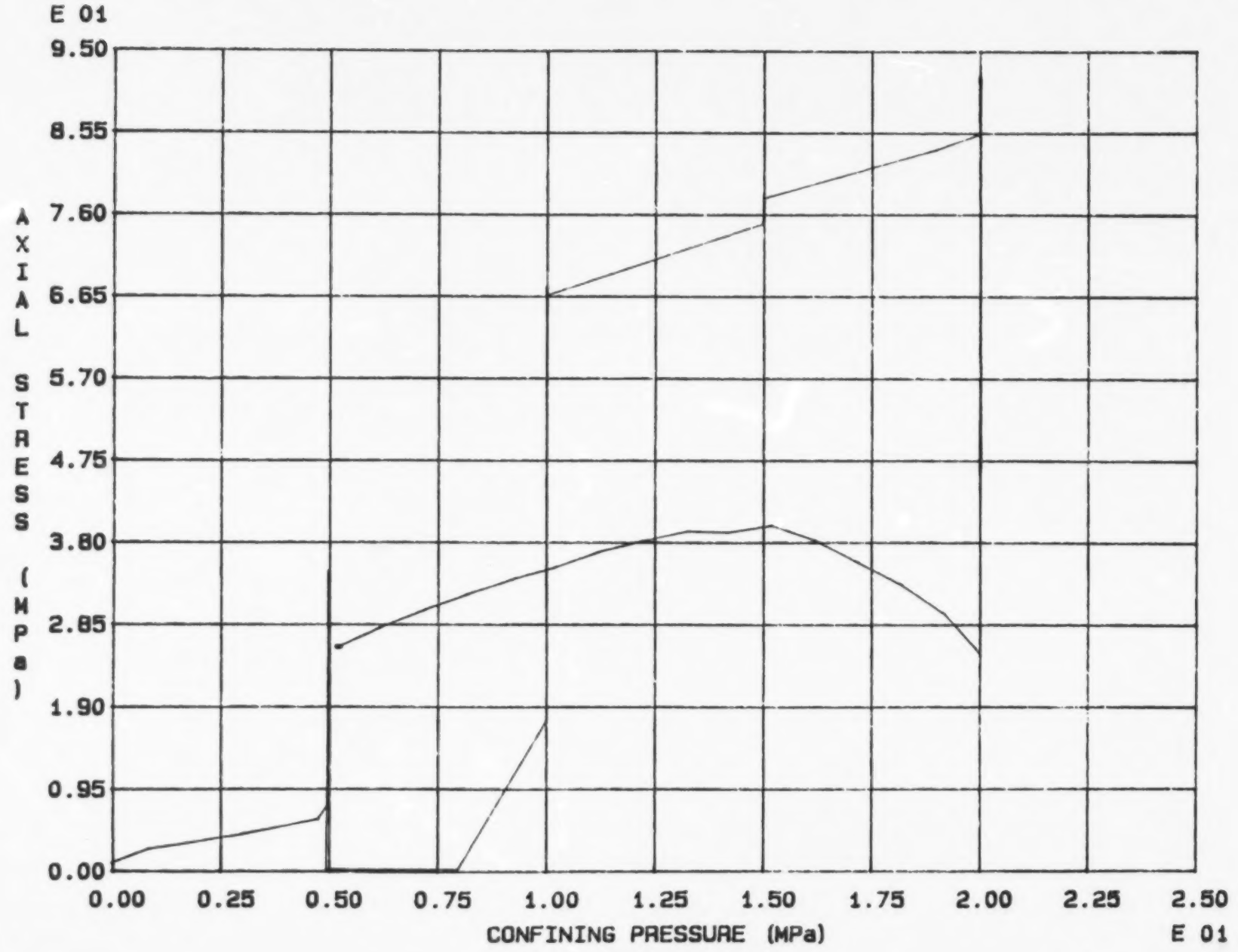

Fig. 7 - 29 Specimen M72T

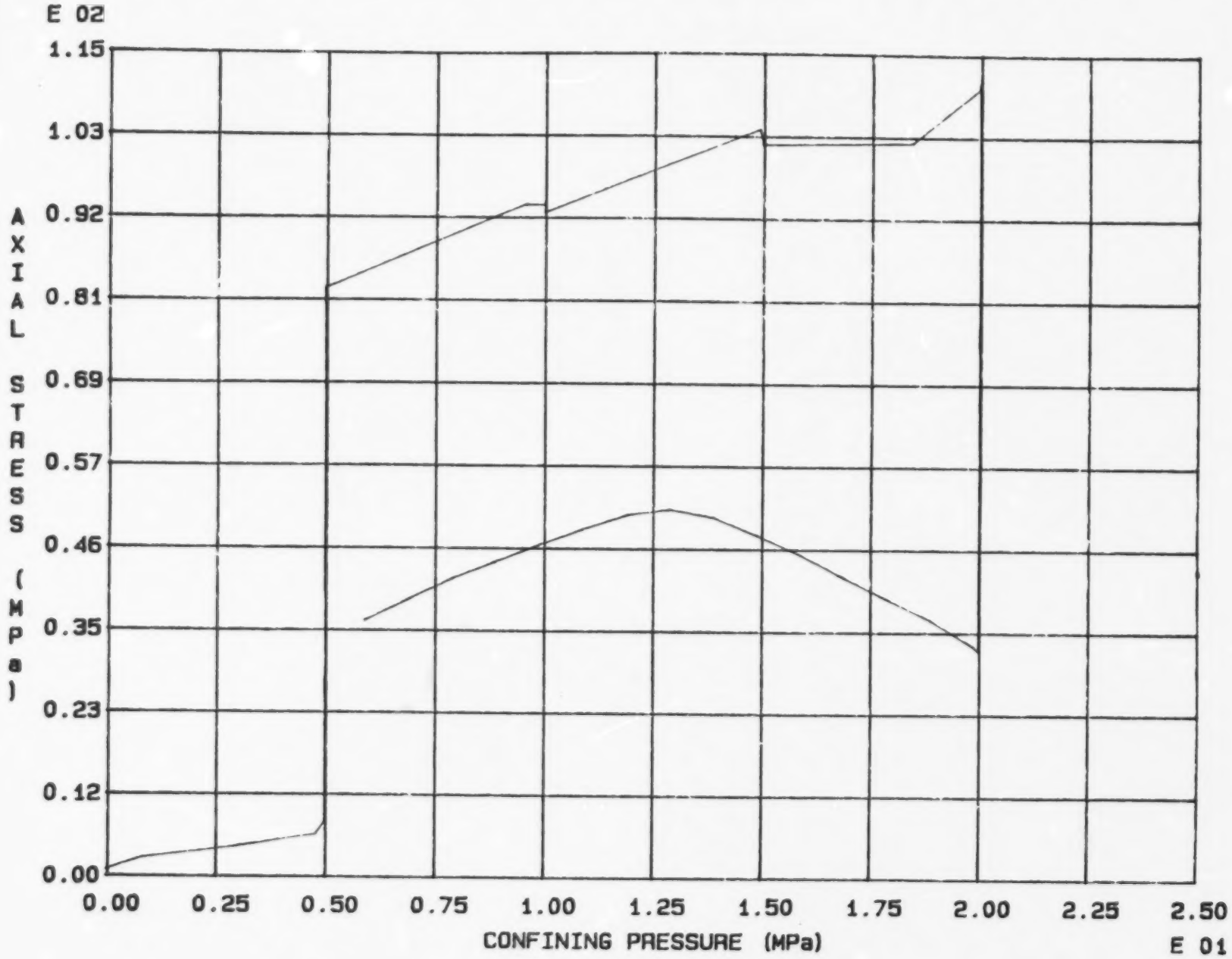

Fig. 7 - 30 Specimen M73T

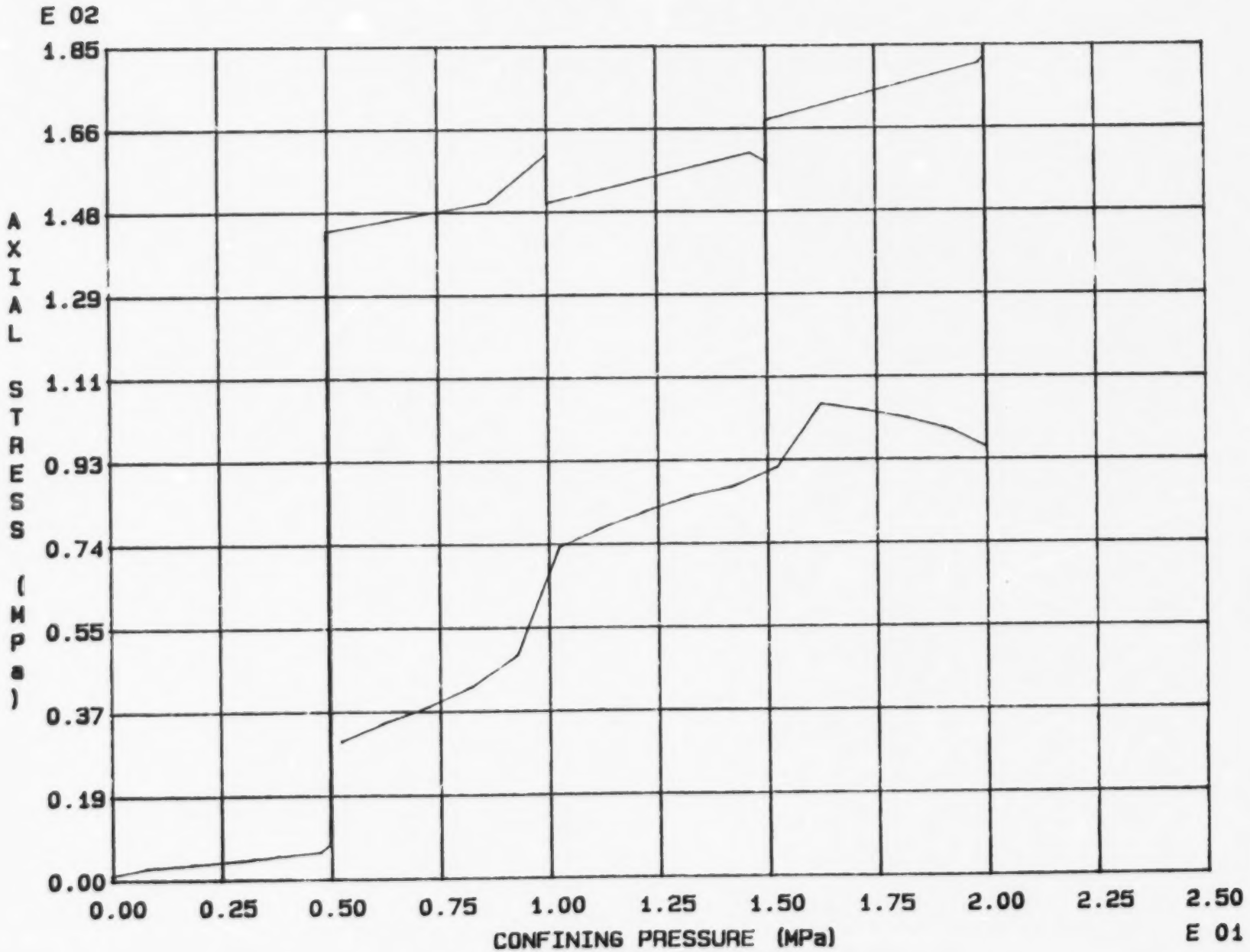

Fig. 7 - 31 Specimen M74T

MOHR ENVELOPE

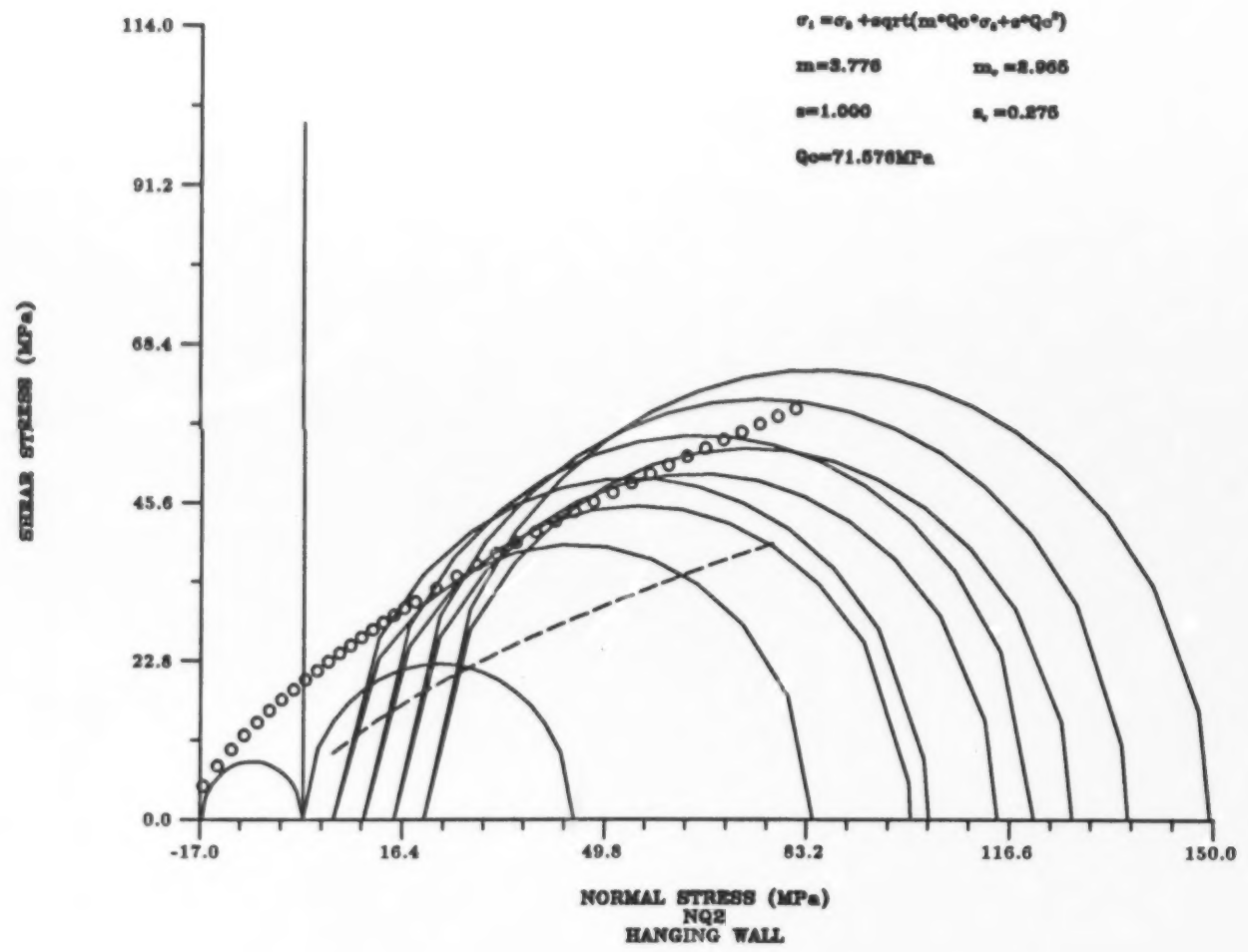

Fig. 8 - 4

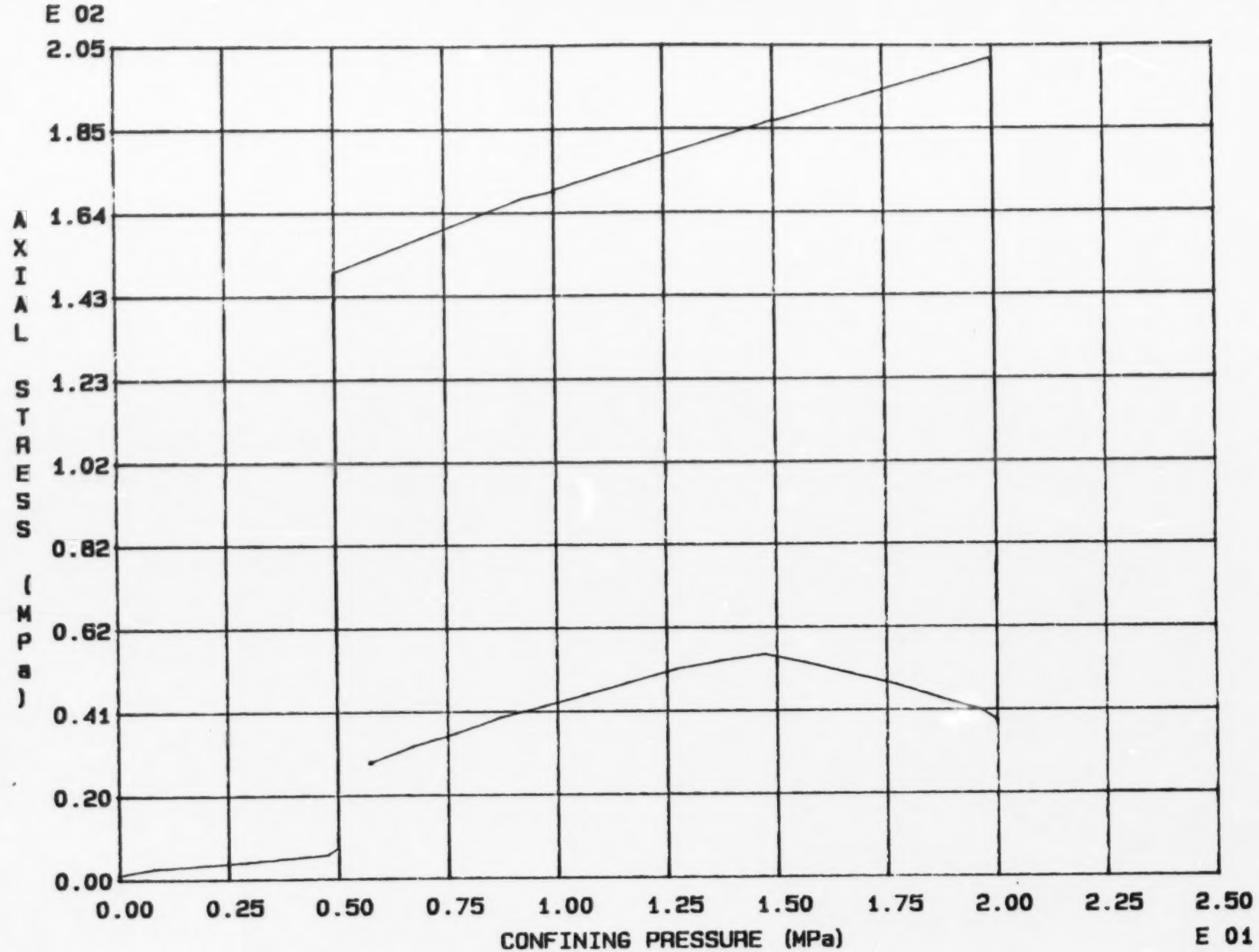

Fig. 7 - 32 Specimen M75T

MOHR ENVELOPE

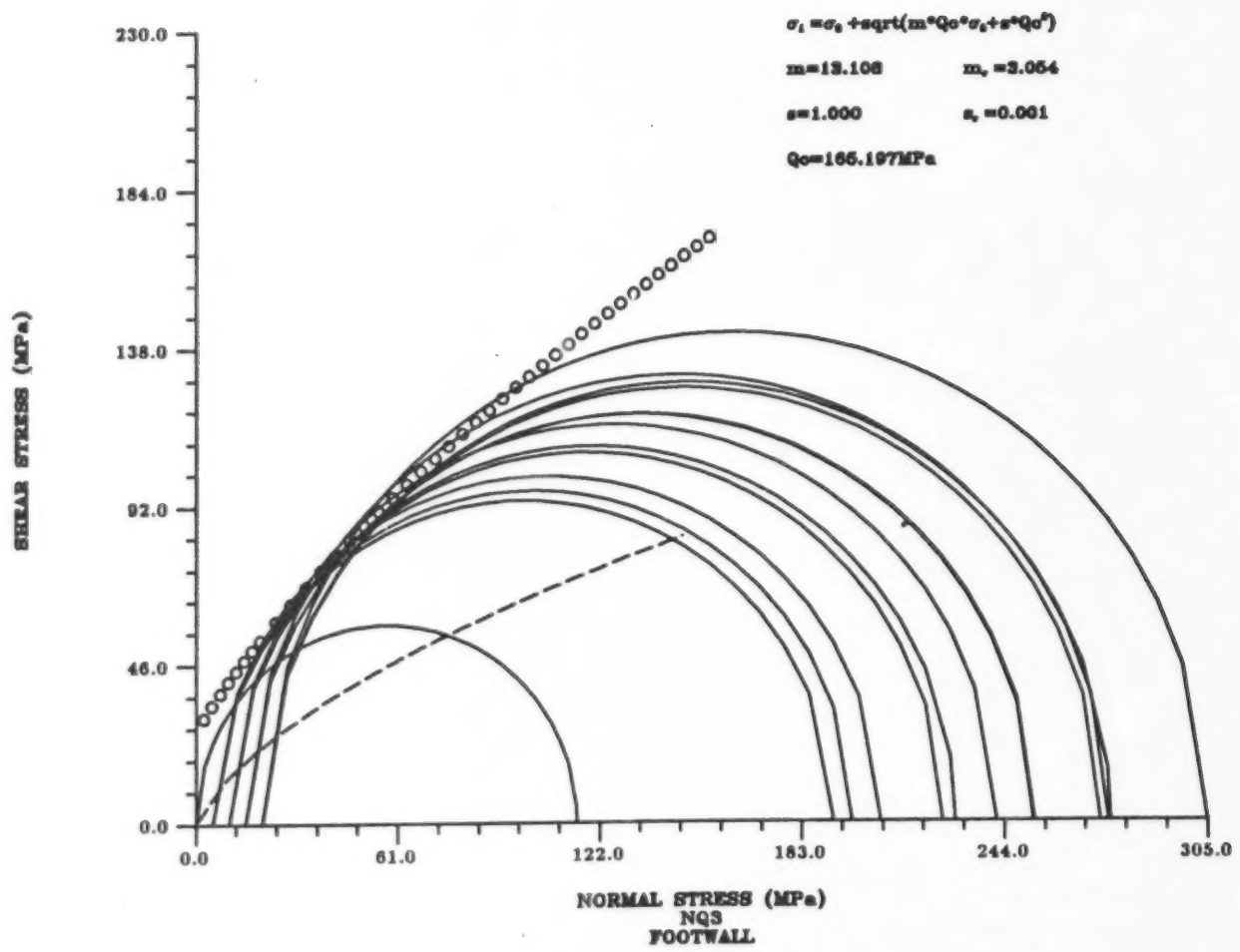

Fig. 8 - 5

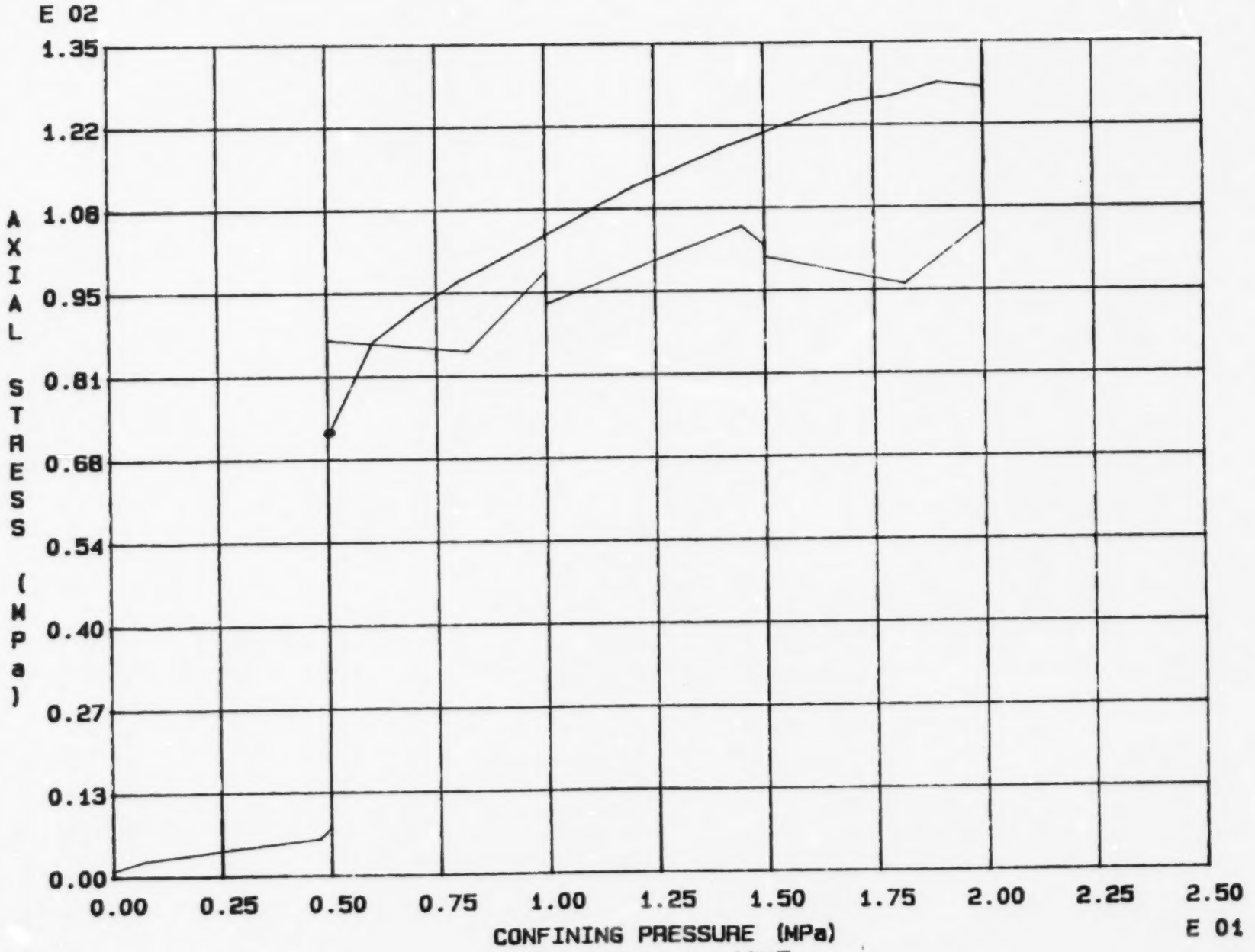

Fig. 7 - 33 Specimen M76T

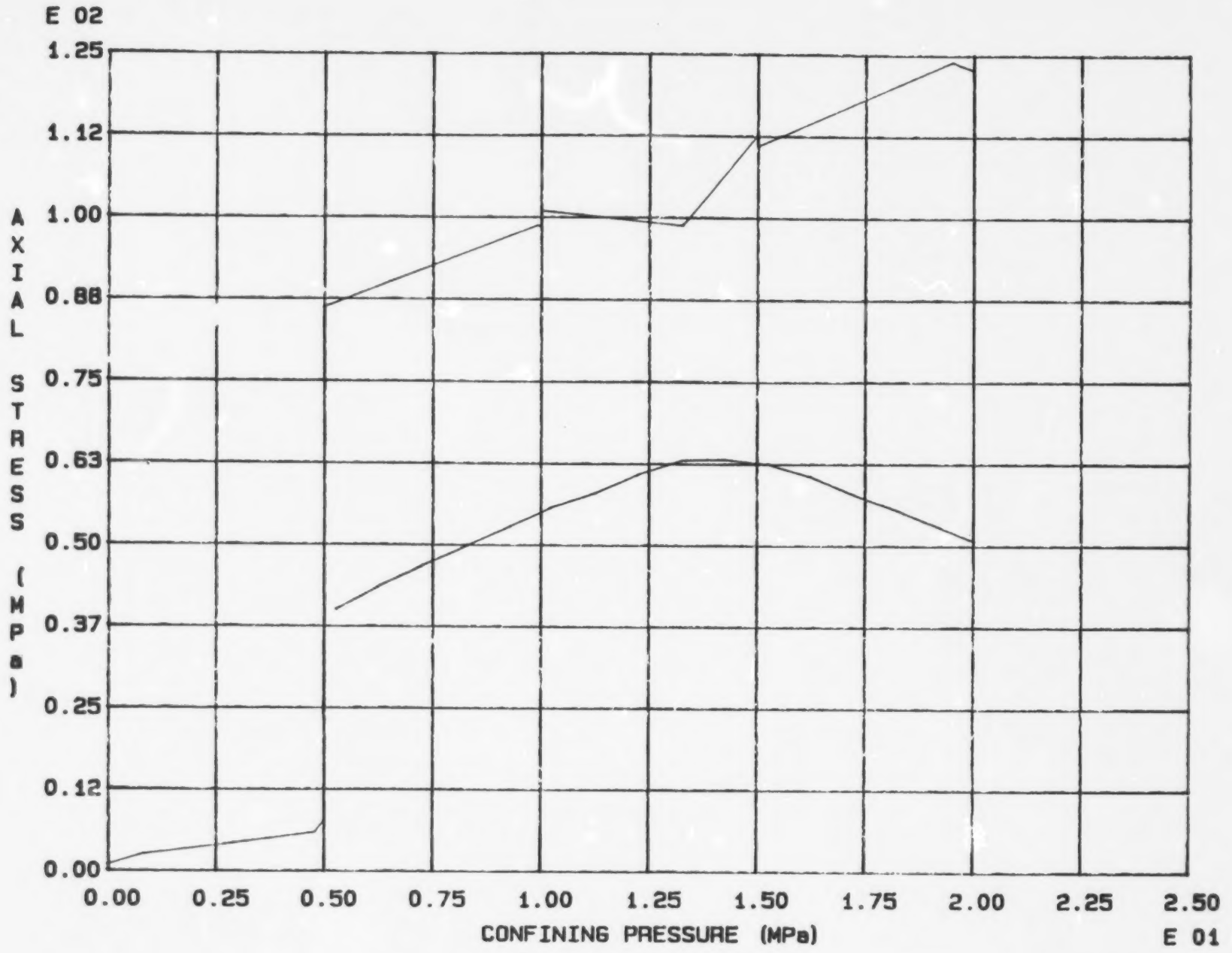

Fig. 7 - 36 Specimen M79T

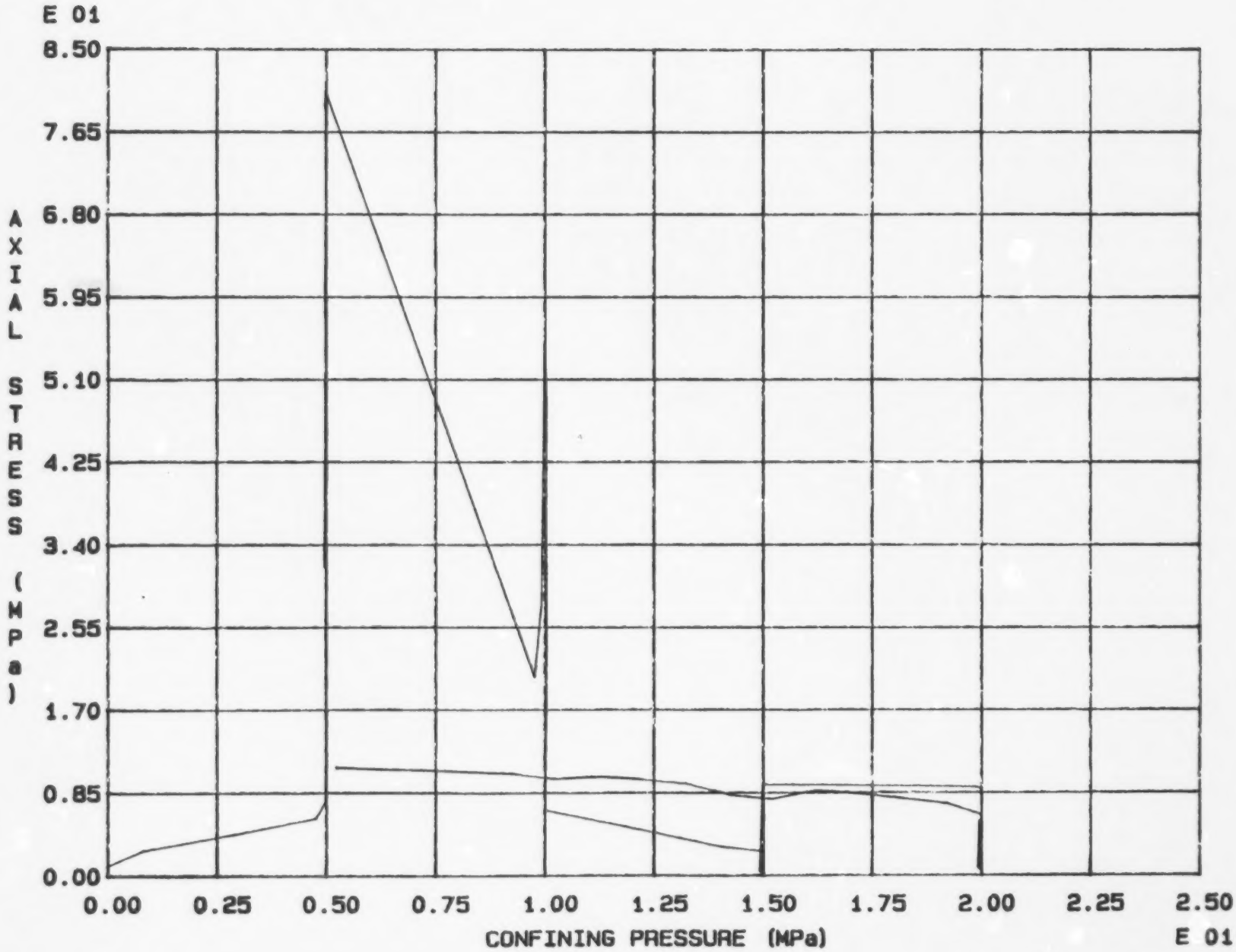

Fig. 7 - 37 Specimen M80T

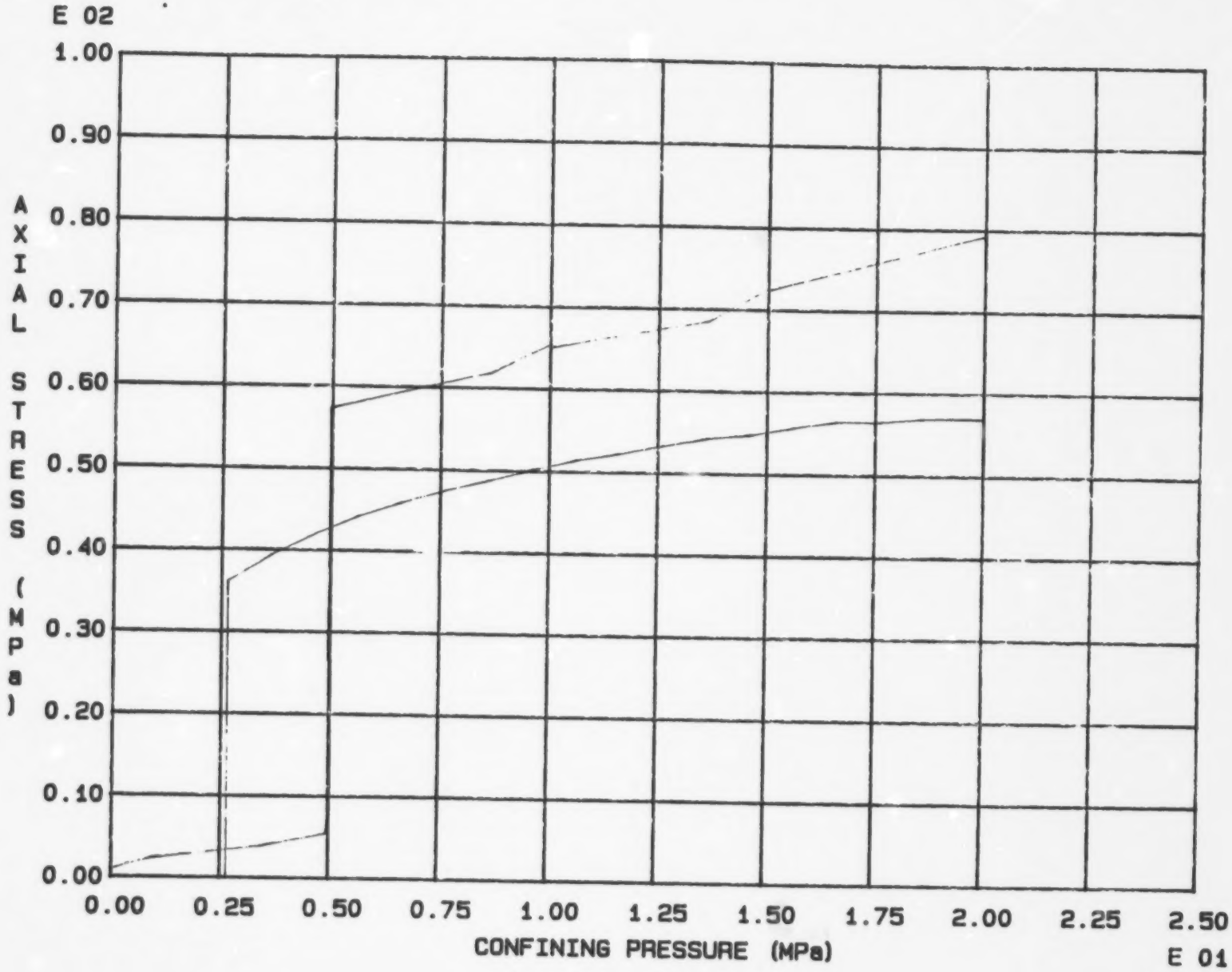

Fig. 7 - 38 Specimen M93T

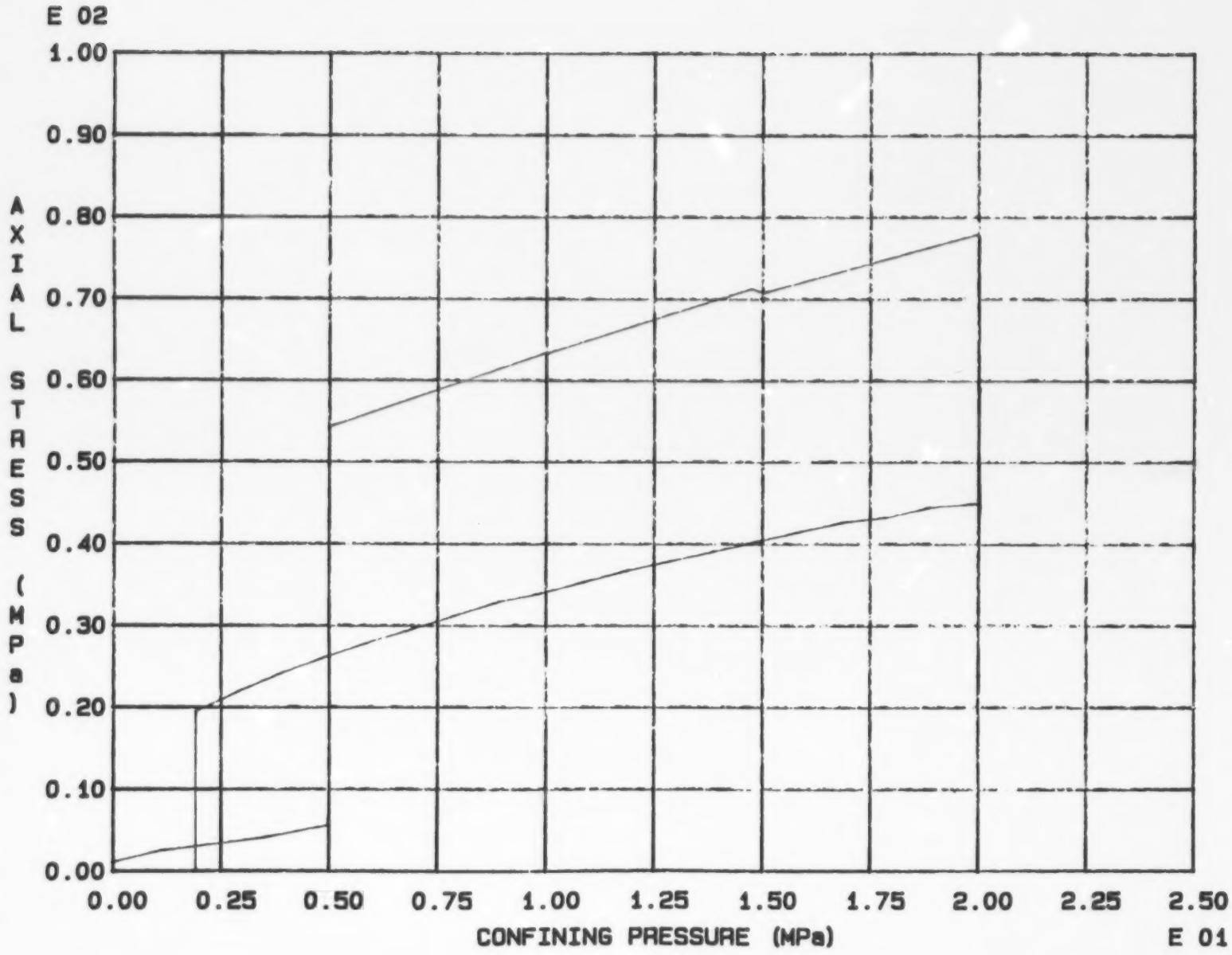

Fig. 7 - 39 Specimen M94T

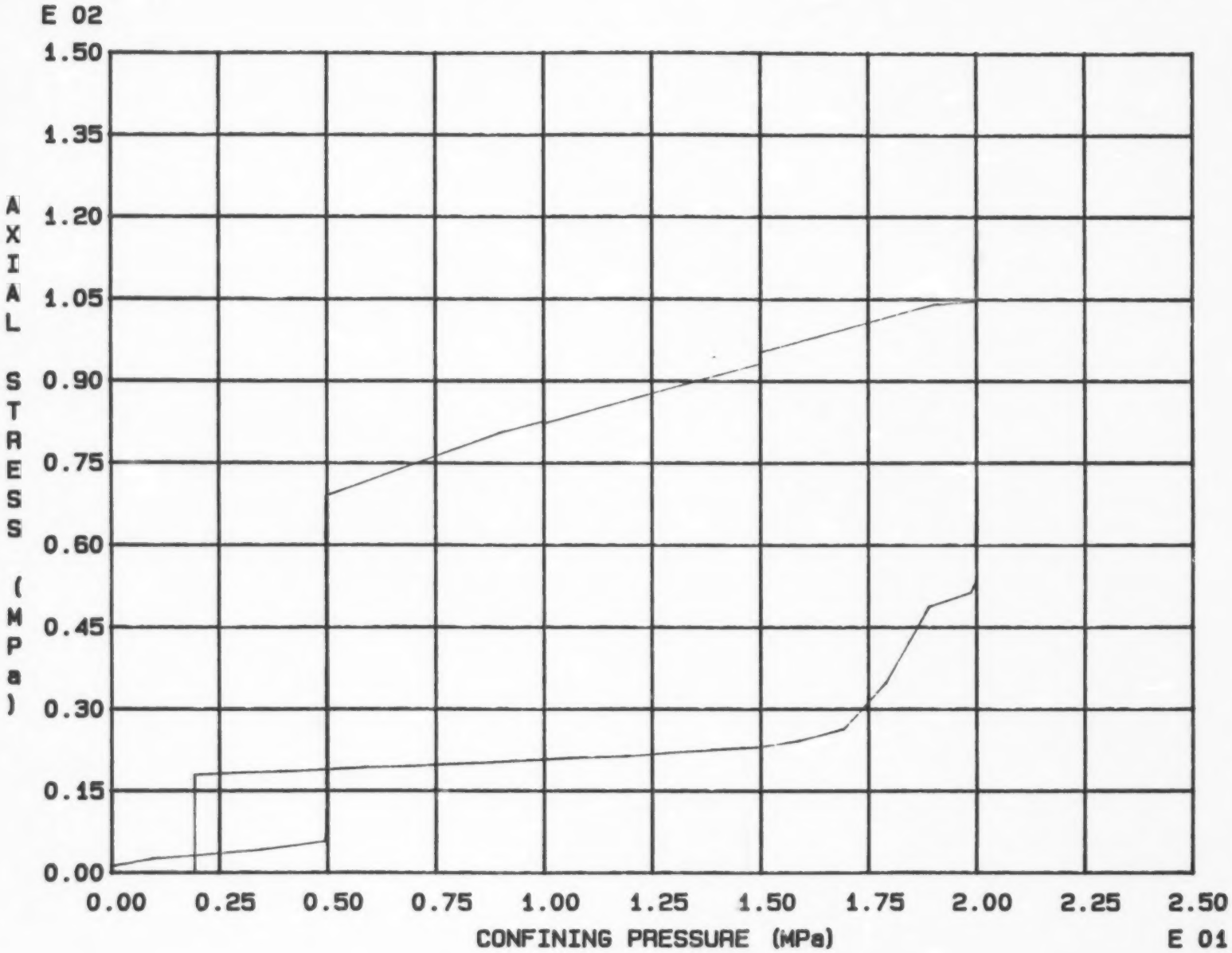

Fig. 7 - 40 Specimen M95T

Appendix 8.

Strength envelopes

MOHR ENVELOPE

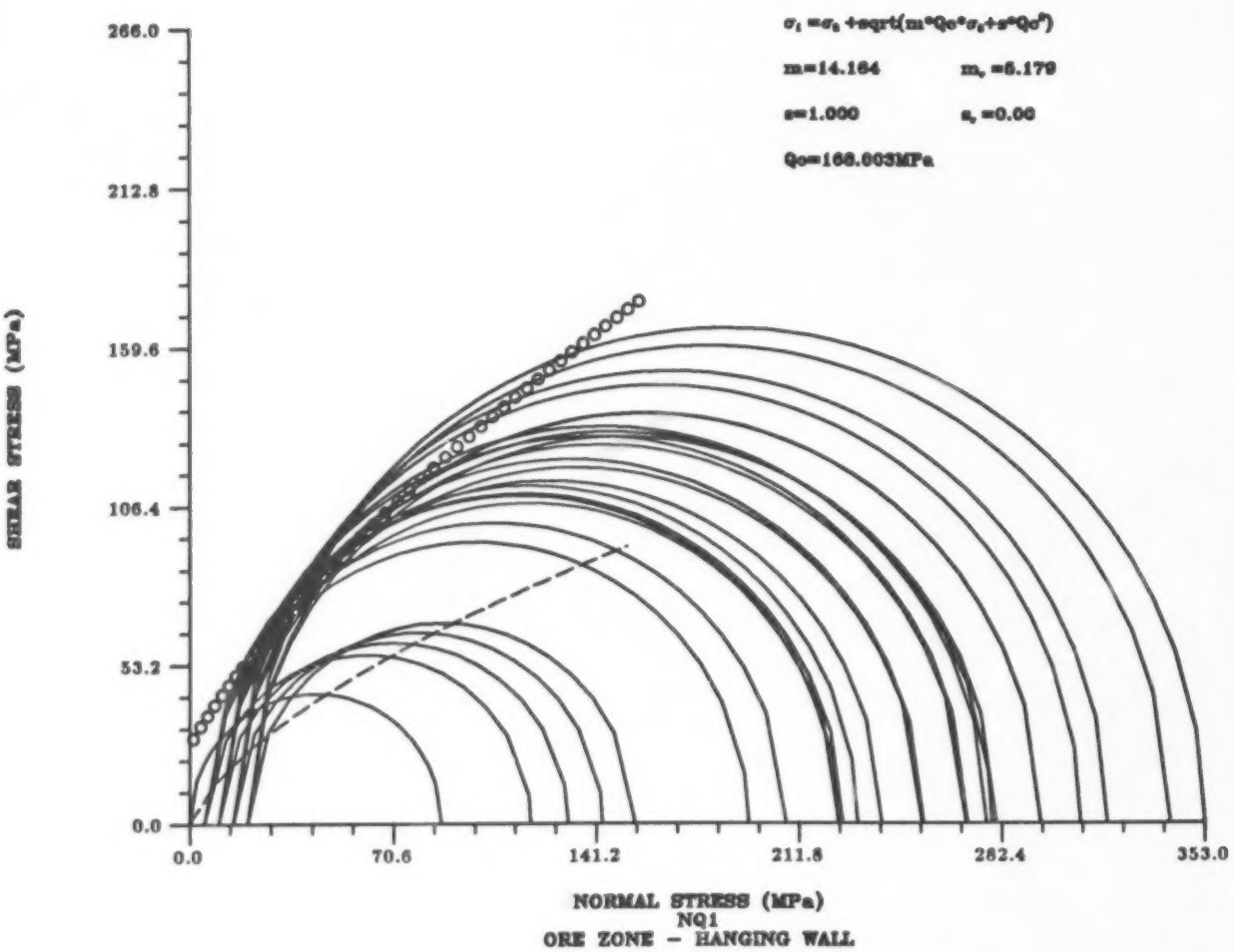

Fig. 8 - 2

MOHR ENVELOPE

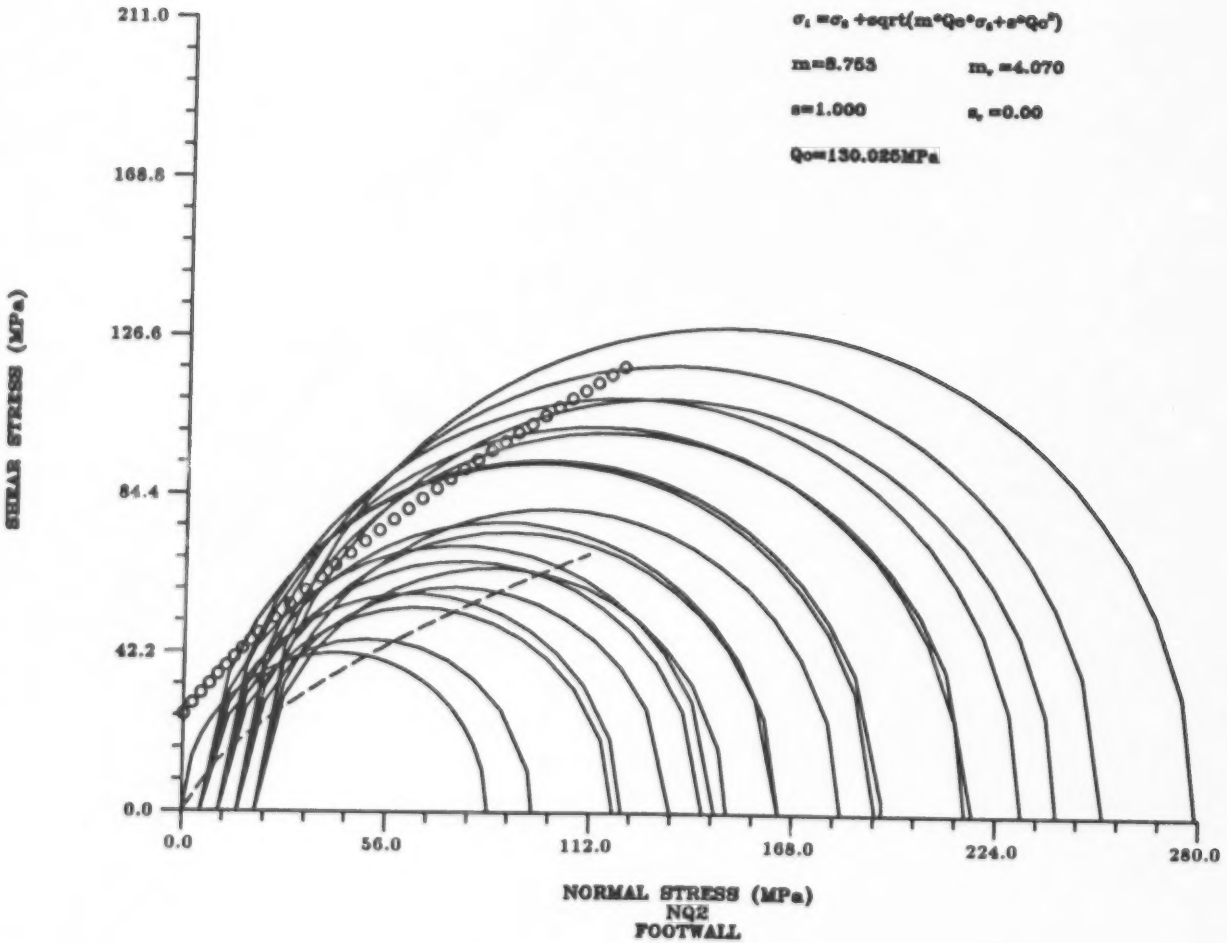

Fig. 8 - 3

MOHR ENVELOPE

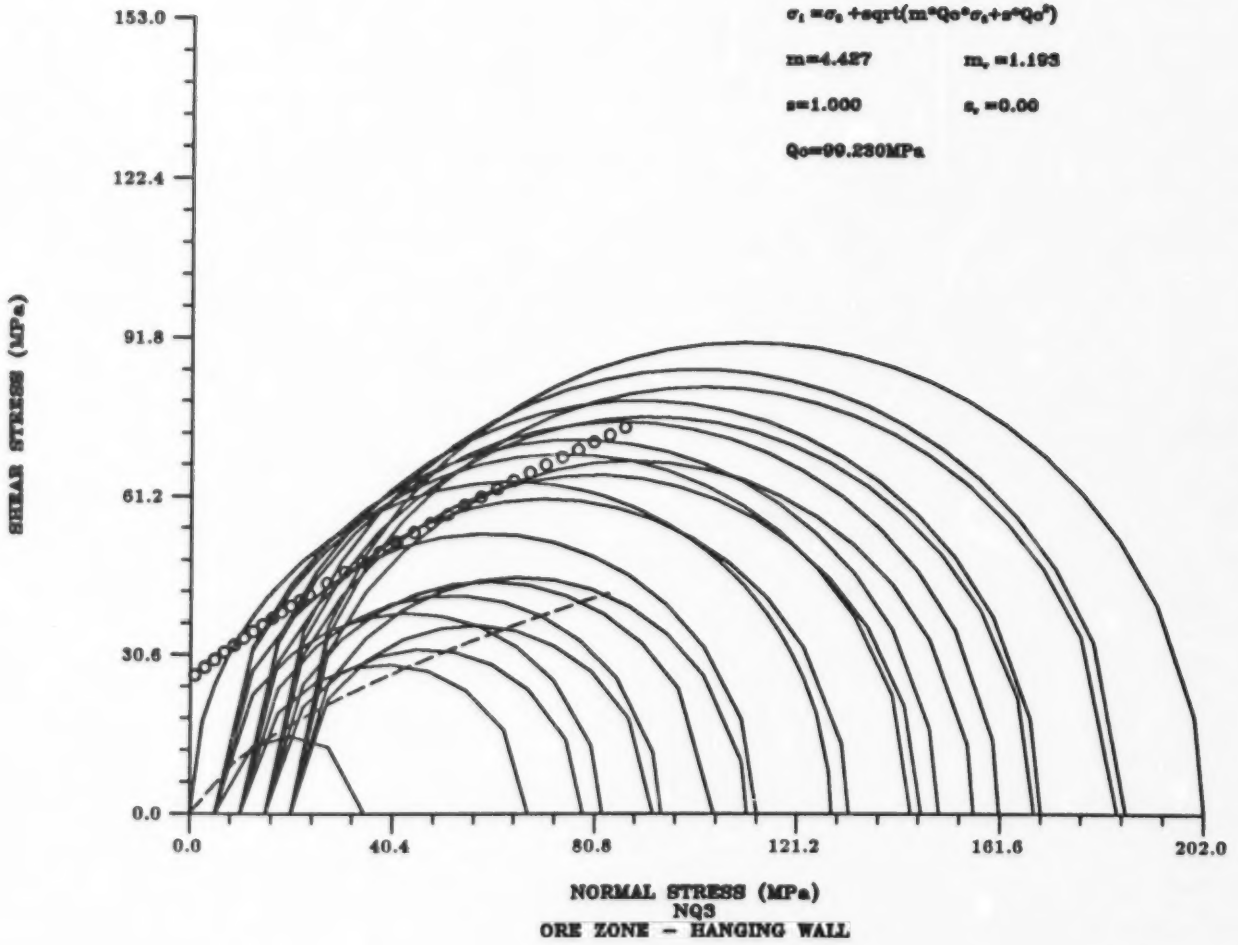

Fig. 8 - 6

MOHR ENVELOPE

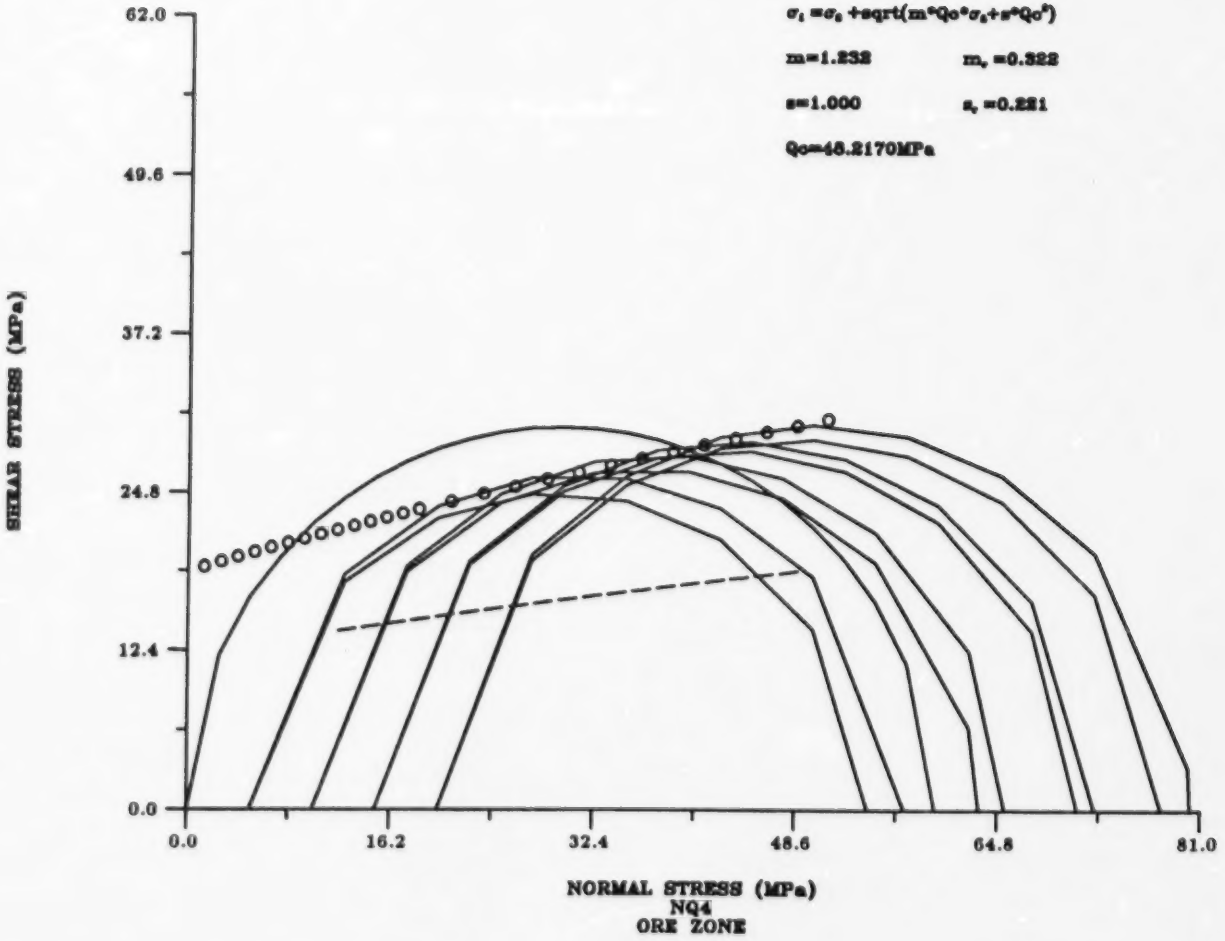

Fig. 8 - 7

MOHR ENVELOPE

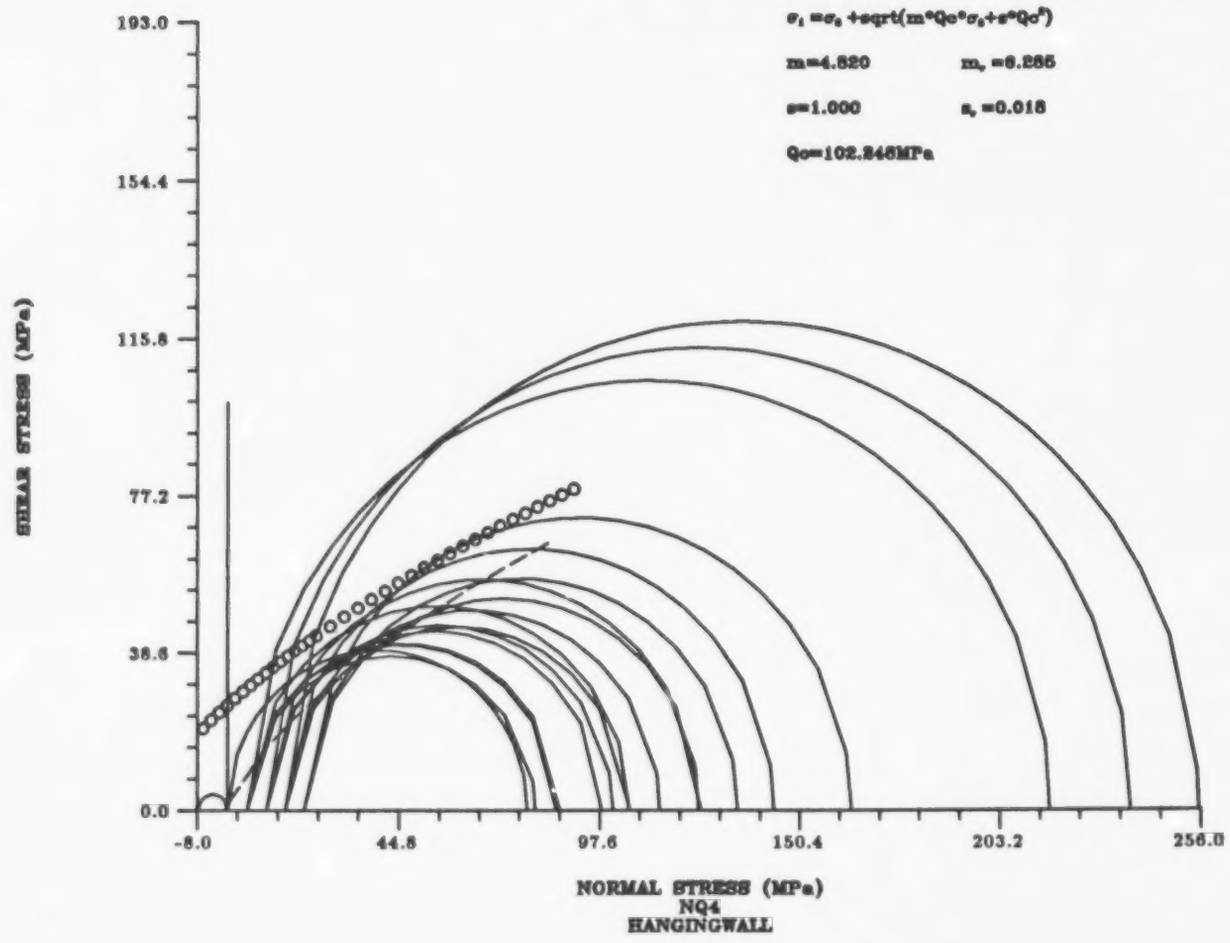

Fig. 8 - 8